THREE DIMENSIONAL RESPONSES OF A STEEL STRUCTURE UNDER BLAST LOADS

by

Young Seo Hwang

A Dissertation Presented to the
FACULTY OF THE USC GRADUATE SCHOOL
UNIVERSITY OF SOUTHERN CALIFORNIA
In Partial Fulfillment of the
Requirements for the Degree
DOCTOR OF PHILOSOPHY
(CIVIL ENGINEERING)

December 2010

Table of Contents

List of Tables

List of Figures

Abstract

The use of vehicle bombs by terrorists to attack building structures has become of increasing concern to structural engineers since the bombing of the marine barracks in Beriut (1982). This is particularly true following attacks on the Murrah building (1995). Due to increasing threat of vehicle bomb attack, structural engineers have developed methods of design and analysis to protect against blast loads. However, the behavior of structures under blast loads is difficult to understand. Current design for air blast loads generally uses simplified analysis procedures that were developed in the late 1950's [19]. More recent modeling and computation capabilities can readily be used to provide a more exact estimate of the structural behavior under these extreme loads. It has been suggested that buildings designed for strong ground motions will also have improved resistance to air blast loads. As an initial attempt to quantify this behavior, the responses of a three story and ten story steel building, designed for the 1994 building code, with lateral resistance provided by perimeter moment frames, are considered. An analytical model of the building is developed and the magnitude and distribution of blast loads on the structure are estimated using available computer software that is based on empirical methods.

To obtain the relationship between pressure, time duration, and standoff distance, these programs are used to obtain an accurate model of the air blast loading. A hemispherical surface burst for various explosive weights and standoff distances is considered for generating the air blast loading and determining the structural responses. Linear and nonlinear analyses are conducted for these loadings. Air blast demands on the structure are compared to current seismic guidelines. These studies present the displacement responses, story drifts, demand/capacity ratio, diaphragm analysis and inelastic demands for these structures.

Chapter 1 : Introduction and Literature Review

1.1. Introduction

Vehicle bombing attacks against buildings have been a weapon of choice used by many terrorist organizations. The use of vehicle bombs to attack a structure has been a common type of terrorist attack. Terror attacks against buildings have been of great concern among the structure analysts since September 11, 2001. Accordingly it is important to protect critical buildings against blast loads and to consider how blast loads may affect the building.

Due to the threat from vehicle bomb attacks, structural engineers have developed methods of structural design and analysis against blast loads. The analysis and design of structures subjected to blast loads requires a detailed understanding of the air blast phenomena and the dynamic response of structure. The analysis of structures against blast loads is very difficult because the uniform highly transient loads produced by the nearby detonation of a conventional weapon, combined with the localized structural response, results in an extremely complex structural analysis problem. The assumptions necessary in developing a simplified analysis procedure usually lead to overly conservative design because they fail to accurately account for the localized nature of the structural response, the large variation of pressure over a relatively small area, and the fact that the pressure does not arrive at every point on the structure at the same time as shown in Figure 1.1.

Engineers in the military or their contractors developed empirical methods to predict peak pressure and time duration of blast loads. Army TM5-855-1 and Army TM5-1300 are representative criteria of structural design and analysis against blast loads.

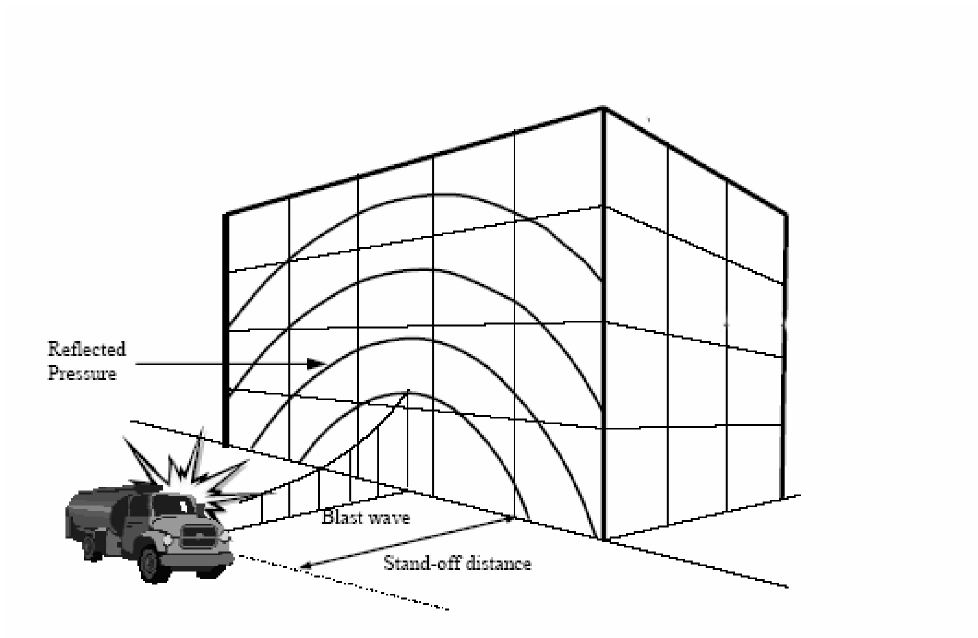

Figure 1.1 : Blast Loads on Structure

The purpose of this research is to examine linear and nonlinear structural responses of two buildings due to the stand-off distance and charge size. In this study, blast loads were applied 3 story and 10 story buildings with welded steel moment frames that are representative of earthquake resistant design in California.

To investigate structural behavior in different conditions, explosive weights of 100 lb, 500 lb, 1,000 lb, and 2,000 lb are applied to a steel frame at stand-off distance 20 ft. Using a explosive weight of 1,000 lb, the effect of stand-off distance is evaluated for distances of 15 ft, 30 ft, 50 ft, and 100 ft. This study also considers the size of the blast crater along with the different structural responses that include story displacements, demand/capacity ratio of columns and floor diaphragm, drifts and plastic rotation demands. These parameters are then compared with limit values suggested by seismic guidelines.

1.2. Literature Review

1.2.1. Blast Wave Scaling Law

Sachs blast wave scaling was proposed in 1944 as a more general one that was consisted of parameters having a function of scaled distance (Baker, 1973).

$$\bar{R} = \frac{R p_0^{\frac{1}{3}}}{E^{\frac{1}{3}}}$$

Where, R is the range, P_0 is the ambient pressure and E is the energy of charge. Sachs Law assumes that air behaves as perfect gas and gravity and viscosity are negligible.

Hopkins-Cranz blast wave scaling was described as cube-root scaling referenced by Baker (1973). The blast wave scaling law defined by Hopkins (1915) states two different weights of the same explosive have same blast characteristics at some scaled distances in similar atmospheric conditions. The Hopkins scaling distance is

$$Z = \frac{R}{W^{\frac{1}{3}}}$$

Where, R is the range from the blast center to the point of structure and W is the weight of charge

1.2.2. Blast Wave Parameters

Incident Pressure

The release of energy from a detonation leads to a sudden pressure increase and then the increase is from the ambient pressure to a peak incident or shock front pressure (p_s). The incident pressure is the pressure on a surface parallel to the direction of the blast wave. Brode (1955) estimated not only incident pressure due to spherical blast based on the Hopkins scaling distance but also expressed in terms of near field and far field.

$$p_s = \frac{6.7}{z^3} + 1\,bar \qquad (p_s \rangle 10\ bar)$$

$$p_s = \frac{0.975}{z} + \frac{1.455}{z^2} + \frac{5.85}{z^3} - 0.019\ bar \qquad (0.1 bar \langle\, p_s \,\langle 10 bar)$$

Newmark and Hansen (1961) introduced blast overpressure in terms of range and explosive weight at the ground surface.

$$p_s = 6784\frac{W}{R^3} + 93\left(\frac{W}{R^3}\right)^{\frac{1}{2}}$$

Another expression of blast overpressure in KPa was introduced by Mills (1987) in terms of equivalent charge weight and scaled distance.

$$p_s = \frac{1772}{z^3} - \frac{114}{z^2} + \frac{108}{z}$$

Reflected Pressure

As the blast wave propagates through the air, the air behind shock front has lower velocity. The velocity depends on incident pressure and is associated with dynamic pressure. If such a blast wave encounters an obstacle perpendicular to the direction of wave direction, the reflection changes the pressure to reflected pressure (p_r). Rankin and Hugoniot (1870) suggested the velocity of blast wave and dynamic pressure in terms of incident pressure.

$$U_s = \sqrt{\frac{6p_s + 7p_0}{7p_0}} \cdot a_0$$

$$q_s = \frac{5p_s^2}{2(p_s + 7p_0)}$$

Where, U_s is the velocity of wavefront, p_s is the overpressure, p_0 is the ambient of air pressure, a_0 is the speed of sound in air and q_s is the dynamic pressure.

Rankine and Hugoniot also derived the equation for reflected overpressure p_r.

$$p_r = 2p_s \left[\frac{7p_0 + 4p_s}{7p_0 + p_s} \right]$$

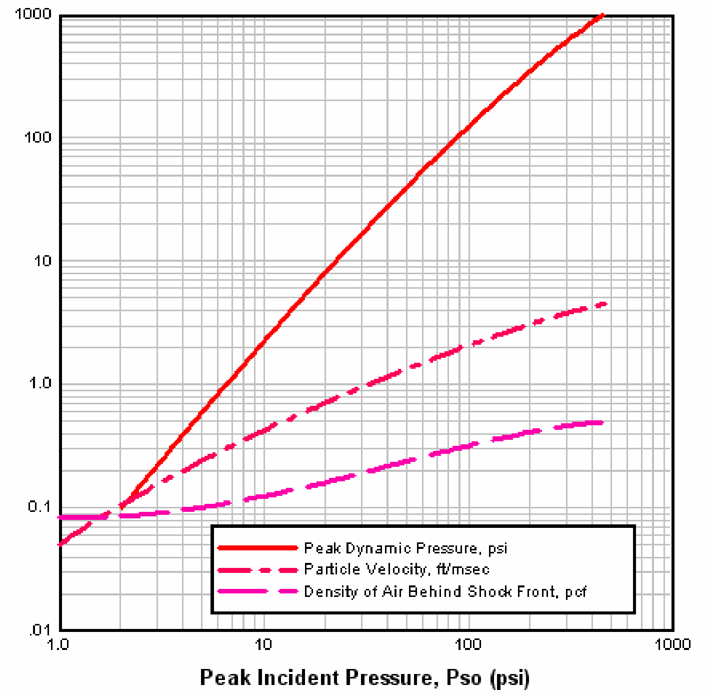

Figure 1.2 : Peak Incident Pressure vs. Peak Dynamic Pressure, Particle Velocity & Density of Air (SOURCE : Army TM5-1300, Navy NAVFAC)

Blast Wave pressure Profiles

The pressure-time history of a blast wave was modeled using exponential functions such as the Friendlander equation. Thus, a conservative estimation used a linear decay and neglected negative phase.

$$p(t) = p_s\left[1-\frac{t}{T_s}\right]\exp\left\{-\frac{bt}{T_s}\right\}$$

Where p_s is the peak overpressure, T_s is the positive phase duration and b is the decay constant.

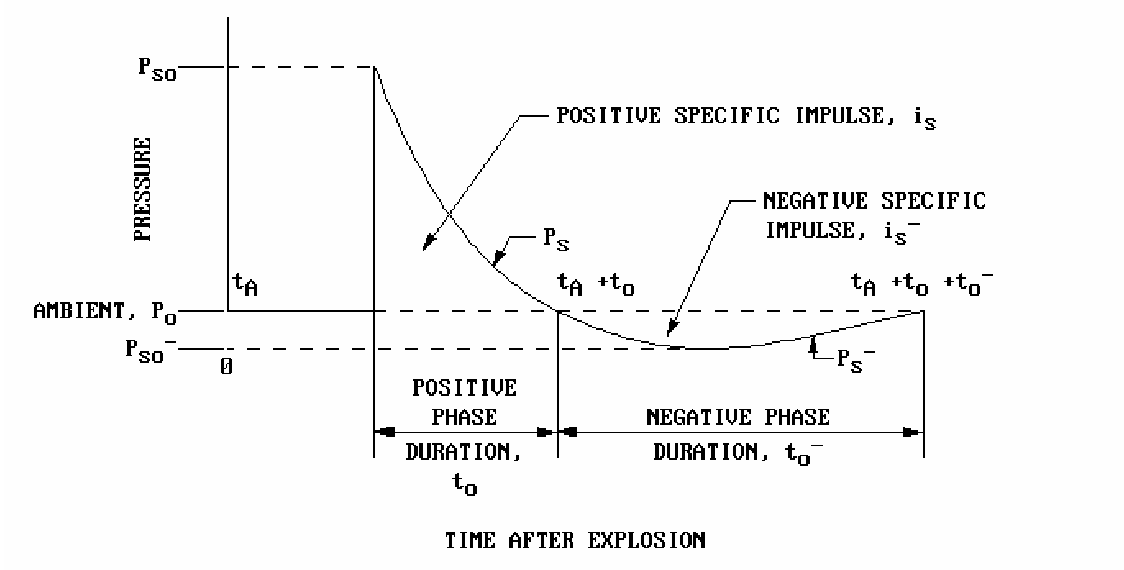

Figure 1.3 : Exponential Decay of Pressure-Time History

Typical blast pressure profile is in shown as Figure 1.3. At the arrival time following the explosion, pressure at the position suddenly increases to a peak overpressure, P_{so}, over ambient pressure, P_o, and pressure decays to ambient pressure at time t_A+t_o, then decays further to an under pressure, p_{so}^-, before returning to ambient level. Most design case ignore negative phase because of little effect on structure.

1.2.3. Blast Wave External Loading on Structure

To obtain the pressure on a structure, a charge placed on or very near the ground surface, such as a vehicle bomb attack, is considered to be a surface burst. The initial wave of the explosion is reflected and reinforced by the ground surface to produce a reflected wave. The Figure 1.4 is shown that how the reflected wave propagates through the atmosphere (TM 5-855-1).

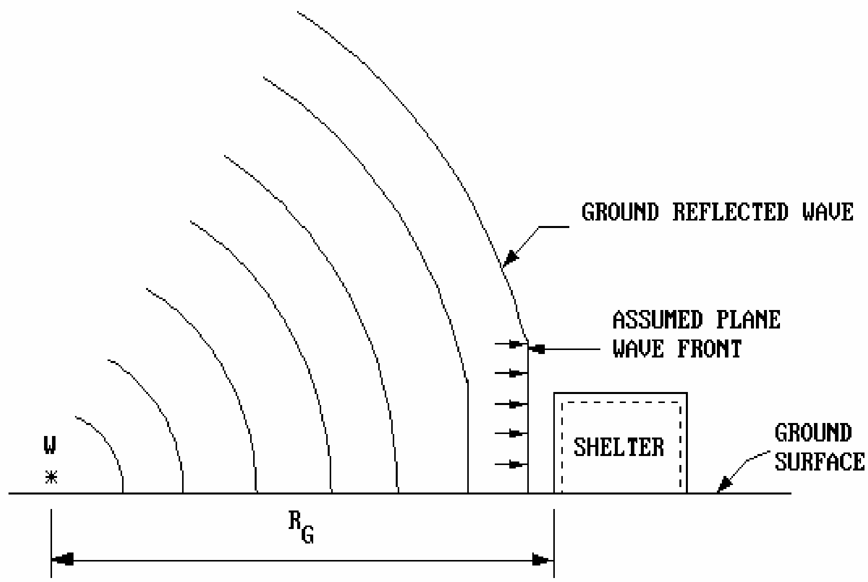

Figure 1.4 : Surface Burst Blast Environmental

TM5-1300 provided reflected pressure, incident pressure, arrival time, time duration, wave length, and the impulse of incident and reflected pressure in terms of scaled distance. Figure 1.5 is shown that various data was given by TM5-1300. In addition, Figure 1.6 is shown that the variation of the pressure and impulse patterns on a reflecting surface is a function of the angle and magnitude of the incident pressure p_s.

For the calculation of reflected pressure, incident pressure is interpolated in Figure 1.6 and then a coefficient ,C_r , is determined for the angle of incident. This coefficient is used to obtain the reflected pressure for applied to the structure.

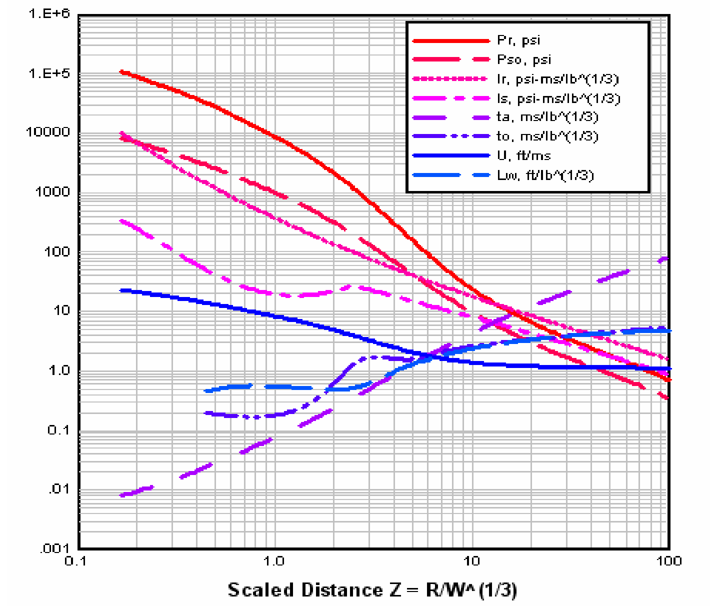

Figure 1.5 : Wave Parameters of Hemispherical TNT Explosions

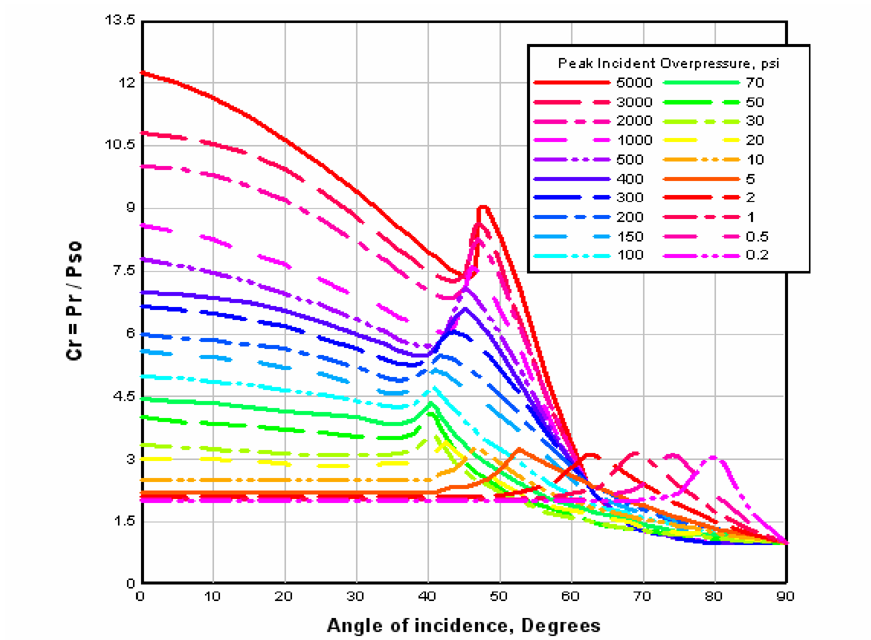

Figure 1.6 : Reflected Pressure Coefficient vs. Angle of Incidence (SOURCE : Army TM5-1300, Navy NAVFAC)

Chapter 2 : Finite Element Model of Steel Structures

The welded steel moment frame (WSMF) buildings are designed to resist earthquake ground shaking, based on the assumption that they are capable of extensive yielding and inelastic deformation. This building system was based on the 1994 Uniform Building Code (UBC). However, the design of the frame didn't provide any deliberate resistance against a vehicle bomb attack. This chapter describes the building details as well as shows a model of building using SAP2000 FEM Software [21].

2.1. Description of 3 Story Building

Figure 2.1 shows the 3 story building with a typical floor to floor height of 13'-0" is rectangular in shape and main roof with same dimension of typical floor in Figure 2.2. The floor was consisted of concrete over metal deck diaphragm. The building plane is 180'*120'and divided into 30-feet bays in each direction, six in the longitudinal direction and four in the transverse direction. The lateral force resisting systems in each direction consist of 3-bay WSMF frames on each side of the building perimeter. The remainder of the steel framing is provided for gravity loads. The base of the frame columns are assumed to be fixed. Concrete grade beams at the foundation level are utilized to resist the moments at the base of the columns. Figure 2.3 shows details of WSMF frames. The gravity beams and columns conform to ASTM A36 and ASTM A572 Gr.50, as specified. The Welded Frame girders conform to ASTM A36 and the Welded Frame columns conform to ASTM A572 Gr.50.

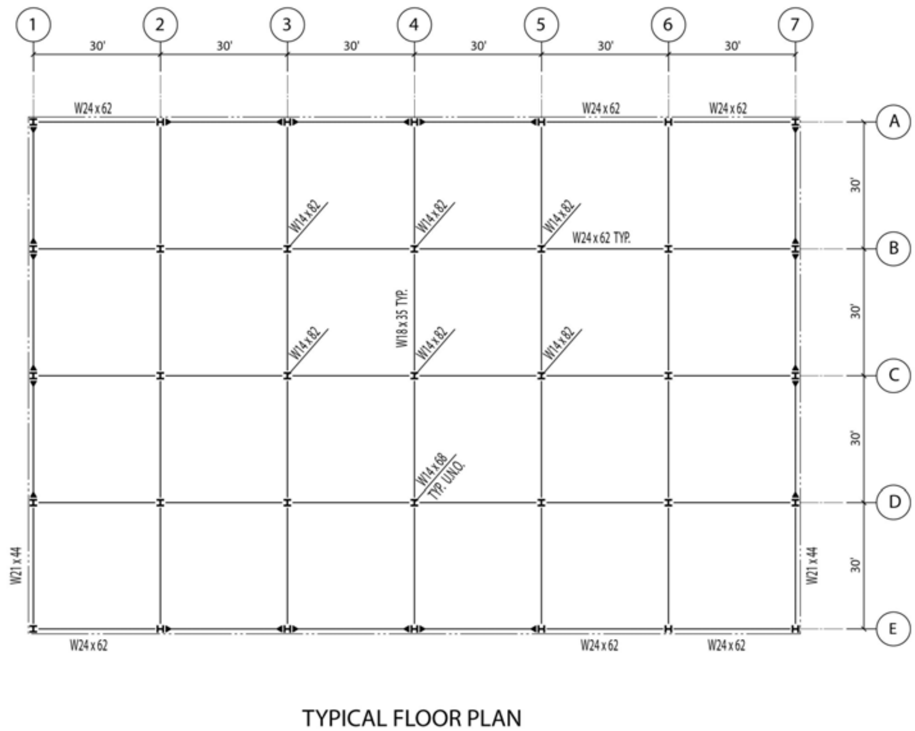

Figure 2.1 : Typical Floor Plan

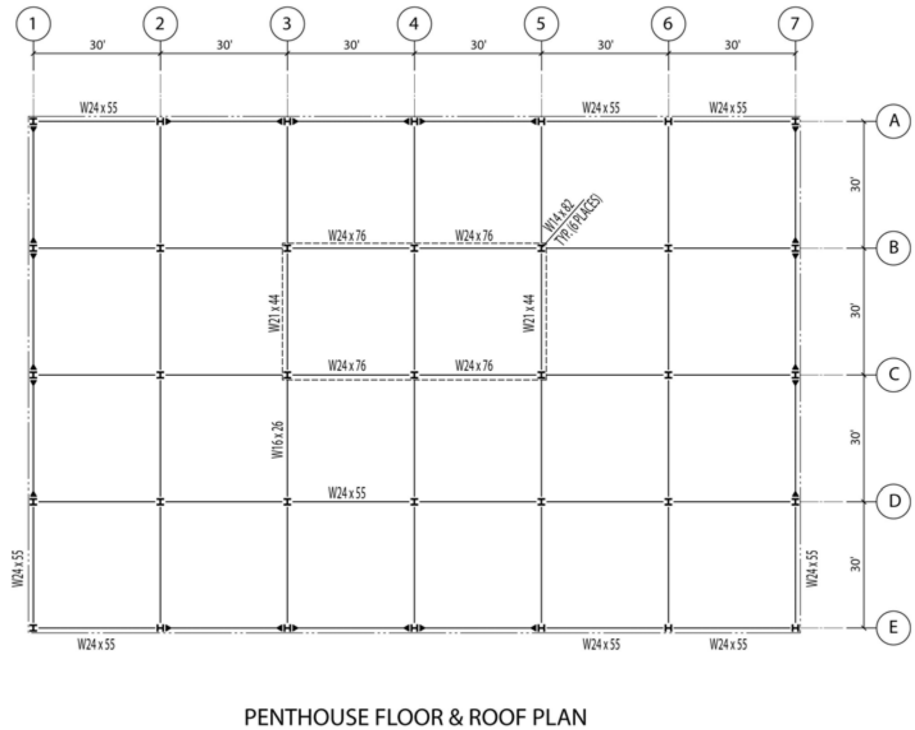

Figure 2.2 : Roof Plan

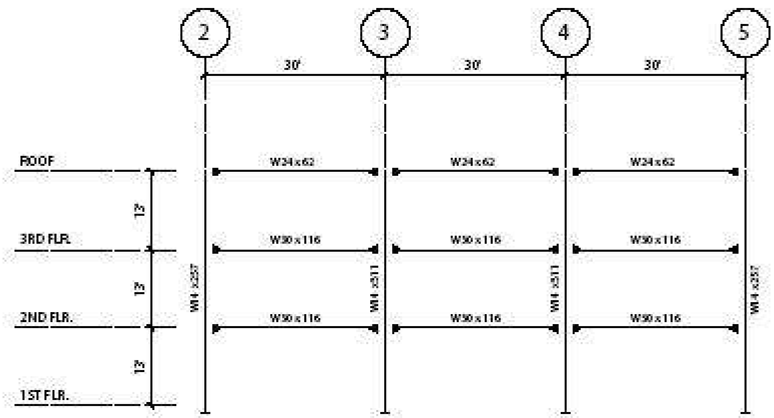

ELEVATION AT LINES "A" & "E"

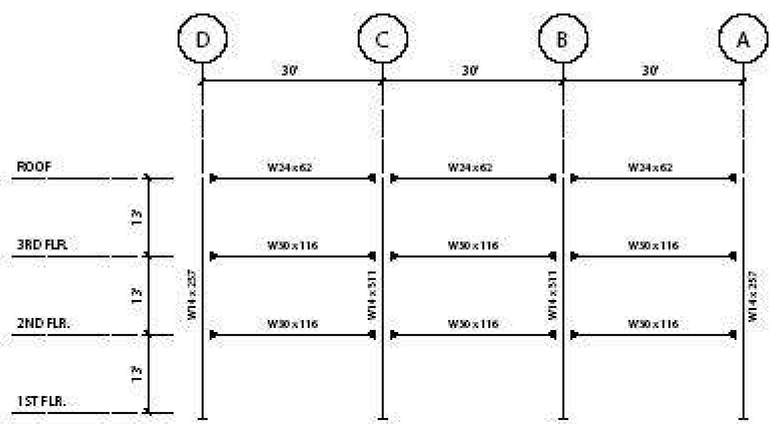

ELEVATION AT LINES "1" & "7"

Figure 2.3 : Welded Steel Moment Frame (WSMF) – Transverse & Longitudinal Direction

2.2. Description of 10 Story Building

Figure 2.4, Figure 2.5 and Figure 2.7 show the 10 story building with a typical floor to floor height of 13’-0” with exception of 12’ for the 1st floor and 18’ for the 2nd floor. The plane is square in shape with the main roof and the same dimension of typical roof in Figure 2.6. The floor was also consisted of concrete over metal deck diaphragm. The building plane is 150’*150’and divided into 30-feet bays in each direction, five in the longitudinal direction and five in the transverse direction. The lateral force resisting systems in each direction consist of 5-bay WSMF frames on each side of the building perimeter. The remainder of the steel framing is provided for gravity loads. The base of the frame columns are designed fixed. Figure 2.7 and Figure 2.8 show details of WSMF frames as well as Figure 2.9 also shows frame elevation of steel column. The gravity beams and columns conform to ASTM A36 and ASTM A572 Gr.50, as specified. The Welded Frame girders and the Welded Frame columns conform to ASTM A36 and ASTM A572 Gr.50.

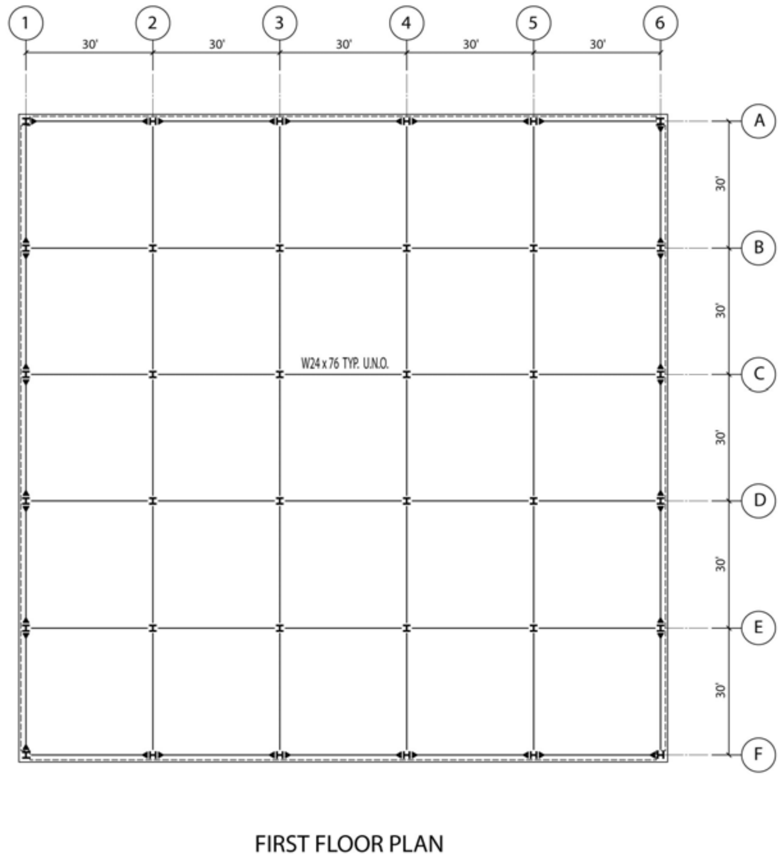

Figure 2.4 : First Floor Plan

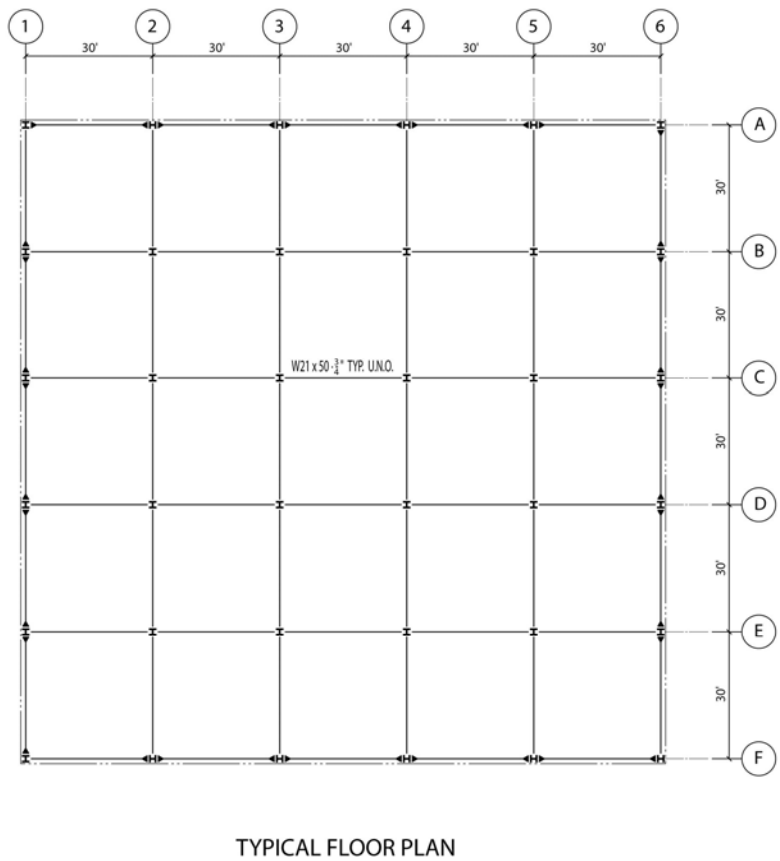

Figure 2.5 : Typical Floor Plan

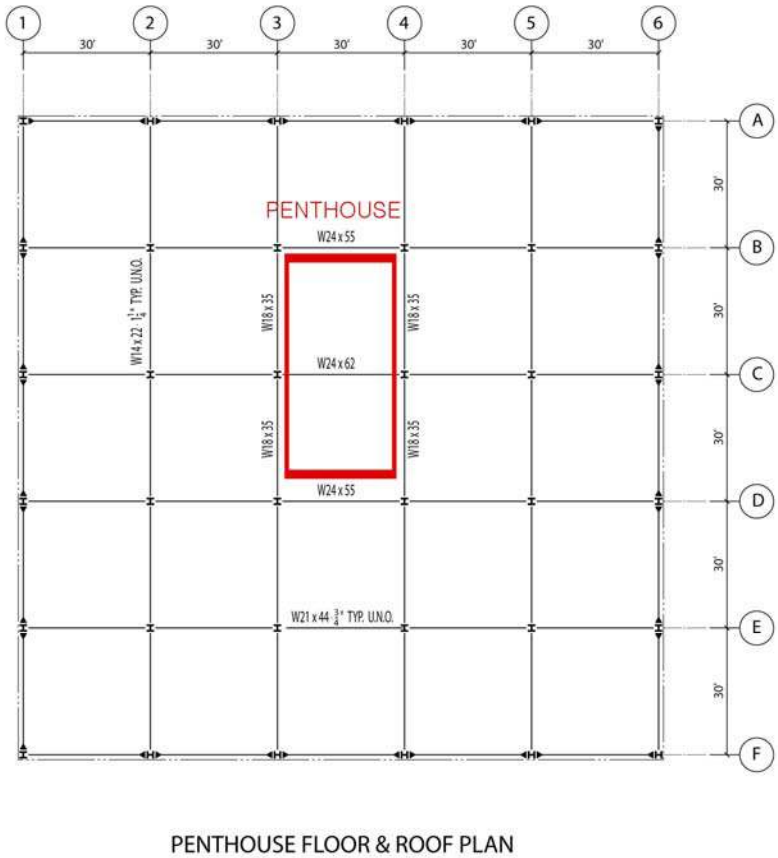

Figure 2.6 : Roof Plan

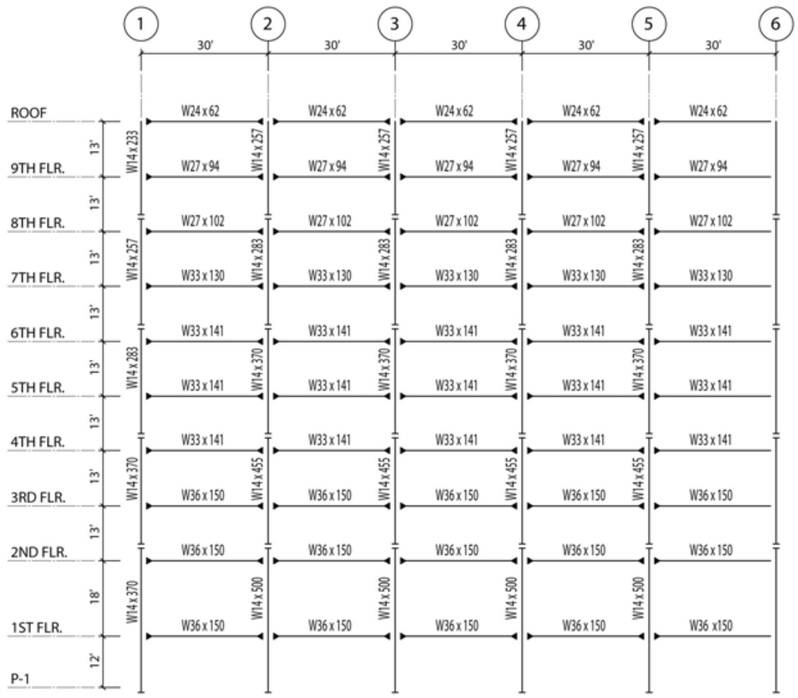

ELEVATION AT LINES "A" & "F"

Figure 2.7 : Welded Steel Moment Frame (WSMF) – Transverse Direction

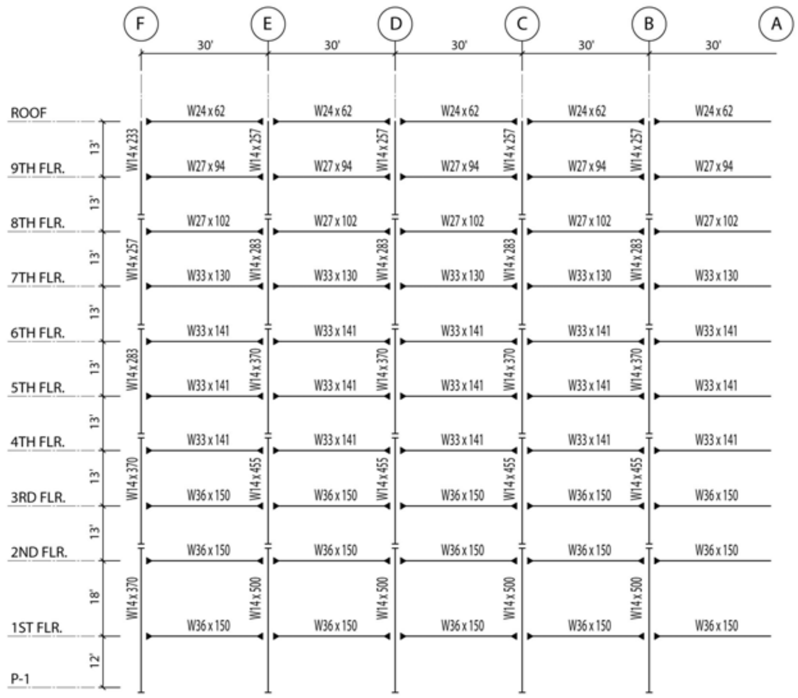

ELEVATION AT LINES "1" & "6"

Figure 2.8 : Welded Steel Moment Frame (WSMF) – Longitudinal Direction

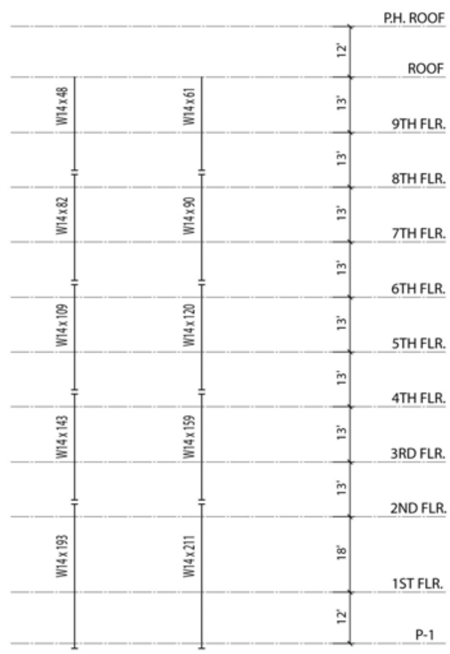

Typical **B-3, B-4**
U.N.O **C-3, C-4**
D-3, D-4

Figure 2.9 : Column Schedule and Steel Frame Elevations

2.3. Description of Building Model

Figure 2.10 and Figure 2.11 show 3D views of the computer model of 3 story building and 10 story building. The floor is assumed to be rigid in its plane due to be consisted of a concrete metal deck diaphragm. The infill beams are not specifically included in the computer model using SAP2000 FEM Software. The base restraint was assumed to be the fixed condition and the concrete over metal deck floor was assumed to be a rigid diaphragm in initial model.

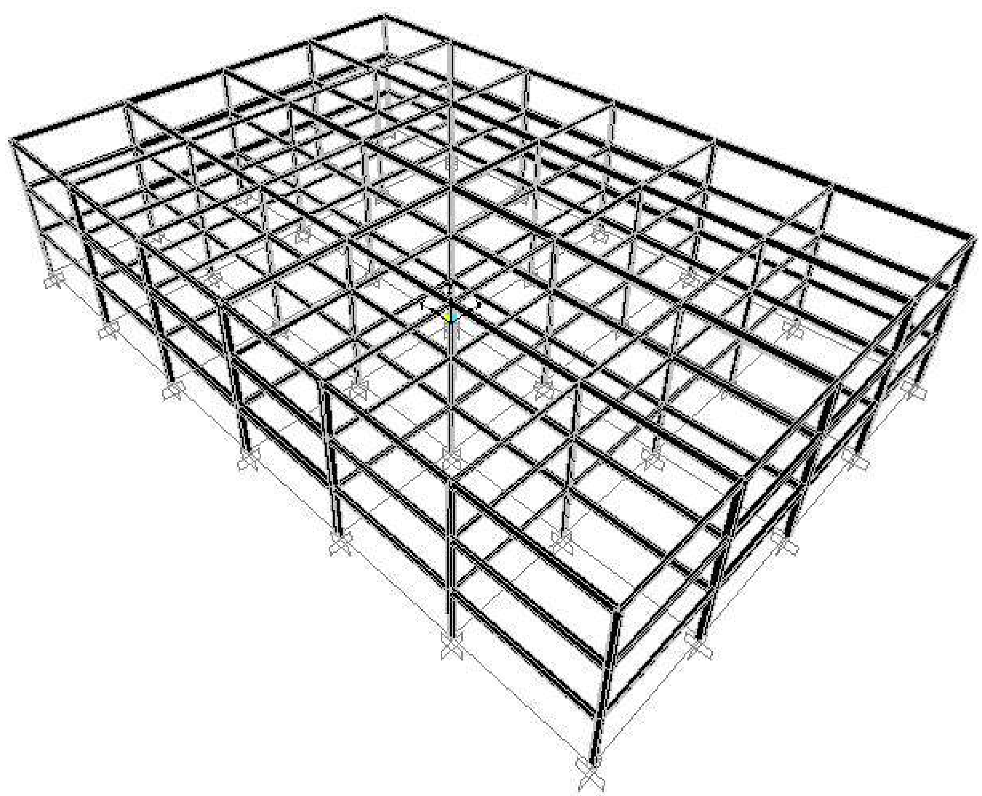

Figure 2.10 : Description of 3 Story Building Model Using SAP2000 FEM Software

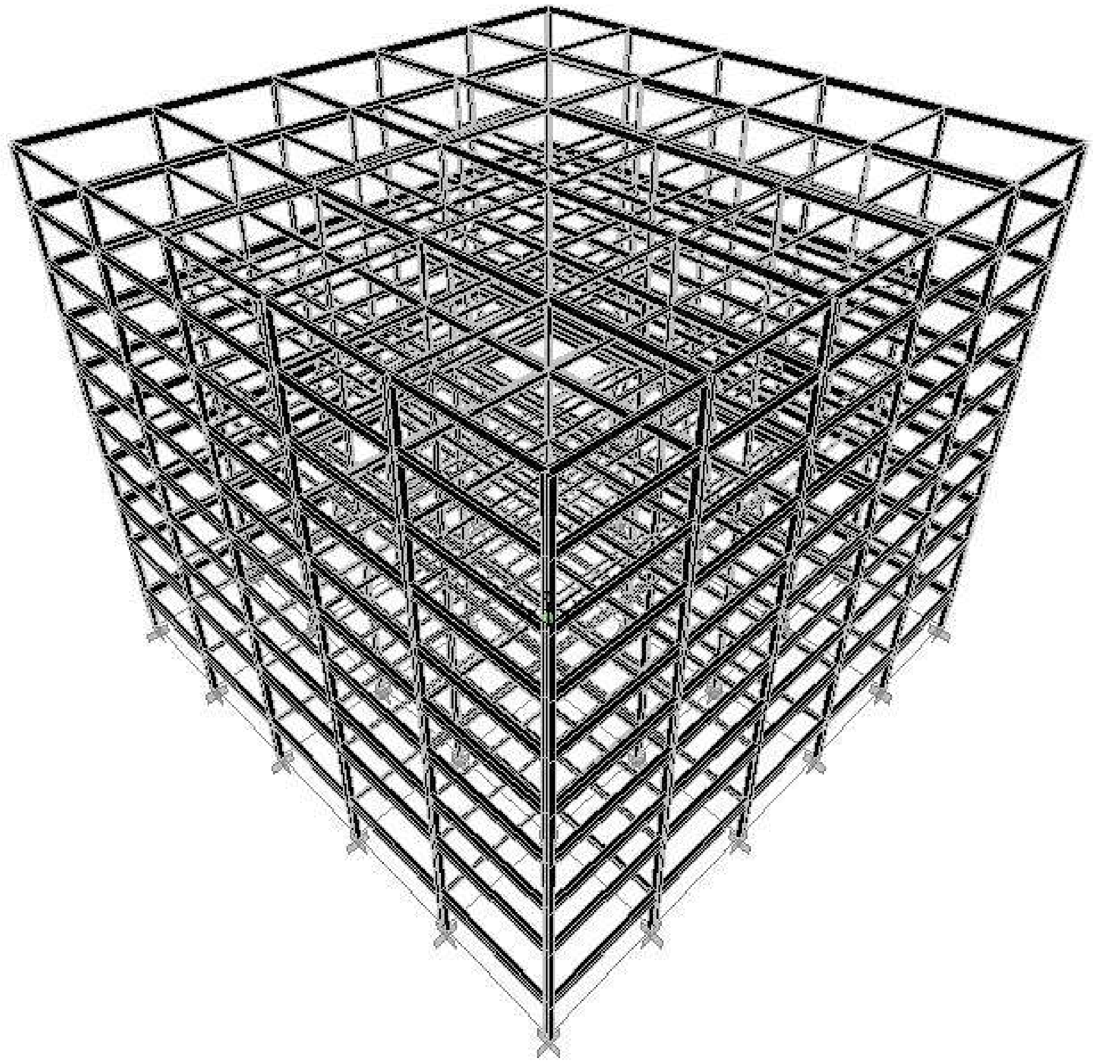

Figure 2.11 : Description of 10 Story Building Model Using SAP 2000 FEM Software

Chapter 3 : Blast Loads and Crater

To confirm the values of incident pressure in Figure 3.1, the CONWEP [26] and ATBLAST [3] program will be used. For example, a vehicle bomb explosion of 2,000 lb TNT weight at 970 ft results in an incident overpressure is 0.5 psi as shown in Figure 3.1. The incident pressure of ATBLAST is 0.5 psi shown in Figure 3.2 and the reflected pressure obtained by ATBLAST is 1.0 psi shown in Figure 3.2 and the reflected pressure obtained by CONWEP is 1.0 psi shown in Figure 3.3. Thus, these programs are able to provide reliable results. In Table 3.1, the incident and reflected pressure have good agreements of four cases at 2,000 lb TNT.

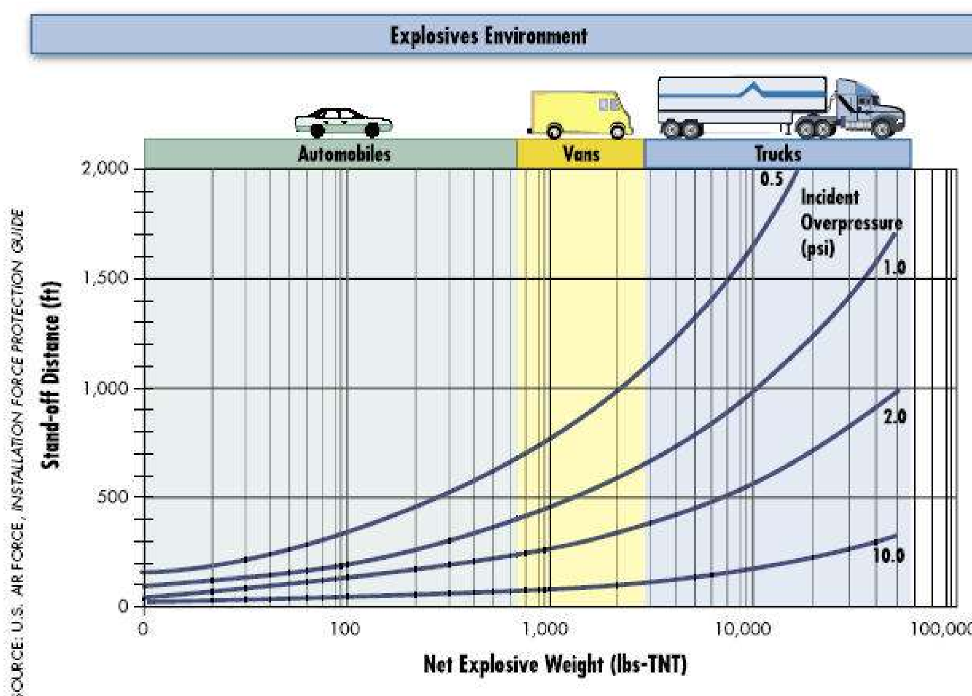

Figure 3.1 : Incident Overpressure Measured in Pounds per Square in, As a Function of Stand-off Distance and Net Explosive Weight (Pounds – TNT)

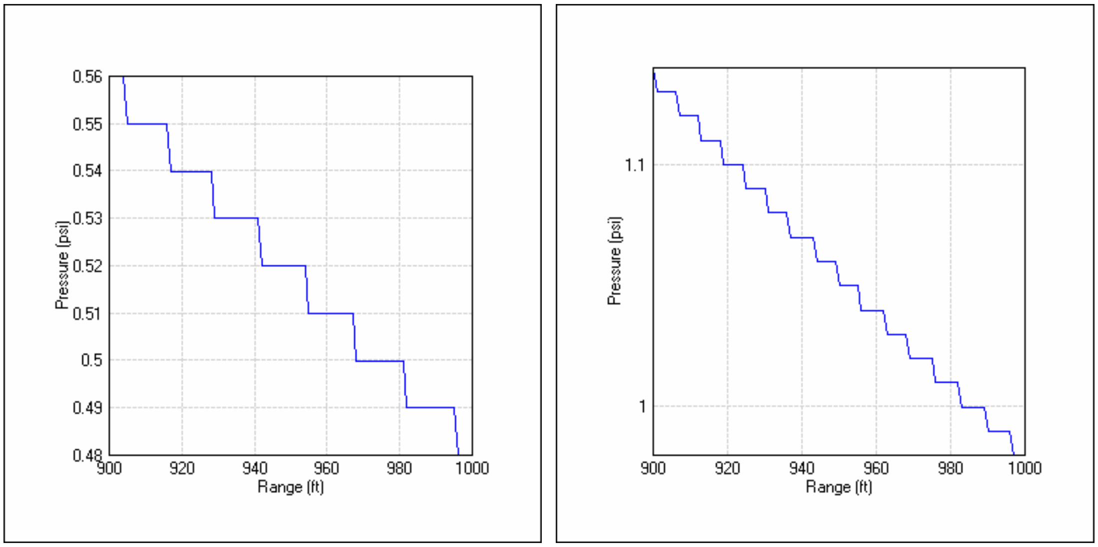

(a) Incident Pressure from ATBLAST (b) Reflected Pressure from ATBLAST

Figure 3.2 : Incident Pressure and Reflected Pressure from ATBLAST Program

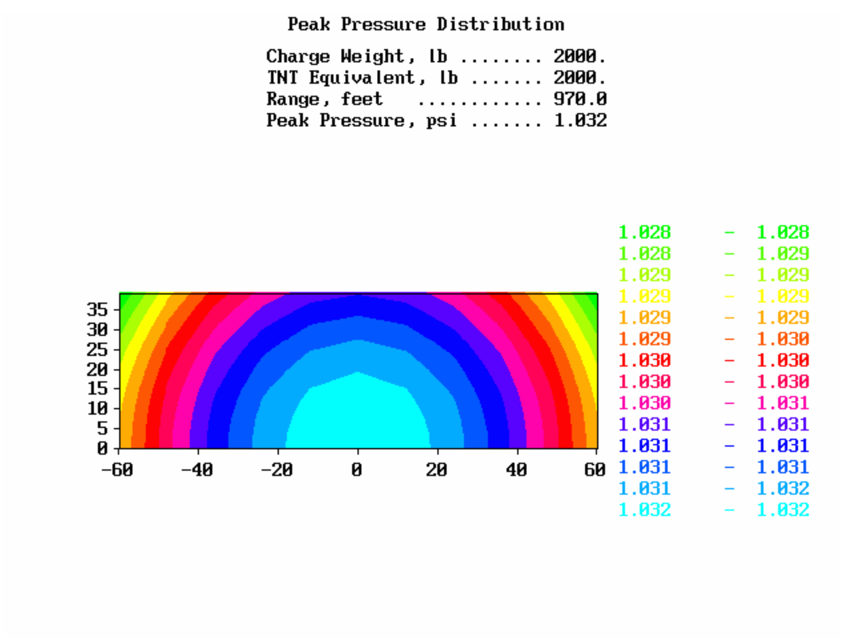

Figure 3.3 : Reflected Pressure from CONWEP Program

Table 3.1 : Comparison of ATBLAST and CONWEP

		ATBLAST	ATBLAST	CONWEP
Case	Range (ft)	Incident Pressure (psi)	Reflected Pressure(psi)	Reflected Pressure(psi)
1	970	0.5	1.02	1.03
2	575	1	2.05	2.04
3	335	2	4.24	4.19
4	123	10.02	25.35	25.05

But incident pressure is not parallel to the direction of the wave's travel, it is reflected and reinforced, producing what is known as reflected pressure. The reflected pressure is always greater than the incident pressure at the same distance from the explosion. When the shock wave impinges on a surface that is perpendicular to the direction it is traveling, the point of impact will experience the maximum reflected pressure [10]. Therefore, reflected pressure is used in the analysis. The incident pressure and reflected pressure through different stand-off distance are shown in Appendix A.1.

3.1. Blast Loads

To define the blast loads, the CONWEP program based on TM 5-855-1 [26] was used for loads on the structure. This program defines peak reflected pressure (Pr) and time duration (td) at a given distance. Prior to obtaining peak pressure and time duration, the type of blast, weapon, direction of target and stand-off distance were selected as given conditions. The input procedures of CONWEP program is shown in Appendix A.2. Table 3.2 shows input data and Table 3.3 shows peak reflected pressure (P_r), time duration (t_d) and time of arrival (t_A) at node points on the transverse face of the structure. These input data were assumed under vehicle bomb attack with 1,000 lb TNT weight at 15 ft. Also, time history functions were defined to input data for SAP2000 FEM software [21] using these results. Figure 3.4 – Figure 3.7 show generation of blast loads on 3 story building using SAP2000.

Table 3.2 : Input Data in CONWEP Program

Type of Blast	Air Blast
Type of Air Blast	Loads on Structure
Select of Weapon and Weight	TNT, 1,000 lb
Direction of Target	Hemispherical Surface Burst
Stand-off Distance	15 ft

Table 3.3 : Output of CONWEP Program

No of Joint	Time of Arrival (msec)	Time of Duration (msec)	Force (kips)
2	19.75	16.8	1178.38
3	22.01	17.65	976.48
4	25.66	18.73	405.23
30	6.92	14.07	26295.09
31	9.44	16.24	8527.47
32	13.53	16.48	1844.86
58	2.35	12.41	49547.16
59	4.95	16.33	14635.30
60	9.17	16.08	2727.27

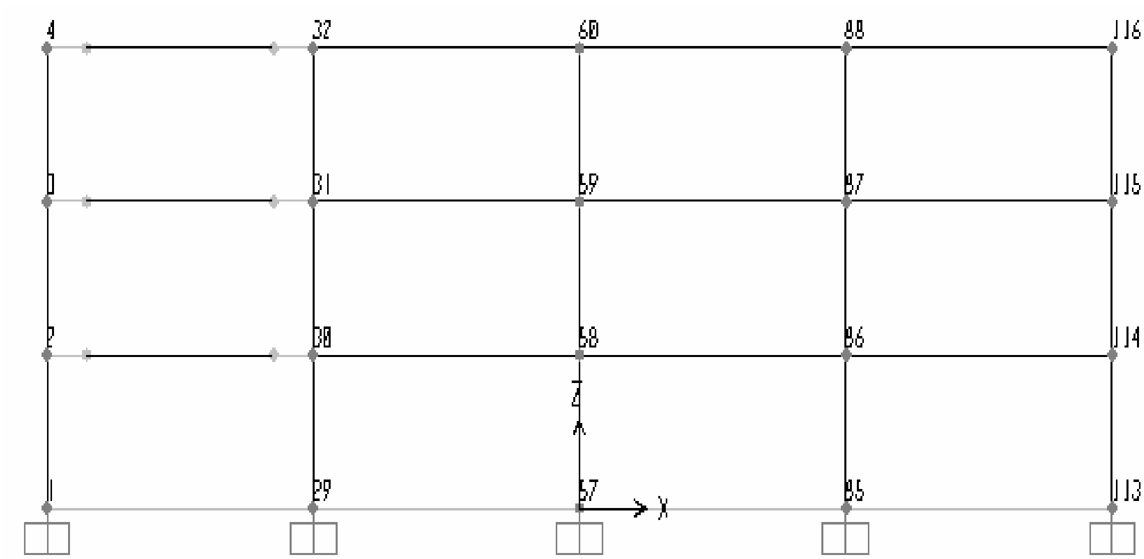

Figure 3.4 : Front Frame (Transverse Direction)

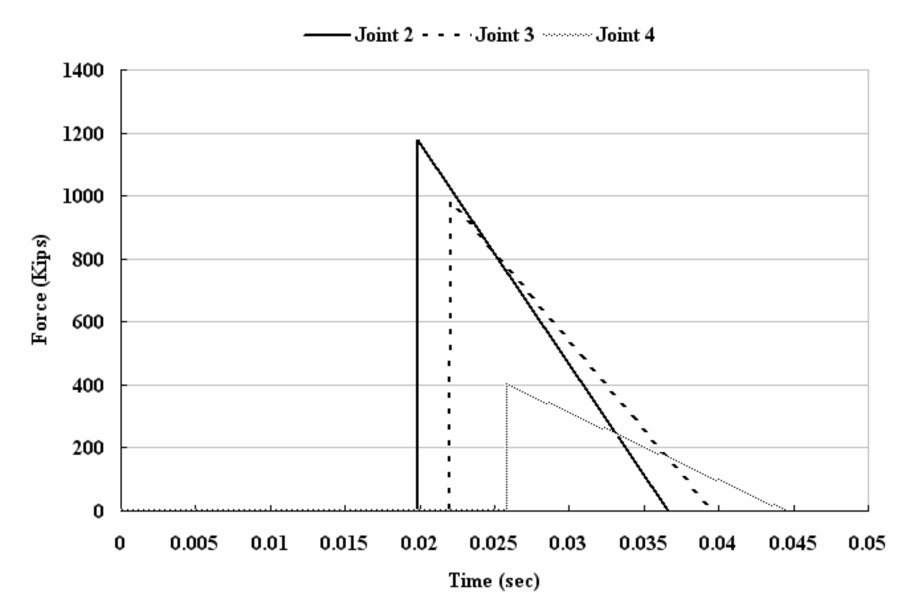

Figure 3.5 : Applied Blast Loads on Joint 2, 3, 4

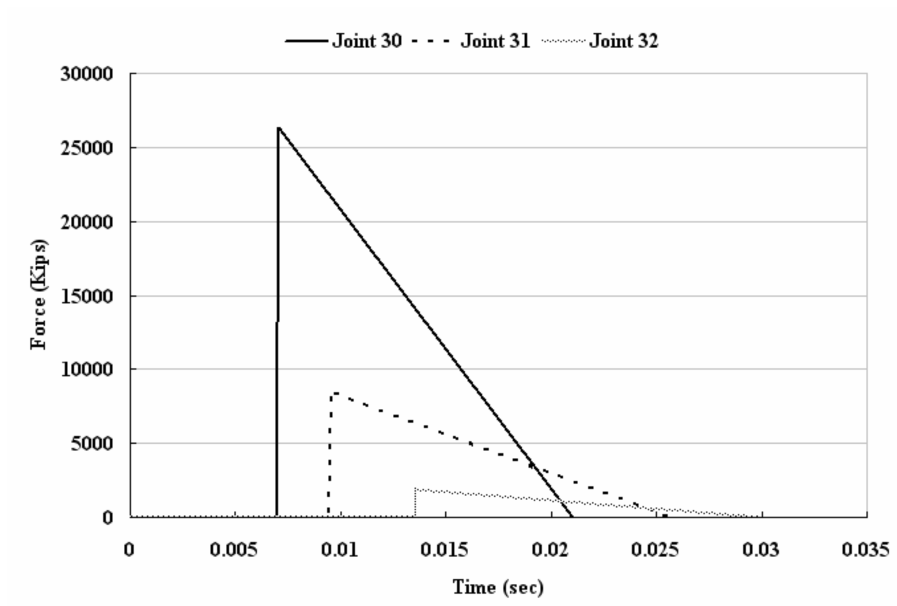

Figure 3.6 : Applied Blast Loads on Joint 30, 31, 32

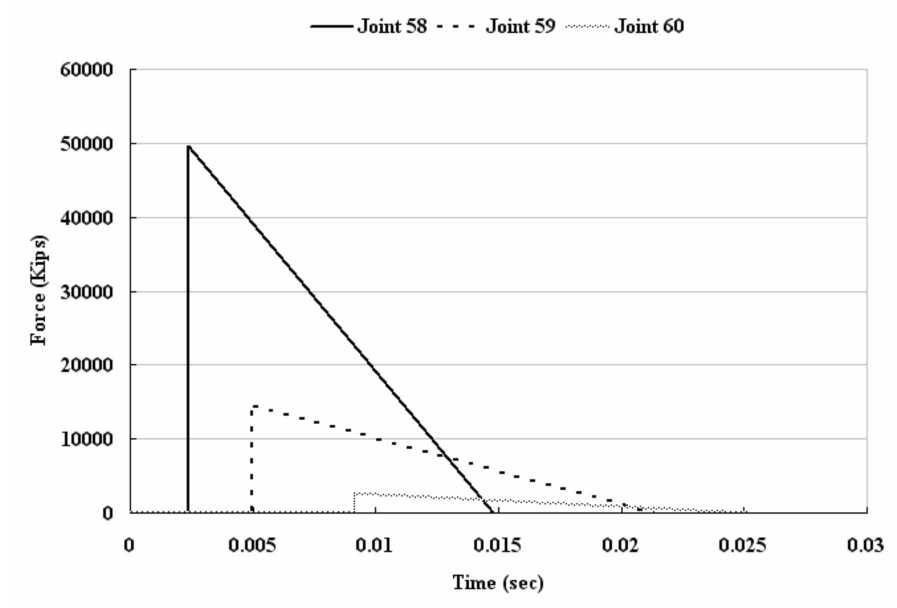

Figure 3.7 : Applied Blast Loads on Joint 58, 59, 60

3.2. Crater

For bursts near the ground surface, the yield and quantity of explosive detonation inferred the dimension of the crater formed as well as distance of window breakage. To verify crater dimension in this study, the crater dimension of Murrah Building [14] was compared with methods used for the analysis of conventional weapons effects on structure (CONWEP). In Murrah Building, the detonation of TNT weight was estimated to be approximately 4,000 lb at 4.5 ft above 18 in thick pavement on soil which resulted in a crater whose dimensions are 28 ft diameter and 6.8 ft in depth.

Table 3.4 shows the dimension of crater measured and the dimension of crater analyzed by CONWEP. As shown in Table 3.4, the prediction of crater dimension using CONWEP provides confidence due to its close approximation to the measured dimension. Therefore, this study was used methods of CONWEP to calculate the dimension of the expected crater for all cases. The results of CONWEP are shown in Figure 3.8. It can be seen that in these cases the apparent crater is almost exactly equal to the true crater.

Table 3.4 : Comparison with Estimates of Crater Dimensions

Condition	Depth (ft)	Diameter (ft)	Distance of Window Breakage (ft)
Measured at Murrah Bldg	6.8	28	N.A.
By F, Mlakar Sr(1998)	7.2	27	N.A.
This Report	7.4	28.64	1937

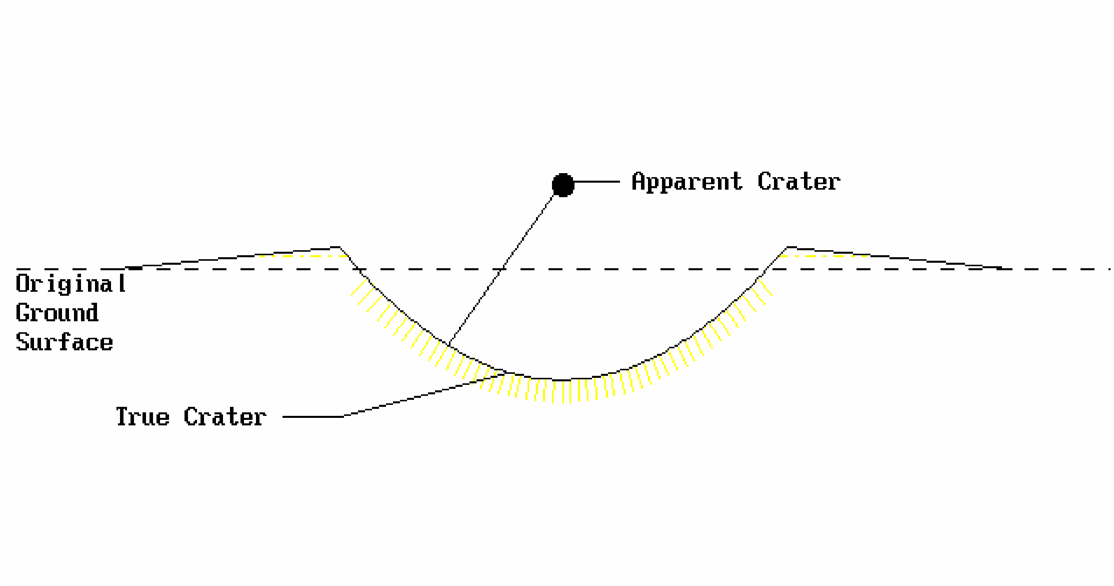

Figure 3.8 : Dimension of 4,000 lb TNT Weight assumed Dry Sand Clay Soil

Chapter 4 : Analyses of Models of Three Story Building

A three dimensional analytical model of the building is developed and the magnitude and distribution of blast loads on the structure are estimated using available computer software based on empirical methods. To obtain the relationship between pressure, time duration, and standoff distance, these tools are used to obtain an accurate model of the air blast loading. A hemispherical surface burst for various explosive weights and standoff distances are considered for the air blast loading. The earthquake loading is represented by an acceleration record obtained during the Northridge earthquake (1994). In this chapter, various air blast loads and stand-off distances are applied to a three story building. Lateral resistance is provided by welded steel moment frames on the perimeter. To investigate effect of the constraints, cases are divided into 3 parts such as beams with pinned connection, beams with welded connection, and alternative orientation of the column axes with welded connection. This chapter also considers the size of the blast crater along with the different linear structural responses that include story displacements, demand/capacity ratio, and diaphragm analysis as well as nonlinear plastic hinge behavior. These parameters are then compared with limit values suggested by seismic guidelines.

4.1. Structural Response to Variable Stand-off Distance

To investigate the effect of variable stand-off distance, this study assumes an explosive weight of 1,000 lb TNT. The reflected overpressure of variable stand-off distances is shown in Figure 4.1. These pressures are obtained by ATBLAST program. In this study, stand-off distance is assumed over 15, 30, 50 and 100 ft. The responded pressure is 4057 psi, 731 psi, 157 psi, 23.98 psi respectively.

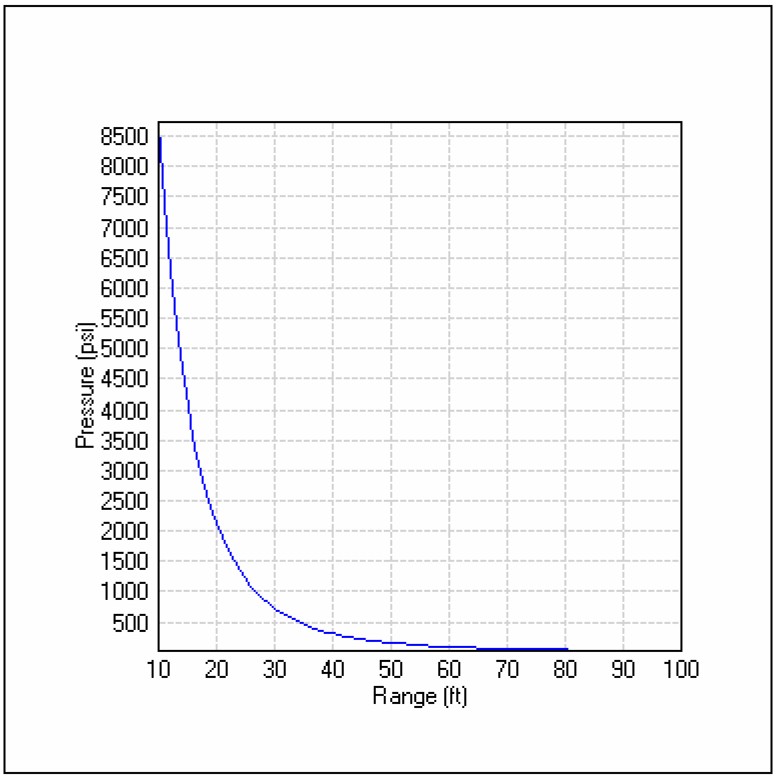

Figure 4.1 : Reflected Pressure of Variable Stand-Off Distances (ATBLAST)

4.1.1. Crater

To investigate the dimension of the bomb crater, the CONWEP computer program is used in case of 1,000 lb TNT explosion. The dimension of crater may affect the collapse of main member of building. In this study, stand-off distance was assumed over 15, 30, 50 and 100 ft. The Dimension of crater is shown in Figure 4.2 applied 1,000 lb TNT and Table 4.1 shows results of applied case.

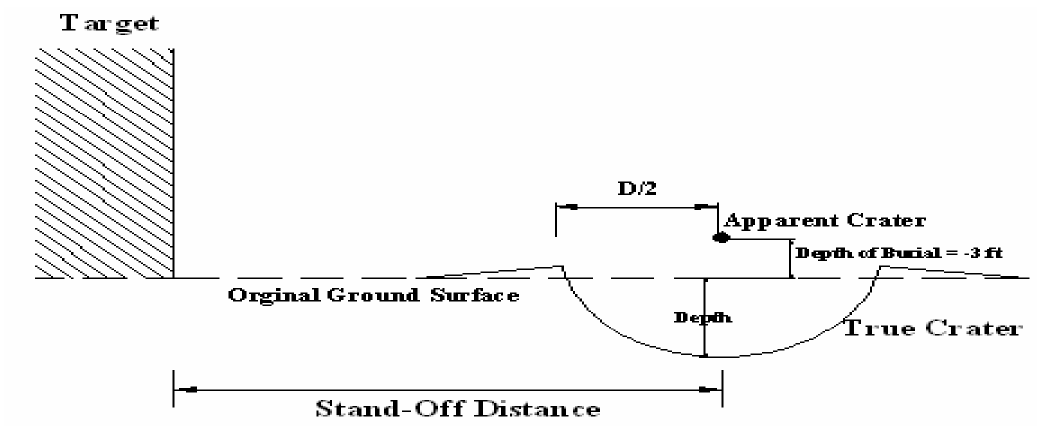

Figure 4.2 : The Dimension of Crater

Table 4.1 : Results of CONWEP in 1,000 lb TNT with Dry Sandy Clay

Charge Weight (lb)	1,000
Depth of Burial (ft)	-3
Depth (ft)	5.186
Radius (ft)	9.43
Window Breakage Range (ft)	1220

4.1.2. Blast Loads

A frame is subjected to 1,000 lb TNT explosive weight at 15 ft, 30 ft, 50 ft and 100 ft stand-off distance. Cases are defined along various distances. The blast wave propagates by compressing the air with supersonic velocity, and it is reflected by the building, amplifying the over pressure. To find blast loads on the 3 story building at each joint, the CONWEP program was used. Figure 4.3, 4.4, 4.5 and 4.6 show time duration and peak reflected pressure on front frame of the structure. Results of using the CONWEP program are summarized for each case in Table 4.2 - 4.9. Using these results, reflected pressure and time duration are defined for each node on the side of building facing the blast and used as input data for SAP2000 software [21].

When a blast with 1,000 lb TNT explosive weight impinges on a structure, a higher pressure is developed, termed the reflected pressure. The calculated (CONWEP) peak overpressures on the front frame are shown in Figure 4.3 – Figure 4.6. These range from a maximum of 4172 psi (15 ft), 731 psi (30 ft), 157 psi (50 ft), 24 psi (100 ft) at the point closest to the detonation to a minimum of 22.43 psi (15 ft), 25.18 psi (30 ft), 28.55 psi (50 ft), 15 psi (100 ft) at the upper west/east corner.

While these pressures are extremely large, they act for a limited duration, as shown in Figure 4.3 – Figure 4.6. The duration ranges from a maximum of 21.12 msec (15 ft), 22.21 msec (30 ft), 24.20 msec (50 ft), 26.20 msec (100 ft) in the upper west/east corner to a minimum of 2.87 msec (15 ft), 16.62 msec (30 ft), 15.73 msec (50 ft), 28.20 msec (100 ft) at the point closest to the blast.

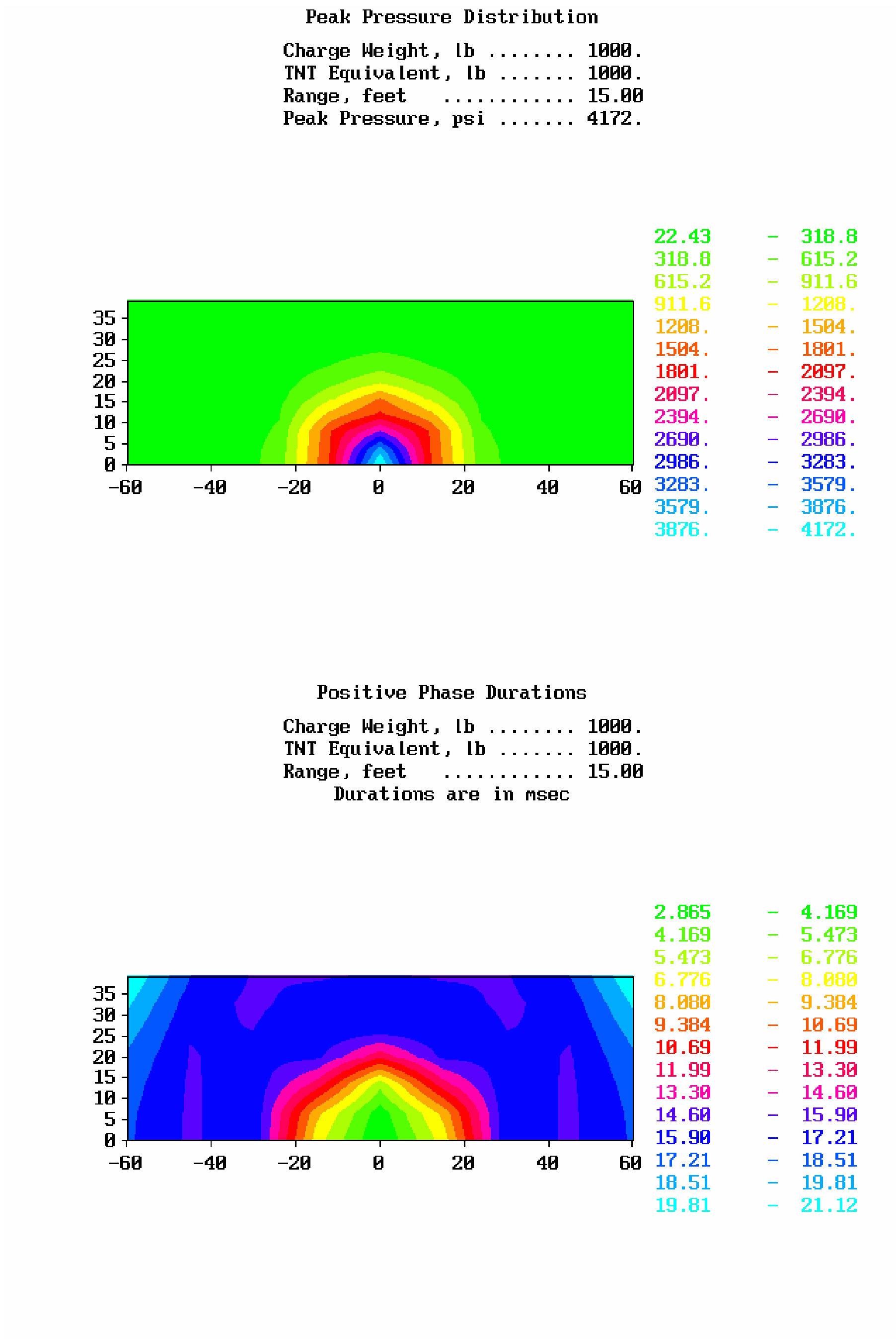

Figure 4.3 : Distribution of Peak Reflected Pressure and Time Duration at 15 ft Stand-Off

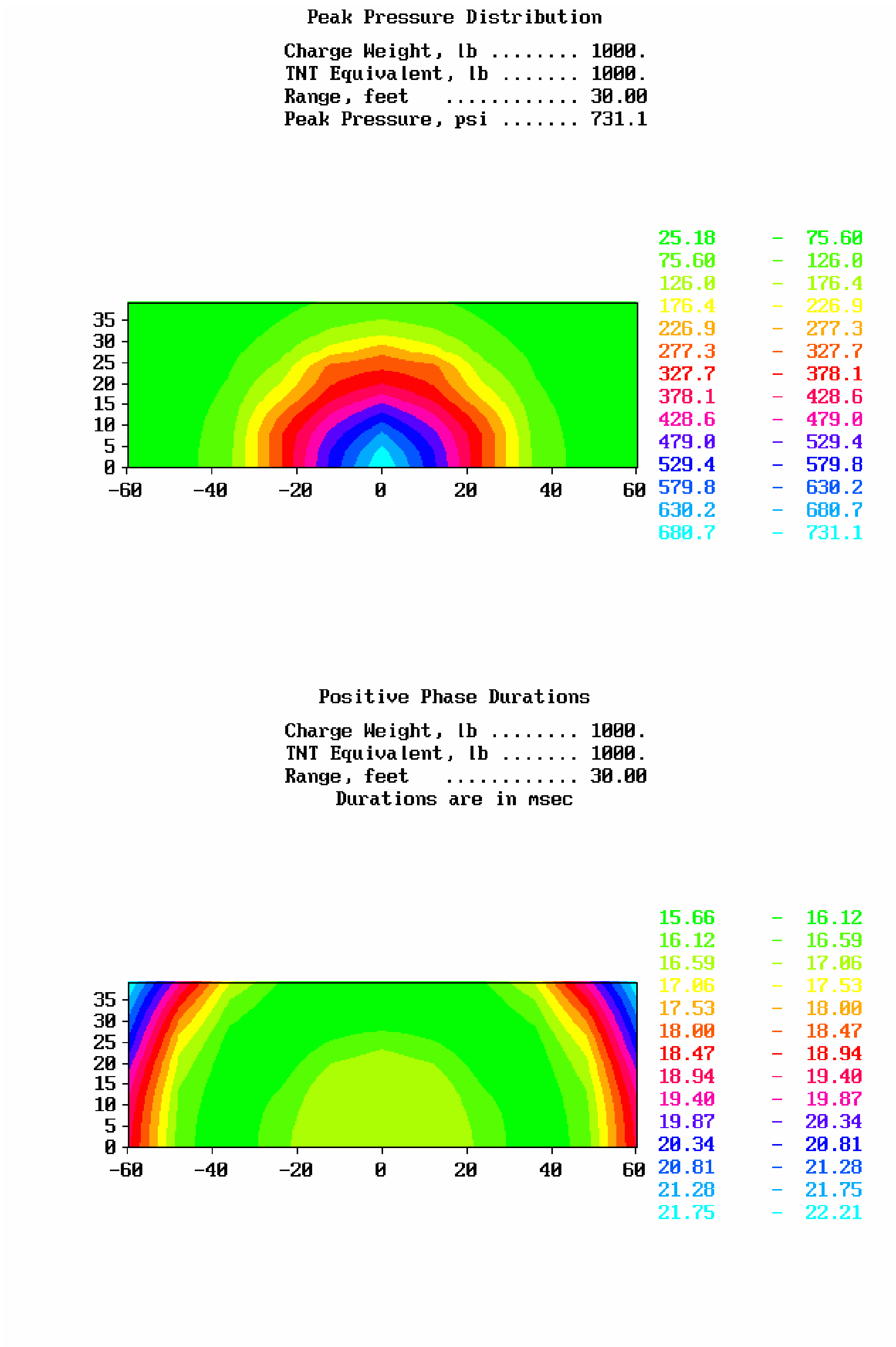

Figure 4.4 : Distribution of Peak Reflected Pressure and Time Duration at 30 ft Stand-Off

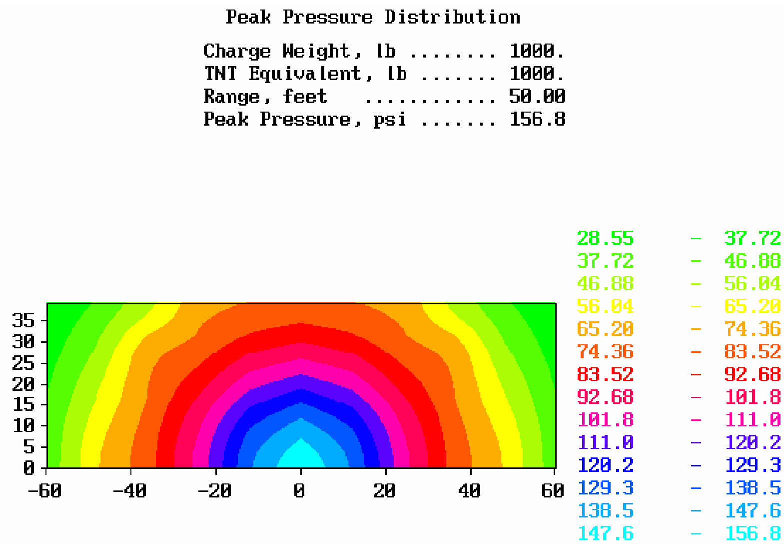

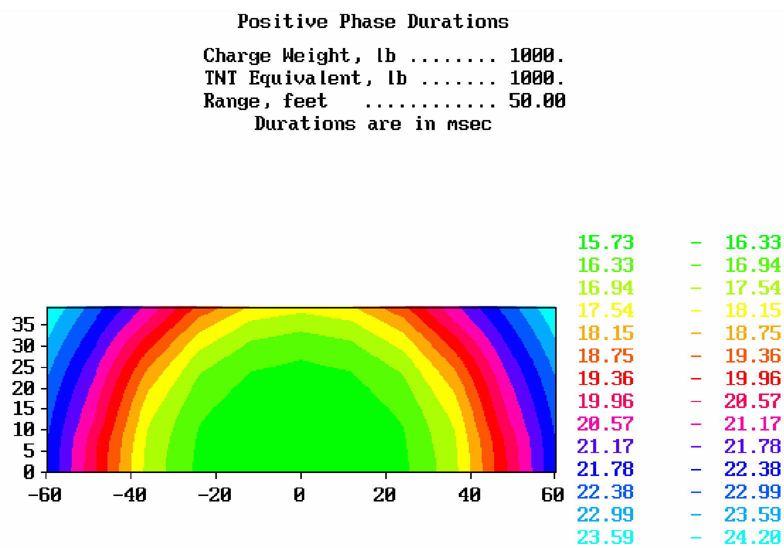

Figure 4.5 : Distribution of Peak Reflected Pressure and Time Duration at 50 ft Stand-Off

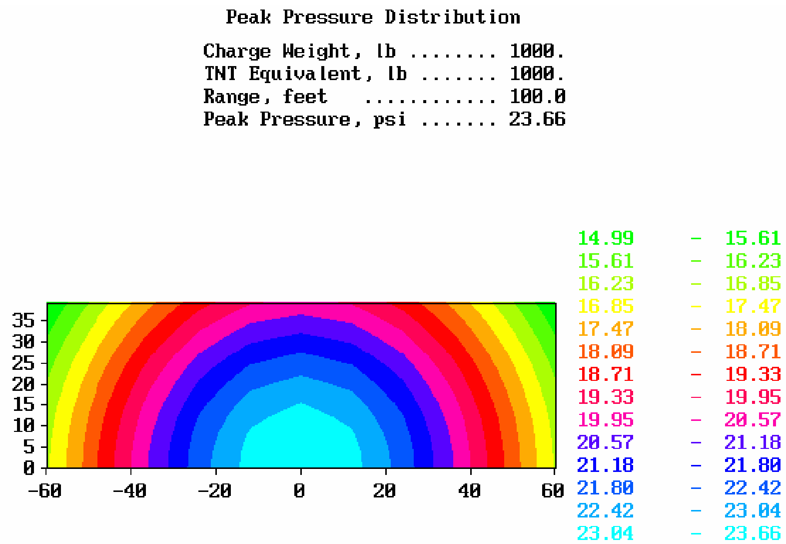

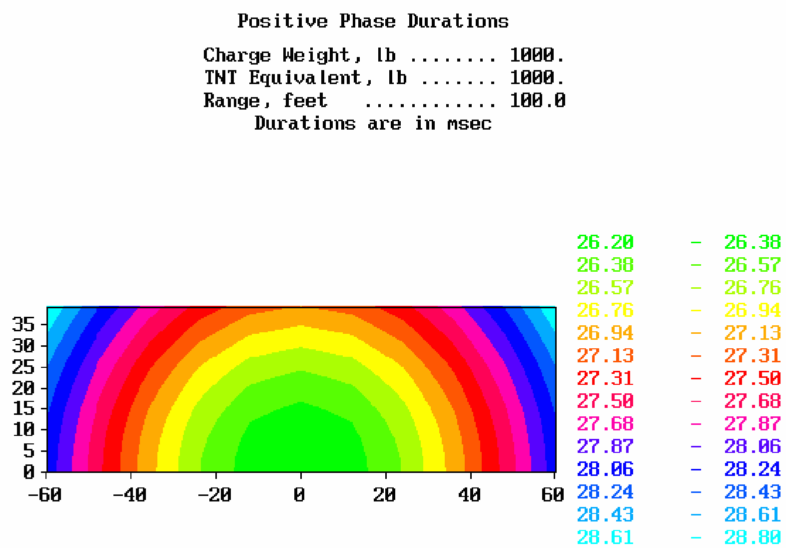

Figure 4.6 : Distribution of Peak Reflected Pressure and Time Duration at 100 ft Stand-Off

Table 4.2 : Reflected Pressure with 1,000 lb TNT Blast at 15 ft Stand-Off (psi)

Width (ft) / Height (ft)	-60	-45	-30	-15	0	15	30	45	60
0.0	31.39	60.31	199.90	1630.00	4172.00	1630.00	199.90	60.31	31.39
6.5	31.03	58.90	186.90	1364.00	3024.00	1364.00	186.90	58.90	31.03
13.0	30.01	55.00	156.50	816.40	1789.00	816.40	156.50	55.00	30.01
19.5	28.46	49.47	120.80	400.50	859.20	400.50	120.80	49.47	28.46
26.0	26.55	42.86	86.30	199.60	324.40	199.60	86.30	42.86	26.55
32.5	24.47	36.70	62.75	120.70	159.20	120.70	62.75	36.70	24.47
39.0	22.43	31.85	49.08	73.55	91.53	73.55	49.08	31.85	22.43

Table 4.3 : Reflected Pressure with 1,000 lb TNT Blast at 30 ft Stand-Off (psi)

Width (ft) / Height (ft)	-60	-45	-30	-15	0	15	30	45	60
0.0	34.77	62.41	194.5	478	731.1	478	194.5	62.41	34.77
6.5	34.34	60.69	181.5	448.1	660.7	448.1	181.5	60.69	34.34
13.0	33.12	56.23	149.6	372.4	522.8	372.4	149.6	56.23	33.12
19.5	31.55	50.57	112.6	319.9	379.7	319.9	112.6	50.57	31.55
26.0	29.67	45.72	85.19	194.2	306.2	194.2	85.19	45.72	29.67
32.5	27.5	40.73	65.34	112.5	152.1	112.5	65.34	40.73	27.5
39.0	25.18	35.32	50.2	75.49	88.79	75.49	50.2	35.32	25.18

Table 4.4 : Reflected Pressure with 1,000 lb TNT Blast at 50 ft Stand-Off (psi)

Width (ft) / Height (ft)	-60	-45	-30	-15	0	15	30	45	60
0.0	41.13	71.57	91.40	129.80	156.80	129.80	91.40	71.57	41.13
6.5	40.64	71.51	89.87	126.10	148.60	126.10	89.87	71.51	40.64
13.0	39.20	68.09	85.67	116.60	135.10	116.60	85.67	68.09	39.20
19.5	36.97	61.00	80.15	103.90	117.50	103.90	80.15	61.00	36.97
26.0	34.17	54.47	74.83	91.36	100.60	91.36	74.83	54.47	34.17
32.5	31.45	48.03	71.87	80.12	86.07	80.12	71.87	48.03	31.45
39.0	28.55	41.78	60.48	73.51	75.14	73.51	60.48	41.78	28.55

Table 4.5 : Reflected Pressure with 1,000 lb TNT Blast at 100 ft Stand-Off (psi)

Width (ft) / Height (ft)	-60	-45	-30	-15	0	15	30	45	60
0.0	16.76	19.16	21.41	23.05	23.66	23.05	21.41	19.16	16.76
6.5	16.70	19.09	21.31	22.94	23.54	22.94	21.31	19.09	16.70
13.0	16.54	18.87	21.03	22.61	23.20	22.61	21.03	18.87	16.54
19.5	16.28	18.52	20.59	22.09	22.65	22.09	20.59	18.52	16.28
26.0	15.92	18.04	19.99	21.40	21.92	21.40	19.99	18.04	15.92
32.5	15.49	17.47	19.29	20.58	21.06	20.58	19.29	17.47	15.49
39.0	14.99	16.83	18.49	19.67	20.10	19.67	18.49	16.83	14.99

Table 4.6 : Time Duration with 1,000 lb TNT Blast at 15 ft Stand-Off (msec)

Width (ft) / Height (ft)	-60.00	-45.00	-30.00	-15.00	0.00	15.00	30.00	45.00	60.00
0.0	17.38	15.66	17.04	7.38	2.87	7.38	17.04	15.66	17.38
6.5	17.47	15.66	17.02	8.59	3.46	8.59	17.02	15.66	17.47
13.0	17.76	15.69	16.86	12.76	5.95	12.76	16.86	15.69	17.76
19.5	18.28	15.80	16.43	16.24	12.27	16.24	16.43	15.80	18.28
26.0	19.06	16.04	15.91	17.04	16.63	17.04	15.91	16.04	19.06
32.5	20.05	16.48	15.66	16.42	16.88	16.42	15.66	16.48	20.05
39.0	21.12	17.27	15.81	15.74	15.98	15.74	15.81	17.27	21.12

Table 4.7 : Time Duration with 1,000 lb TNT Blast at 30 ft Stand-Off (msec)

Width (ft) / Height (ft)	-60	-45	-30	-15	0	15	30	45	60
0.0	19.06	16.04	15.91	17.04	16.62	17.04	15.91	16.04	19.06
6.5	19.18	16.08	15.86	17.02	16.78	17.02	15.86	16.08	19.18
13.0	19.52	16.22	15.74	16.86	17.03	16.86	15.74	16.22	19.52
19.5	20.05	16.48	15.66	16.43	16.88	16.43	15.66	16.48	20.05
26.0	20.81	16.95	15.71	15.91	16.28	15.91	15.71	16.95	20.81
32.5	21.48	17.73	15.97	15.66	15.75	15.66	15.97	17.73	21.48
39.0	22.21	18.92	16.50	15.81	15.69	15.81	16.50	18.92	22.21

Table 4.8 : Time Duration with 1,000 lb TNT Blast at 50 ft Stand-Off (msec)

Height (ft) \ Width (ft)	-60	-45	-30	-15	0	15	30	45	60
0.0	22.33	19.13	16.62	15.87	15.73	15.87	16.62	19.13	22.33
6.5	22.39	19.24	16.68	15.90	15.75	15.90	16.68	19.24	22.39
13.0	22.57	19.58	16.89	16.01	15.83	16.01	16.89	19.58	22.57
19.5	22.86	20.29	17.29	16.23	16.00	16.23	17.29	20.29	22.86
26.0	23.24	20.86	17.95	16.62	16.31	16.62	17.95	20.86	23.24
32.5	23.69	21.52	18.94	17.29	16.87	17.29	18.94	21.52	23.69
39.0	24.20	22.25	20.32	18.38	17.82	18.38	20.32	22.25	24.20

Table 4.9 : Time Duration with 1,000 lb TNT Blast at 100 ft Stand-Off (msec)

Height (ft) \ Width (ft)	-60	-45	-30	-15	0	15	30	45	60
0.0	28.17	27.41	26.78	26.35	26.20	26.35	26.78	27.41	28.17
6.5	28.19	27.43	26.80	26.38	26.23	26.38	26.80	27.43	28.19
13.0	28.25	27.50	26.88	26.46	26.31	26.46	26.88	27.50	28.25
19.5	28.34	27.61	27.00	26.60	26.45	26.60	27.00	27.61	28.34
26.0	28.46	27.75	27.17	26.78	26.64	26.78	27.17	27.75	28.46
32.5	28.62	27.94	27.38	27.00	26.87	27.00	27.38	27.94	28.62
39.0	28.80	28.15	27.62	27.26	27.14	27.26	27.62	28.15	28.80

4.1.3. Effect of Framing Conditions

To obtain the response of 3 story building, SAP2000 FEM Software was used. The blast loads are generated at each joint as peak reflected pressure from CONWEP. The dynamic time history indicates that number of output time steps is 1,000 and output time step size is 0.005. The damping ratio is assumed as 5 %. In addition, the constraint of joints are divided into three parts : case 1 is beam with pinned connection, case 2 is beam with welded connection, and case 3 is alternative orientation of the column axes with welded connection in shown as Figure 4.7 – Figure 4.12.

CASE 1 : Beams with Pinned Connection

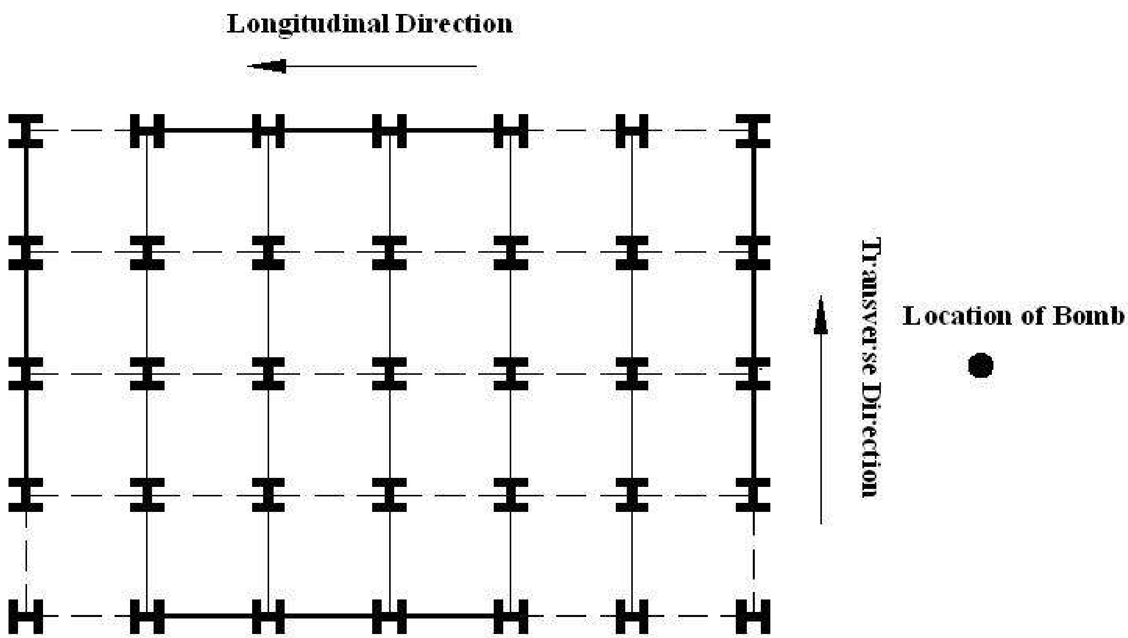

Figure 4.7 : Orientation of the Column (CASE 1)

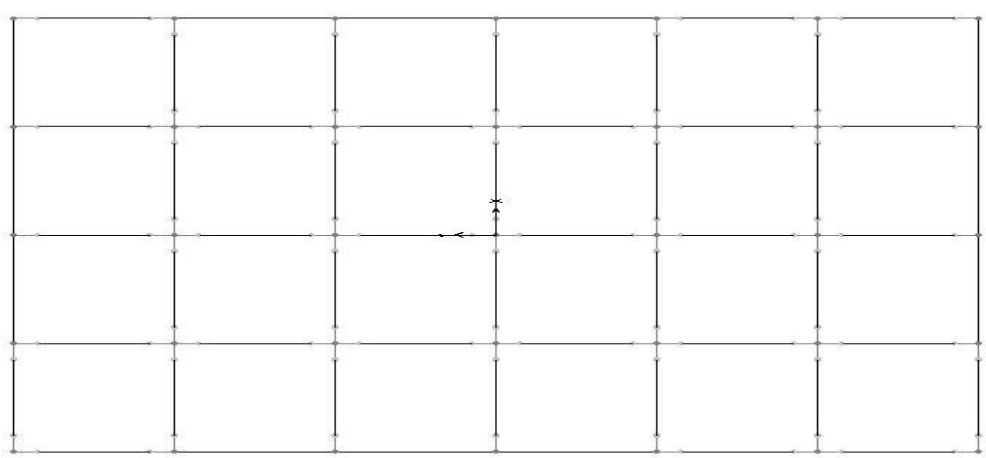

Figure 4.8 : Constraints of Joints by SAP2000 Modeling (CASE 1)

CASE 2 : Beams with Welded Connection

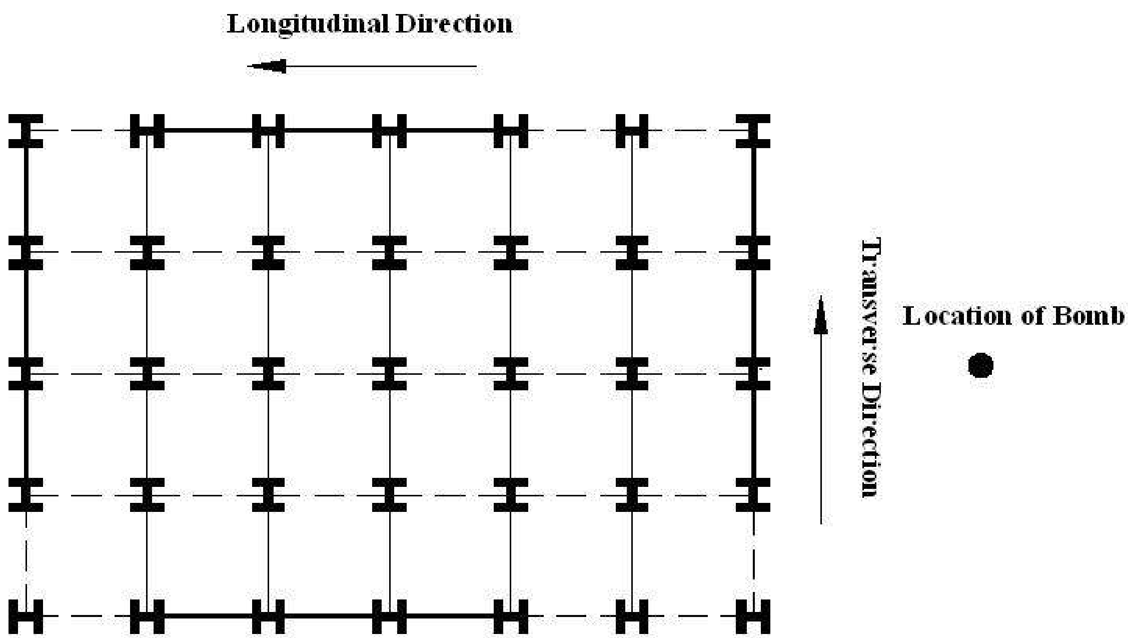

Figure 4.9 : Orientation of the Column (CASE 2)

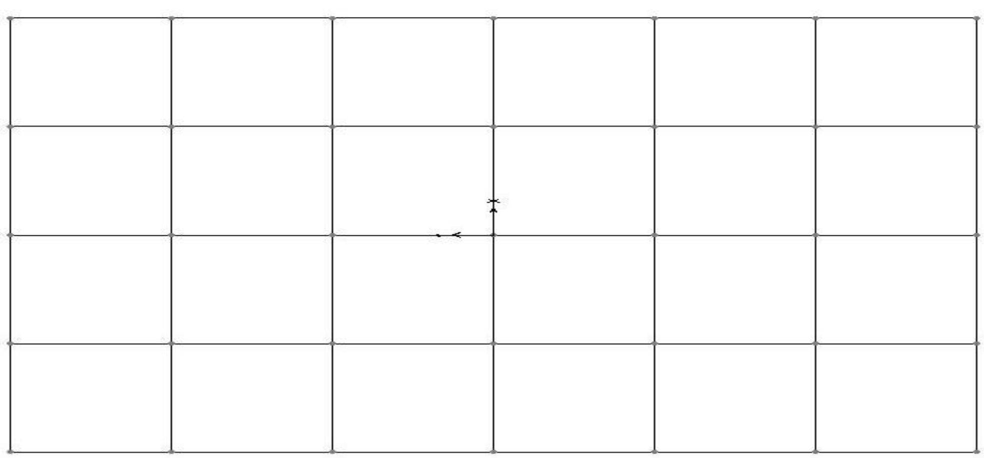

Figure 4.10 : Constraints of Joints by SAP2000 Modeling (CASE 2)

CASE 3 : Alternative Orientation of the Column Axes with Welded Connection

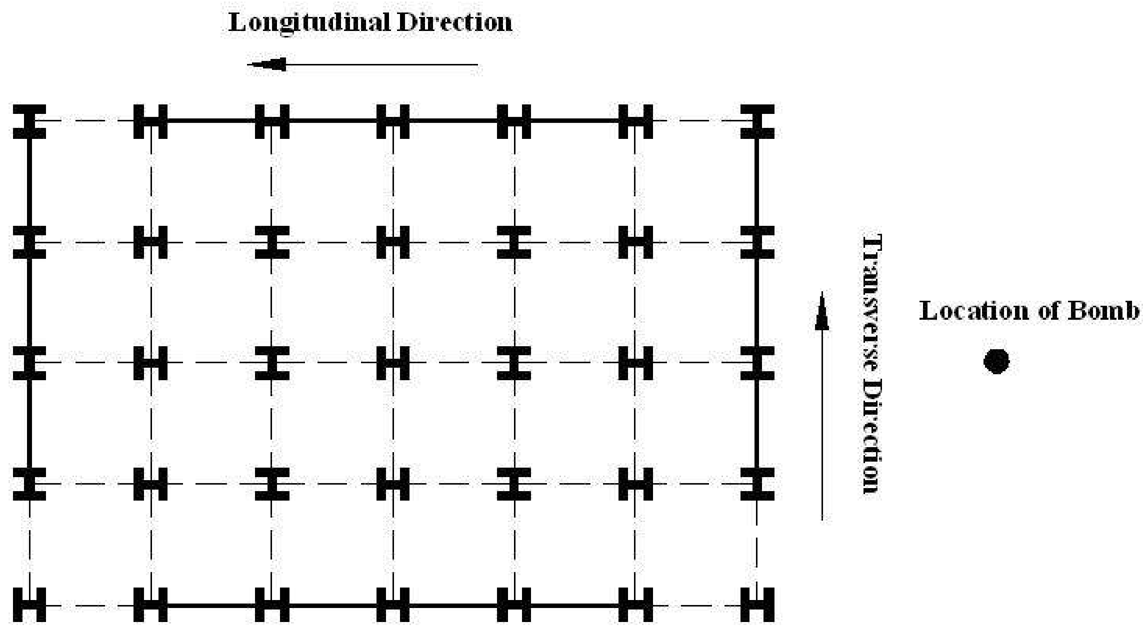

Figure 4.11 : Orientation of the Column (CASE 3)

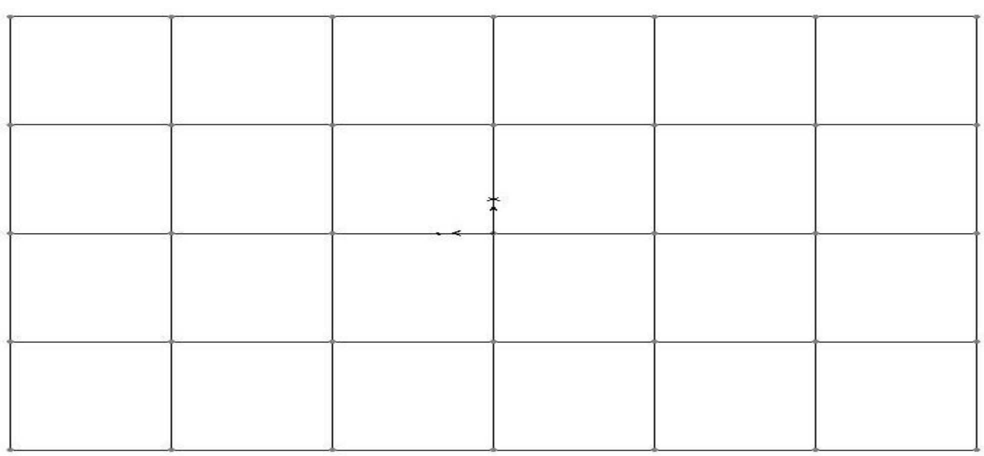

Figure 4.12 : Constraints of Joints by SAP2000 Modeling (CASE 3)

In this chapter, dynamic time history curves are obtained by each case. The cases of different condition are shown : case 1 indicates joints have beams pinned connection (moment released) with normal column distribution, case 2 indicates joints have beams welded connection (moment fixed) with normal column distribution and case 3 shows that joints have alternative orientation of the column axes with welded connection (moment fixed and alternative column distribution). All cases applied a loading condition of 1,000 lb TNT explosive weight at 15 ft, 30 ft, 50 ft, and 100 ft. The results of case 1, case 2 and case 3 are shown in Figure 4.13 – Figure 4.15 respectively.

CASE 1 : Beams with Pinned connection (Moment Released)

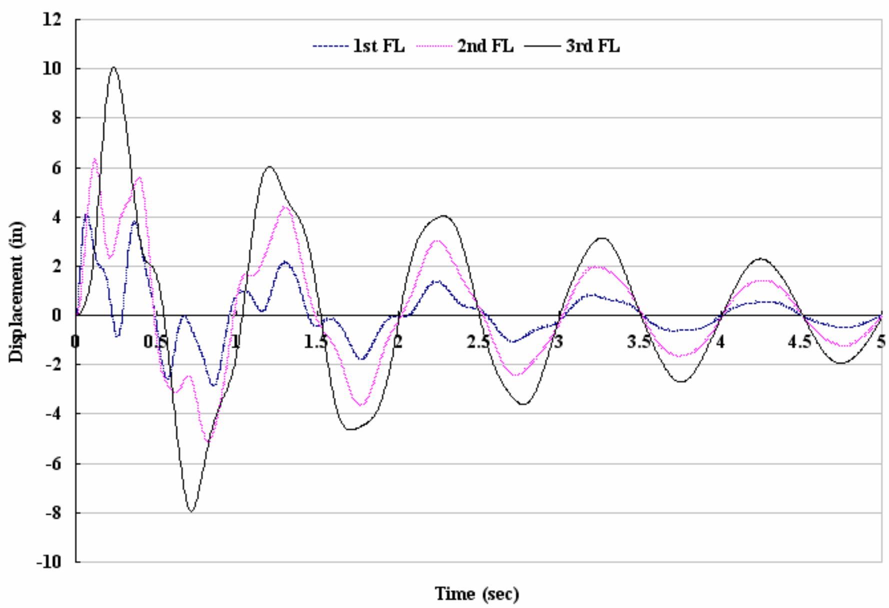

(a) 1,000 lb TNT Weight at 15 ft Stand-Off

Figure 4.13 : Linear Dynamic Time History to Variable Stand-Off Distances (Moment Released)

“Figure 4.13 : Continued”

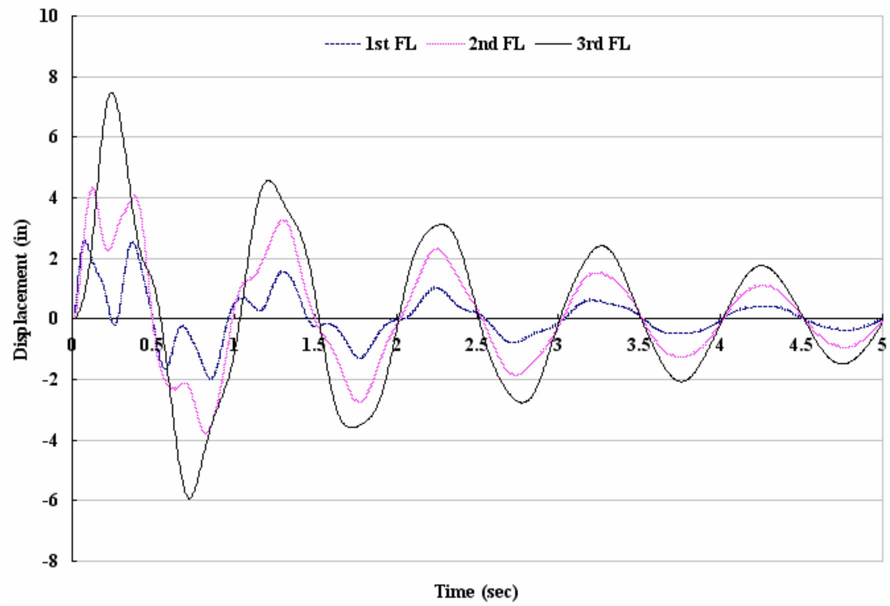

(b) 1,000 lb TNT Weight at 30 ft Stand-Off

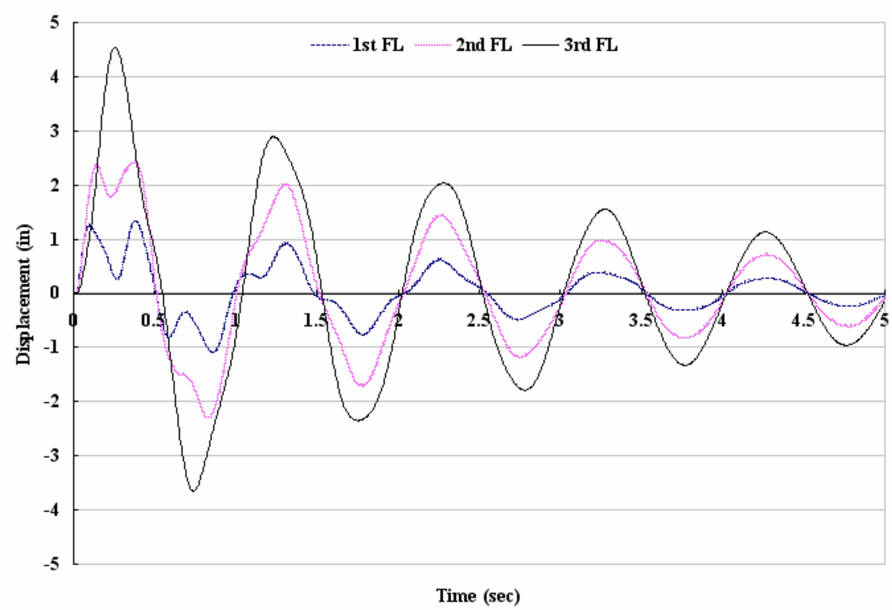

(c) 1,000 lb TNT Weight at 50 ft Stand-Off

"Figure 4.13 : Continued"

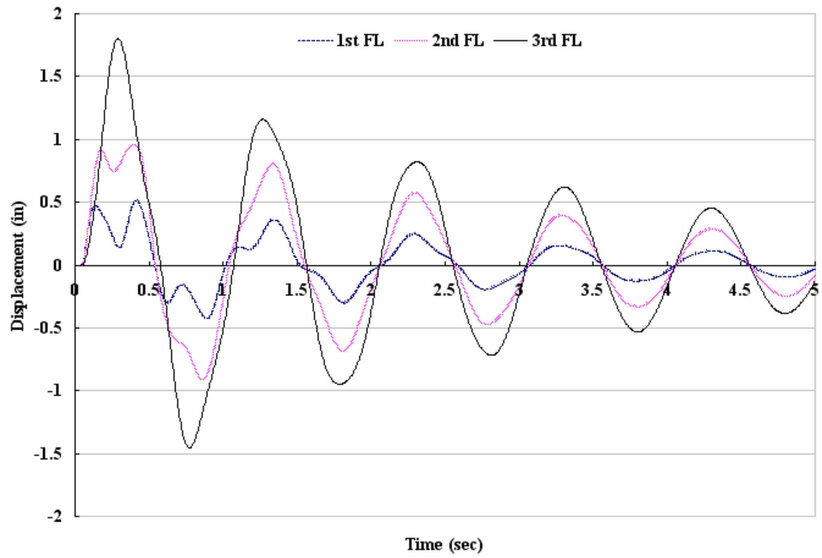

(d) 1,000 lb TNT Weight at 100 ft Stand-Off

CASE 2 : Beams with Welded Connection (Moment Fixed)

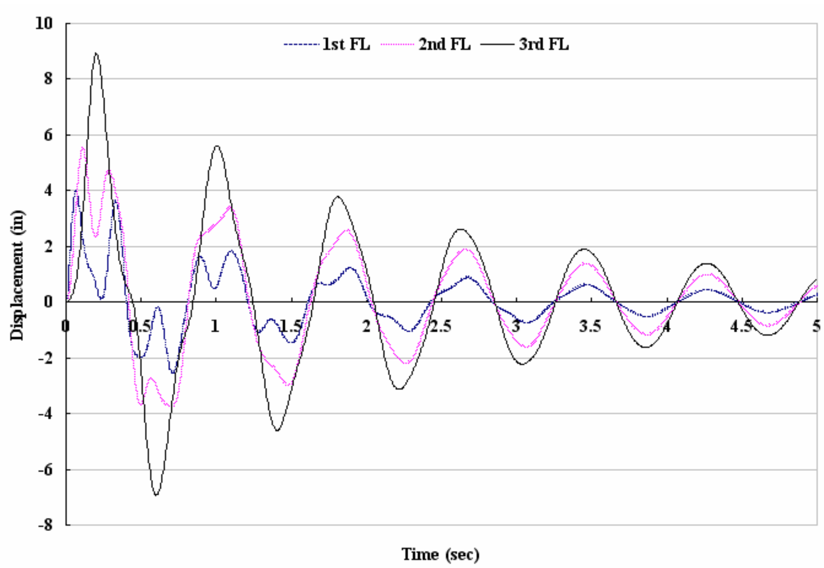

(a) 1,000 lb TNT Weight at 15 ft Stand-Off

Figure 4.14 : Linear Dynamic Time History to Variable Stand-Off Distances (Moment Fixed)

“Figure 4.14 : Continued”

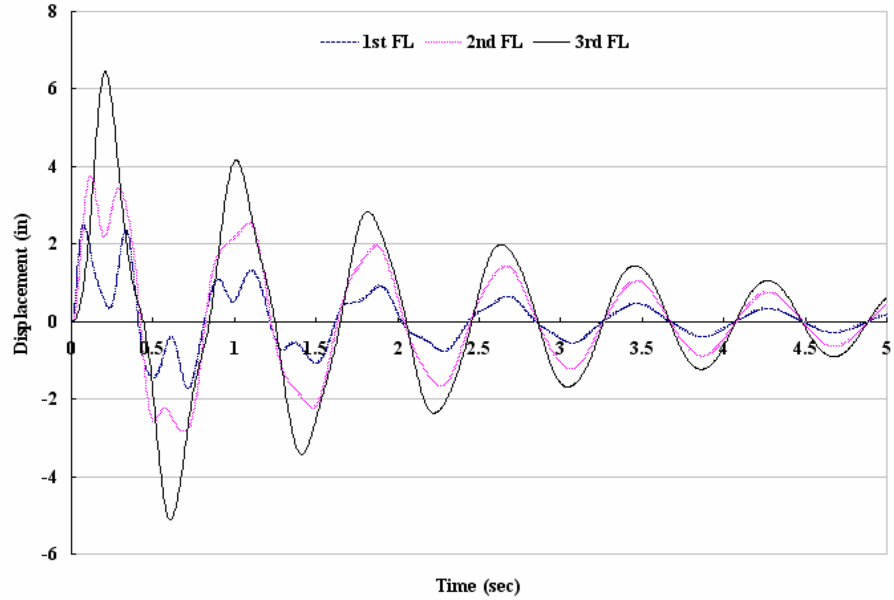

(b) 1,000 lb TNT Weight at 30 ft Stand-Off

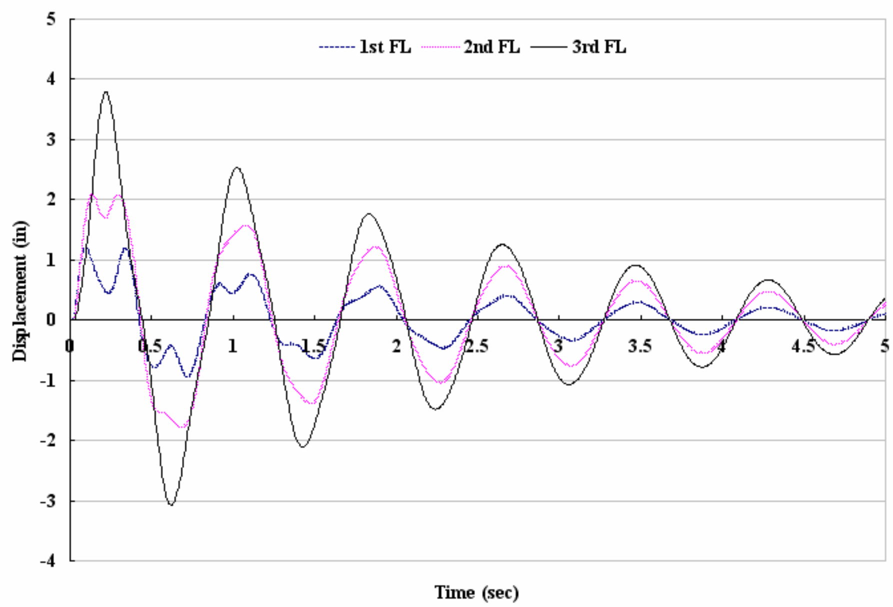

(c) 1,000 lb TNT Weight at 50 ft Stand-Off

"Figure 4.14 : Continued"

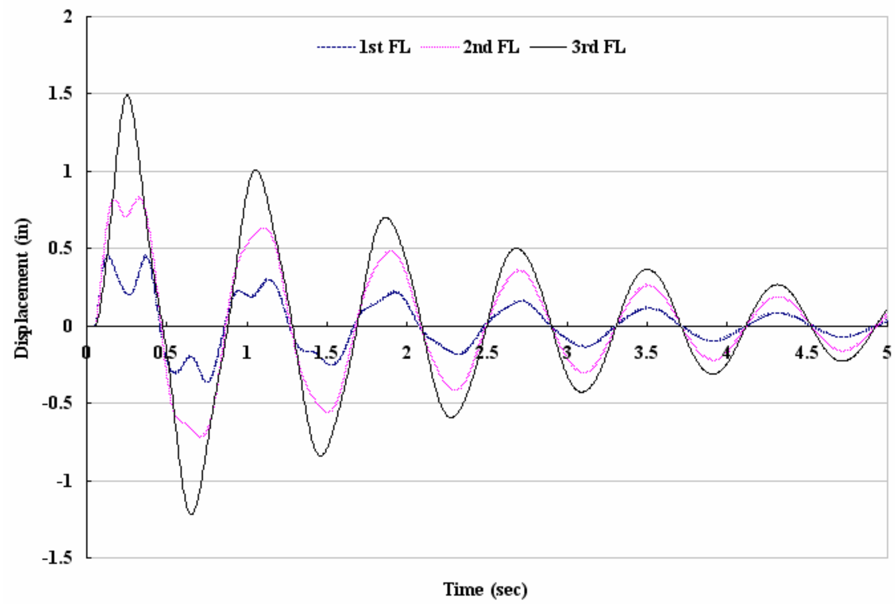

(d) 1,000 lb TNT Weight at 100 ft Stand-Off

CASE 3 : Alternative Orientation of the Column Axes with Welded Connection

(Alternative Rotation)

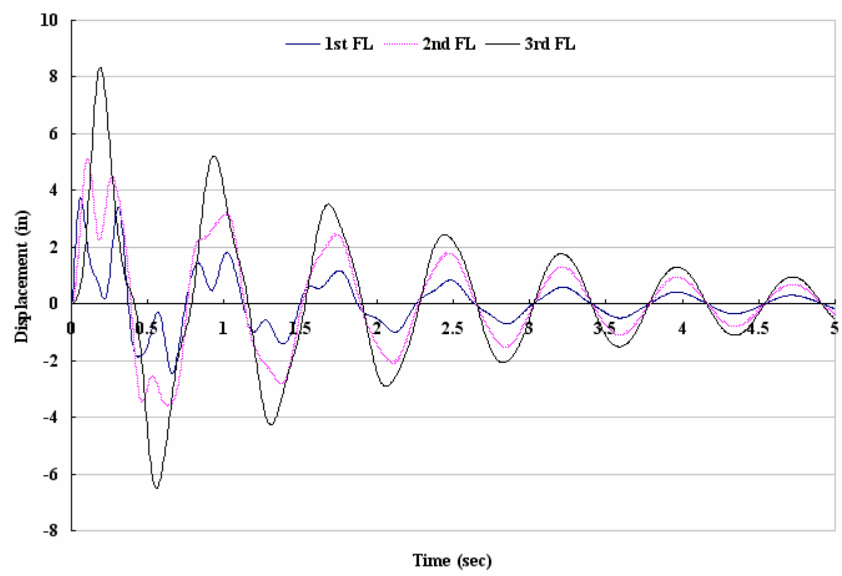

(a) 1,000 lb TNT Weight at 15 ft Stand-Off

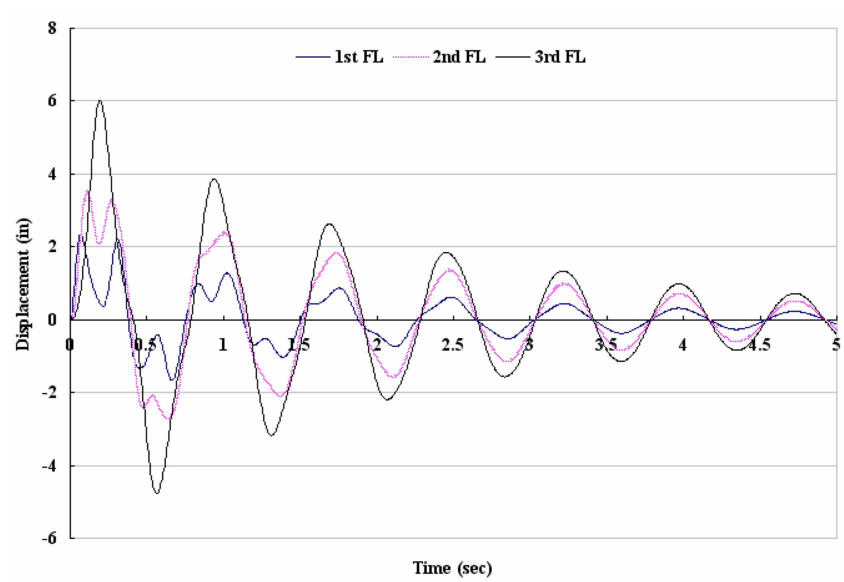

(b) 1,000 lb TNT Weight at 30 ft Stand-Off

Figure 4.15 : Linear Dynamic Time History to Variable Stand-Off Distances (Alternative Rotation)

“Figure 4.15 : Continued”

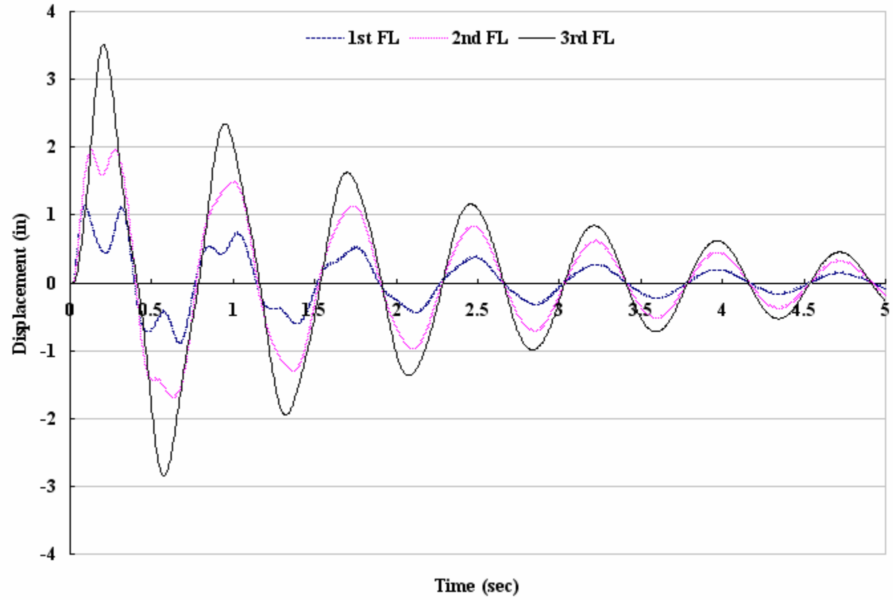

(c) Maximum Deflection with 1,000 lb TNT Weight at 50 ft Stand-Off

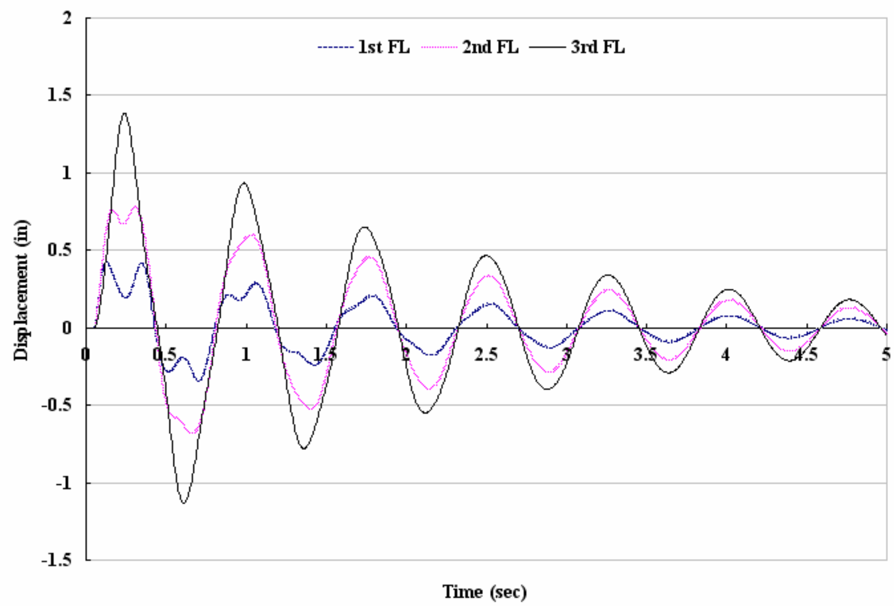

(d) 1,000 lb TNT Weight at 100 ft Stand-Off

To find critical column corresponding to each case, the result of analysis from SAP2000 based on UBC 97 LRFD design code shows demand/capacity ratio of all frames shown in Appendix B.1. These values are obtained by combination of dead load, live load and blast loads. As a result, critical column (Frame 43) on transverse direction was found at closest distance of blast source. The moments were compared by defined code value and value of analysis using SAP2000. The comparison with moment of code and analysis was shown in Table 4.10.

Table 4.10 : Comparison with Code and Analysis value of moment (Frame 43)

CASE	Time(sec)	M_u (kips-in)	M_n (kips-in)	Demand/Capacity Ratio	Status
1,000 lb_15 ft	0.075	44196.30	13680	3.23	over stress
1,000 lb_30 ft	0.08	26148.06	13680	1.91	over stress
1,000 lb_50 ft	0.1	11597.19	13680	0.85	OK
1,000 lb_100 ft	0.135	4208.96	13680	0.31	OK

$$where, \quad \Phi = 0.9, \quad M_n = \varphi \cdot F_y \cdot Z_y$$
$$F_y = Yield\ Stress = 50\,ksi$$
$$Z_y = Plastic\ Section\ Modulus$$

4.1.4. Summary

As results of dynamic time history analysis with different joint constraint and column rotation, maximum deflections are shown in Figure 4.16 for each case. As might be expected, the maximum deflection occurs for the 1,000 TNT weight @ 15 ft standoff distance. The maximum displacement is 10 in, 8.92 in and 8.4 in at the roof for respective case and occurs at 0.2 sec. However, for the 1,000 lb TNT weight at 100 ft stand off distance, the maximum displacement of 1.8 in, 1.49 in and 1.38 in is at the roof level for respective case and occurs at 0.3 seconds.

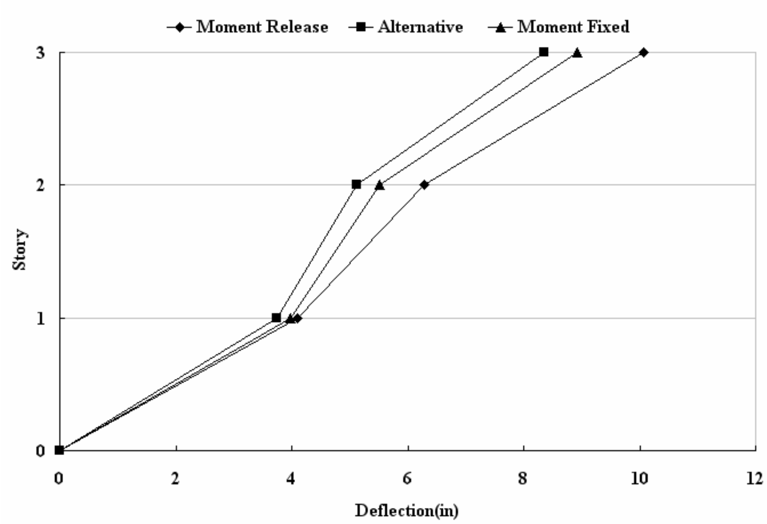

(a) 1,000 lb Weight at 15 ft Stand-off

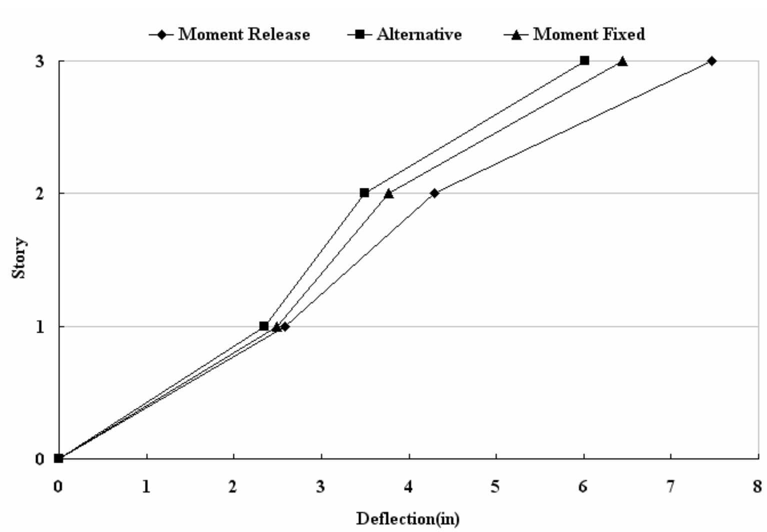

(b) 1,000 lb Weight at 30 ft Stand-off

Figure 4.16 : Maximum Deflection on Each Floor to Variable Stand-Off Distance

"Figure 4.16 : Continued"

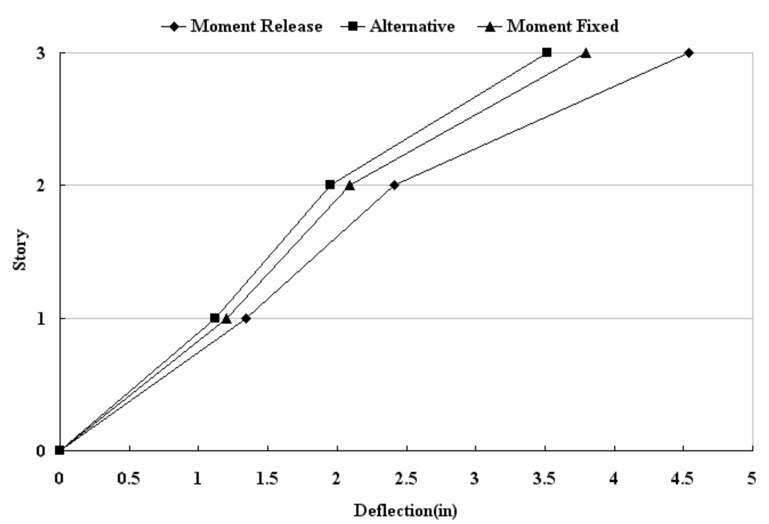

(c) 1,000 lb Weight at 50 ft Stand-off

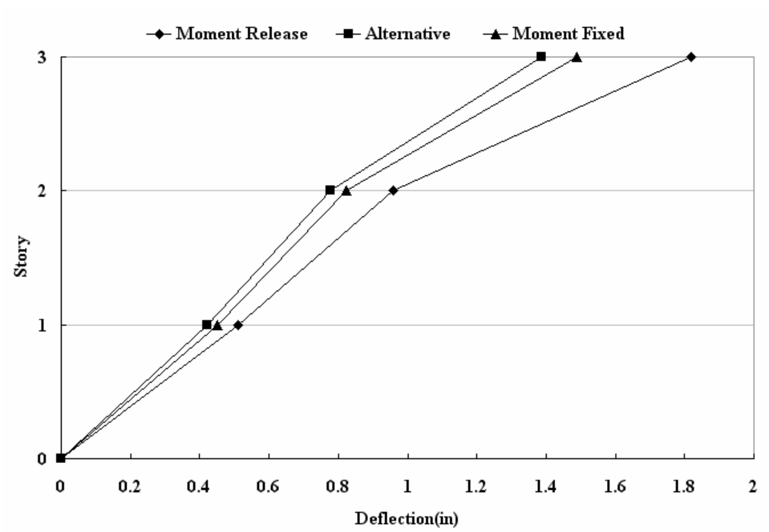

(d) 1,000 lb Weight at 100 ft Stand-off

Based on maximum displacements, interstory drifts are shown in Figure 4.17. The code limitation of drift ratio based on UBC'97 is 0.02 and the responses of all conditions satisfy this loading with the exception of the 1,000 lb explosive @ 15 ft. However, in this case, the drift of 0.027, 0.023, 0.021 respectively which should be sustained with proper welded connections.

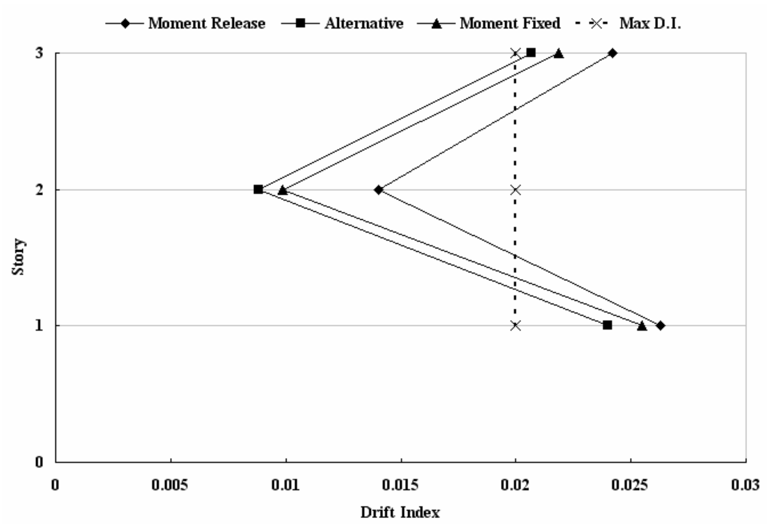

(a) 1,000 lb Weight at 15 ft Stand-off

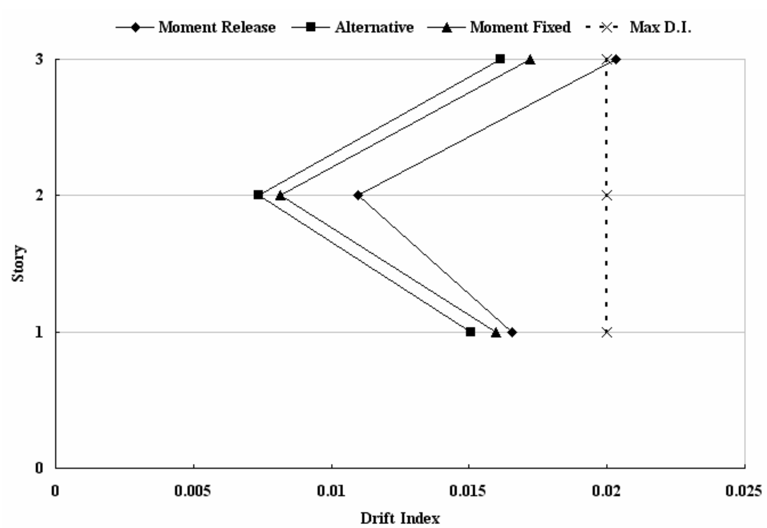

(b) 1,000 lb Weight at 30 ft Stand-off

Figure 4.17 : Interstory Drift to Variable Stand-Off Distance

“Figure 4.17 : Continued”

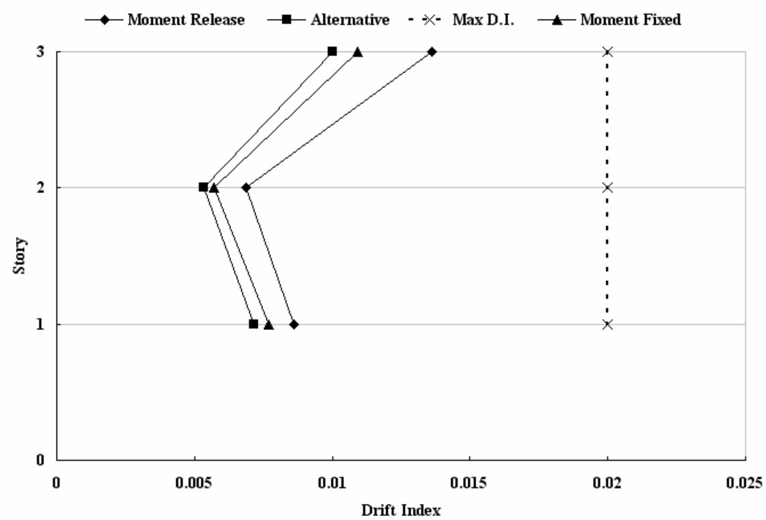

(c) 1,000 lb Weight at 50 ft Stand-off

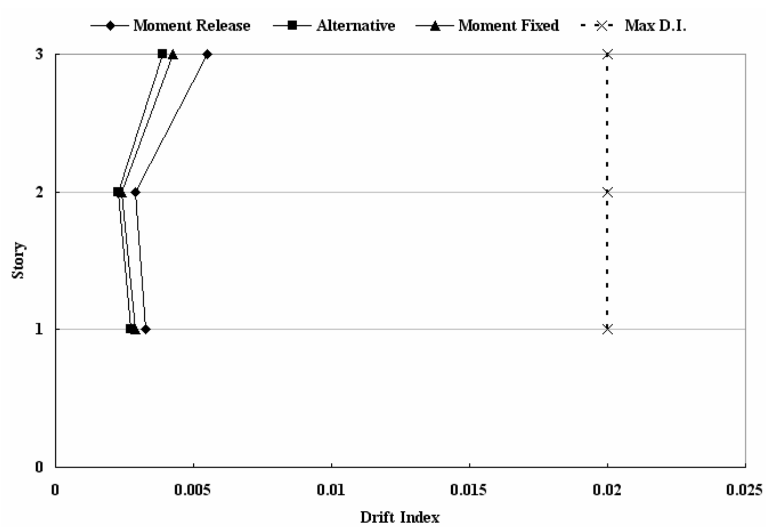

(d) 1,000 lb Weight at 100 ft Stand-off

The maximum D/C ratios for the columns in each story of the transverse frame and longitudinal frame for an explosive weight of 1,000 lb with different joint constraints are summarized in Figure 4.18 and Figure 4.19. Here it can be seen that for two of the blast conditions (c,d) the D/C demands are all less than unity indicating elastic behavior. The two blast conditions (a,b) with the shortest standoff result in D/C demands greater than unity with a maximum of about 2.8. Each ratio was shown in Appendix B.1.

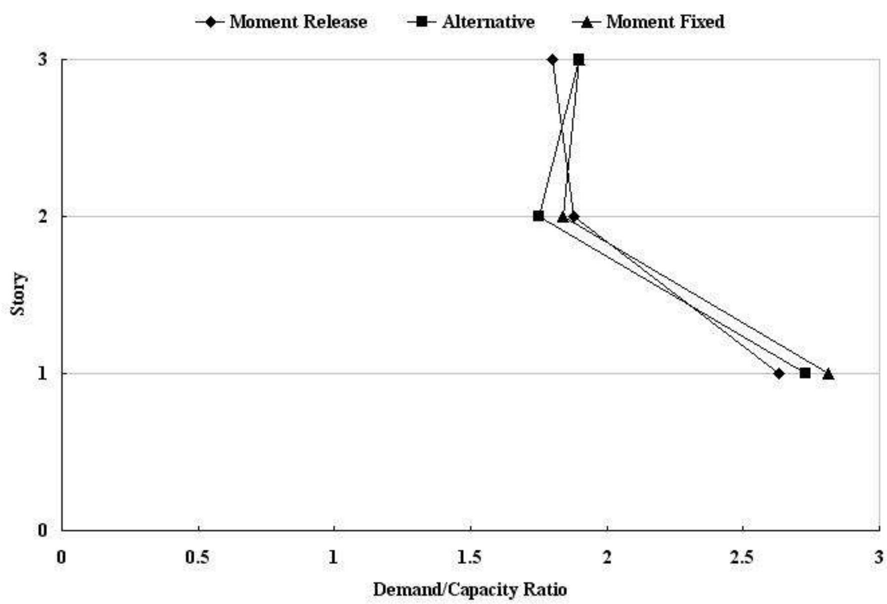

(a) 1,000 lb Weight at 15 ft Stand-off

Figure 4.18 : Demand/Capacity Ratio to Variable Stand-Off Distance on Transverse MRF

“Figure 4.18 : Continued”

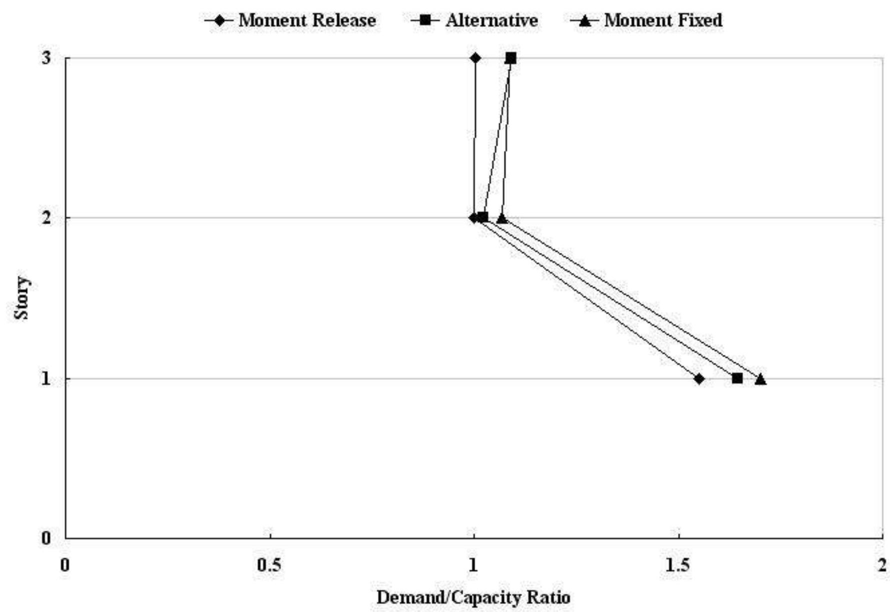

(b) 1,000 lb Weight at 30 ft Stand-off

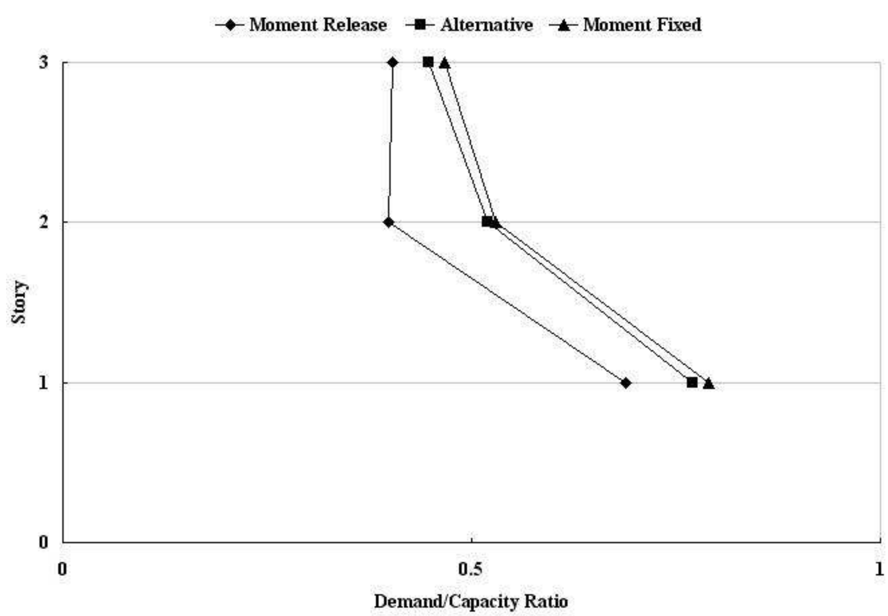

(c) 1,000 lb Weight at 50 ft Stand-off

“Figure 4.18 : Continued”

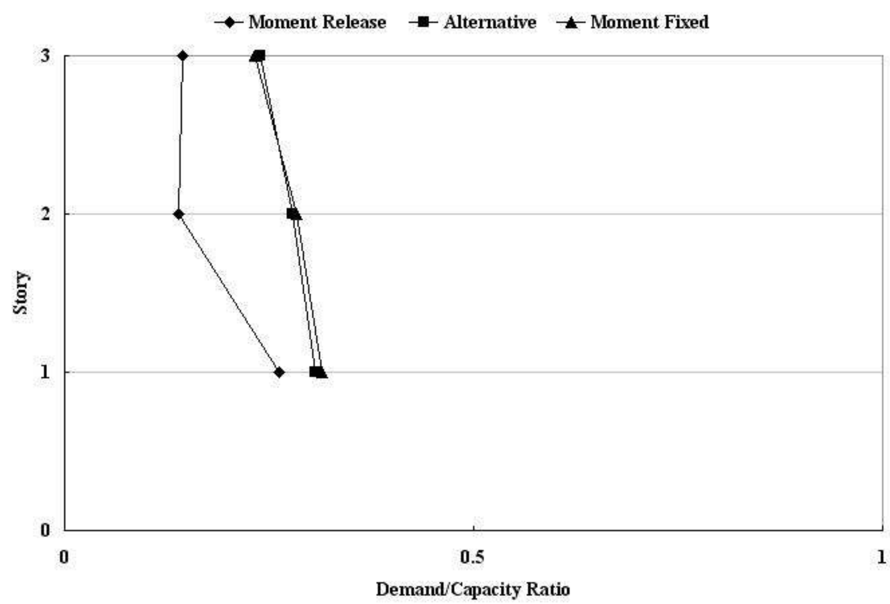

(d) 1,000 lb Weight at 100 ft Stand-off (Transverse Direction)

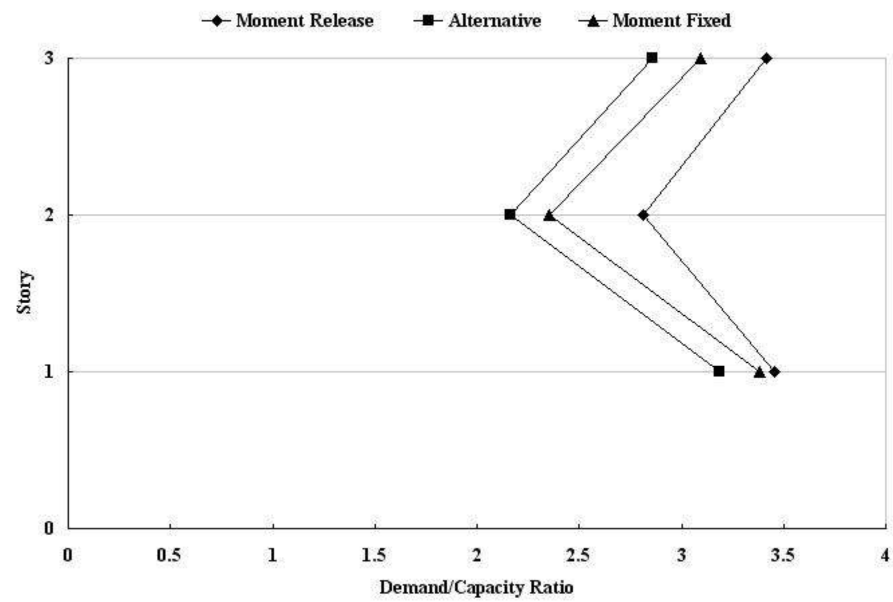

(a) 1,000 lb Weight at 15 ft Stand-off

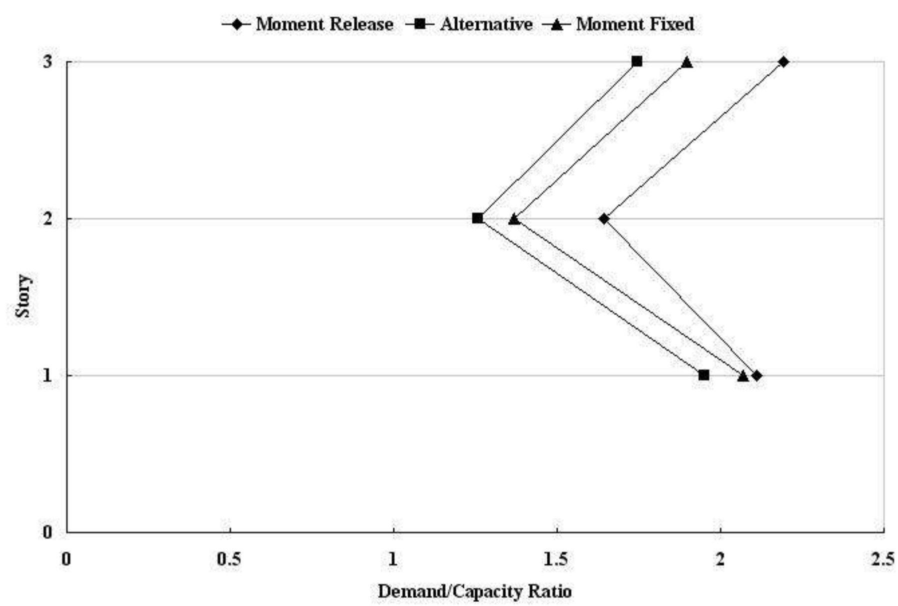

(b) 1,000 lb Weight at 30 ft Stand-off

Figure 4.19 : Demand/Capacity Ratio to Variable Stand-Off Distance on Longitudinal MRF

“Figure 4.19 : Continued”

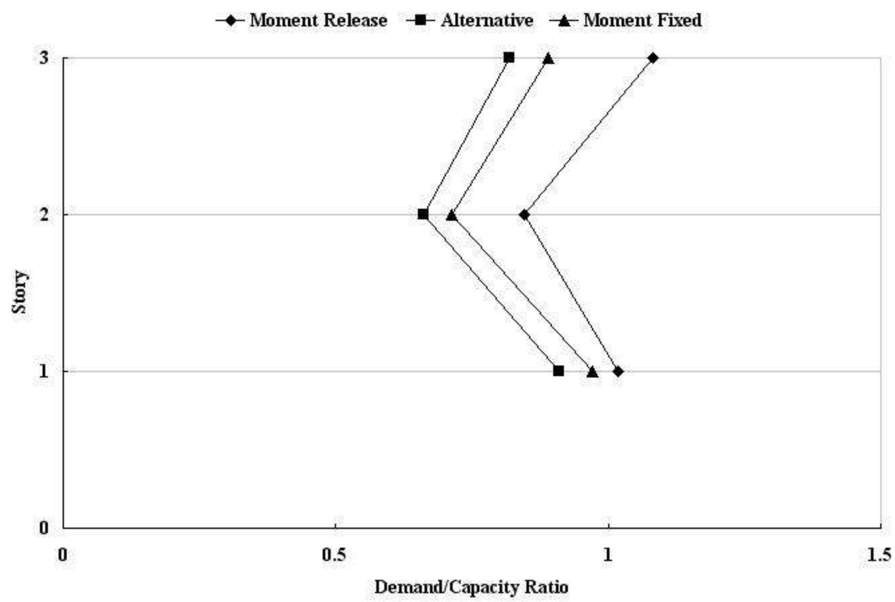

(c) 1,000 lb Weight at 50 ft Stand-off

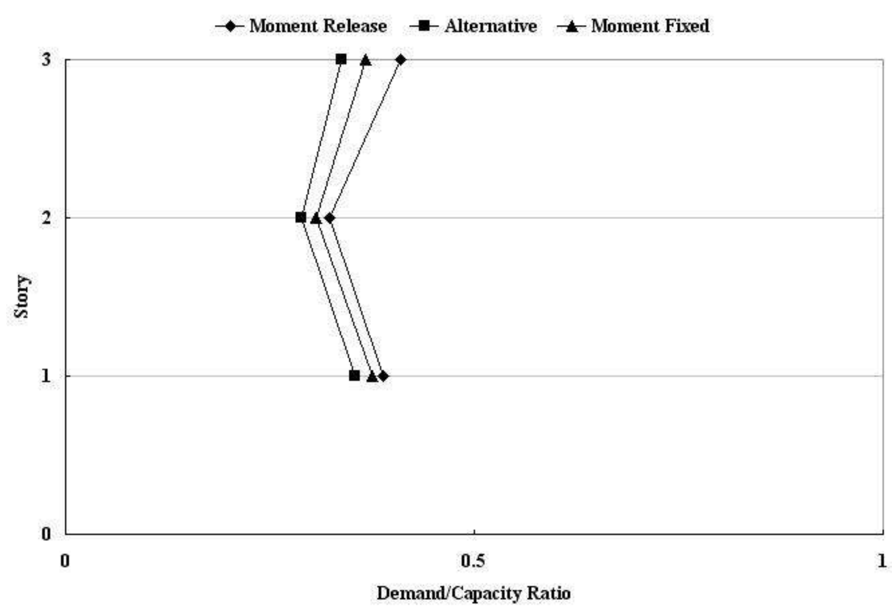

(d) 1,000 lb Weight at 100 ft Stand-off

4.2. Linear Structural Response to Variable TNT Weight

To know effect of variable TNT weight, this study is assumed explosive weight is 100 lb, 500 lb, 1,000 lb, and 2,000 lb at stand-off 20 ft. A scenario is constructed that these explosive values range from automobiles to van bomb attack on 3 story building as shown in Figure 3.1. Table 4.11 shows incident pressure, reflected pressure, time of arrival, time duration at each case. In this chapter, the crater dimension also is estimated by different TNT weight.

Table 4.11 : Incident Pressure and Reflected Pressure at each TNT Weight

TNT weight	Range (ft)	T_A (msec)	T_{di} (msec)	T_{dr} (msec)	Incident pressure (psi)	Reflected pressure (psi)
100 lb	20	4.51	2.74	1.85	59.1	246.72
500 lb	20	2.85	2.12	1.32	196.94	1182.55
1,000 lb	20	2.38	1.42	1.27	314.72	2133.71
2,000 lb	20	2.02	1.01	1.32	481.91	3602.49

Where, T_A : Time of arrival, T_{di} : Time duration of incident pressure, T_{dr} : Time of duration of reflected pressure

4.2.1. Crater

To investigate dimension of crater, CONWEP computer program used in cases of 100 lb, 500 lb, 1,000 lb, 2,000 lb and stand-off distance was assumed 20 ft. The dimension of variable TNT weight is shown in Figure 4.20 and Table 4.12.

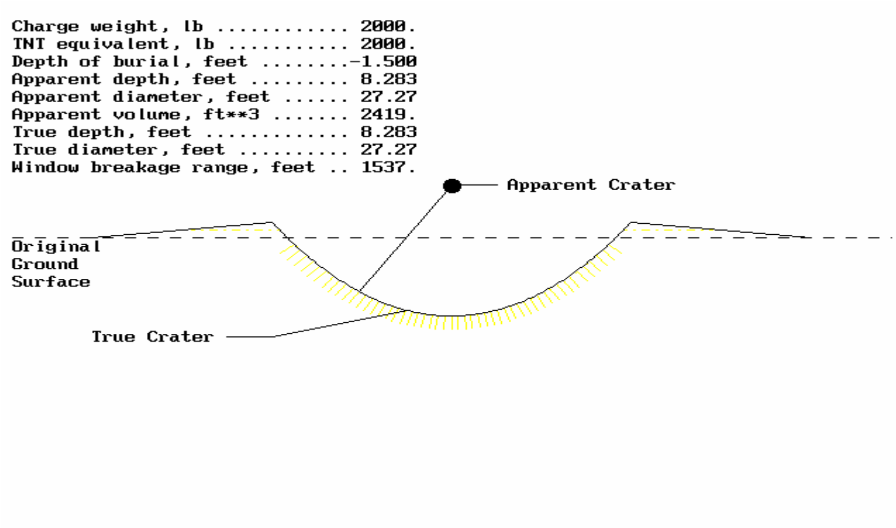

Figure 4.20 : Dimension of Crater with 2,000 lb TNT Weight

Table 4.12 : Results of CONWEP in Variable TNT with Dry Sandy Clay

Charge weight (lb)	Depth of Burial (ft)	Depth (ft)	Diameter (ft)	Breakage range (ft)
100	-3	N.A	N.A	N.A
500	-3	3.7	14.32	968.3
1,000	-3	5.19	18.95	1220
2,000	-3	7.12	24.94	1537

4.2.2. Blast Loads

A frame is subjected to 100 lb, 500 lb, 1,000 lb and 2,000 lb TNT blast at 20 ft stand-off distance. Cases are defined along various TNT weight. To find blast loads on 3 story building at each joint, the CONWEP program was used. Figure 4.21 - Figure 4.24 show time duration and peak reflected pressure on front frame of structure. Table 4.13 – Table 4.20 shows the summary of results using CONWEP Program at each case.

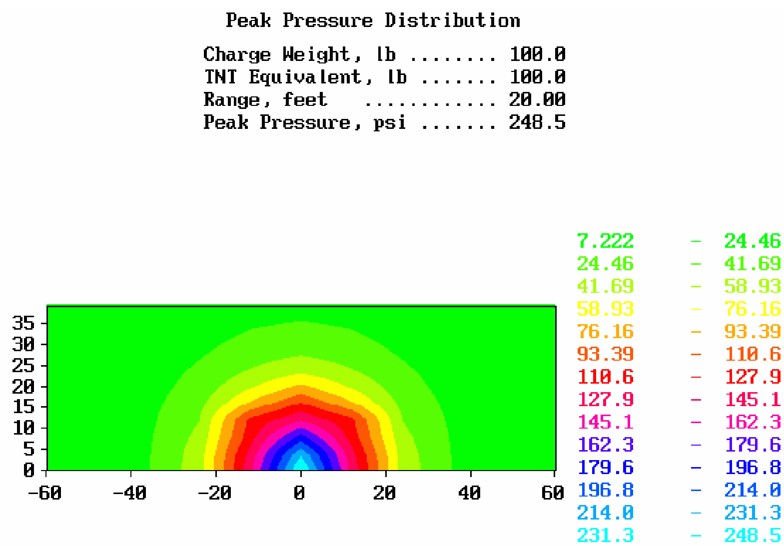

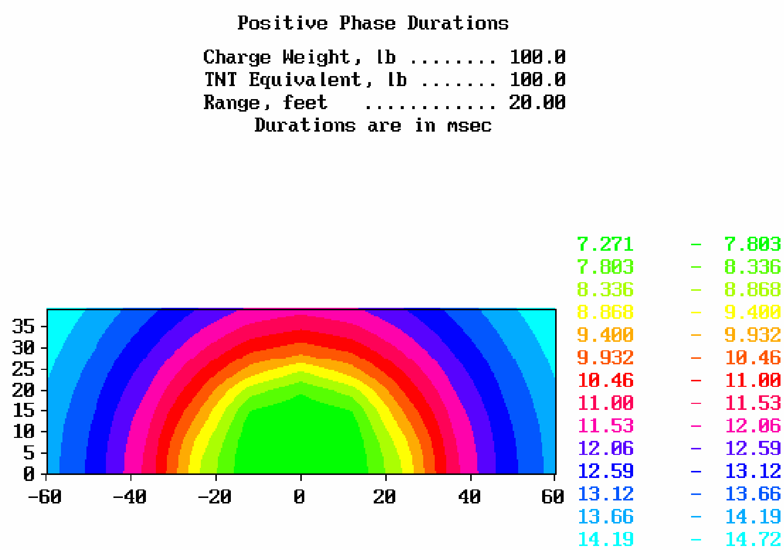

Figure 4.21 : Distribution of Peak Reflected Pressure and Time Duration 100 lb TNT

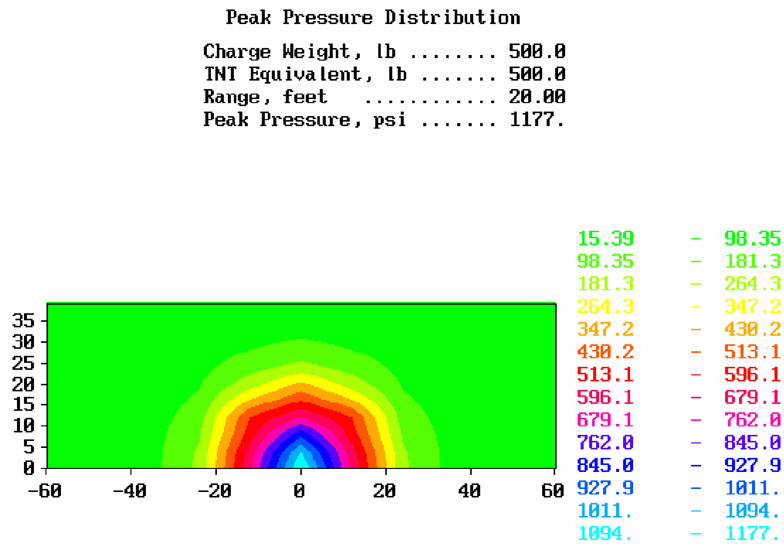

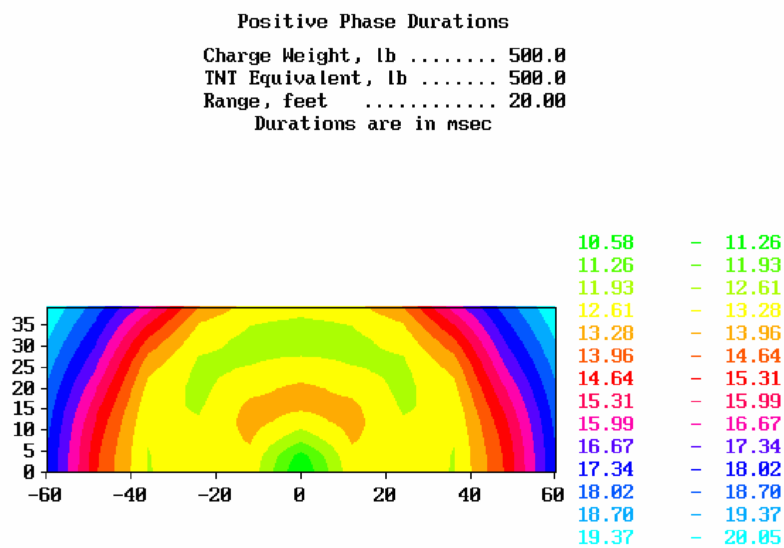

Figure 4.22 : Distribution of Peak Reflected Pressure and Time Duration 500 lb TNT

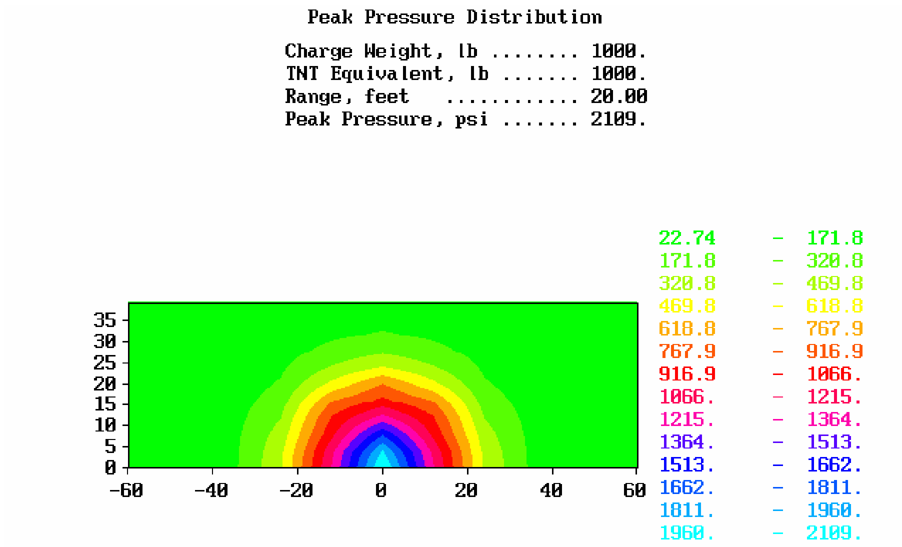

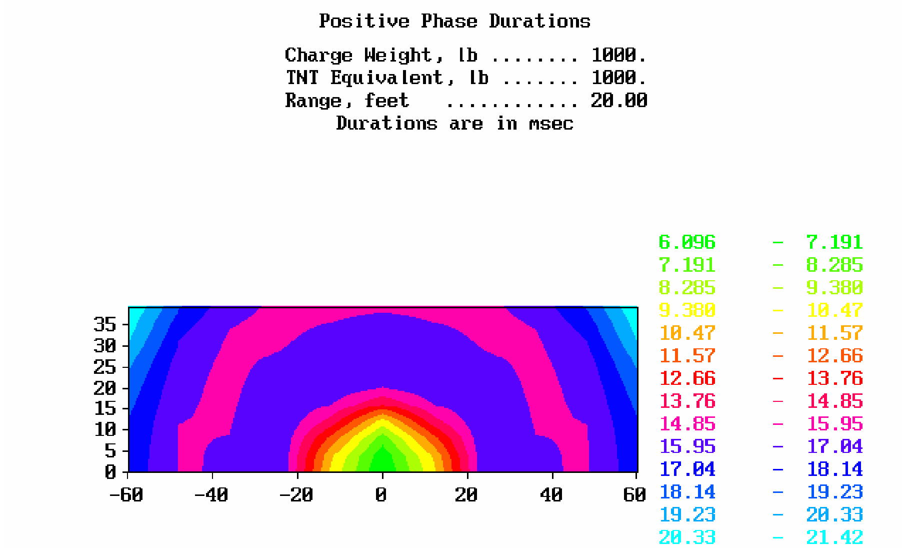

Figure 4.23 : Distribution of Peak Reflected Pressure and Time Duration 1,000 lb TNT

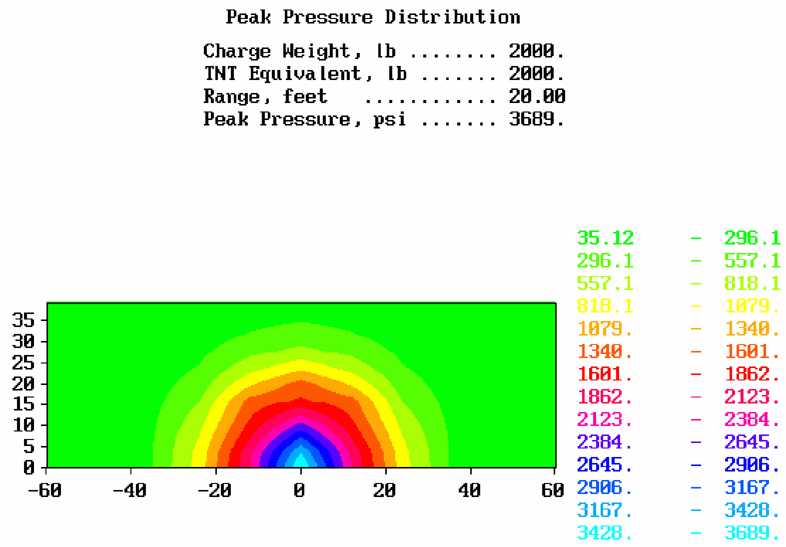

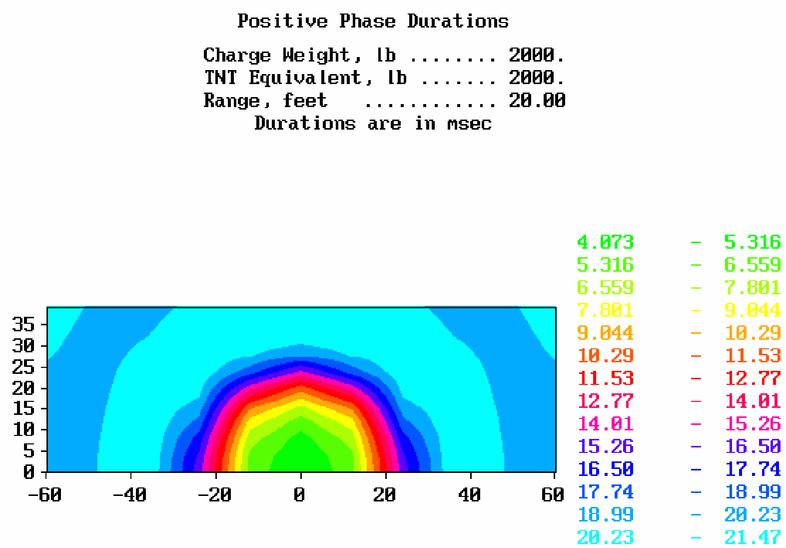

Figure 4.24 : Distribution of Peak Reflected Pressure and Time Duration 2,000 lb TNT

Table 4.13 : Reflected Pressure with 100 lb TNT Blast At 20 ft Stand-Off (psi)

Width (ft) / Height (ft)	-60	-45	-30	-15	0	15	30	45	60
0.0	9.693	15.79	32.93	115.8	248.5	115.8	32.93	15.79	9.693
6.5	9.587	15.54	31.39	113.8	199.9	113.8	31.39	15.54	9.587
13.0	9.282	14.83	27.95	77.17	129.7	77.17	27.95	14.83	9.282
19.5	8.809	13.74	23.46	48.82	80.3	48.82	23.46	13.74	8.809
26.0	8.298	12.46	19.01	32.89	43.25	32.89	19.01	12.46	8.298
32.5	7.787	11.16	16.2	23.44	28.27	23.44	16.2	11.16	7.787
39.0	7.222	9.83	13.66	17.5	19.7	17.5	13.66	9.83	7.222

Table 4.14 : Reflected Pressure with 500 lb TNT Blast At 20 ft Stand-Off (psi)

Width (ft) / Height (ft)	-60	-45	-30	-15	0	15	30	45	60
0.0	21.58	37.67	99.77	534.8	1177	534.8	99.77	37.67	21.58
6.5	21.36	37	93.67	516.4	971.8	516.4	93.67	37	21.36
13.0	20.71	35.13	78.77	353.7	611.1	353.7	78.77	35.13	20.71
19.5	19.72	32.37	62.4	184.3	372.3	184.3	62.4	32.37	19.72
26.0	18.51	28.68	48.16	99.62	153.5	99.62	48.16	28.68	18.51
32.5	16.98	24.94	38.8	62.34	80.05	62.34	38.8	24.94	16.98
39.0	15.39	21.88	32.18	42.7	50.41	42.7	32.18	21.88	15.39

Table 4.15 : Table 4.16 Reflected Pressure with 1,000 lb TNT Blast At 20 ft Stand-Off (psi)

Width (ft) / Height (ft)	-60.00	-45.00	-30.00	-15.00	0.00	15.00	30.00	45.00	60.00
0.0	32.41	60.77	209.3	985.8	2109	985.8	209.3	60.77	32.41
6.5	32.03	59.35	192.8	935.2	1762	935.2	192.8	59.35	32.03
13.0	30.91	55.41	158.6	746.5	1128	746.5	158.6	55.41	30.91
19.5	29.16	49.81	120.5	410.7	773.6	410.7	120.5	49.81	29.16
26.0	26.97	43.36	85.21	208.8	344.1	208.8	85.21	43.36	26.97
32.5	24.79	37.69	63.23	120.3	161.5	120.3	63.23	37.69	24.79
39.0	22.74	32.91	49.43	71.97	90.5	71.97	49.43	32.91	22.74

Table 4.16 : Reflected Pressure with 2,000 lb TNT Blast At 20 ft Stand-Off (psi)

Width (ft) / Height (ft)	-60.00	-45.00	-30.00	-15.00	0.00	15.00	30.00	45.00	60.00
0.00	52.95	121.7	464.7	1704	3689	1704	464.7	121.7	52.95
6.50	52.25	118.1	426.1	1603	3003	1603	426.1	118.1	52.25
13.00	50.24	107.9	336.1	1420	1970	1420	336.1	107.9	50.24
19.50	47.2	92.71	244.2	862.3	1464	862.3	244.2	92.71	47.2
26.00	43.48	76.53	173.7	463.7	731.5	463.7	173.7	76.53	43.48
32.50	39.16	63.24	127.8	243.9	343.7	243.9	127.8	63.24	39.16
39.00	35.12	53.88	91.73	149.9	183.5	149.9	91.73	53.88	35.12

Table 4.17 : Time Duration with 100 lb TNT Blast at 20 ft Stand-Off (msec)

Width (ft) / Height (ft)	-60	-45	-30	-15	0	15	30	45	60
0.0	13.91	12.53	10.32	7.433	7.353	7.433	10.32	12.53	13.91
6.5	13.94	12.58	10.45	7.528	7.285	7.528	10.45	12.58	13.94
13.0	14.01	12.73	10.81	7.939	7.337	7.939	10.81	12.73	14.01
19.5	14.14	12.95	11.32	9.055	7.884	9.055	11.32	12.95	14.14
26.0	14.31	13.23	11.88	10.32	9.498	10.32	11.88	13.23	14.31
32.5	14.5	13.55	12.44	11.32	10.78	11.32	12.44	13.55	14.5
39.0	14.72	13.87	12.97	12.15	11.78	12.15	12.97	13.87	14.72

Table 4.18 : Time Duration with 500 lb TNT Blast at 20 ft Stand-Off (msec)

Width (ft) / Height (ft)	-60	-45	-30	-15	0	15	30	45	60
0.0	18	13.84	12.45	13.43	10.58	13.43	12.45	13.84	18
6.5	18.08	13.95	12.44	13.51	11.77	13.51	12.44	13.95	18.08
13.0	18.29	14.33	12.43	13.43	13.2	13.43	12.43	14.33	18.29
19.5	18.62	15.03	12.56	12.89	13.45	12.89	12.56	15.03	18.62
26.0	19.04	16.13	12.91	12.45	12.73	12.45	12.91	16.13	19.04
32.5	19.53	17.01	13.66	12.56	12.43	12.56	13.66	17.01	19.53
39.0	20.05	17.91	15.08	13.2	12.83	13.2	15.08	17.91	20.05

Table 4.19 : Time Duration with 1,000 lb TNT Blast at 20 ft Stand-Off (msec)

Width (ft) / Height (ft)	-60.00	-45.00	-30.00	-15.00	0.00	15.00	30.00	45.00	60.00
0.0	17.77	15.69	16.85	12.97	6.096	12.97	16.85	15.69	17.77
6.5	17.87	15.71	16.77	14.09	7.173	14.09	16.77	15.71	17.87
13.0	18.18	15.78	16.5	15.97	11.03	15.97	16.5	15.78	18.18
19.5	18.74	15.93	16.09	16.94	15.85	16.94	16.09	15.93	18.74
26.0	19.54	16.22	15.74	16.85	17.03	16.85	15.74	16.22	19.54
32.5	20.58	16.75	15.67	16.09	16.53	16.09	15.67	16.75	20.58
39.0	21.42	17.65	15.94	15.66	15.78	15.66	15.94	17.65	21.42

Table 4.20 : Time Duration with 2,000 lb TNT Blast at 20 ft Stand-Off (msec)

Width (ft) / Height (ft)	-60.00	-45.00	-30.00	-15.00	0.00	15.00	30.00	45.00	60.00
0.00	19.83	20.64	20.37	7.491	4.073	7.491	20.37	20.64	19.83
6.50	19.84	20.57	20.59	8.316	4.589	8.316	20.59	20.57	19.84
13.00	19.9	20.37	21.07	11.12	6.485	11.12	21.07	20.37	19.9
19.50	20.02	20.1	21.44	16.72	10.79	16.72	21.44	20.1	20.02
26.00	20.23	19.85	21.34	20.37	18.07	20.37	21.34	19.85	20.23
32.50	20.57	19.73	20.75	21.44	21.03	21.44	20.75	19.73	20.57
39.00	21.09	19.8	20.08	21.1	21.4	21.1	20.08	19.8	21.09

When blast with 100 lb, 500 lb, 1,000 lb, 2,000 lb TNT weight at 20 ft stand-off distance impinges on a structure, a higher pressure is developed, termed the reflected pressure. The calculated (CONWEP) peak overpressures on the front frame are shown in Figure 4.21 – Figure 4.24 These range from a maximum of 248.5 psi (100 lb), 1177 psi (500 lb), 2109 psi (1,000 lb), 3689 psi (2,000 lb) at the point closest to the detonation to a minimum of 7.22 psi (100 lb), 15.39 psi (500 lb), 22.74 psi (1,000 lb), 35.12 psi (2,000 lb) at the upper west/east corner.

While these pressures are extremely large, they act for a limited duration, as shown in Figure 4. 21 – Figure 4.24. The duration ranges from a maximum of 14.72 msec (100 lb), 20.05 msec (500 lb), 21.42 msec (1,000 lb), 21.09 msec (2,000 lb) in the upper west/east corner to a minimum of 7.35 msec (100 lb), 10.58 msec (500 lb), 6.09 msec (1,000 lb), 4.07 msec(2,000 lb) at the point closest to the blast. Table 4.21 shows summary of results from CONWEP program.

Table 4.21 : Table 4.22 Summary of Results from CONWEP Program

Weight (lb)	Pressure (psi)		Duration of Load (msec)	
	Max.	Min.	Max.	Min.
100	248.5	7.22	14.72	7.53
500	1177	15.39	20.05	10.58
1,000	2109	22.74	21.42	6.09
2,000	3689	35.12	21.09	4.07

4.2.3. Effects of Framing Conditions

To obtain the response of 3 story building, SAP2000 FEM Software was used. The blast loads are generated at each joint as peak reflected pressure from CONWEP. The dynamic time history indicates that number of output time steps is 1,000 and output time step size is 0.005. The damping ratio is assumed as 5 %. This structure was analyzed 4 different cases to obtain dynamic time history curve at each floor. Dynamic time history curves of each floor at 20 ft stand-off distance with 100 lb, 500 lb, 1,000 lb, 2,000 lb TNT weight are shown in Figure 4.25 – Figure 4.27. In addition, the constraint of joints are also divided into 3 cases such as moment released, moment fixed and moment fixed with different rotation of columns as previous chapter.

CASE 1 : Moment Released

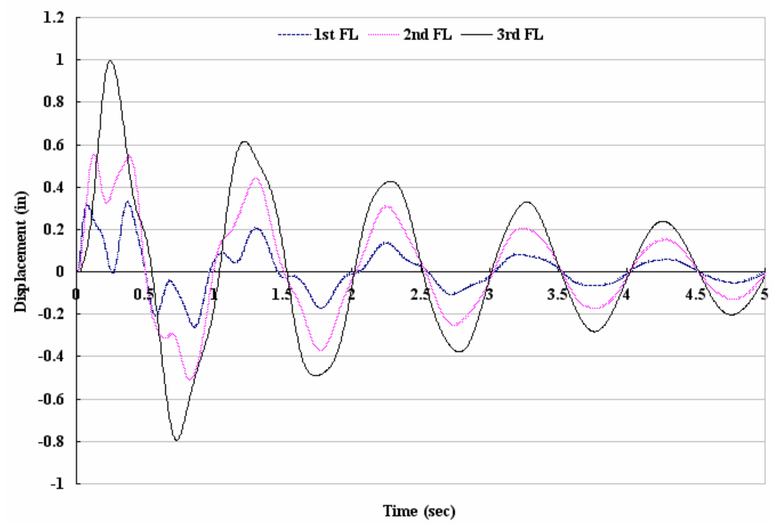

(a) 100 lb TNT Weight at 20 ft Stand-Off

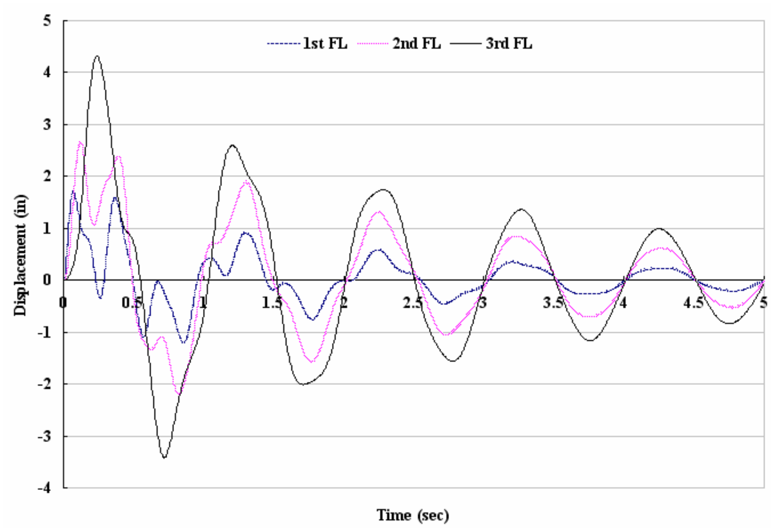

(b) TNT Weight at 20 ft Stand-Off

Figure 4.25 : Linear Dynamic Time History to Variable TNT Weight (Moment Released)

"Figure 4.25 : Continued"

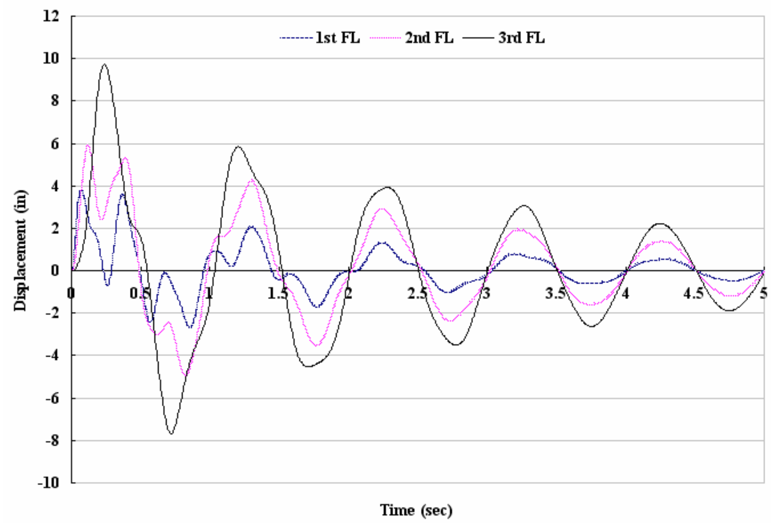

(c) 1,000 lb TNT Weight at 20 ft Stand-Off

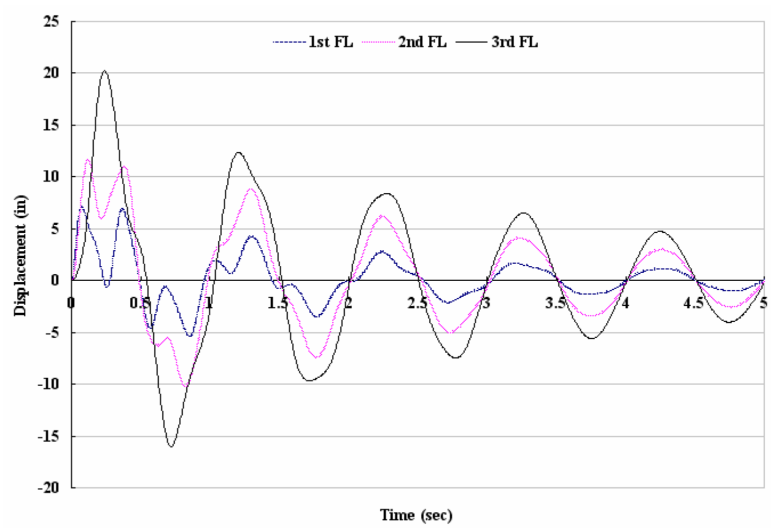

(d) 2,000 lb TNT Weight at 20 ft Stand-Off

CASE 2 : Moment Fixed

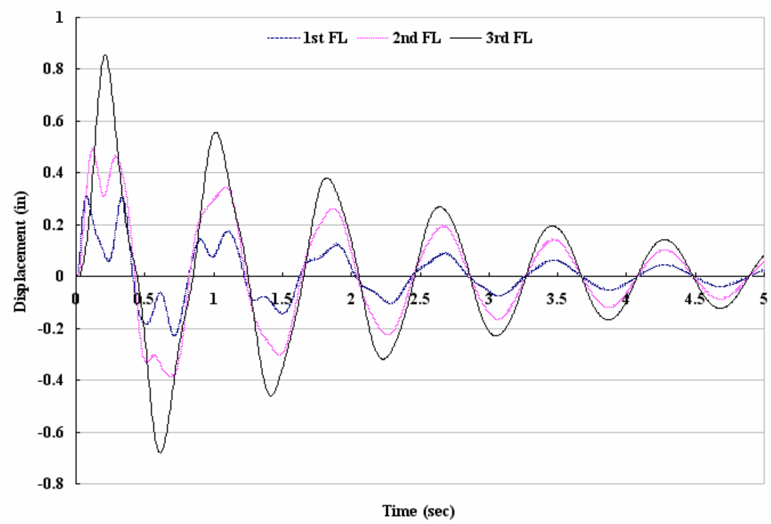

(a) 100 lb TNT Weight at 20 ft Stand-Off

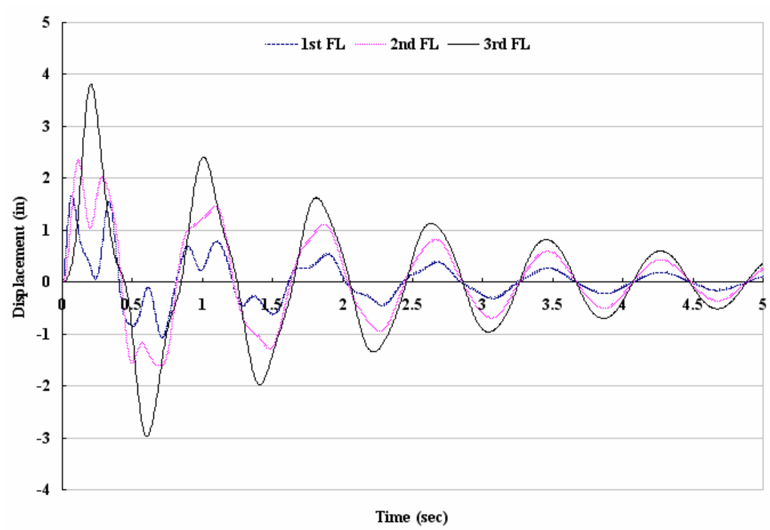

(b) 500 lb TNT Weight at 20 ft Stand-Off

Figure 4.26 : Linear Dynamic Time History to Variable TNT Weight (Moment Fixed)

“Figure 4.26 : Continued”

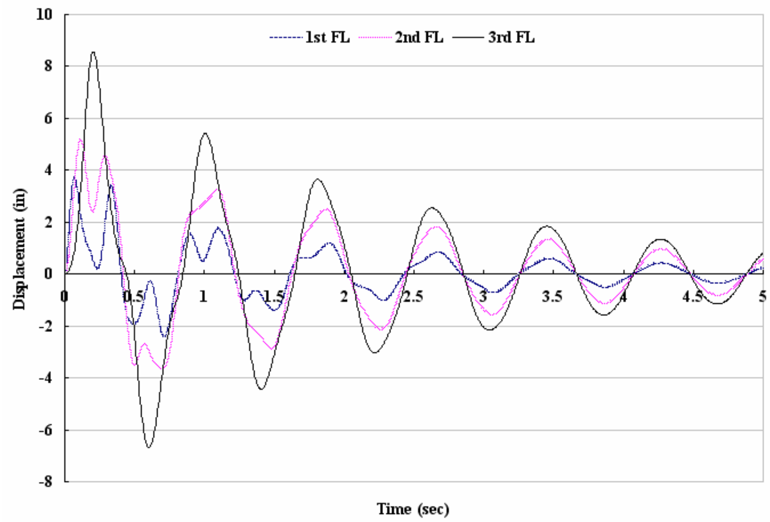

(c) 1,000 lb TNT Weight at 20 ft Stand-Off

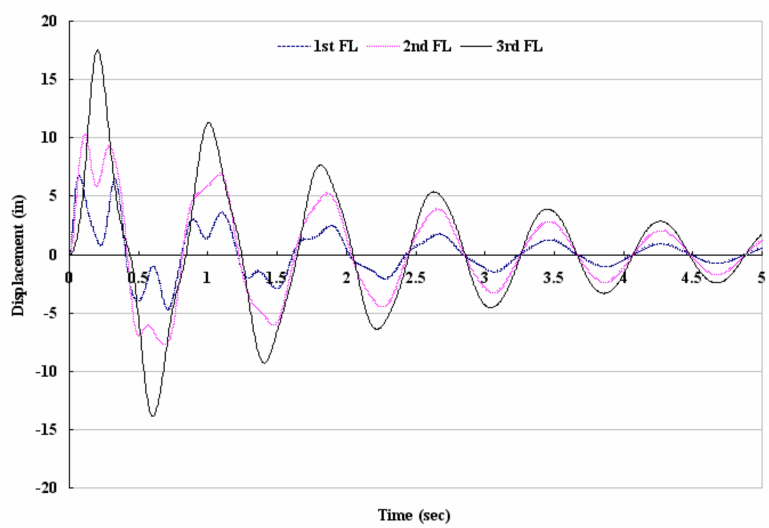

(d) 2,000 lb TNT Weight at 20 ft Stand-Off

CASE 3 : Moment Fixed (Alternative Rotation)

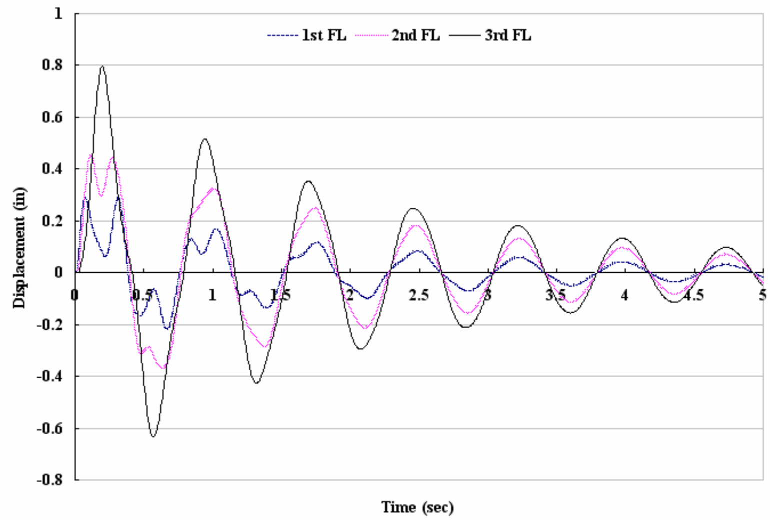

(a) 100 lb TNT Weight at 20 ft Stand-Off

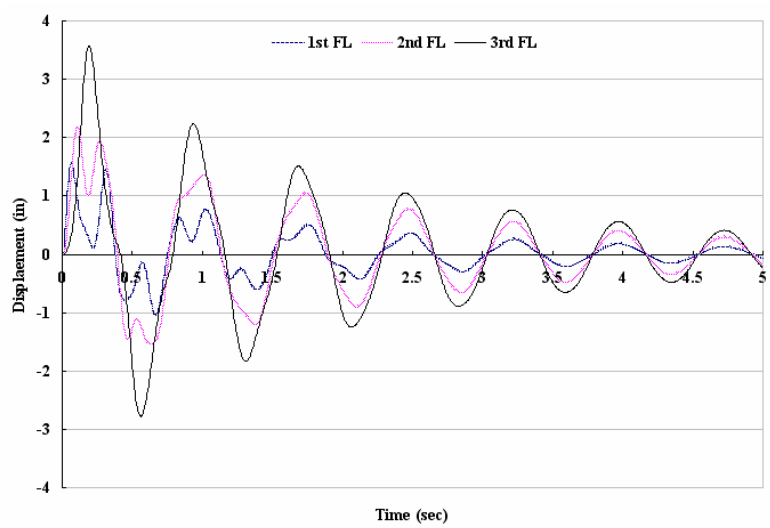

(b) 500 lb TNT Weight at 20 ft Stand-Off

Figure 4.27 : Linear Dynamic Time History to Variable TNT Weight (Moment Fixed (Alternative Rotation))

"Figure 4.27 : Continued"

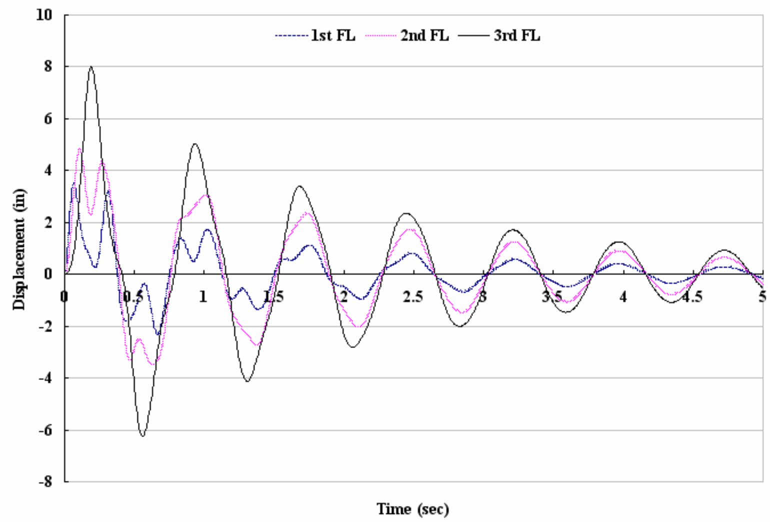

(c) 1,000 lb TNT Weight at 20 ft Stand-Off

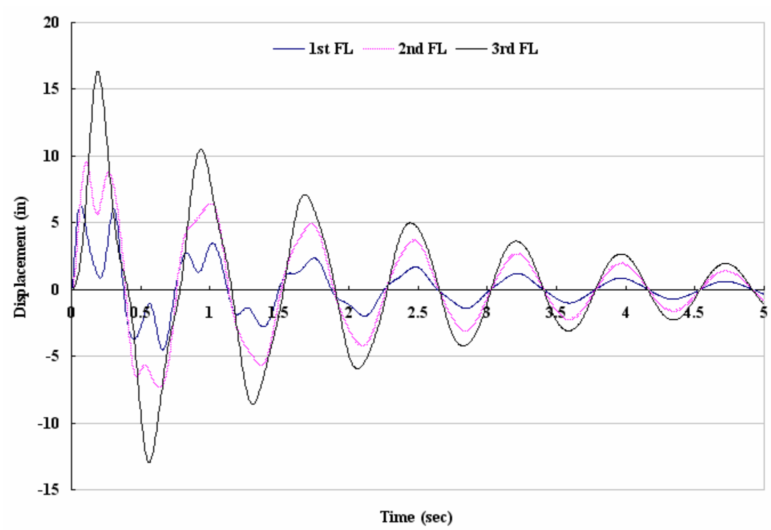

(d) 2,000 lb TNT Weight at 20 ft Stand-Off

To find demand/capacity ratio of members corresponding to each case, the result of analysis from SAP2000 based on UBC 97 LRFD design code shows demand/capacity ratio of all frame. These values are obtained by combination of dead load, live load and blast loads. All Demand/Capacity ratio of each frame against applied loads shows in appendix B. As a result, critical column was found at closest distance of blast source. The moments were compared by defined code value with value of analysis using SAP 2000. The comparison with moment of code defined by UBC 97 and analysis was shown in Table 4.22.

Table 4.22 : Comparison with Code and Analysis value of moment

CASE(Fram43)	Time (sec)	Mu (kips-in)	Mn (kips-in)	Demand/capacity ratio	Status
100 lb_20 ft	0.08	3253.1	13680	0.24	Ok
500 lb_20 ft	0.07	18435.7	13680	1.35	over stress
1,000 lb_20 ft	0.075	40686	13680	2.97	over stress
2,000 lb_20 ft	0.075	70498	13680	5.15	over stress

$$where, \quad \Phi = 0.9, \quad M_n = \varphi \cdot F_y \cdot Z_y$$

$$F_y = Yield\ \ Stress = 50\,ksi$$

$$Z_y = Plastic\ \ Section\ \ Modulus$$

4.2.4. Summary

As results of dynamic time history analysis with different joint constraint and column rotation, maximum deflections are shown in Figure 4.28 for each case. As might be expected, the maximum deflection occurs for the 2,000 TNT weight @ 20 ft standoff distance. The maximum displacement is 20.2 in 17.5 in and 16.33 in at the roof for respective case and occurs at 0.24 sec, 0.2 sec. 0.19 sec. However, for the 100 lb TNT weight at 20 ft stand-off distance, the maximum displacement of 0.99 in, 0.85 in and 0.8 in is at the roof level for respective case and occurs at 0.2 seconds.

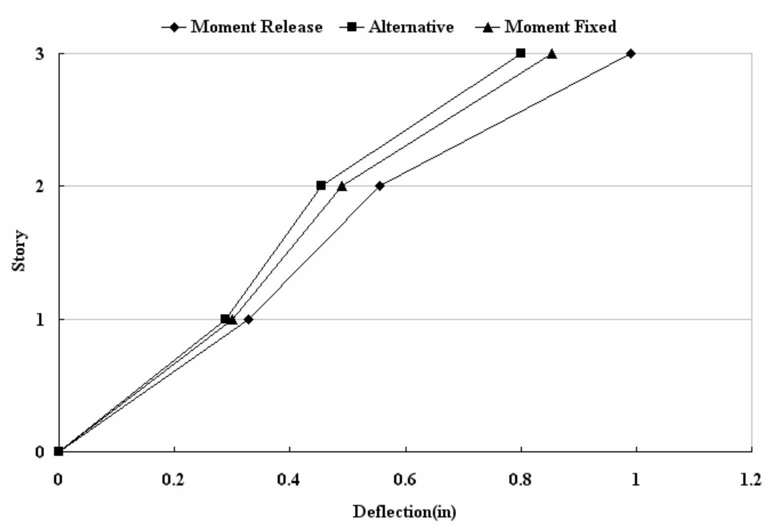

(a) 100 lb TNT Weight at 20 ft Stand-off

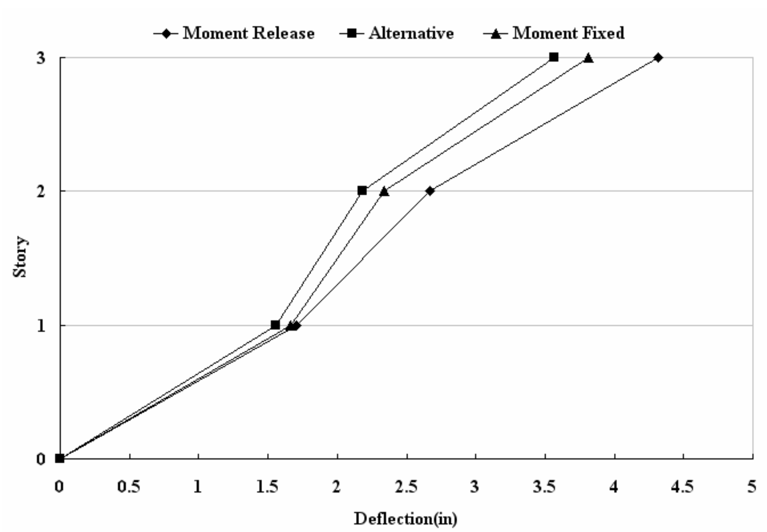

(b) 500 lb TNT Weight at 20 ft Stand-off

Figure 4.28 : Maximum Deflection on Each Floor to Variable TNT Weight

"Figure 4.28 : Continued"

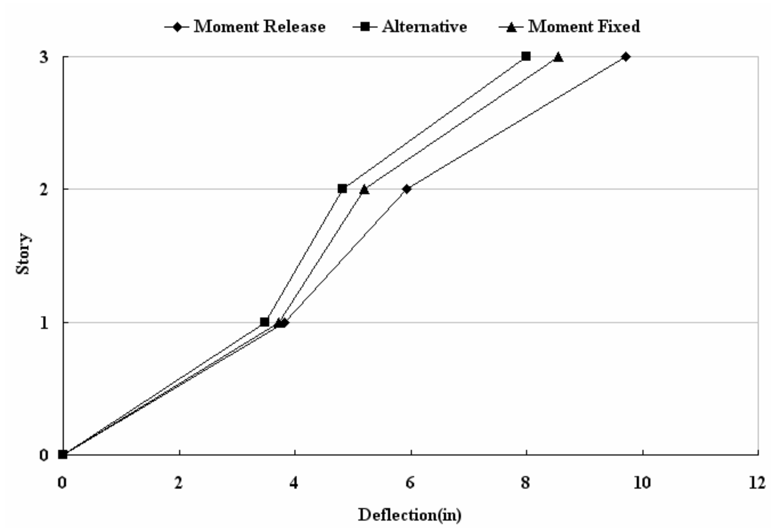

(c) 1,000 lb TNT Weight at 20 ft Stand-off

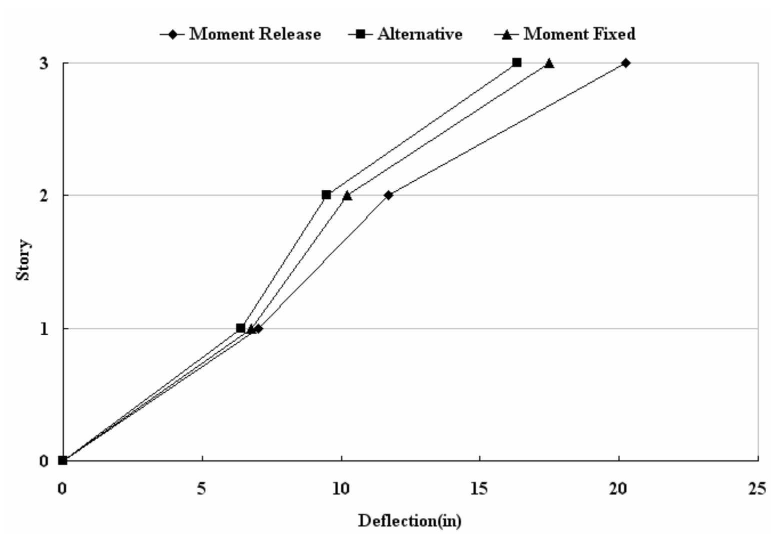

(d) 2,000 lb TNT Weight at 20 ft Stand-off

Based on maximum displacements, interstory drifts are shown in Figure 4.29. The code limitation of drift ratio for seismic load based on UBC 97 is 0.02 and the responses of all conditions satisfy this loading with the exception of the 1,000 lb, 2,000 lb explosive @ 20 ft. However, in this case, the drift of 0.025, 0.023, 0.022 with 1,000 lb @ 20 ft standoff distance which should be sustained with proper welded connections. The 2,000 lb explosive @ 20 ft has a drift of 0.055 at the roof and 0.045 at the first story. These are high and may not be sustainable.

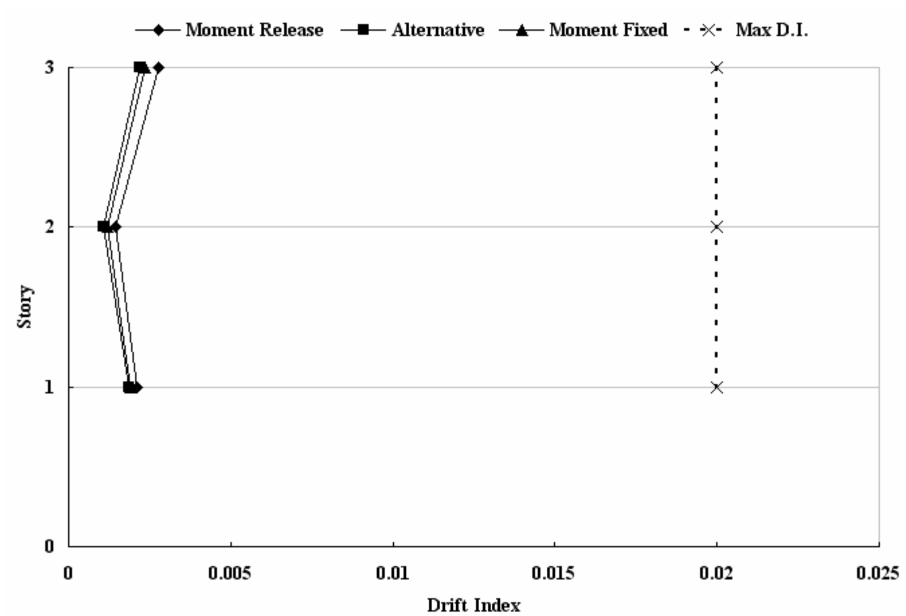

(a) 100 lb TNT Weight at 20 ft Stand-off

Figure 4.29 : Interstory Drift to Variable TNT Weight

“Figure 4.29 : Continued”

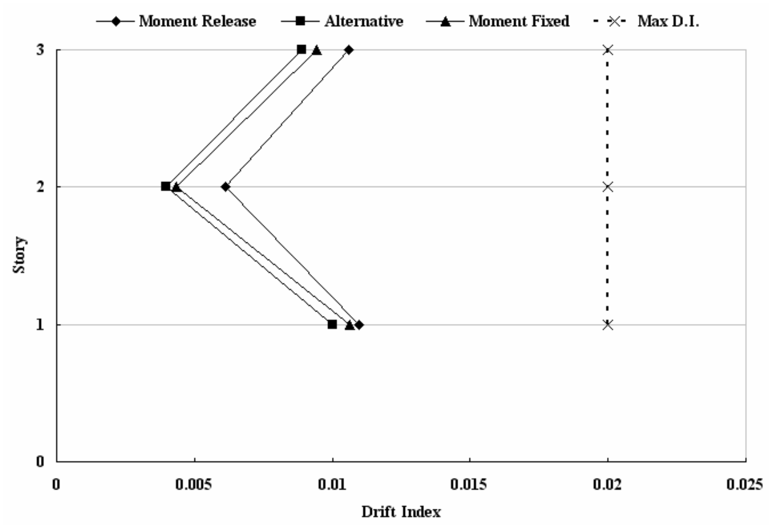

(b) 500 lb TNT Weight at 20 ft Stand-off

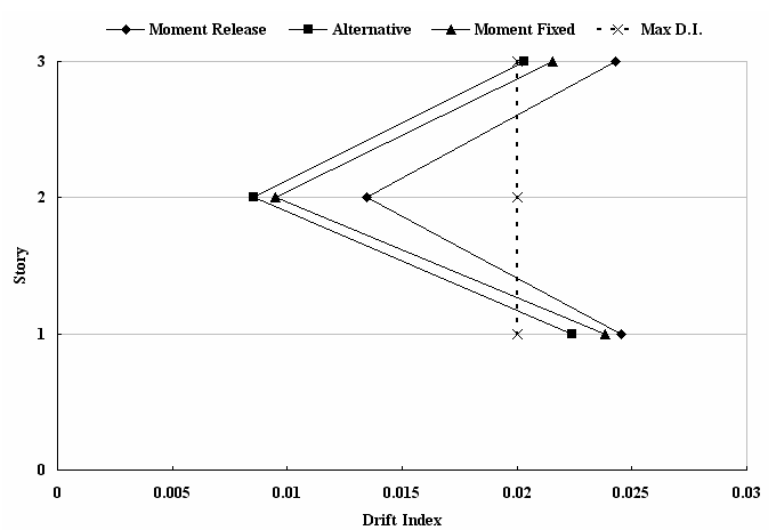

(c) 1,000 lb TNT Weight at 20 ft Stand-off

“Figure 4.29 : Continued”

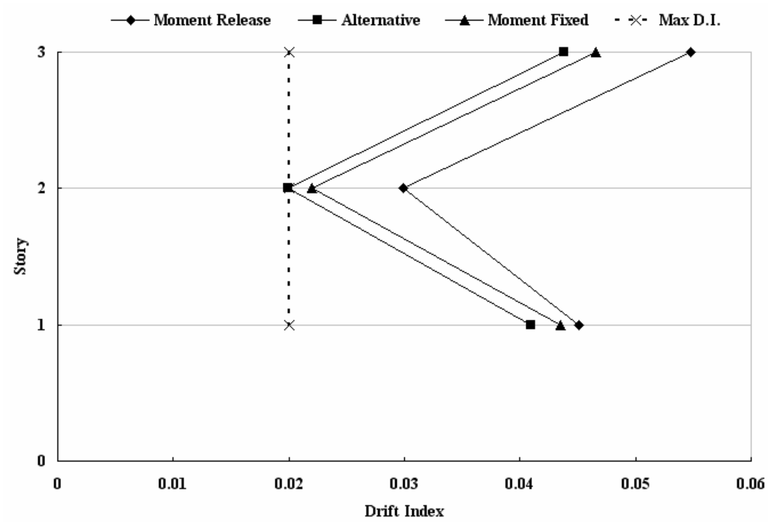

(d) 2,000 lb TNT Weight at 20 ft Stand-off

The maximum D/C ratios for the columns under explosive weights of 100 lb, 500 lb, 1,000 lb, 2,000 lb at a standoff distance 20 ft are shown in Figure 4.30 and Figure 4.31. Elastic behavior occurs for the two smaller explosive weights (a, b). For the two larger weights (c, d), three maximum D/C values are 2.5 and 4.5 indicating inelastic behavior and the use of a nonlinear analysis. In the longitudinal frame, the 500 lb explosive weight may cause weakly nonlinear behavior, however, the two larger weights result in D/C ratios of 3.2 and 6.7. Each ratio was shown in Appendix B.2.

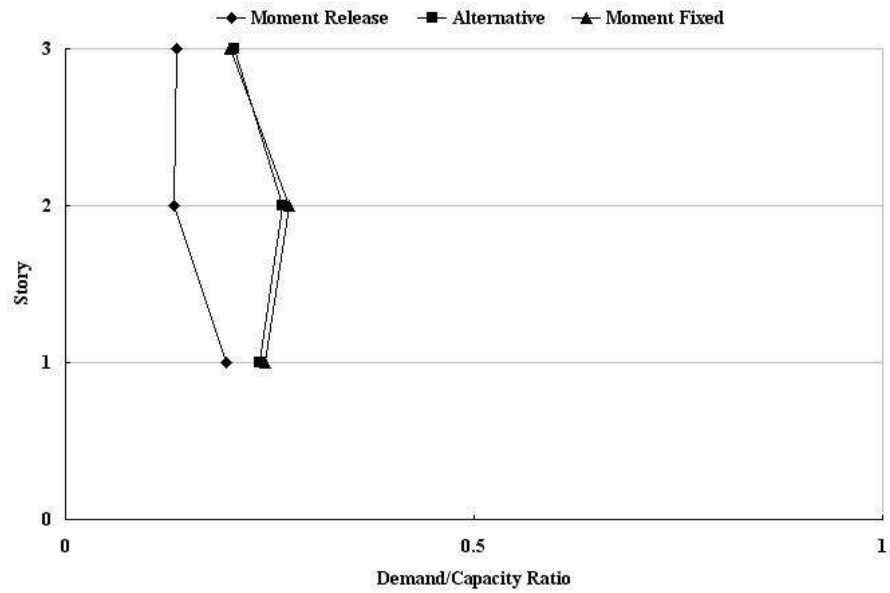

(a) 100 lb TNT Weight at 20 ft Stand-off

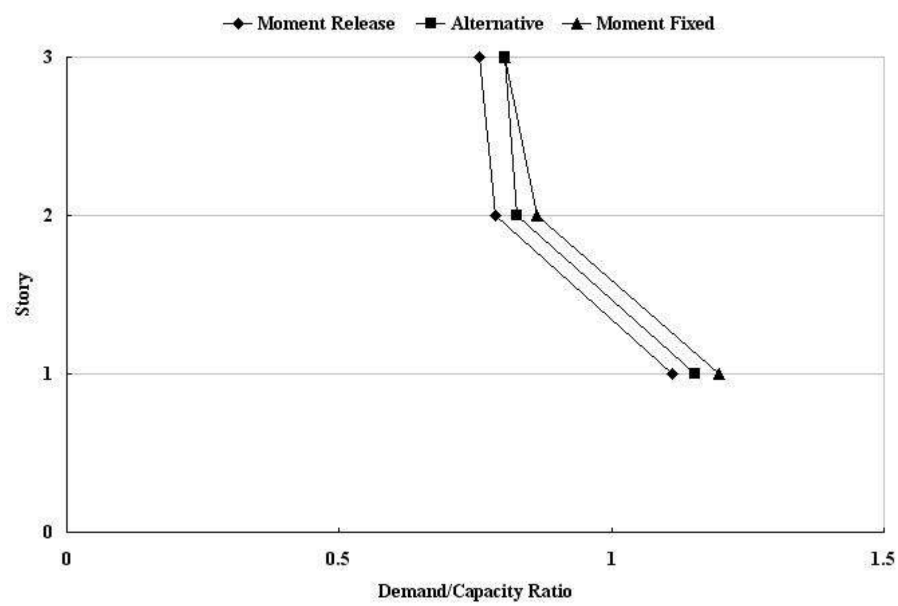

(b) 500 lb TNT Weight at 20 ft Stand-off

Figure 4.30 : Demand/Capacity Ratio to Variable TNT Weight on Transverse MRF

"Figure 4.30 : Continued"

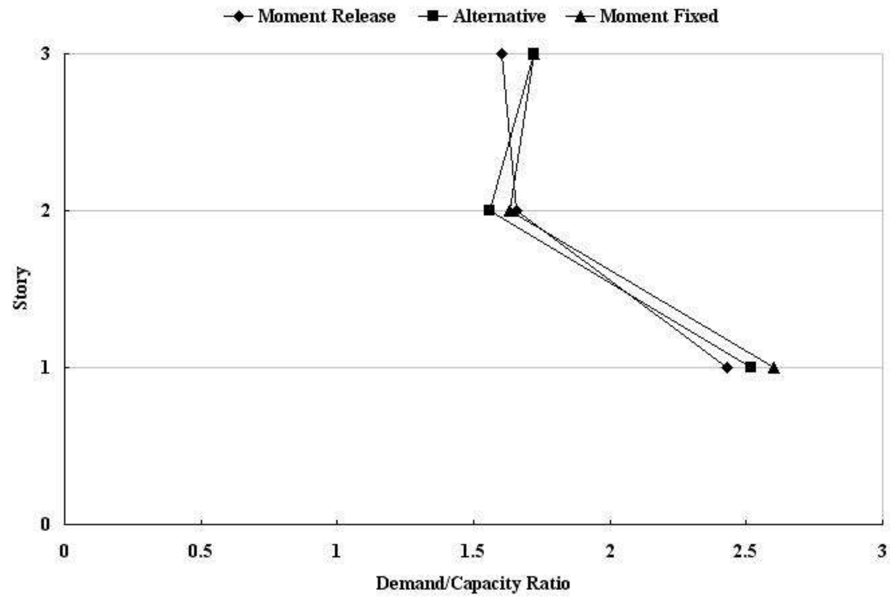

(c) 1,000 lb TNT Weight at 20 ft Stand-off

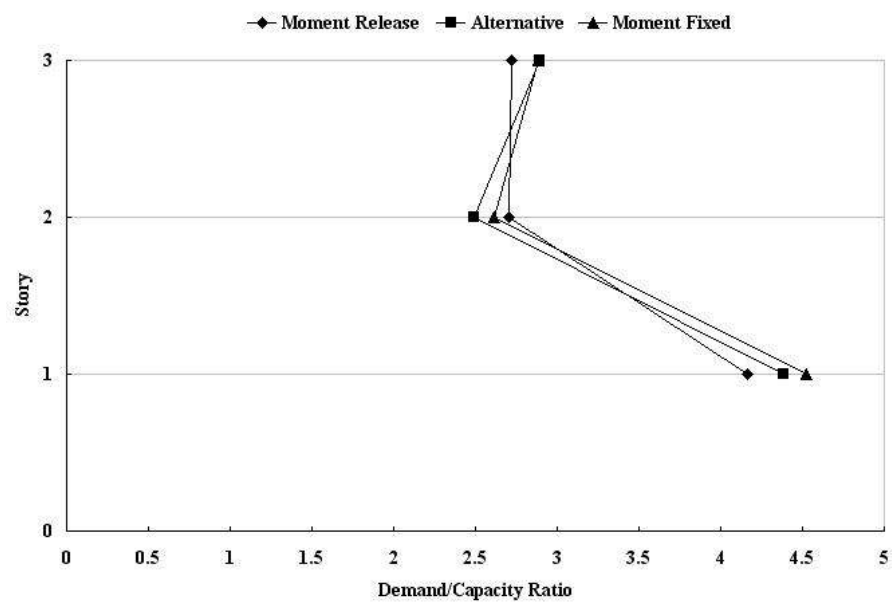

(d) 2,000 lb TNT Weight at 20 ft Stand-off

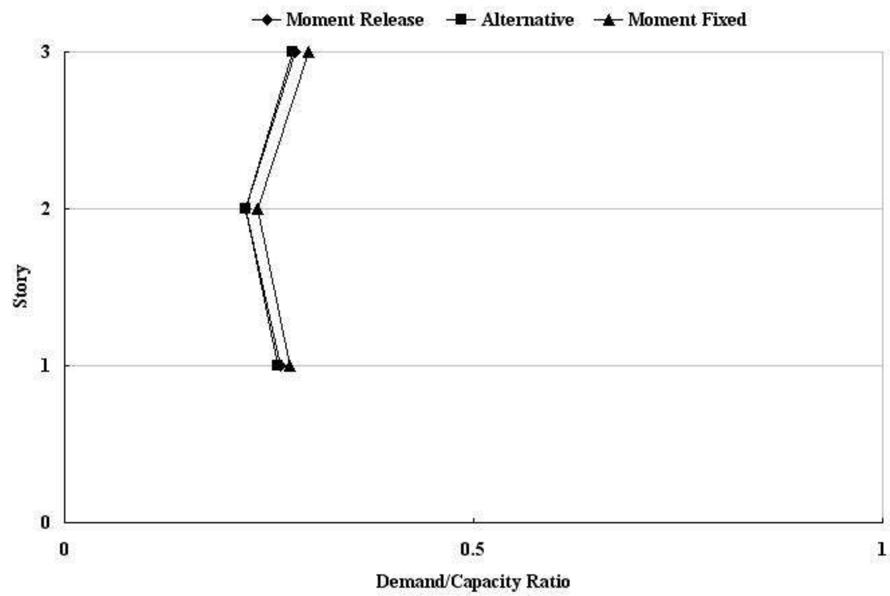

(a) 100 lb TNT Weight at 20 ft Stand-off

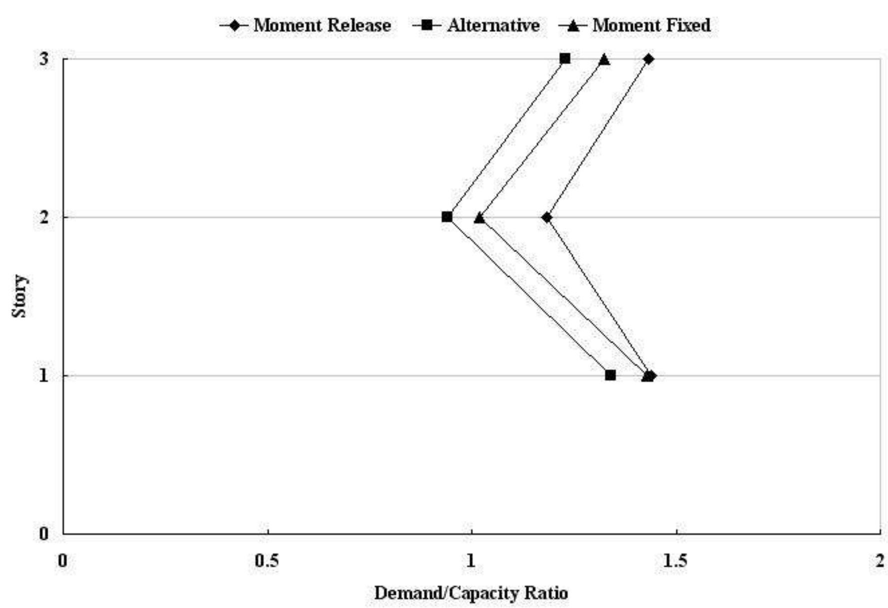

(b) 500 lb TNT Weight at 20 ft Stand-off

Figure 4.31 : Demand/Capacity Ratio to Variable TNT Weight on Longitudinal MRF

“Figure 4.31 : Continued”

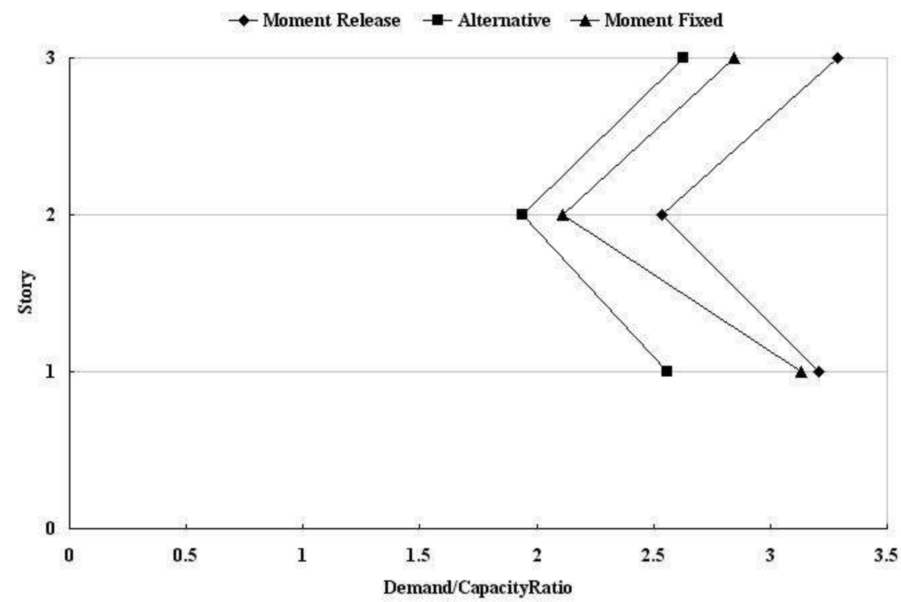

(c) 1,000 lb TNT Weight at 20 ft Stand-off

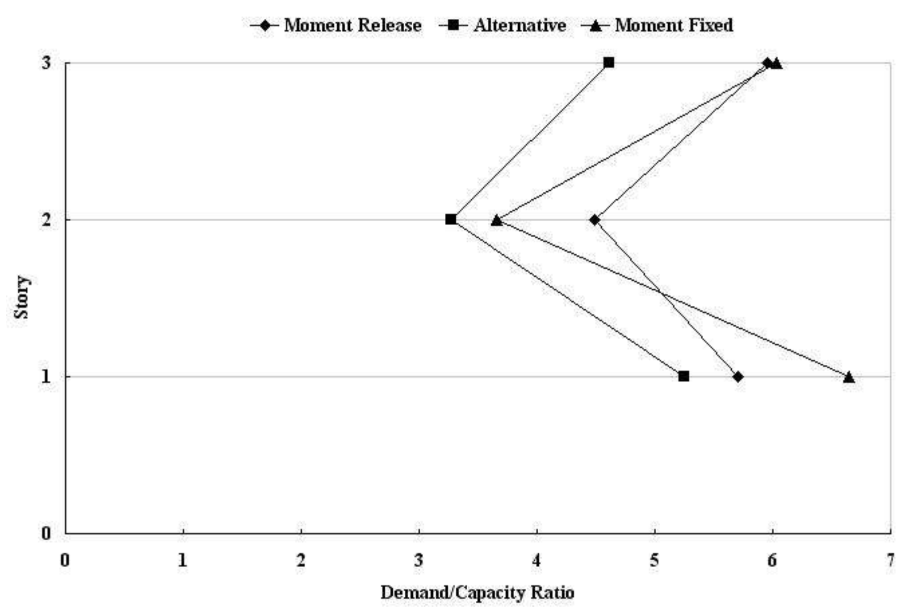

(d) 2,000 lb TNT Weight at 20 ft Stand-off (Longitudinal Direction)

4.3. Diaphragm Analysis of Using Shell Elements of 3 Story Building

4.3.1. Flexible Diaphragm Analysis

The floor diaphragms in the structure are often assumed to be rigid in their plane. However, they can also be represented by flexible diaphragm resulting in shear force and bending moment contours shown in Figure 4.41 – Figure 4.42 for a linear analysis against 1,000 lb @ 20 ft stand-off distance. These contours indicate how the blast loading that occurs on the face perpendicular to the blast is distributed to the moment frames on the sides parallel to the blast force. Maximum shear forces and maximum moment in slab are investigated against 500 lb, 1,000 lb, 2,000 lb, 3,000 lb TNT @ 20 ft stand-off distance. For reference, the member locations, identification numbers and member sizes are shown Figure 4.32 for typical longitudinal frame. Table 4.23 – 4.30 and Figure 4.33 – 4.40 show comparison of developed shear force and bending moment with capacity of each moment resistance frames. The results of flexible diaphragm analysis are also shown in Figure 4.43- 4.44 and Table 4.31.

In addition, maximum shear forces and bending moments of Moment Resistant Frame are investigated as compared with capacity defined by AISC-LRFD [2] respectively.

Moment Capacity : $\boldsymbol{\phi M_n = F_y \cdot Z_x}$

Shear Capacity : $\boldsymbol{\phi V_n = 0.9\left(0.6F_y\right)A_w}$

Where, F_y : yielding stress of section

Z_x : section modulus

A_w : area of the web

Hence, the moment capacity of W14*257 is calculated as 24,350 k-in and the one of W14*311 is 30,105 k-in. The other side, the shear capacity is estimated to be 522.5 k/in and 651.8 k/in at each member.

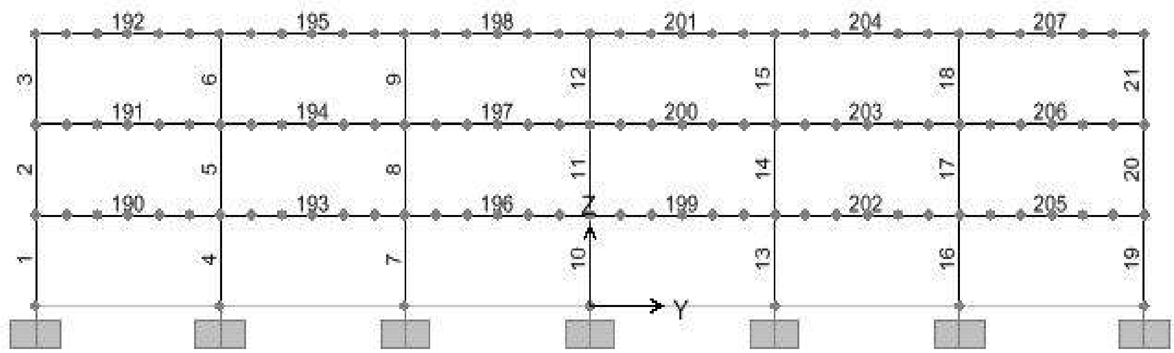

(a) Generated Member Numbers along the Longitudinal Direction

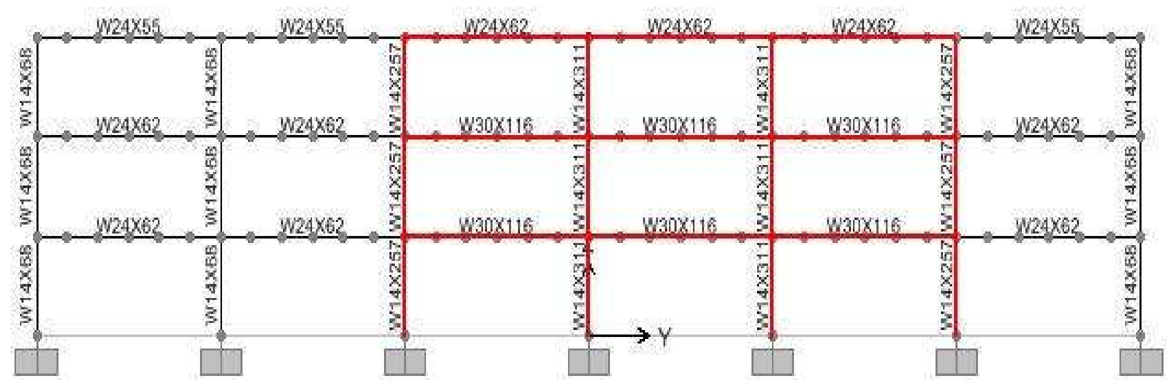

(b) Generated Frame Sections and Moment Resistant Frames

Figure 4.32 : Generated Member Numbers and Frame Section along the Longitudinal direction

Table 4.23 : Max. Shear Force at Moment Resistant Frames (500 lb TNT Weight @ 20 ft)

Frame No.	Frame Section	Shear Force (V_u)	Shear Strength (ϕV_n)
7	W14*257	203.041	522.5
8	W14*257	71.804	522.5
9	W14*257	160.915	522.5
10	W14*311	282.494	651.8
11	W14*311	128.896	651.8
12	W14*311	263.333	651.8
13	W14*311	281.920	651.8
14	W14*311	128.846	651.8
15	W14*311	262.719	651.8
16	W14*257	201.901	522.5
17	W14*257	72.721	522.5
18	W14*257	160.143	522.5

(unit : k/in)

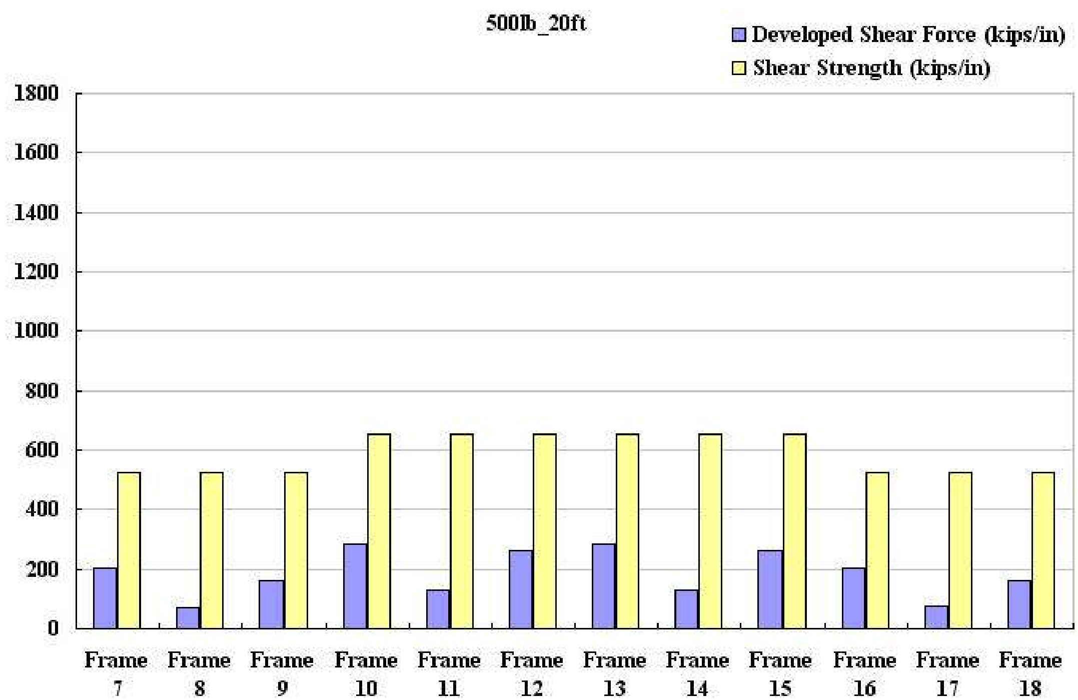

Figure 4.33 : Developed Shear Force vs. Shear Capacity of Flexible Diaphragm (500 lb @ 20 ft)

Table 4.24 : Max. Shear Force at MRF Frames (1,000 lb TNT Weight @ 20 ft)

Frame No.	Frame Section	Shear Force (V_u)	Shear Strength (ϕV_n)
7	W14*257	454.739	522.5
8	W14*257	161.143	522.5
9	W14*257	360.384	522.5
10	W14*311	632.945	651.8
11	W14*311	284.777	651.8
12	W14*311	589.780	651.8
13	W14*311	631.663	651.8
14	W14*311	284.663	651.8
15	W14*311	588.403	651.8
16	W14*257	452.196	522.5
17	W14*257	160.956	522.5
18	W14*257	358.856	522.5

(unit : k/in)

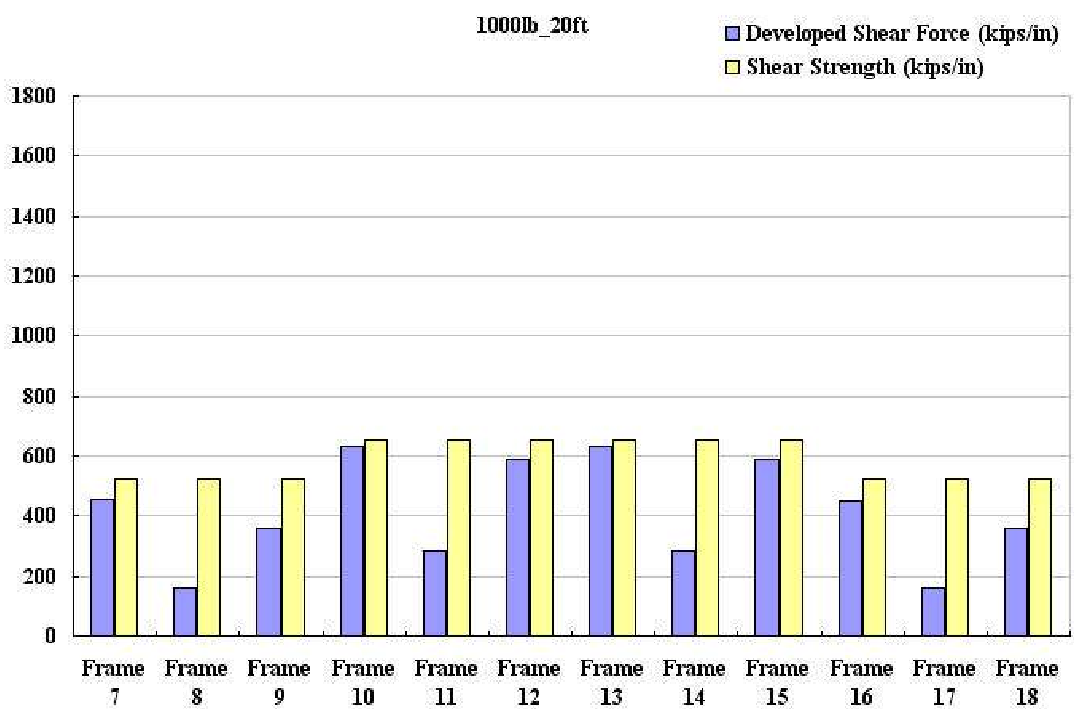

Figure 4.34 : Developed Shear Force vs. Shear Capacity of Flexible Diaphragm (1,000 lb @ 20 ft)

Table 4.25 : Max. Shear Force at MRF Frames (2,000 lb TNT Weight @ 20 ft)

Frame No.	Frame Section	Shear Force (Vu)	Shear Strength (φVn)
7	W14*257	882.270	522.5
8	W14*257	344.787	522.5
9	W14*257	703.573	522.5
10	W14*311	1230.401	651.8
11	W14*311	607.375	651.8
12	W14*311	1156.027	651.8
13	W14*311	1227.981	651.8
14	W14*311	607.112	651.8
15	W14*311	1153.410	651.8
16	W14*257	877.488	522.5
17	W14*257	344.368	522.5
18	W14*257	700.320	522.5

(unit : k/in)

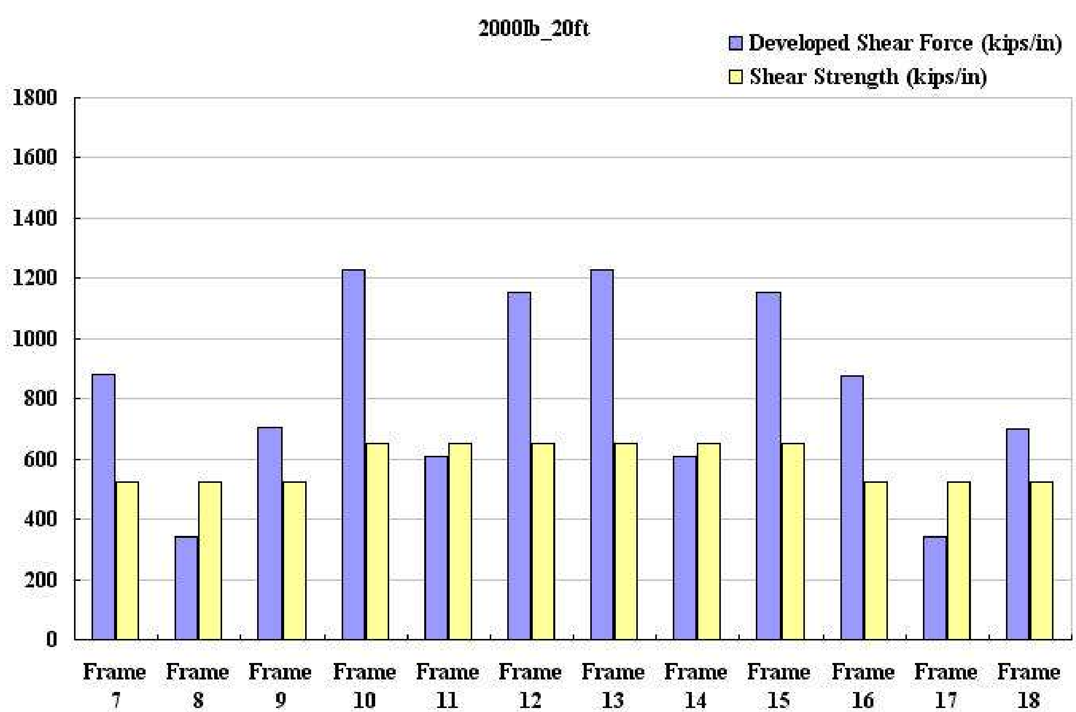

Figure 4.35 : Developed Shear Force vs. Shear Capacity of Flexible Diaphragm (2,000 lb @ 20 ft)

Table 4.26 : Max. Shear Force at MRF Frames (3,000 lb TNT Weight @ 20 ft)

Frame No.	Frame Section	Shear Force (Vu)	Shear Strength (ϕVn)
7	W14*257	1169.521	522.5
8	W14*257	493.059	522.5
9	W14*257	937.343	522.5
10	W14*311	1633.678	651.8
11	W14*311	866.517	651.8
12	W14*311	1545.583	651.8
13	W14*311	1630.550	651.8
14	W14*311	866.119	651.8
15	W14*311	1542.178	651.8
16	W14*257	1163.356	522.5
17	W14*257	492.436	522.5
18	W14*257	933.344	522.5

(unit : k/in)

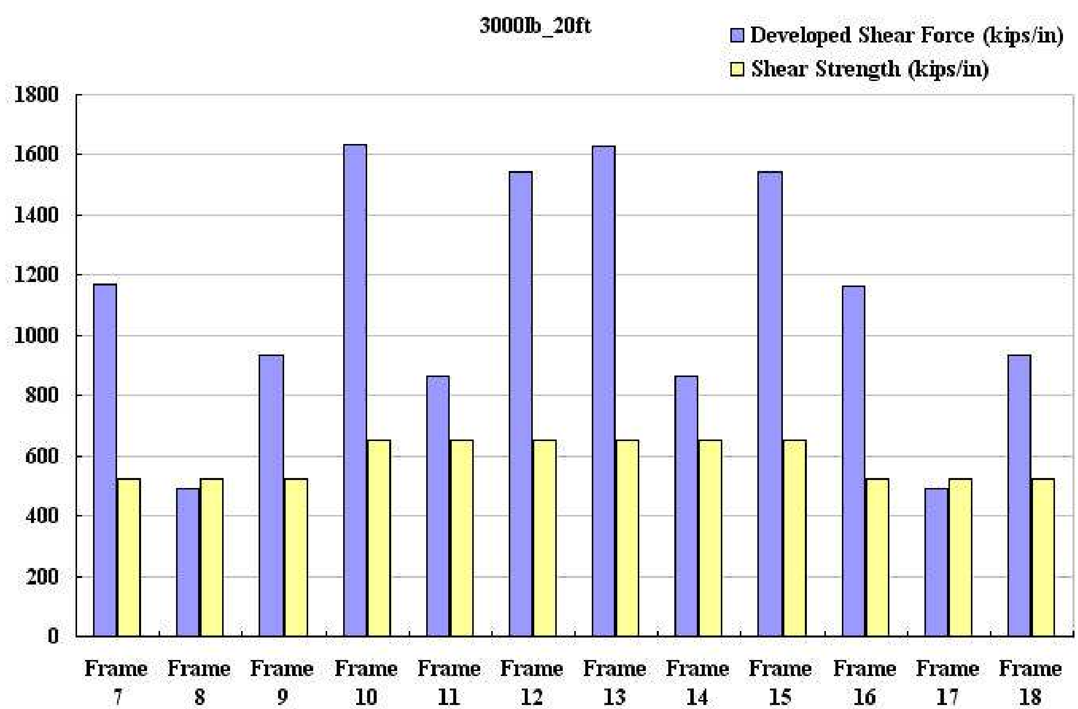

Figure 4.36 : Developed Shear Force vs. Shear Capacity of Flexible Diaphragm (3,000 lb @ 20 ft)

Table 4.27 : Max. Bending Moment at MRF Frames (500 lb TNT Weight @ 20 ft)

Frame No.	Frame Section	Bending Moment (Mu)	Moment Capacity (ϕMn)
7	W14*257	19159.5	24350
8	W14*257	9348.2	24350
9	W14*257	15308.8	24350
10	W14*311	25405.9	30150
11	W14*311	13737.2	30150
12	W14*311	24098.9	30150
13	W14*311	25357.3	30150
14	W14*311	13724.4	30150
15	W14*311	24044.9	30150
16	W14*257	19051.5	24350
17	W14*257	9306.6	24350
18	W14*257	15220.2	24350

(unit : k-in)

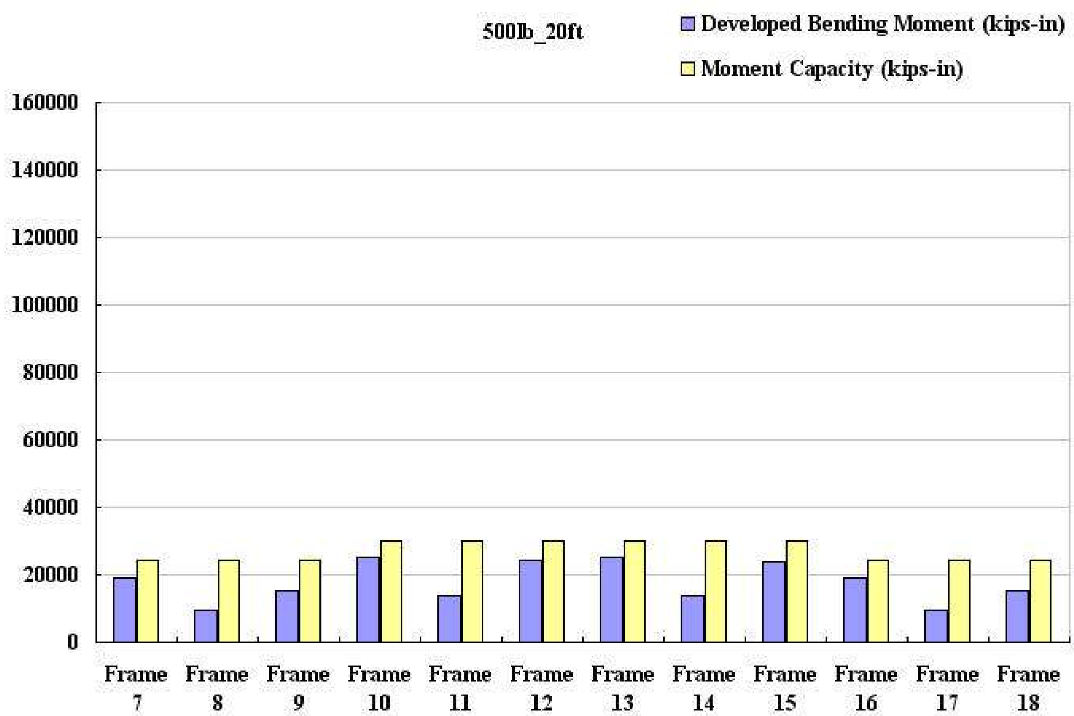

Figure 4.37 : Developed Bending Moment vs. Moment Capacity of Flexible Diaphragm (500 lb @ 20 ft)

Table 4.28 : Max. Bending Moment at MRF Frames (1,000 lb TNT Weight @ 20 ft)

Frame No.	Frame Section	Bending Moment (Mu)	Moment Capacity (ϕMn)
7	W14*257	42593.3	24350
8	W14*257	20946.8	24350
9	W14*257	34283.7	24350
10	W14*311	56967.8	30150
11	W14*311	30798.5	30150
12	W14*311	53971.7	30150
13	W14*311	56859.1	30150
14	W14*311	30769.7	30150
15	W14*311	53850.3	30150
16	W14*257	42712.3	24350
17	W14*257	20853.4	24350
18	W14*257	34085.5	24350

(unit : k-in)

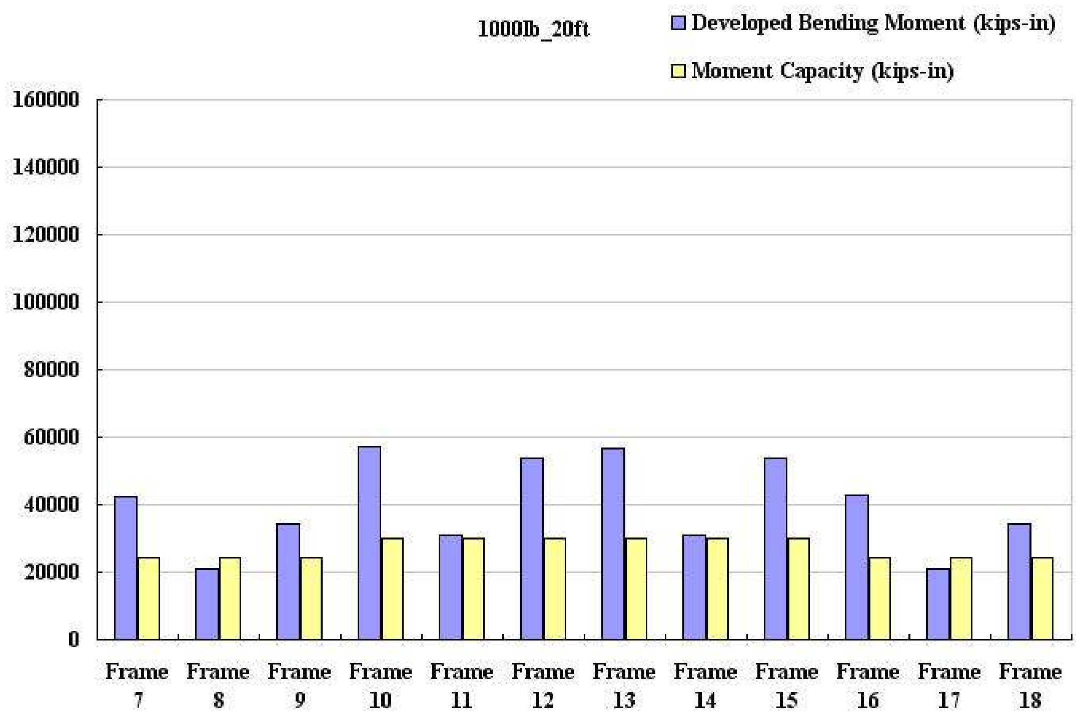

Figure 4.38 : Developed Bending Moment vs. Moment Capacity of Flexible Diaphragm (1,000 lb @ 20 ft)

Table 4.29 : Max. Bending Moment at MRF Frames (2,000 lb TNT Weight @ 20 ft)

Frame No.	Frame Section	Bending Moment (Mu)	Moment Capacity (ϕMn)
7	W14*257	83726.8	24350
8	W14*257	42681.1	24350
9	W14*257	66523.4	24350
10	W14*311	111143.9	30150
11	W14*311	63560.9	30150
12	W14*311	105334.9	30150
13	W14*311	110938.7	30150
14	W14*311	63502.5	30150
15	W14*311	105104.9	30150
16	W14*257	83272.4	24350
17	W14*257	42497.9	24350
18	W14*257	66150.2	24350

(unit : k-in)

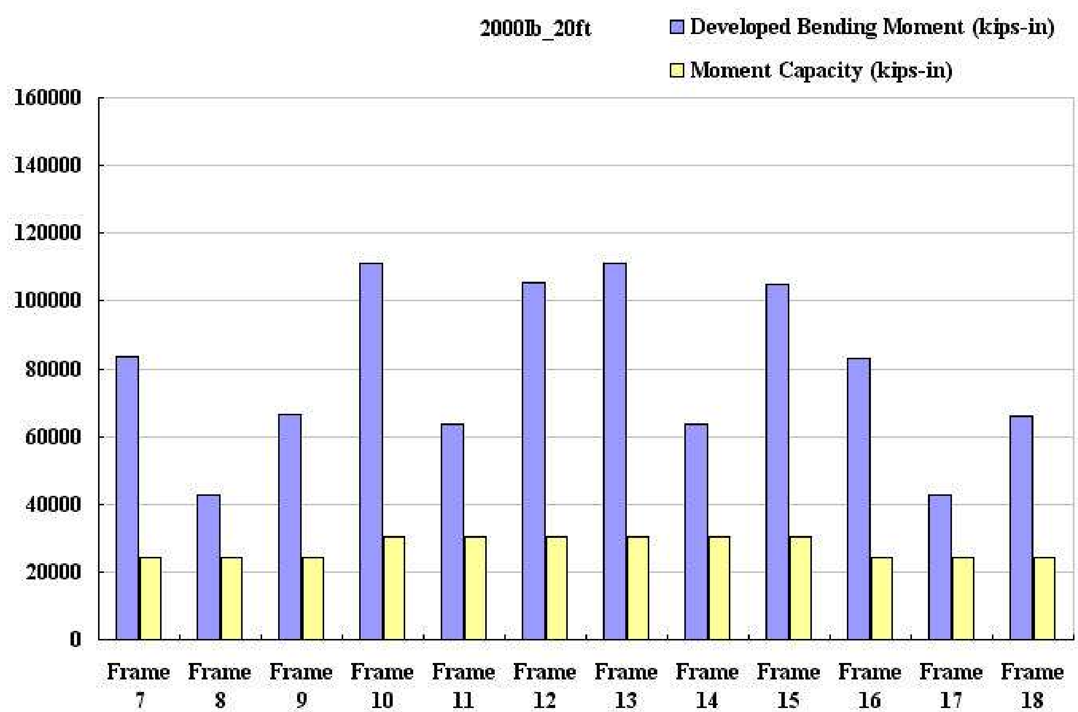

Figure 4.39 : Developed Bending Moment vs. Moment Capacity of Flexible Diaphragm (2,000 lb @ 20 ft)

Table 4.30 : Max. Bending Moment at MRF Frames (3,000 lb TNT Weight @ 20 ft)

Frame No.	Frame Section	Bending Moment (Mu)	Moment Capacity (ϕMn)
7	W14*257	111426.0	24350
8	W14*257	58862.2	24350
9	W14*257	88191.3	24350
10	W14*311	148039.0	30150
11	W14*311	88514.9	30150
12	W14*311	140326.5	30150
13	W14*311	147778.5	30150
14	W14*311	88434.7	30150
15	W14*311	140028.0	30150
16	W14*257	110838.9	24350
17	W14*257	58617.5	24350
18	W14*257	87709.8	24350

(unit : k-in)

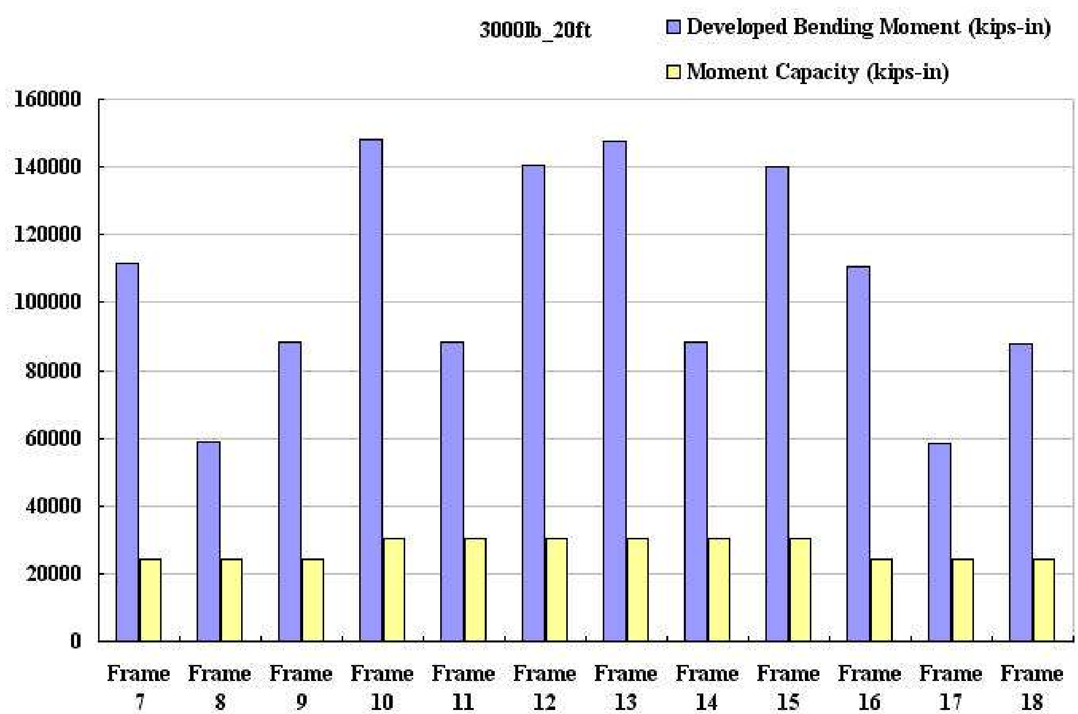

Figure 4.40 : Developed Bending Moment vs. Moment Capacity of Flexible Diaphragm (3,000 lb @ 20 ft)

Bending moment and shear capacity of concrete slab is provided by followed equations from ACI 318 [1]. In these equations, the effective thickness of concrete is assumed 3.5 in as shown in Appendix C and steel ratio is less than 0.01. Also f'_c is 4,000 psi and f_y is 60,000 psi.

Moment Capacity : $$\frac{\phi M_n}{\phi k_n} = \frac{bd^2}{12{,}000}$$

$$\phi k_n = \phi\left[f_c^{'} \omega (1 - 0.59\omega) \right], \varpi = \rho f_y / f_c^{'}$$

Shear Capacity : $\phi V_n = 2\sqrt{f_c^{'}}\, b_w d$

Where, b : width of concrete slab

d : depth of concrete slab

ω : mechanical reinforcement ratio

ρ : steel ratio

Hence, the moment capacity is calculated as 212.5 k-in and the shear capacity is 0.76 k/in.

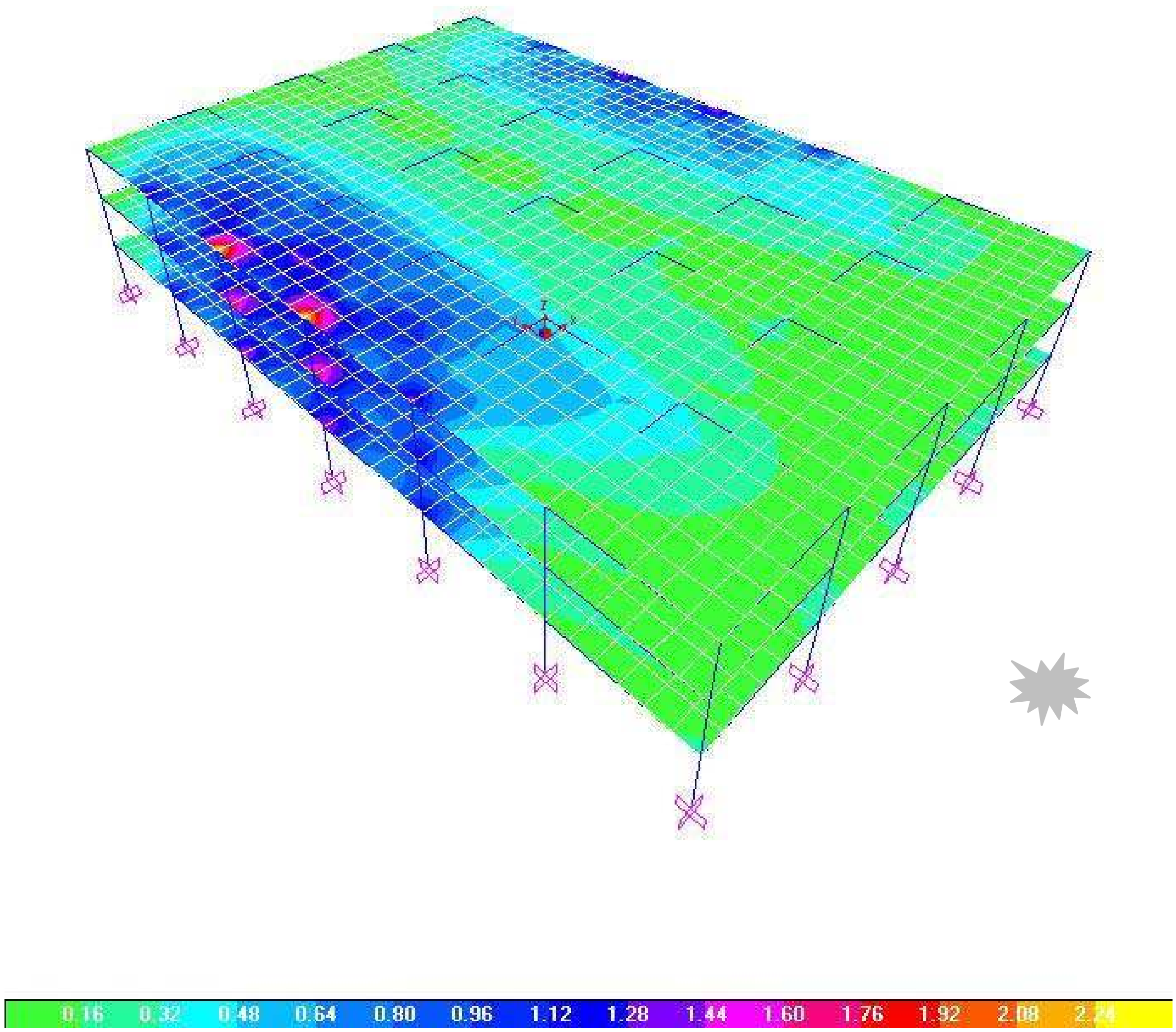

(a) Shear Force Distribution on Whole Structure (1,000 lb TNT Weight@20 ft Stand-Off Distance)

Figure 4.41 : Shear Force Distribution on Three Story Building (1,000 lb TNT Weight @ 20 ft Stand-Off Distance)

"Figure 4.41 : Continued"

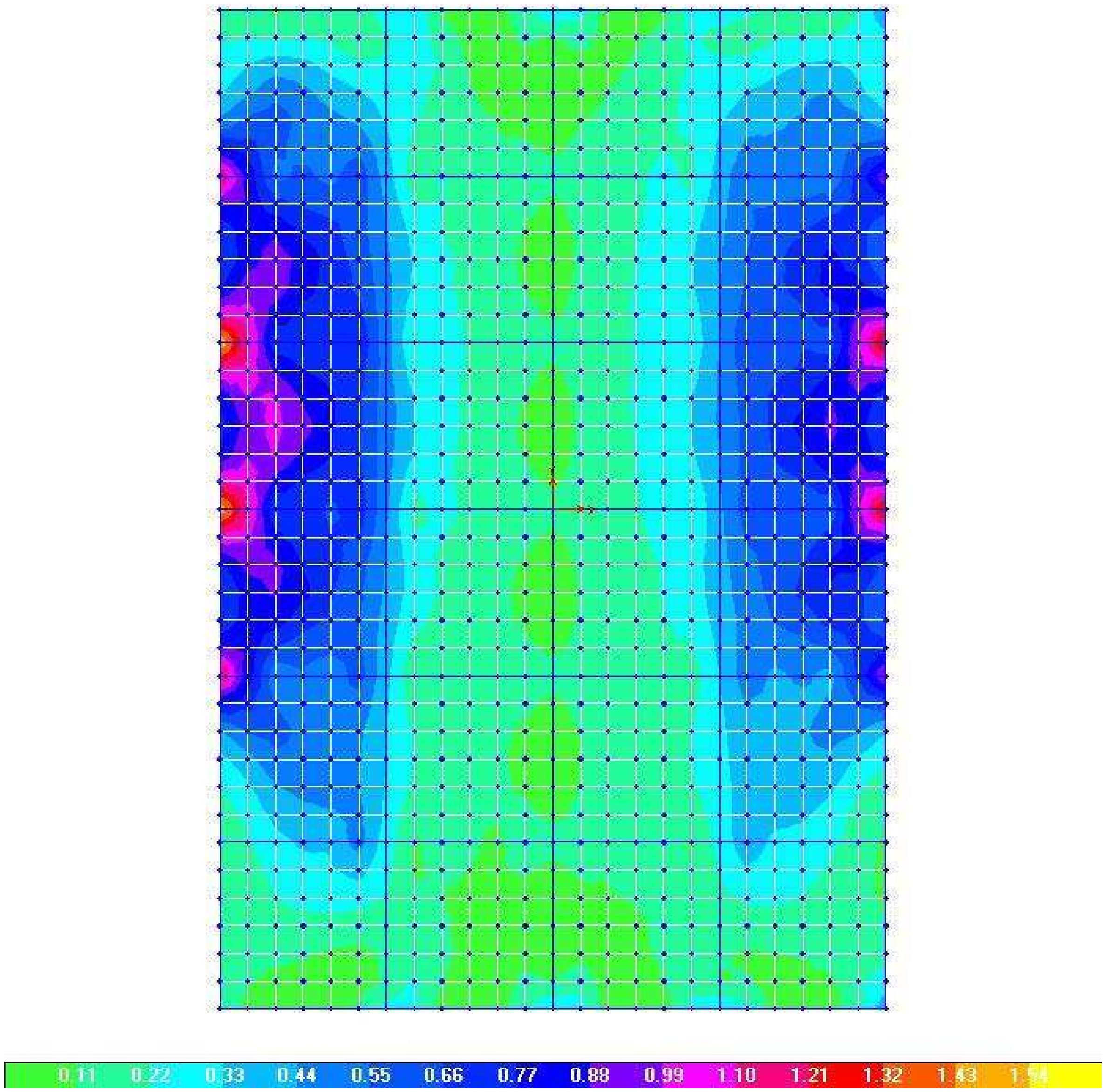

(b) Shear Force Distribution at 2nd Floor (1,000 lb TNT Weight@20 ft Stand-Off Distance)

“Figure 4.41 : Continued”

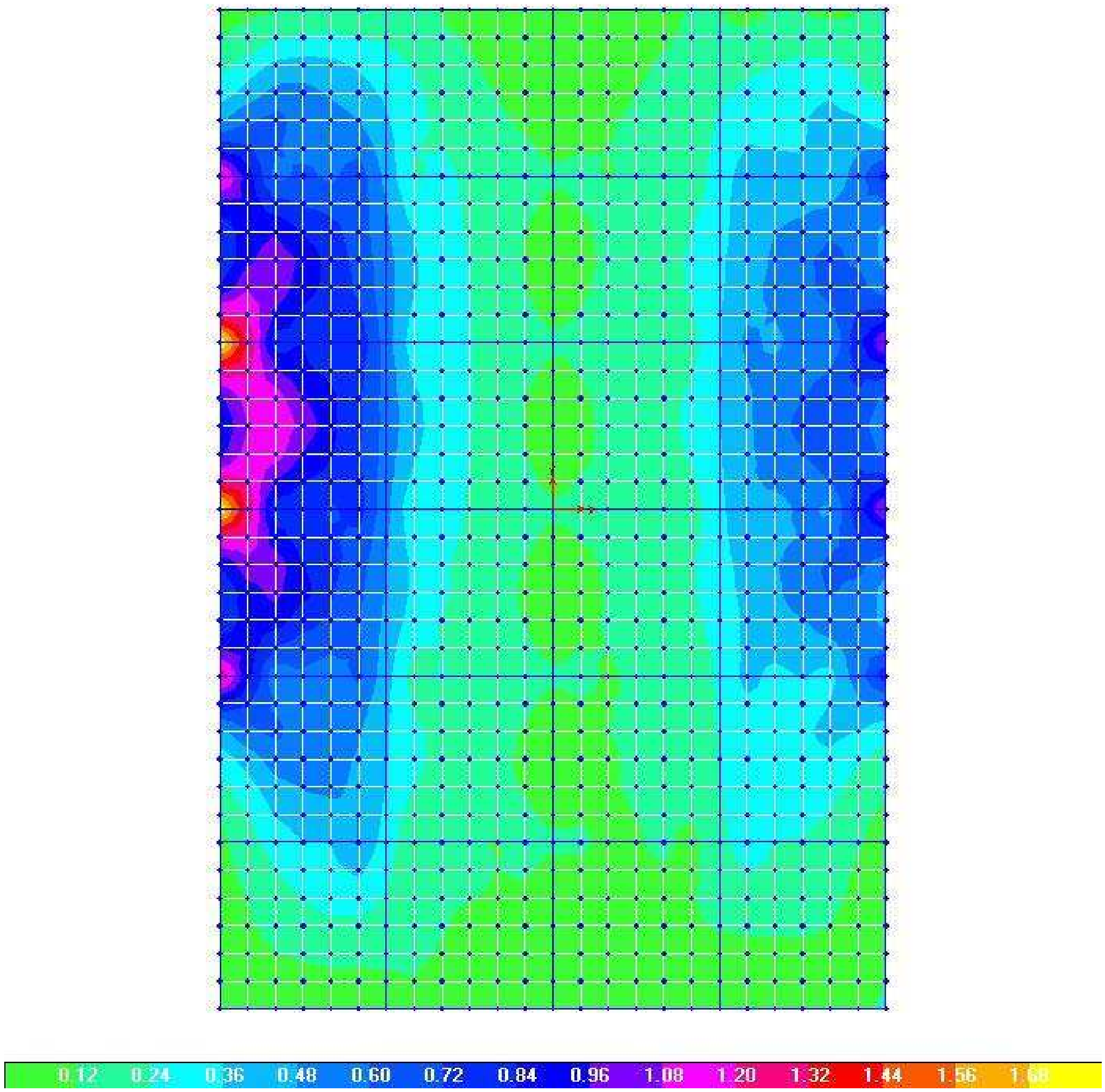

(c) Shear Force Distribution at 3rd Floor (1,000 lb TNT Weight@20 ft Stand-Off Distance)

"Figure 4.41 : Continued"

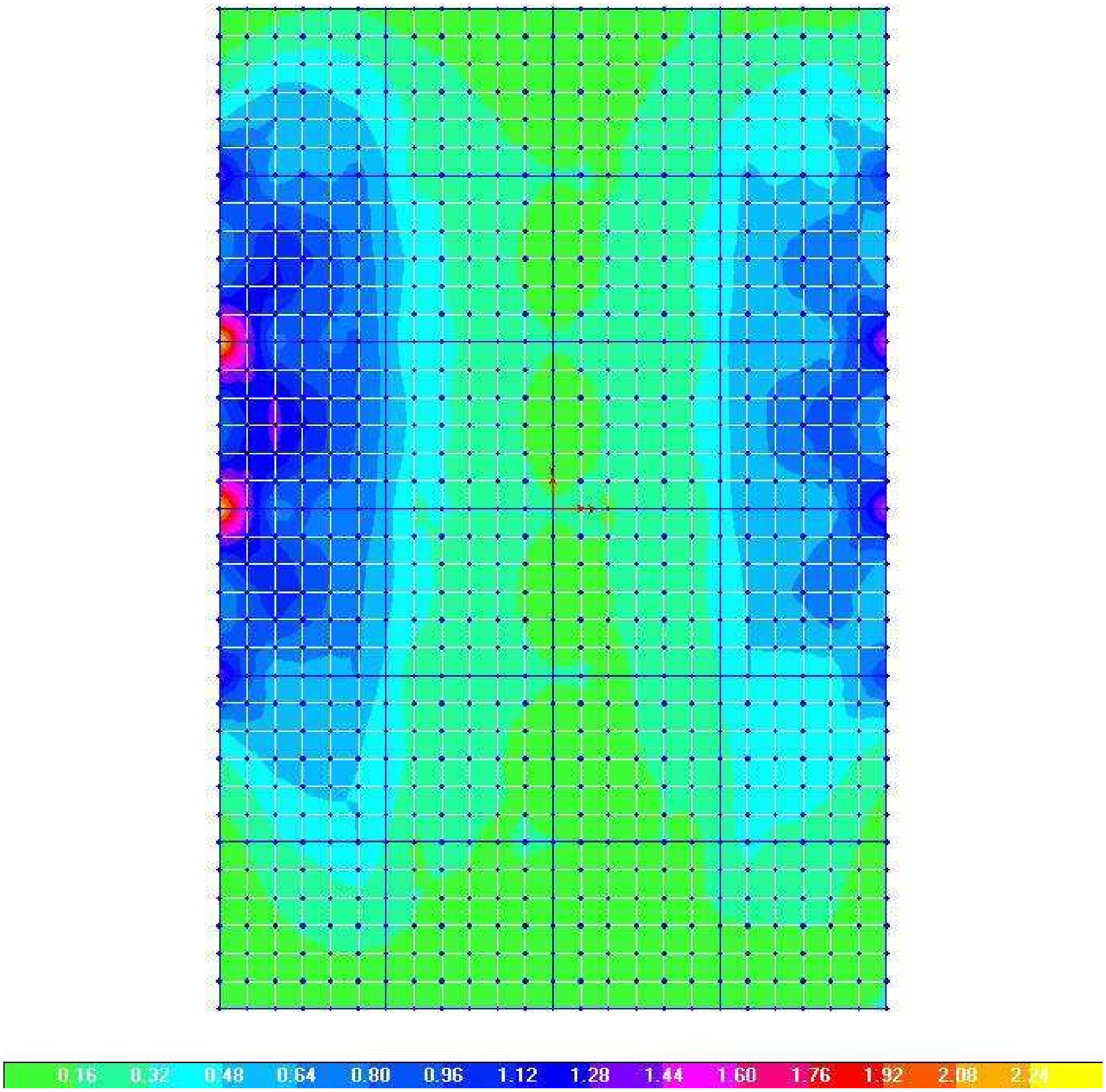

(d) Shear Force Distribution at Roof (1,000 lb TNT Weight@20 ft Stand-Off Distance)

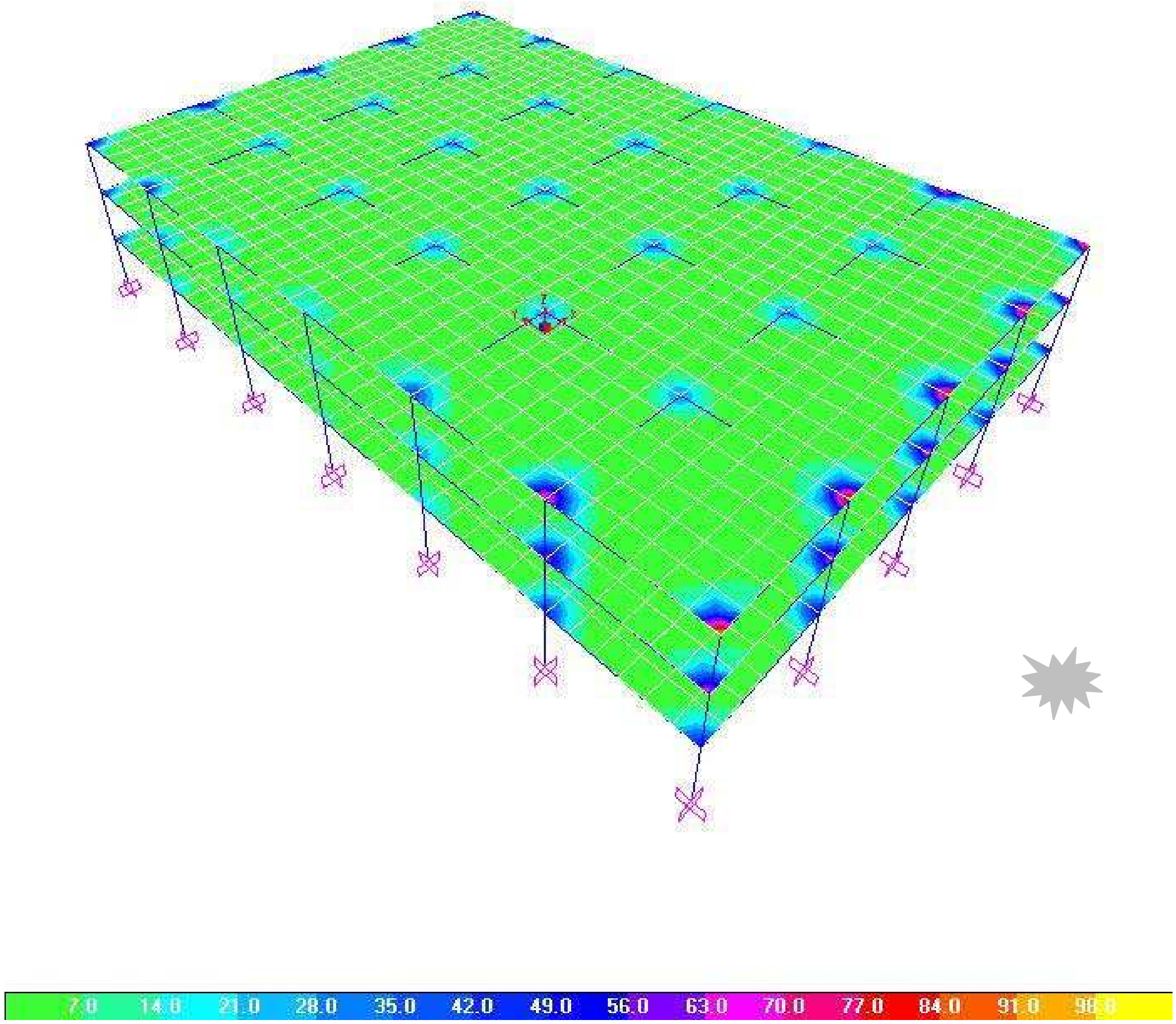

(a) Moment Distribution on Whole Structure (1,000 lb TNT Weight@20 ft Stand-Off Distance)

Figure 4.42 : Moment Distribution on Three Story Building (1,000 lb TNT Weight @ 20 ft Stand-Off Distance)

"Figure 4.42 : Continued"

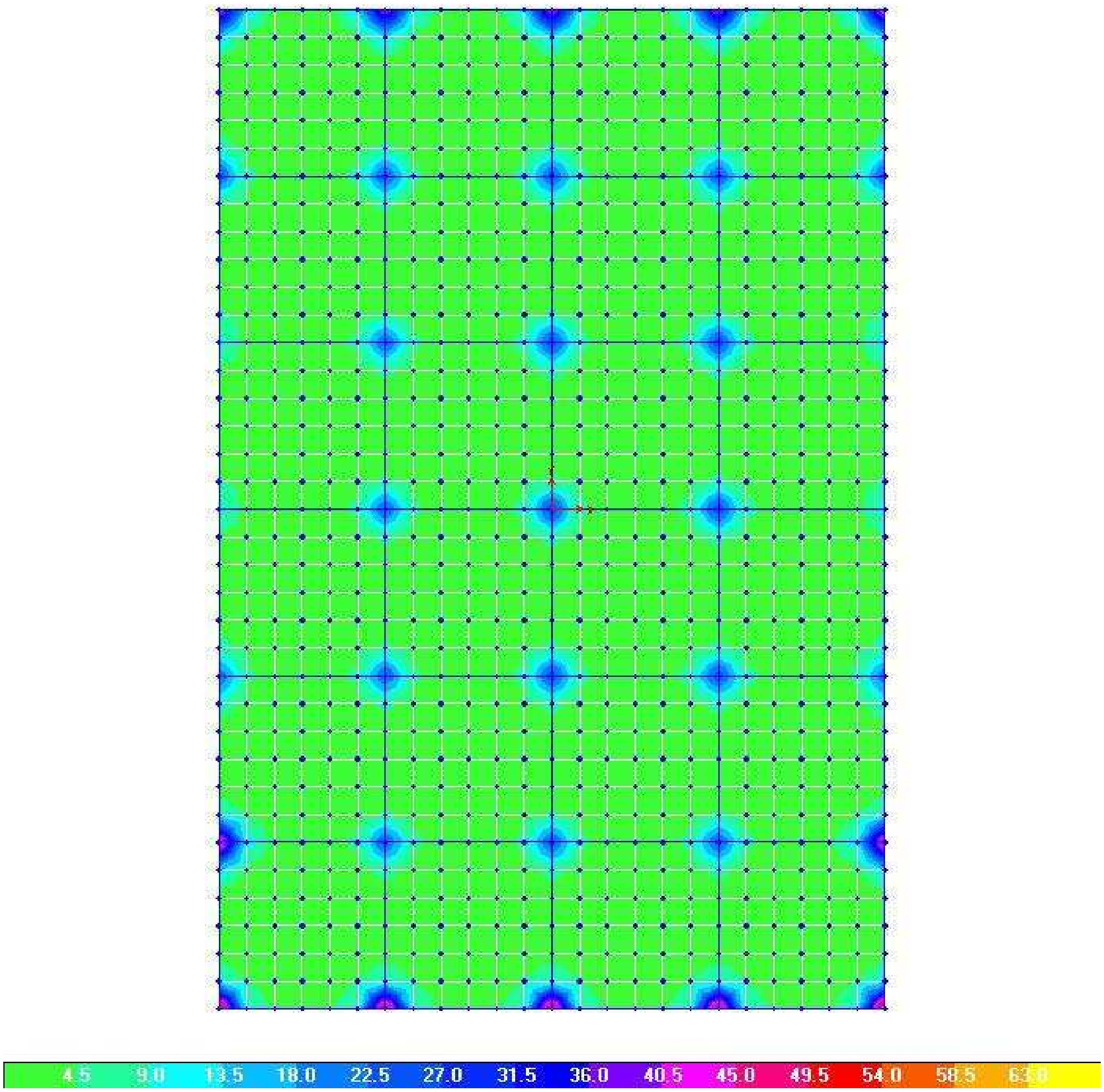

(b) Moment Distribution at 2nd Floor (1,000 lb TNT Weight@20 ft Stand-Off Distance)

“Figure 4.42 : Continued”

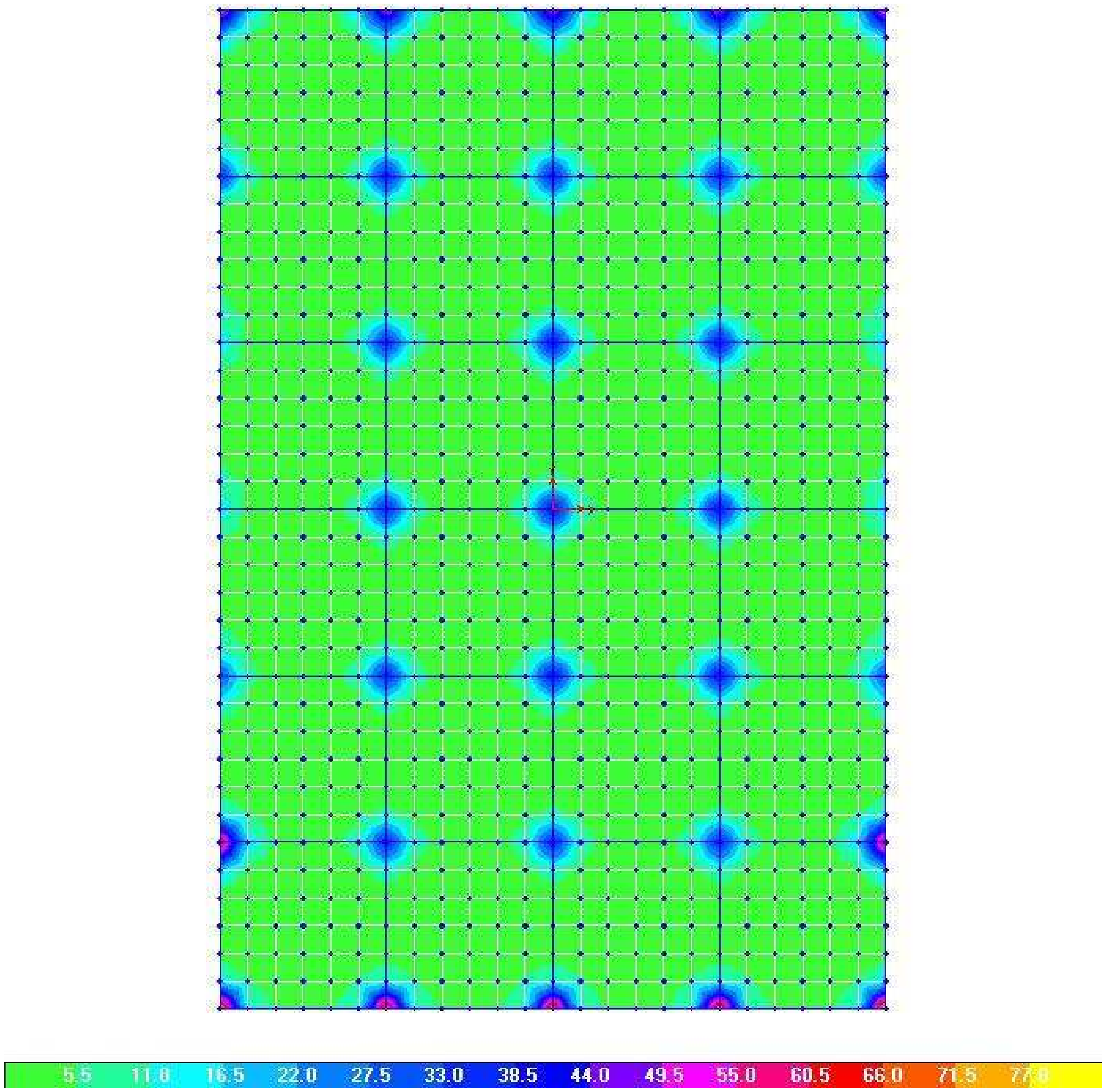

(c) Moment Distribution at 3rd Floor (1,000 lb TNT Weight@20 ft Stand-Off Distance)

“Figure 4.42 : Continued”

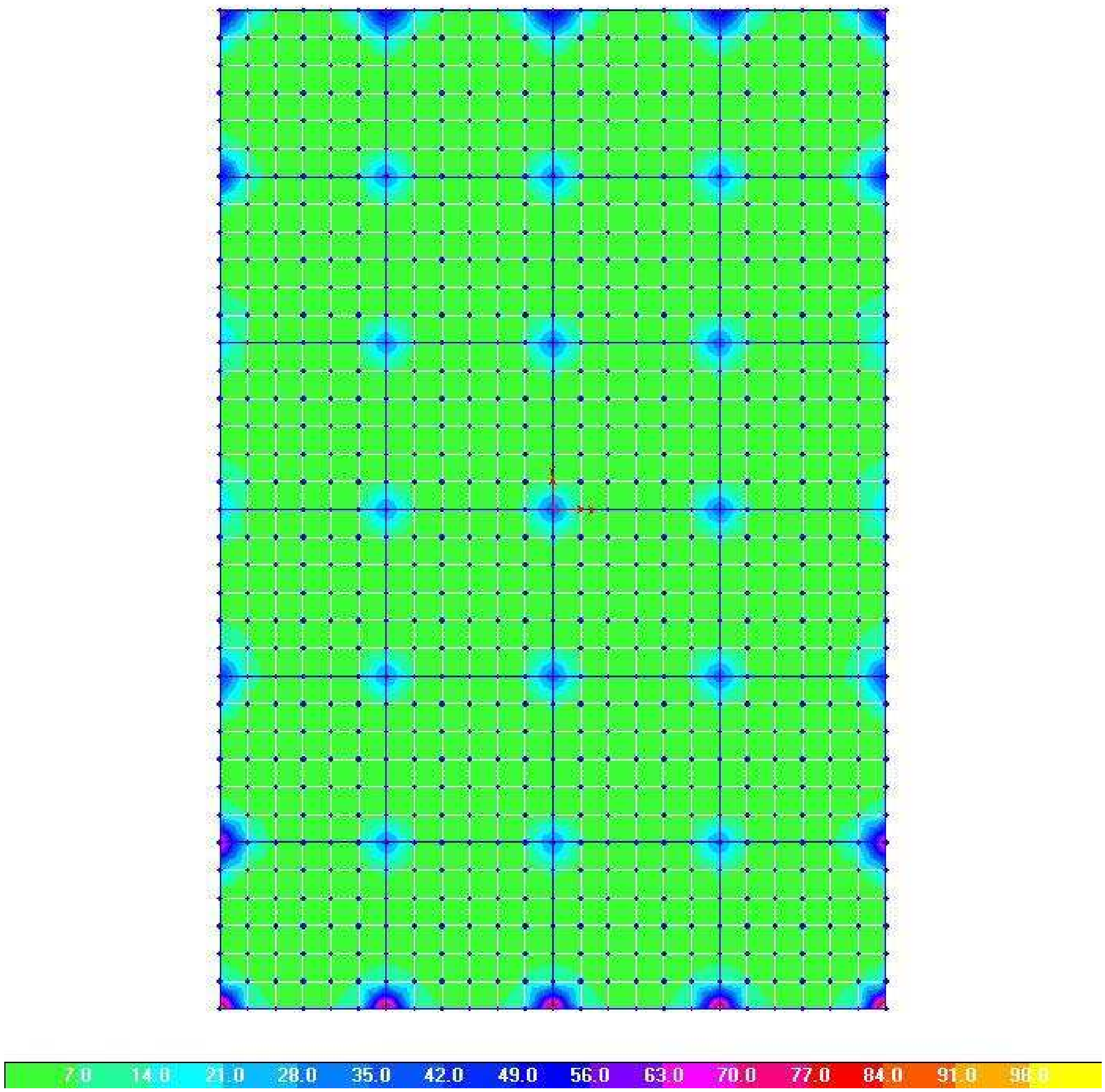

(d) Moment Distribution at Roof (1,000 lb TNT Weight@20 ft Stand-Off Distance)

Table 4.31 : The Results of Flexible Diaphragm Analysis

CASE	Story	Flexible Diaphragm			
		Moment (k-in)	Moment Capacity (k-in)	Shear Force (k/in)	Shear Capacity (k/in)
500 lb_20 ft	Roof	45.772	212.5	1.037	0.76
	3^{rd}	34.815	212.5	0.801	0.76
	2^{nd}	26.720	212.5	0.680	0.76
1,000 lb_20 ft	Roof	102.661	212.5	2.323	0.76
	3^{rd}	78.162	212.5	1.793	0.76
	2^{nd}	60.102	212.5	1.520	0.76
2,000 lb_20 ft	Roof	202.027	212.5	4.555	0.76
	3^{rd}	157.417	212.5	3.434	0.76
	2^{nd}	119.508	212.5	2.868	0.76
3,000 lb_20 ft	Roof	270.985	212.5	6.092	0.76
	3^{rd}	215.120	212.5	4.501	0.76
	2^{nd}	161.779	212.5	3.709	0.76

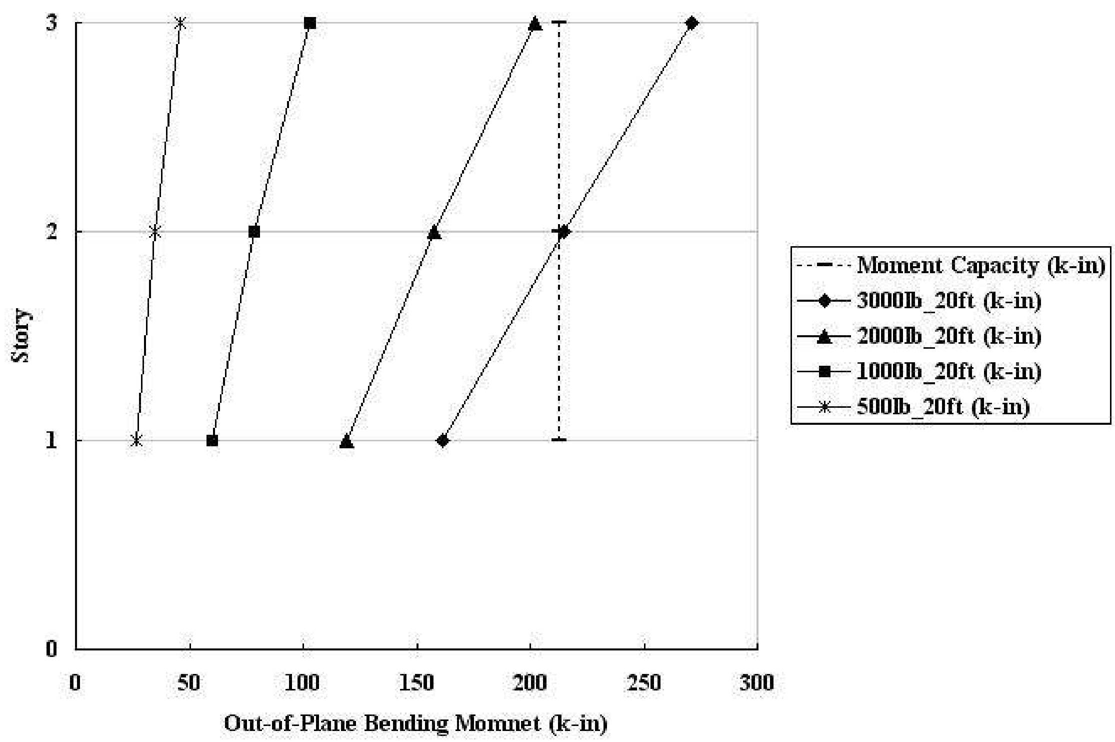

Figure 4.43 : Developed Bending Moment vs. Moment Capacity of Concrete Slab Based on Flexible Diaphragm Analysis

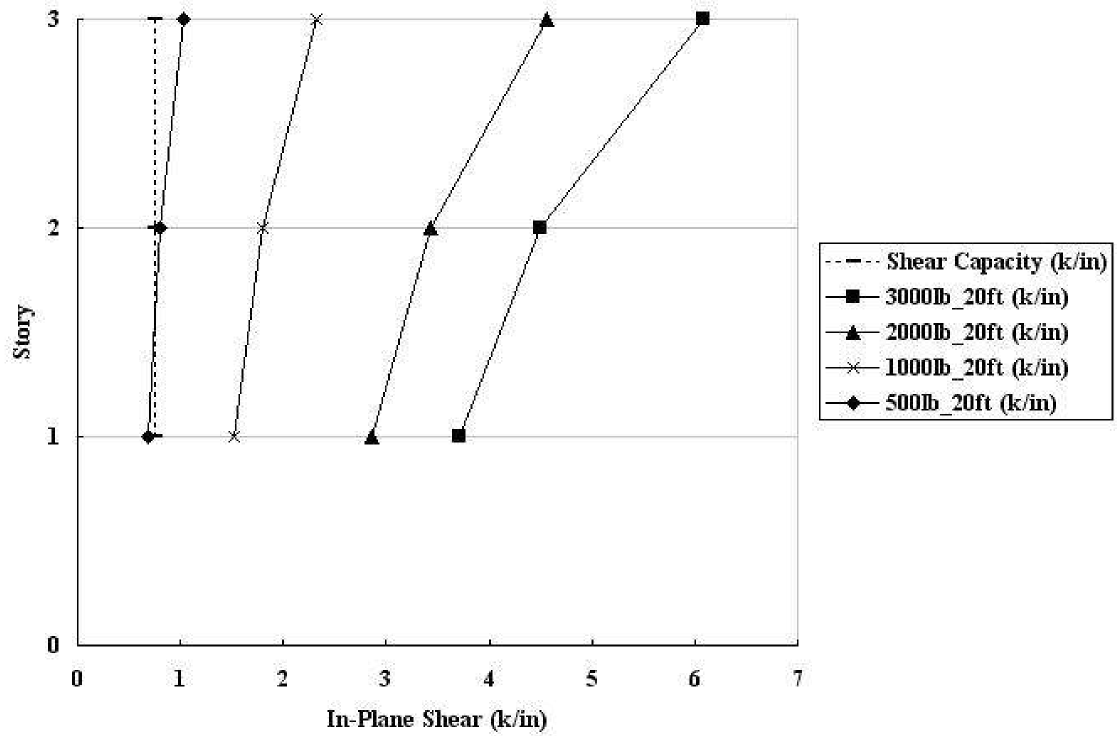

Figure 4.44 : Developed Shear Force vs. Shear Capacity of Concrete Slab Based on Flexible Diaphragm Analysis

As a result, the flexural strength of this system is well provided but shear failure is expected to this concrete slab.

4.3.2. Rigid Diaphragm Analysis

Most floor diaphragm in the structure is often assumed to be rigid in their plane. It means that model floors in building structure, which typically have very high in-plane stiffness. Maximum shear forces and bending moment of Moment Resistant Frame are investigated as compared with capacity of member shown in Figure 4.46- 4.53 and Table 4.32 – 4.39. For reference, the member locations, identification numbers and member sizes are shown in Figure 4.45 for typical longitudinal frame. The distribution of moment on rigid diaphragm is shown in Figure 4.54 and the results of rigid diaphragm analysis are shown in Table 4.40 and Figure 4.55.

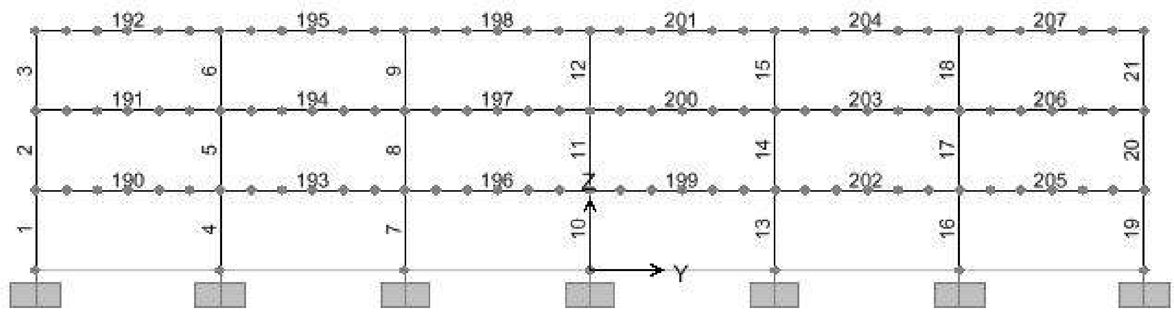

(a) Generated Member Numbers along the Longitudinal Direction

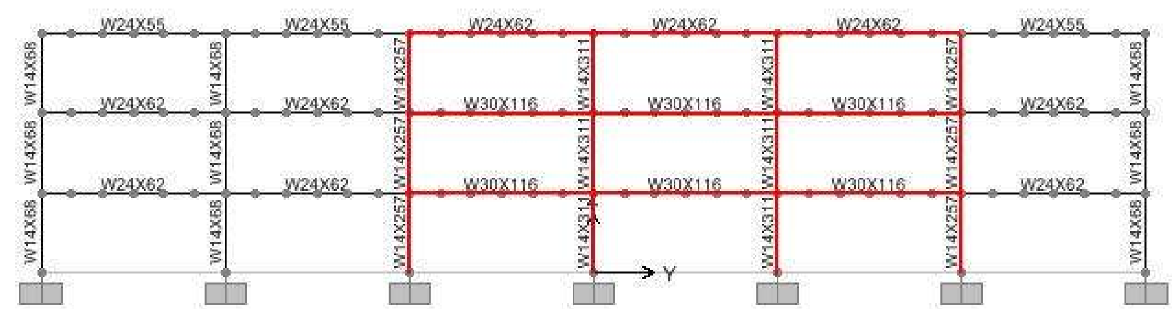

(b) Generated Frame Sections and Moment Resistant Frames

Figure 4.45 : Generated Member Numbers and Frame Section along the Longitudinal Direction

Table 4.32 : Max. Shear Force at MRF Frames (500 lb TNT Weight @ 20 ft)

Frame No.	Frame Section	Shear Force (Vu)	Shear Strength (ϕVn)
7	W14*257	203.5	522.5
8	W14*257	72.1	522.5
9	W14*257	161.5	522.5
10	W14*311	284.3	651.8
11	W14*311	127.3	651.8
12	W14*311	266.1	651.8
13	W14*311	284.3	651.8
14	W14*311	127.3	651.8
15	W14*311	266.1	651.8
16	W14*257	203.5	522.5
17	W14*257	72.1	522.5
18	W14*257	161.5	522.5

(unit : k/in)

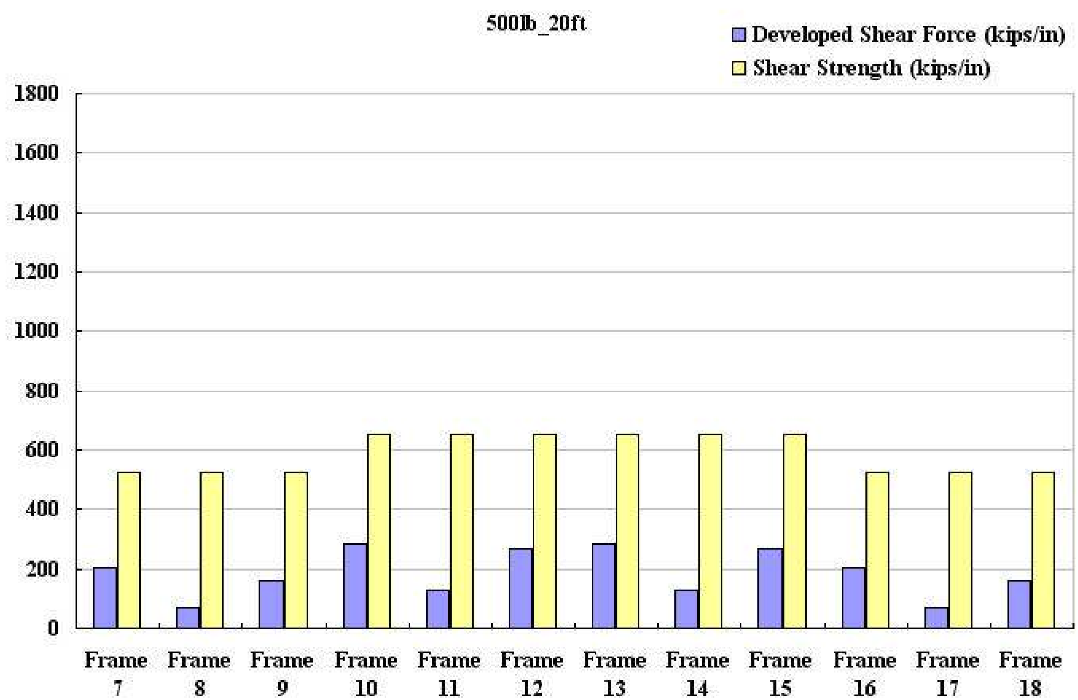

Figure 4.46 : Developed Shear Force vs. Shear Capacity of Rigid Diaphragm (500 lb @ 20 ft)

Table 4.33 : Max. Shear Force at MRF Frames (1,000 lb TNT Weight @ 20 ft)

Frame No.	Frame Section	Shear Force (Vu)	Shear Strength (ϕVn)
7	W14*257	455.75	522.5
8	W14*257	161.9	522.5
9	W14*257	361.6	522.5
10	W14*311	636.8	651.8
11	W14*311	285.9	651.8
12	W14*311	595.8	651.8
13	W14*311	636.8	651.8
14	W14*311	285.9	651.8
15	W14*311	285.9	651.8
16	W14*257	455.75	522.5
17	W14*257	161.9	522.5
18	W14*257	361.6	522.5

(unit : k/in)

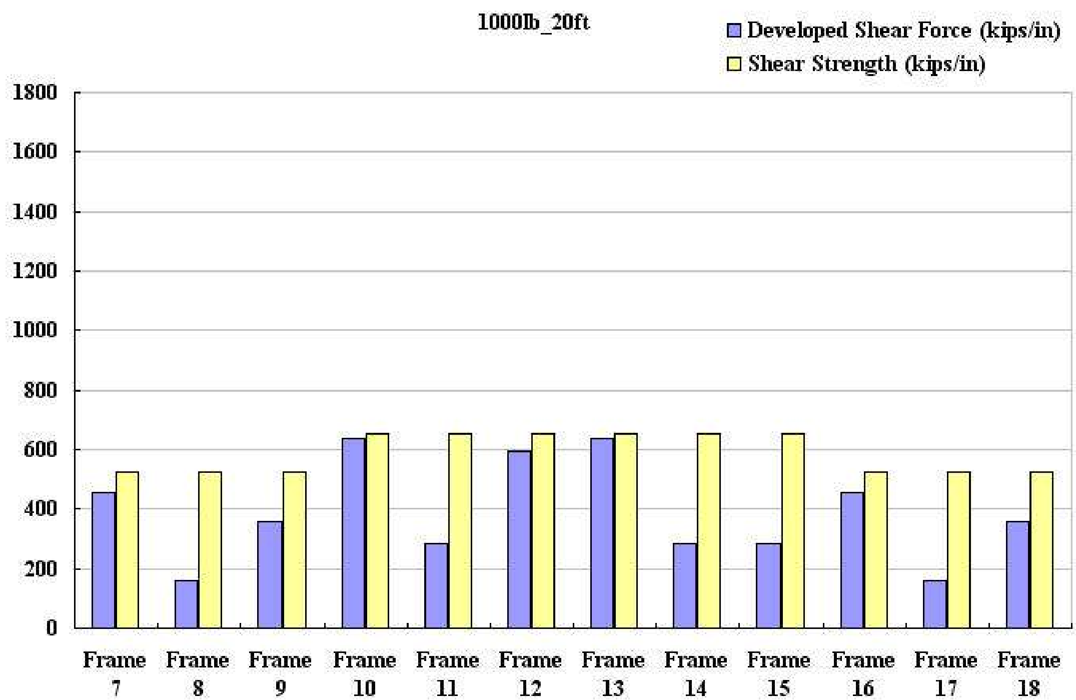

Figure 4.47 : Developed Shear Force vs. Shear Capacity of Rigid Diaphragm (1,000 lb @ 20 ft)

Table 4.34 : Max. Shear Force at MRF Frames (2,000 lb TNT Weight @ 20 ft)

Frame No.	Frame Section	Shear Force (Vu)	Shear Strength (ϕVn)
7	W14*257	888.8	522.5
8	W14*257	346.2	522.5
9	W14*257	705.6	522.5
10	W14*311	1237.4	651.8
11	W14*311	609.6	651.8
12	W14*311	1167.0	651.8
13	W14*311	1237.4	651.8
14	W14*311	609.6	651.8
15	W14*311	1167.0	651.8
16	W14*257	888.8	522.5
17	W14*257	346.2	522.5
18	W14*257	705.6	522.5

(unit : k/in)

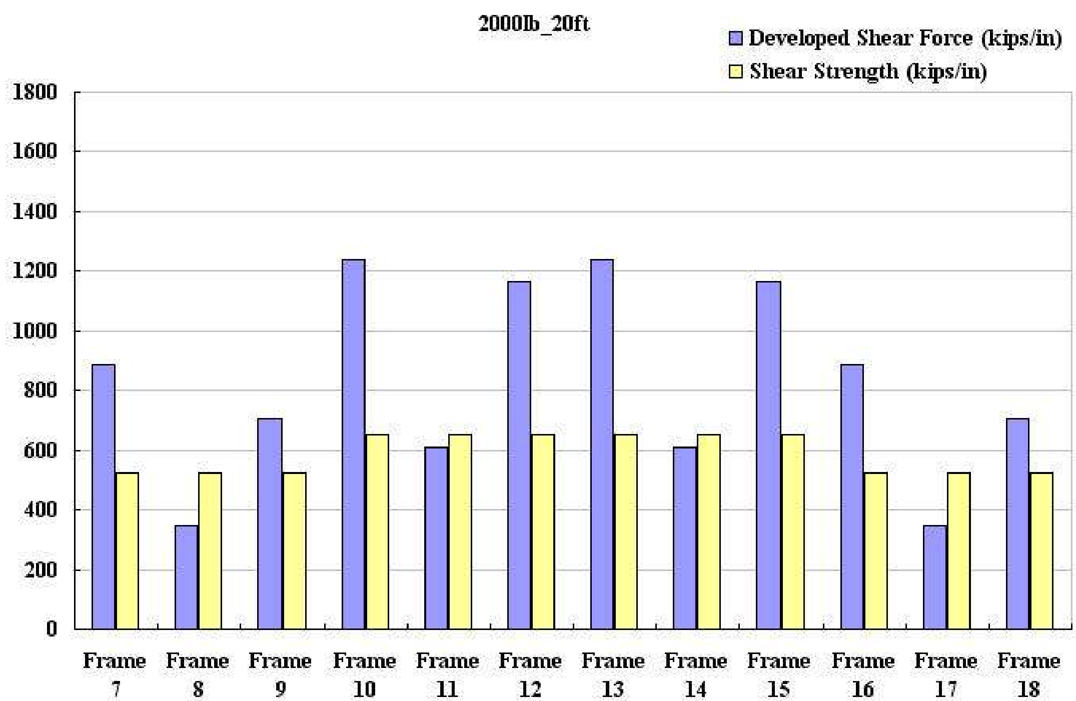

Figure 4.48 : Developed Shear Force vs. Shear Capacity of Rigid Diaphragm (2,000 lb @ 20 ft)

Table 4.35 : Shear Force at MRF Frames (3,000 lb TNT Weight @ 20 ft)

Frame No.	Frame Section	Shear Force (Vu)	Shear Strength (ϕVn)
7	W14*257	1171.5	522.5
8	W14*257	494.9	522.5
9	W14*257	940.0	522.5
10	W14*311	1642.6	651.8
11	W14*311	869.7	651.8
12	W14*311	1559.7	651.8
13	W14*311	1642.6	651.8
14	W14*311	869.7	651.8
15	W14*311	1559.7	651.8
16	W14*257	1171.5	522.5
17	W14*257	494.9	522.5
18	W14*257	940.0	522.5

(unit : k/in)

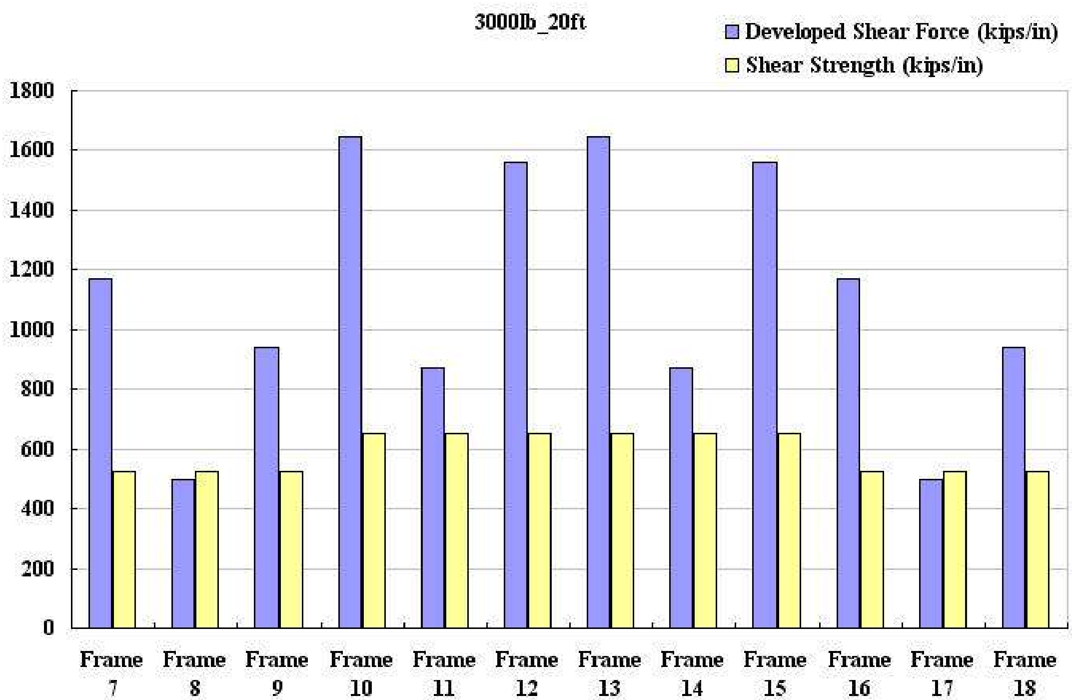

Figure 4.49 : Developed Shear Force vs. Shear Capacity of Rigid Diaphragm (3,000 lb @ 20 ft)

Table 4.36 : Max. Bending Moment at MRF Frames (500 lb TNT Weight @ 20 ft)

Frame No.	Frame Section	Bending Moment (Mu)	Moment Capacity (ϕMn)
7	W14*257	19203.7	24350
8	W14*257	9372.2	24350
9	W14*257	15367.4	24350
10	W14*311	25582.1	30150
11	W14*311	13823.0	30150
12	W14*311	24375.2	30150
13	W14*311	25581.1	30150
14	W14*311	13824.1	30150
15	W14*311	24371.6	30150
16	W14*257	19205.4	24350
17	W14*257	9371.0	24350
18	W14*257	15375.8	24350

(unit : k-in)

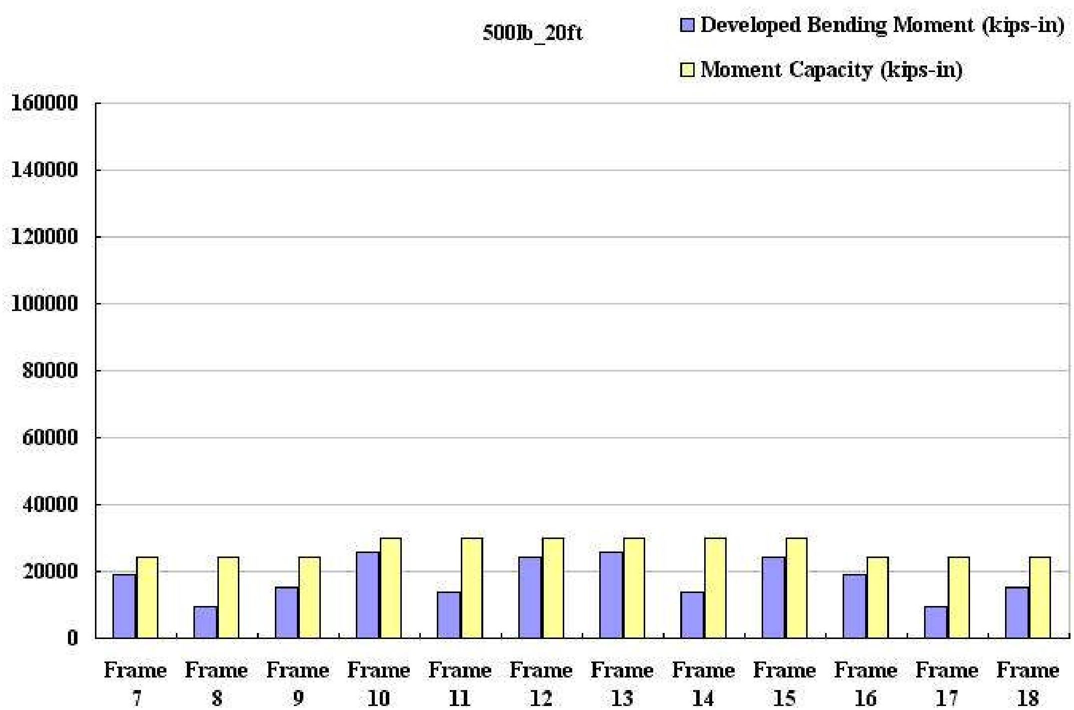

Figure 4.50 : Developed Bending Moment vs. Moment Capacity of Rigid Diaphragm (500 lb @ 20 ft)

Table 4.37 : Max. Bending Moment at MRF Frames (1,000 lb TNT Weight @ 20 ft)

Frame No.	Frame Section	Bending Moment (Mu)	Moment Capacity (ϕMn)
7	W14*257	43030.3	24350
8	W14*257	21010.0	24350
9	W14*257	34385.1	24350
10	W14*311	57331.1	30150
11	W14*311	30931.5	30150
12	W14*311	54551.5	30150
13	W14*311	57328.9	30150
14	W14*311	30994.0	30150
15	W14*311	54543.3	30150
16	W14*257	43034.1	24350
17	W14*257	21007.2	24350
18	W14*257	34403.7	24350

(unit : k-in)

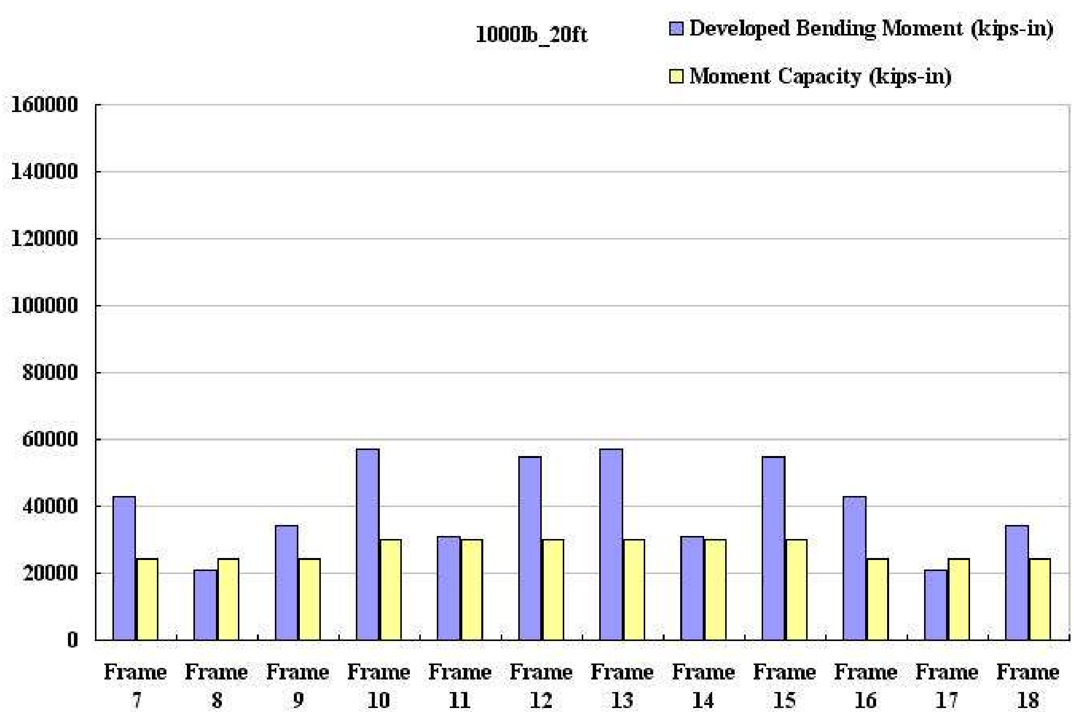

Figure 4.51 : Developed Bending Moment vs. Moment Capacity of Rigid Diaphragm (1,000 lb @ 20 ft)

Table 4.38 : Max. Bending Moment at MRF Frames (2,000 lb TNT Weight @ 20 ft)

Frame No.	Frame Section	Bending Moment (Mu)	Moment Capacity (ϕMn)
7	W14*257	83855.6	24350
8	W14*257	42792.1	24350
9	W14*257	66690.2	24350
10	W14*311	111799.2	30150
11	W14*311	63939.7	30150
12	W14*311	106395.1	30150
13	W14*311	111794.8	30150
14	W14*311	63944.1	30150
15	W14*311	106379.3	30150
16	W14*257	83862.9	24350
17	W14*257	42787.7	24350
18	W14*257	66726.0	24350

(unit : k-in)

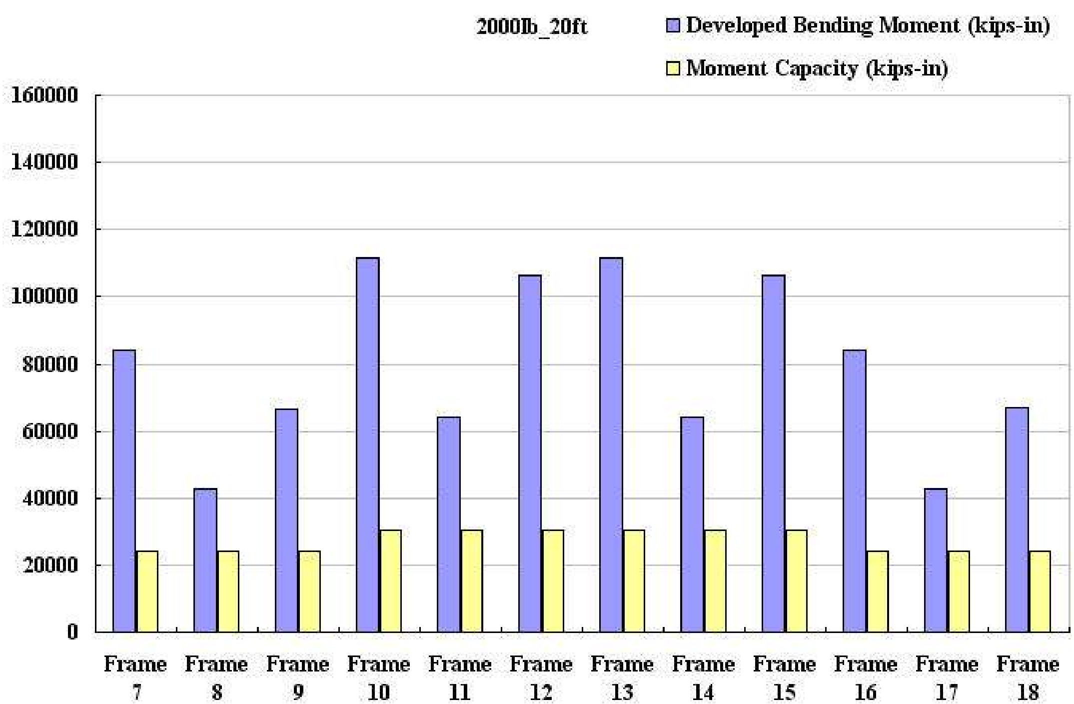

Figure 4.52 : Developed Bending Moment vs. Moment Capacity of Rigid Diaphragm (2,000 lb @ 20 ft)

Table 4.39 : Max. Bending Moment at MRF Frames (3,000 lb TNT Weight @ 20 ft)

Frame No.	Frame Section	Bending Moment (Mu)	Moment Capacity (ϕMn)
7	W14*257	111593.3	24350
8	W14*257	59002.4	24350
9	W14*257	88393.9	24350
10	W14*311	148863.7	30150
11	W14*311	89031.8	30150
12	W14*311	141682.5	30150
13	W14*311	148858.0	30150
14	W14*311	89037.0	30150
15	W14*311	141661.6	30150
16	W14*257	11602.9	24350
17	W14*257	58997.6	24350
18	W14*257	88441.4	24350

(unit : k-in)

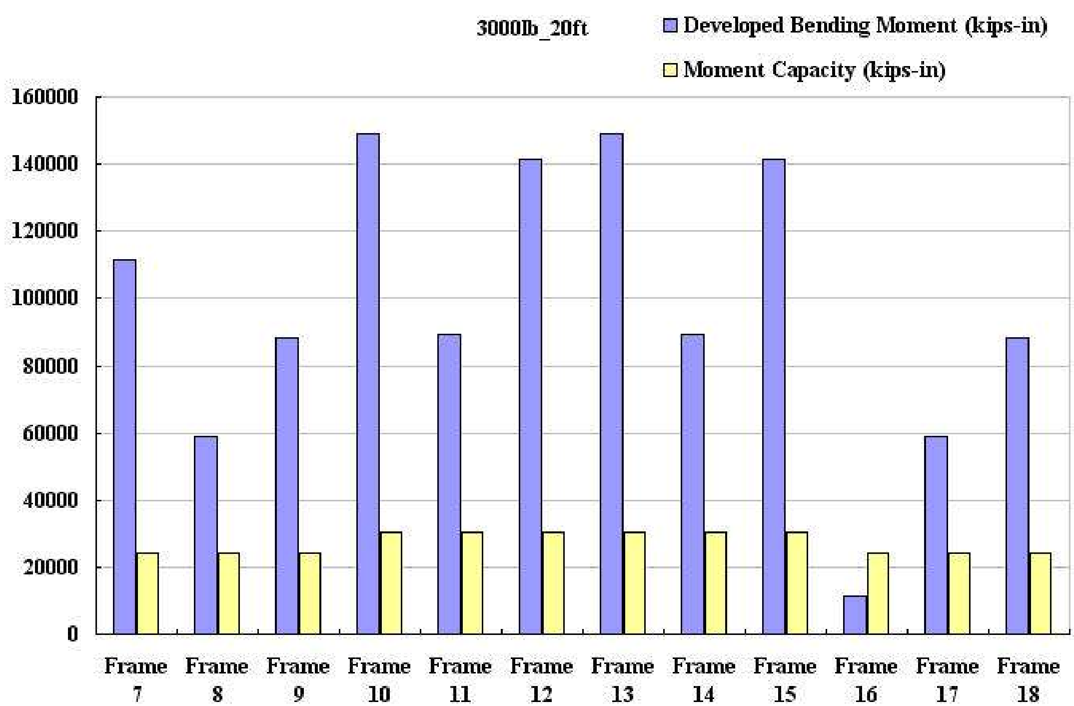

Figure 4.53 : Developed Bending Moment vs. Moment Capacity of Rigid Diaphragm (3,000 lb @ 20 ft)

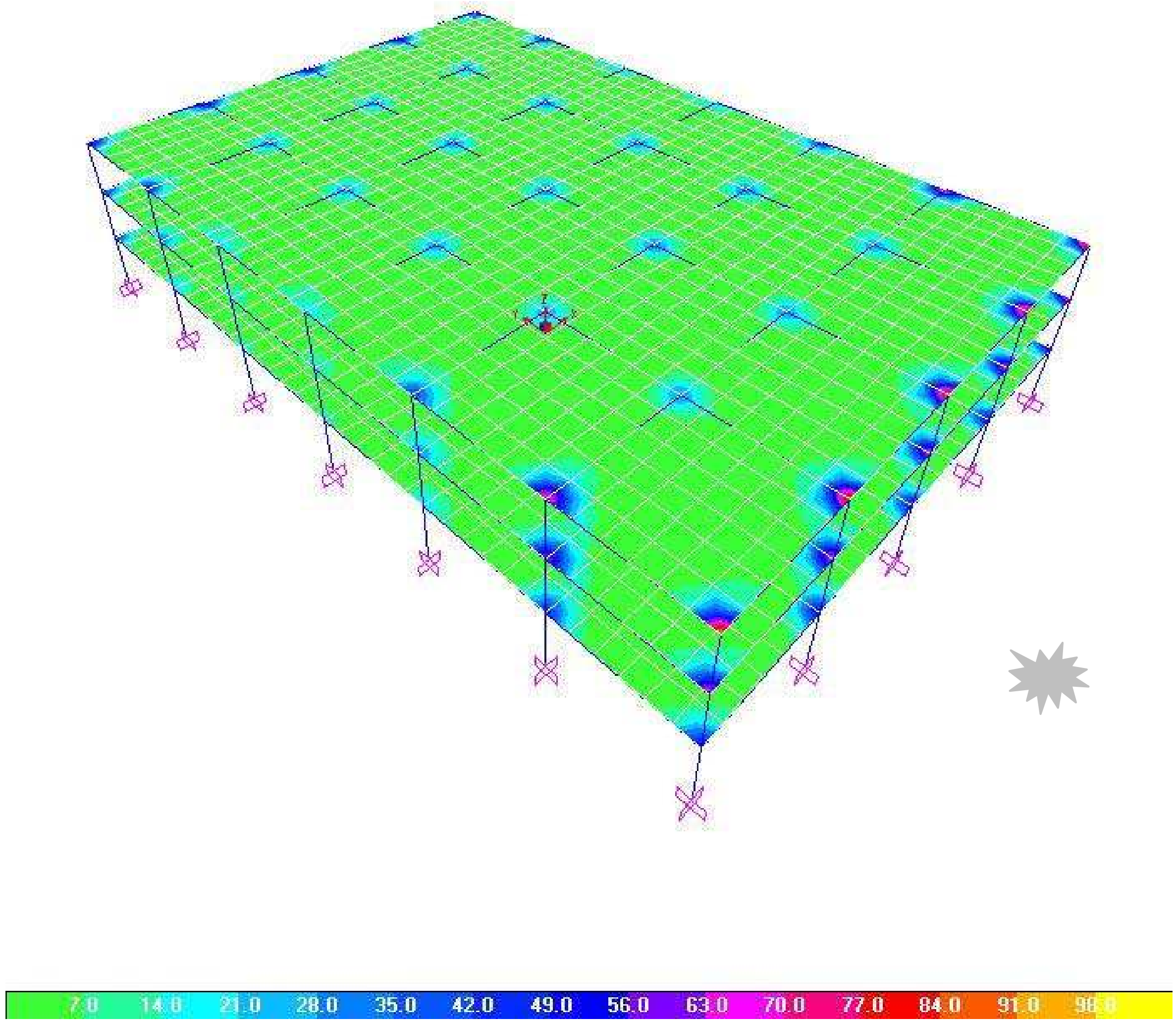

(a) Moment Distribution on Whole Structure (1,000 lb TNT Weight@20 ft Stand-Off Distance)

Figure 4.54 : Moment Distribution on Three Story Building (1,000 lb TNT Weight@20 ft Stand-Off Distance)

“Figure 4.54 : Continued”

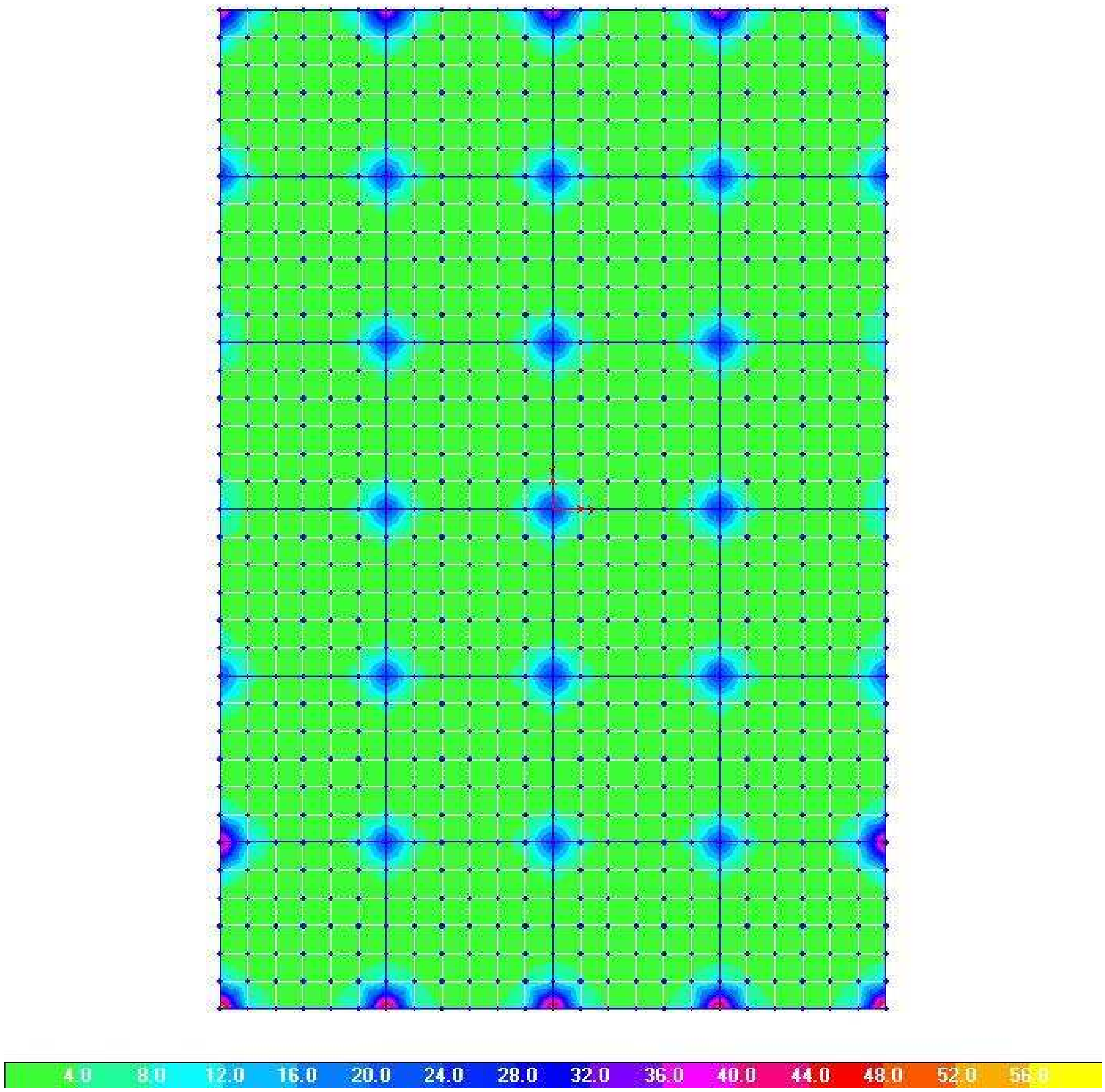

(b) Moment Distribution at 2nd Floor (1,000 lb TNT Weight@20 ft Stand-Off Distance)

"Figure 4.54 : Continued"

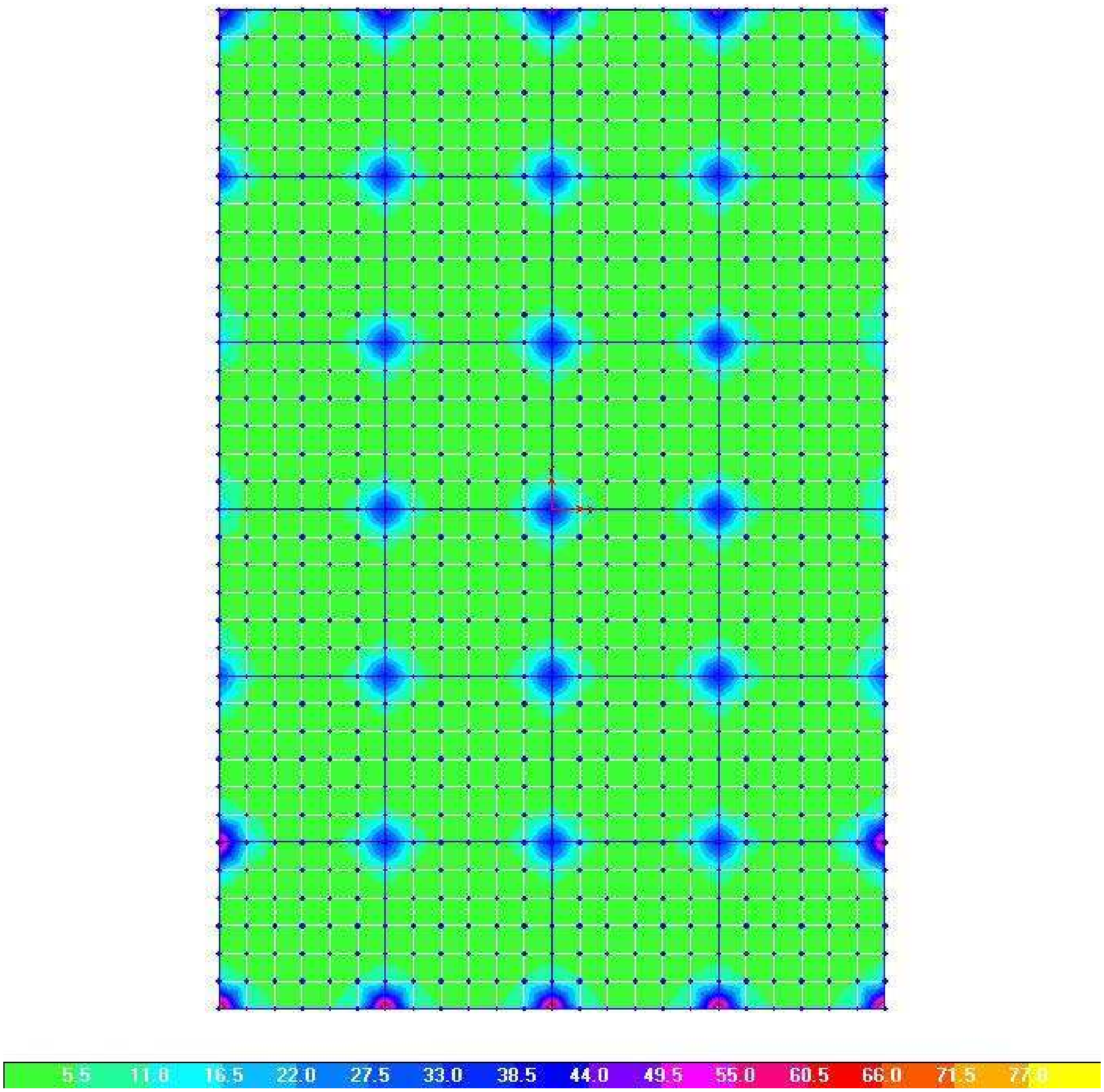

(c) Moment Distribution at 3rd Floor (1,000 lb TNT Weight@20 ft Stand-Off Distance)

“Figure 4.54 : Continued”

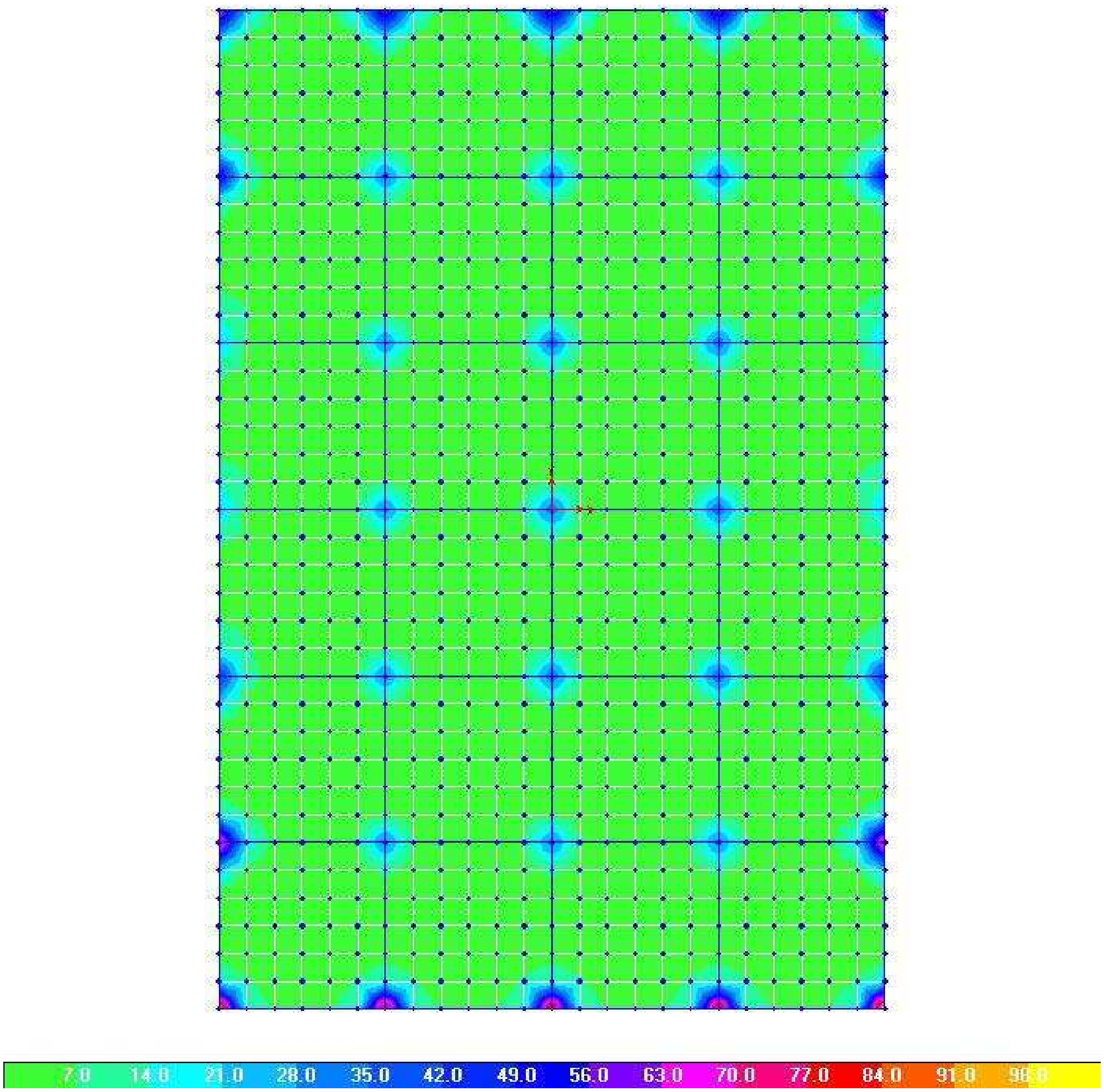

(d) Moment Distribution at Roof (1,000 lb TNT Weight@20 ft Stand-Off Distance)

Table 4.40 : The Results of Rigid Diaphragm Analysis

CASE	Story	Rigid Diaphragm	
		Developed Moment (k-in)	Moment Capacity (k-in)
500 lb_20 ft	Roof	45.319	212.5
	3rd	34.562	212.5
	2nd	26.472	212.5
1,000 lb_20 ft	Roof	101.587	212.5
	3rd	77.611	212.5
	2nd	59.525	212.5
2,000 lb_20 ft	Roof	199.913	212.5
	3rd	156.265	212.5
	2nd	118.391	212.5
3,000 lb_20 ft	Roof	268.192	212.5
	3rd	213.529	212.5
	2nd	160.245	212.5

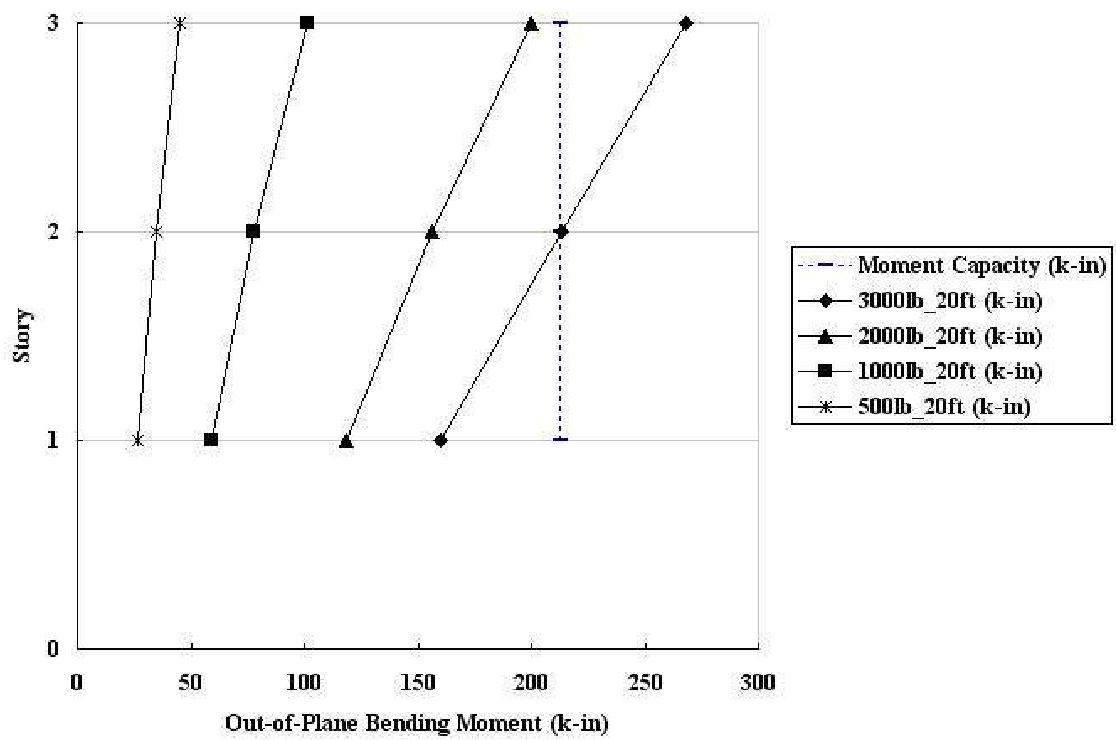

Figure 4.55 : Developed Bending Moment vs. Moment Capacity of Concrete Slab Based on Rigid Diaphragm Analysis

4.4. Nonlinear Structural Response of Three Story Building

4.4.1. Nonlinear Reponses of Three Story Building

The time history of the floor displacements obtained from nonlinear analyses are shown Figure 4.56. Here it can be seen that displacement for 1,000 lb @15 ft and 1,000 lb @20 ft has same value. However, the displacement for the 2,000 lb @20 ft has increased to 26 inches shown in Figure 4.57. In addition, it has been damped out be inelastic deformations that have occurred throughout the frame.

An important parameter in earthquake resistant design is the interstory drift index that is obtained by dividing the maximum relative story displacement by the story height. The UBC requires that for structures having a period greater than 0.7 seconds the interstory drift be limited to 0.02. The graph shown in Figure 4.58 indicates that the drift is slightly satisfied with limit for the 1,000 lb @15 ft and 1,000 lb @20 ft. However, for the 2,000 lb @20 ft, the interstory drift ratio is well above the limiting value.

Nonlinear dynamic analyses can also be used to calculate the demand/capacity (D/C) ratios for the structural members. Calculated demand/capacity ratios for the three loading conditions are shown Figure 4.59 - Figure 4.62. In these figures the largest demands occur in the perimeter moment frames as might be expected. However, there is also a significant demand in the columns of the transverse frames which are normal to the blast loading. The value of D/C ratio is lower than one of D/C ratio obtained linear analyses.

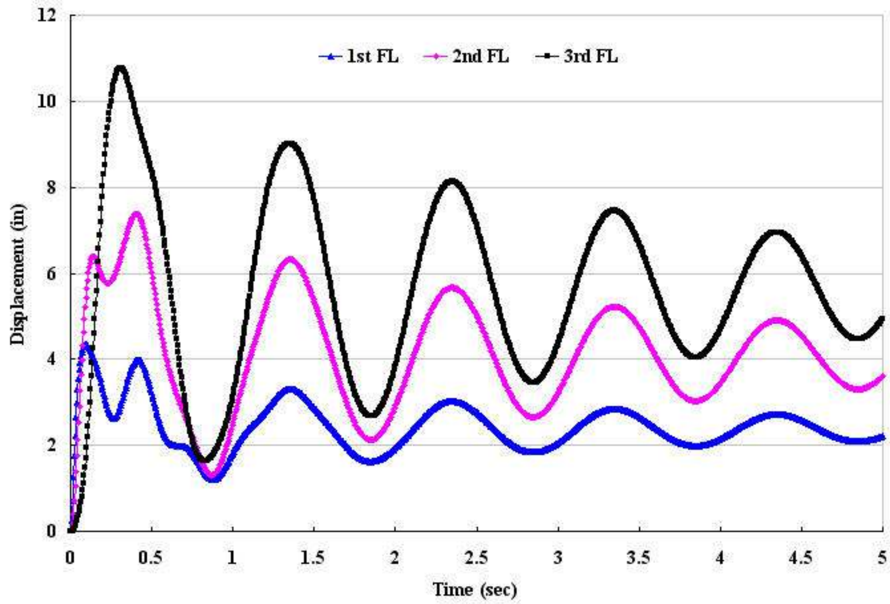

(a) 1,000 lb TNT Weight @ 15 ft Stand-Off Distance

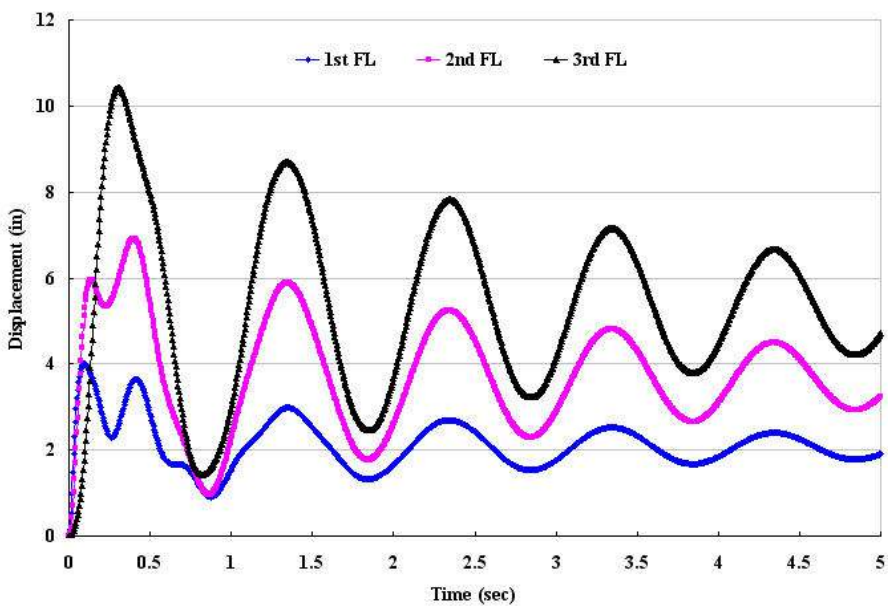

(b) 1,000 lb TNT Weight @ 20 ft Stand-Off Distance

Figure 4.56 : Nonlinear Dynamic Time History

"Figure 4.56 : Continued"

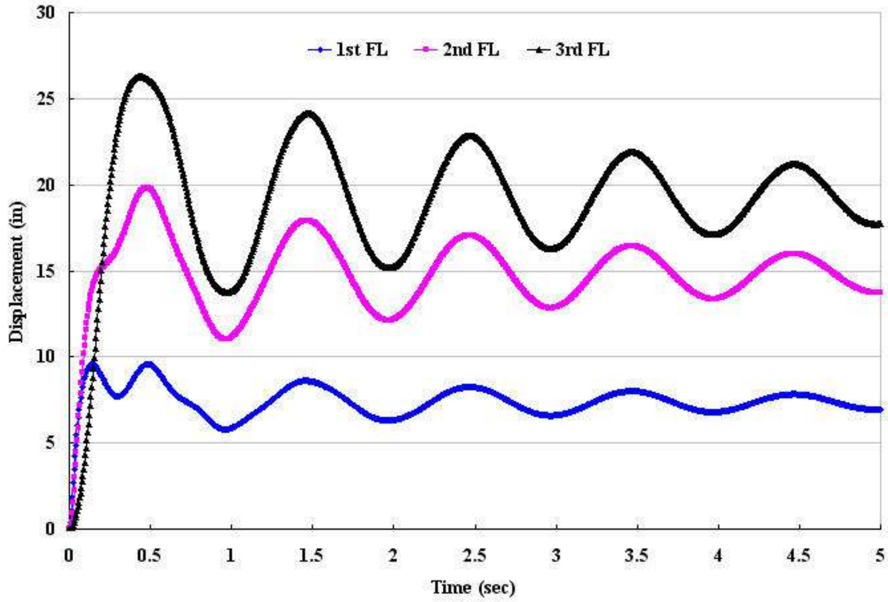

(c) 2,000 lb TNT Weight @ 20 ft Stand-Off Distance

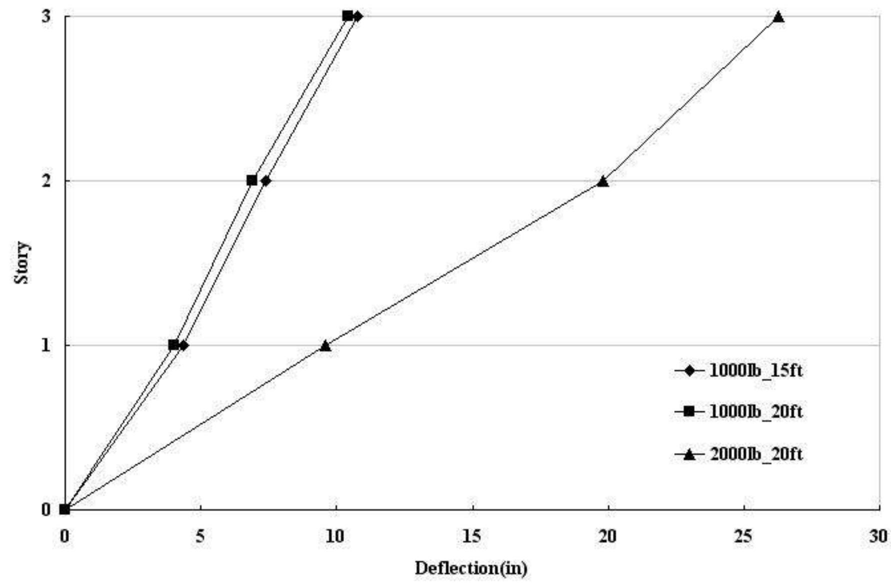

Figure 4.57 : Maximum Deflection on Each Floor By Nonlinear Analysis

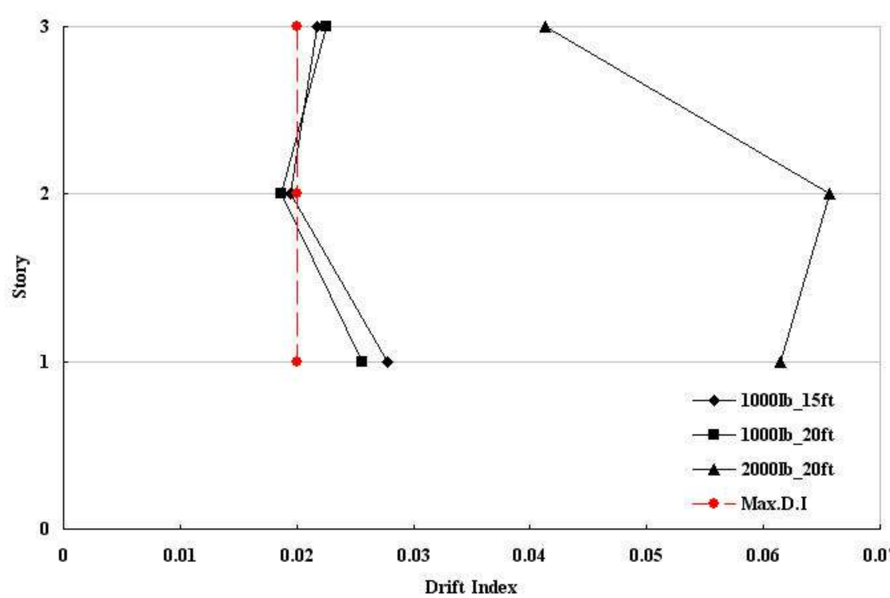

Figure 4.58 : Maximum Drift Ratio Analyzed By Nonlinear Analysis

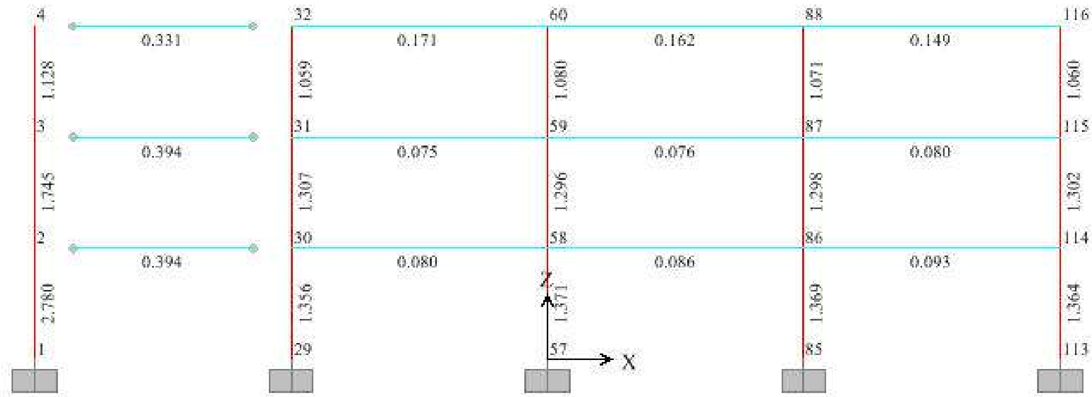

(a) 1,000 lb TNT Weight at 15 ft Stand-Off Distance

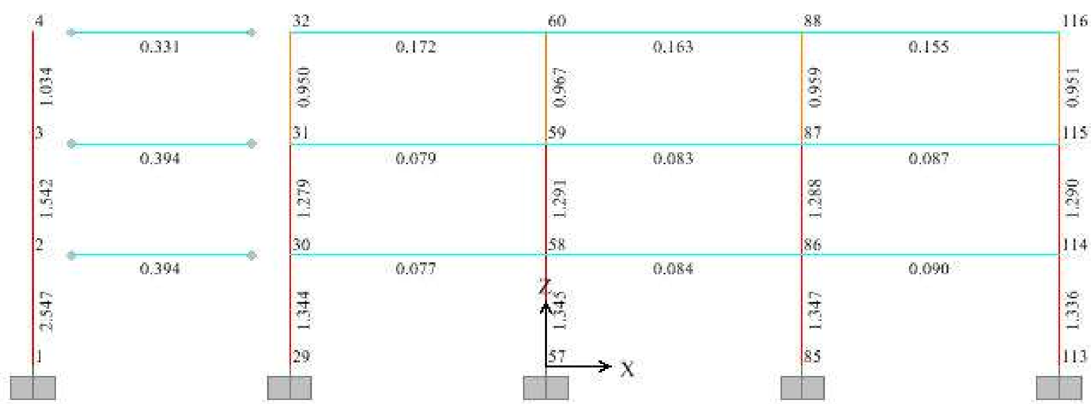

(b) 1,000 lb TNT Weight at 20 ft Stand-Off Distance

Figure 4.59 : Nonlinear Demand/Capacity Ratio on Transverse Direction

"Figure 4.59 : Continued"

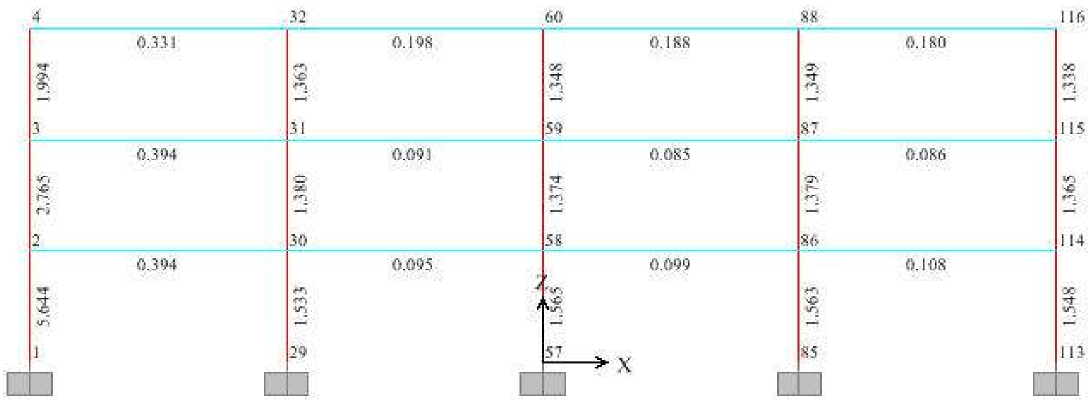

(c) 2,000 lb TNT Weight at 20 ft Stand-Off Distance

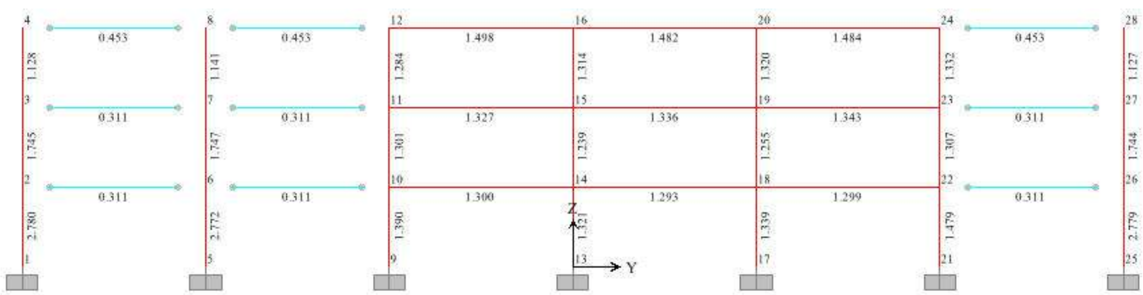

(a) 1,000 lb TNT Weight at 15 ft Stand-Off Distance

Figure 4.60 : Nonlinear Demand/Capacity Ratio on Longitudinal Direction

"Figure 4.60 : Continued"

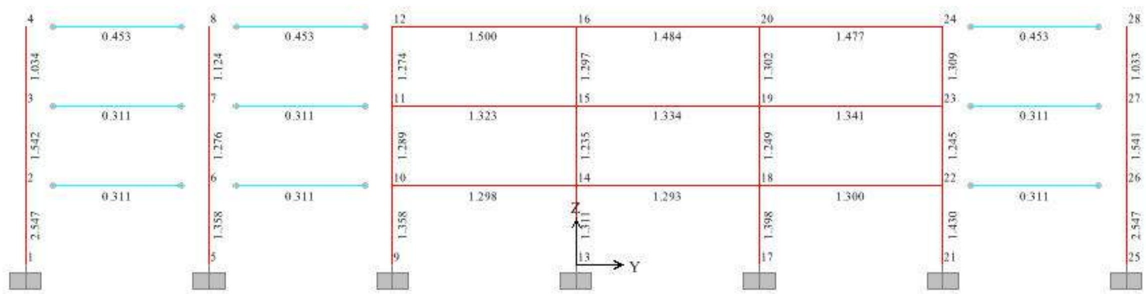

(b) 1,000 lb TNT Weight at 20 ft Stand-Off Distance

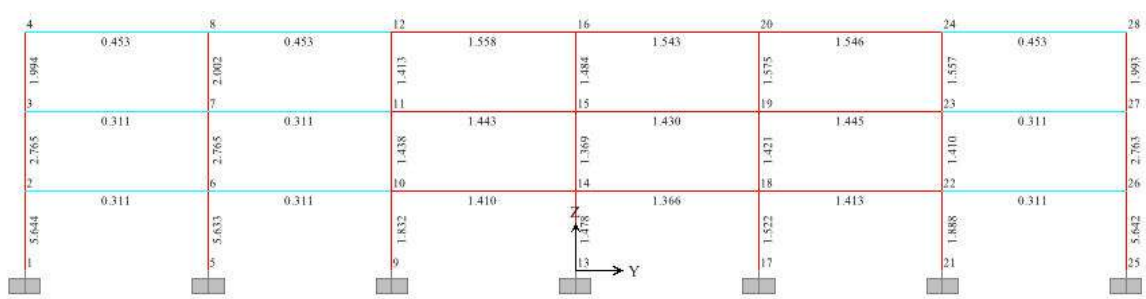

(c) 2,000 lb TNT Weight at 20 ft Stand-Off Distance

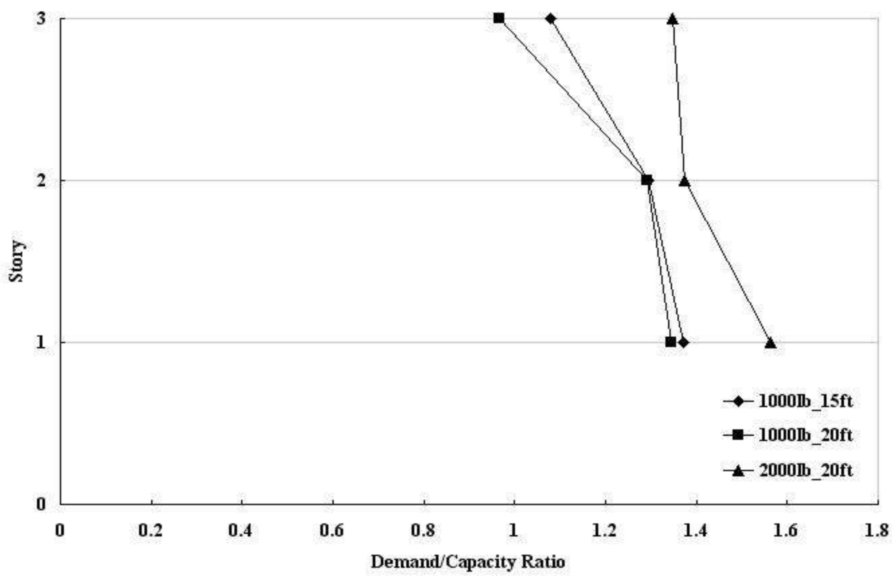

Figure 4.61 : Demand/Capacity Ratio Analyzed by Nonlinear Analysis (Transverse Direction)

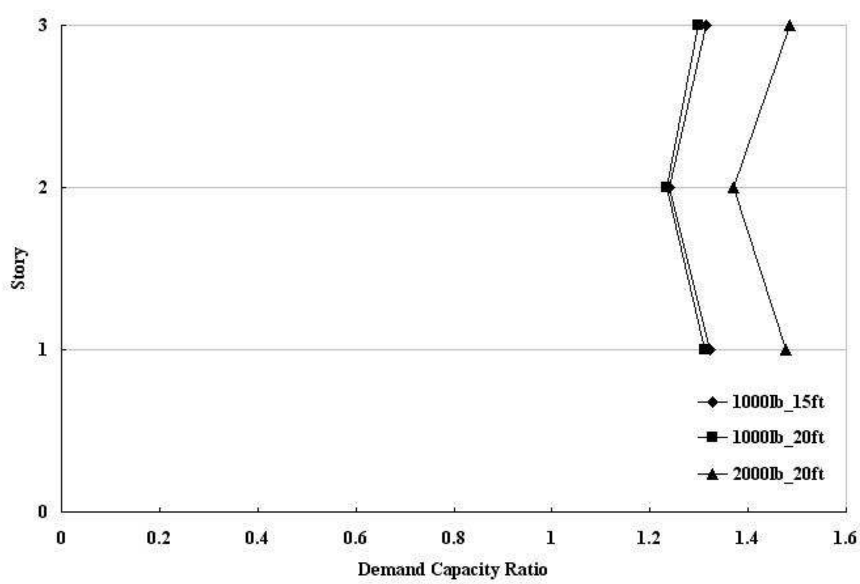

Figure 4.62 : Demand/Capacity Ratio Analyzed by Nonlinear Analysis (Longitudinal Direction)

4.4.2. Nonlinear Plastic Hinge Behavior

The default plastic hinge properties in SAP2000 are used for the analyses. These properties are based on the recommendations made in FEMA-273 for steel moment hinges. The moment-rotation curve that gives the yield value and the plastic deformation following yield is shown Figure 4.63. It should be noted that point B represents yielding and this rotation is subtracted from the deformations at point C, D and E. Therefore, only the plastic deformation is indicted by the hinge.

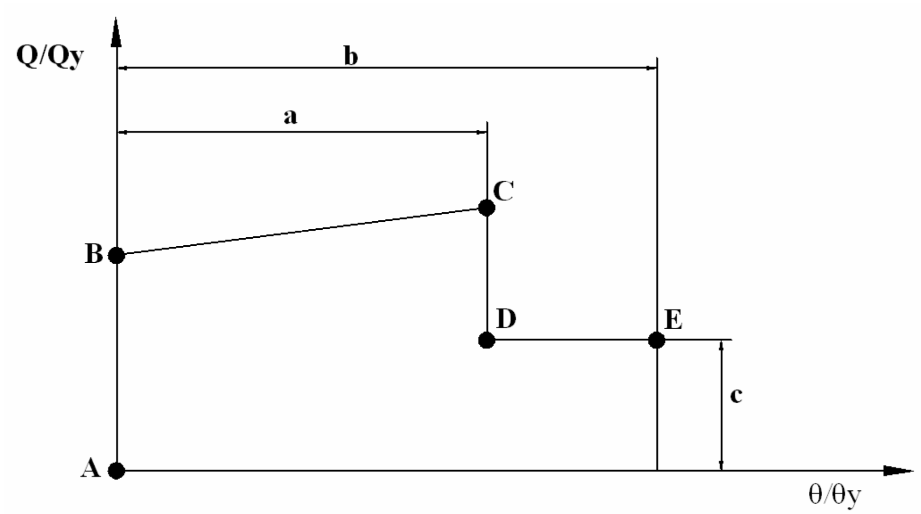

Figure 4.63 : Generalized Force-Deformation Relation for Steel Elements or Components (FEMA 356, Fig 5-1)

The hinge parameters are summarized in Figure 4.64 along with the FEMA condition assessment. To calculate the yield rotation, θy, is used from FEMA 356 equations.

Table 5-6 ***Modeling Parameters and Acceptance Criteria for Nonlinear Procedures—Structural Steel Components***

Component/Action	Modeling Parameters: Plastic Rotation Angle, Radians a	Modeling Parameters: Plastic Rotation Angle, Radians b	Residual Strength Ratio c	Acceptance Criteria (Plastic Rotation Angle, Radians): IO	Primary LS	Primary CP	Secondary LS	Secondary CP
Beams—flexure								
a. $\frac{b_f}{2t_f} \le \frac{52}{\sqrt{F_{ye}}}$ and $\frac{h}{t_w} \le \frac{418}{\sqrt{F_{ye}}}$	$9\theta_y$	$11\theta_y$	0.6	$1\theta_y$	$6\theta_y$	$8\theta_y$	$9\theta_y$	$11\theta_y$
b. $\frac{b_f}{2t_f} \ge \frac{65}{\sqrt{F_{ye}}}$ or $\frac{h}{t_w} \ge \frac{640}{\sqrt{F_{ye}}}$	$4\theta_y$	$6\theta_y$	0.2	$0.25\theta_y$	$2\theta_y$	$3\theta_y$	$3\theta_y$	$4\theta_y$
c. Other	Linear interpolation between the values on lines a and b for both flange slenderness (first term) and web slenderness (second term) shall be performed, and the lowest resulting value shall be used							
Columns—flexure [2, 7]								
For $P/P_{CL} < 0.20$								
a. $\frac{b_f}{2t_f} \le \frac{52}{\sqrt{F_{ye}}}$ and $\frac{h}{t_w} \le \frac{300}{\sqrt{F_{ye}}}$	$9\theta_y$	$11\theta_y$	0.6	$1\theta_y$	$6\theta_y$	$8\theta_y$	$9\theta_y$	$11\theta_y$
b. $d\ \frac{b_f}{2t_f} \ge \frac{65}{\sqrt{F_{ye}}}$ or $\frac{h}{t_w} \ge \frac{460}{\sqrt{F_{ye}}}$	$4\theta_y$	$6\theta_y$	0.2	$0.25\theta_y$	$2\theta_y$	$3\theta_y$	$3\theta_y$	$4\theta_y$
c. Other	Linear interpolation between the values on lines a and b for both flange slenderness (first term) and web slenderness (second term) shall be performed, and the lowest resulting value shall be used							

Figure 4.64 : Modeling Parameters and Acceptance Criteria for Nonlinear Procedures

$$\text{Beams:} \quad \theta_y = \frac{ZF_{ye}l_b}{6EI_b}$$

$$\text{Columns:} \quad \theta_y = \frac{ZF_{ye}l_c}{6EI_c}\left(1 - \frac{P}{P_{ye}}\right)$$

For reference, the member locations and identification numbers are shown in Figure 4.65 and Figure 4.66 for typical transverse and longitudinal frames. Figure 4.67 shows the criteria of plastic hinge behavior. The plastic rotation demands in critical members of the transverse and longitudinal frame are summarized in Figure 4.68 – Figure 4.70.

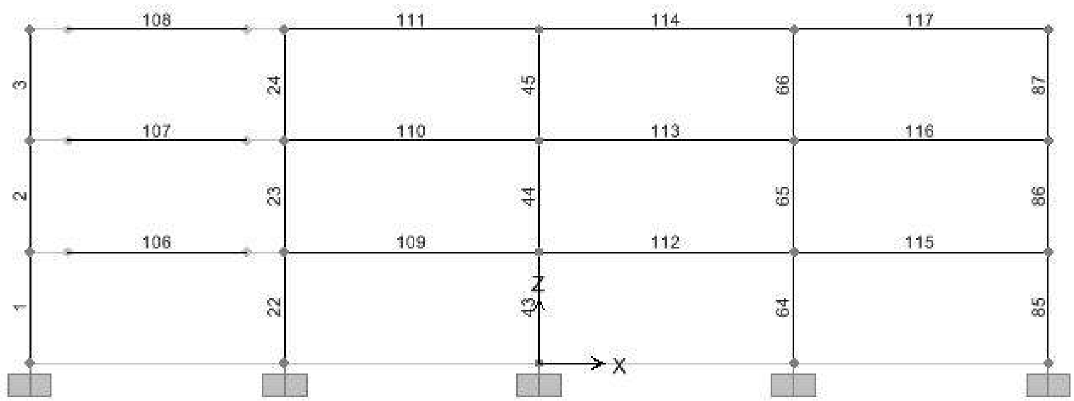

Figure 4.65 : Generated Member Numbers along the Transverse Direction

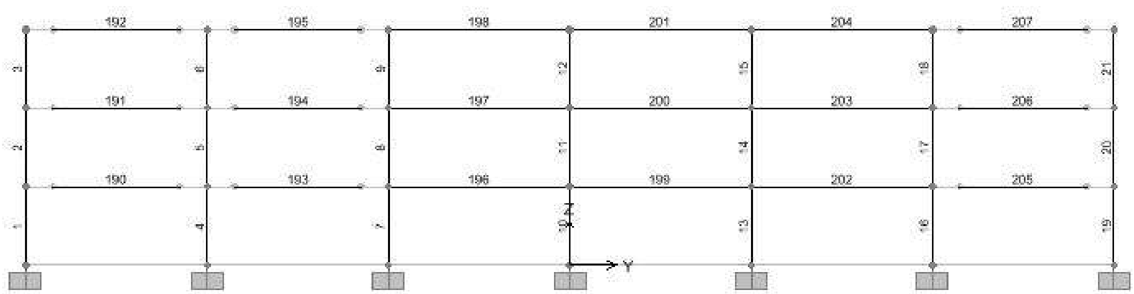

Figure 4.66 : Generated Member Numbers along the Longitudinal Direction

Demands for the 1,000 lb TNT weight @ 15 ft and 1,000 lb TNT weight @ 20 ft are summarized in Figure 4.68 and Figure 4.69. Figure 4.68 is shown that the beams and columns that exceed the elastic limit are only weakly nonlinear with small plastic rotation demands along both directions. In Figure 4.69, the behaviors of the transverse columns at the 3rd and roof level are elastic and similar behaviors can be seen on 1,000 lb TNT weight @ 15 ft case. According to the FEMA recommendations, this building would be classified as suitable for immediate occupancy (IO). The maximum member demands for the condition of 2,000 lb @ 20 ft are summarized in Figure 4.70. Here it can be seen that there is yielding in the column over the direction of the frame with plastic rotation demands ranging from 0.049 radians at the first floor of longitudinal direction to -0.009 radians at the roof level of transverse direction. There is also yielding in the beams over the height of the frame with plastic rotation demands ranging from 0.0459 radians at the 2nd floor to 0.031 at first floor.

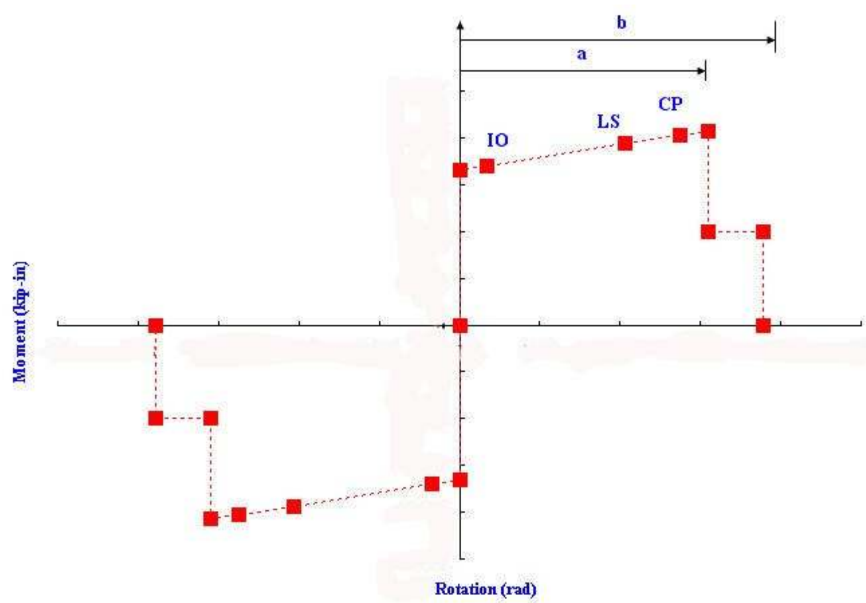

Figure 4.67 : Criteria of Plastic Hinge Behavior

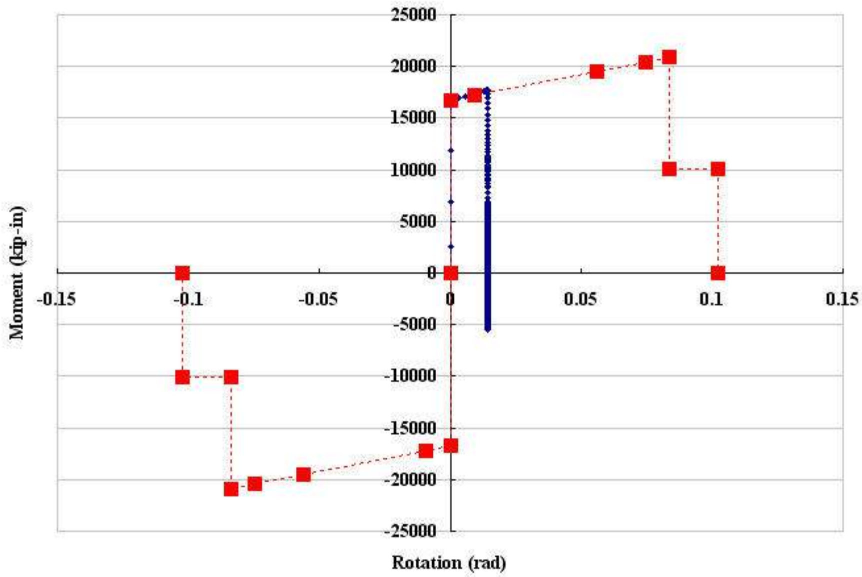

(a) Moment-Rotation Relationship on Transverse Direction (Column 43)

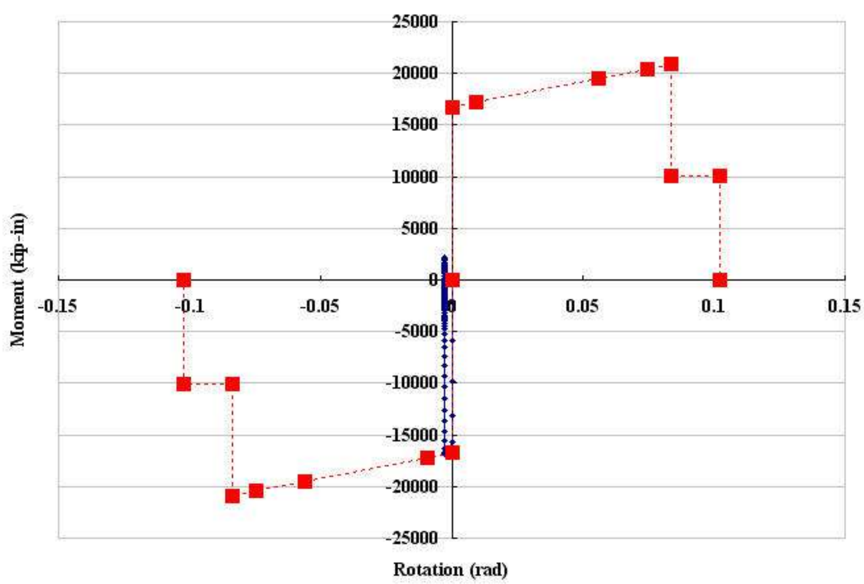

(b) Moment-Rotation Relationship on Transverse Direction (Column 44)

Figure 4.68 : Moment-Rotation Relation In Case Of 1,000 lb TNT Weight at 15 ft Stand-Off Distance

"Figure 4.68 : Continued"

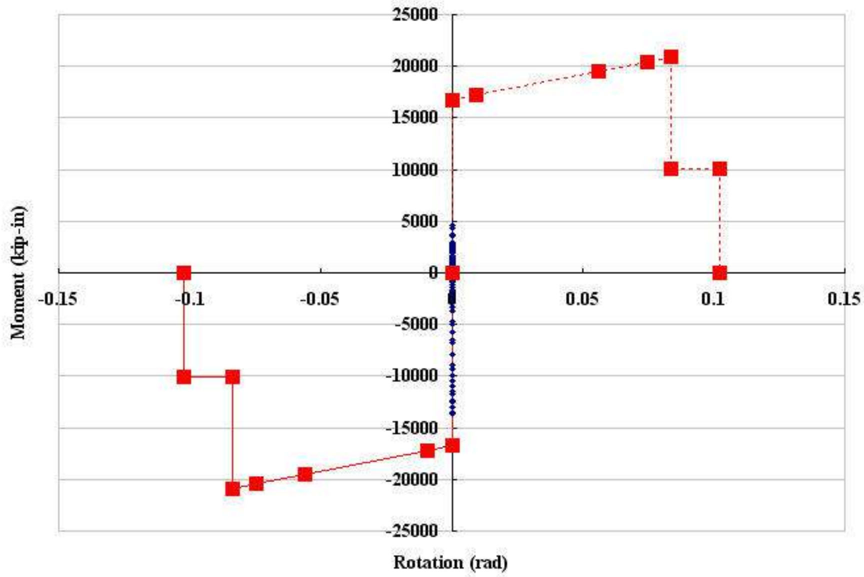

(c) Moment-Rotation Relationship on Transverse Direction (Column 45)

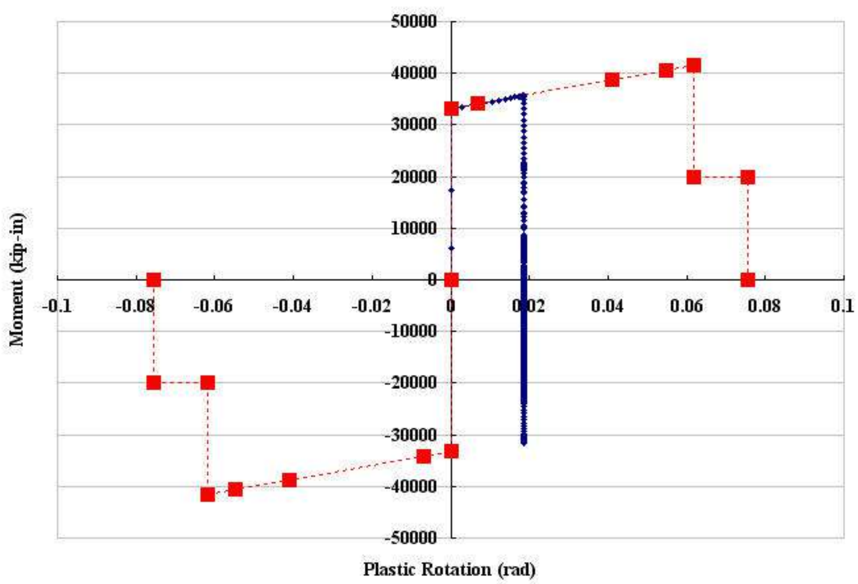

(d) Moment-Rotation Relationship on Longitudinal Direction (Column 10)

"Figure 4.68 : Continued"

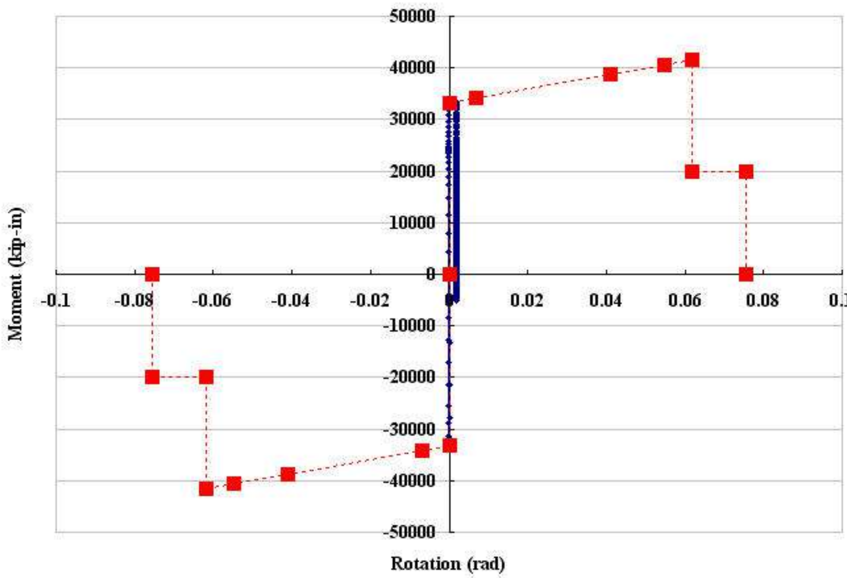

(e) Moment-Rotation Relationship on Longitudinal Direction (Column 11)

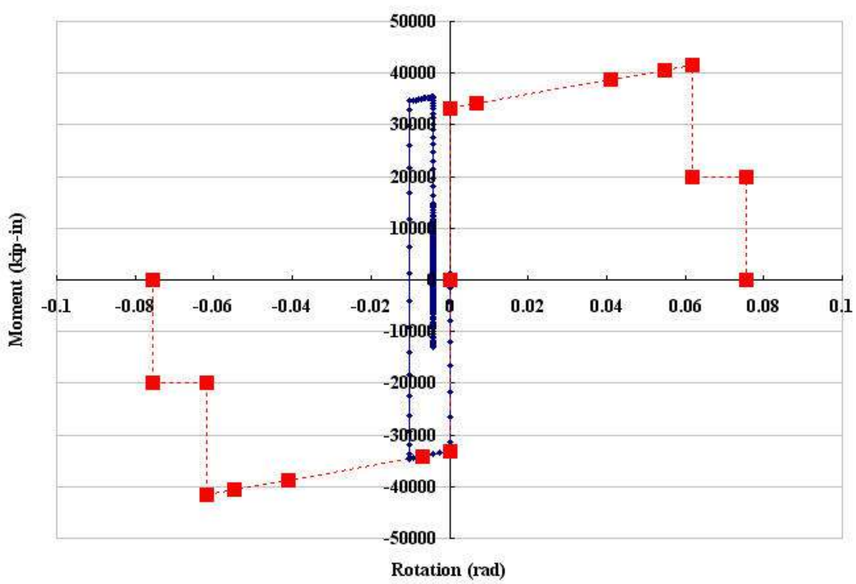

(f) Moment-Rotation Relationship on Longitudinal Direction (Column 12)

"Figure 4.68 : Continued"

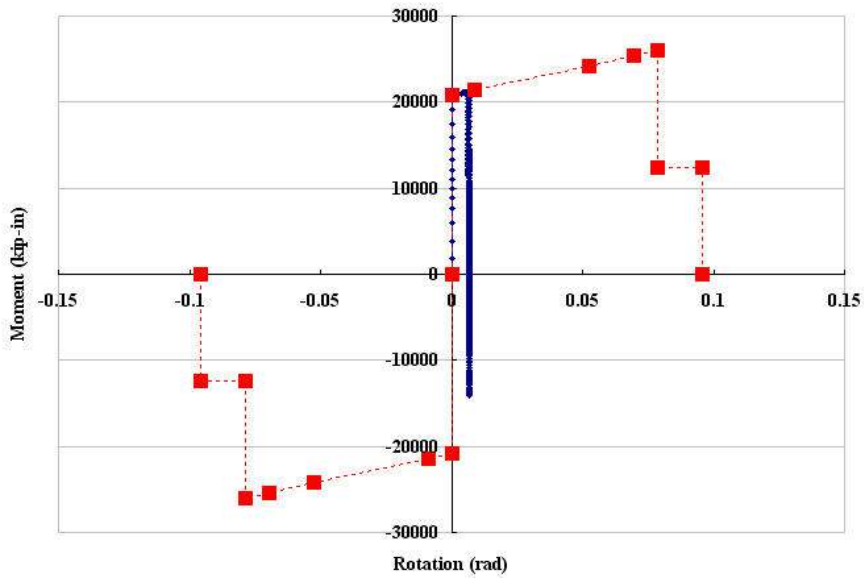

(g) Moment-Rotation Relationship on Longitudinal Direction (Beam 196)

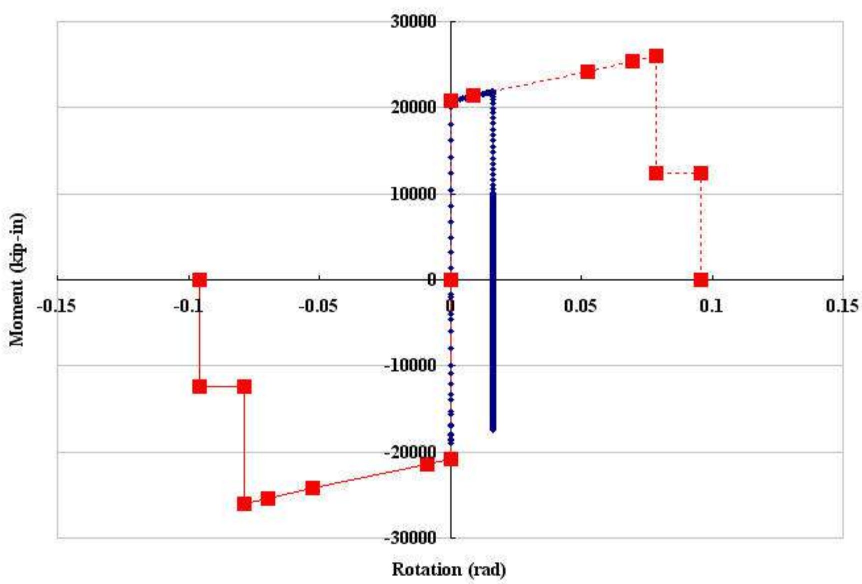

(h) Moment-Rotation Relationship on Longitudinal Direction (Beam 197)

"Figure 4.68 : Continued"

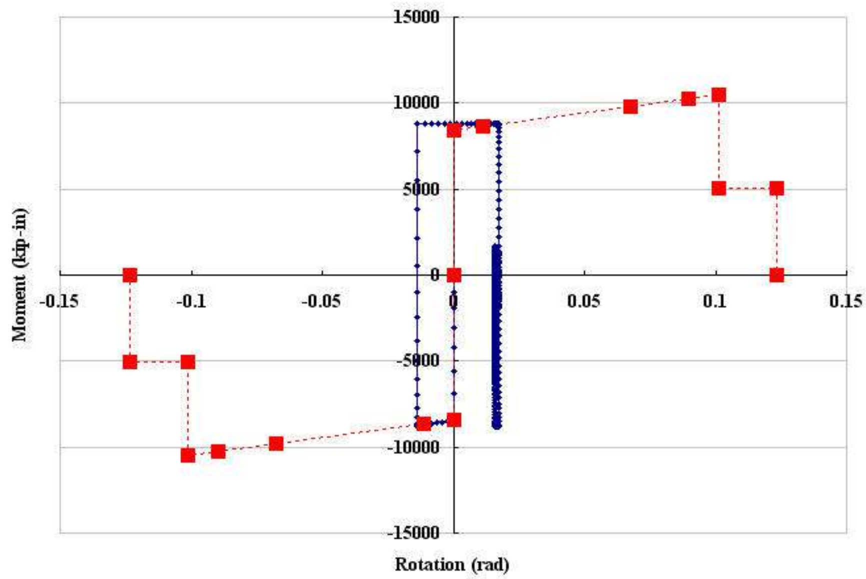

(i) Moment-Rotation Relationship on Longitudinal Direction (Beam 198)

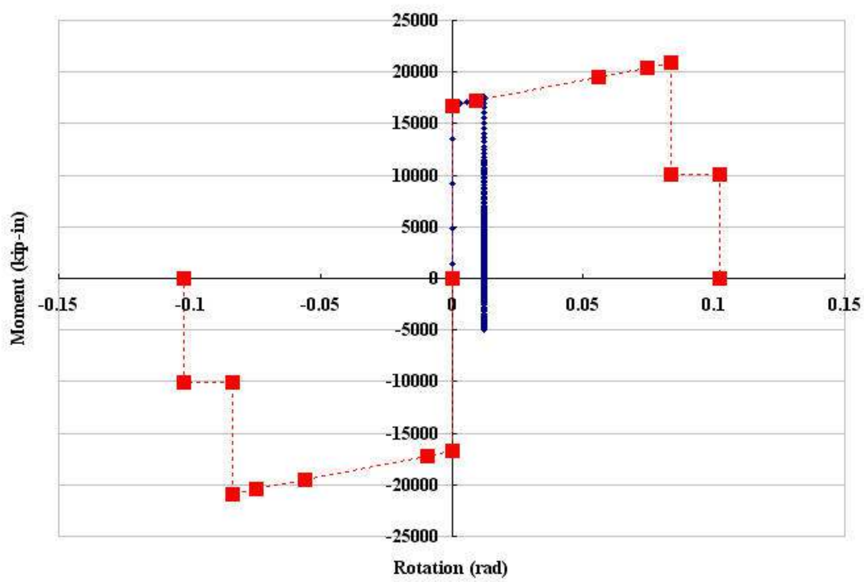

(a) Moment-Rotation Relationship on Transverse Direction (Column 43)

Figure 4.69 : Moment-Rotation Relation In Case Of 1,000 lb TNT Weight at 20 ft Stand-Off Distance

“Figure 4.69 : Continued”

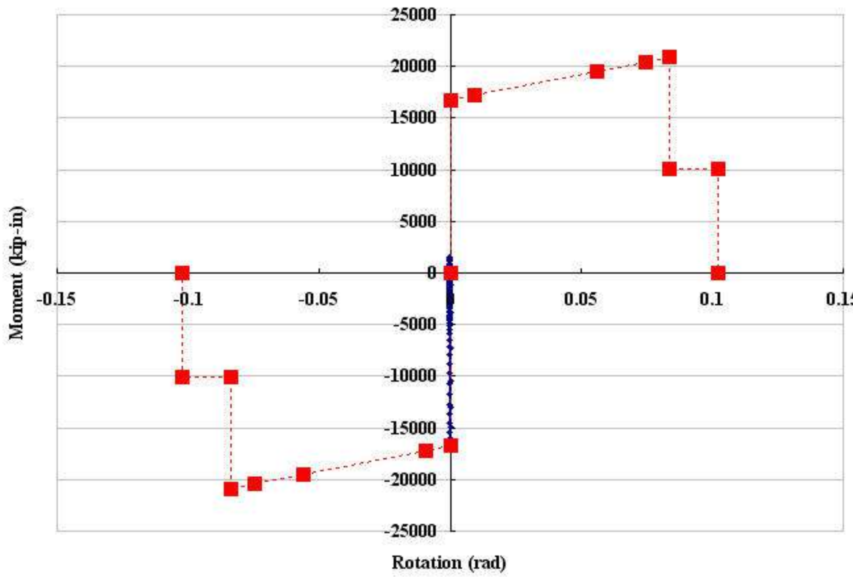

(b) Moment-Rotation Relationship on Transverse Direction (Column 44)

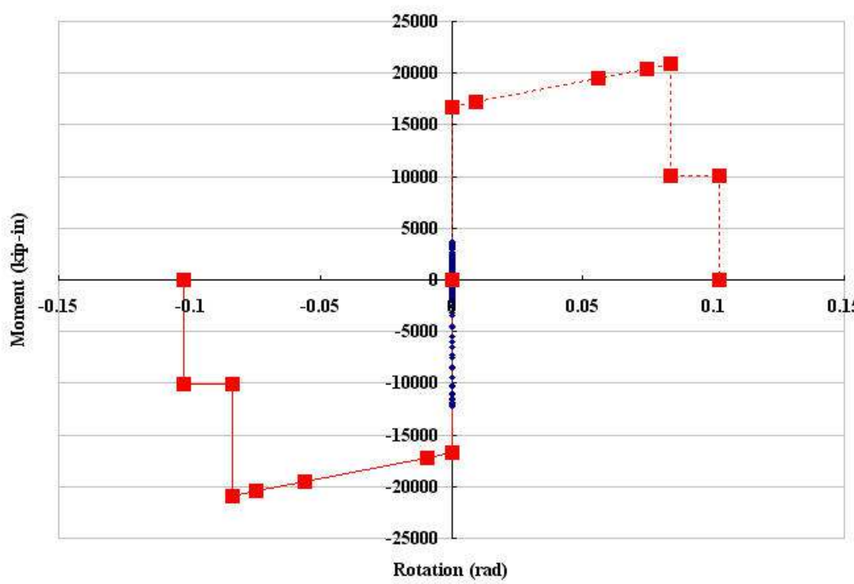

(c) Moment-Rotation Relationship on Transverse Direction (Column 45)

“Figure 4.69 : Continued”

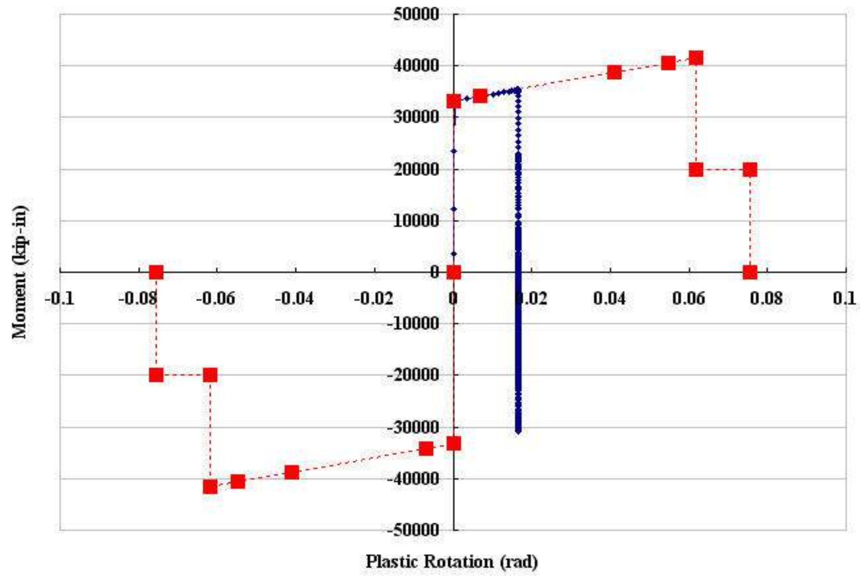

(d) Moment-Rotation Relationship on Longitudinal Direction (Column 10)

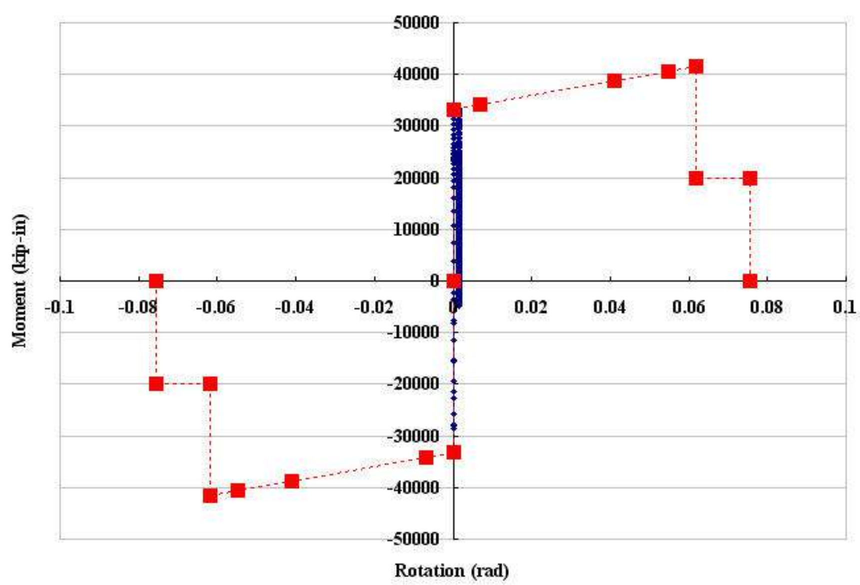

(e) Moment-Rotation Relationship on Longitudinal Direction (Column 11)

"Figure 4.69 : Continued"

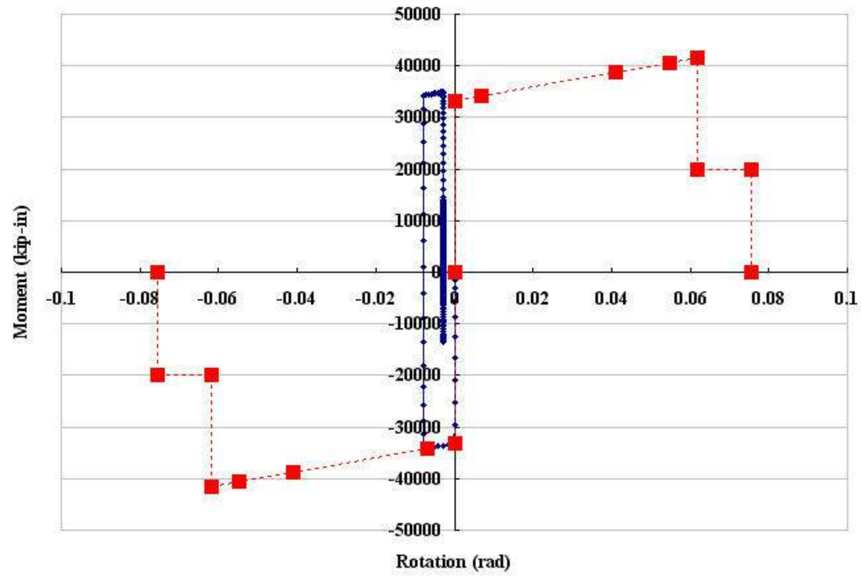

(f) Moment-Rotation Relationship on Longitudinal Direction (Column 12)

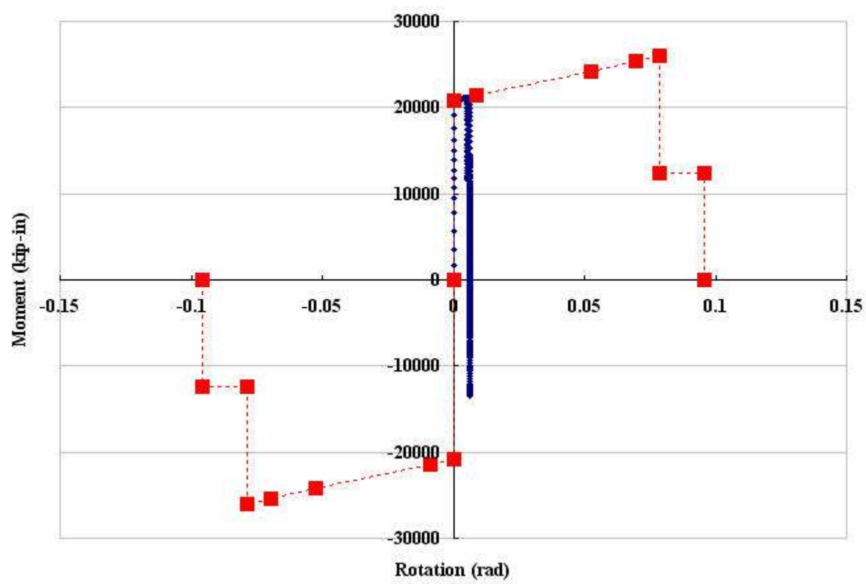

(g) Moment-Rotation Relationship on Longitudinal Direction (Beam 196)

“Figure 4.69 : Continued”

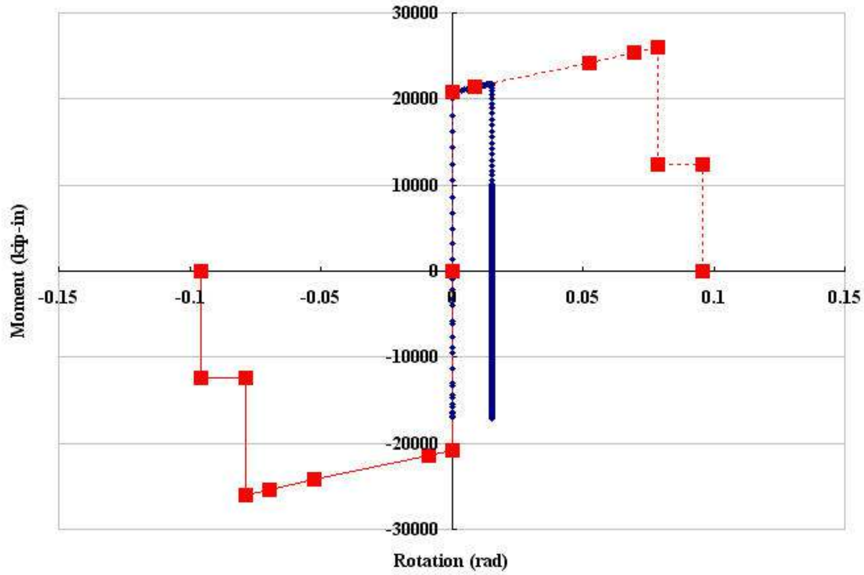

(h) Moment-Rotation Relationship on Longitudinal Direction (Beam 197)

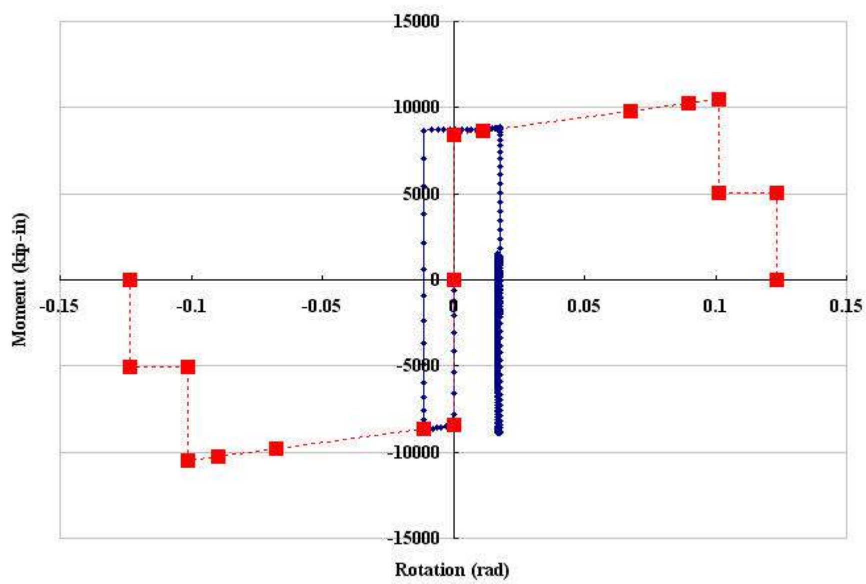

(i) Moment-Rotation Relationship on Longitudinal Direction (Beam 198)

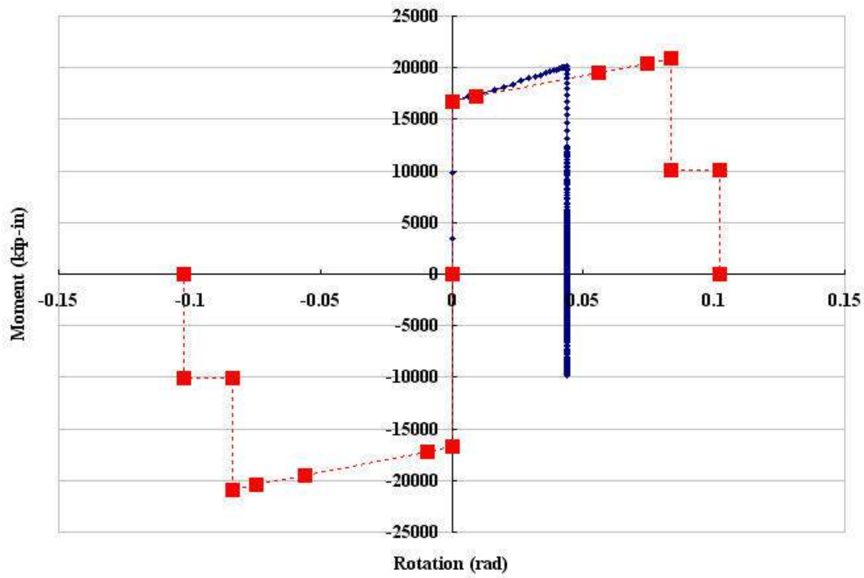

(a) Moment-Rotation Relationship on Transverse Direction (Column 43)

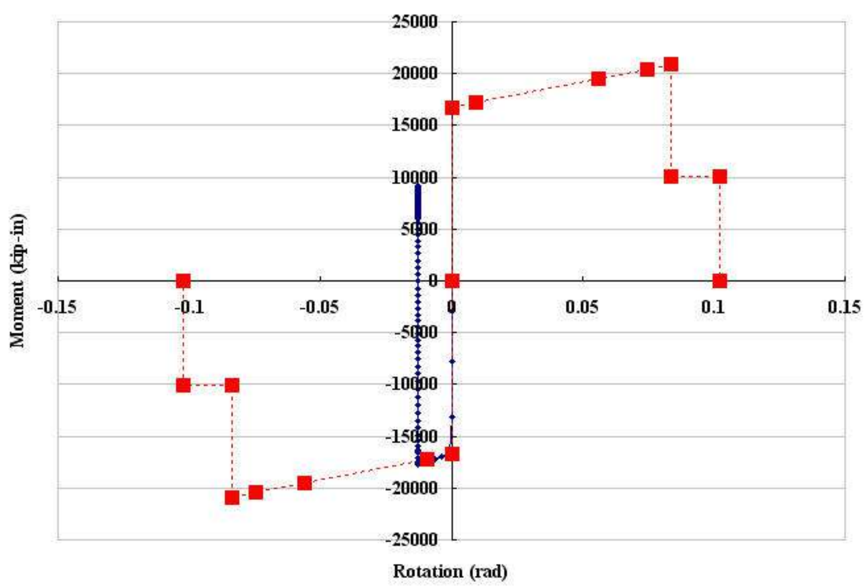

(b) Moment-Rotation Relationship on Transverse Direction (Column 44)

Figure 4.70 : Moment-Rotation Relation In Case Of 2,000 lb TNT Weight at 20 ft Stand-Off Distance

"Figure 4.70 : Continued"

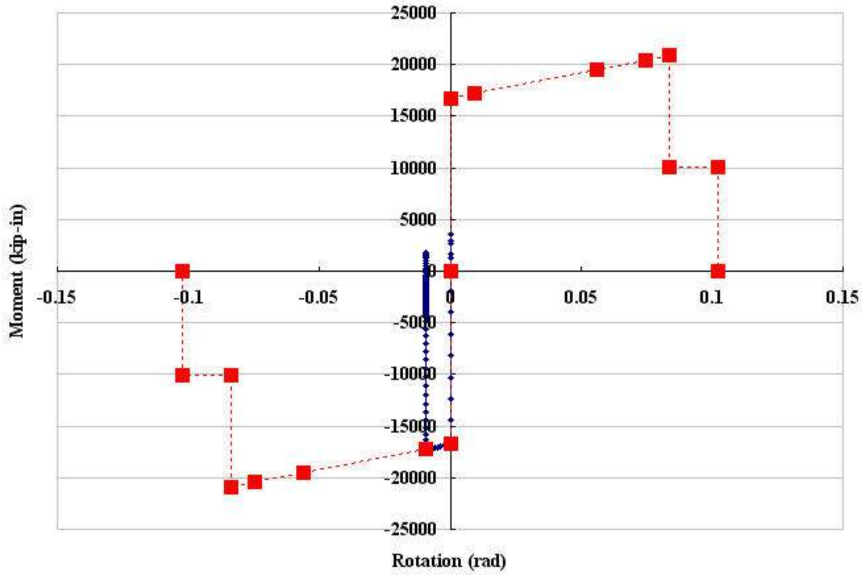

(c) Moment-Rotation Relationship on Transverse Direction (Column 45)

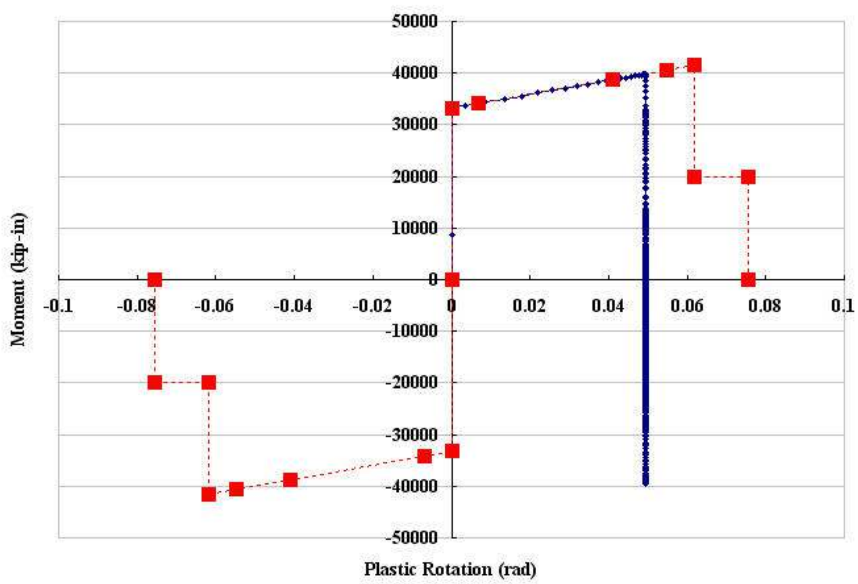

(d) Moment-Rotation Relationship on Longitudinal Direction (Column 10)

“Figure 4.70 : Continued”

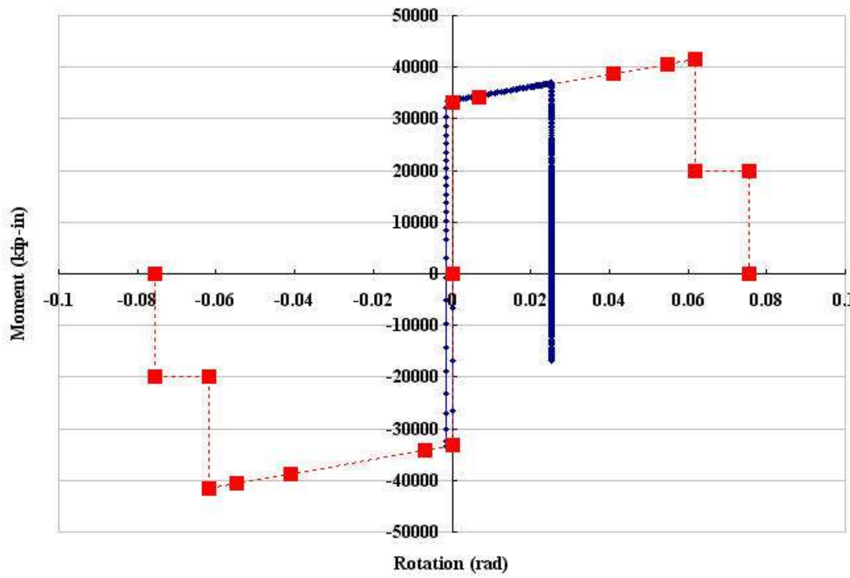

(e) Moment-Rotation Relationship on Longitudinal Direction (Column 11)

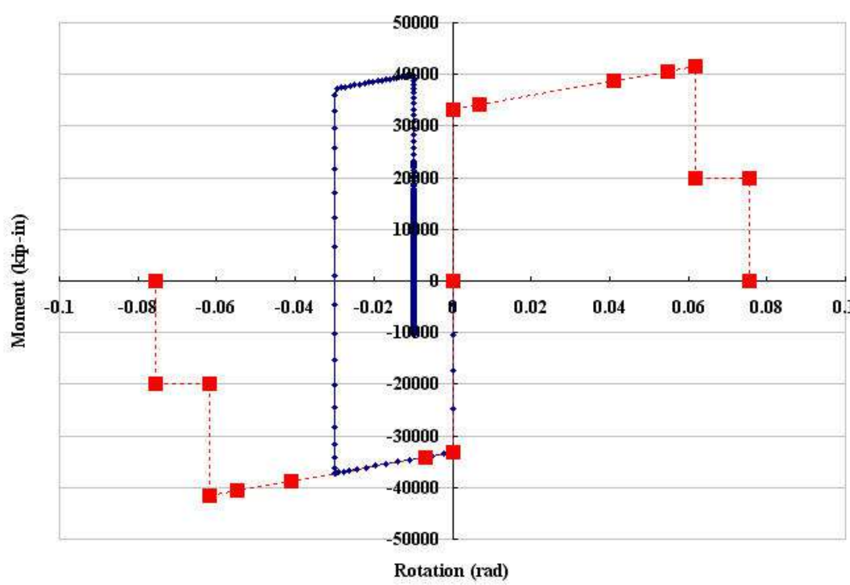

(f) Moment-Rotation Relationship on Longitudinal Direction (Column 12)

"Figure 4.70 : Continued"

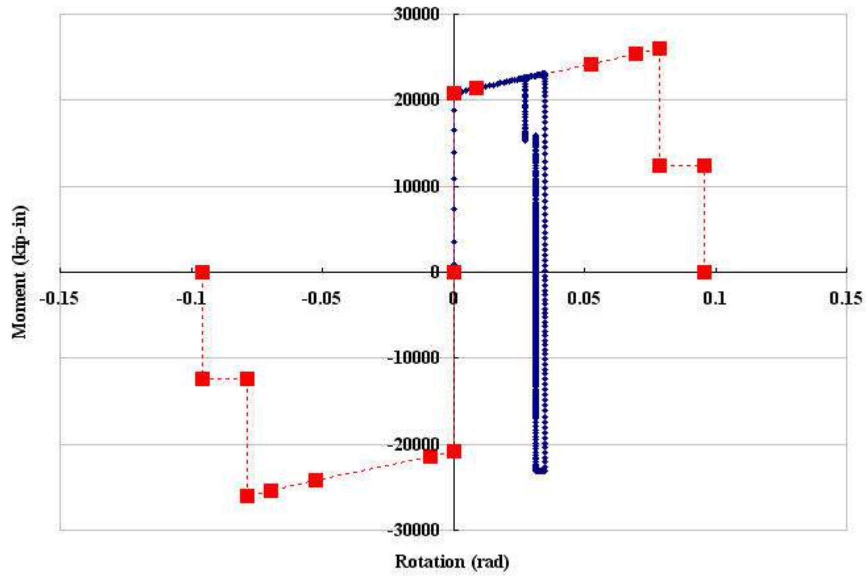

(g) Moment-Rotation Relationship on Longitudinal Direction (Beam 196)

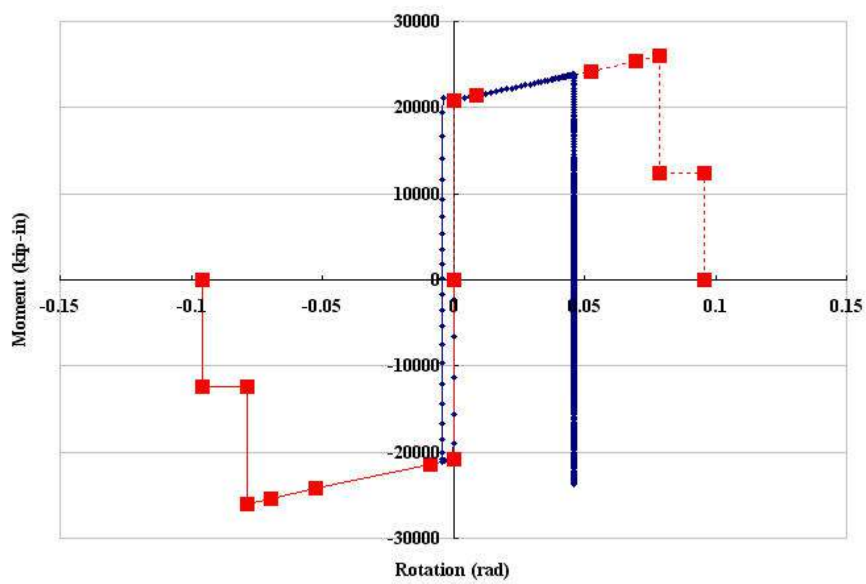

(h) Moment-Rotation Relationship on Longitudinal Direction (Beam 197)

“Figure 4.70 : Continued”

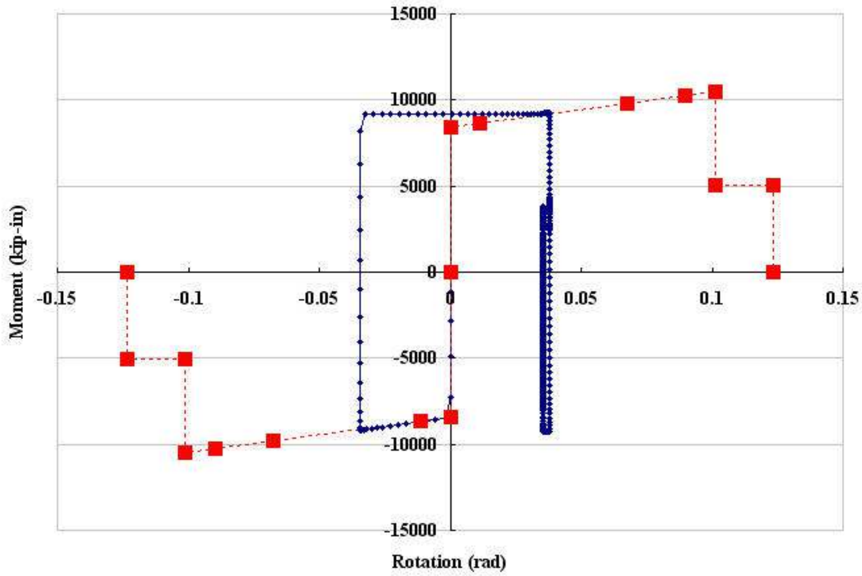

(i) Moment-Rotation Relationship on Longitudinal Direction (Beam 198)

Chapter 5 : Analyses of Model of Ten Story Building

To investigate effects of middle rise building against various cases of bomb attack, similar cases from previous chapter are applied to a ten story building. Various air blast loads and stand-off distances are applied to ten story building with welded steel moment frames on the parameter. In addition, extreme load cases, 3,000 lb and 4,000 lb TNT weight @ 20 ft stand-off distance, add to this chapter. It also considers the size of the blast crater along with the different structural responses that include story displacements, demand/capacity ratio, and diaphragm analysis as well as nonlinear plastic hinge behavior. These parameters are then compared with limit values suggested by seismic guidelines.

5.1. Structural Response to Variable Stand-off Distance

5.1.1. Blast Loads

A frame is subjected to 1,000 lb TNT explosive weight at 15 ft, 30 ft, 50 ft and 100 ft stand-off distance. Cases are defined along various distances. The blast wave propagates by compressing the air with supersonic velocity, and it is reflected by the building, amplifying over pressure. To find blast loads on the ten story building at each joint, the CONWEP program was used. Figure 5.1, 5.2, 5.3 and 5.4 show time duration and peak reflected pressure on front frame of structure.

When a blast with 1,000 lb TNT explosive weight impinges on a structure, a higher pressure is developed, termed the reflected pressure. The calculated (CONWEP) peak overpressures on the front frame are shown in Figure 5.1 – Figure 5.4. These range from a maximum of 4172 psi (15 ft), 731 psi (30 ft), 157 psi (50 ft), 24 psi (100 ft) at the point closest to the detonation to a minimum of 5.43 psi (15 ft), 6.30 psi (30 ft), 7.84 psi (50 ft), 8.89 psi (100 ft) at the upper west/east corner.

While these pressures are extremely large, they act for a limited duration, as shown in Figure 5.1 – Figure 5.4. The duration ranges from a maximum of 31.32 msec (15 ft), 31.47 msec (30 ft), 31.81 msec (50 ft), 33.17 msec (100 ft) in the upper west/east corner to a minimum of 2.87 msec (15 ft), 16.62 msec (30 ft), 15.73 msec (50 ft), 28.20 msec (100 ft) at the point closest to the blast.

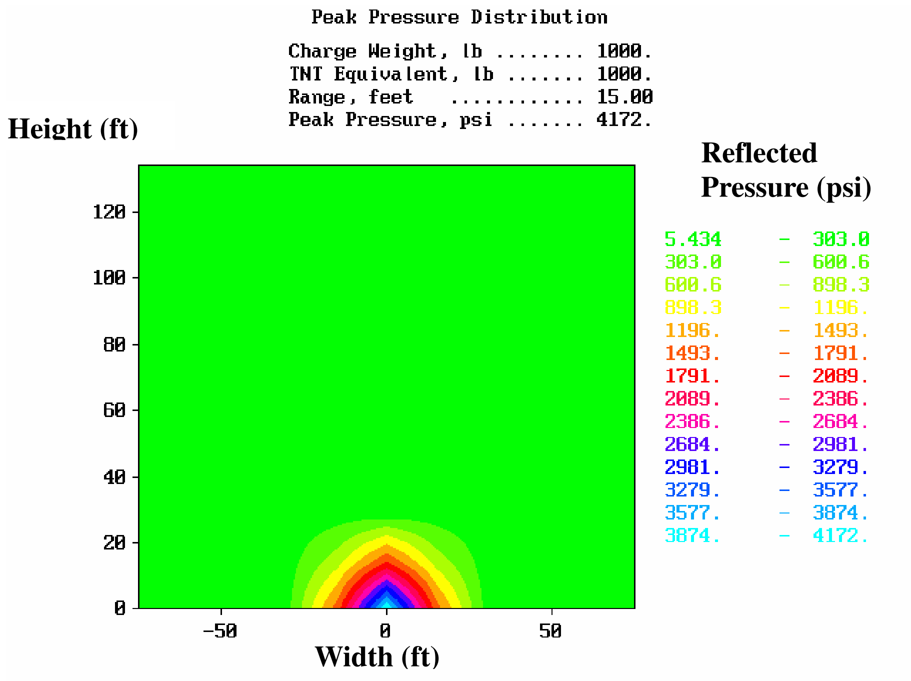

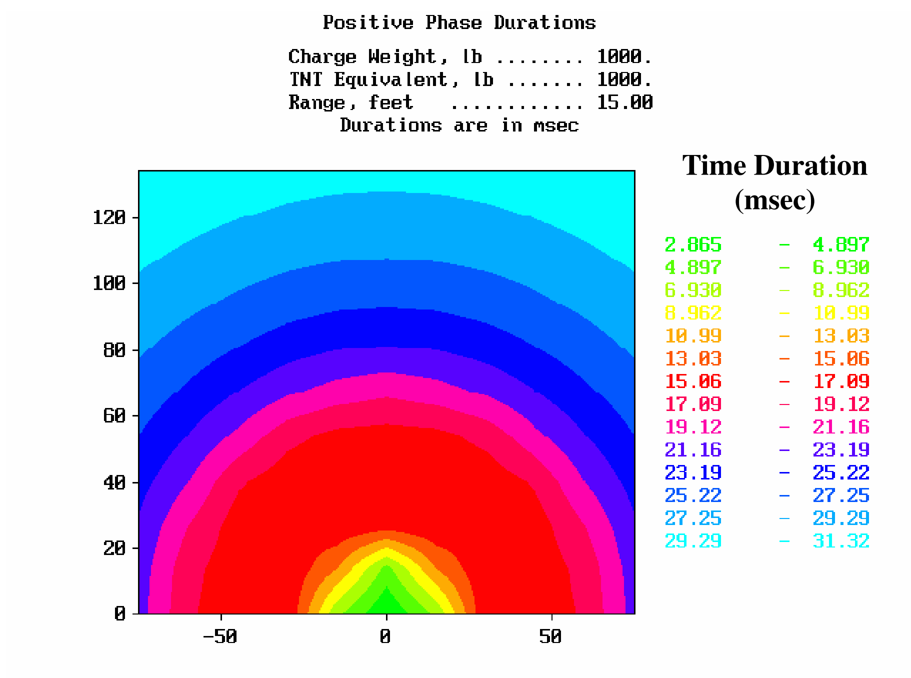

Figure 5.1 : Distribution of Peak Reflected Pressure and Time Duration at 15 ft Stand-Off

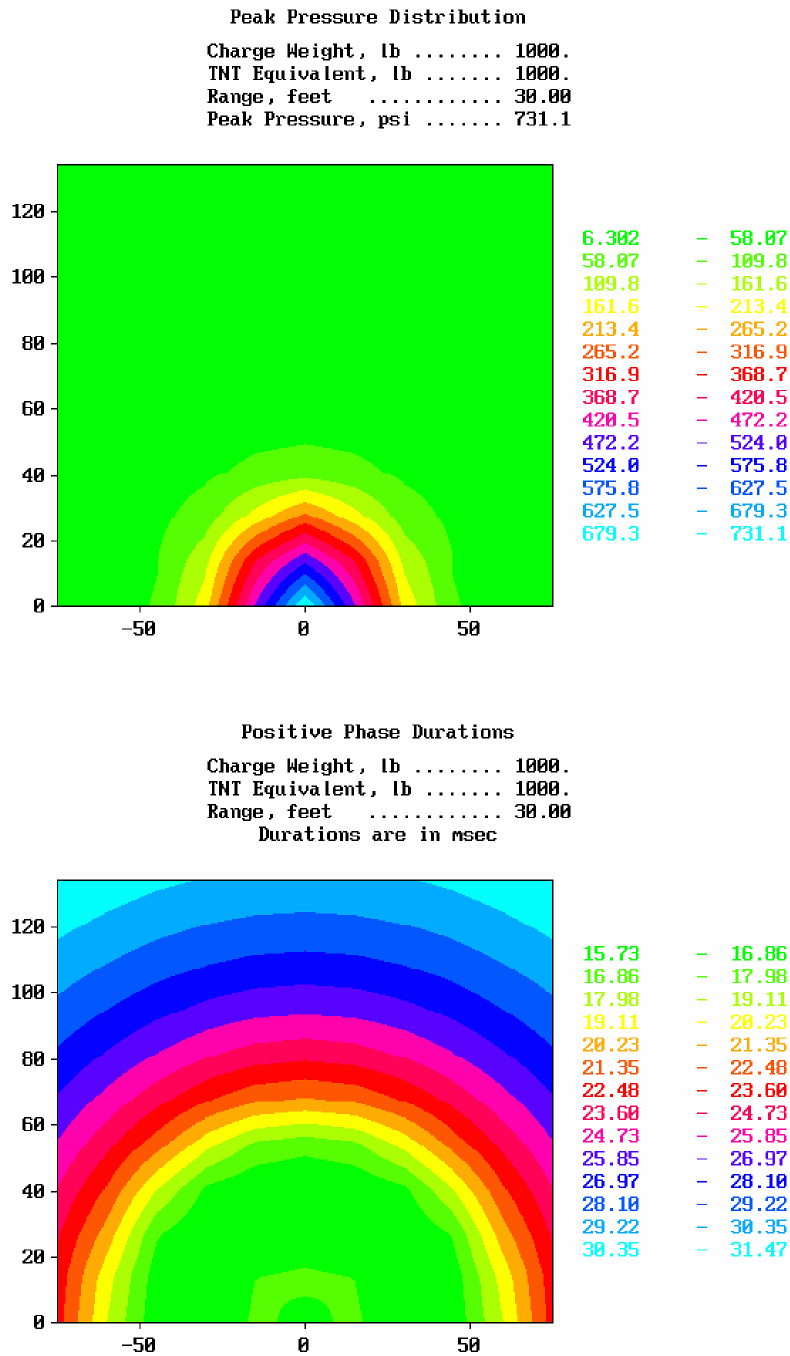

Figure 5.2 : Distribution of Peak Reflected Pressure and Time Duration at 30 ft Stand-Off

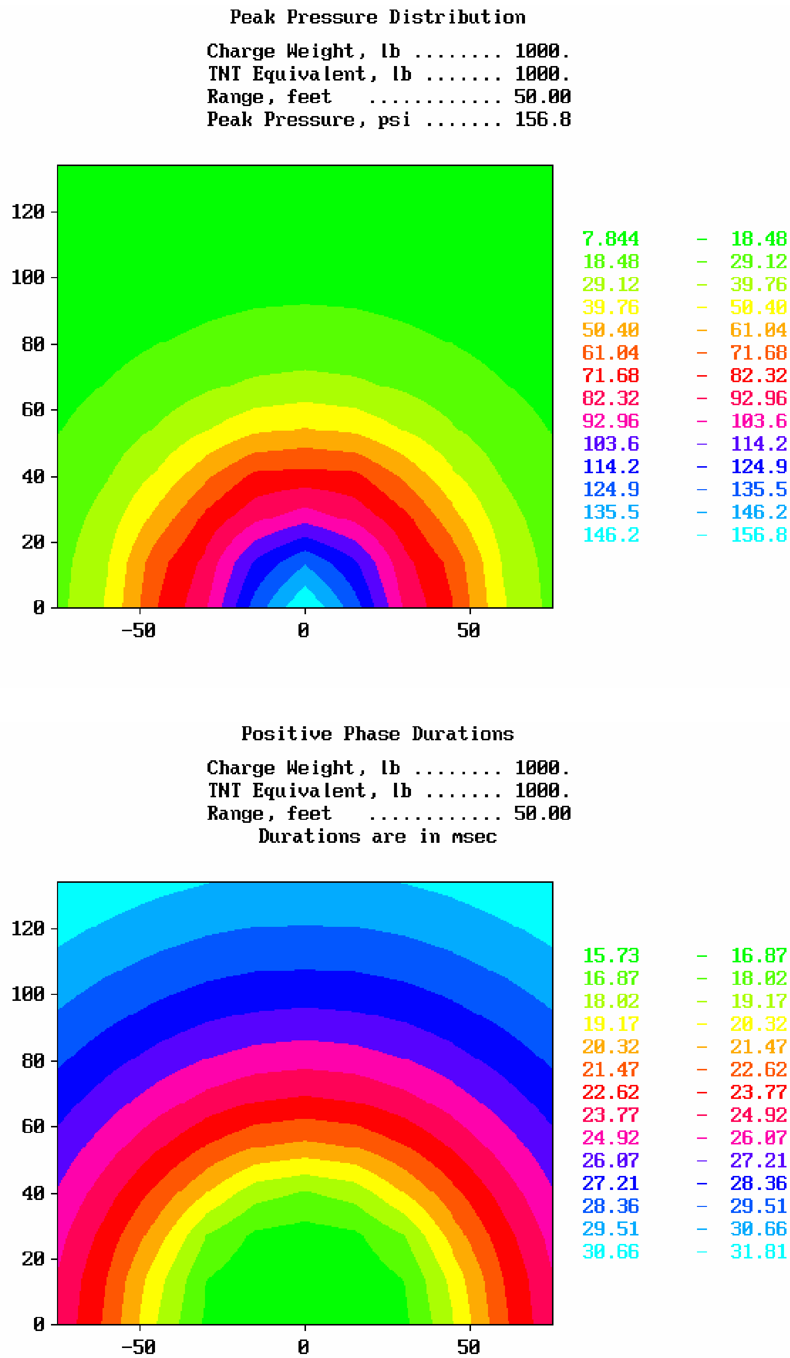

Figure 5.3 : Distribution of Peak Reflected Pressure and Time Duration at 50 ft Stand-Off

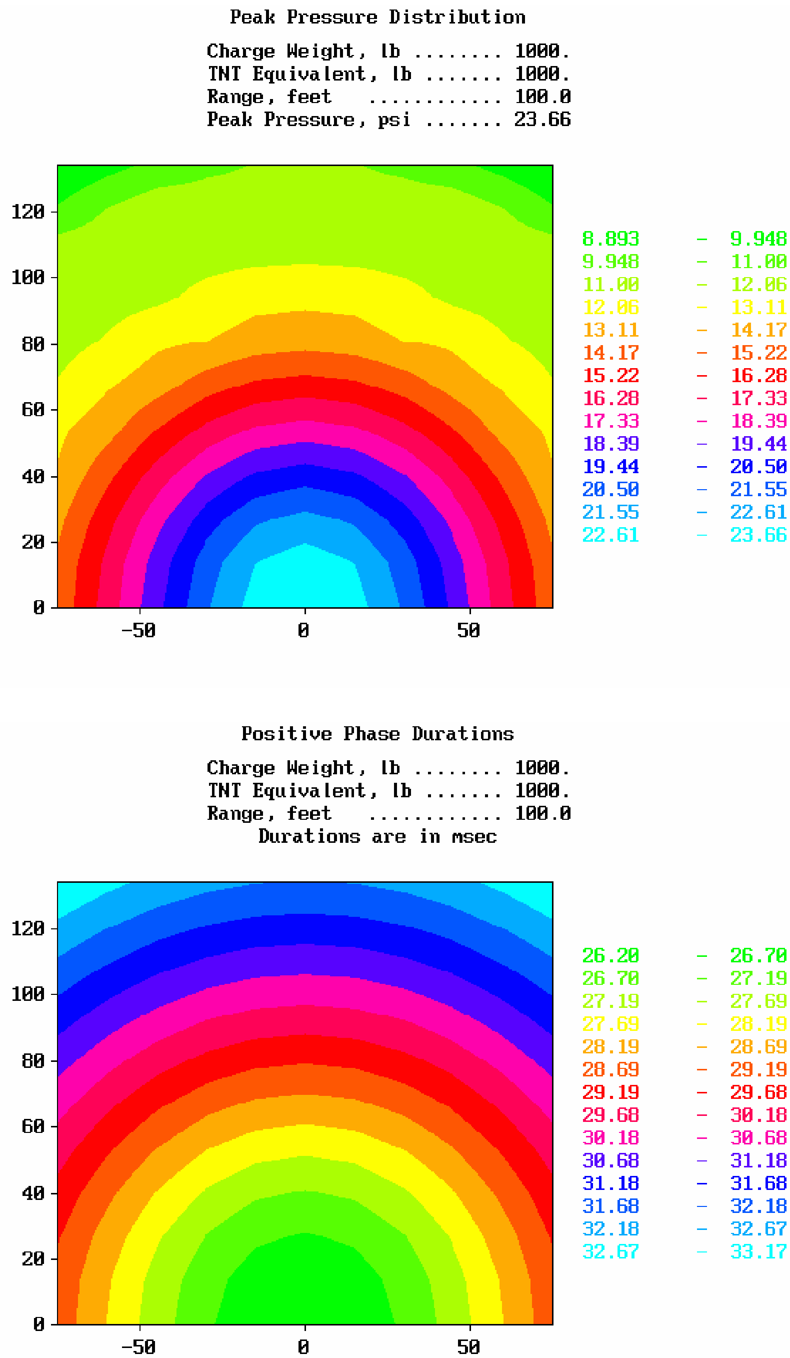

Figure 5.4 : Distribution of Peak Reflected Pressure and Time Duration at 100 ft Stand-Off

5.1.2. Responses of Ten Story Building

To obtain the response of ten story building, SAP2000 FEM Software was used. The blast loads are generated at each joint as Figure 5.1- Figure 5.4. The dynamic time history indicates that number of output time steps is 1,000 and output time step size is 0.005. The damping ratio is assumed as 5 %.

In this chapter, dynamic time history curves are obtained by each case. All cases applied a loading condition of 1,000 lb TNT explosive weight at 15 ft, 30 ft, 50 ft, and 100 ft. The results are shown in Figure 5.5.

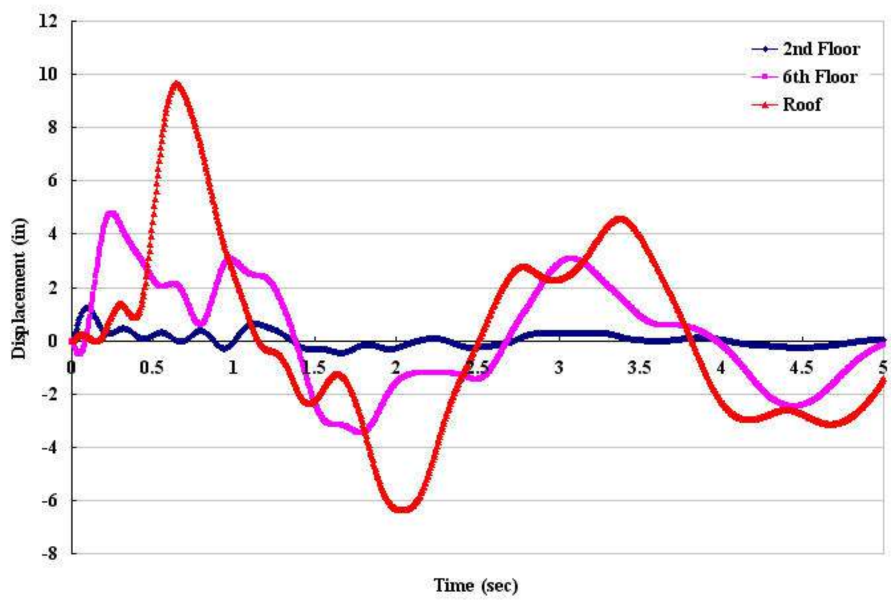

(a) 1,000 lb TNT Weight at 15 ft Stand-Off

Figure 5.5 : Linear Dynamic Time History to Variable Stand-Off Distances

"Figure 5.5 : Continued"

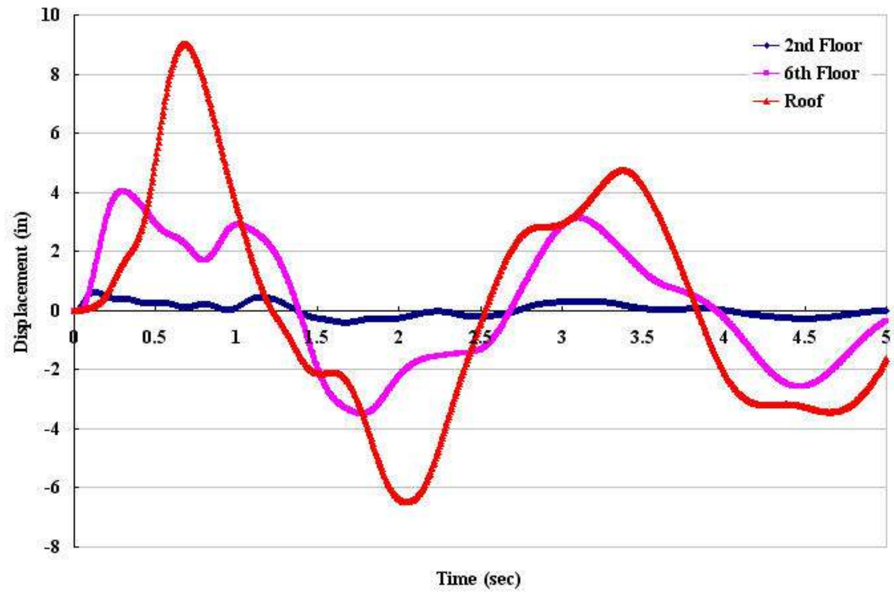

(b) 1,000 lb TNT Weight at 30 ft Stand-Off

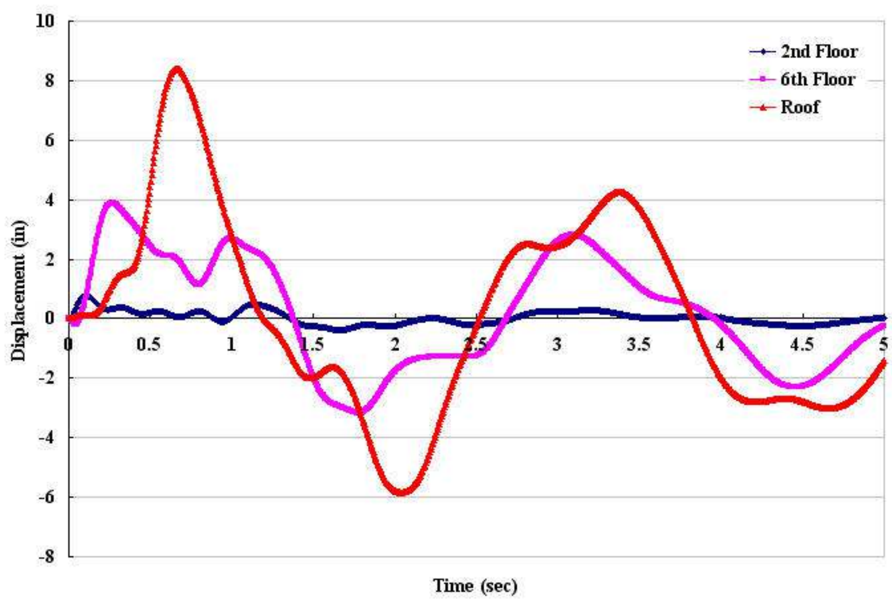

(c) 1,000 lb TNT Weight at 50 ft Stand-Off

“Figure 5.5 : Continued”

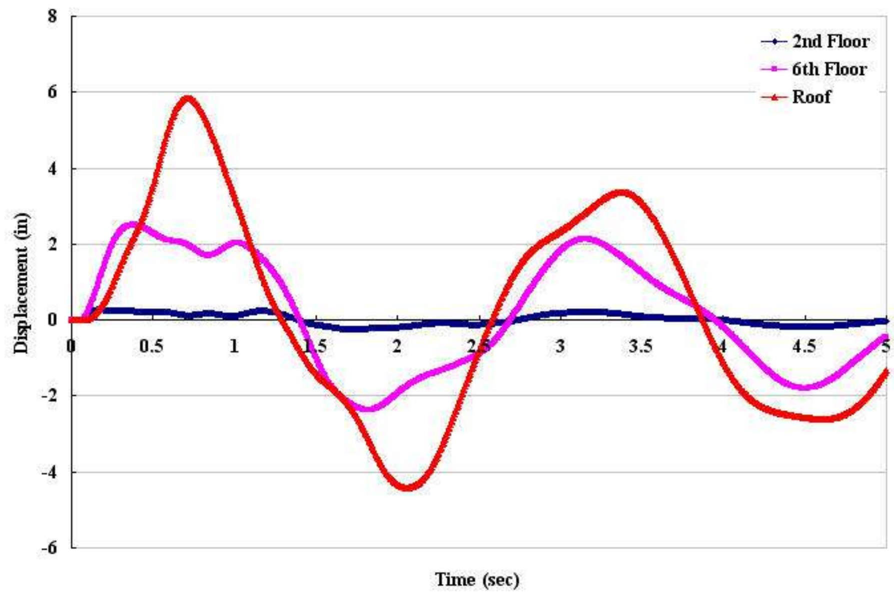

(d) 1,000 lb TNT Weight at 100 ft Stand-Off

To find critical column corresponding to each case, the result of analysis from SAP2000 based on UBC 97 LRFD design code shows demand/capacity ratio of all frame. These values are obtained by combination of dead load, live load and blast loads. Figure 5.6 – Figure 5.7 show demand/capacity ratio of each frame against applied loads along both directions. As a result, critical column on transverse direction was found at closest distance of blast source.

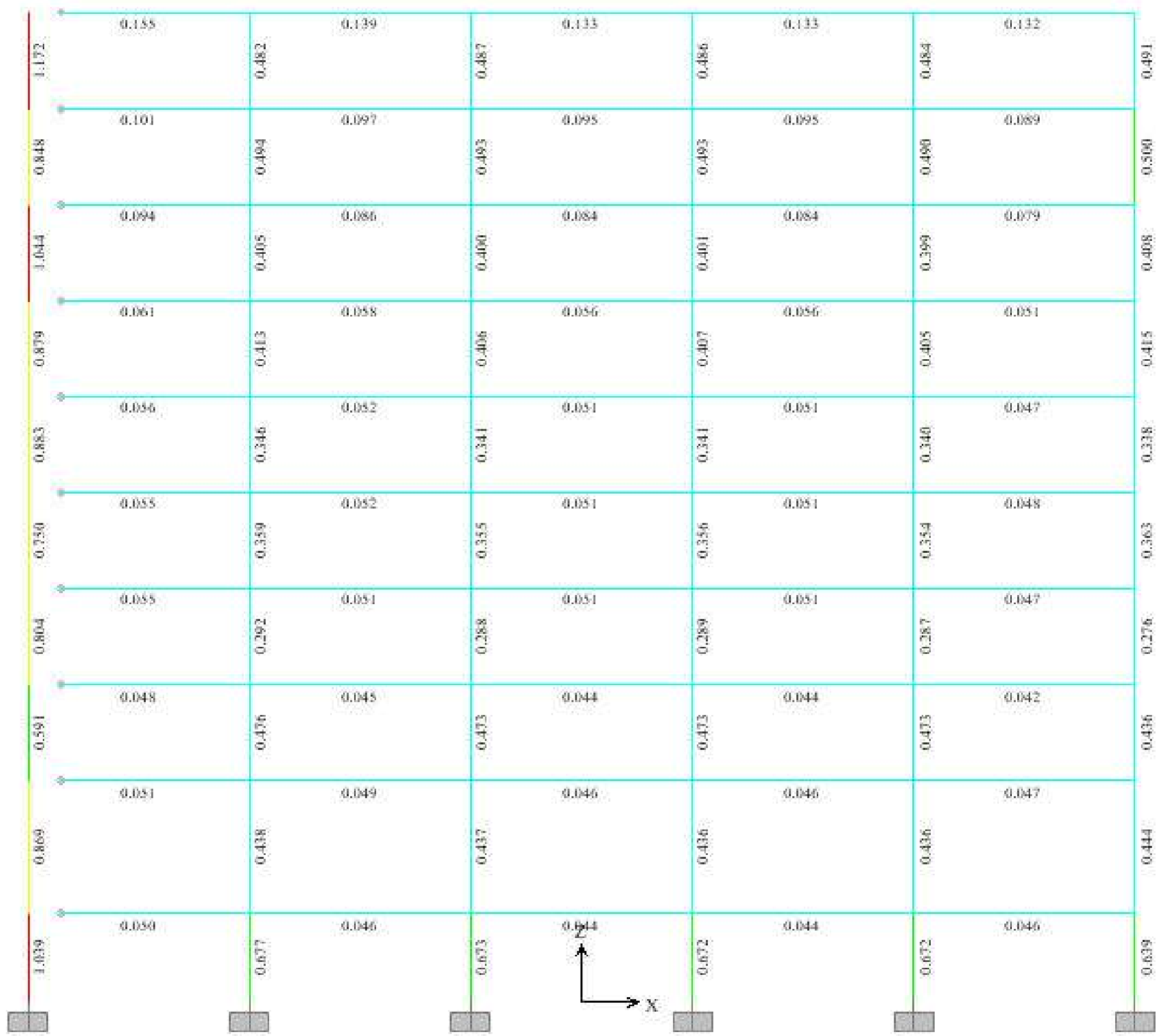

(a) 1,000 lb Weight at 15 ft Stand-off

Figure 5.6 : Demand/Capacity Ratio on Transverse MRF to Variable Stand-Off Distances

“Figure 5.6 : Continued”

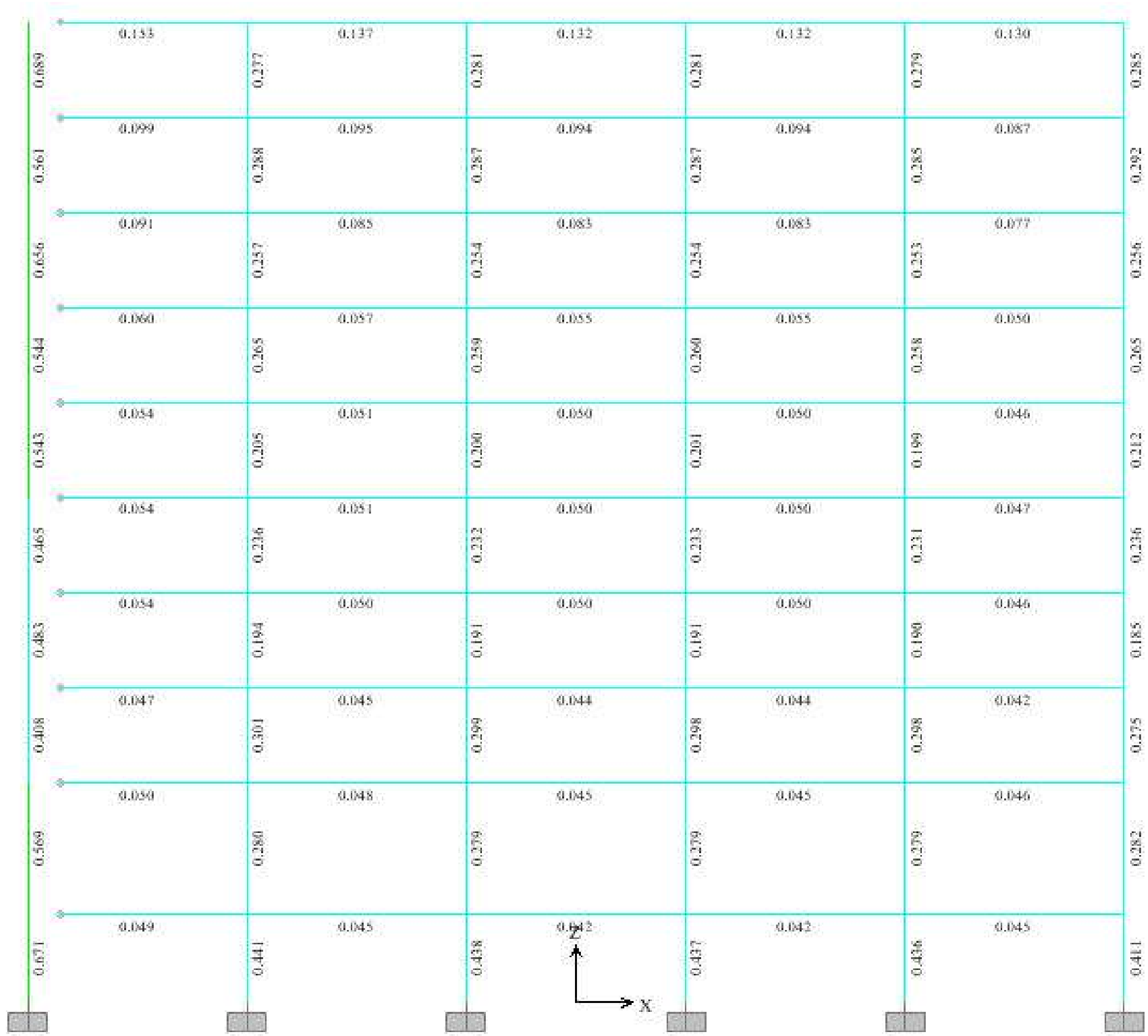

(b) 1,000 lb Weight at 30 ft Stand-off

“Figure 5.6 : Continued”

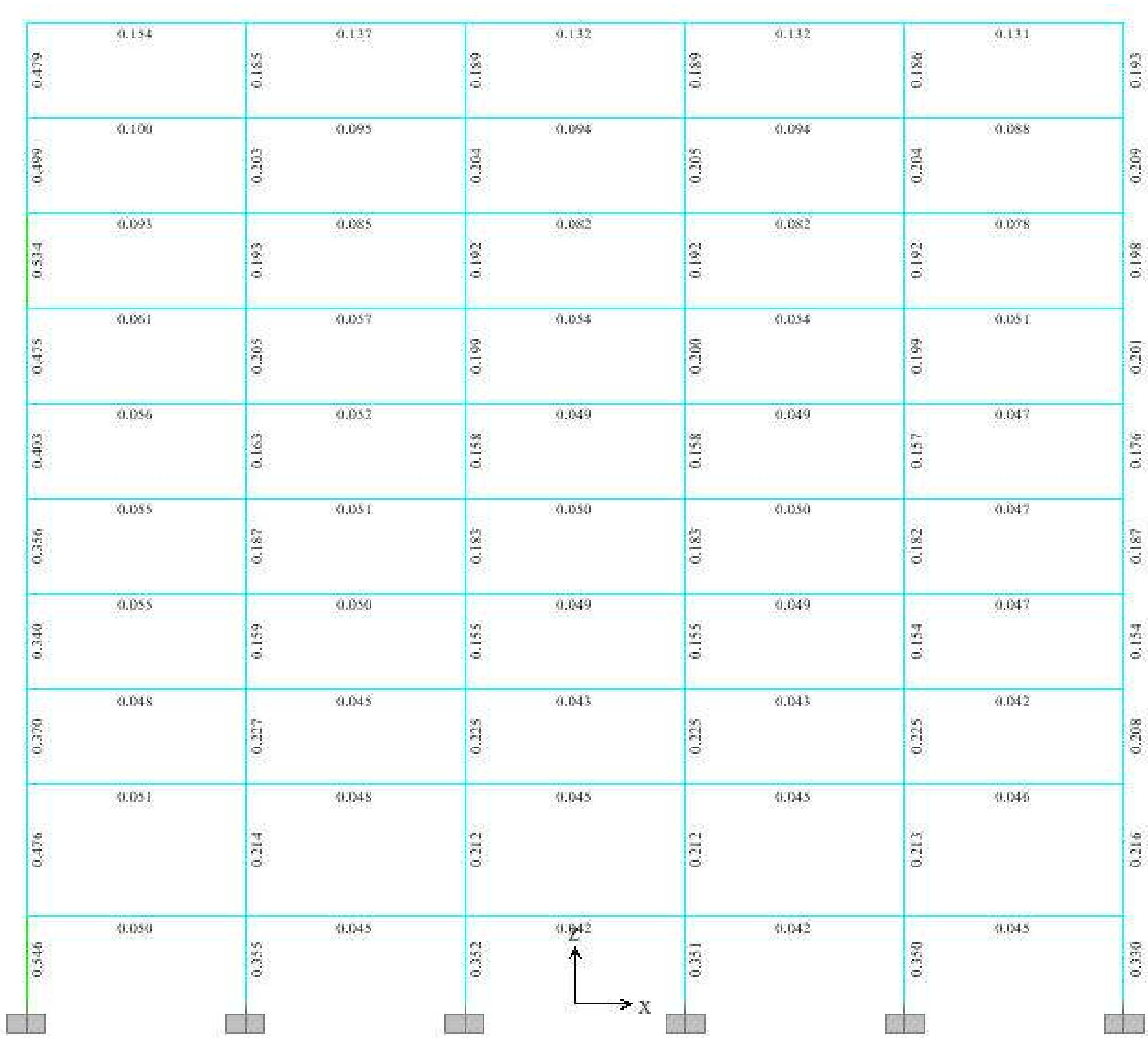

(c) Demand/capacity ratio with 1,000 lb Weight at 50 ft Stand-off

“Figure 5.6 : Continued”

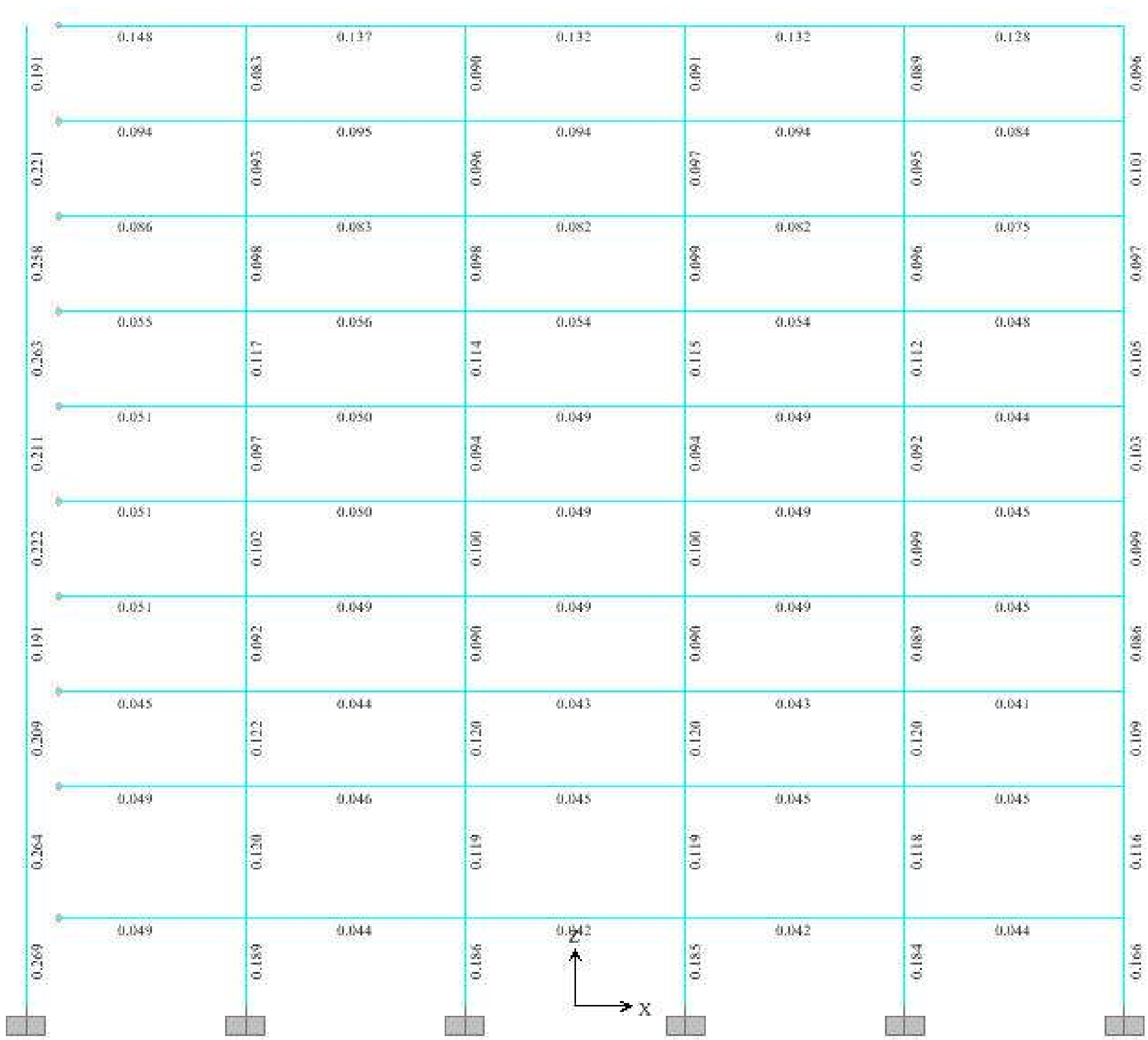

(d) Demand/capacity ratio with 1,000 lb Weight at 100 ft Stand-off

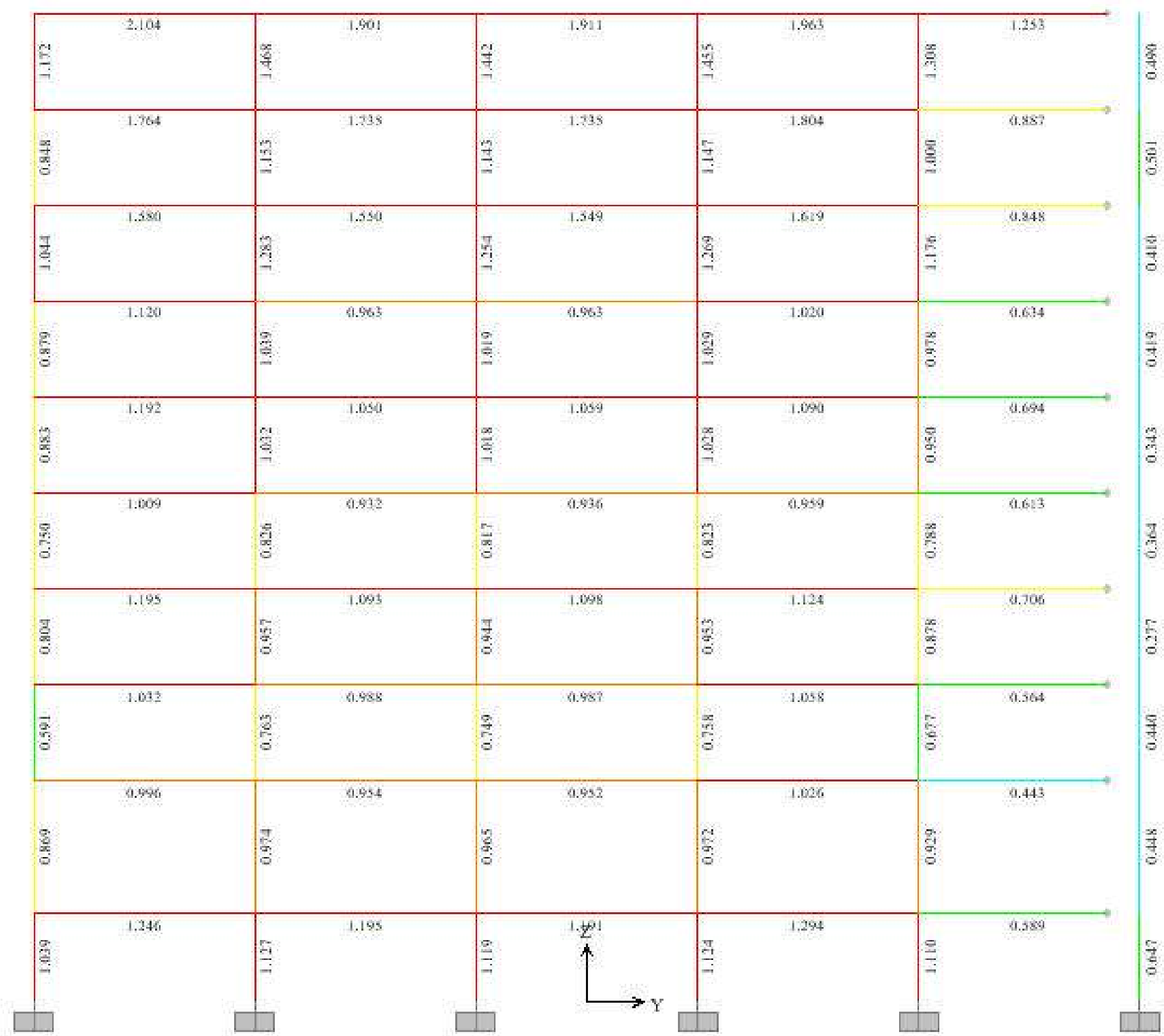

(a) 1,000 lb Weight at 15 ft Stand-off

Figure 5.7 : Demand/Capacity Ratio on Longitudinal MRF to Variable Stand-Off distances

"**Figure 5.7 : Continued**"

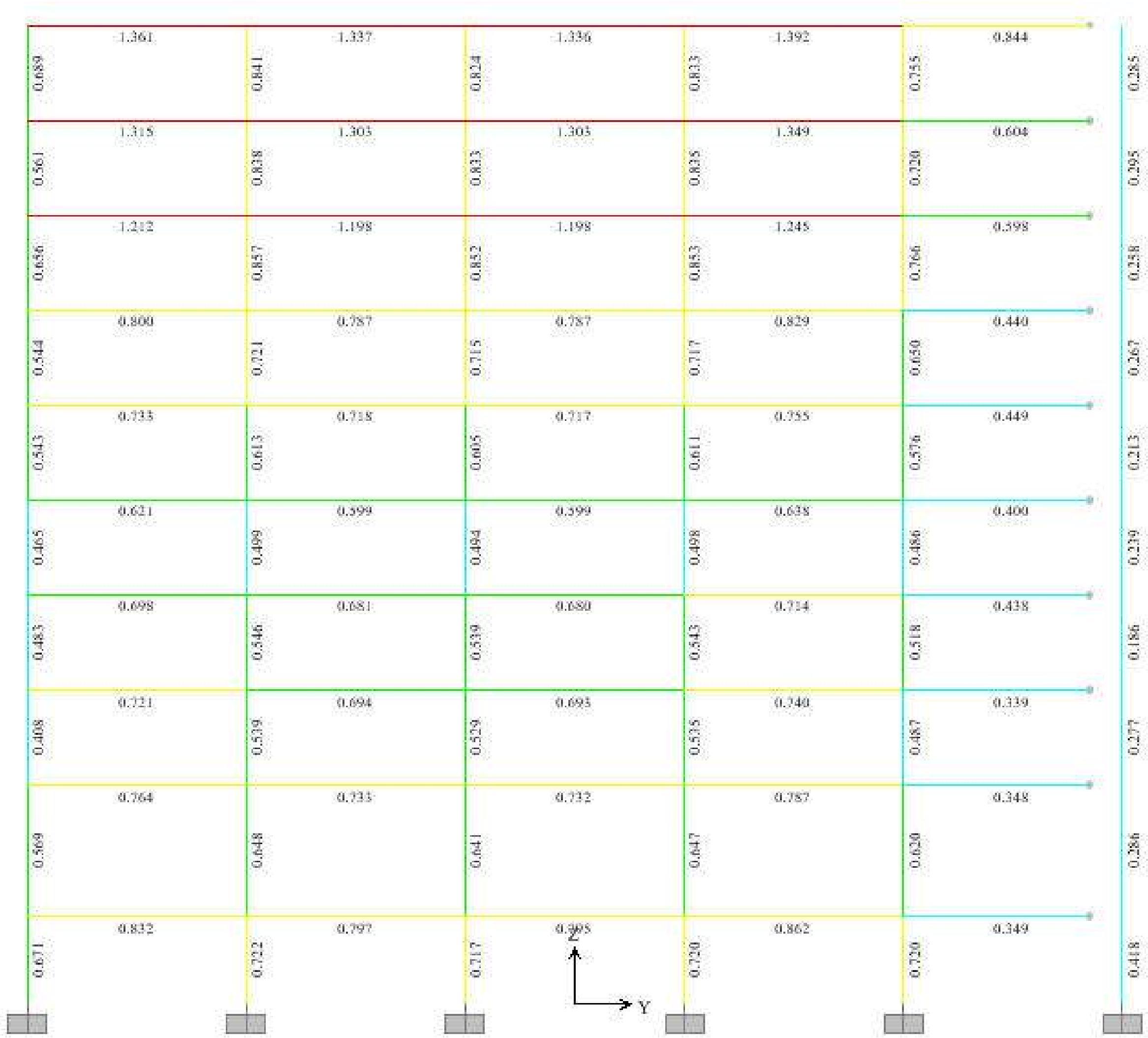

(b) 1,000 lb Weight at 30 ft Stand-off

“Figure 5.7 : Continued”

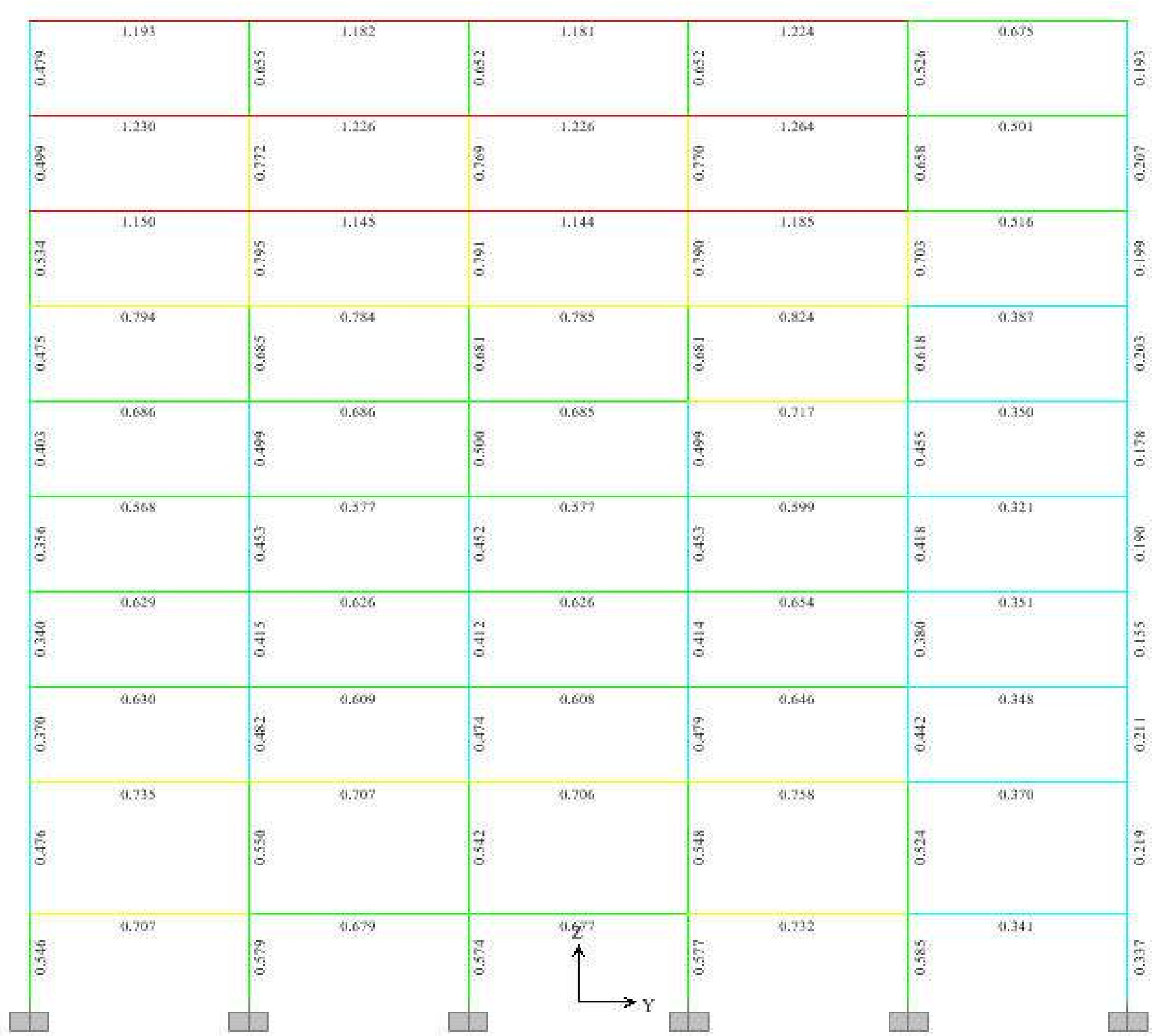

(c) 1,000 lb Weight at 50 ft Stand-off

"Figure 5.7 : Continued"

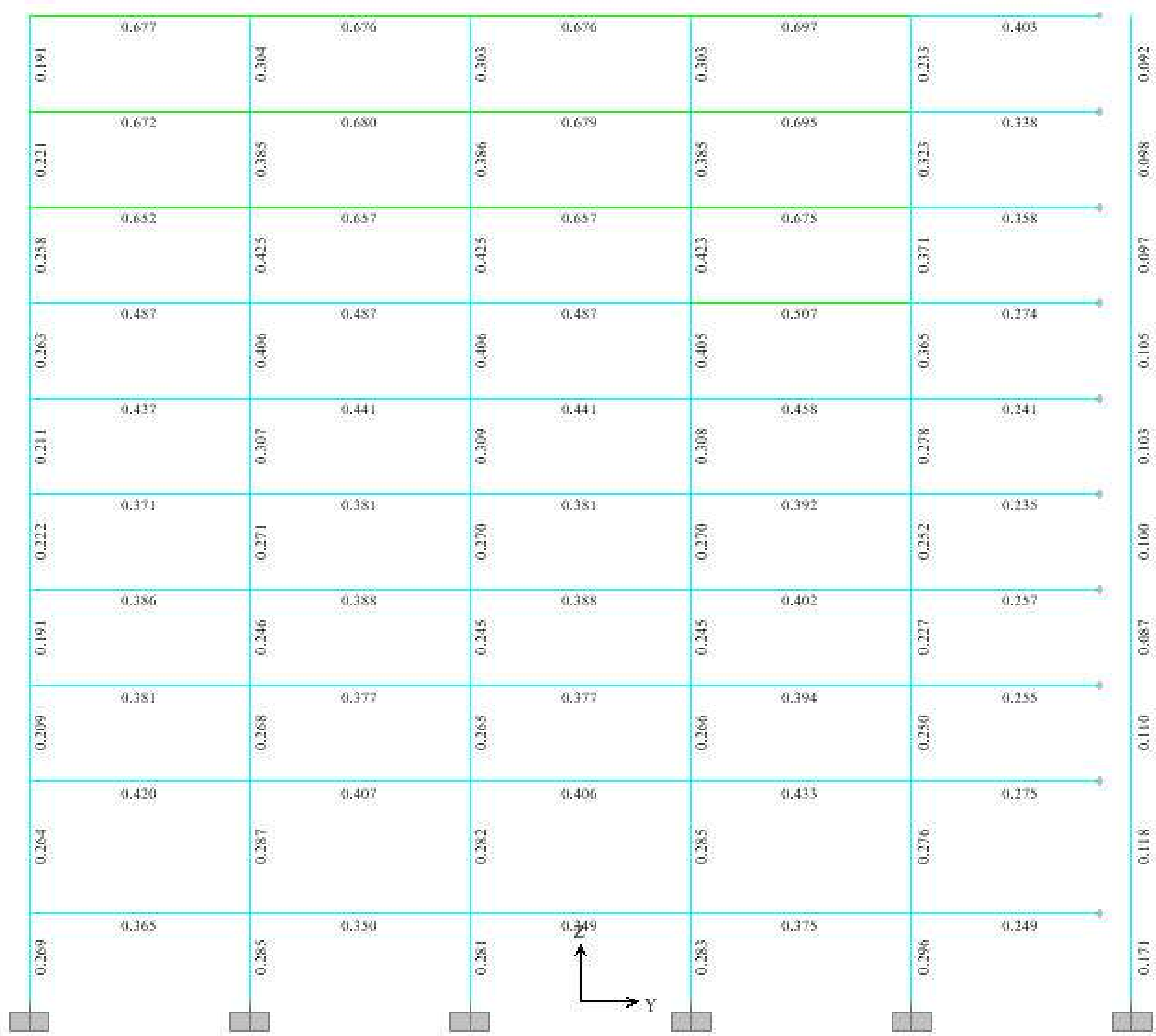

(d) 1,000 lb Weight at 100 ft Stand-off

5.1.3. Summary

As results of dynamic time history analysis with variable stand-off distance, maximum deflections are shown in Figure 5.8. As might be expected, the maximum deflection occurs for the 1,000 TNT weight @ 15 ft standoff distance. The maximum displacement occurs at Roof and minimum displacement occurs at 2nd floor. The maximum displacements are 9.64 in, 9.02 in, 8.39 in and 5.84 in and minimum displacements are 1.24 in, 0.77 in, 0.61 in and 0.27 in respectively.

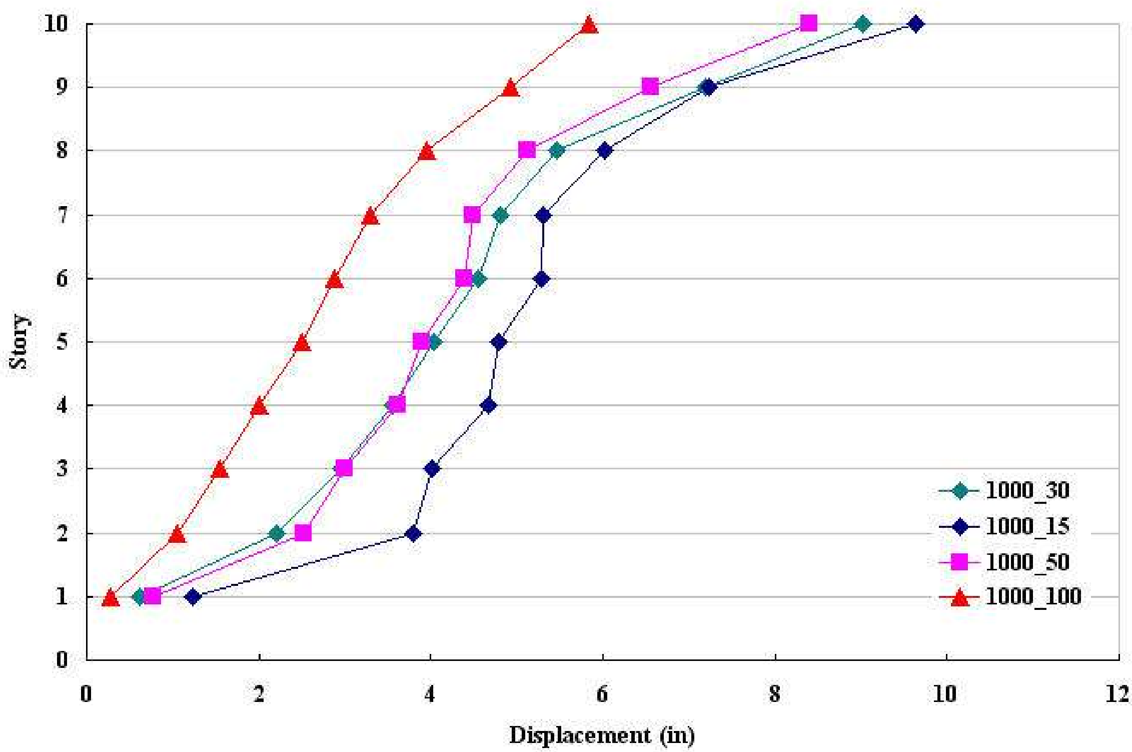

Figure 5.8 : Maximum Deflection on Each Floor to Variable Stand-Off Distance

Based on maximum displacements, instestory drifts are shown in Figure 5.9. The code limitation of drift ratio based on UBC'97 for earthquake is 0.02 and the responses of all conditions satisfy with code limitation.

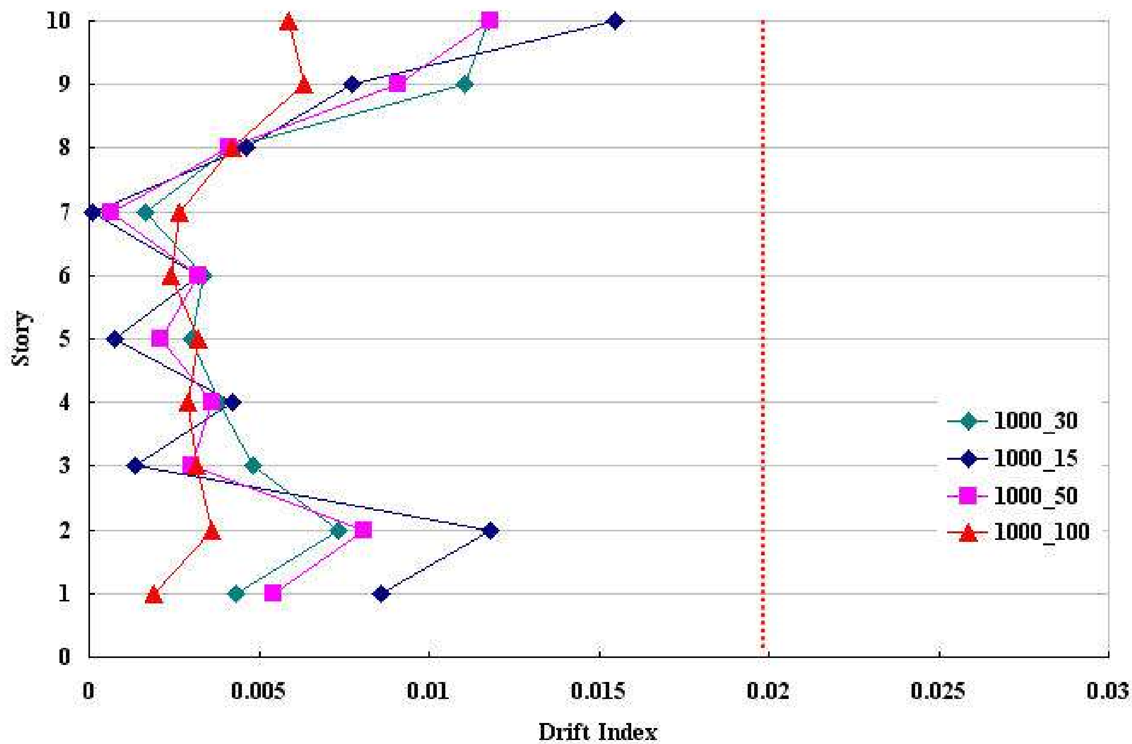

Figure 5.9 : Interstory Drift to Variable Stand-Off Distance

The maximum demand/capacity ratios for the columns in each story of the transverse frame and longitudinal frame for an explosive weight of 1,000 lb are summarized in Figure 5.10 and Figure 5.11. Here it can be seen that the D/C ratio are all less than unity indicating elastic behavior. However, one case of longitudinal direction with 1,000 TNT weight at 15 ft stand-off distance, is greater than unity with a maximum of about 1.5.

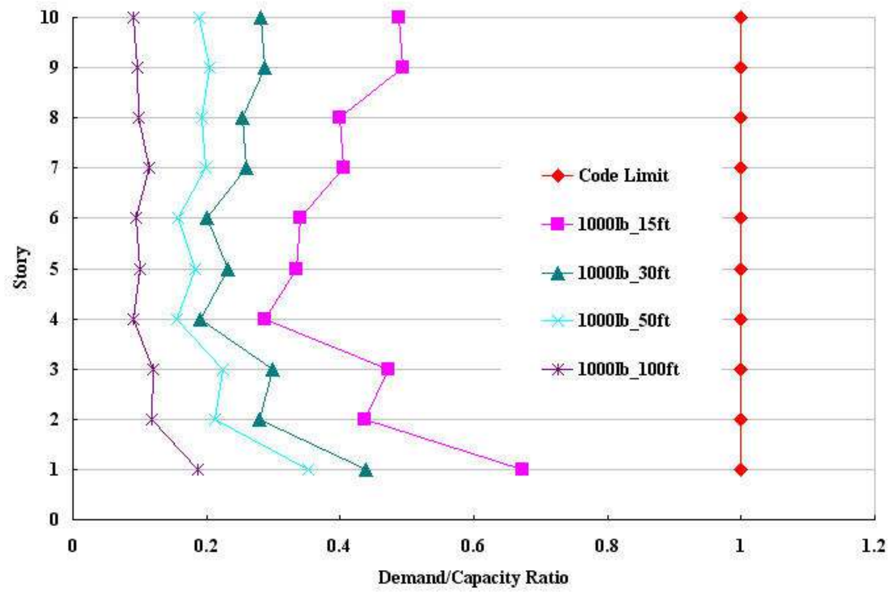

Figure 5.10 : Demand/Capacity Ratio to Variable Stand-Off Distance on Transverse MRF

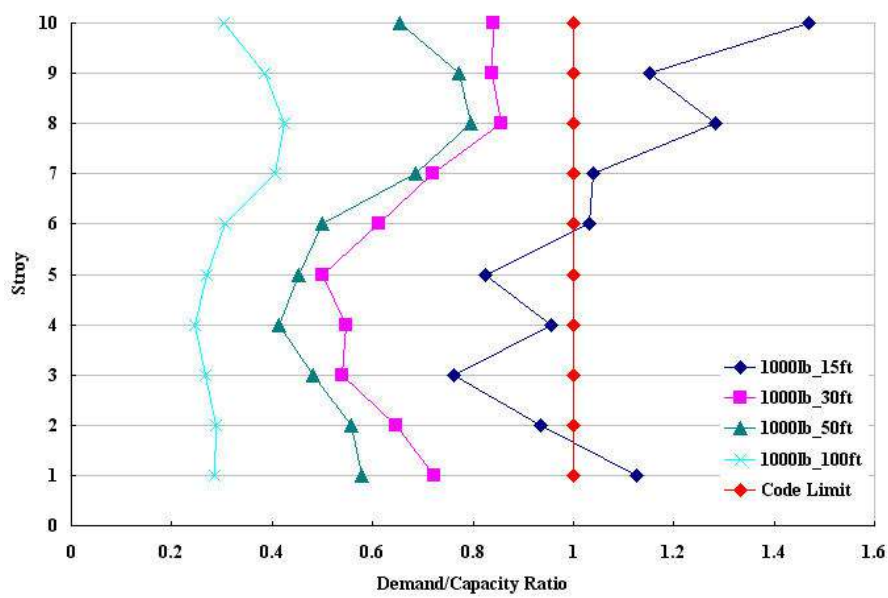

Figure 5.11 : Demand/Capacity Ratio to Variable Stand-Off Distance on Longitudinal MRF

5.2. Structural Response to Variable TNT Weight

5.2.1. Blast Loads

A frame is subjected to 100 lb, 500 lb, 1,000 lb and 2,000 lb TNT blast at 20 ft stand-off distance in this chapter. To find blast loads on ten story building at each joint, the CONWEP program was used. Figure 5.12 - Figure 5.15 show time duration and peak reflected pressure on front frame of structure.

When blast with 100 lb, 500 lb, 1,000 lb, 2,000 lb TNT weight at 20 ft stand-off distance impinges on a structure, a higher pressure is developed, termed the reflected pressure. The calculated (CONWEP) peak overpressures on the front frame are shown in Figure 5.12 – Figure 15. These range from a maximum of 248.5 psi (100 lb), 1177 psi (500 lb), 2109 psi (1,000 lb), 3689 psi (2,000 lb) at the point closest to the detonation to a minimum of 2.13 psi (100 lb), 4.11 psi (500 lb), 5.67 psi (1,000 lb), 8.09 psi (2,000 lb) at the upper west/east corner.

While these pressures are extremely large, they act for a limited duration, as shown in Figure 5.12 – Figure 5.15. The duration ranges from a maximum of 18.68 msec (100 lb), 26.87 msec (500 lb), 31.36 msec (1,000 lb), 36.28 msec (2,000 lb) in the upper west/east corner to a minimum of 7.35 msec (100 lb), 10.58 msec (500 lb), 6.09 msec (1,000 lb), 4.07 msec(2,000 lb) at the upper west/east corner.

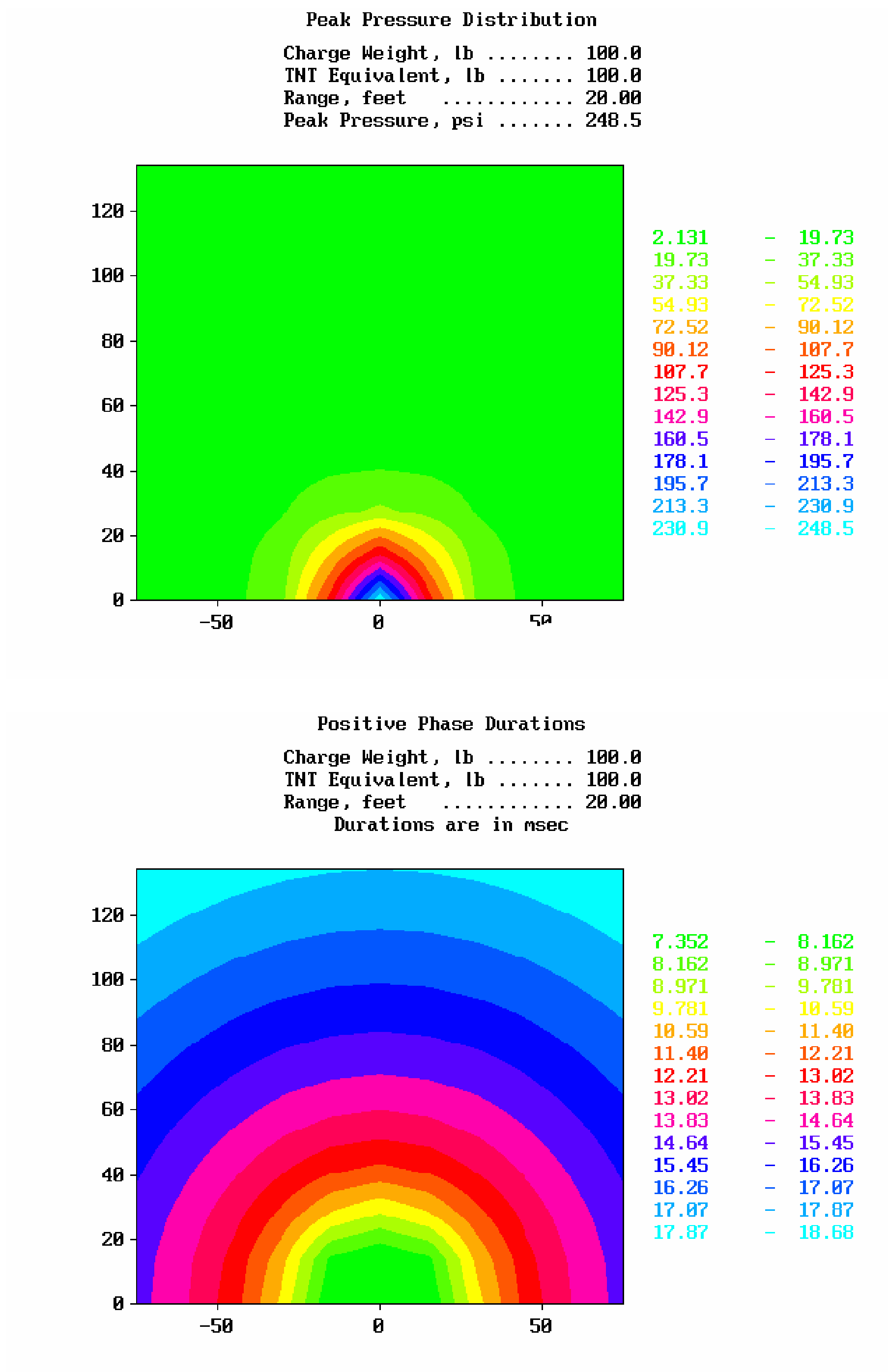

Figure 5.12 : Distribution of Peak Reflected Pressure and Time Duration on 100 lb TNT weight

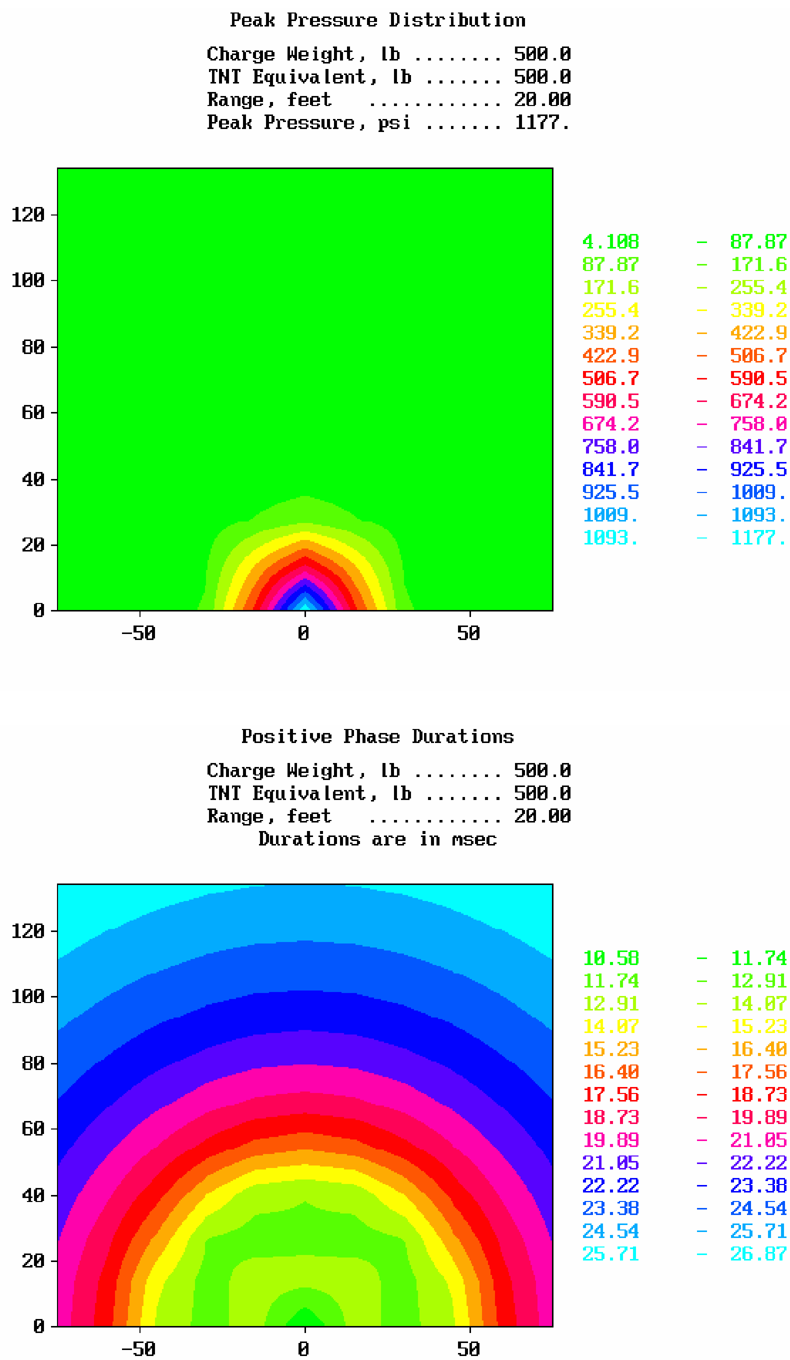

Figure 5.13 : Distribution of Peak Reflected Pressure and Time Duration on 500 lb TNT weight

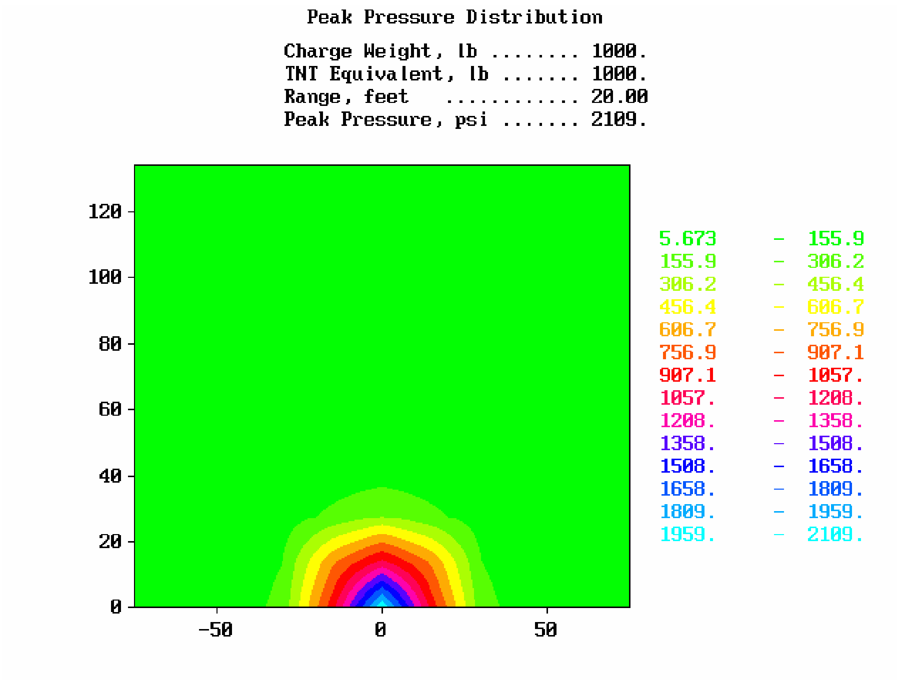

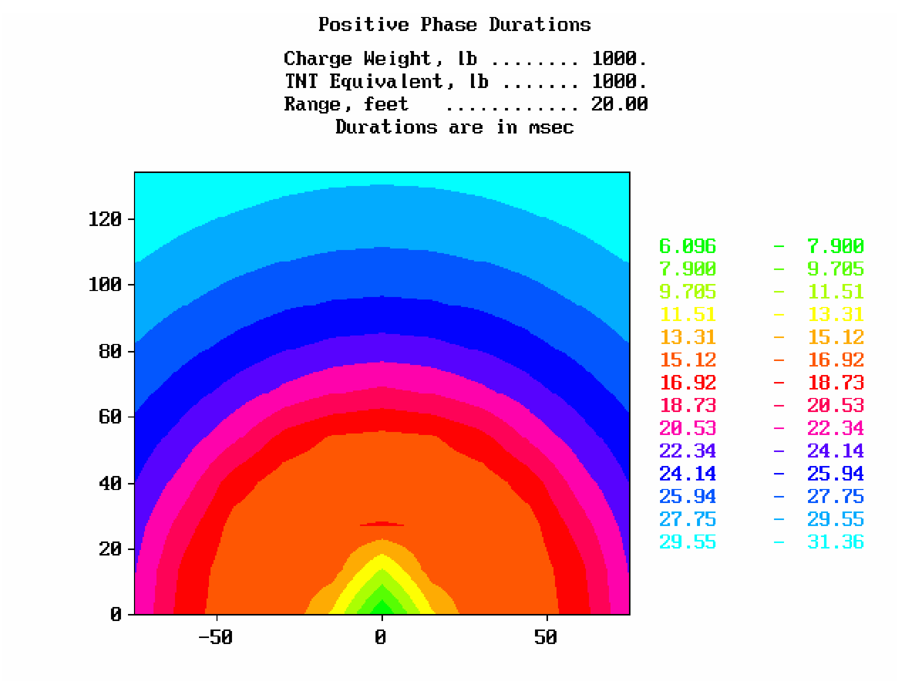

Figure 5.14 : Distribution of Peak Reflected Pressure and Time Duration on 1,000 lb TNT weight

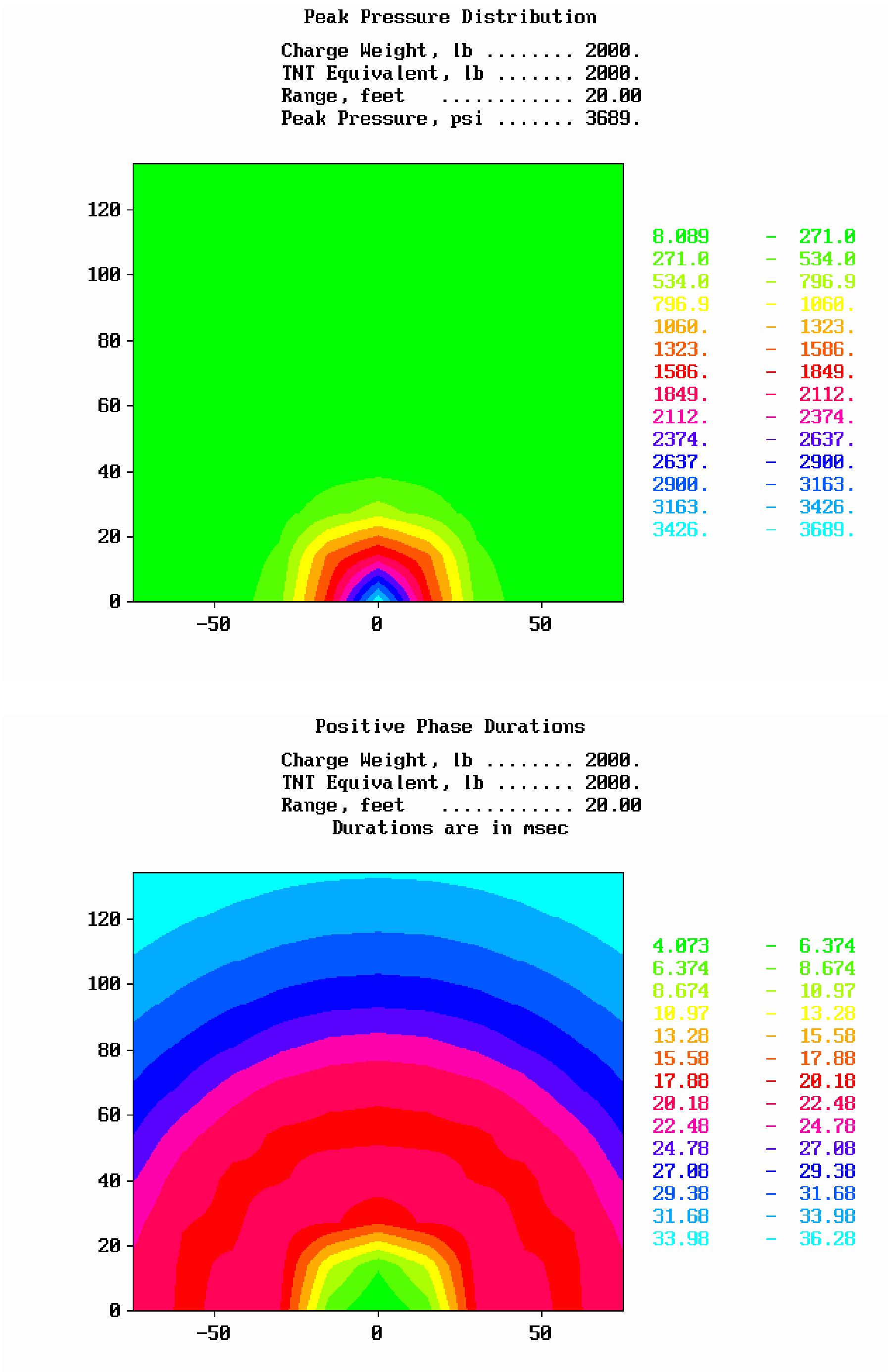

Figure 5.15 : Distribution of Peak Reflected Pressure and Time Duration on 2,000 lb TNT weight

5.2.2. Responses of Ten Story Building

To obtain the response of ten story building, SAP2000 FEM Software was used. The blast loads are generated at each joint as peak reflected pressure from CONWEP. The dynamic time history indicates that number of output time steps is 1,000 and output time step size is 0.005. The damping ratio is assumed as 5%. Dynamic time history curves of each floor at 20 ft with 100 lb, 500 lb, 1,000 lb, 2,000 lb TNT weight are shown in Figure 5.16.

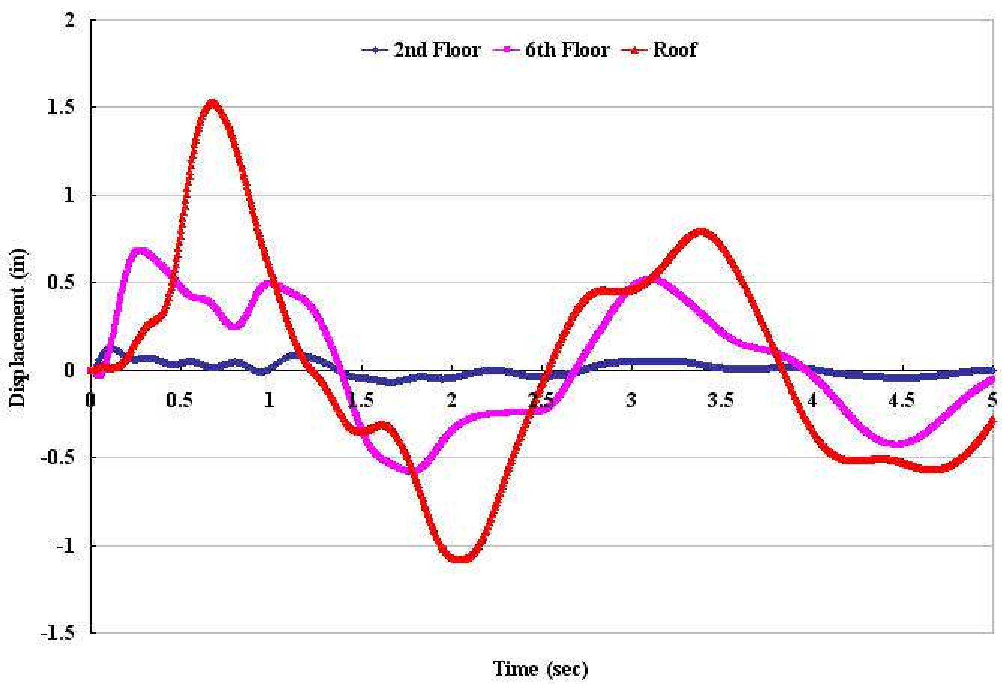

(a) 100 lb TNT Weight at 20 ft Stand-Off

Figure 5.16 : Linear Dynamic Time History to Variable Stand-Off Distances

“Figure 5.16 : Continued”

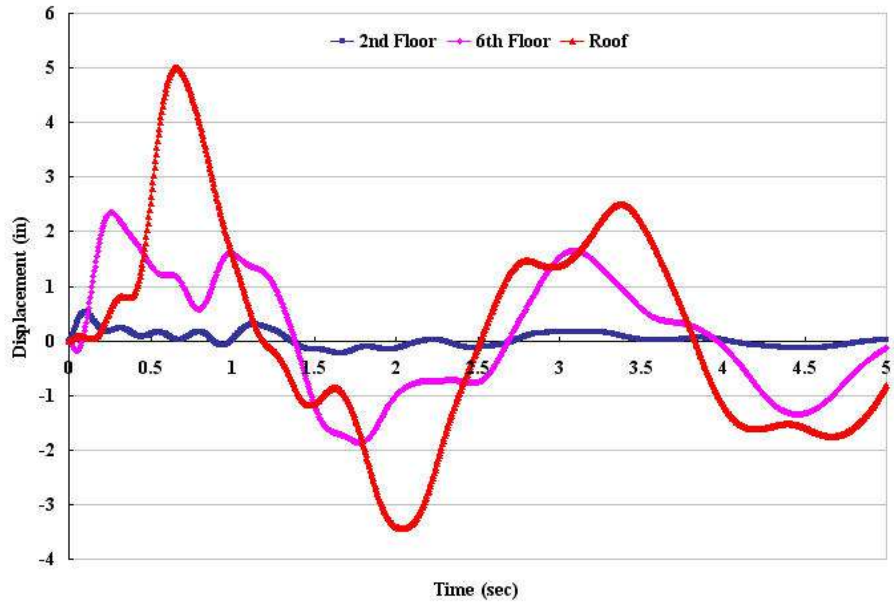

(b) 500 lb TNT Weight at 20 ft Stand-Off

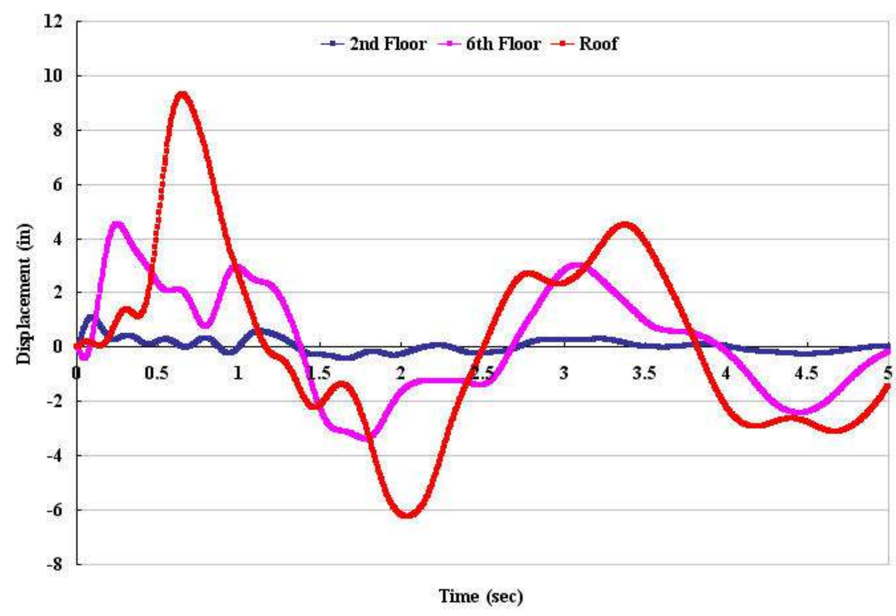

(c) 1,000 lb TNT Weight at 20 ft Stand-Off

“Figure 5.16 : Continued”

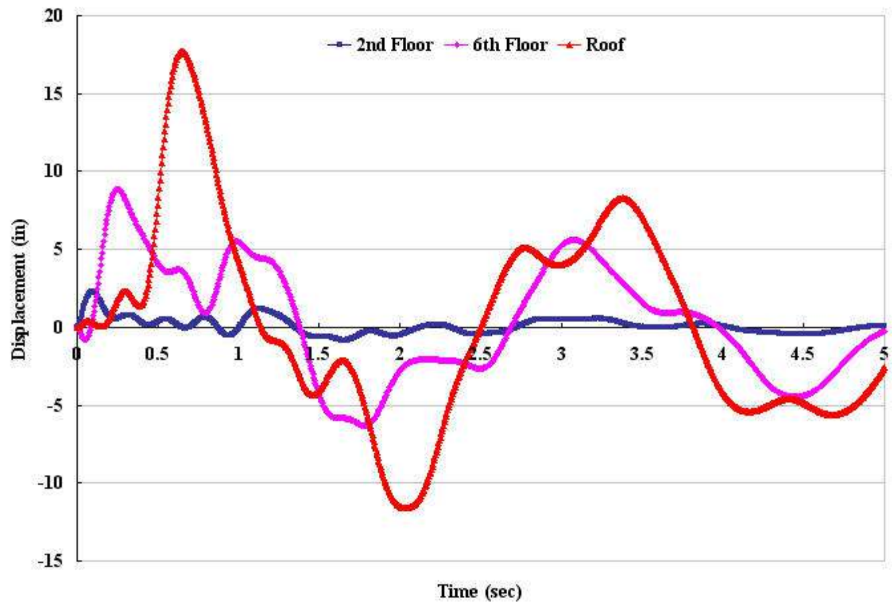

(d) 2,000 lb TNT Weight at 20 ft Stand-Off

To find critical column corresponding to each case, the result of analysis from SAP2000 based on UBC 97 LRFD design code shows demand/capacity ratio of all frame. These values are obtained by combination of dead load, live load and blast loads. Figure 5.17 and Figure 5.18 show demand/capacity ratio of each frame against applied loads along both directions. As a result, critical column on transverse direction was found at closest distance of blast source.

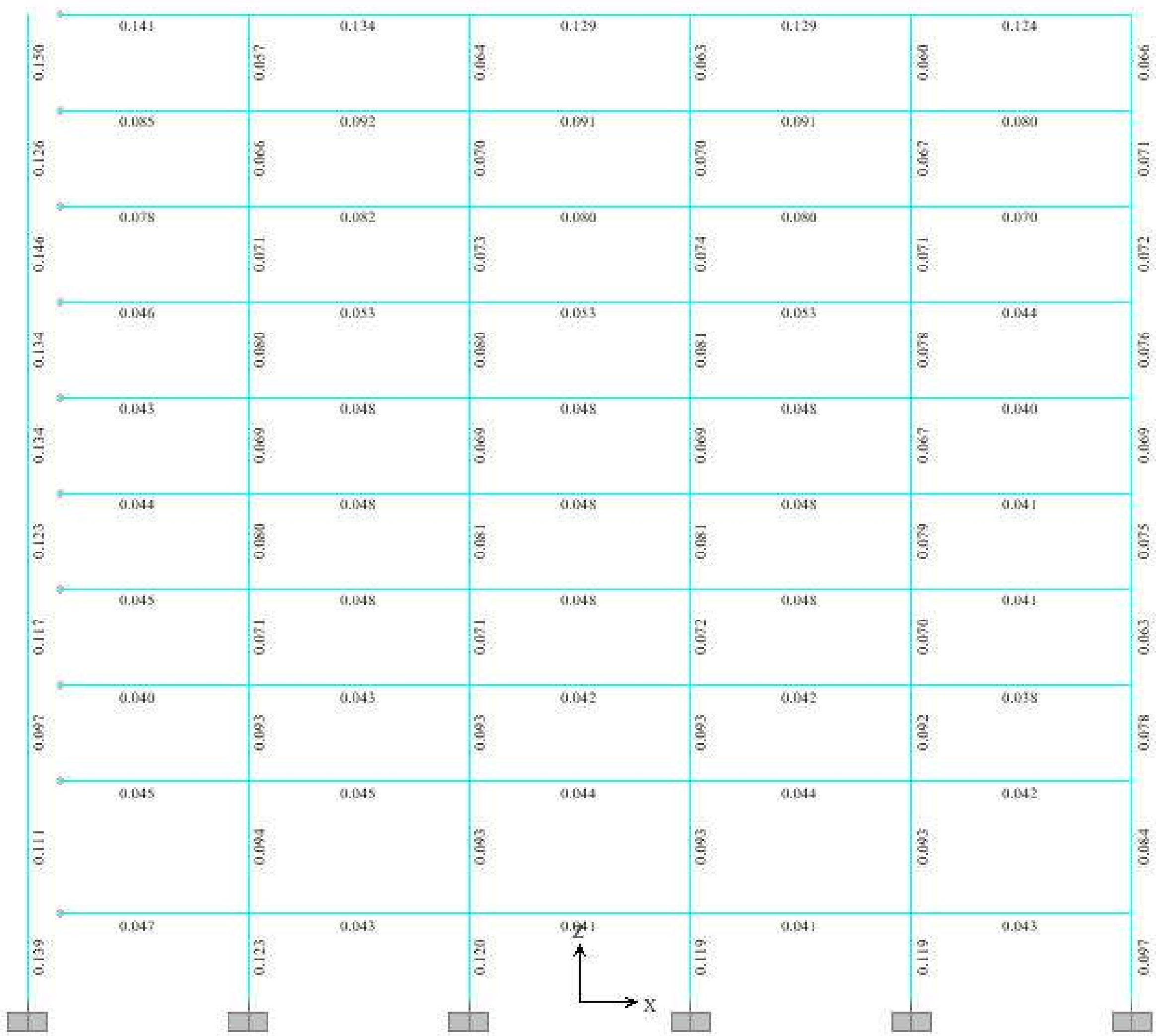

(a) 100 lb Weight at 20 ft Stand-off

Figure 5.17 : Demand/Capacity Ratio on Transverse MRF to Variable TNT Weight

“Figure 5.17 : Continued”

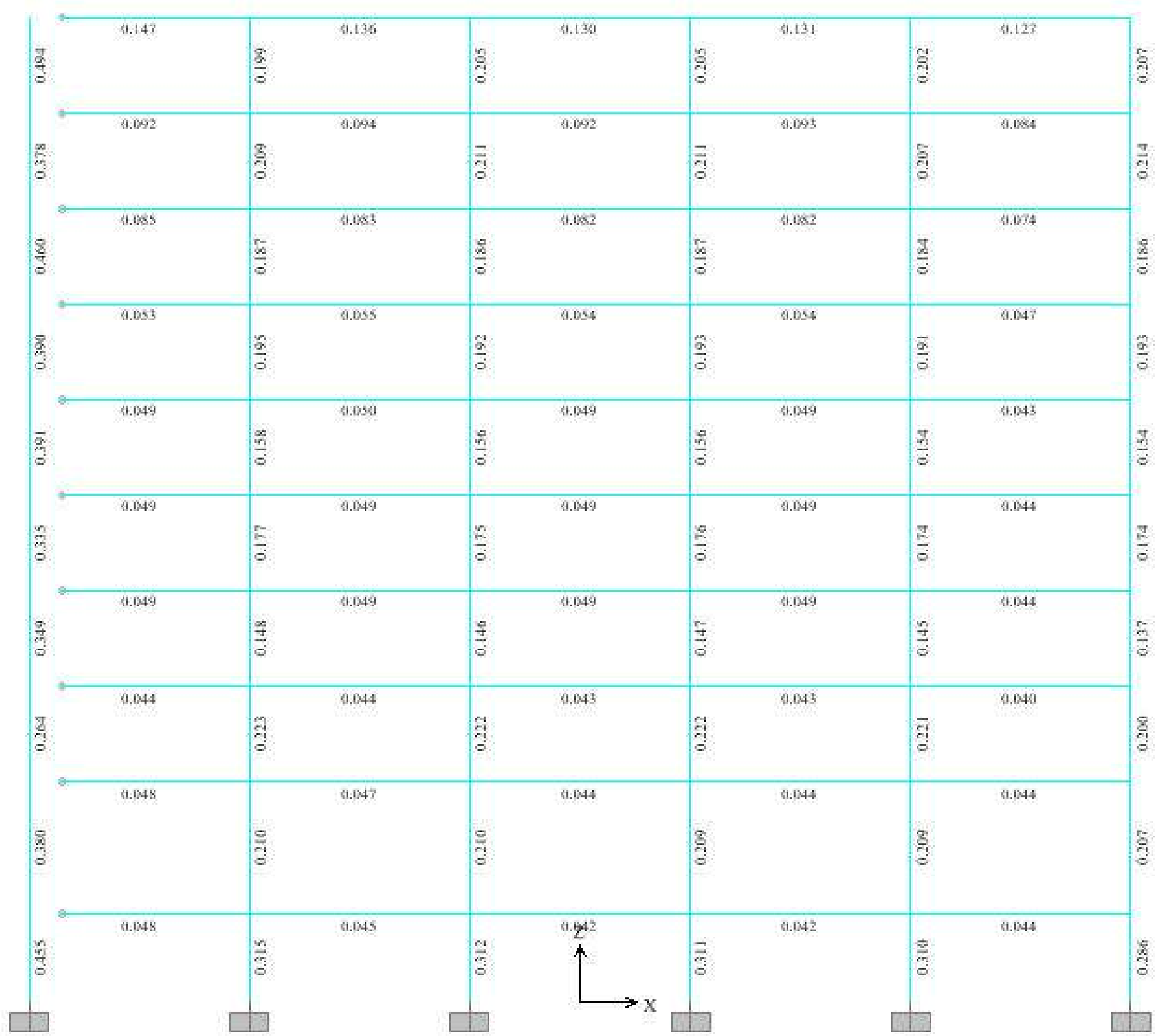

(b) 500 lb Weight at 20 ft Stand-off

“Figure 5.17 : Continued”

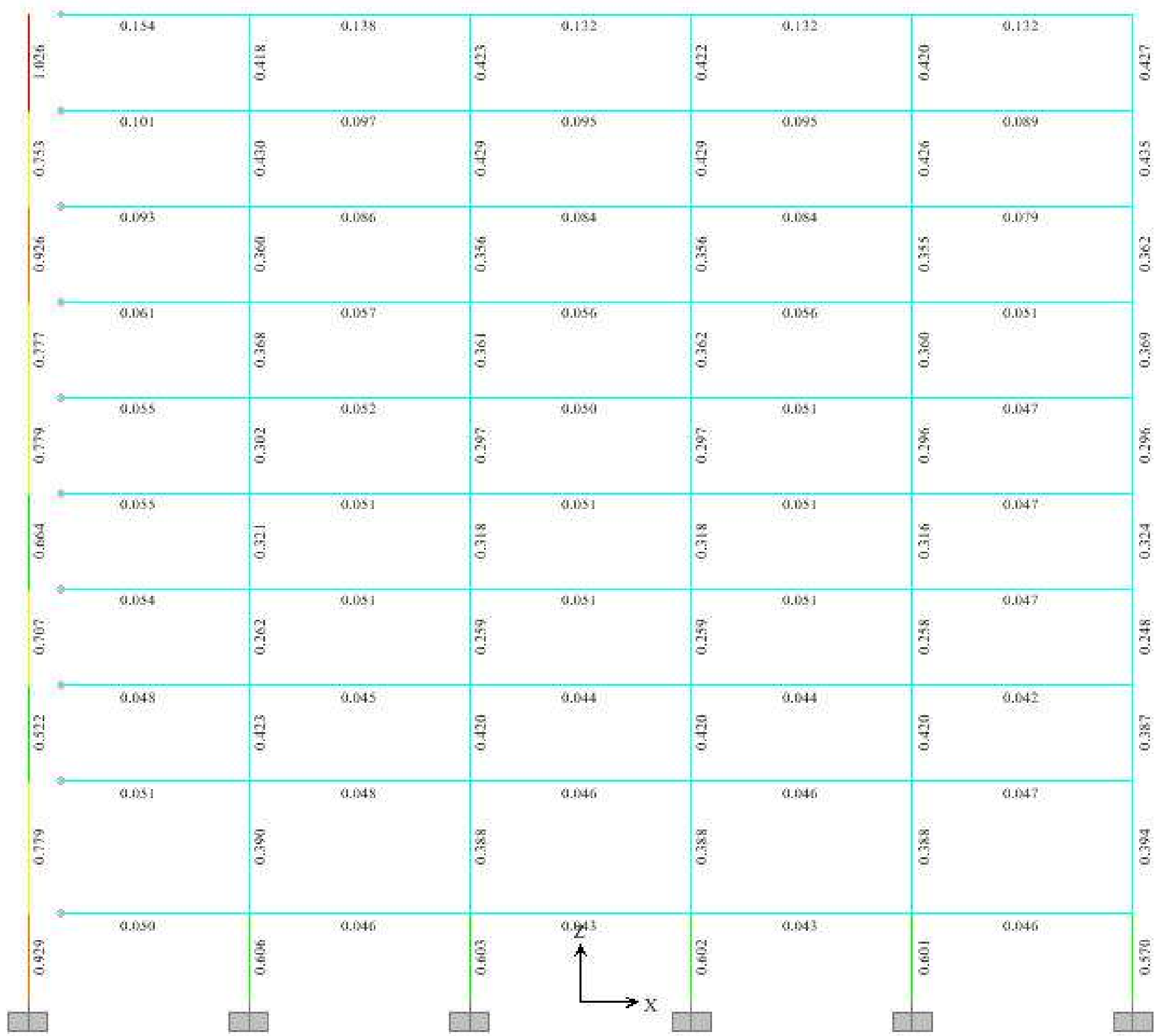

(c) 1,000 lb Weight at 20 ft Stand-off

“Figure 5.17 : Continued”

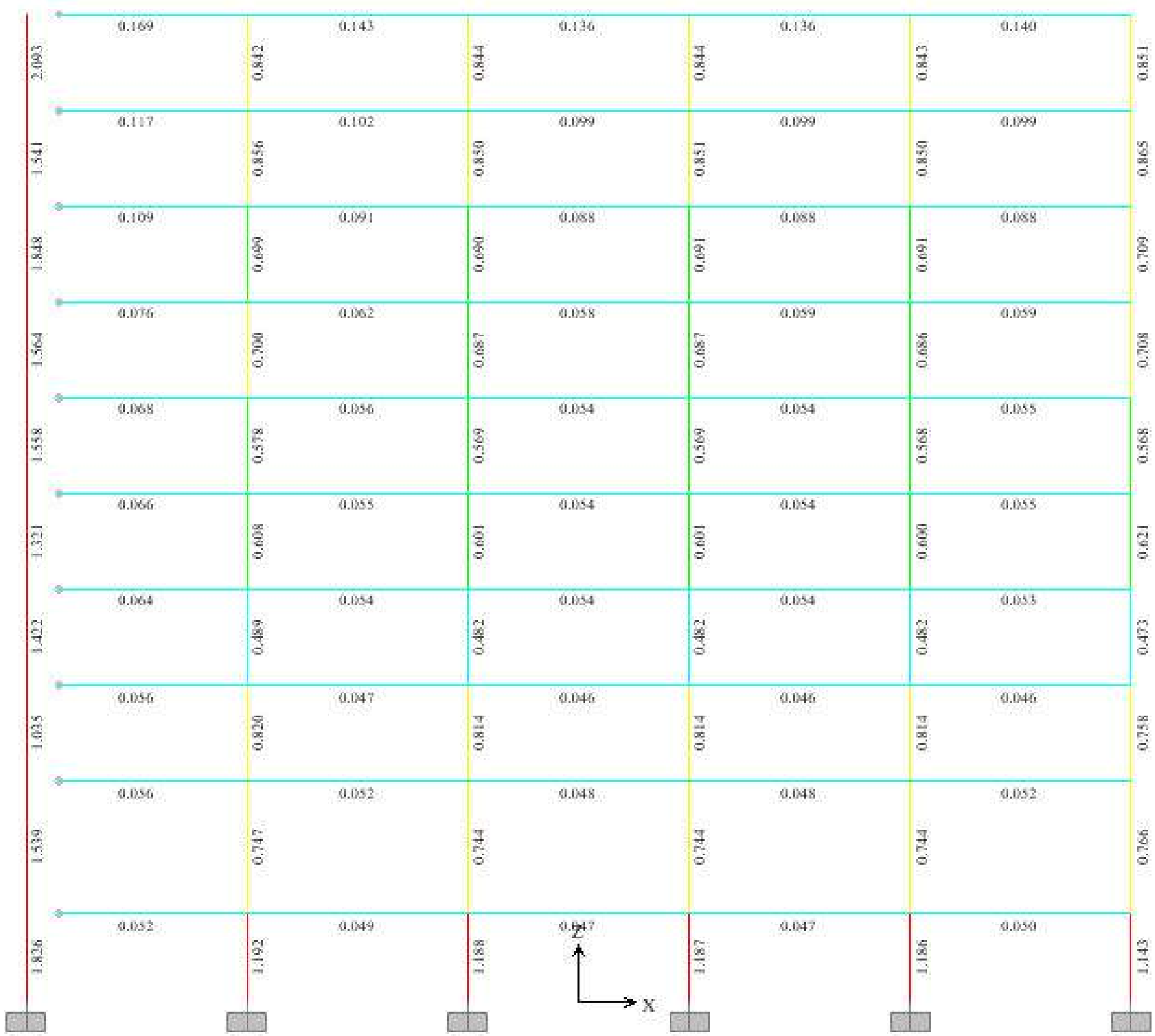

(d) 2,000 lb Weight at 20 ft Stand-off

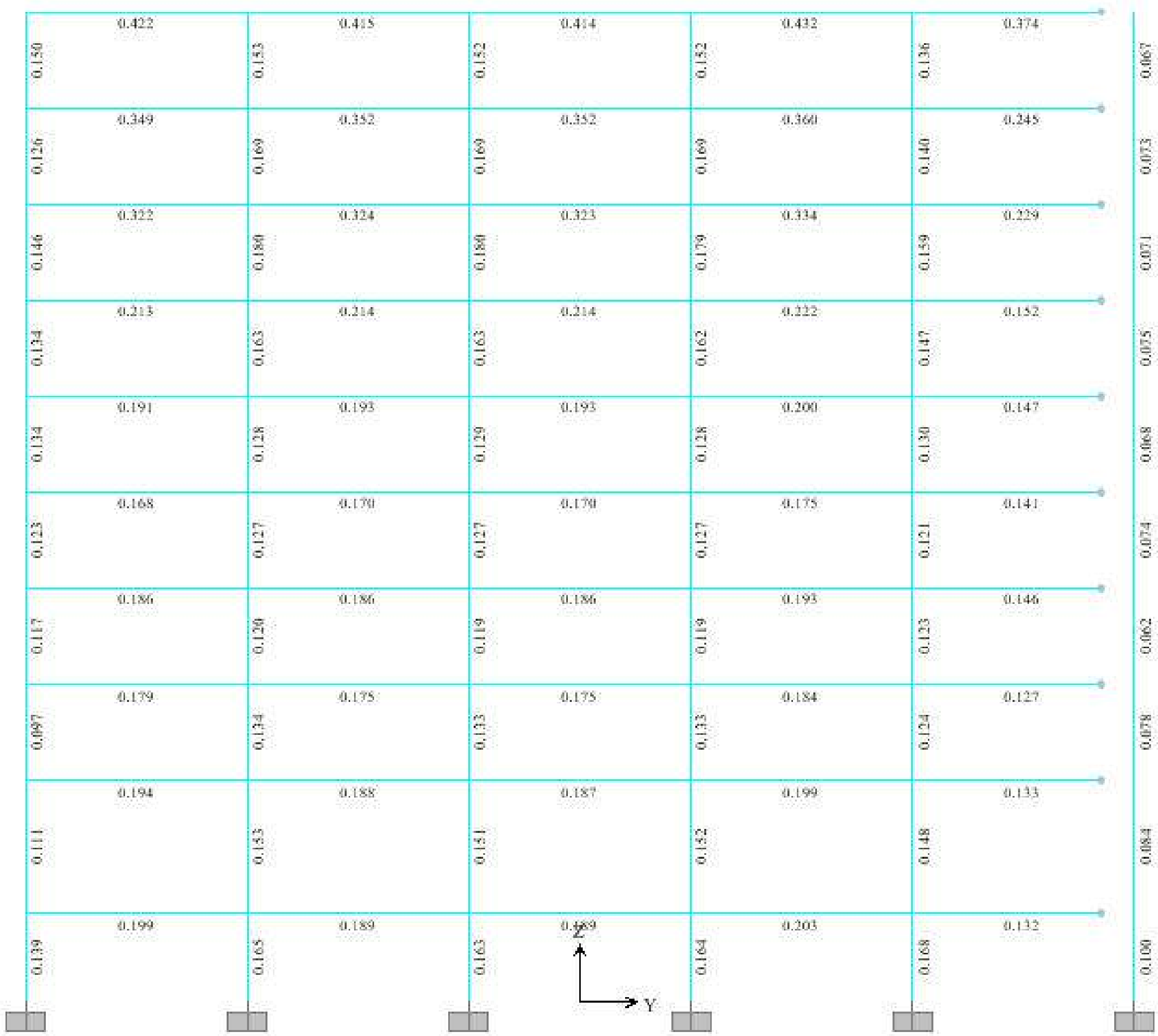

(a) 100 lb Weight at 20 ft Stand-off

Figure 5.18 : Demand/Capacity Ratio on Longitudinal MRF to Variable TNT Weight

“Figure 5.18 : Continued”

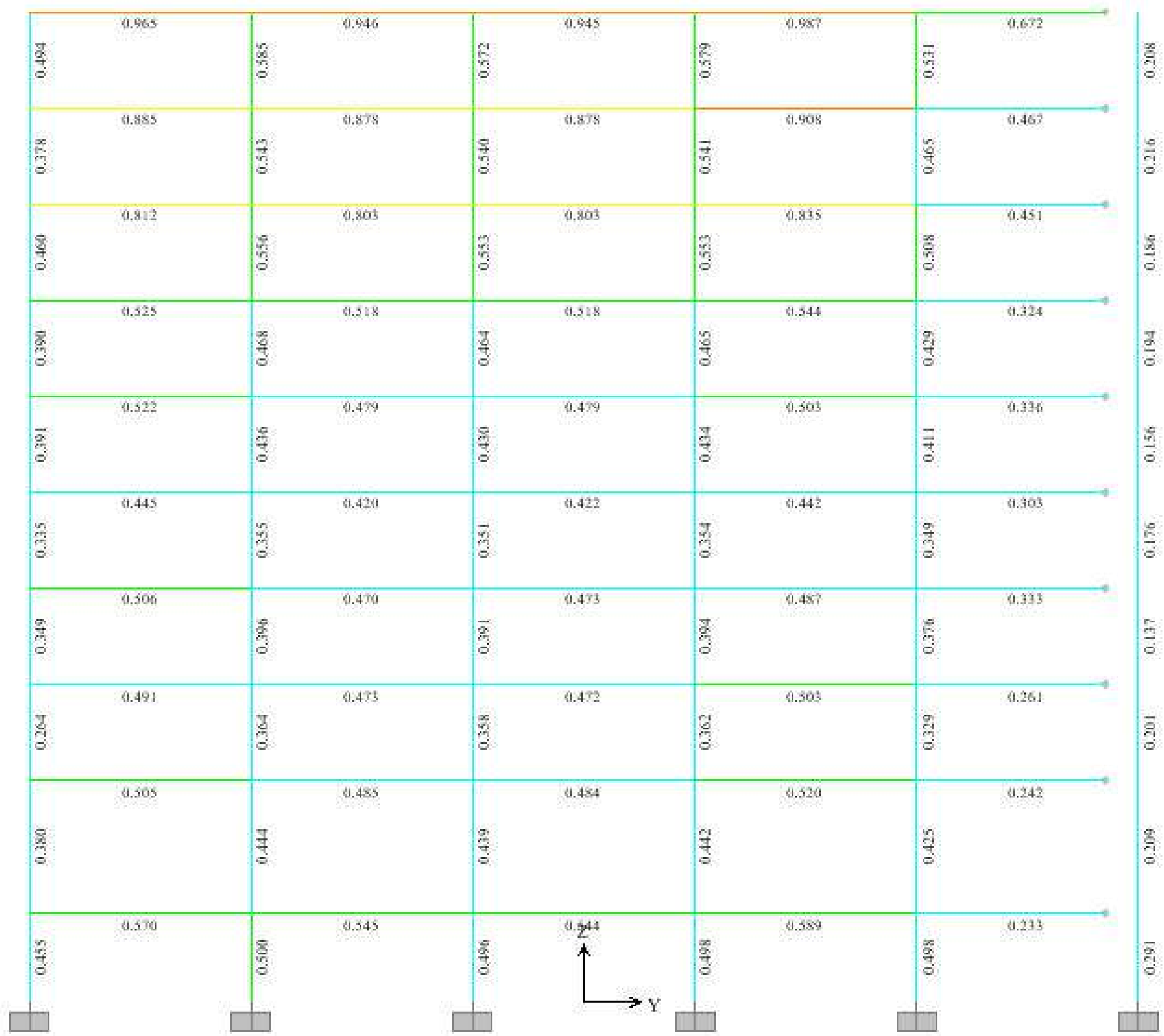

(b) 500 lb Weight at 20 ft Stand-off

“Figure 5.18 : Continued”

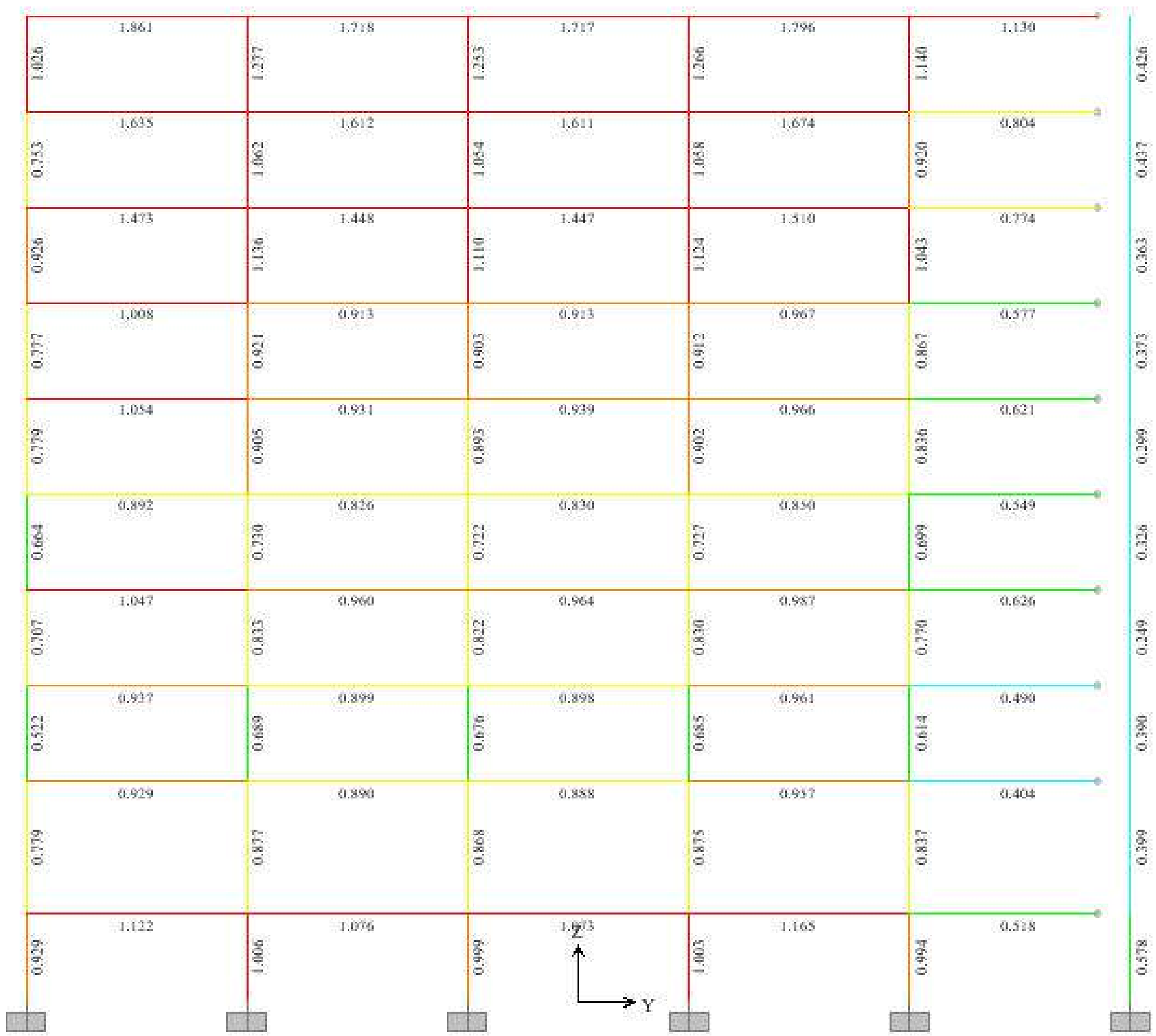

(c) 1,000 lb Weight at 20 ft Stand-off

“Figure 5.18 : Continued”

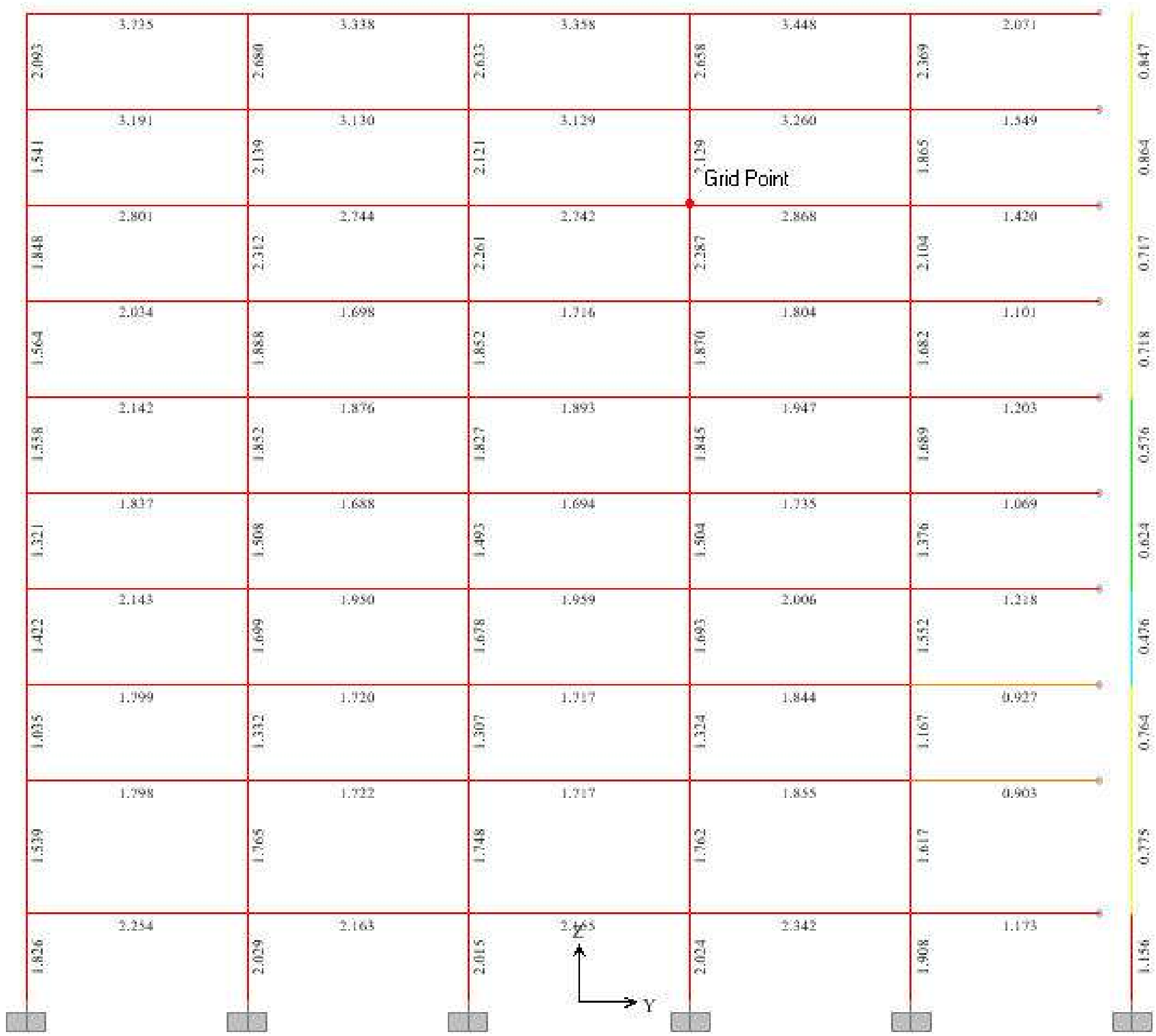

(d) 2,000 lb Weight at 20 ft Stand-off

5.2.3. Summary

As results of dynamic time history analysis with variable TNT weight, maximum deflections are shown in Figure 5.19. As might be expected, the maximum deflection occurs for the 2,000 TNT weight @ 20 ft standoff distance. The maximum displacement occurs at roof and minimum displacement occurs at 1st floor. The maximum displacements are 17.73 in, 9.3 in, 5.0 in and 1.53 in and minimum displacements are 2.29 in, 1.10 in, 0.51 in and 0.13 in respectively.

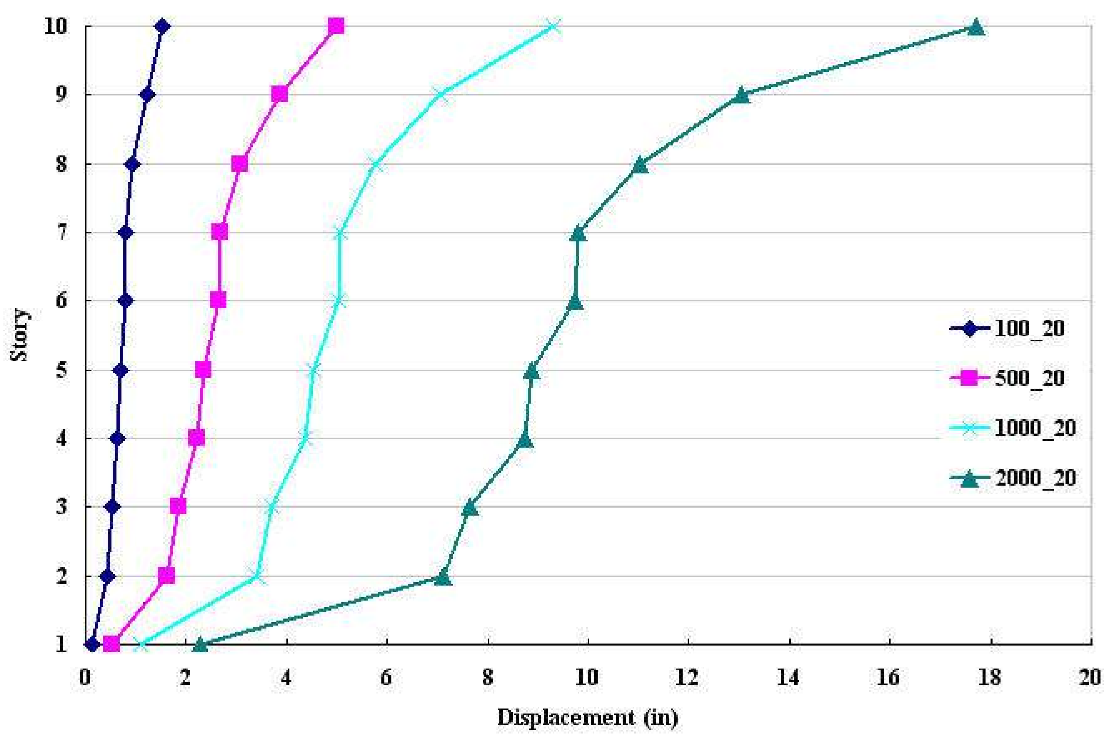

Figure 5.19 : Maximum Deflection on Each Floor to Variable TNT Weight

Based on maximum displacements, instestory drifts are shown in Figure 5.20. The code limitation of drift ratio based on UBC'97 for earthquake is 0.02 and the responses of all conditions satisfy with code limitation but 2,000 lb@20 ft case.

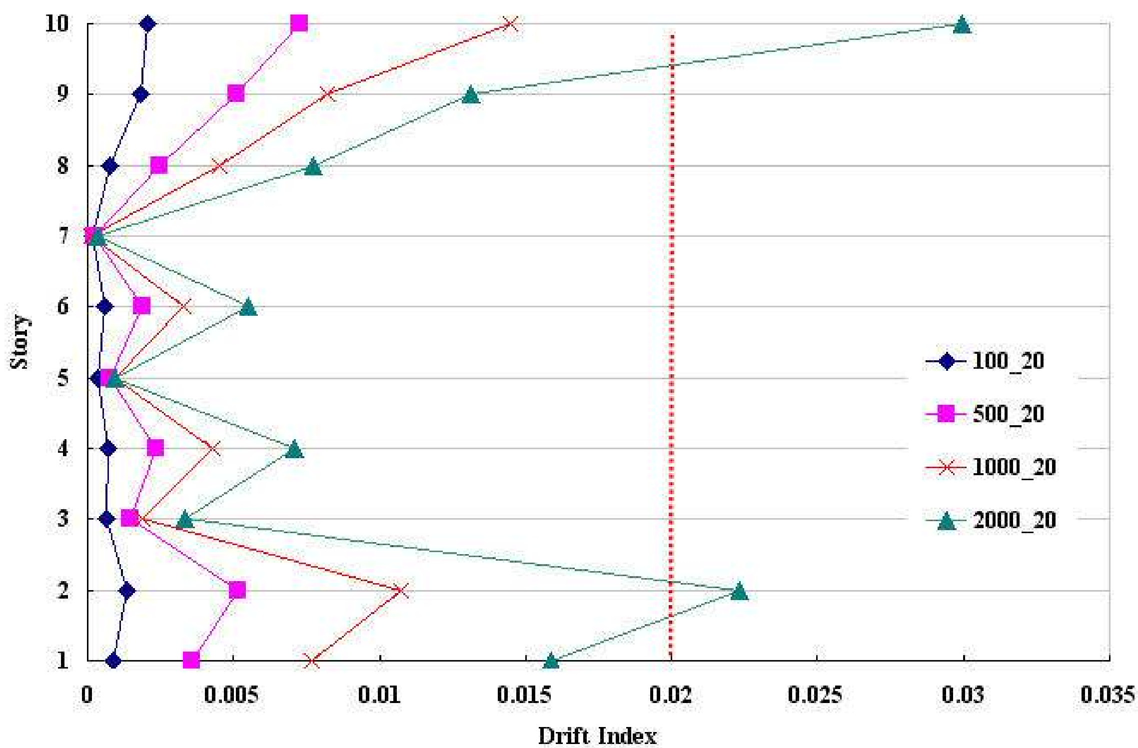

Figure 5.20 : Interstory Drift to Variable TNT Weight

The maximum demand/capacity ratios for the columns in each story of the transverse frame and longitudinal frame for a stand-off distance 20 ft are summarized in Figure 5.21 and Figure 5.22. Here it can be seen that the D/C demands are all less than unity indicating elastic behavior However, two cases of longitudinal direction with 2,000 TNT weight and 1,000 lb TNT weight at 20 ft stand-off distance, is greater than unity with a maximum of about 1.3 and 2.6 respectively.

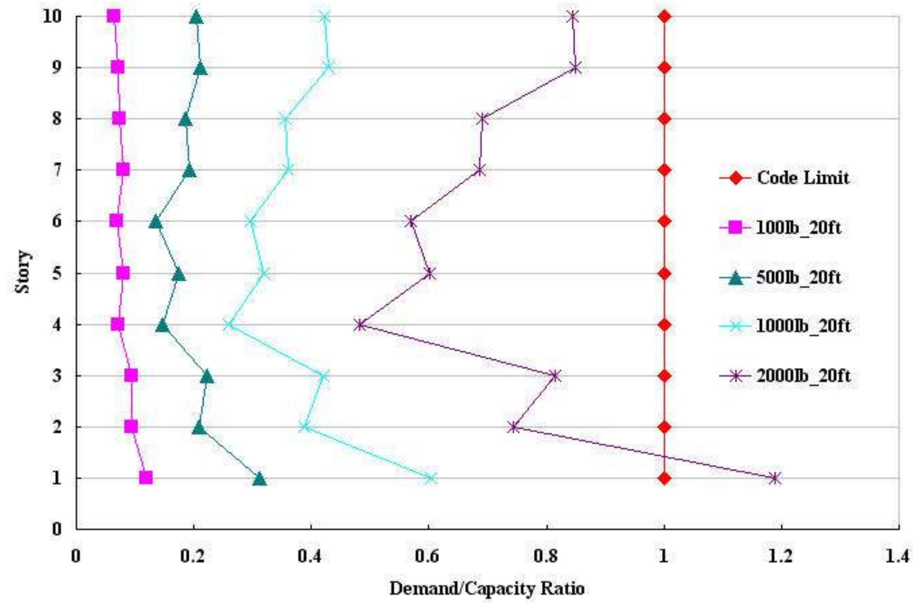

Figure 5.21 : Demand/Capacity Ratio to Variable TNT Weight on Transverse MRF

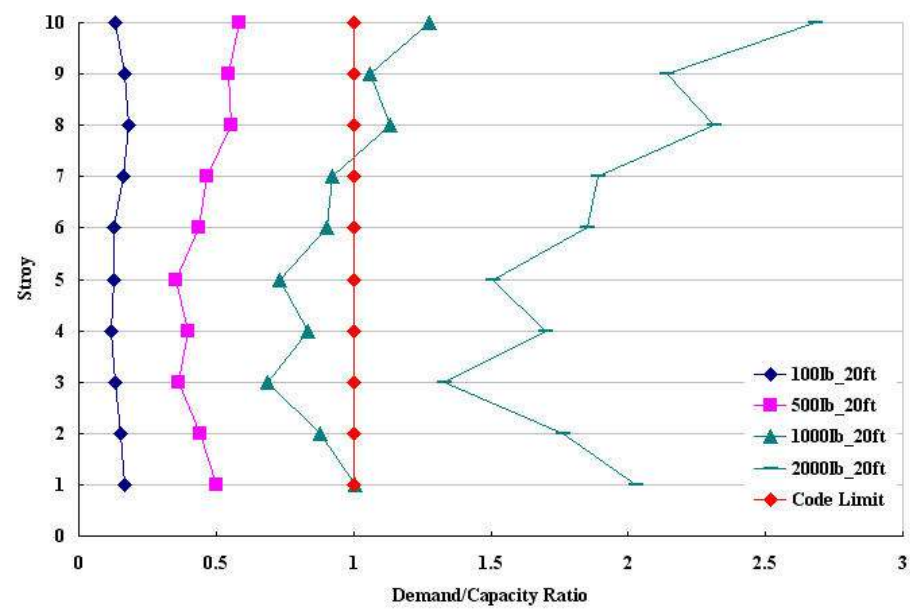

Figure 5.22 : Demand/Capacity Ratio to Variable TNT Weight on Longitudinal MRF

5.3. Structural Response to Extreme Blast Loads

5.3.1. Crater

To investigate dimension of crater, CONWEP computer program is used in case of 3,000 lb TNT weight and 4,000 lb TNT weight. In this study, stand-off distance was assumed over 20 ft. Table 5.1 shows results of applied cases.

Table 5.1 : Results of CONWEP in 3,000 lb and 4,000 lb TNT Weight with Dry Sandy Clay

Charge Weight (lb)	3,000	4,000
Depth of Burial (ft)	-3	-3
Depth (ft)	8.46	9.55
Radius (ft)	29.19	32.59
Window Breakage Range (ft)	1760	1937

Accordingly window breakage range is over bay width, the window should be broken by the weight both cases.

5.3.2. Blast Loads

A frame is subjected to 3,000 lb and 4,000 lb TNT blast at 20 ft stand-off distance in this chapter. To find blast loads on ten story building at each joint, the CONWEP program was used. Figure 5.23 - Figure 5.24 show time duration and peak reflected pressure on front frame of structure.

The calculated (CONWEP) peak overpressures on the front frame are shown in Figure 5.23 – Figure 5.24. These range from a maximum of 4084 psi (3,000 lb), 4870 psi (4,000 lb) at the point closest to the detonation to a minimum of 10.09 psi (3,000 lb), 11.84 psi (4,000 lb) at the upper west/east corner.

While these pressures are extremely large, they act for a limited duration, as shown in Figure 5.23 – Figure 5.24. The duration ranges from a maximum of 41.04 msec (3,000 lb), 39.15msec (4,000 lb) in the upper west/east corner to a minimum of 3.86 msec (3,000 lb), 3.63 msec (4,000 lb), at the upper west/east corner.

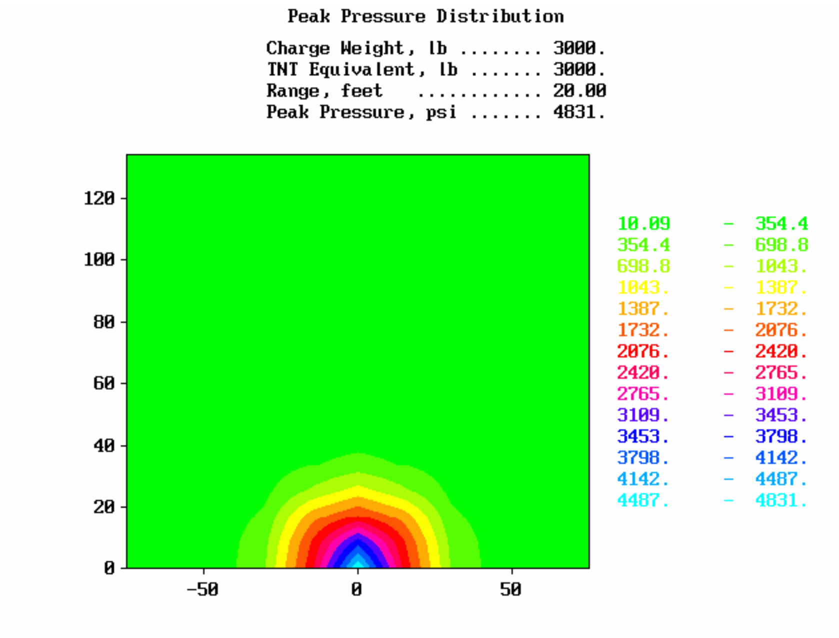

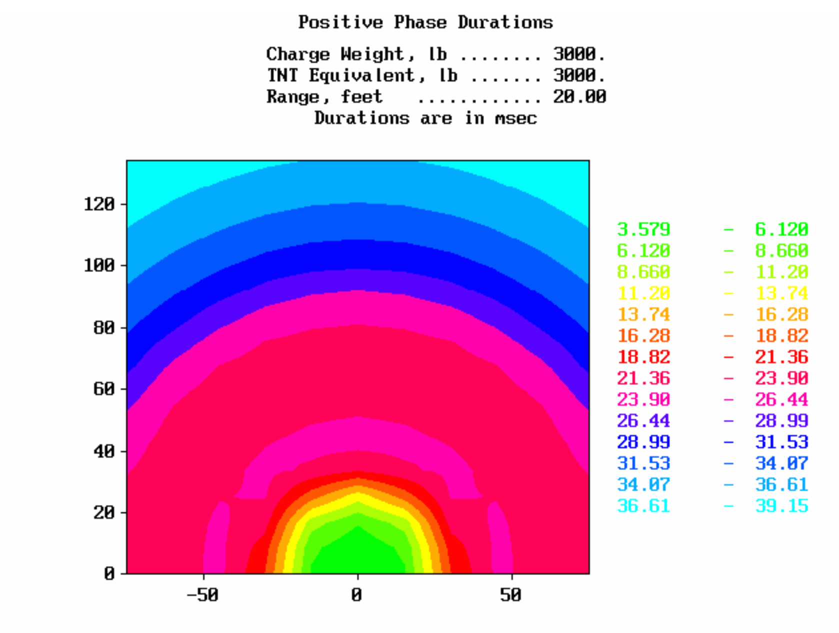

Figure 5.23 : Distribution of Peak Reflected Pressure and Time Duration on 3,000 lb TNT weight

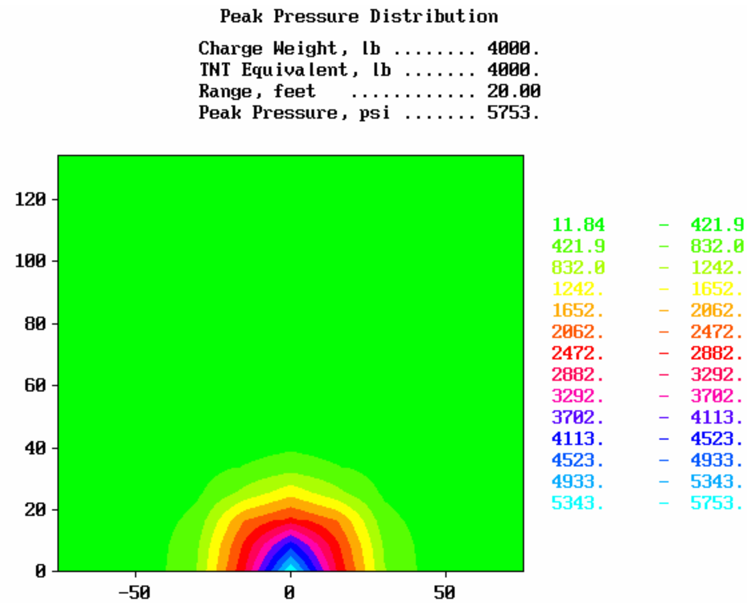

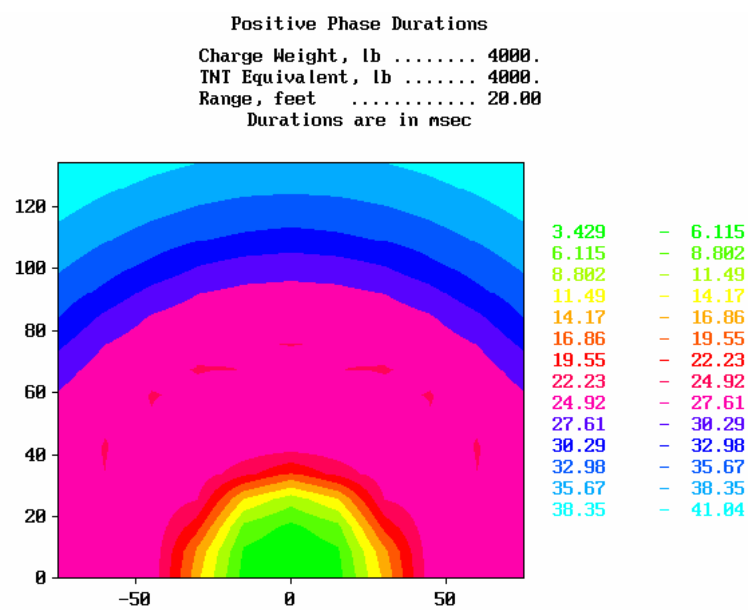

Figure 5.24 : Distribution of Peak Reflected Pressure and Time Duration on 4,000 lb TNT weight

5.3.3. Responses of Ten Story Building

To obtain the response of extreme blast loads on ten story building, SAP2000 FEM Software was used. The blast loads are generated at each joint as peak reflected pressure from CONWEP. The dynamic time history indicates that number of output time steps is 1,000 and output time step size is 0.005. The damping ratio is assumed as 5%. Dynamic time history curves of each floor at 20 ft with 3,000 lb, 4,000 lb TNT weight are shown in Figure 5.25.

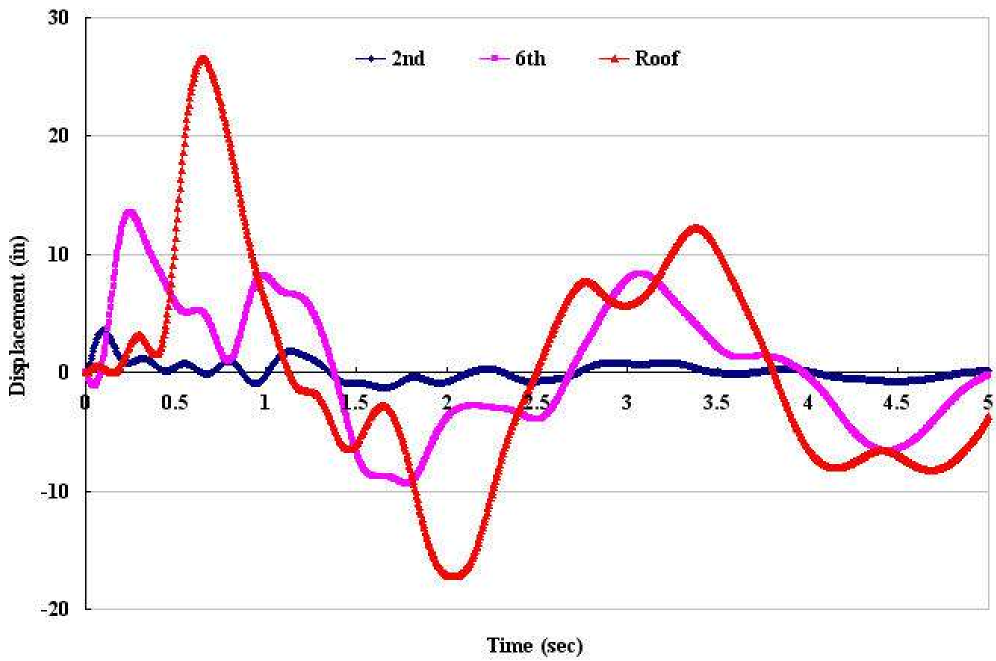

(a) 3,000 lb TNT Weight @ 20 ft Stand-Off Distance

Figure 5.25 : Linear Dynamic Time History to Extreme Blast Loads

"Figure 5.25 : Continued"

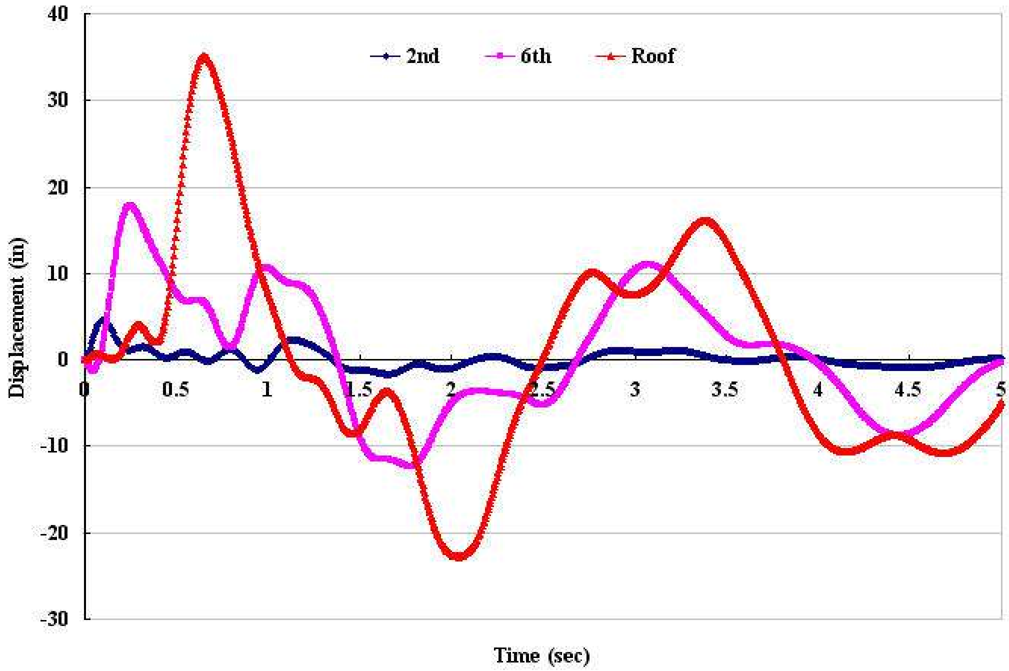

(b) 4,000 lb TNT Weight at 20 ft Stand-Off

To find critical column corresponding to each case, the result of analysis from SAP2000 based on UBC 97 LRFD design code shows demand/capacity ratio of all frame. These values are obtained by combination of dead load, live load and blast loads. Figure 5.26 and Figure 5.27 show demand/capacity ratio of each frame against applied loads along both directions. As a result, critical column on transverse direction was found at closest distance of blast source.

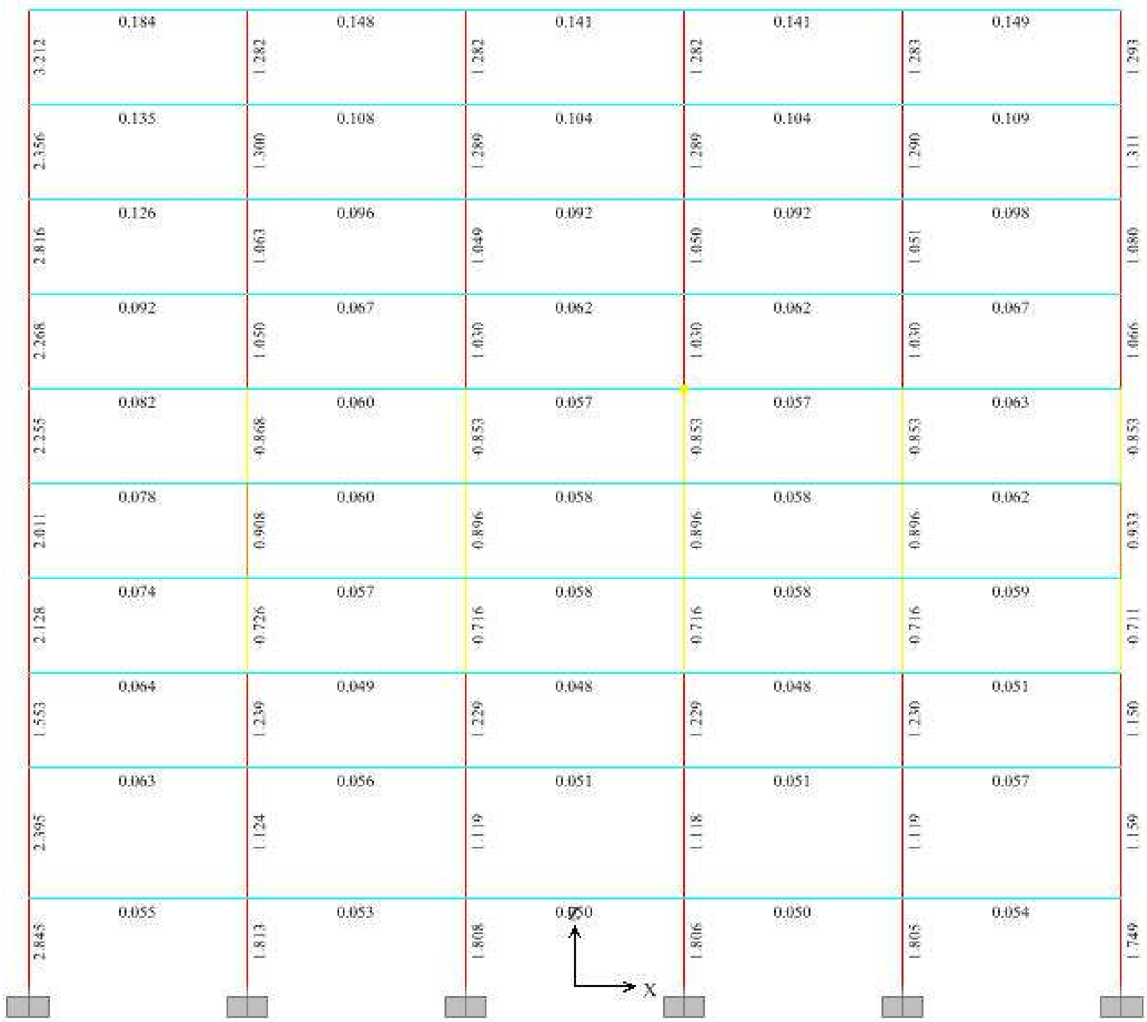

(a) 3,000 lb Weight at 20 ft Stand-off

Figure 5.26 : Demand/Capacity Ratio on Transverse MRF to Extreme Blast Loads

“Figure 5.26 : Continued”

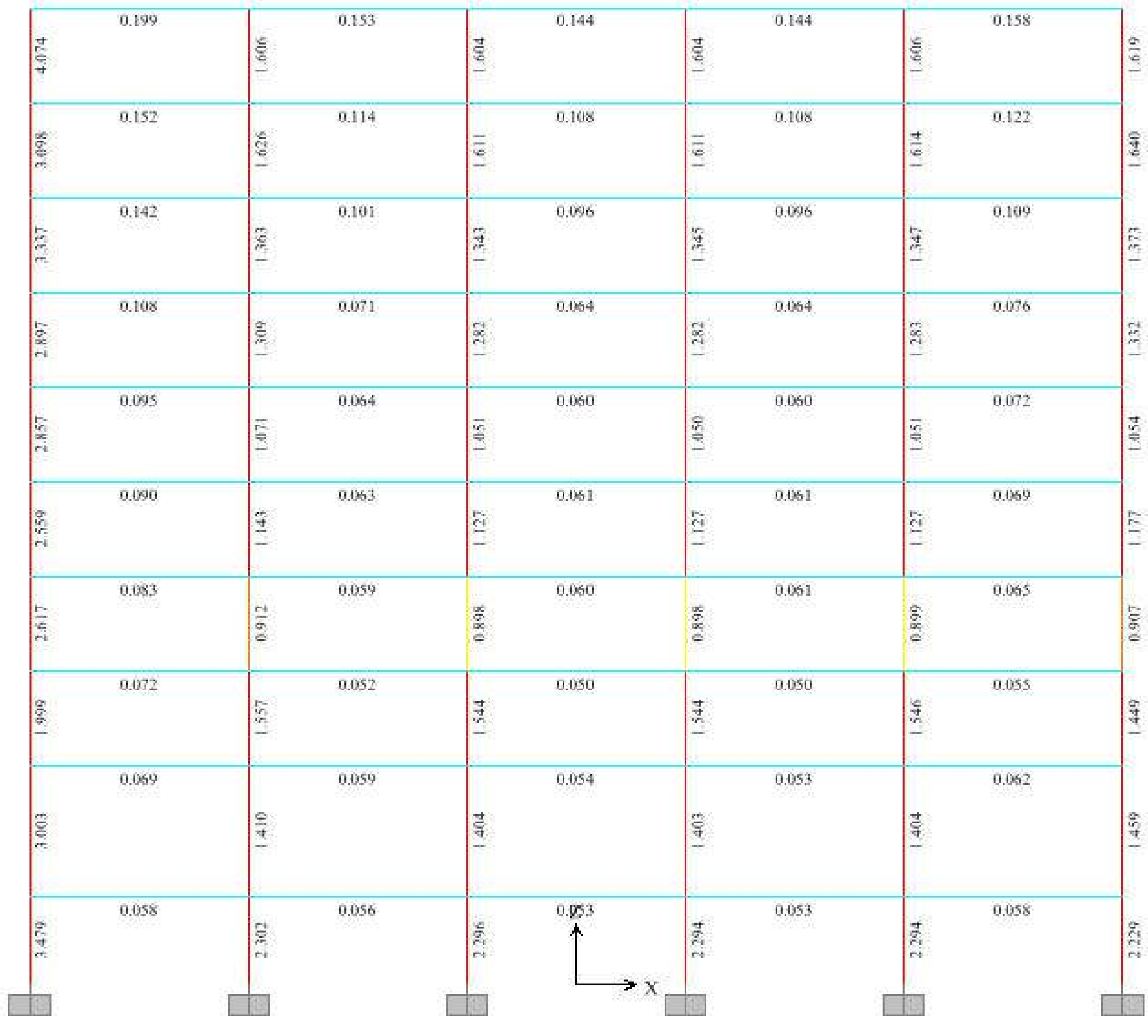

(b) 4,000 lb Weight at 20 ft Stand-off

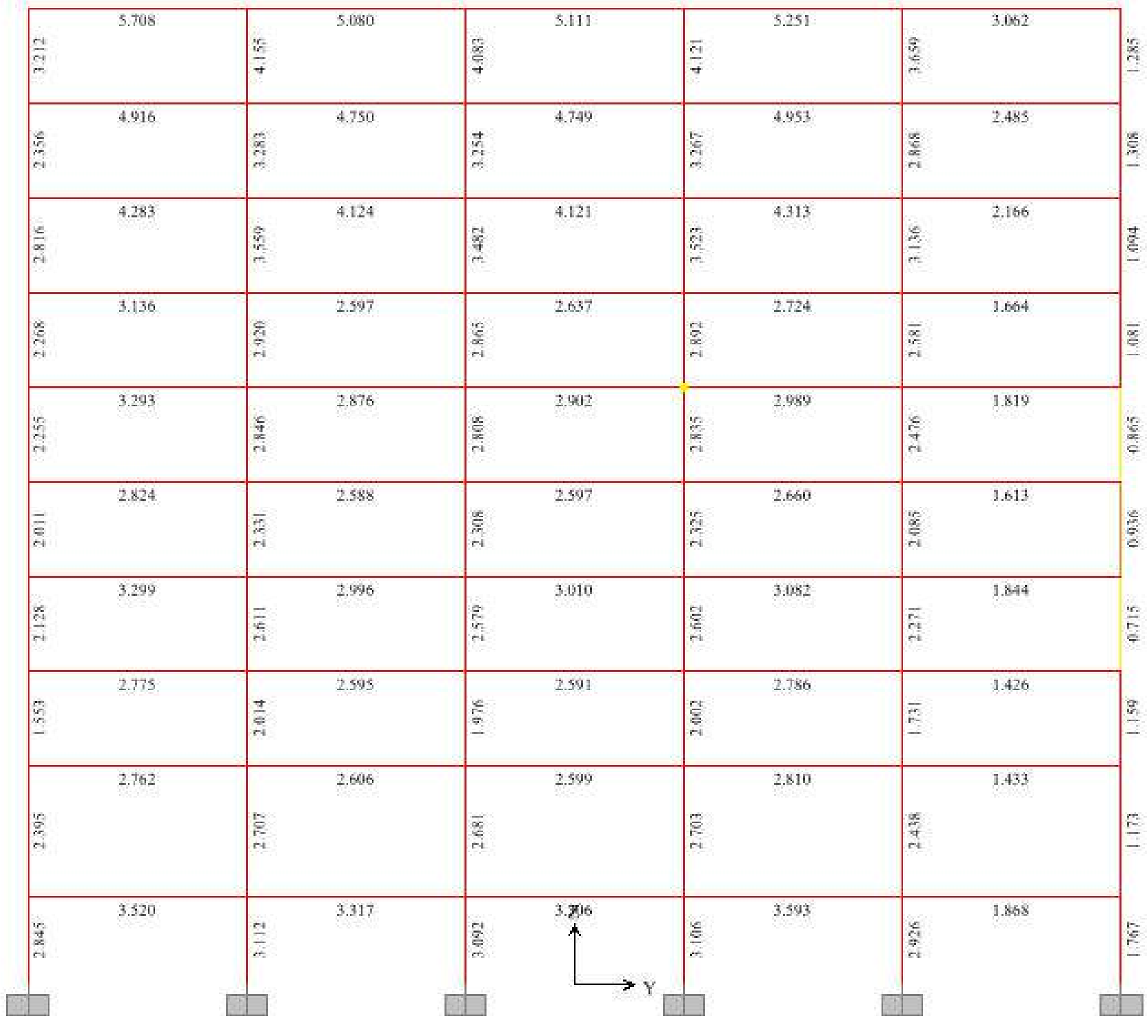

(a) 3,000 lb Weight at 20 ft Stand-off

Figure 5.27 : Demand/Capacity Ratio on Longitudinal MRF to Extreme Blast Loads

"Figure 5.27 : Continued"

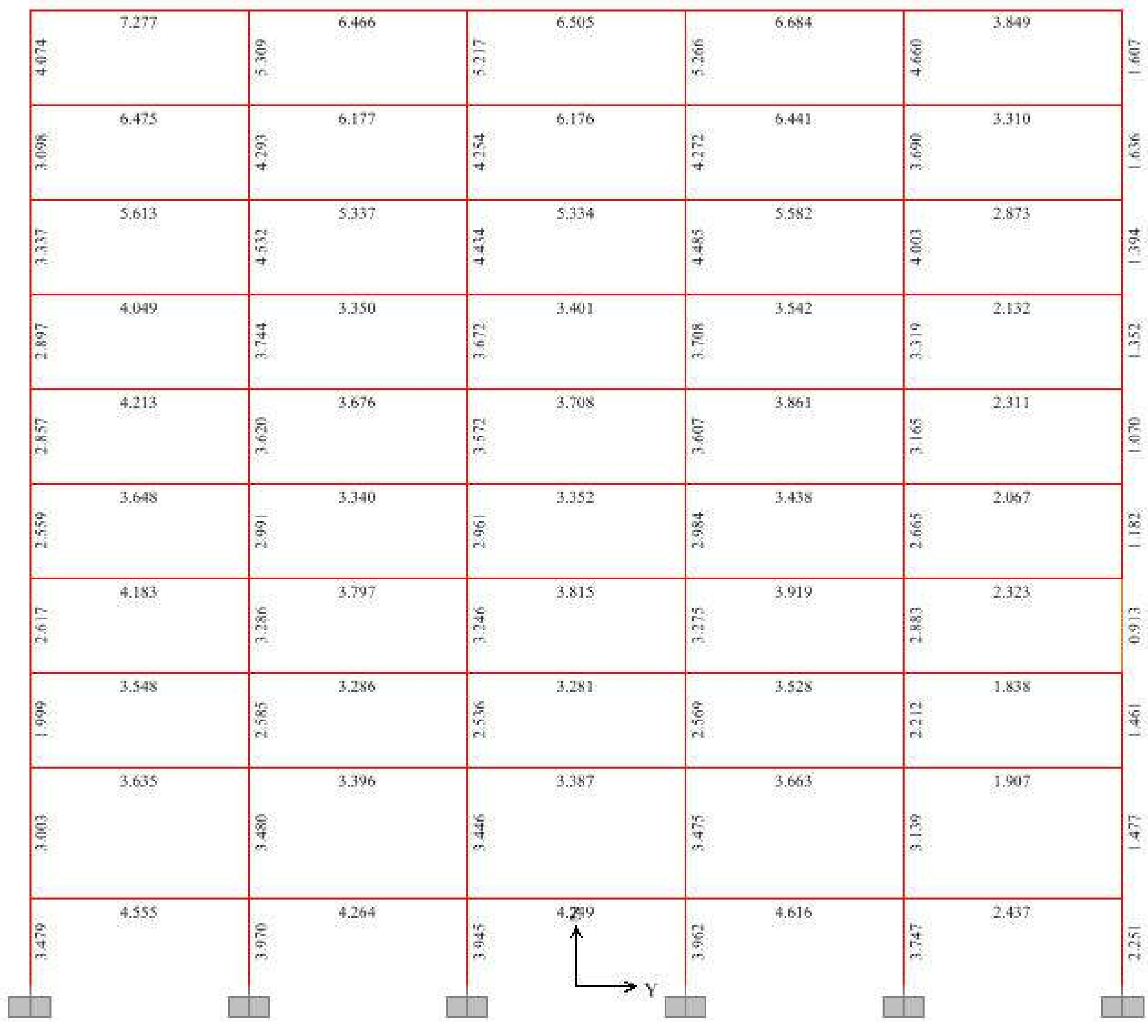

(b) 4,000 lb Weight at 20 ft Stand-off

5.3.4. Summary

As results of dynamic time history analysis with extreme TNT weights, maximum deflections are shown in Figure 5.28. As might be expected, the maximum deflection occurs for the 4,000 TNT weight @ 20 ft standoff distance. The maximum displacement occurs at roof and minimum displacement occurs at 1st floor. The maximum displacements are 26.61 in, 35.05 in and minimum displacements are 3.55 in, 4.56 in respectively.

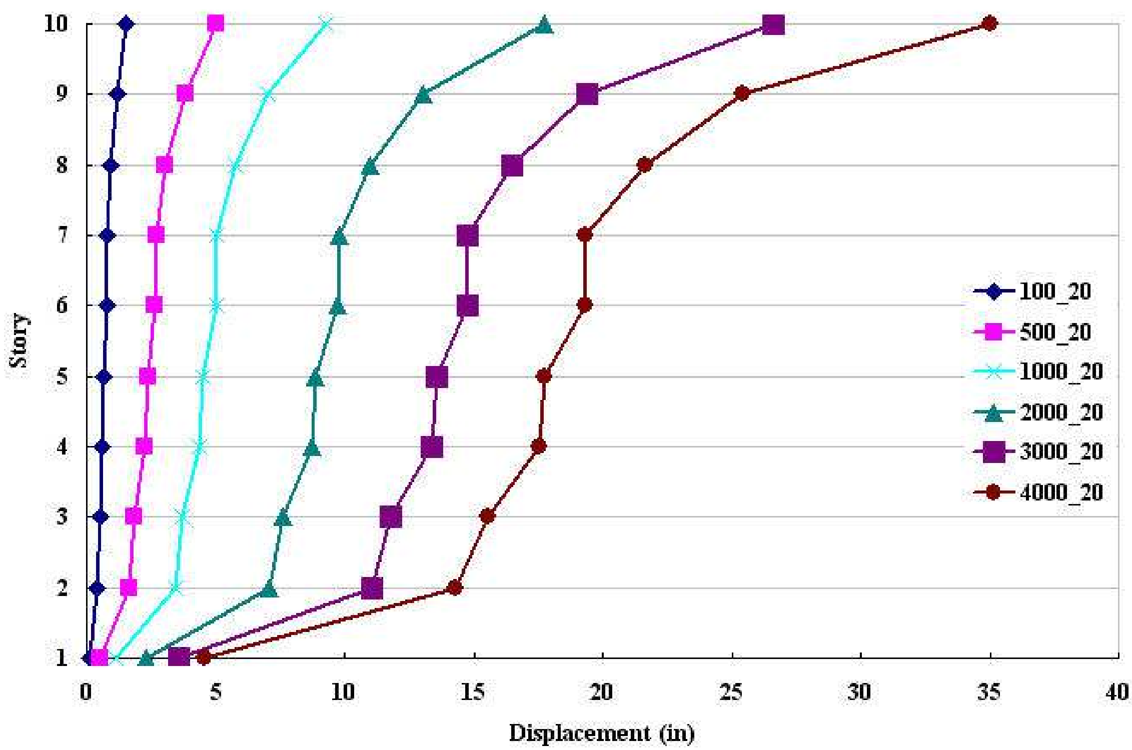

Figure 5.28 : Maximum Deflection on Each Floor to Extreme Blast Loads

Based on maximum displacements, instestory drifts are shown in Figure 5.29. The code limitation of drift ratio based on UBC'97 for earthquake is 0.02 and the responses of two extreme condition are out of range.

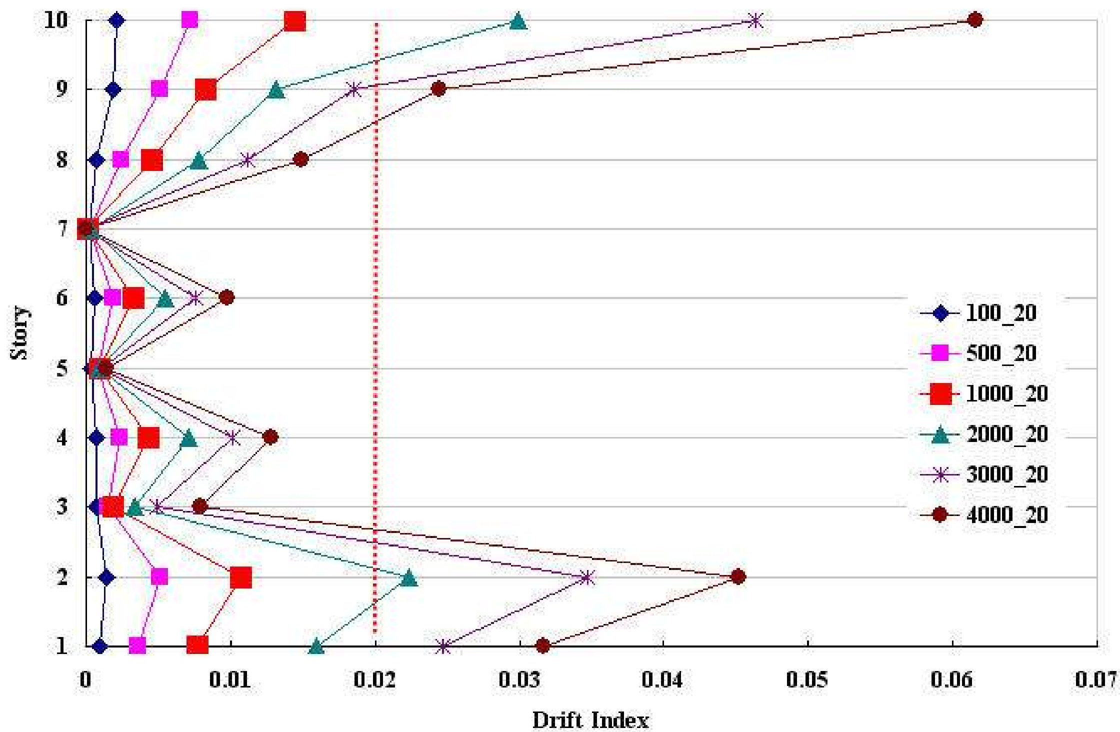

Figure 5.29 : Interstory Drift to Extreme Blast Loads

The maximum demand/capacity ratios for the columns in each story of the transverse frame and longitudinal frame for a stand-off distance 20 ft are summarized in Figure 5.30 and Figure 5.31. Here it can be seen that for two (3,000 lb and 4,000 lb TNT) of the blast conditions the D/C ratios are all more than unity indicating inelastic behavior.

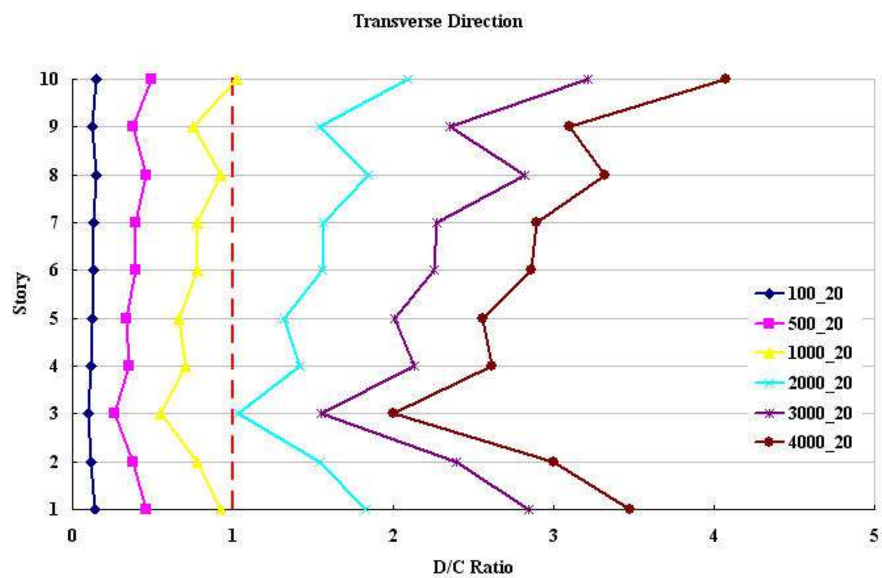

Figure 5.30 : Demand/Capacity Ratio to Extreme Blast Loads on Transverse MRF

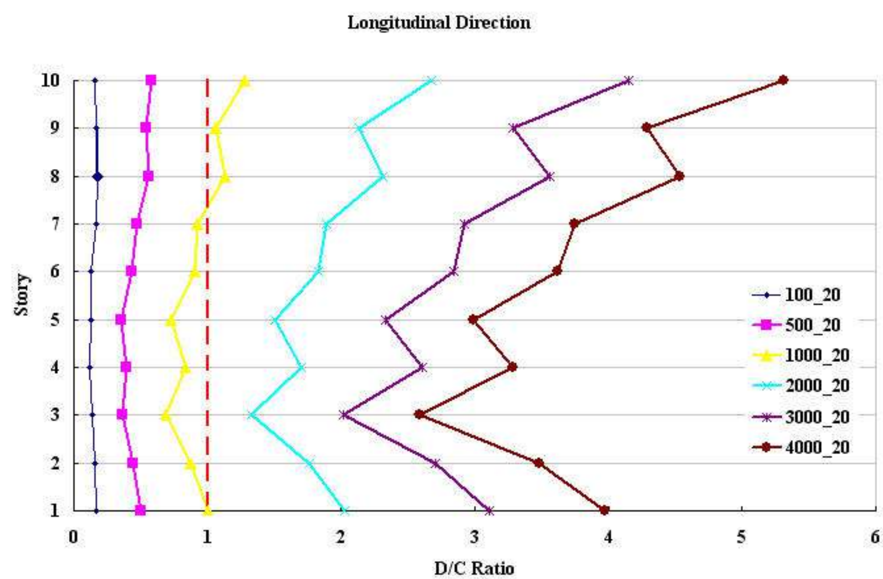

Figure 5.31 : Demand/Capacity Ratio to Extreme Blast Loads on Longitudinal MRF

5.4. Diaphragm Analysis of Using Shell Elements of Ten Story Building

5.4.1. Flexible Diaphragm Analysis

The floor diaphragm is assumed flexible diaphragm and rigid diaphragm as shown in chapter 4.3. The floor diaphragm is represented by flexible diaphragm resulting in shear force and bending moment contour shown in Figure 5.41 – Figure 5.42 for a linear analysis against 1,000 lb @ 20 ft stand-off distance. These contours indicate the blast loading is distributed to the moment frame on the sides parallel to the blast force. For reference, the member locations, identification numbers and member sizes are shown in Figure 5.32 for typical longitudinal frame. Table 5.2 – 5.9 and Figure 5.33 – 5.40 show comparison of developed shear force and bending moment with capacity of each moment resistance frames. The results of flexible diaphragm analysis are also shown in Figure 5.41- 5.44 and Table 5.10.

In addition, maximum shear forces and bending moments of Moment Resistant Frame are investigated as compared with capacity defined by AISC-LRFD [2] shown in chapter 4.3. Hence, the shear capacity of W14*500, W14*455, W14*370, W14*283, W14*257 is calculated as **1,159 k/in, 1,035 k/in, 801 k/in, 583 k/in, 523 k/in** respectively and the moment capacity of W14*500, W14*455, W14*370, W14*283, W14*257 is also calculated as **52,500 k-in, 46,800 k-in, 36,800 k-in, 29,150 k-in, 24,350 k-in**.

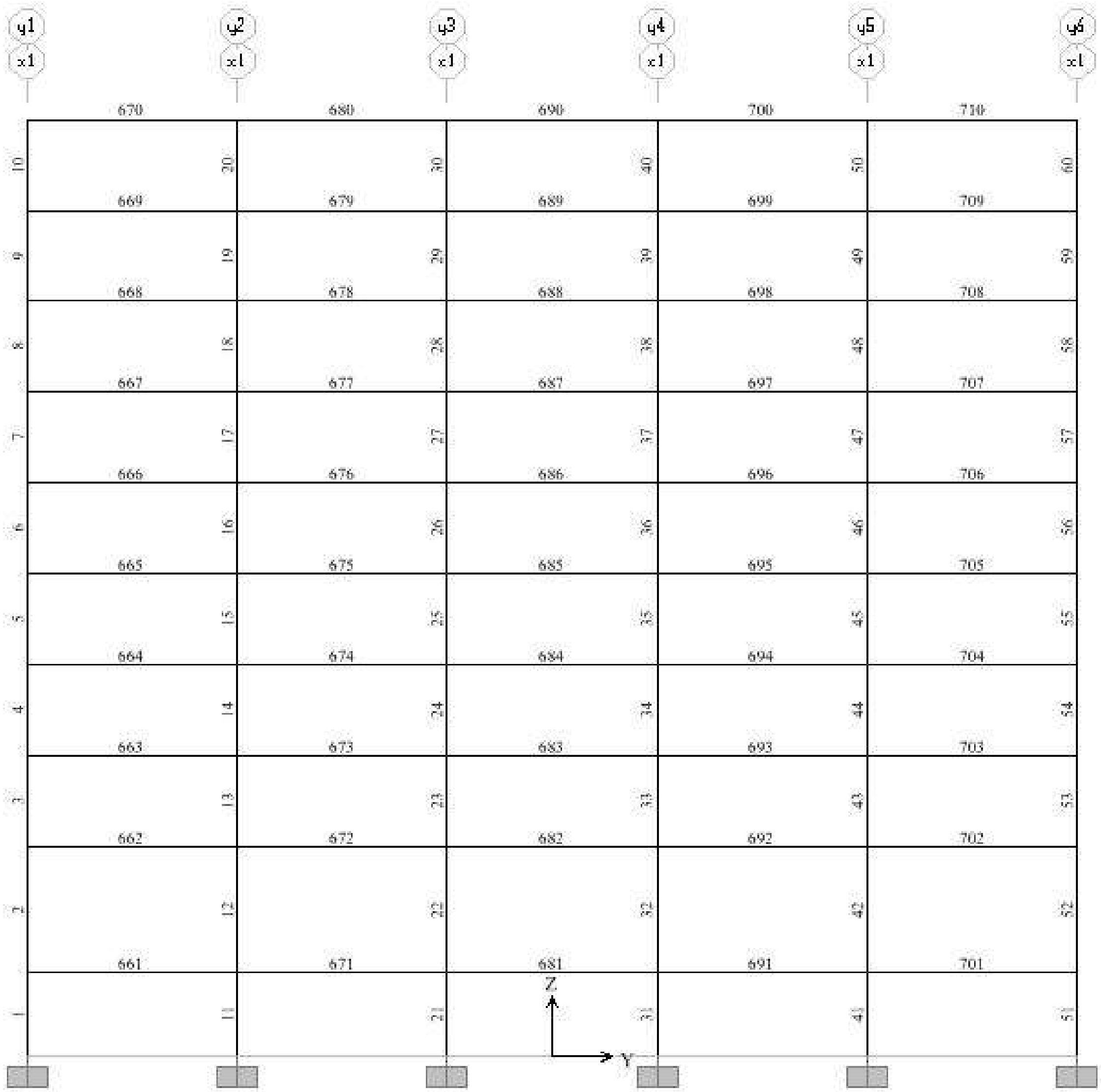

(a) Generated Member Numbers along the Longitudinal Direction

Figure 5.32 : Generated Member Numbers and Frame Section along the Longitudinal Direction

"Figure 5.32 : Continued"

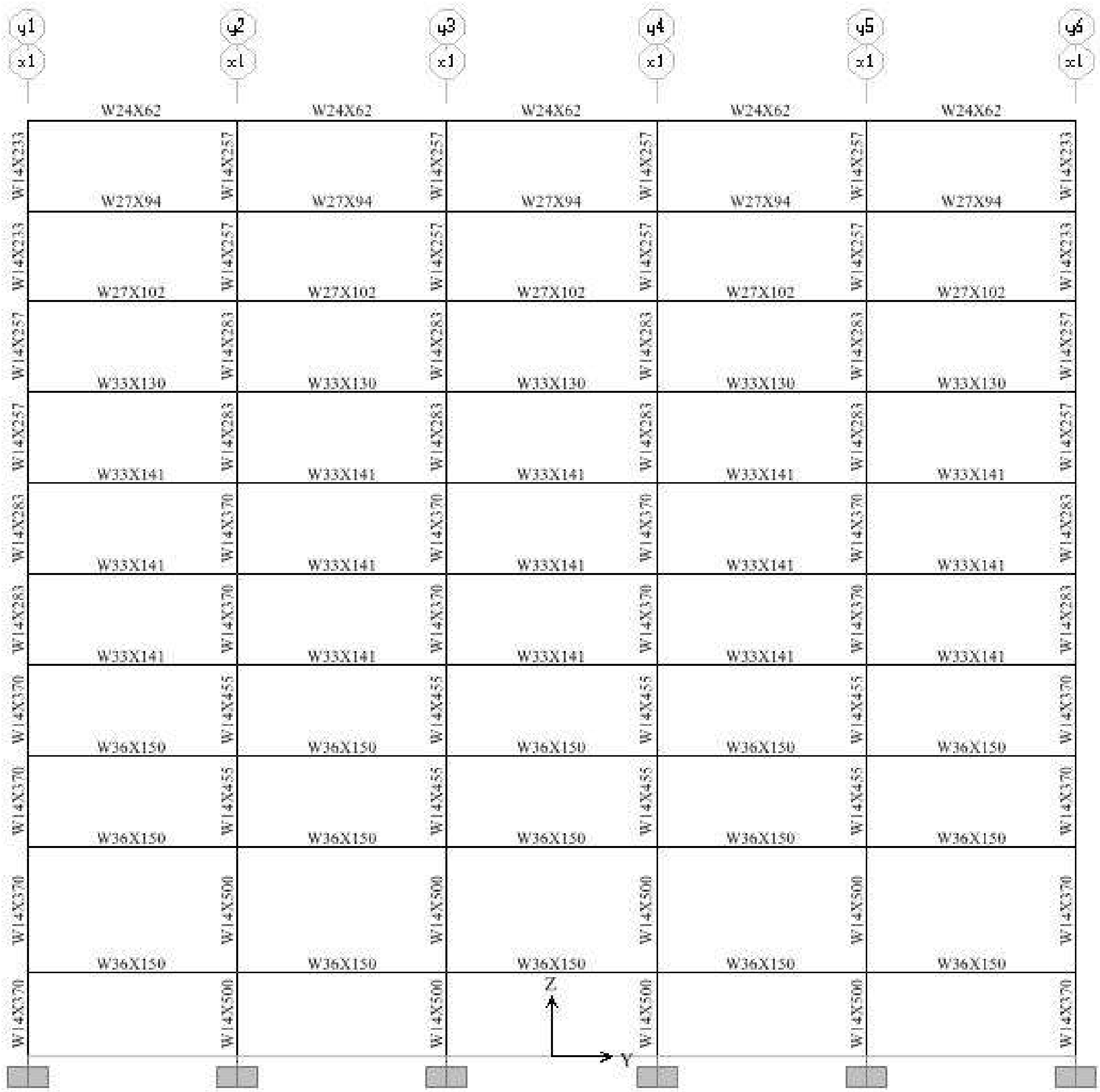

(b) Generated Frame Sections and Moment Resistant Frames

Table 5.2 : Max. Shear Force at MRF Frames (1,000 lb TNT Weight @ 20 ft)

Frame No.	Frame Section	Shear Force (V_u)	Shear Strength (ϕV_n)
11	W14*500	459.2	1159
12	W14*500	313.0	1159
13	W14*455	324.8	1035
14	W14*455	276.5	1035
15	W14*370	222.5	801
16	W14*370	246.4	801
17	W14*283	246.3	583
18	W14*283	264.3	583
19	W14*257	269.0	523
20	W14*257	286.9	523

(unit : k/in)

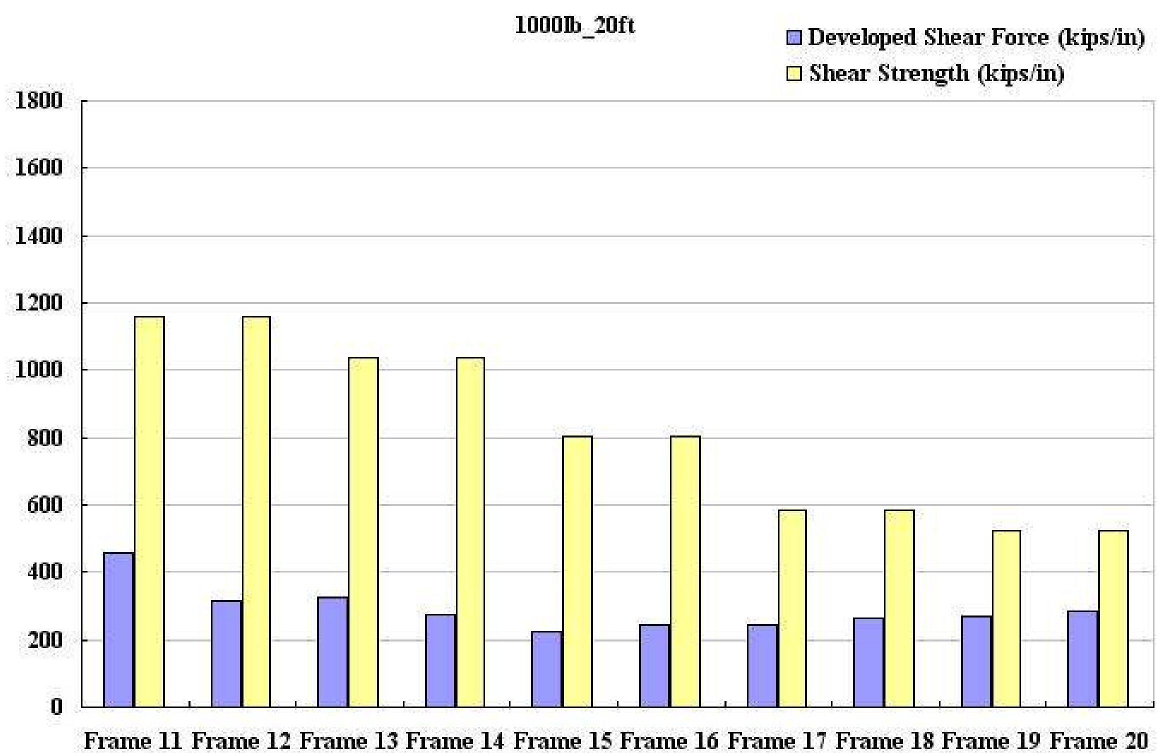

Figure 5.33 : Developed Shear Force vs. Shear Capacity of Flexible Diaphragm (1,000 lb @ 20 ft)

Table 5.3 : Max. Shear Force at MRF Frames (2,000 lb TNT Weight @ 20 ft)

Frame No.	Frame Section	Shear Force (V_u)	Shear Strength (ϕV_n)
11	W14*500	953.9	1159
12	W14*500	651.8	1159
13	W14*455	650.8	1035
14	W14*455	553.3	1035
15	W14*370	452.1	801
16	W14*370	482.1	801
17	W14*283	486.6	583
18	W14*283	522.6	583
19	W14*257	546.1	523
20	W14*257	590.2	523

(unit : k/in)

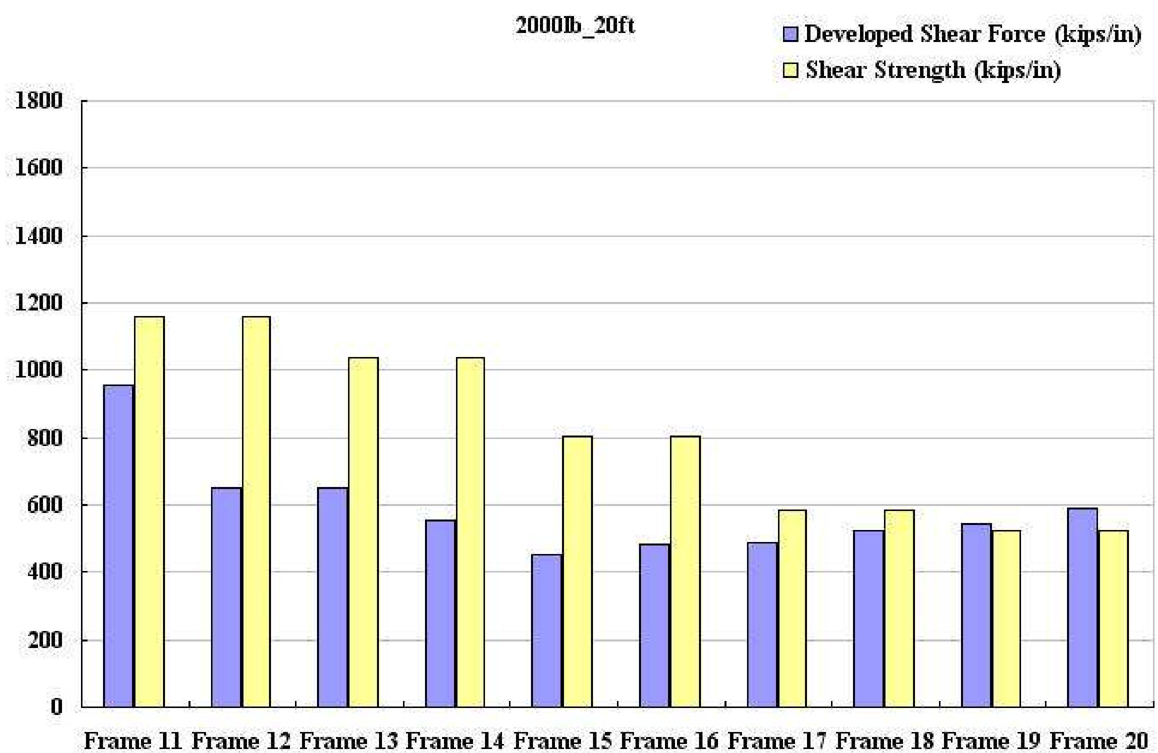

Figure 5.34 : Developed Shear Force vs. Shear Capacity of Flexible Diaphragm (2,000 lb @ 20 ft)

Table 5.4 : Max. Shear Force at MRF Frames (3,000 lb TNT Weight @ 20 ft)

Frame No.	Frame Section	Shear Force (V_u)	Shear Strength (ϕV_n)
11	W14*500	1477.1	1159
12	W14*500	1011.9	1159
13	W14*455	995.9	1035
14	W14*455	849.0	1035
15	W14*370	693.2	801
16	W14*370	730.7	801
17	W14*283	742.1	583
18	W14*283	798.2	583
19	W14*257	839.9	523
20	W14*257	912.3	523

(unit : k/in)

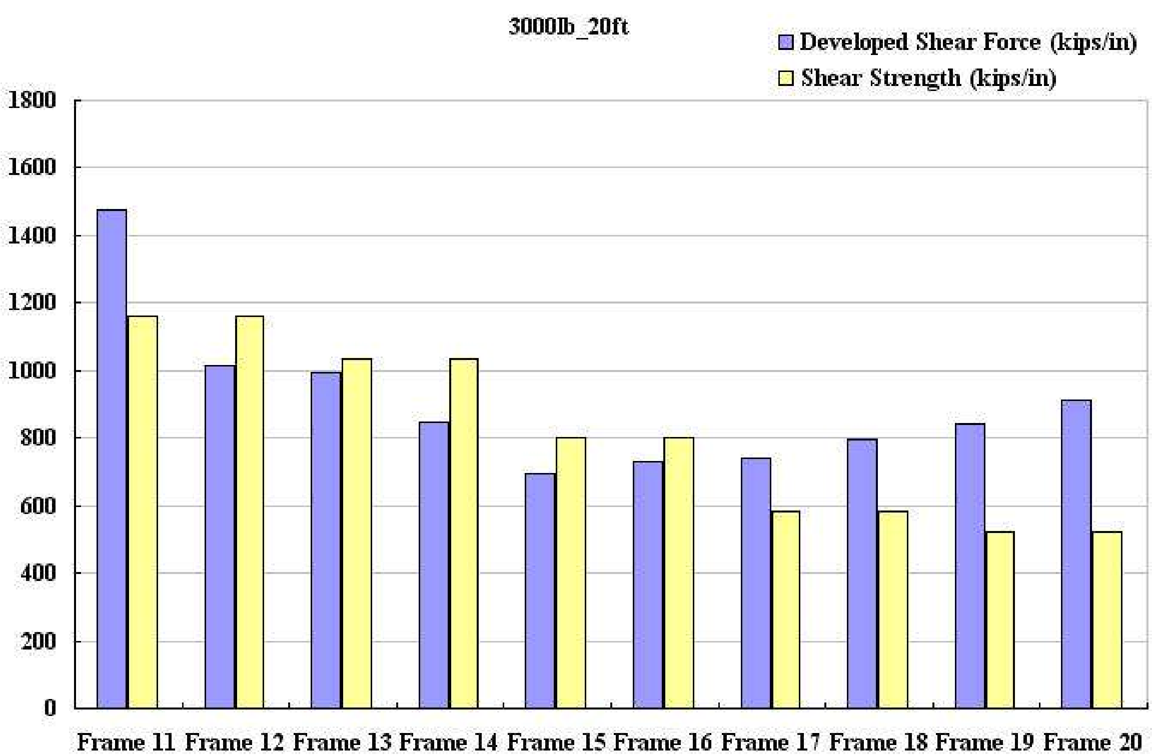

Figure 5.35 : Developed Shear Force vs. Shear Capacity of Flexible Diaphragm (3,000 lb @ 20 ft)

Table 5.5 : Max. Shear Force at MRF Frames (4,000 lb TNT Weight @ 20 ft)

Frame No.	Frame Section	Shear Force (V_u)	Shear Strength (ϕV_n)
11	W14*500	1886.8	1159
12	W14*500	1312.5	1159
13	W14*455	1272.6	1035
14	W14*455	1072.2	1035
15	W14*370	895.5	801
16	W14*370	936.6	801
17	W14*283	960.8	583
18	W14*283	1031.1	583
19	W14*257	1099.2	523
20	W14*257	1169.8	523

(unit : k/in)

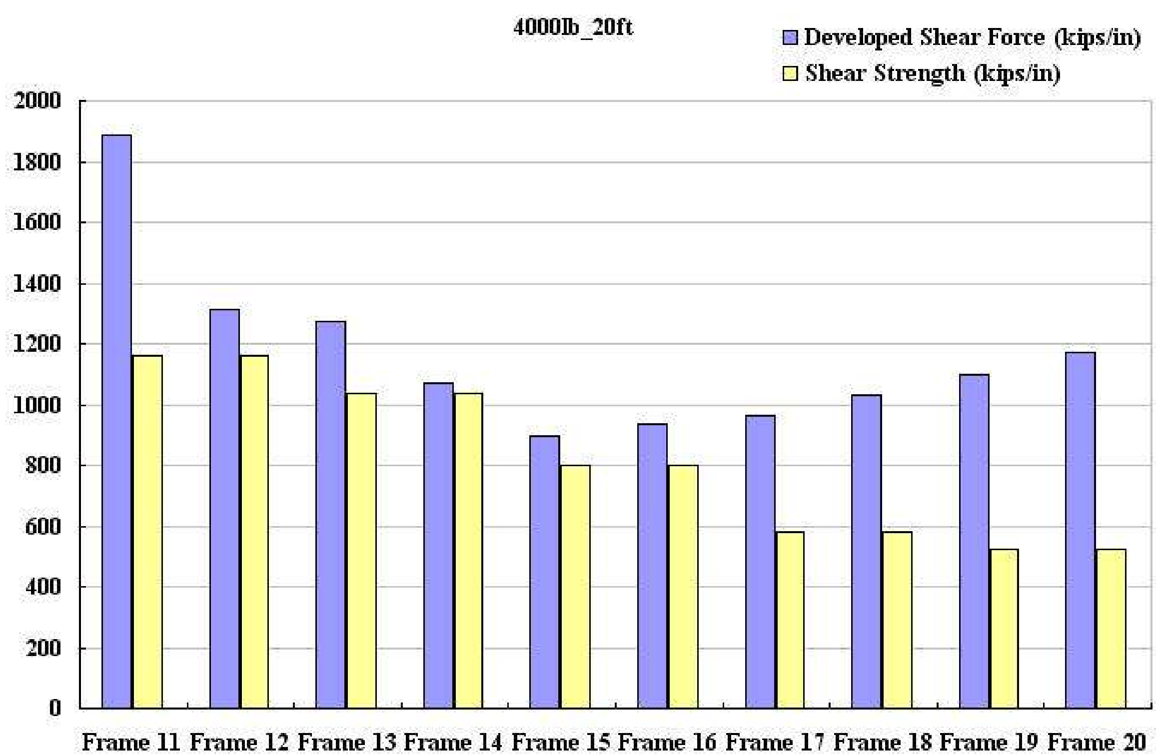

Figure 5.36 : Developed Shear Force vs. Shear Capacity of Flexible Diaphragm (4,000 lb @ 20 ft)

Table 5.6 : Max. Bending Moment at MRF Frames (1,000 lb TNT Weight @ 20 ft)

Frame No.	Frame Section	Bending Moment (Mu)	Moment Capacity (ϕMn)
11	W14*500	43314.0	52500
12	W14*500	30591.9	52500
13	W14*455	25507.7	46800
14	W14*455	22578.7	46800
15	W14*370	18166.2	36800
16	W14*370	20601.0	36800
17	W14*283	19196.9	29150
18	W14*283	24124.7	29150
19	W14*257	21844.8	24350
20	W14*257	23771.2	24350

(unit : k-in)

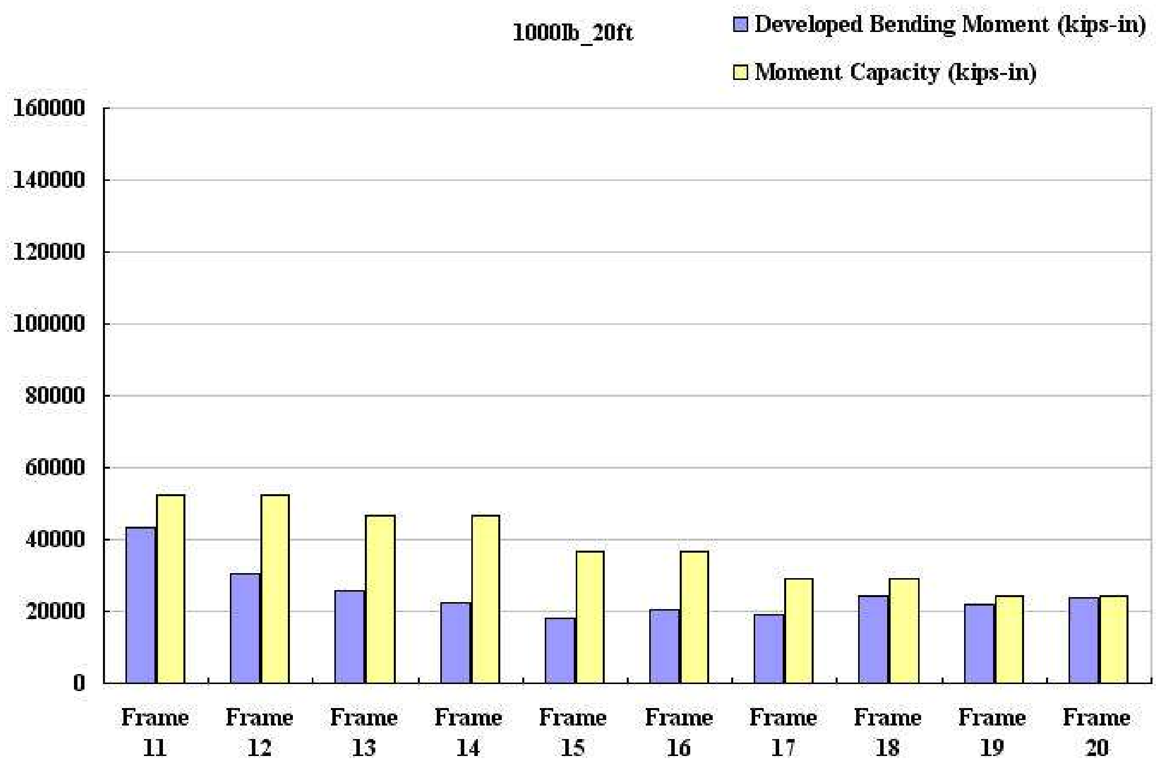

Figure 5.37 : Developed Bending Moment vs. Moment Capacity of Flexible Diaphragm (1,000 lb @ 20 ft)

Table 5.7 : Max. Bending Moment at MRF Frames (2,000 lb TNT Weight @ 20 ft)

Frame No.	Frame Section	Bending Moment (Mu)	Moment Capacity (ϕMn)
11	W14*500	90031.2	52500
12	W14*500	63602.7	52500
13	W14*455	51052.2	46800
14	W14*455	45547.0	46800
15	W14*370	36931.9	36800
16	W14*370	40454.9	36800
17	W14*283	37962.3	29150
18	W14*283	47935.3	29150
19	W14*257	44733.5	24350
20	W14*257	48927.2	24350

(unit : k-in)

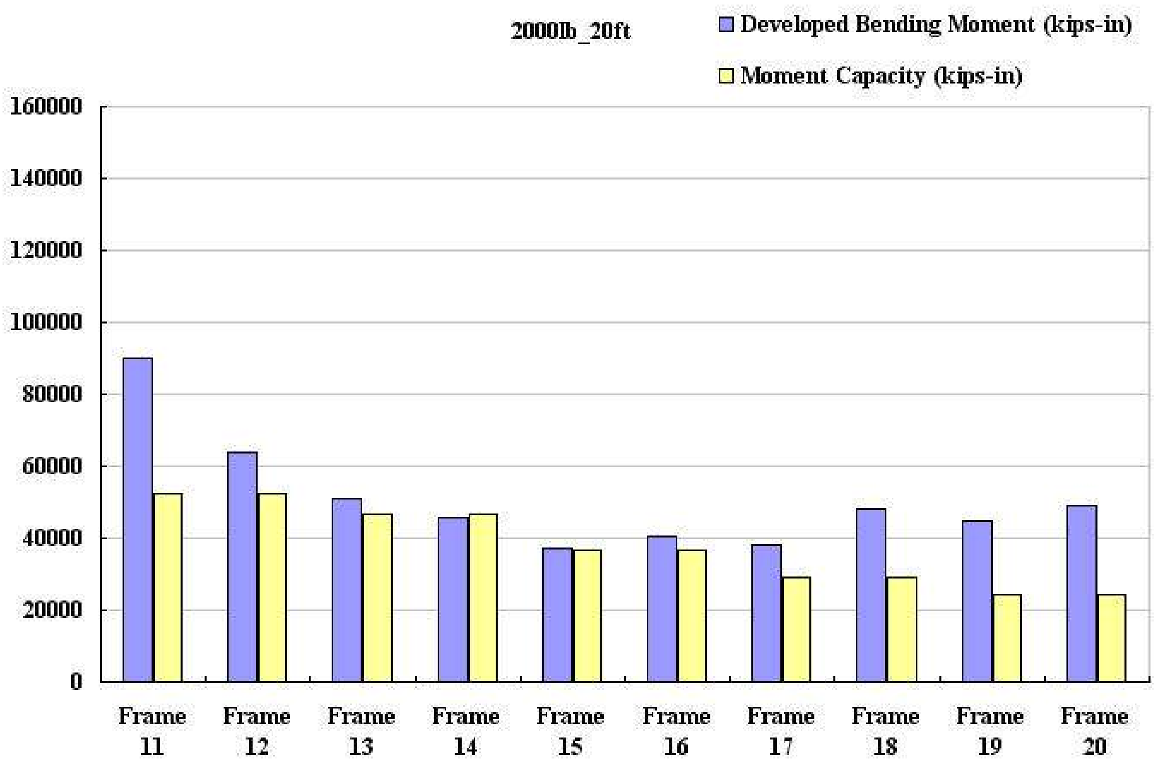

Figure 5.38 : Developed Bending Moment vs. Moment Capacity of Flexible Diaphragm (2,000 lb @ 20 ft)

Table 5.8 : Max. Bending Moment at MRF Frames (3,000 lb TNT Weight @ 20 ft)

Frame No.	Frame Section	Bending Moment (Mu)	Moment Capacity (ϕMn)
11	W14*500	139484.3	52500
12	W14*500	98740.0	52500
13	W14*455	78117.6	46800
14	W14*455	69556.1	46800
15	W14*370	56534.2	36800
16	W14*370	61394.0	36800
17	W14*283	57977.8	29150
18	W14*283	73260.1	29150
19	W14*257	69040.0	24350
20	W14*257	75600.7	24350

(unit : k-in)

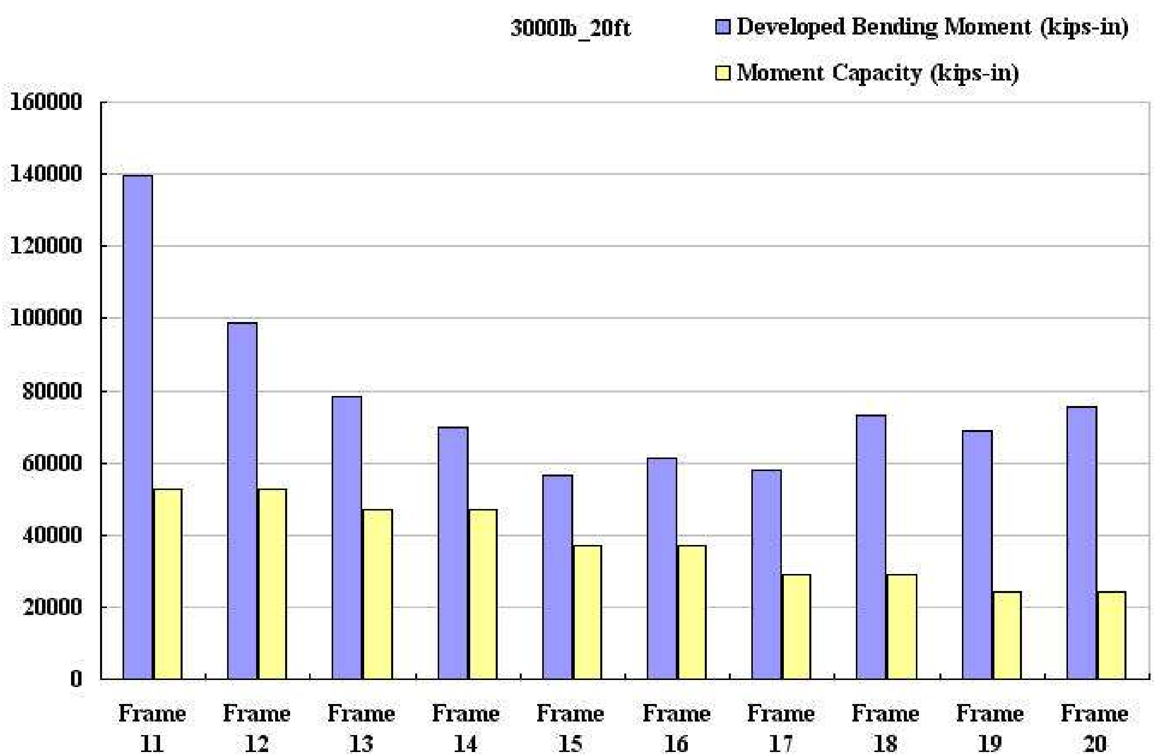

Figure 5.39 : Developed Bending Moment vs. Moment Capacity of Flexible Diaphragm (3,000 lb @ 20 ft)

Table 5.9 : Max. Bending Moment at MRF Frames (4,000 lb TNT Weight @ 20 ft)

Frame No.	Frame Section	Bending Moment (Mu)	Moment Capacity (ϕMn)
11	W14*500	178708.0	52500
12	W14*500	128890.1	52500
13	W14*455	99036.7	46800
14	W14*455	89564.8	46800
15	W14*370	72524.5	36800
16	W14*370	78651.2	36800
17	W14*283	75264.3	29150
18	W14*283	94725.2	29150
19	W14*257	90509.8	24350
20	W14*257	96603.9	24350

(unit : k-in)

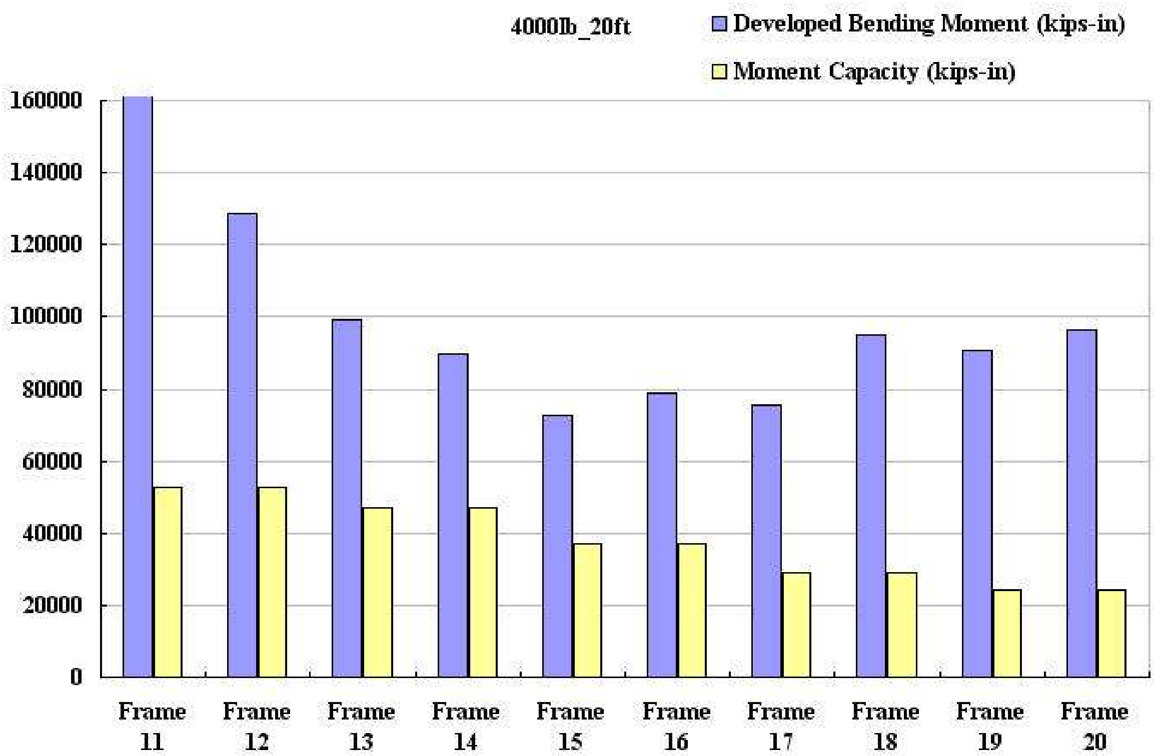

Figure 5.40 : Developed Bending Moment vs. Moment Capacity of Flexible Diaphragm (4,000 lb @ 20 ft)

To compare developed forces obtained by flexible diaphragm analysis with capacity, Bending moment and shear capacity of concrete slab is provided by followed equations from ACI 318-02 [1] as shown in chapter 4.3. Hence, the moment capacity is calculated as **212.5 k-in** and the shear capacity is **0.76 k/in**.

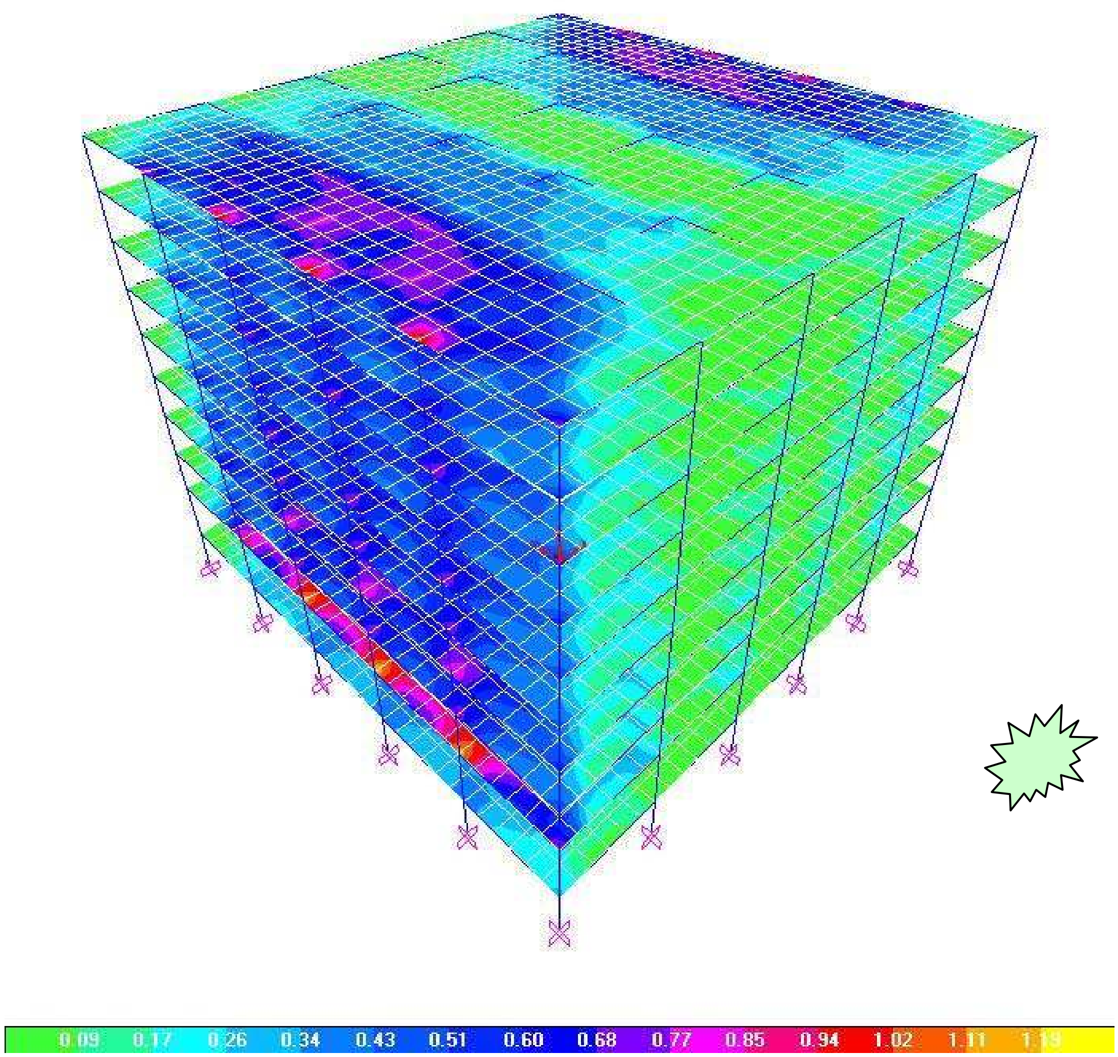

(a) Shear Force Distribution on Whole Structure (1,000 lb TNT Weight@20 ft Stand-Off Distance)

Figure 5.41 : Shear Force Distribution on Ten Story Building (1,000 lb TNT Weight@20 ft Stand-Off Distance)

“Figure 5.41 : Continued”

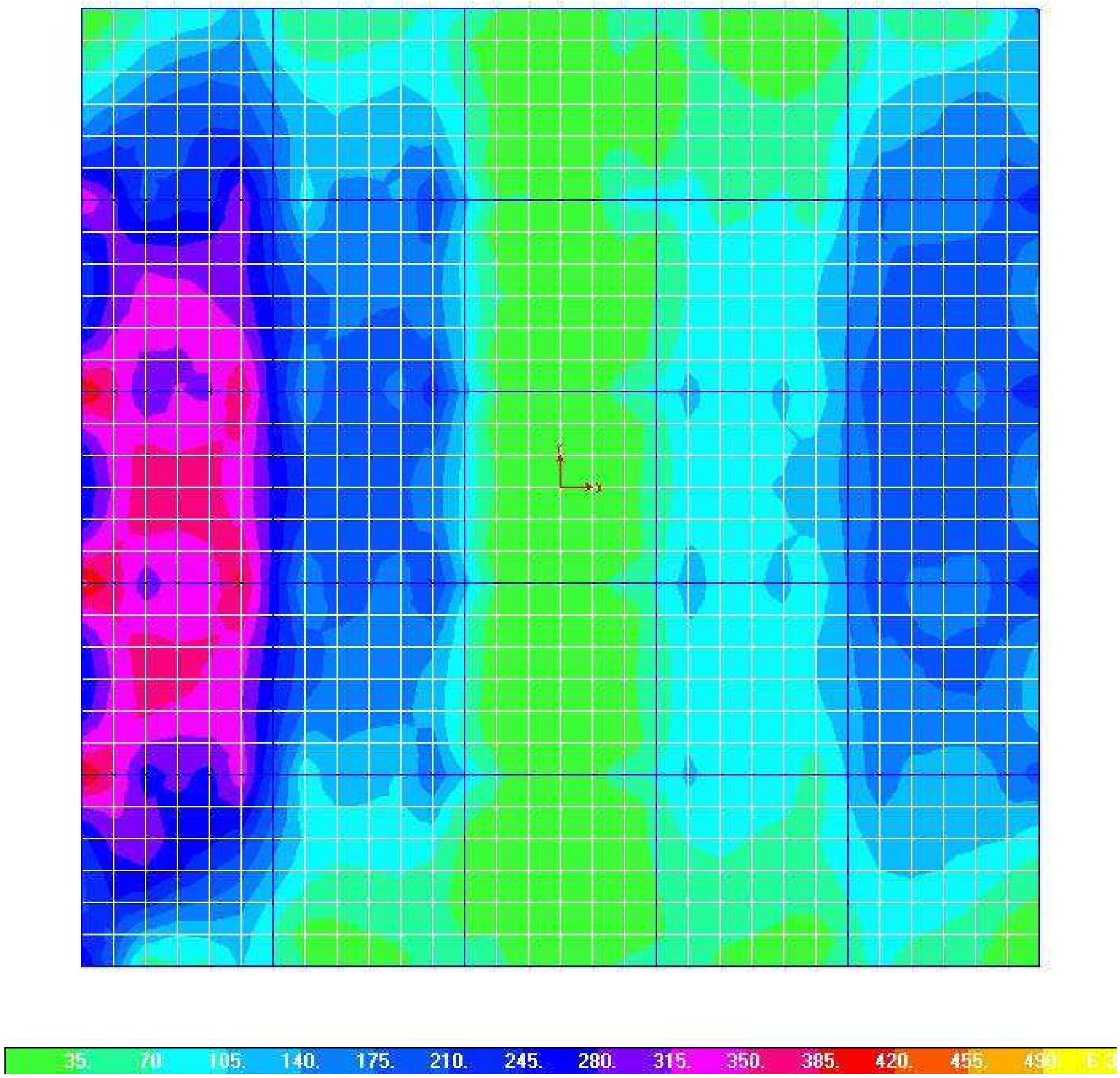

(b) Shear Force Distribution at 1st Floor (1,000 lb TNT Weight@20 ft Stand-Off Distance)

"Figure 5.41 : Continued"

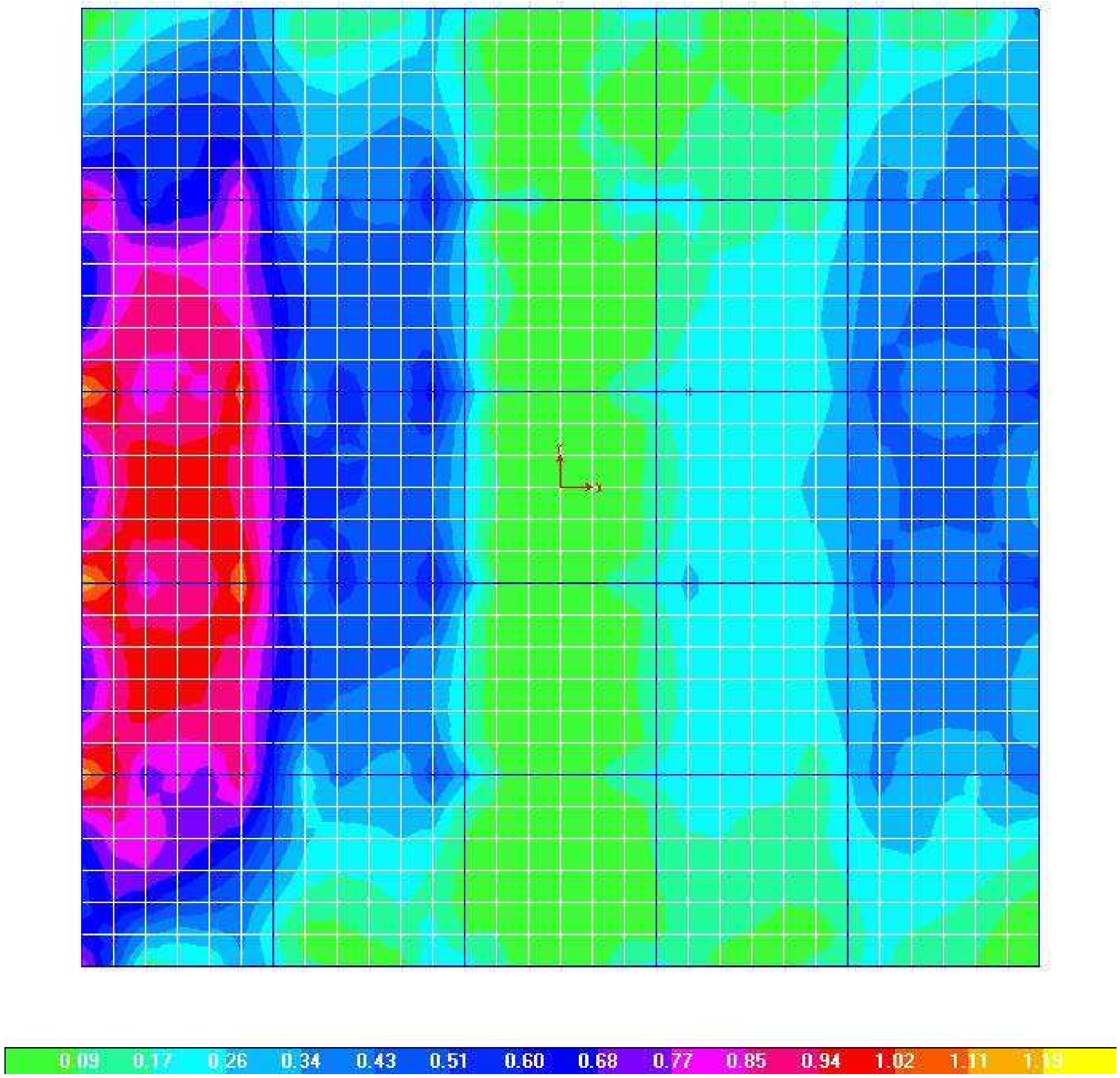

(c) Shear Force Distribution at 2^{nd} Floor (1,000 lb TNT Weight@20 ft Stand-Off Distance)

“Figure 5.41 : Continued”

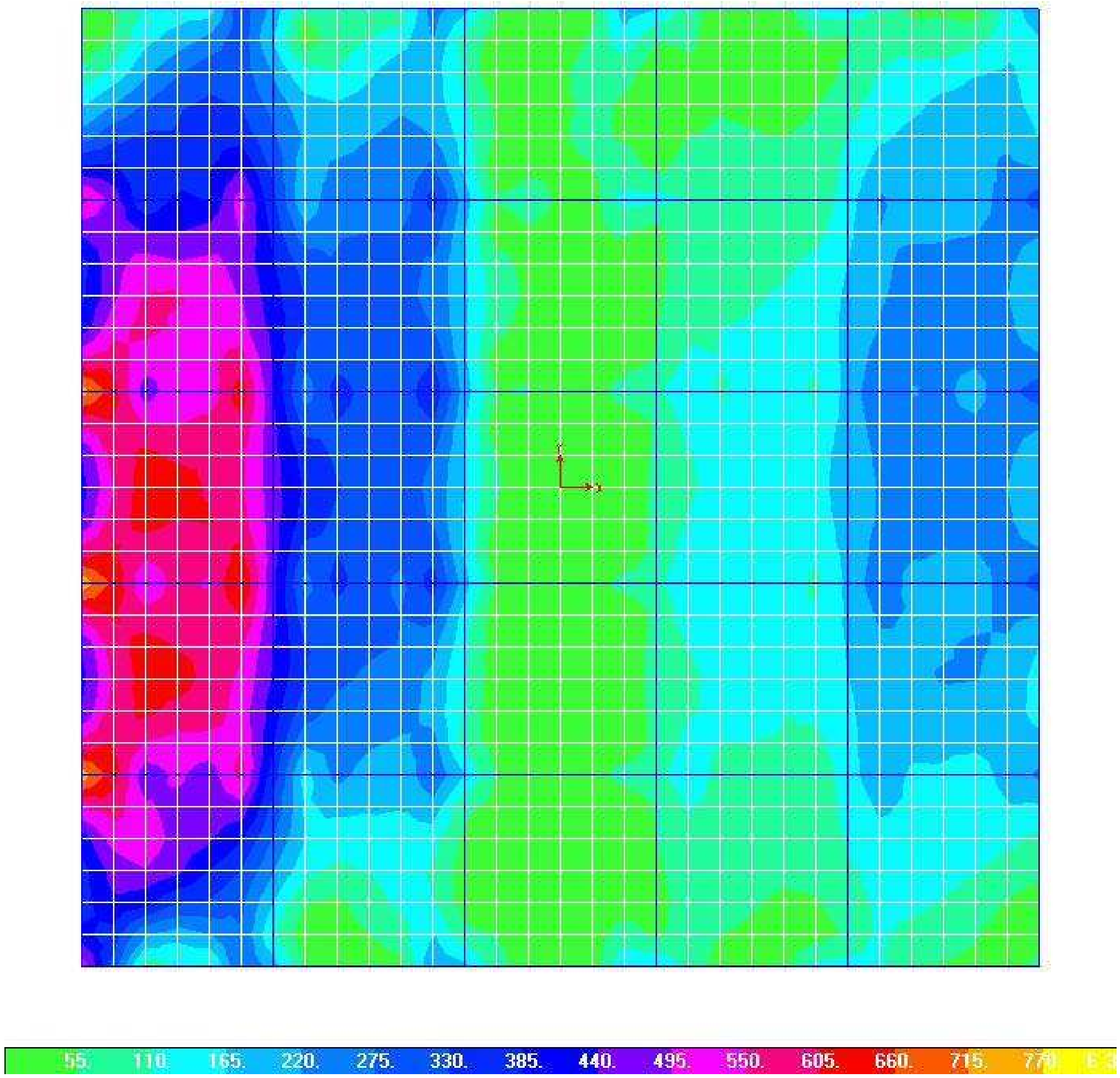

(d) Shear Force Distribution at 3rd Floor (1,000 lb TNT Weight@20 ft Stand-Off Distance)

"Figure 5.41 : Continued"

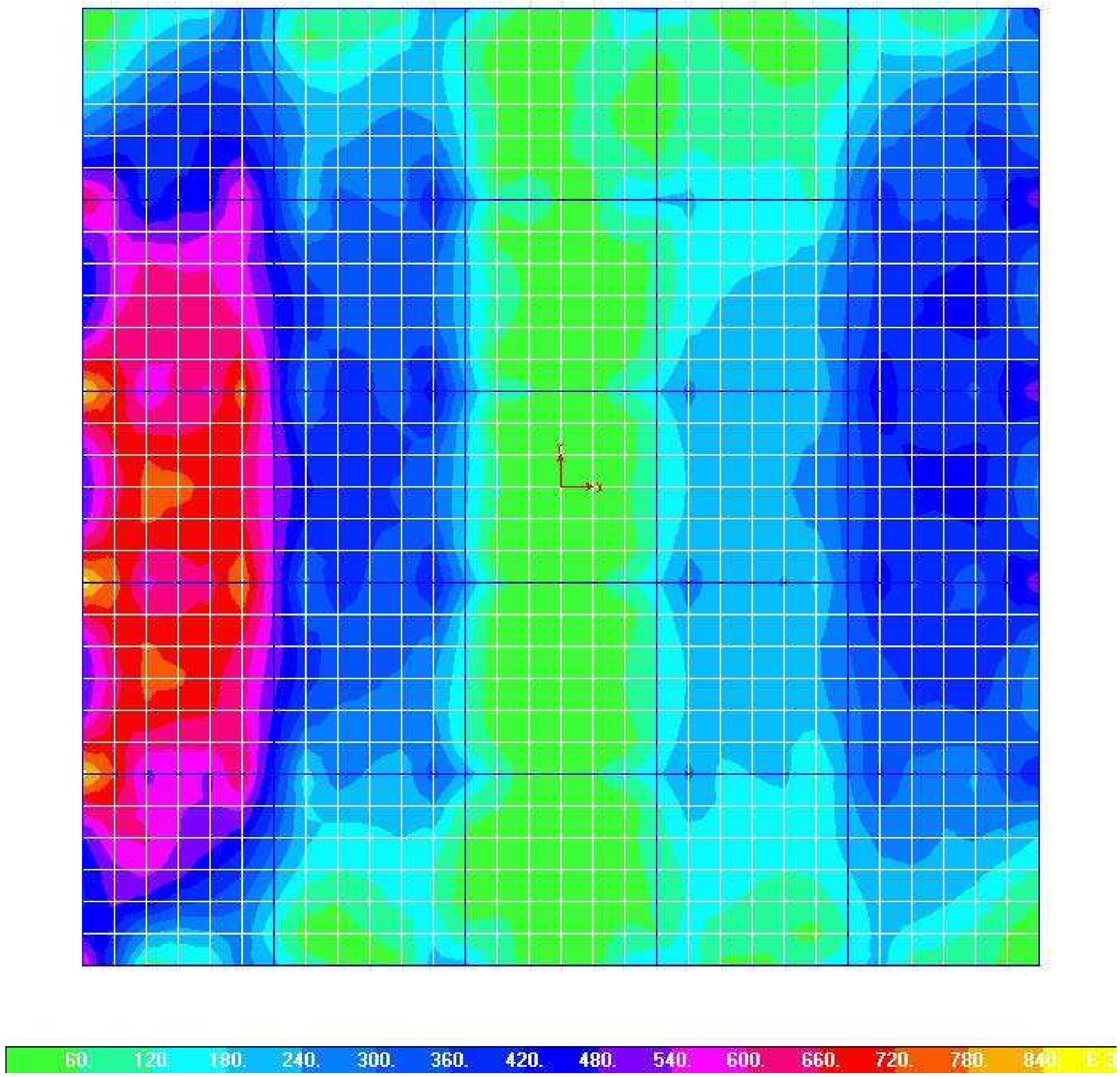

(e) Shear Force Distribution at 4th Floor (1,000 lb TNT Weight@20 ft Stand-Off Distance)

"Figure 5.41 : Continued"

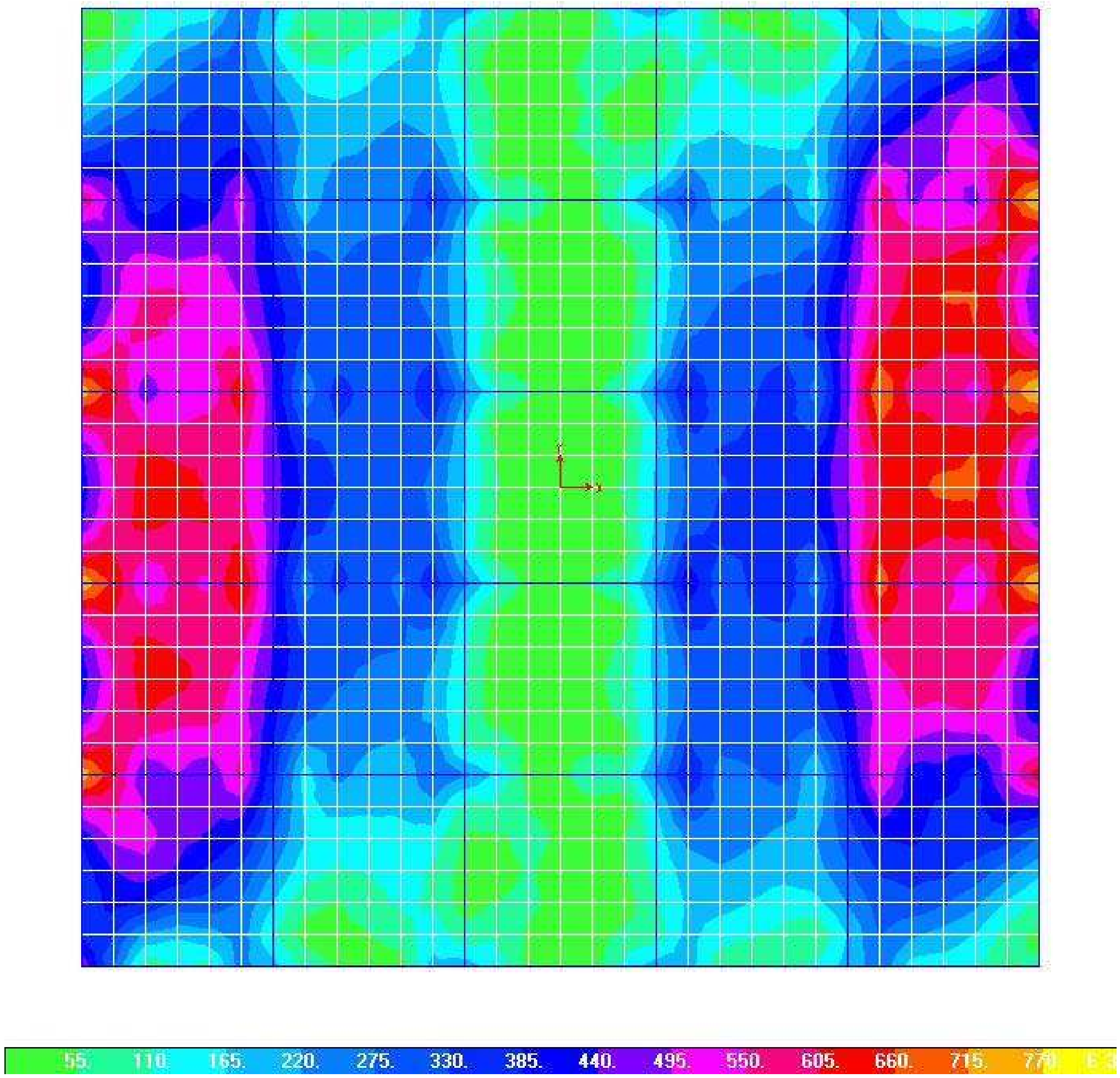

(f) Shear Force Distribution at 5th Floor (1,000 lb TNT Weight@20 ft Stand-Off Distance)

“Figure 5.41 : Continued”

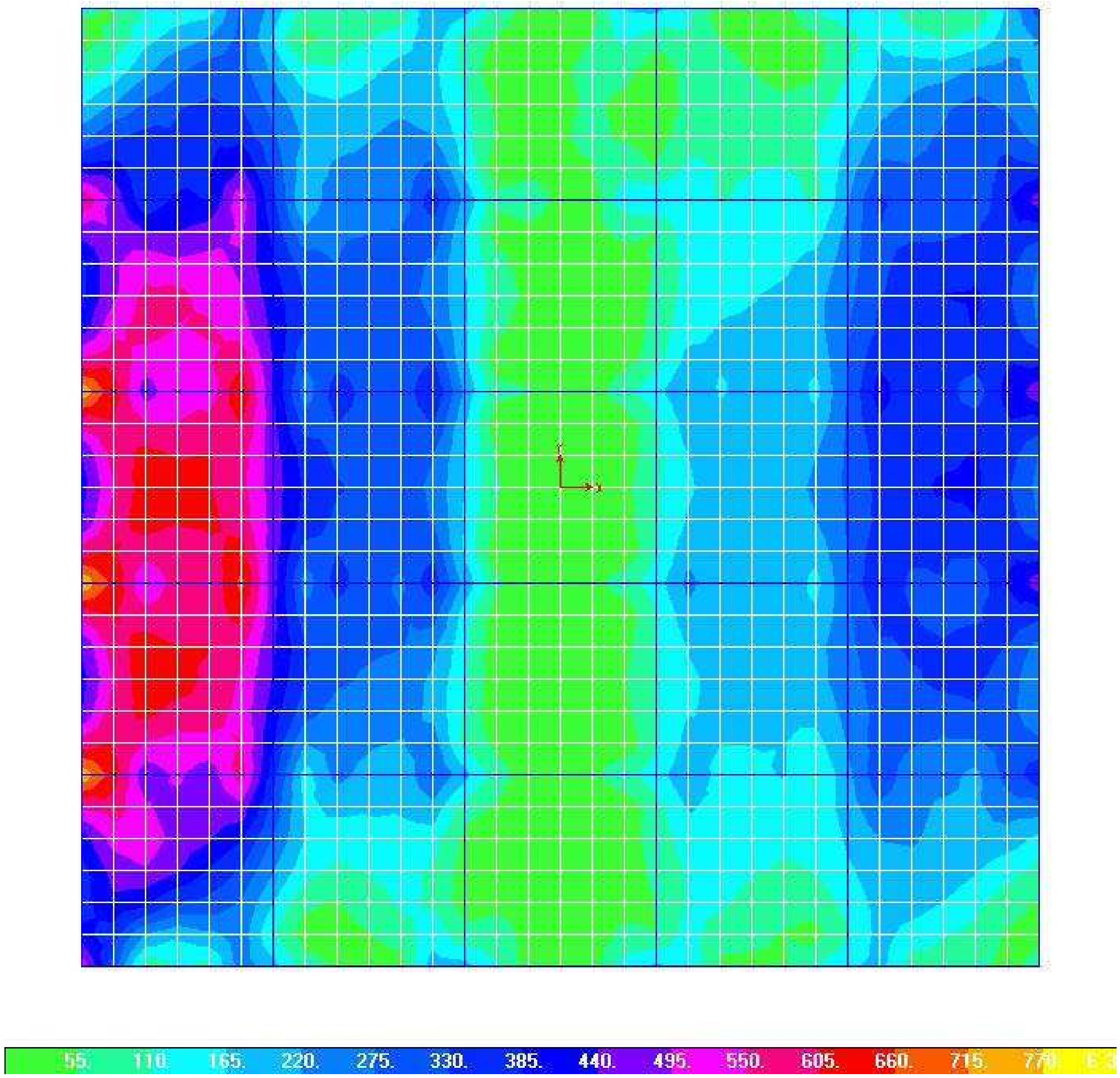

(g) Shear Force Distribution at 6th Floor (1,000 lb TNT Weight@20 ft Stand-Off Distance)

"Figure 5.41 : Continued"

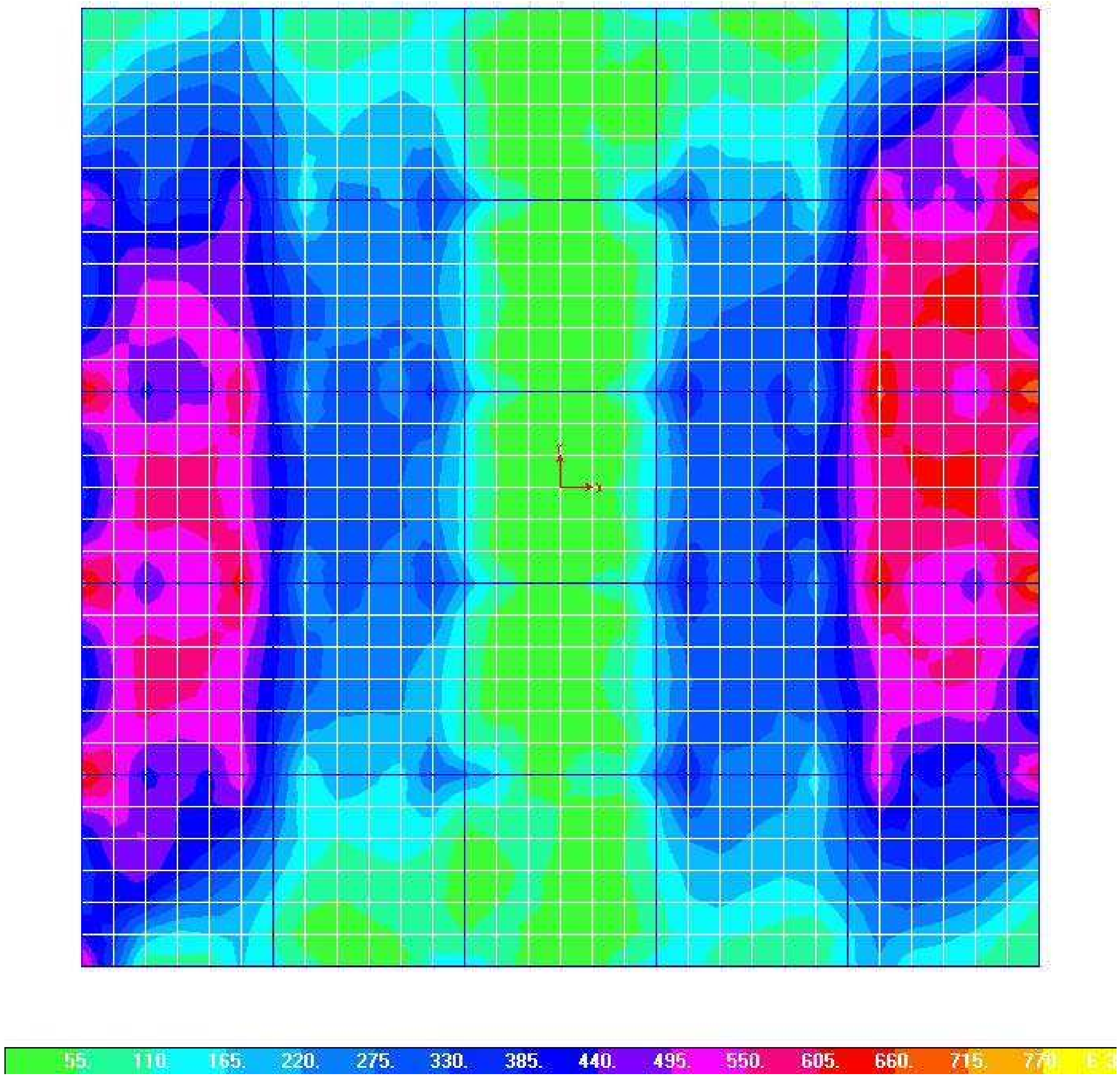

(h) Shear Force Distribution at 7th Floor (1,000 lb TNT Weight@20 ft Stand-Off Distance)

“Figure 5.41 : Continued”

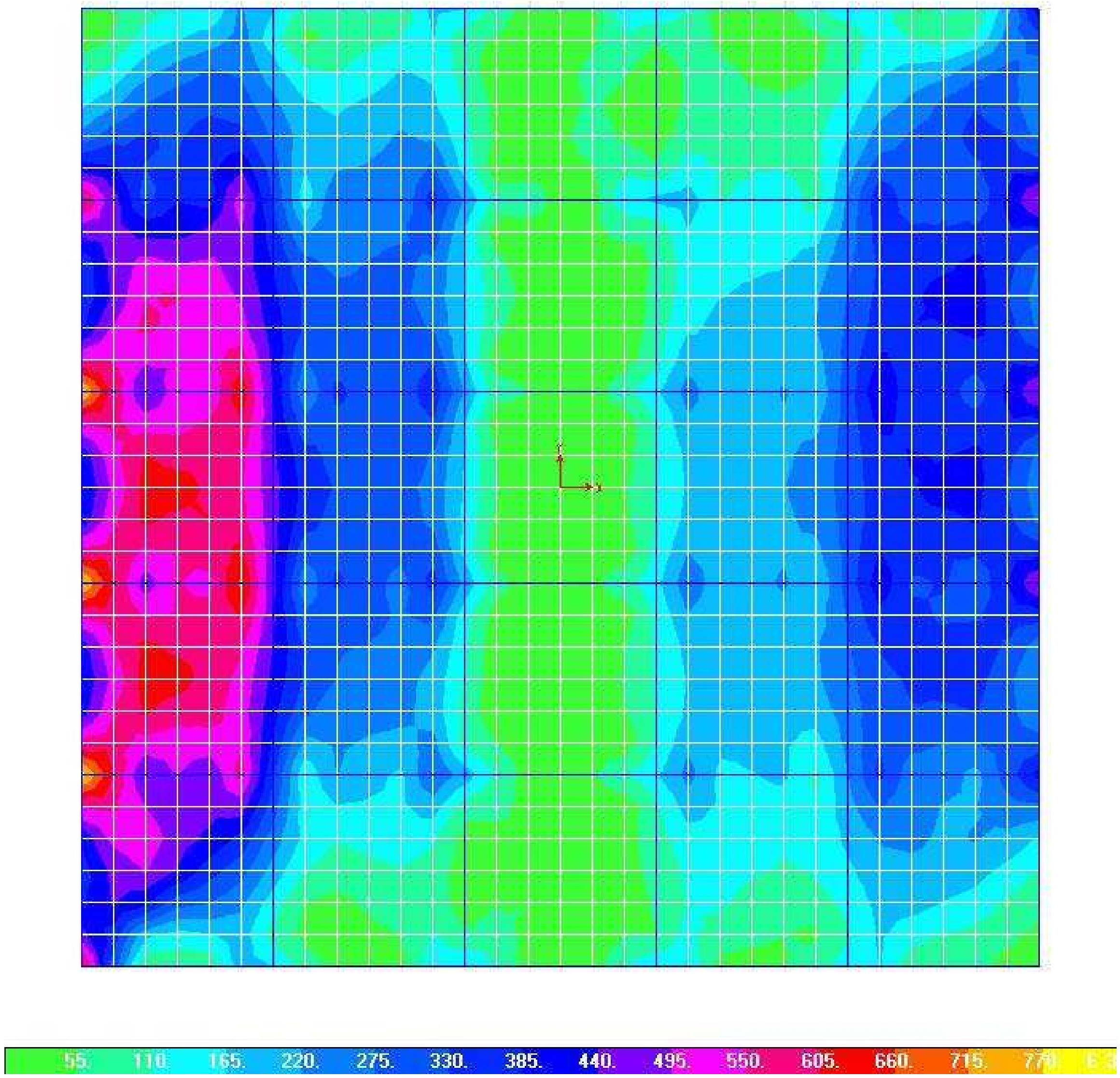

(i) Shear Force Distribution at 8th Floor (1,000 lb TNT Weight@20 ft Stand-Off Distance)

"Figure 5.41 : Continued"

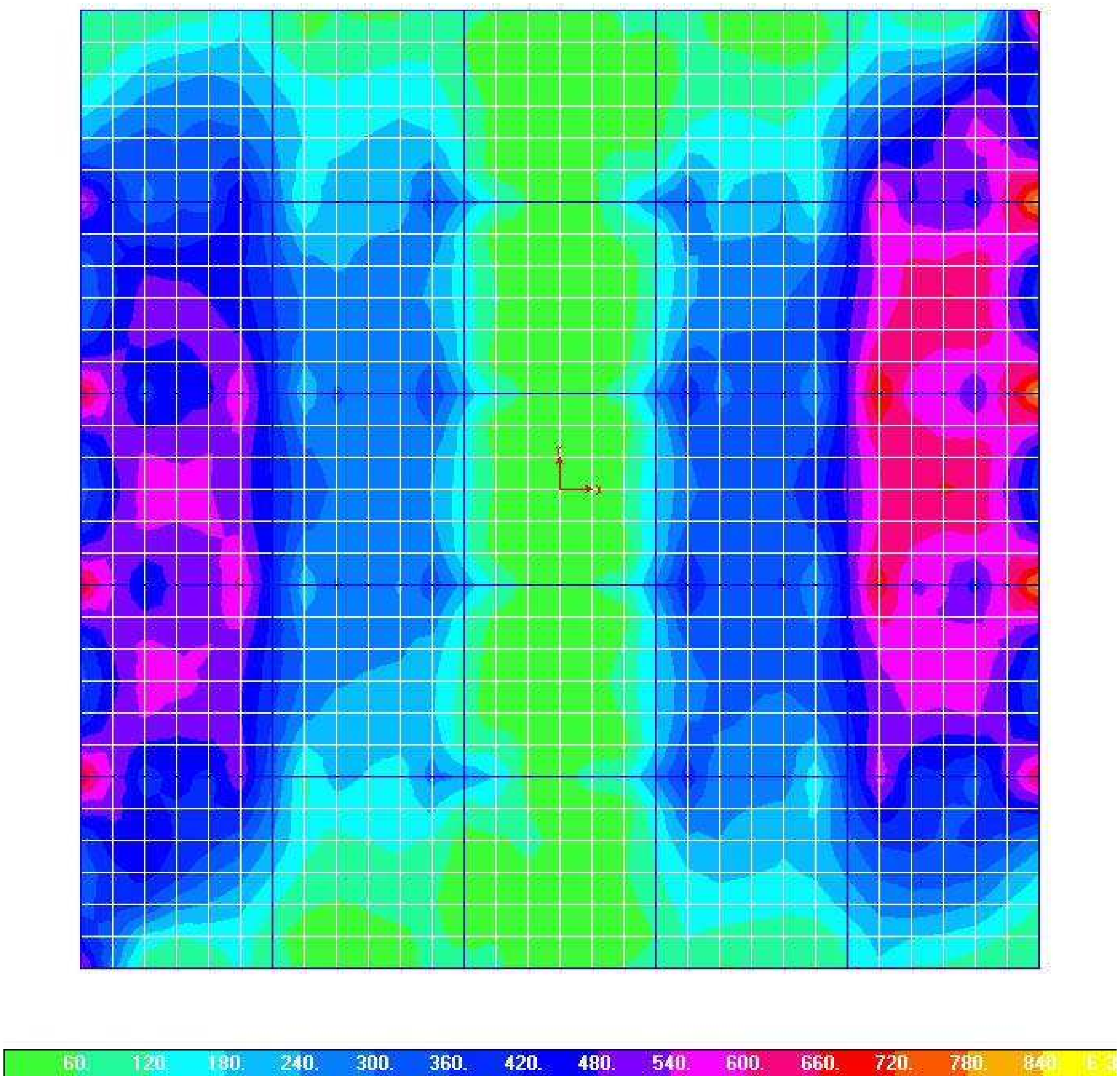

(j) Shear Force Distribution at 9th Floor (1,000 lb TNT Weight@20 ft Stand-Off Distance)

“Figure 5.41 : Continued”

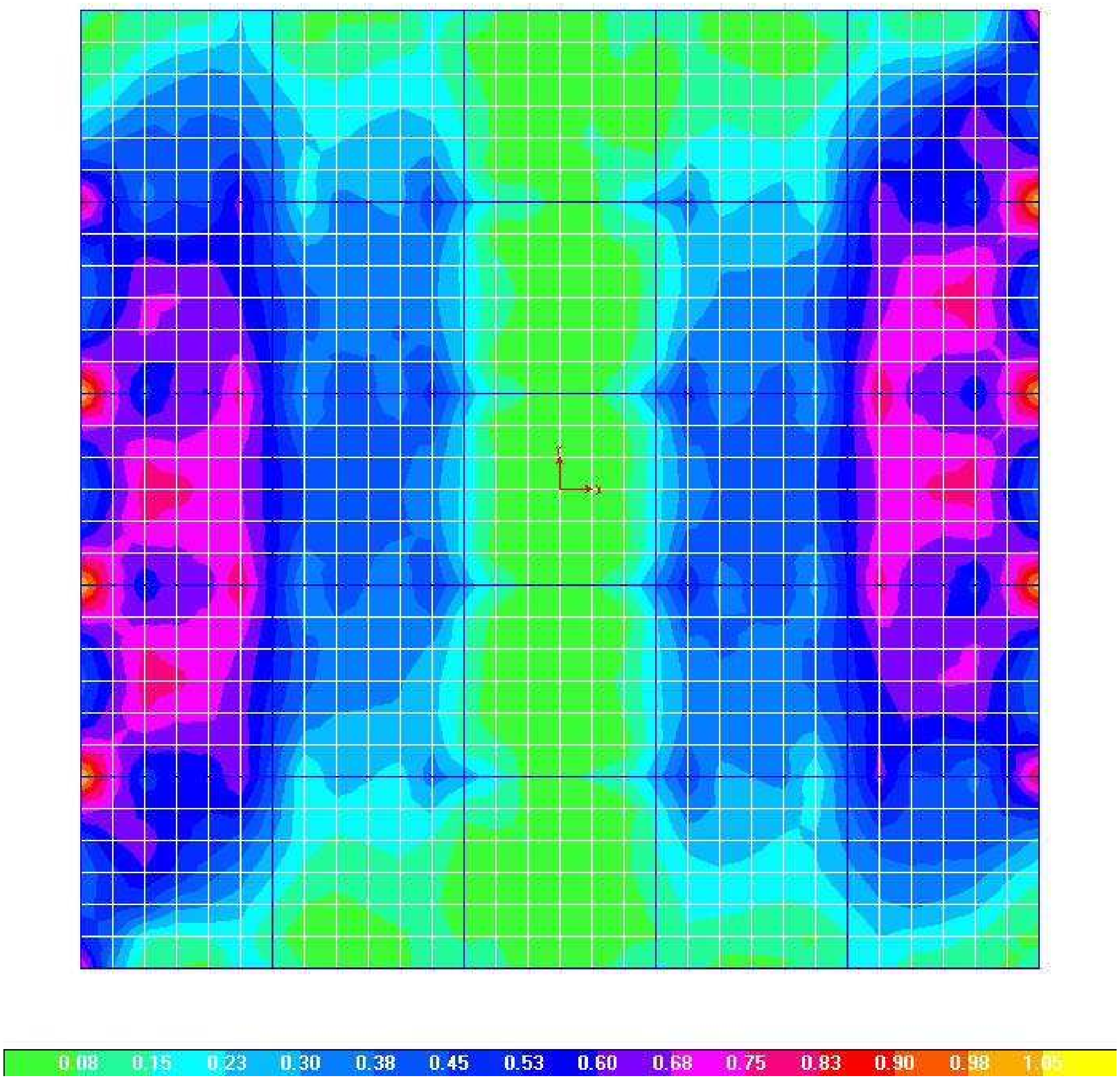

(k) Shear Force Distribution at Roof (1,000 lb TNT Weight@20 ft Stand-Off Distance)

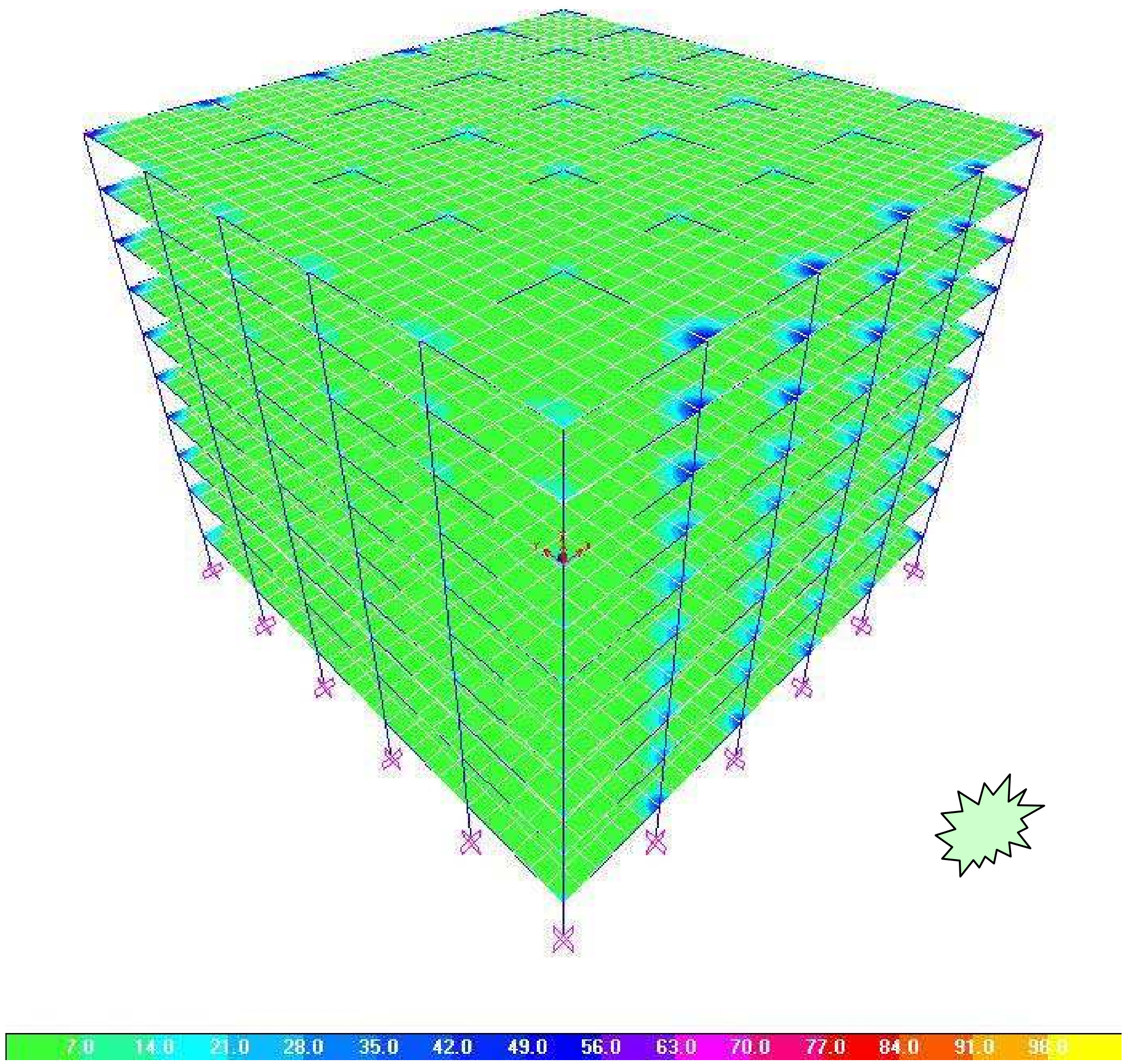

(a) Moment Distribution on Whole Structure (1,000 lb TNT Weight@20 ft Stand-Off Distance)

Figure 5.42 : Moment Distribution on Ten Story Building (1,000 lb TNT Weight@20 ft Stand-Off Distance)

"Figure 5.42 : Continued"

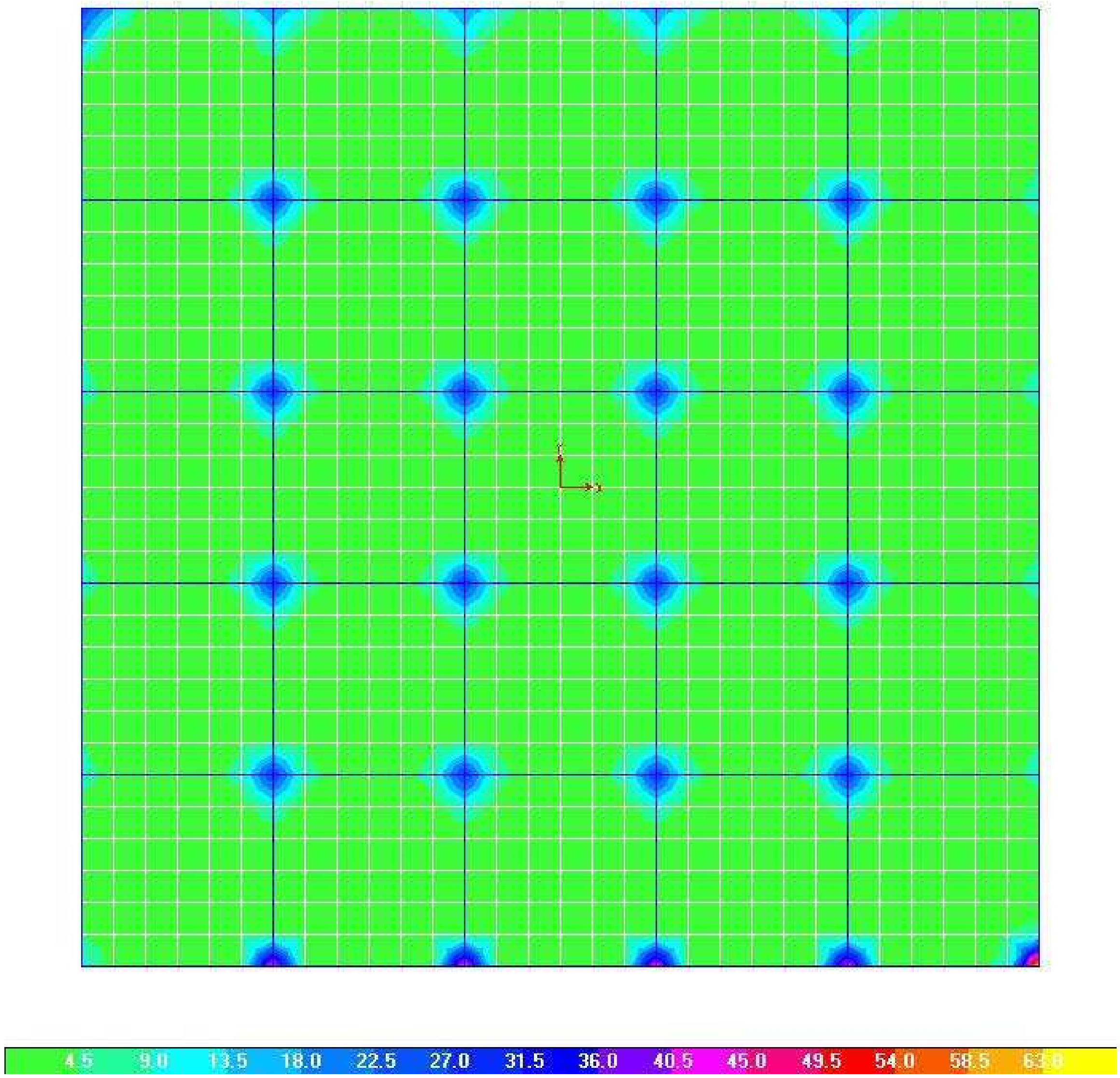

(b) Moment Distribution at 1st Floor (1,000 lb TNT Weight@20 ft Stand-Off Distance)

“Figure 5.42 : Continued”

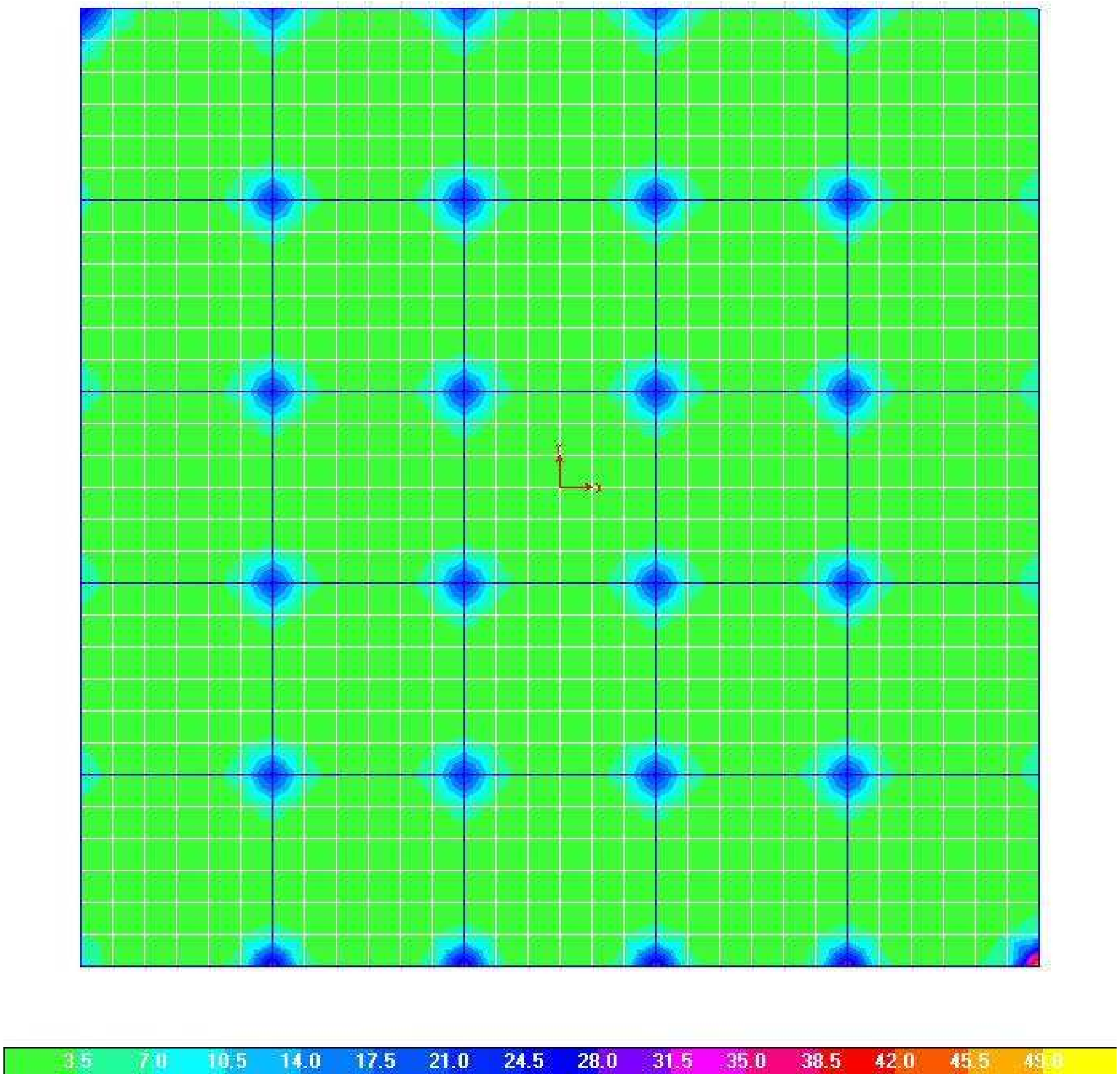

(c) Moment Distribution at 2nd Floor (1,000 lb TNT Weight@20 ft Stand-Off Distance)

“Figure 5.42 : Continued”

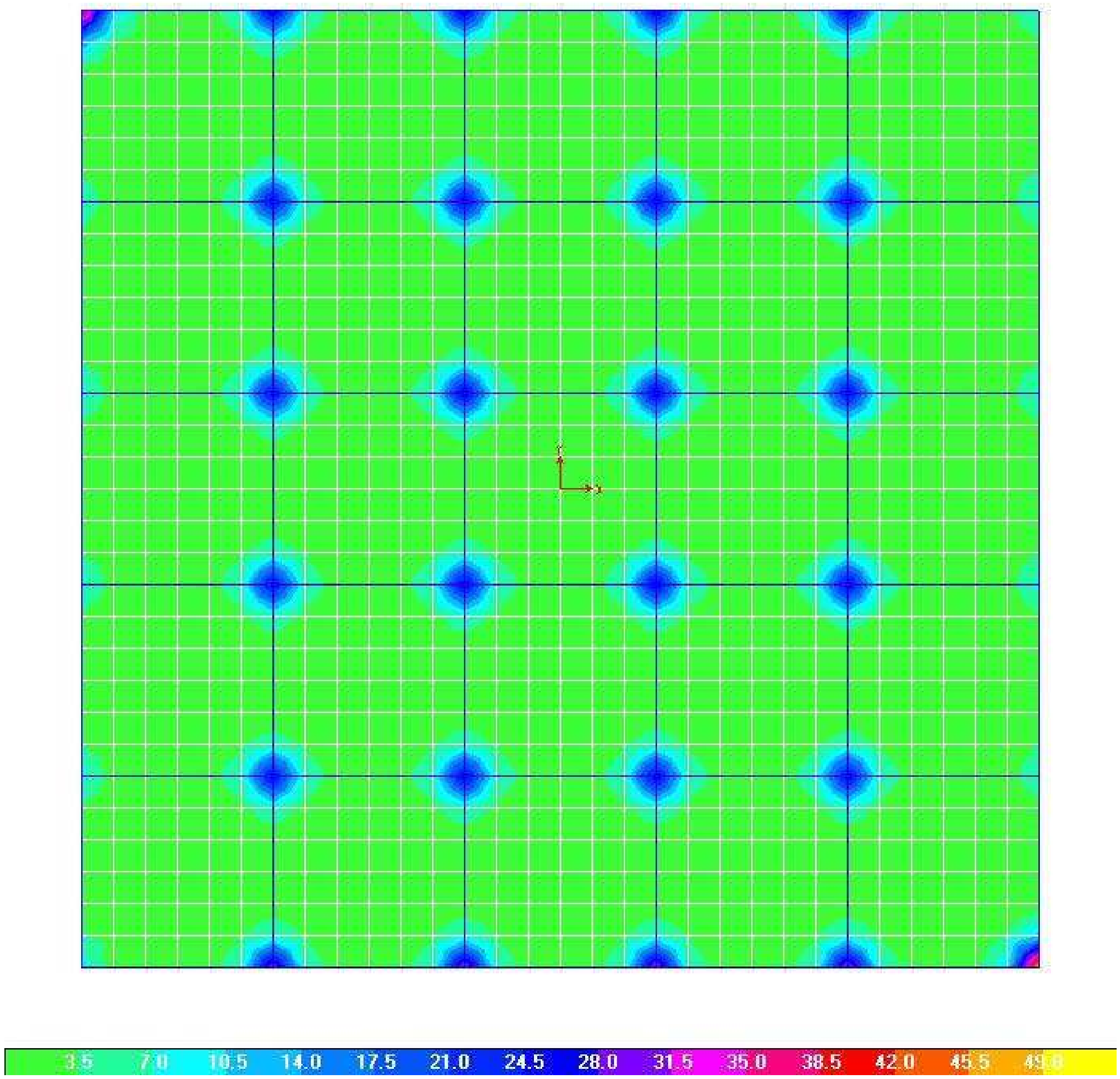

(d) Moment Distribution at 3rd Floor (1,000 lb TNT Weight@20 ft Stand-Off Distance)

“Figure 5.42 : Continued”

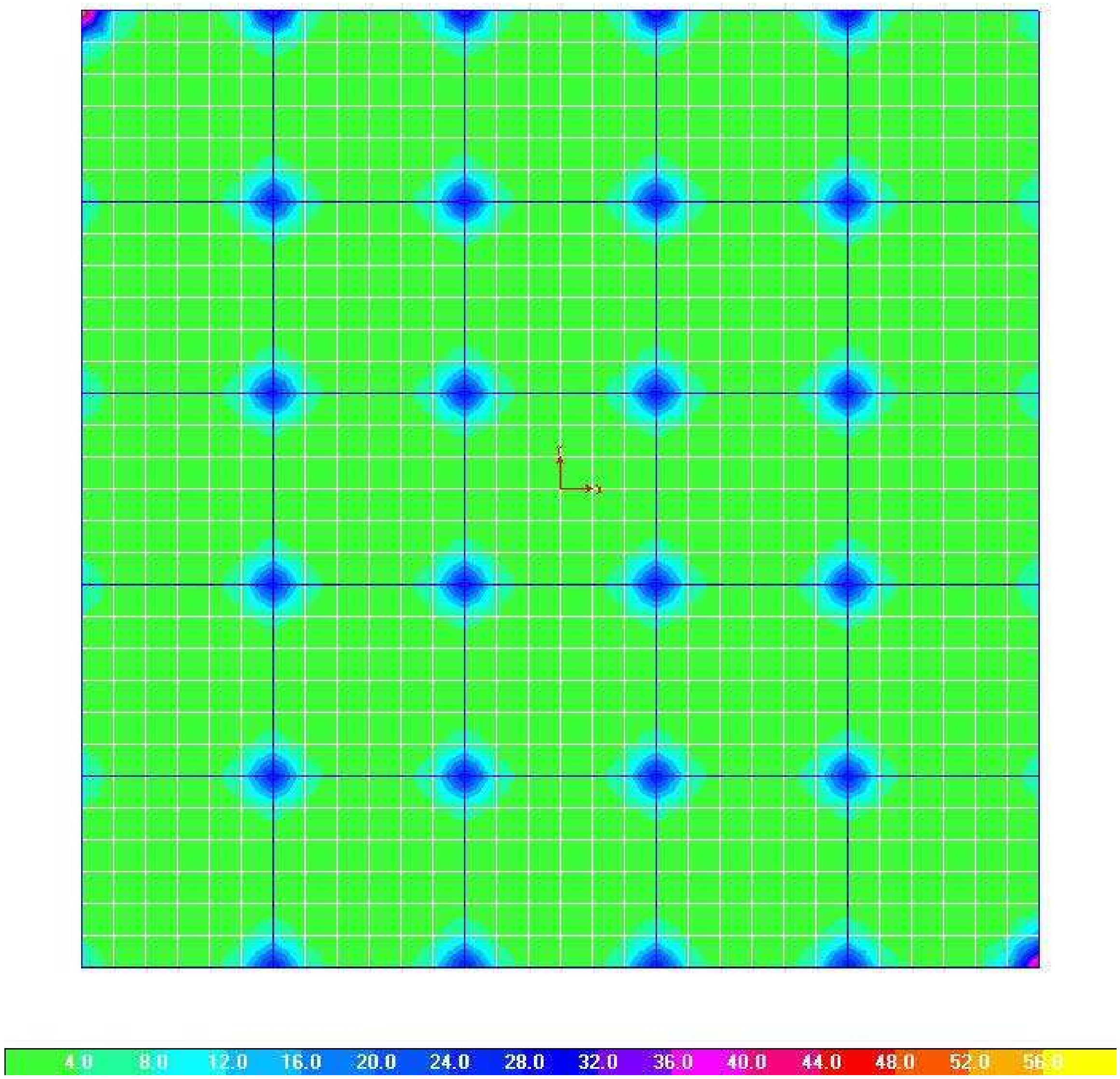

(e) Moment Distribution at 4th Floor (1,000 lb TNT Weight@20 ft Stand-Off Distance)

“Figure 5.42 : Continued”

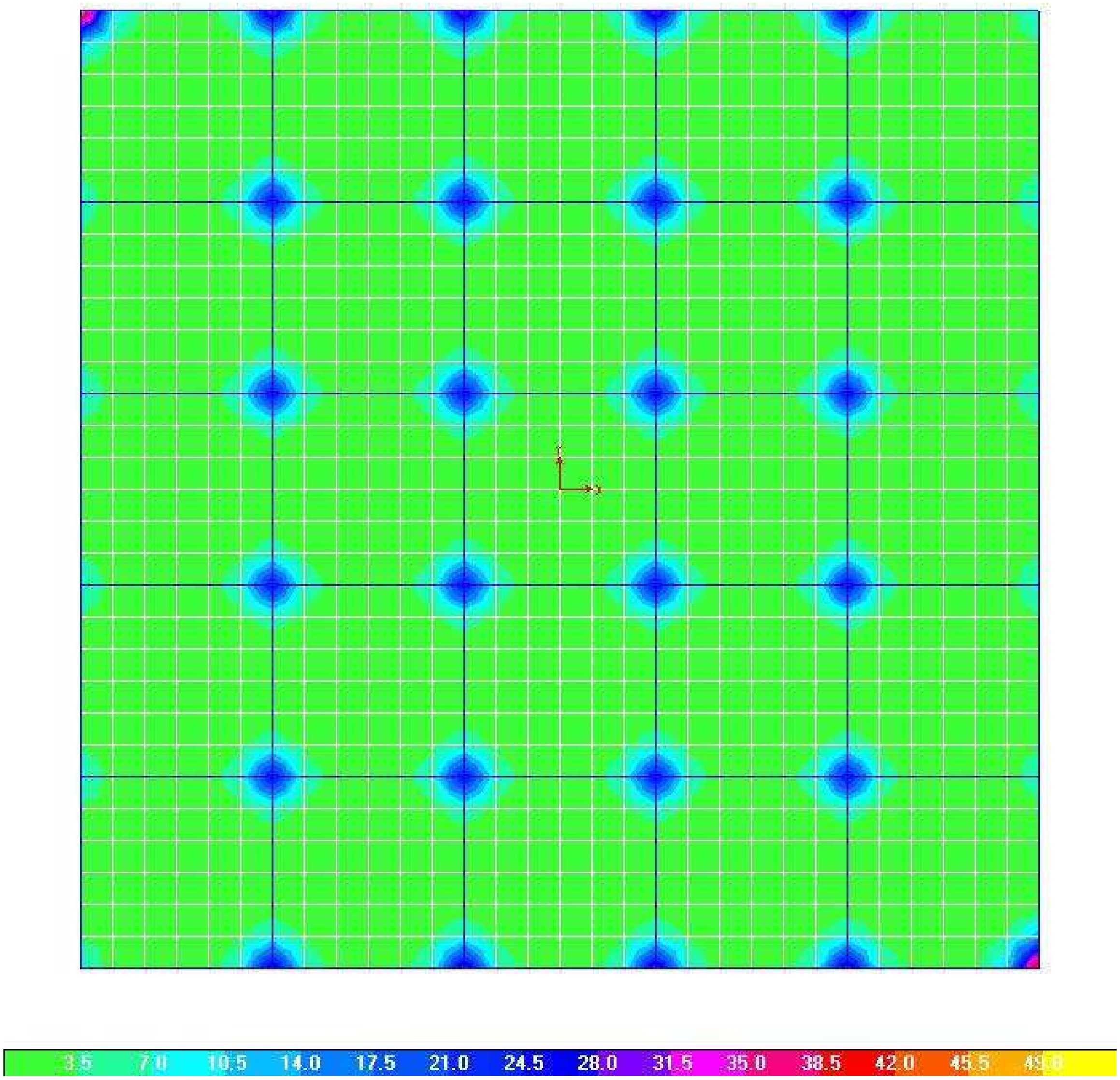

(f) Moment Distribution at 5th Floor (1,000 lb TNT Weight@20 ft Stand-Off Distance)

"Figure 5.42 : Continued"

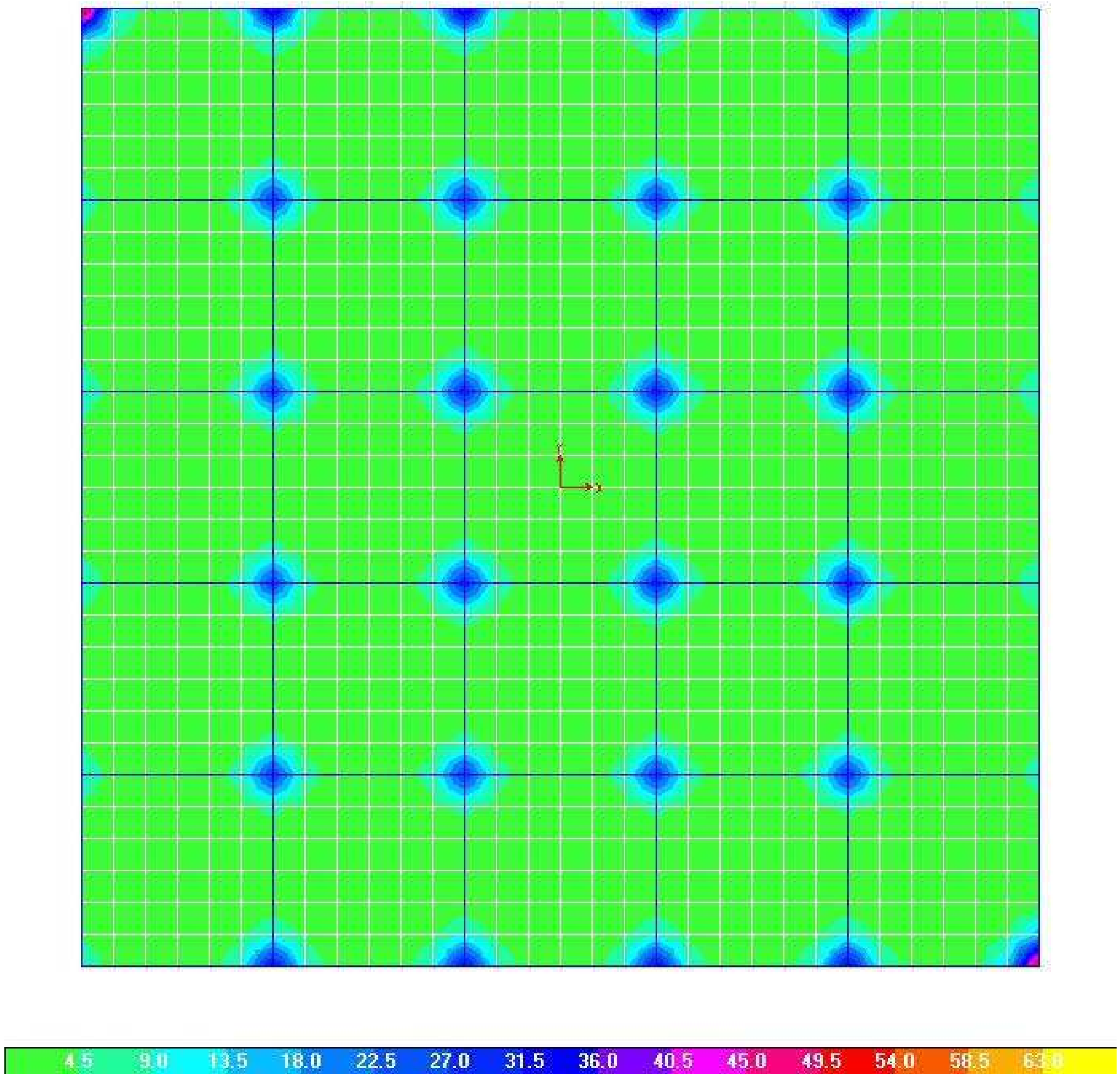

(g) Moment Distribution at 6th Floor (1,000 lb TNT Weight@20 ft Stand-Off Distance)

"Figure 5.42 : Continued"

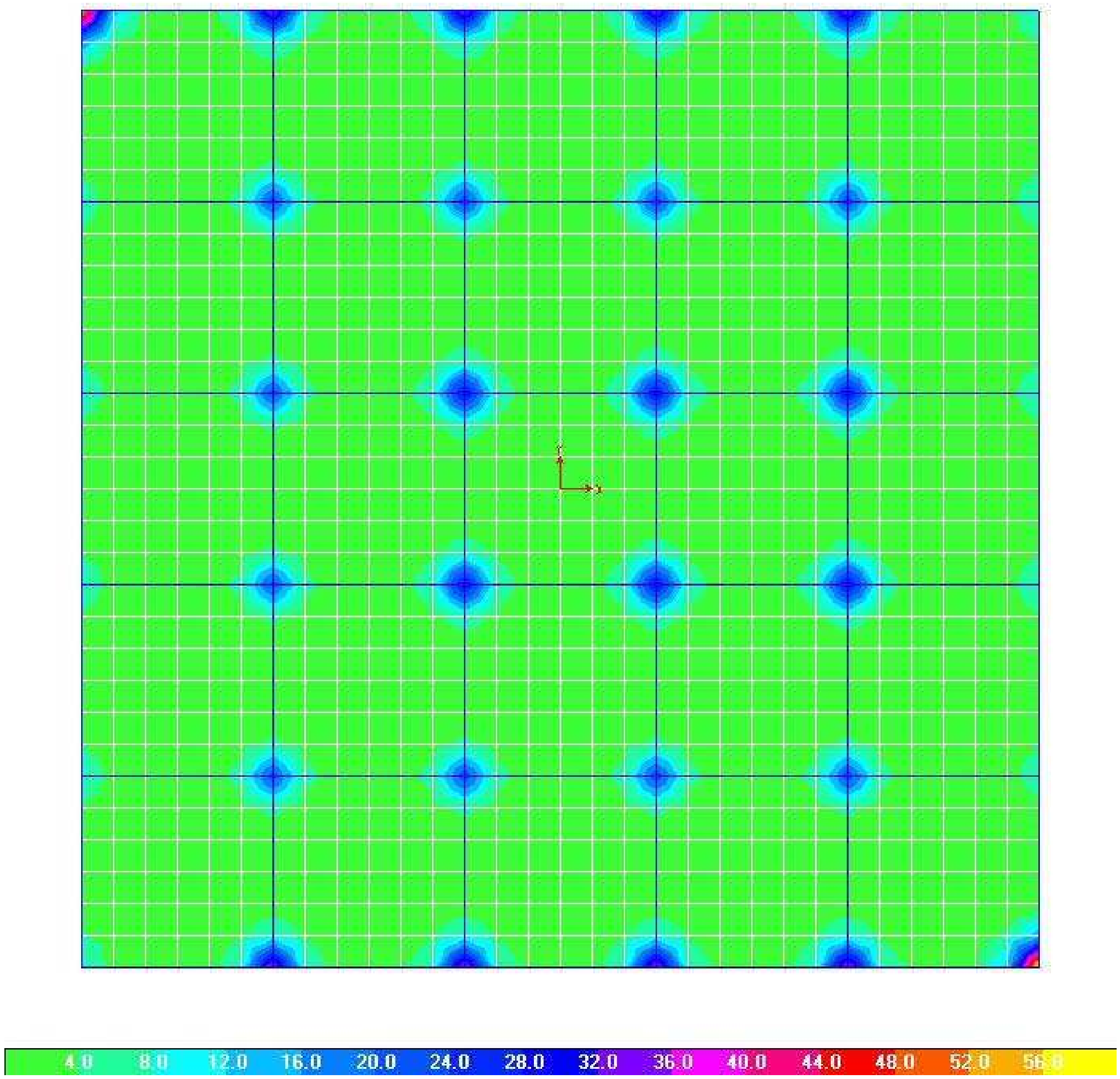

(h) Moment Distribution at 7^{th} Floor (1,000 lb TNT Weight@20 ft Stand-Off Distance)

"Figure 5.42 : Continued"

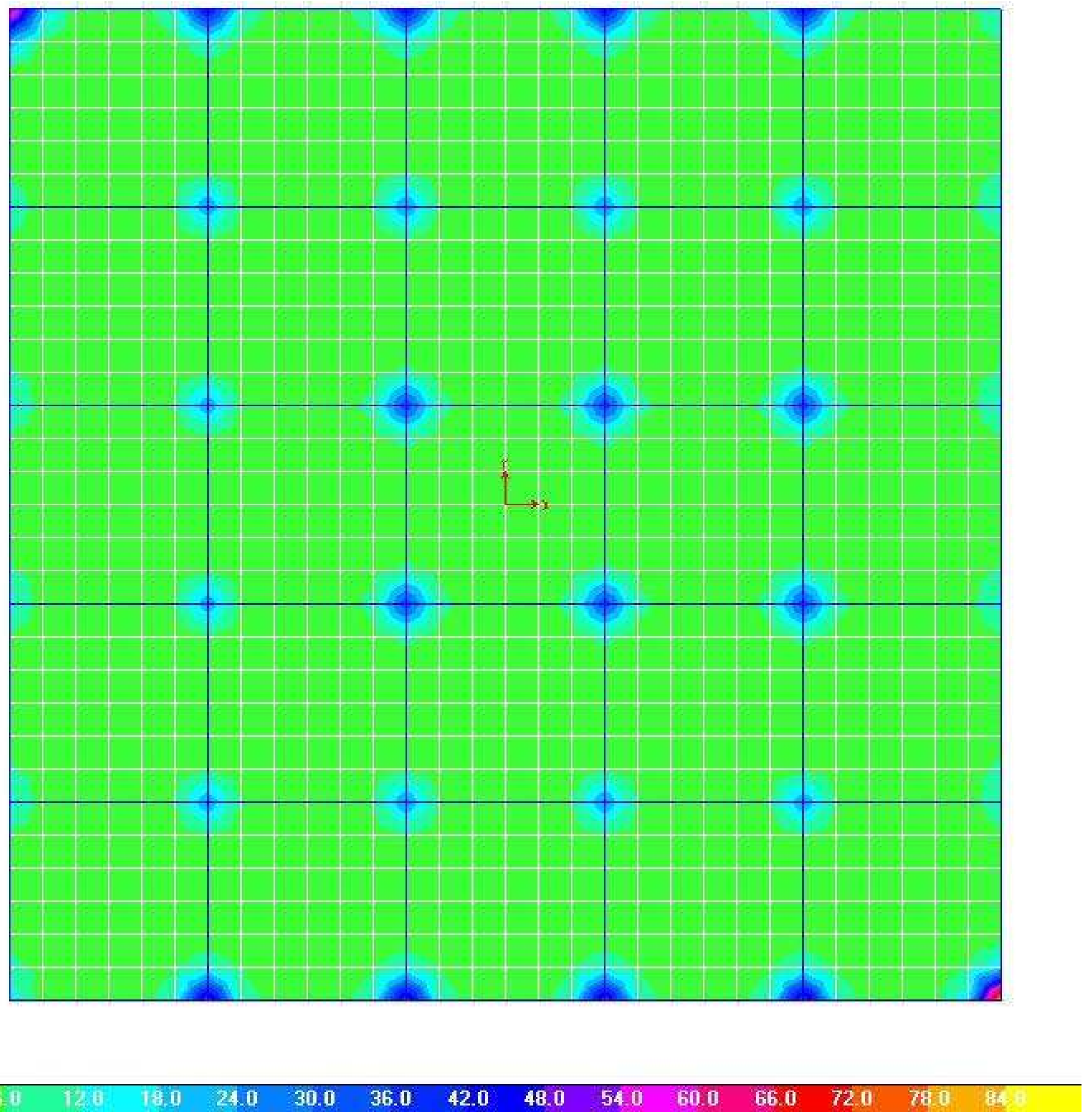

(i) Moment Distribution at 8th Floor (1,000 lb TNT Weight@20 ft Stand-Off Distance)

"Figure 5.42 : Continued"

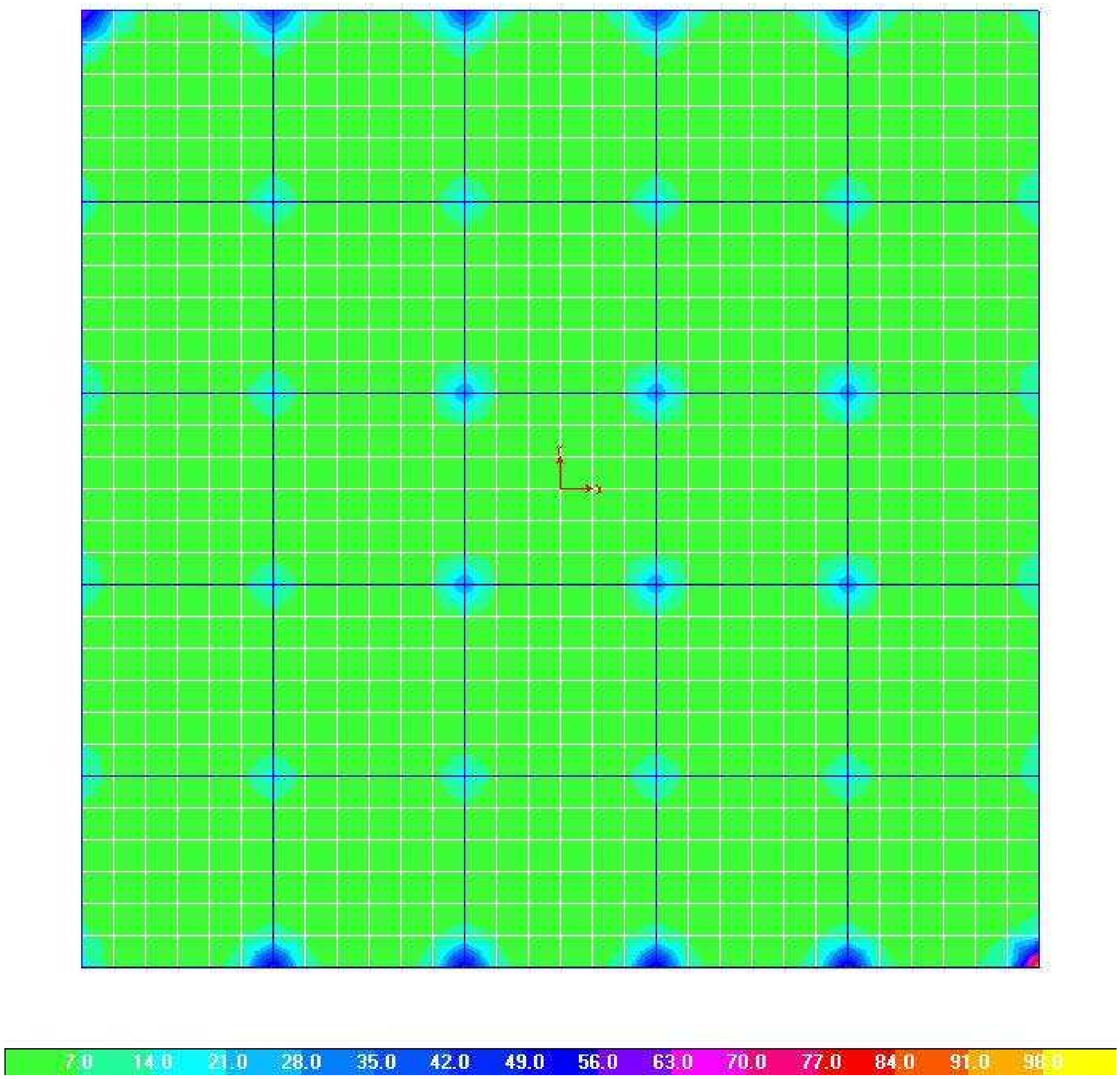

(j) Moment Distribution at 9th Floor (1,000 lb TNT Weight@20 ft Stand-Off Distance)

“Figure 5.42 : Continued”

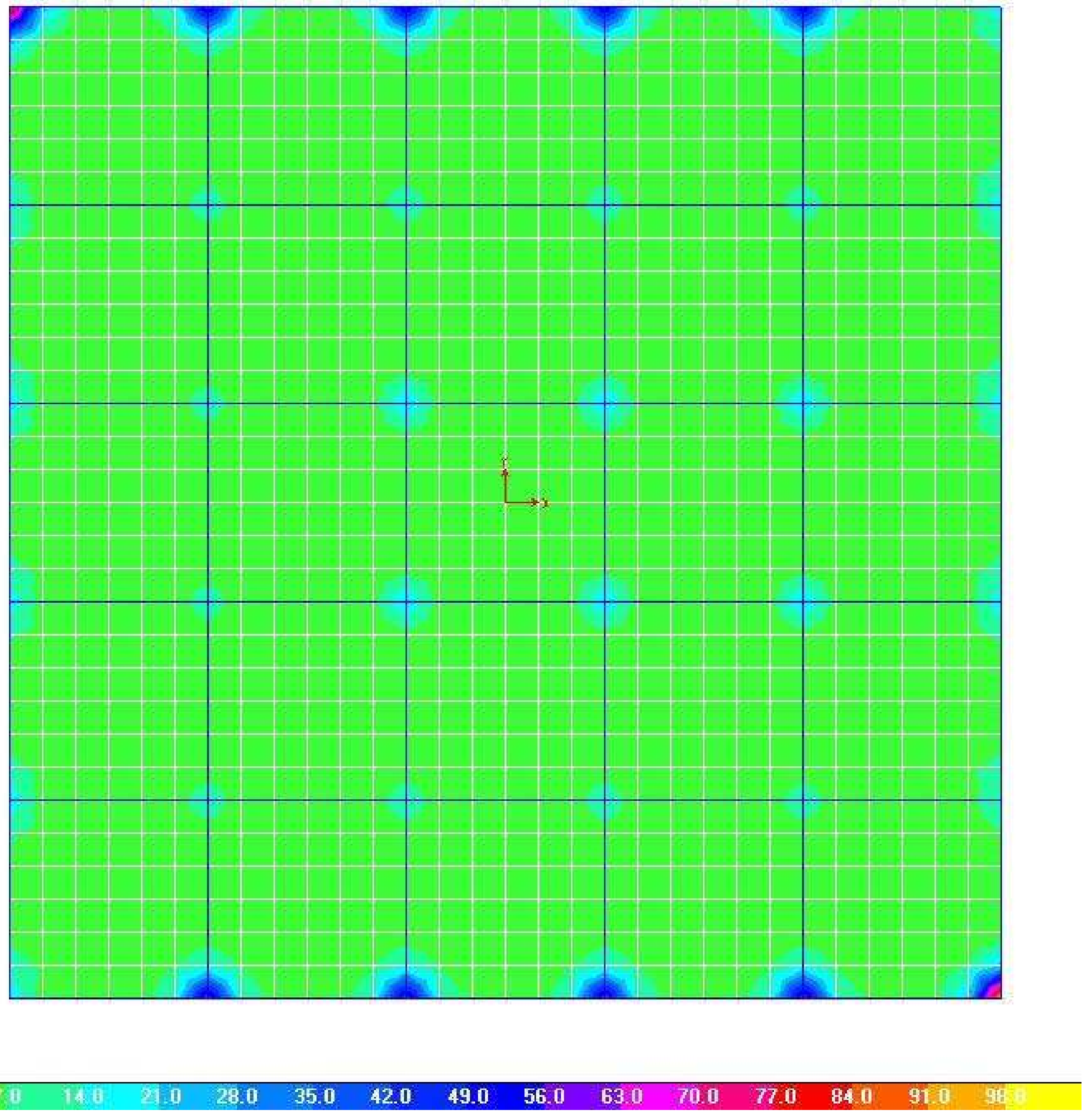

(k) Moment Distribution at Roof (1,000 lb TNT Weight@20 ft Stand-Off Distance)

Table 5.10 : The Results of Flexible Diaphragm Analysis

	1,000 lb @ 20 ft		2,000 lb @ 20 ft		3,000 lb @ 20 ft		4,000 lb @ 20 ft	
Floor	Shear Force (k/in)	Bending Moment (k-in)	Shear Force (k/in)	Bending Moment (k-in)	Shear Force (k/in)	Bending Moment (k-in)	Shear Force (k/in)	Bending Moment (k-in)
Roof	1.07	99.9	2.22	205.1	3.45	316.9	4.41	407.7
9^{th}	0.83	98.4	1.70	201.2	2.60	310.9	3.26	406.1
8^{th}	0.79	87.2	1.70	173.9	2.56	266.0	3.29	346.4
7^{th}	0.77	59.1	1.60	118.6	2.46	184.9	3.08	239.4
6^{th}	0.78	61.1	1.60	127.5	2.46	197.7	3.12	253.3
5^{th}	0.82	49.6	1.70	105.6	2.62	163.9	3.26	212.4
4^{th}	0.90	57.0	1.83	119.9	2.81	186.3	3.55	237.1
3^{rd}	0.78	49.8	1.64	99.4	2.55	152.2	3.31	193.3
2^{nd}	1.25	49.8	2.59	100.6	3.99	154.4	5.02	202.3
1^{st}	0.45	65.0	0.39	133.36	1.43	209.9	1.79	207.5

As a result, the flexural strength of this system is well provided in cases of 1,000 lb, 2,000 lb TNT weight @ 20 ft but other cases is not enough and shear failure is expected to this concrete slab at all cases as shown in Figure 5.43 – Figure 5.44.

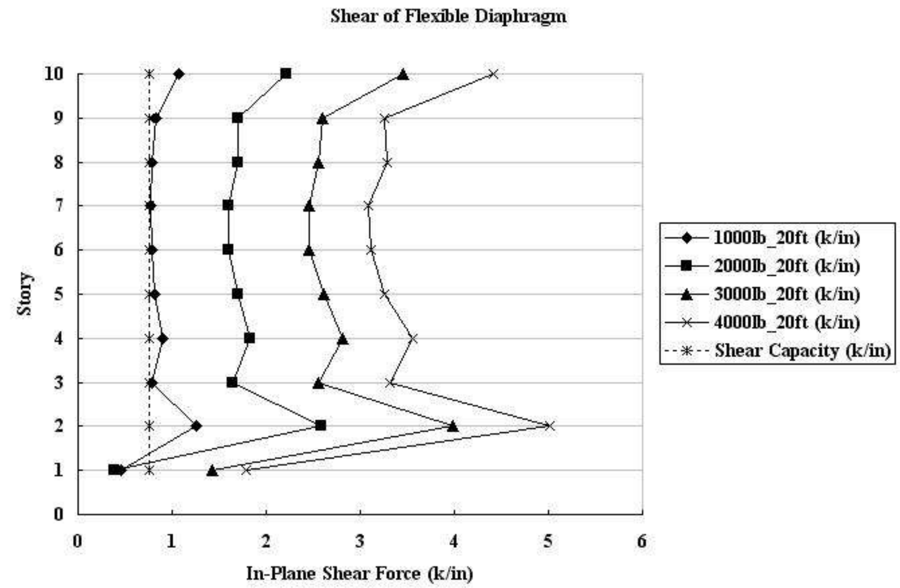

Figure 5.43 : Developed Shear Force vs. Shear Capacity of Concrete Slab Based on Flexible Diaphragm Analysis

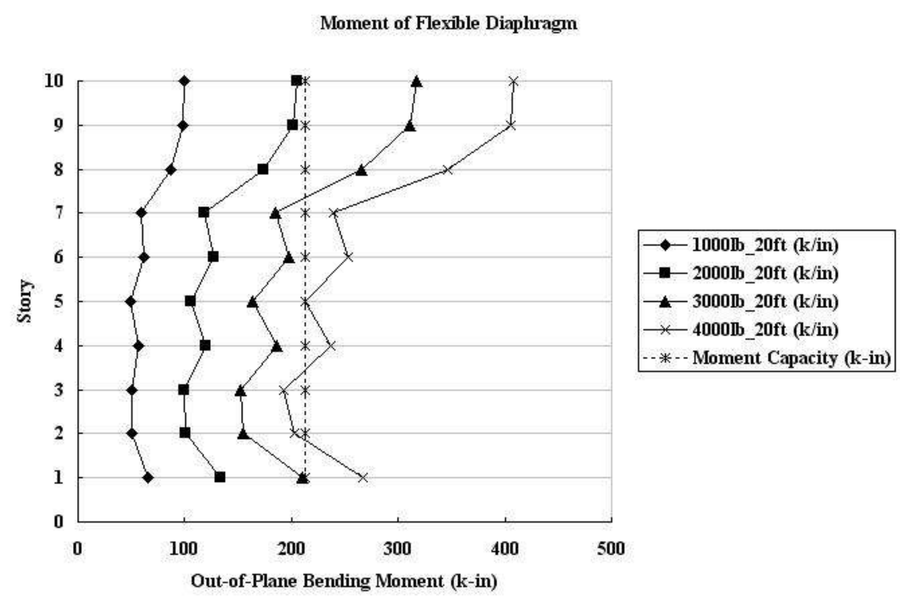

Figure 5.44 : Developed Bending Moment vs. Moment Capacity of Concrete Slab Based on Flexible Diaphragm Analysis

5.4.2. Rigid Diaphragm Analysis

Those models have very high in-plane stiffness due to normal weight concrete fill over 3 in metal deck. The floor systems are also assumed to be rigid in their planes. Maximum shear forces and bending moment of Moment Resistant Frame are investigated as compared with capacity of member shown in Figure 5.46- 5.53 and Table 5.11 – 5.18. For reference, the member locations, identification numbers and member sizes are shown in Figure 5.45 for typical longitudinal frame. The distribution of moment on rigid diaphragm is shown in Figure 5.54 and the results of rigid diaphragm analysis are shown in Table 5.19 and Figure 5.55.

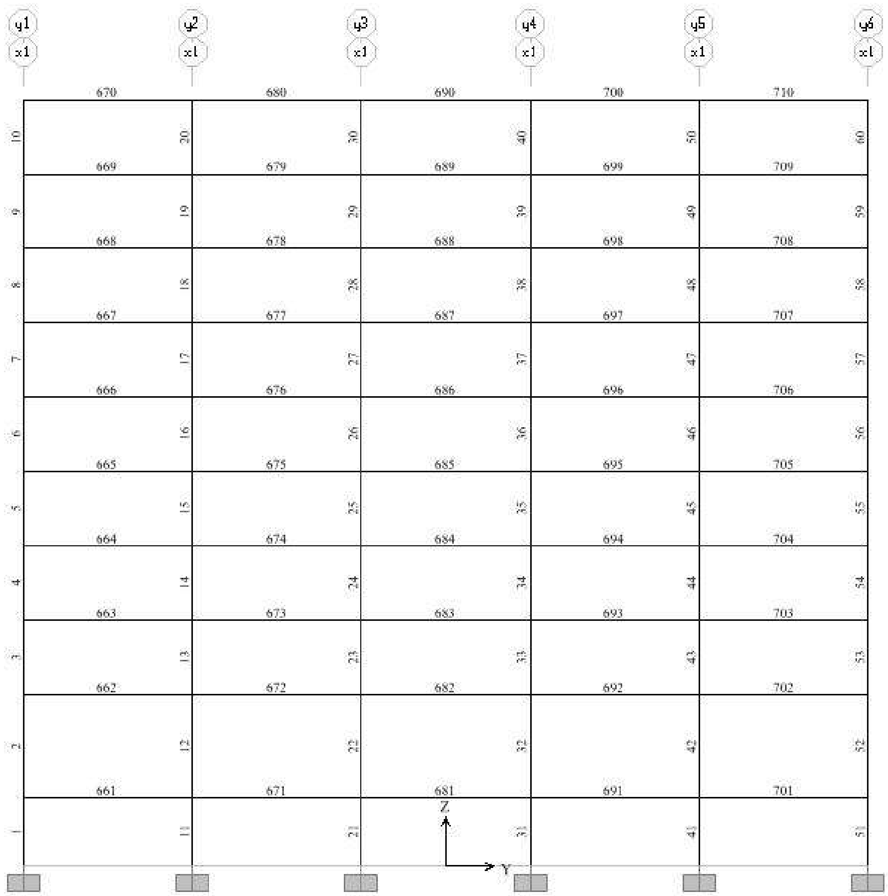

(a) Generated Member Numbers along the Longitudinal Direction

Figure 5.45 : Generated Member Numbers and Frame Section along the Longitudinal Direction

“Figure 5.45 : Continued”

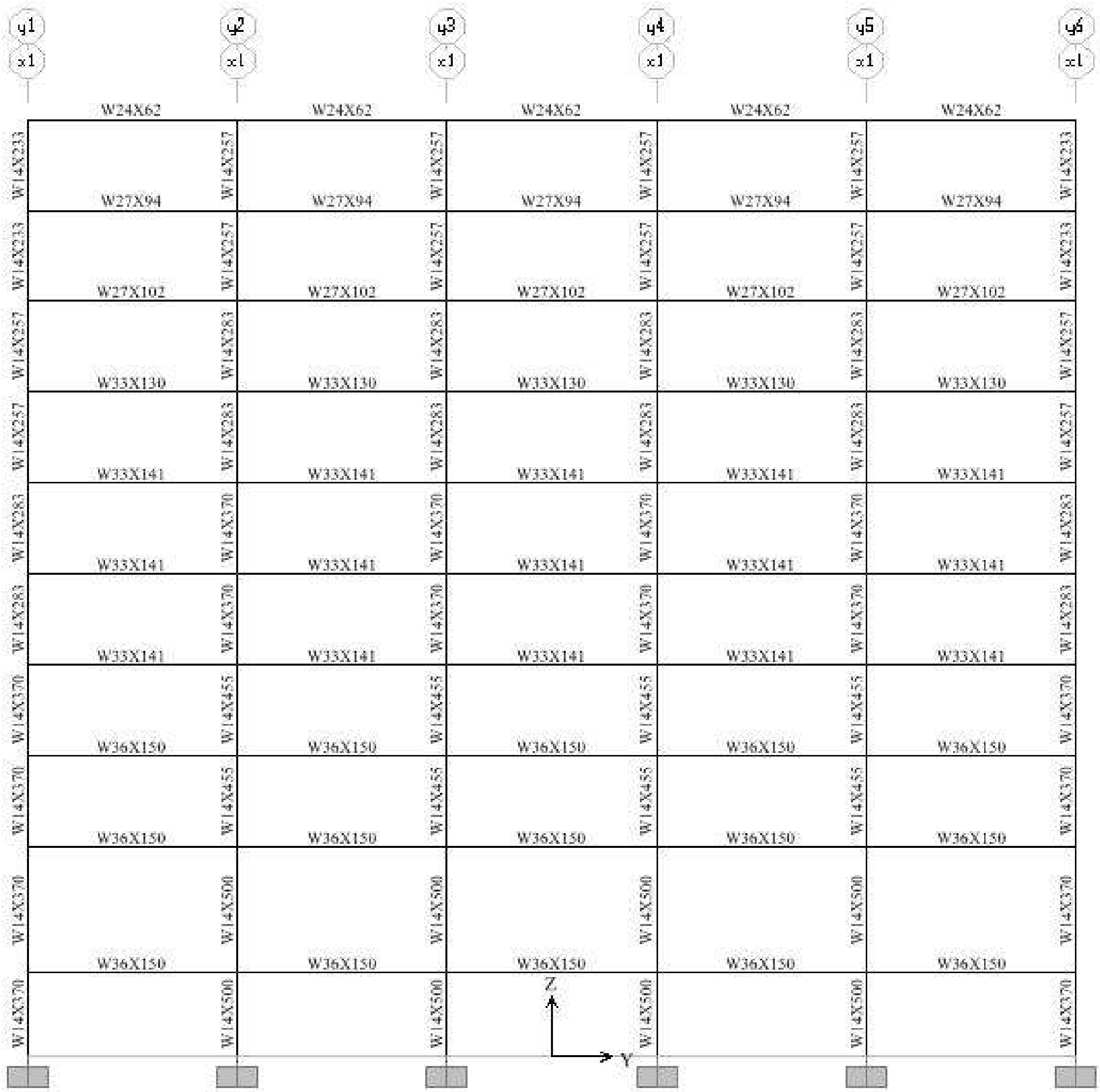

(b) Generated Frame Sections and Moment Resistant Frames

Table 5.11 : Max. Shear Force at MRF Frames (1,000 lb TNT Weight @ 20 ft)

Frame No.	Frame Section	Shear Force (V_u)	Shear Strength (ϕV_n)
11	W14*500	462.4	1159
12	W14*500	313.7	1159
13	W14*455	328.0	1035
14	W14*455	275.9	1035
15	W14*370	221.7	801
16	W14*370	245.3	801
17	W14*283	250.3	583
18	W14*283	263.8	583
19	W14*257	272.9	523
20	W14*257	281.7	523

(unit : k/in)

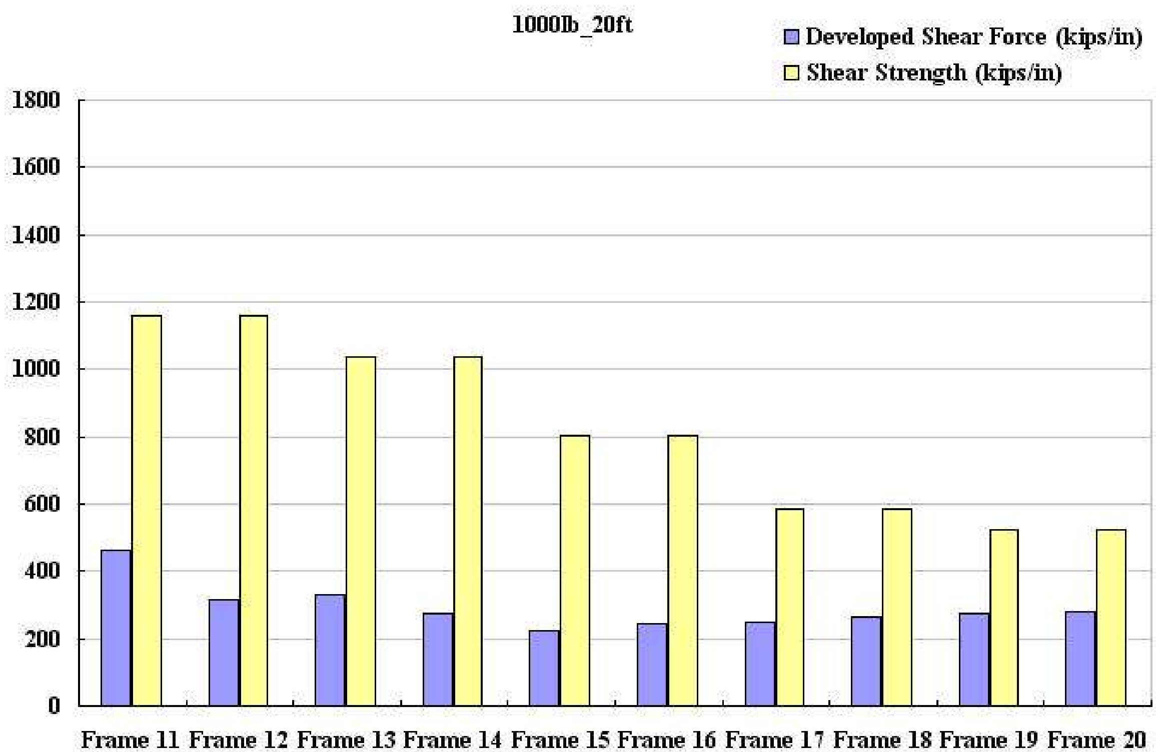

Figure 5.46 : Developed Shear Force vs. Shear Capacity of Rigid Diaphragm (1,000 lb @ 20 ft)

Table 5.12 : Max. Shear Force at MRF Frames (2,000 lb TNT Weight @ 20 ft)

Frame No.	Frame Section	Shear Force (V_u)	Shear Strength (ϕV_n)
11	W14*500	960.4	1159
12	W14*500	653.2	1159
13	W14*455	657.6	1035
14	W14*455	553.7	1035
15	W14*370	450.5	801
16	W14*370	478.5	801
17	W14*283	494.3	583
18	W14*283	521.7	583
19	W14*257	554.1	523
20	W14*257	579.5	523

(unit : k/in)

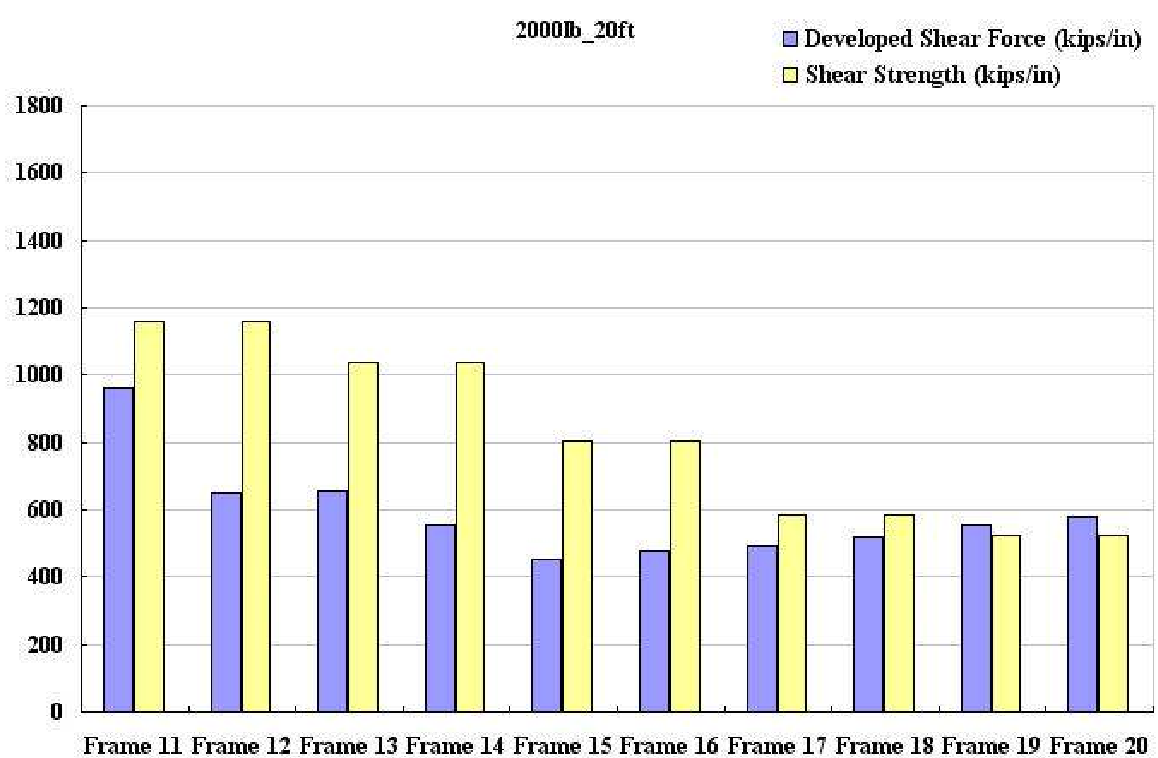

Figure 5.47 : Developed Shear Force vs. Shear Capacity of Rigid Diaphragm (2,000 lb @ 20 ft)

Table 5.13 : Max. Shear Force at MRF Frames (3,000 lb TNT Weight @ 20 ft)

Frame No.	Frame Section	Shear Force (V_u)	Shear Strength (ϕV_n)
11	W14*500	1486.7	1159
12	W14*500	1013.9	1159
13	W14*455	1005.9	1035
14	W14*455	843.9	1035
15	W14*370	690.7	801
16	W14*370	724.5	801
17	W14*283	753.8	583
18	W14*283	796.8	583
19	W14*257	851.9	523
20	W14*257	895.9	523

(unit : k/in)

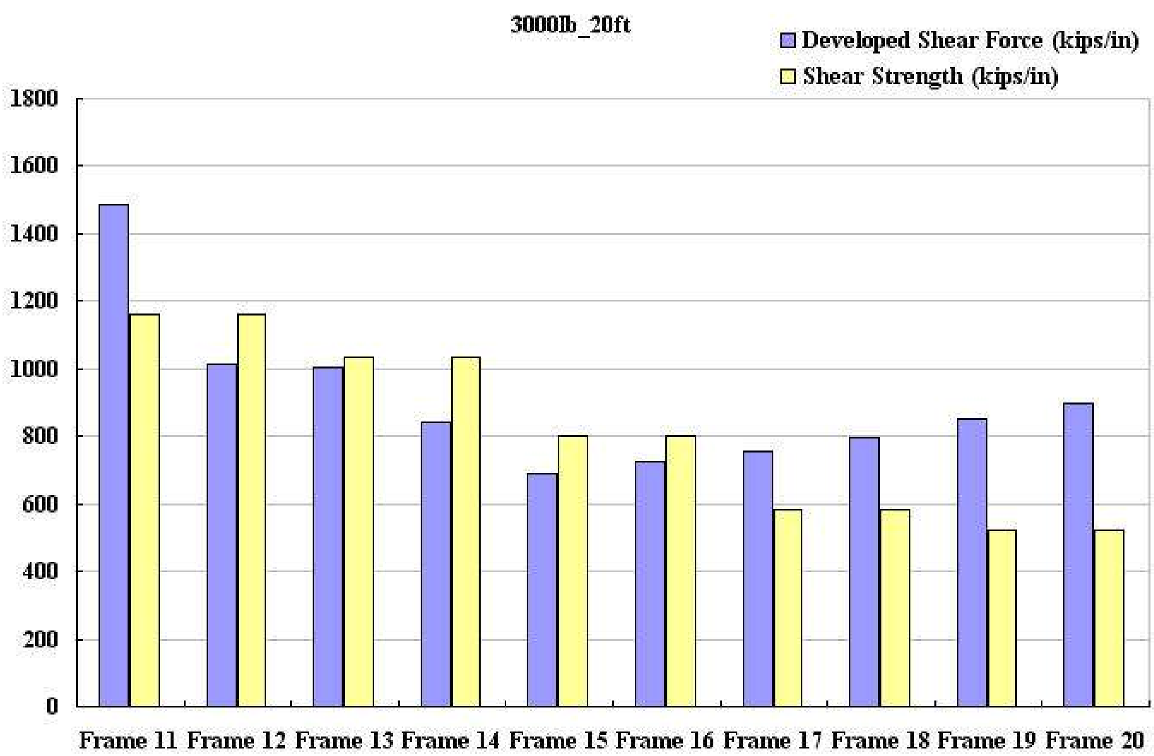

Figure 5.48 : Developed Shear Force vs. Shear Capacity of Rigid Diaphragm (3,000 lb @ 20 ft)

Table 5.14 : Max. Shear Force at MRF Frames (4,000 lb TNT Weight @ 20 ft)

Frame No.	Frame Section	Shear Force (V_u)	Shear Strength (ϕV_n)
11	W14*500	1898.8	1159
12	W14*500	1315.1	1159
13	W14*455	1285.1	1035
14	W14*455	1083.5	1035
15	W14*370	891.3	801
16	W14*370	927.9	801
17	W14*283	975.5	583
18	W14*283	1029.5	583
19	W14*257	1113.9	523
20	W14*257	1148.6	523

(unit : k/in)

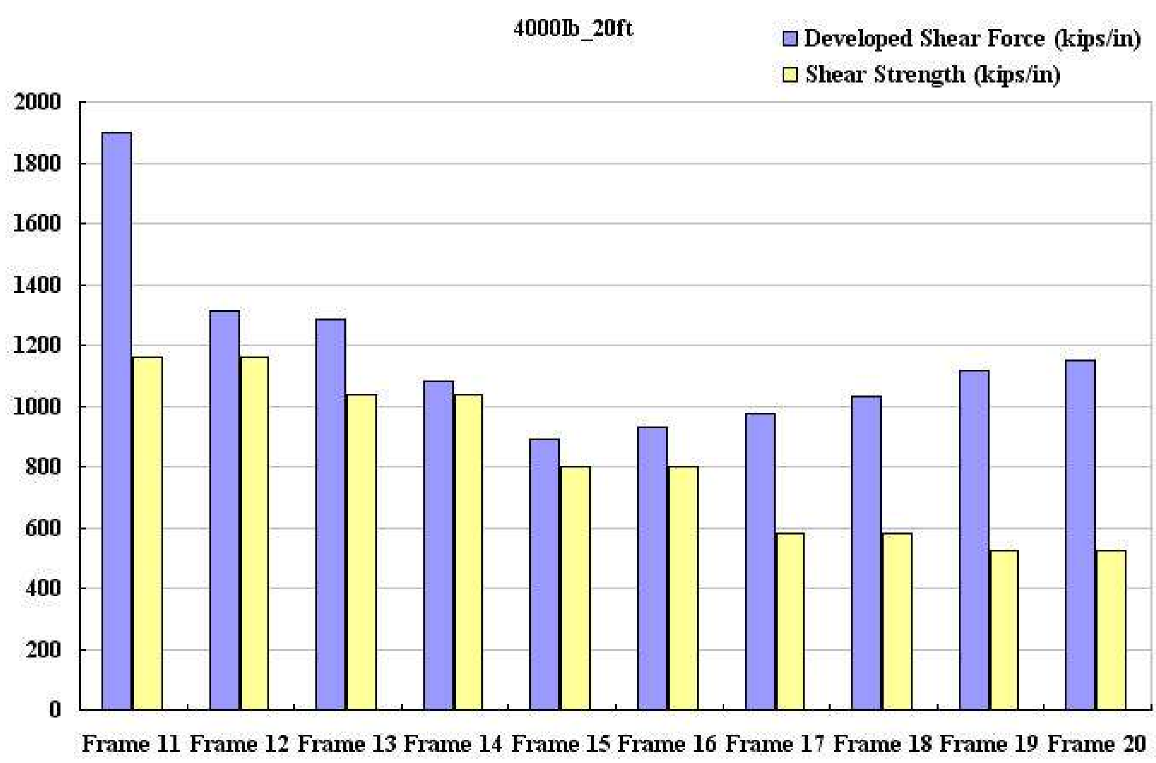

Figure 5.49 : Developed Shear Force vs. Shear Capacity of Rigid Diaphragm (4,000 lb @ 20 ft)

Table 5.15 : Max. Bending Moment at MRF Frames (1,000 lb TNT Weight @ 20 ft)

Frame No.	Frame Section	Bending Moment (Mu)	Moment Capacity (ϕMn)
11	W14*500	43582.9	52500
12	W14*500	30623.2	52500
13	W14*455	25696.3	46800
14	W14*455	22924.0	46800
15	W14*370	18083.2	36800
16	W14*370	20661.3	36800
17	W14*283	19487.0	29150
18	W14*283	24227.6	29150
19	W14*257	22008.0	24350
20	W14*257	23378.2	24350

(unit : k-in)

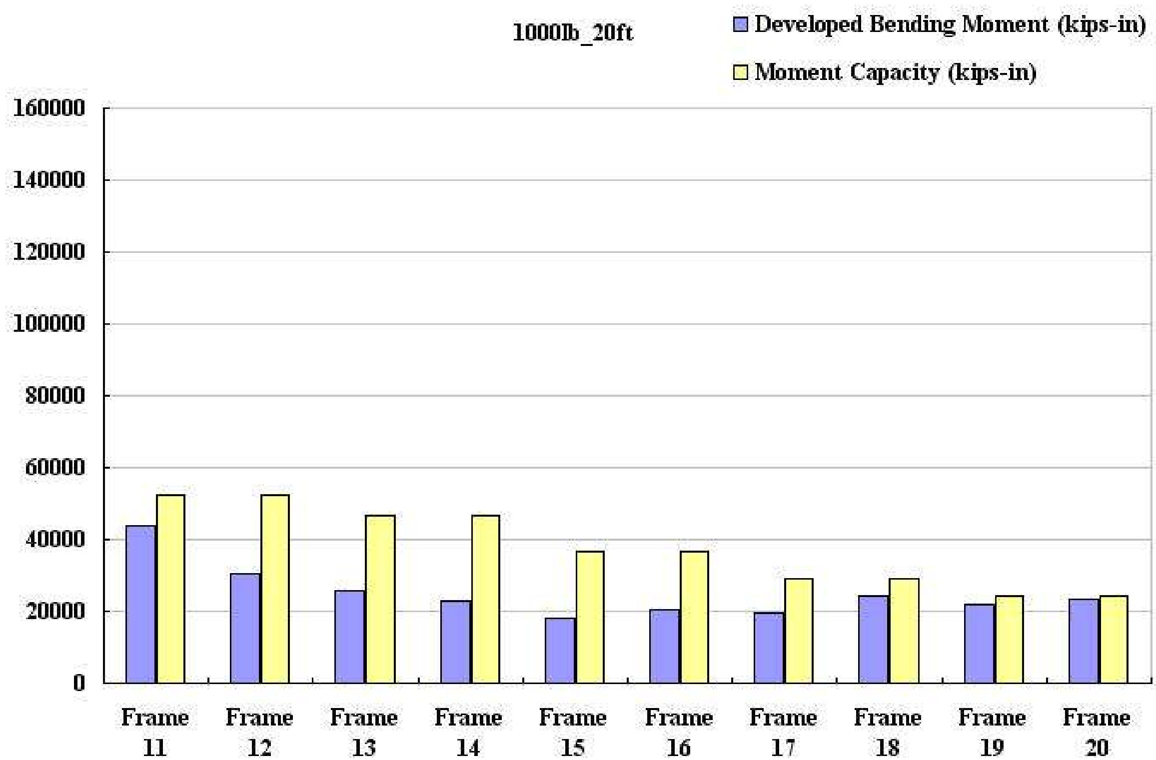

Figure 5.50 : Developed Bending Moment vs. Moment Capacity of Rigid Diaphragm (1,000 lb @ 20 ft)

Table 5.16 : Max. Bending Moment at MRF Frames (2,000 lb TNT Weight @ 20 ft)

Frame No.	Frame Section	Bending Moment (Mu)	Moment Capacity (ϕMn)
11	W14*500	90572.6	52500
12	W14*500	63661.3	52500
13	W14*455	51419.6	46800
14	W14*455	46232.3	46800
15	W14*370	36744.9	36800
16	W14*370	40481.5	36800
17	W14*283	38519.9	29150
18	W14*283	48137.4	29150
19	W14*257	45066.1	24350
20	W14*257	48106.8	24350

(unit : k-in)

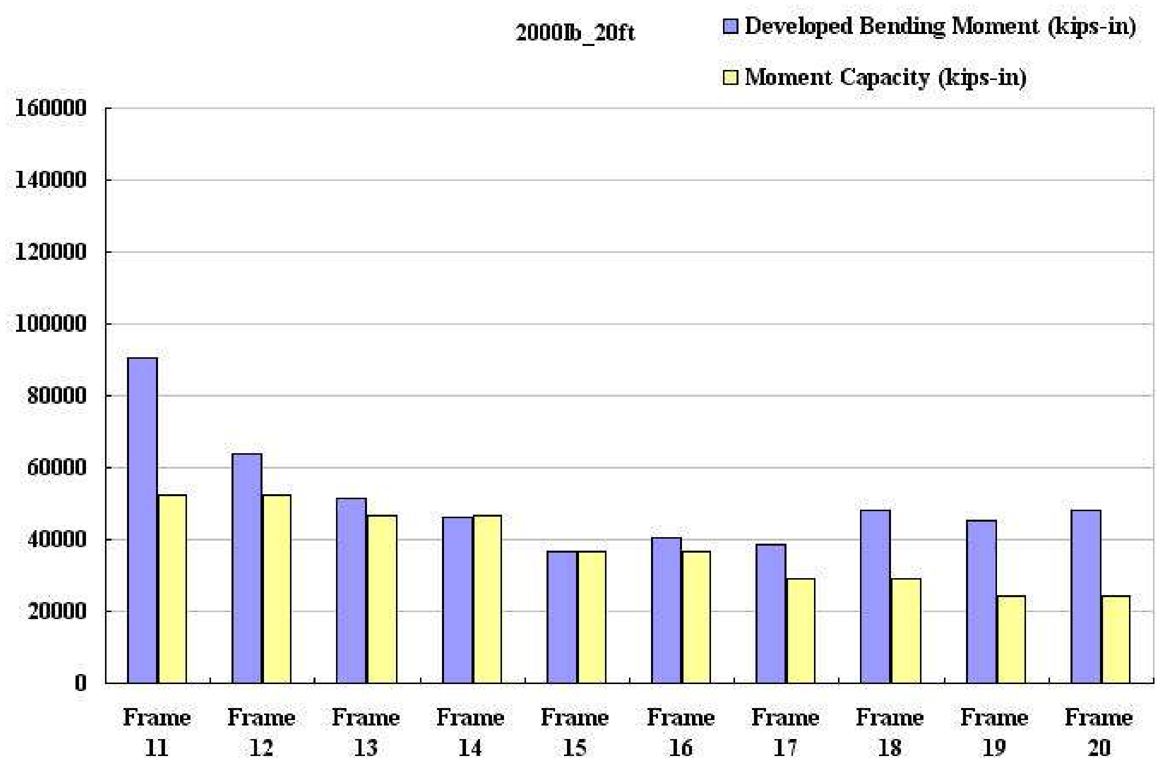

Figure 5.51 : Developed Bending Moment vs. Moment Capacity of Rigid Diaphragm (2,000 lb @ 20 ft)

Table 5.17 : Max. Bending Moment at MRF Frames (3,000 lb TNT Weight @ 20 ft)

Frame No.	Frame Section	Bending Moment (Mu)	Moment Capacity (ϕMn)
11	W14*500	140271.3	52500
12	W14*500	98824.2	52500
13	W14*455	78635.9	46800
14	W14*455	70604.2	46800
15	W14*370	56237.6	36800
16	W14*370	61393.6	36800
17	W14*283	58836.7	29150
18	W14*283	73555.6	29150
19	W14*257	69548.0	24350
20	W14*257	74334.6	24350

(unit : k-in)

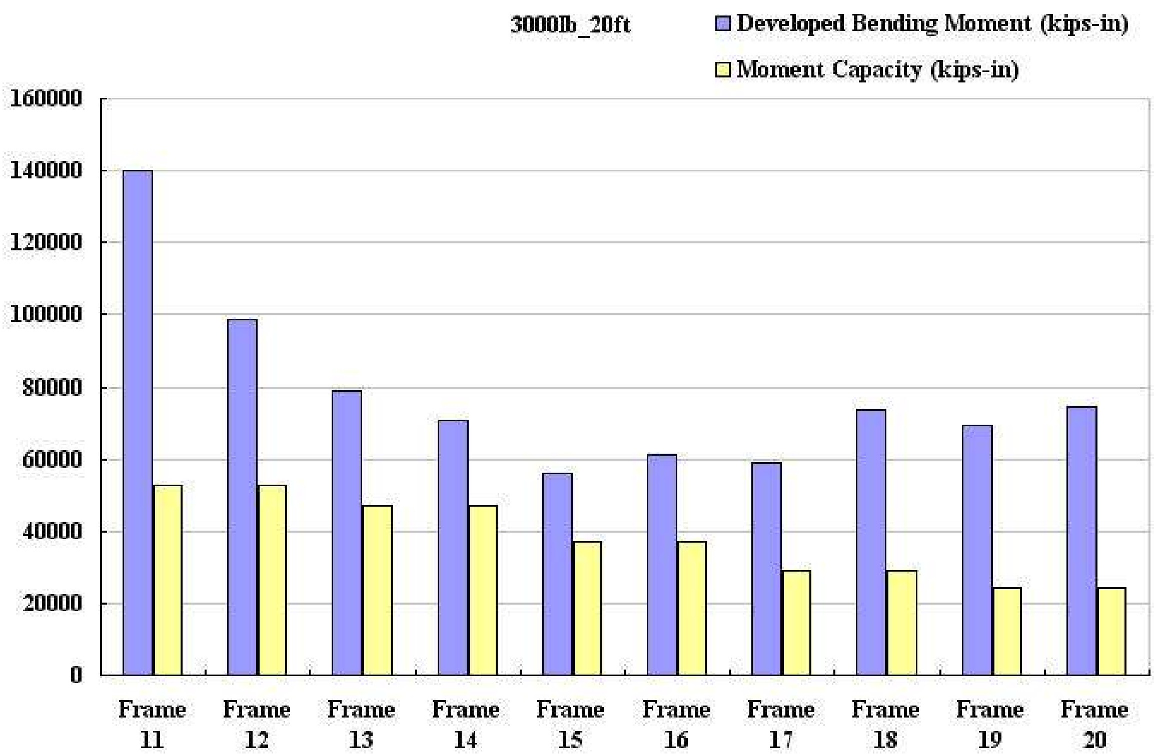

Figure 5.52 : Developed Bending Moment vs. Moment Capacity of Rigid Diaphragm (3,000 lb @ 20 ft)

Table 5.18 : Max. Bending Moment at MRF Frames (4,000 lb TNT Weight @ 20 ft)

Frame No.	Frame Section	Bending Moment (Mu)	Moment Capacity (ϕMn)
11	W14*500	179496.0	52500
12	W14*500	129010.6	52500
13	W14*455	99639.0	46800
14	W14*455	90903.0	46800
15	W14*370	72113.6	36800
16	W14*370	78588.1	36800
17	W14*283	76385.5	29150
18	W14*283	95122.8	29150
19	W14*257	91122.1	24350
20	W14*257	94881.1	24350

(unit : k-in)

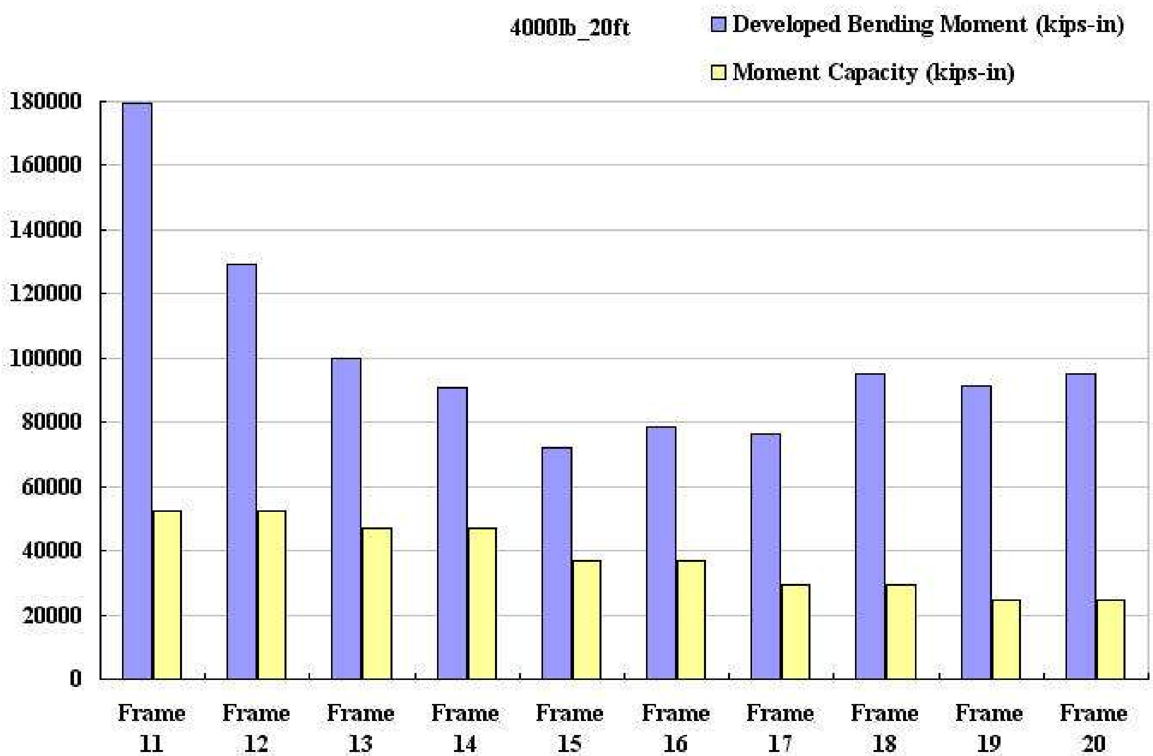

Figure 5.53 : Developed Bending Moment vs. Moment Capacity of Rigid Diaphragm (4,000 lb @ 20 ft)

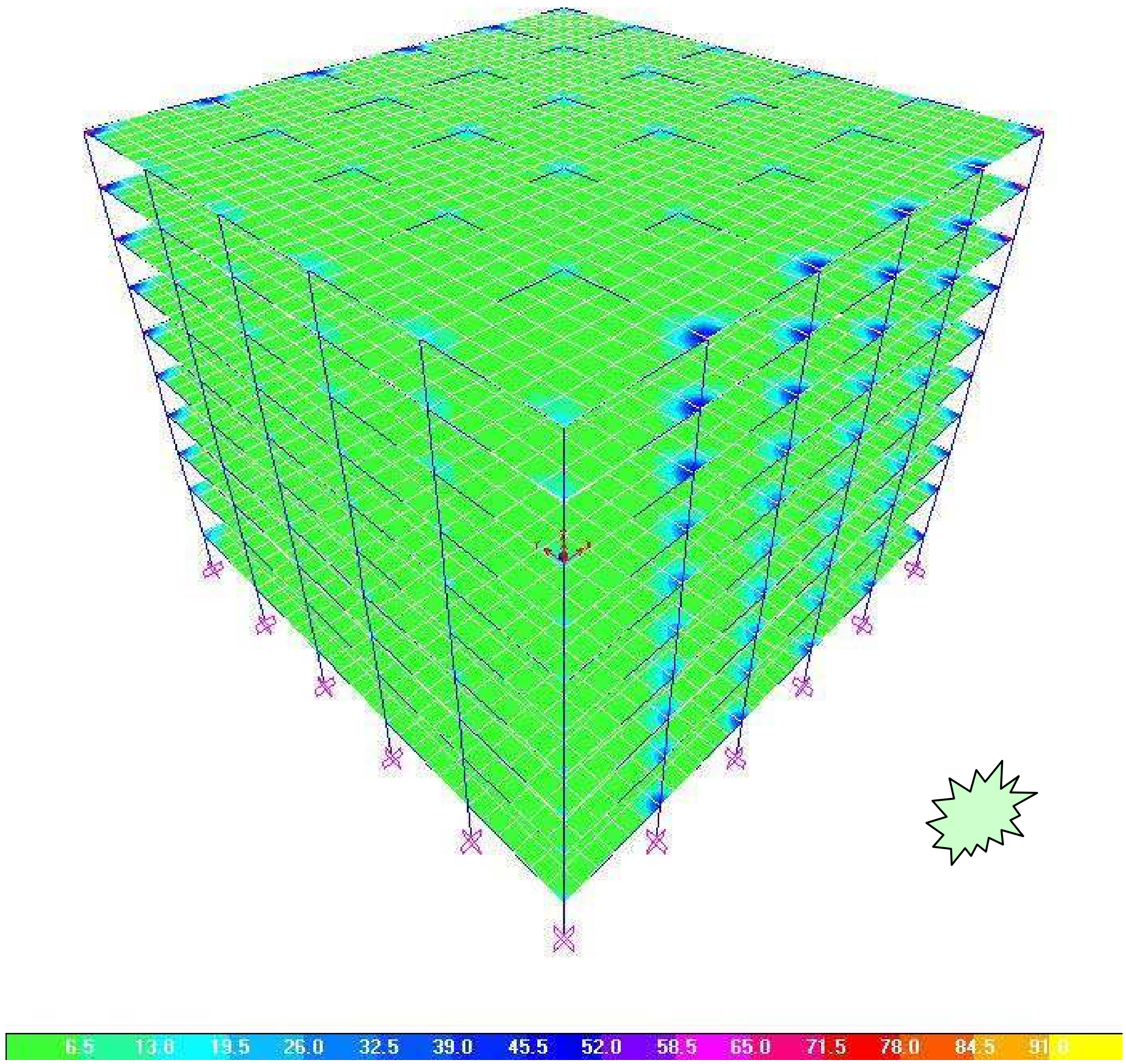

(a) Moment Distribution on Whole Structure (1,000 lb TNT Weight@20 ft Stand-Off Distance)

Figure 5.54 : Moment Distribution on Three Story Building (1,000 lb TNT Weight@20 ft Stand-Off Distance)

“Figure 5.54 : Continued”

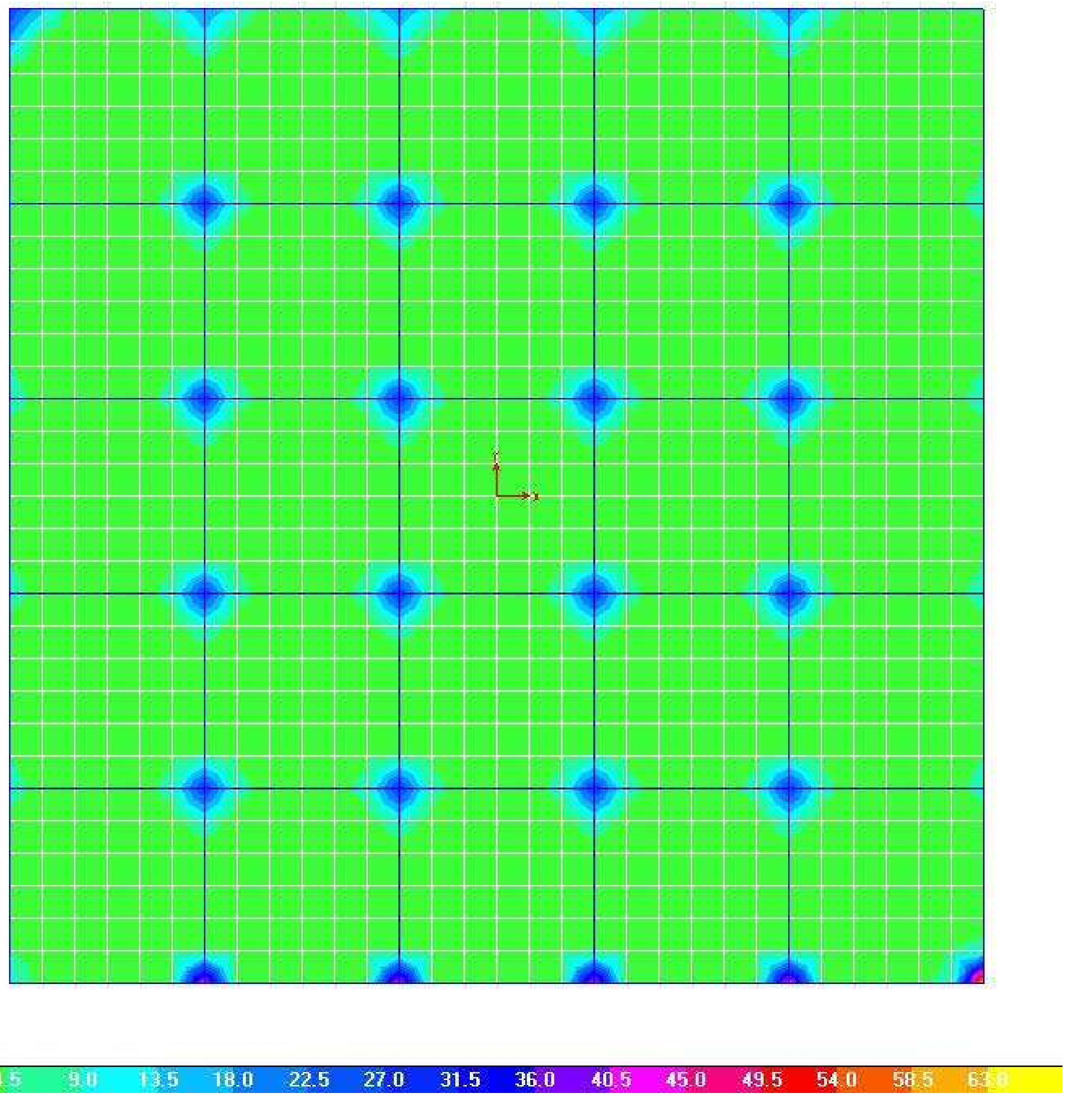

(b) Moment Distribution at 1st Floor (1,000 lb TNT Weight@20 ft Stand-Off Distance)

“Figure 5.54 : Continued”

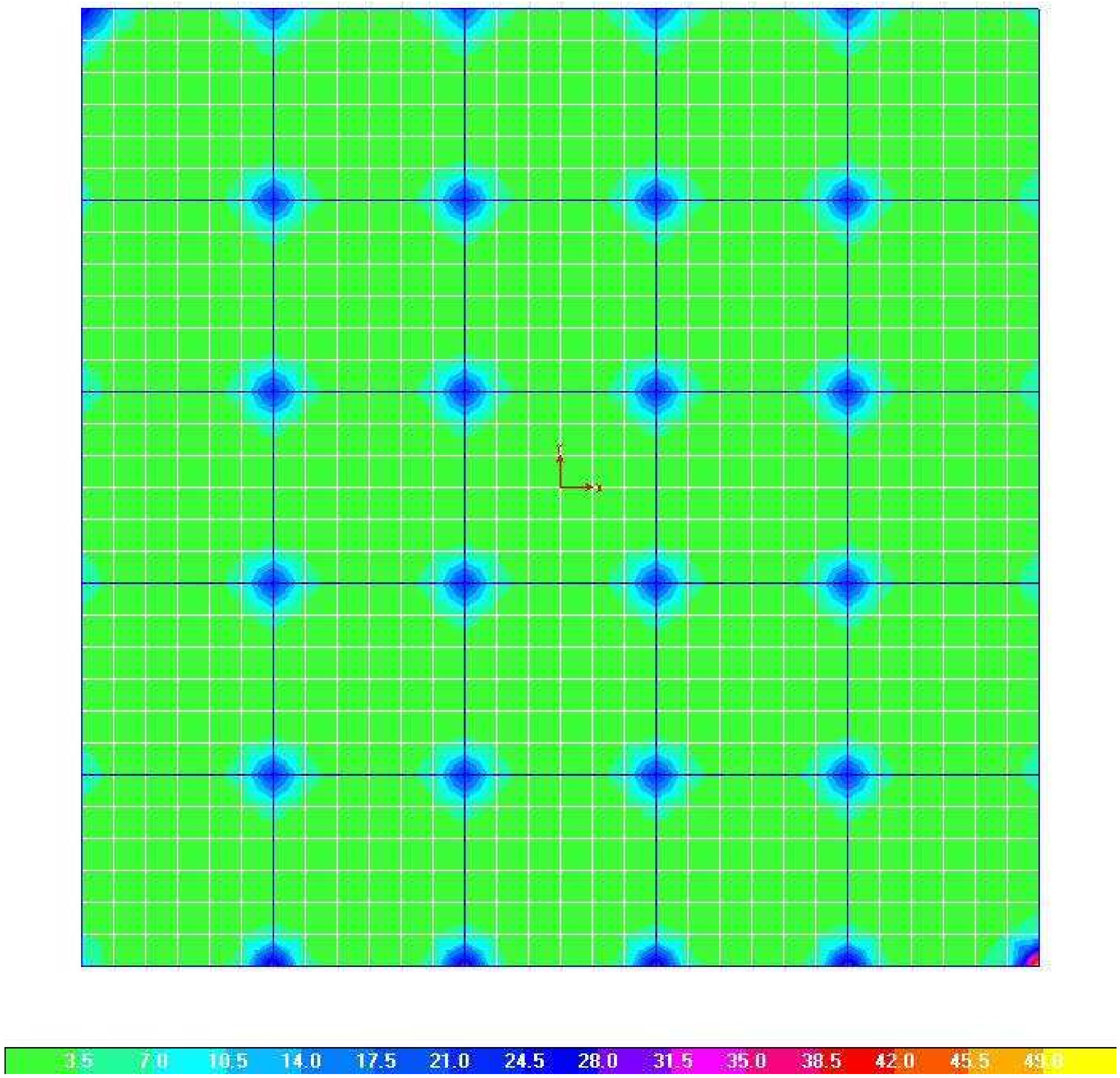

(c) Moment Distribution at 2nd Floor (1,000 lb TNT Weight@20 ft Stand-Off Distance)

“Figure 5.54 : Continued”

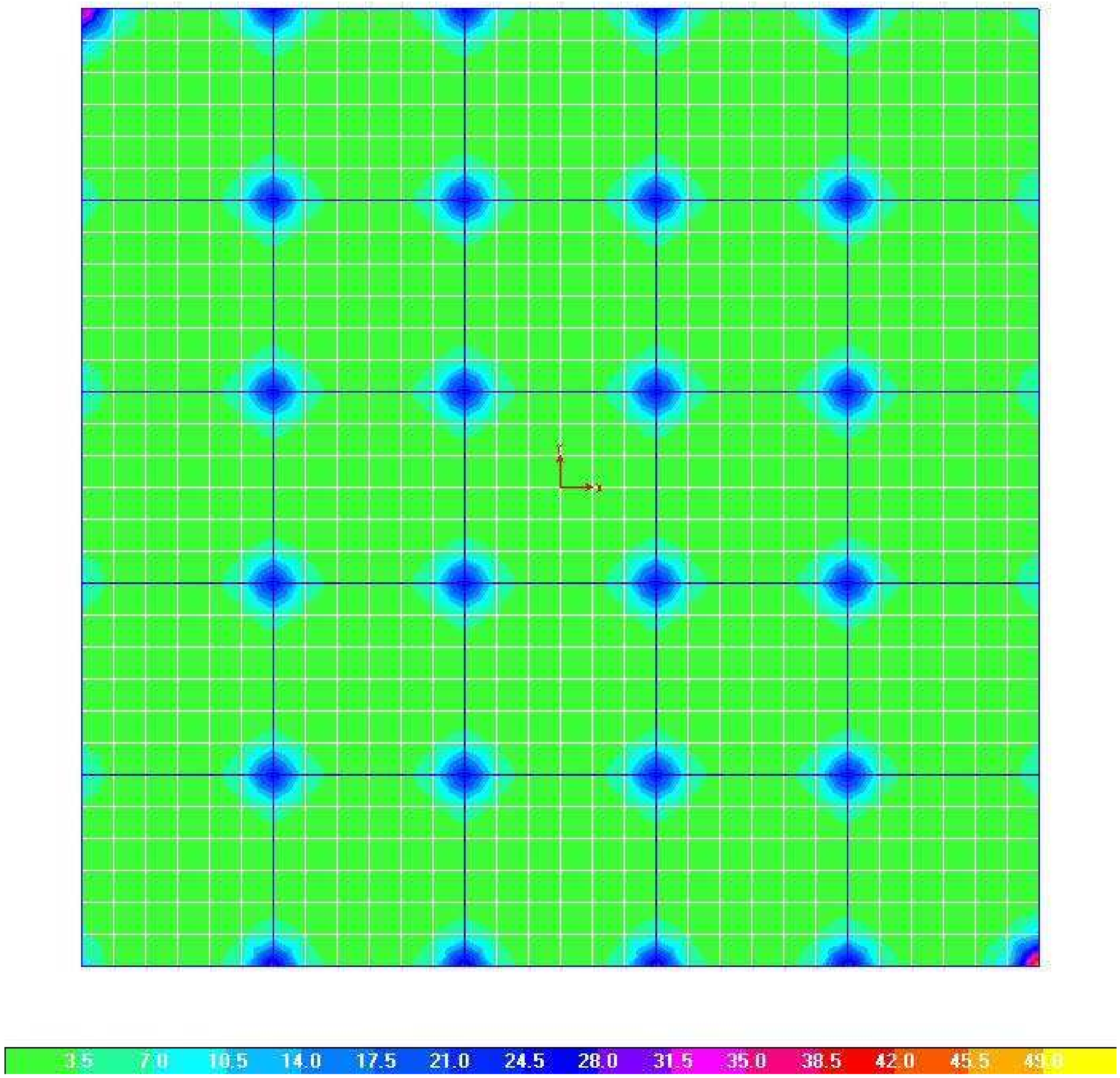

(d) Moment Distribution at 3rd Floor (1,000 lb TNT Weight@20 ft Stand-Off Distance)

“Figure 5.54 : Continued”

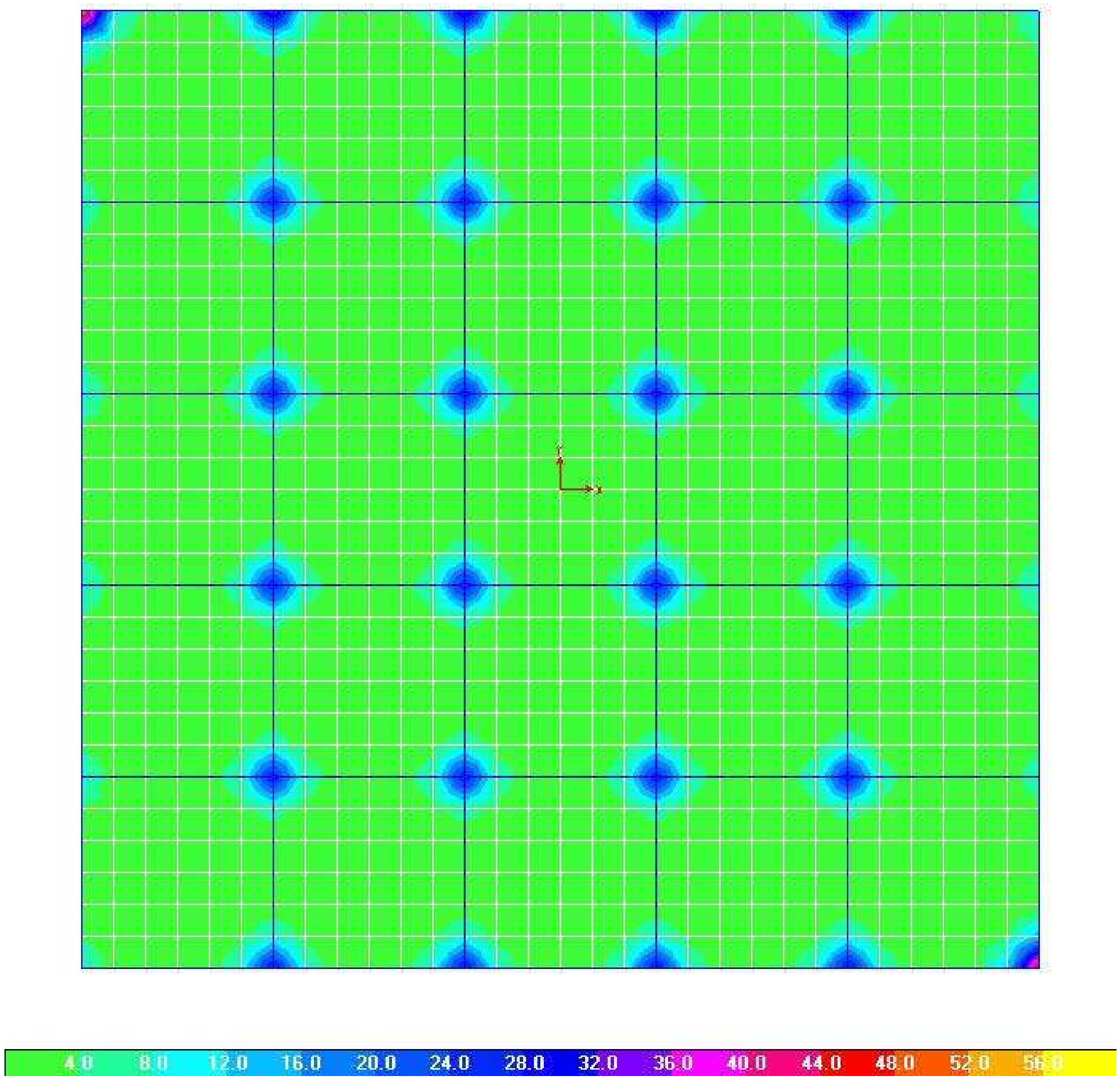

(e) Moment Distribution at 4th Floor (1,000 lb TNT Weight@20 ft Stand-Off Distance)

"Figure 5.54 : Continued"

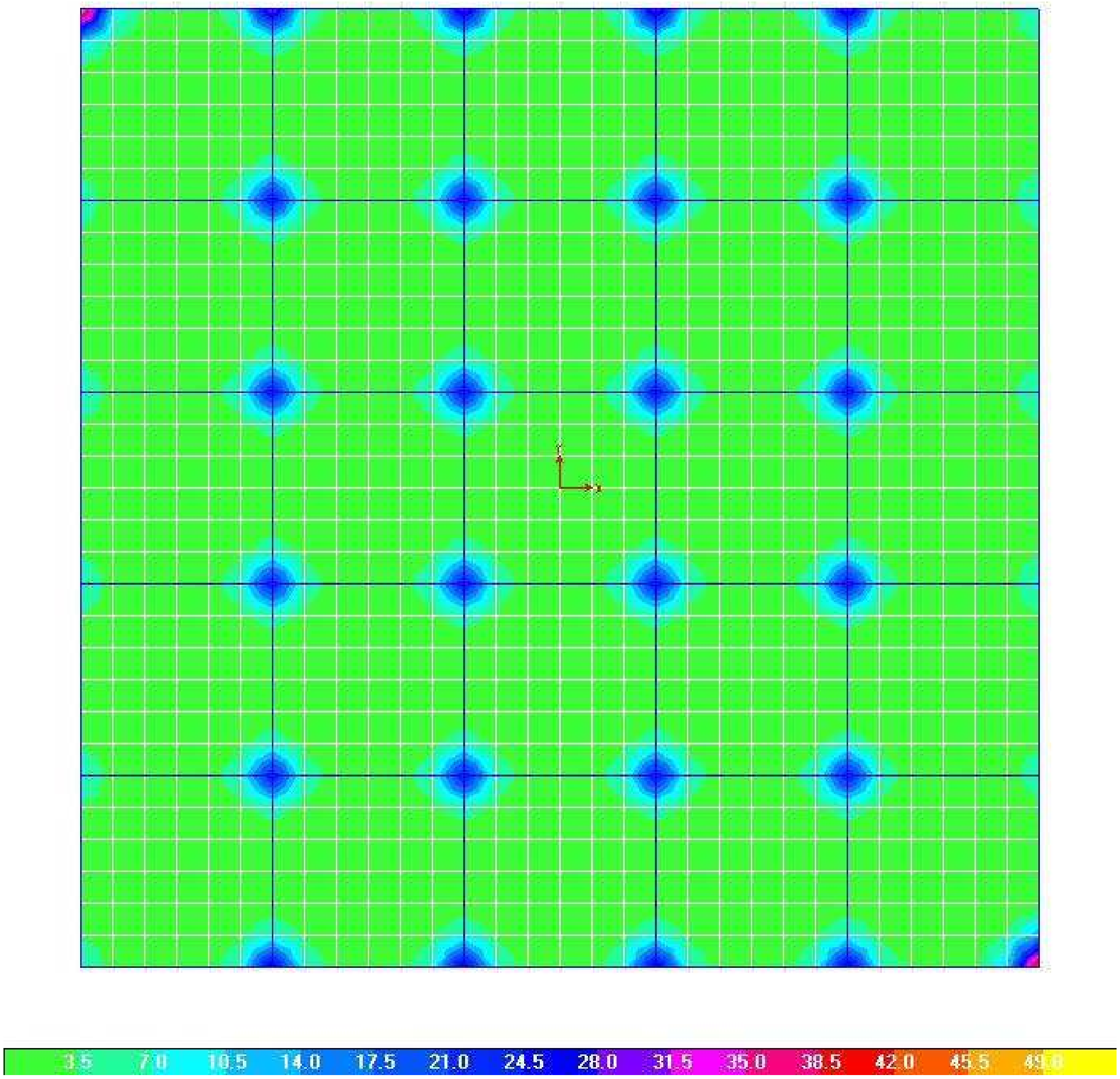

(f) Moment Distribution at 5th Floor (1,000 lb TNT Weight@20 ft Stand-Off Distance)

“Figure 5.54 : Continued”

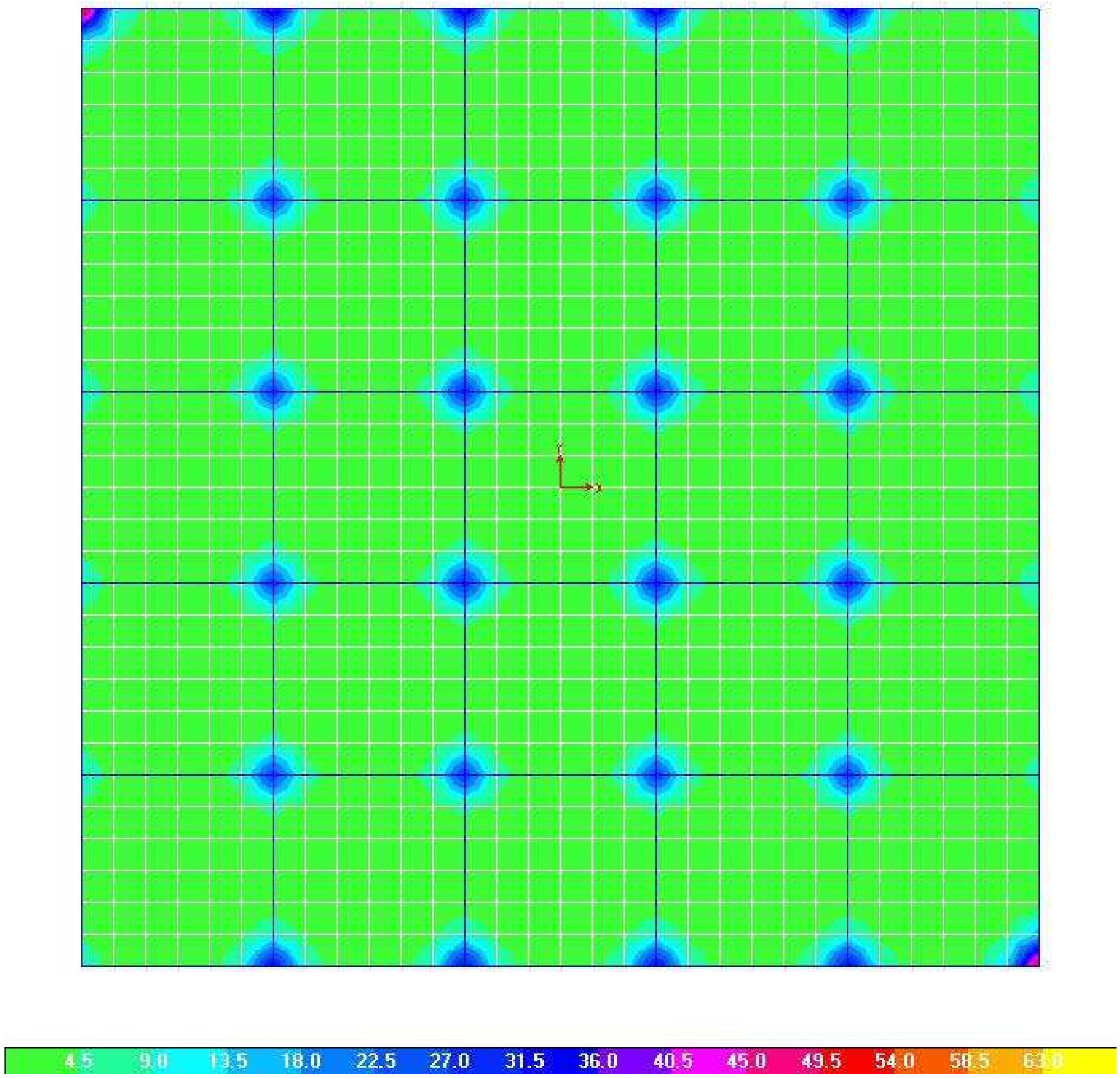

(g) Moment Distribution at 6^{th} Floor (1,000 lb TNT Weight@20 ft Stand-Off Distance)

“Figure 5.54 : Continued”

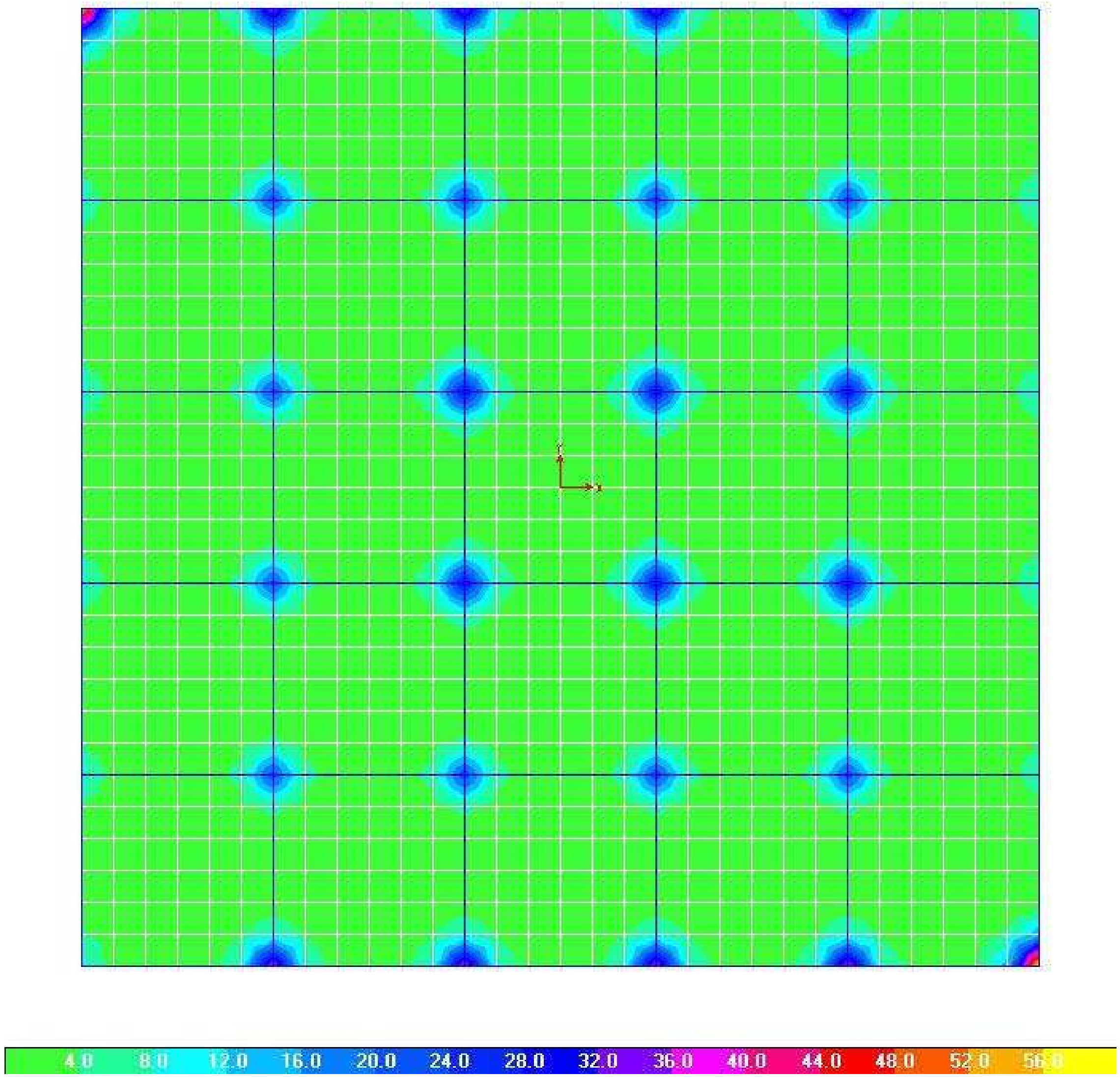

(h) Moment Distribution at 7th Floor (1,000 lb TNT Weight@20 ft Stand-Off Distance)

“Figure 5.54 : Continued”

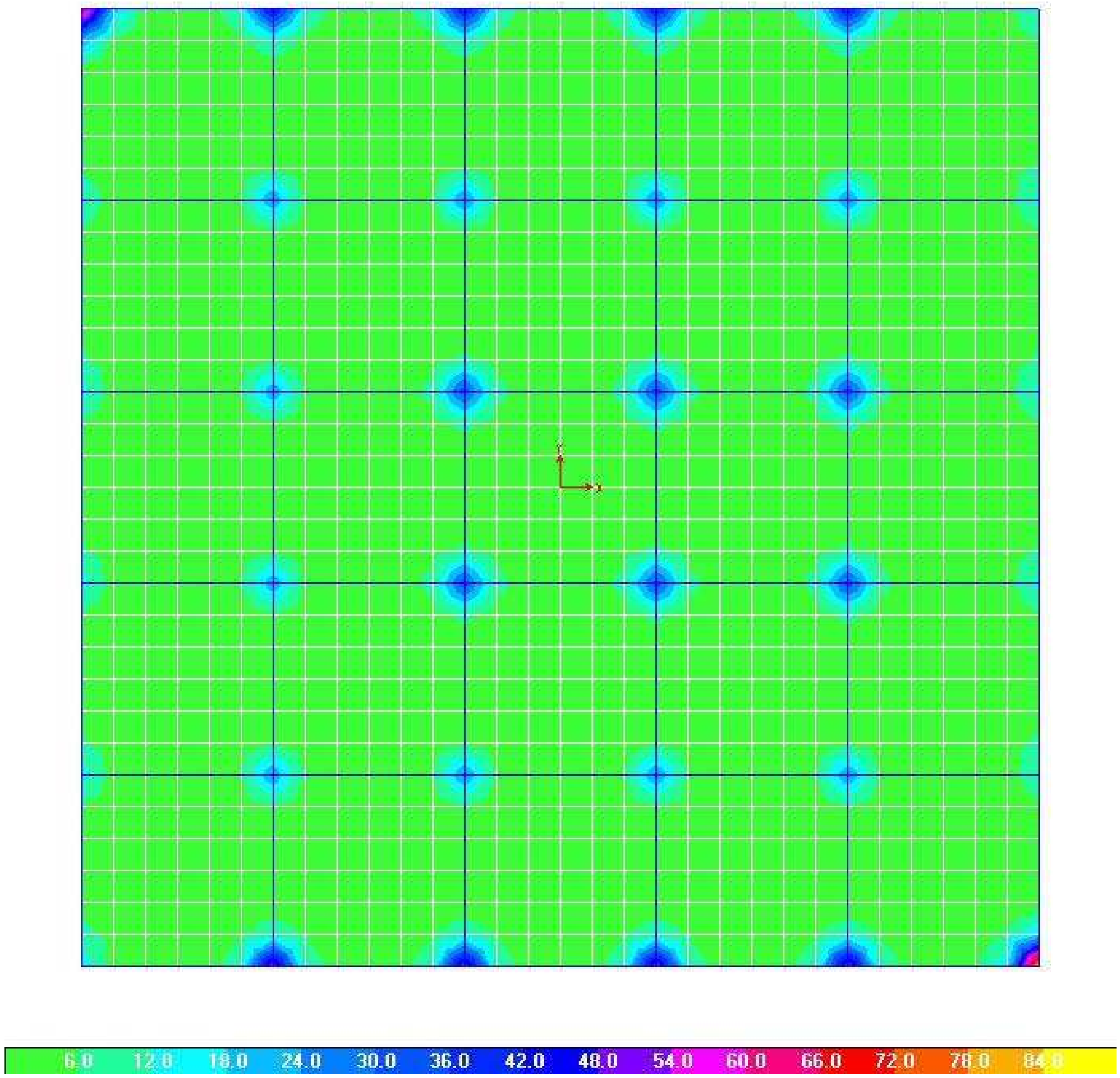

(i) Moment Distribution at 8th Floor (1,000 lb TNT Weight@20 ft Stand-Off Distance)

“Figure 5.54 : Continued”

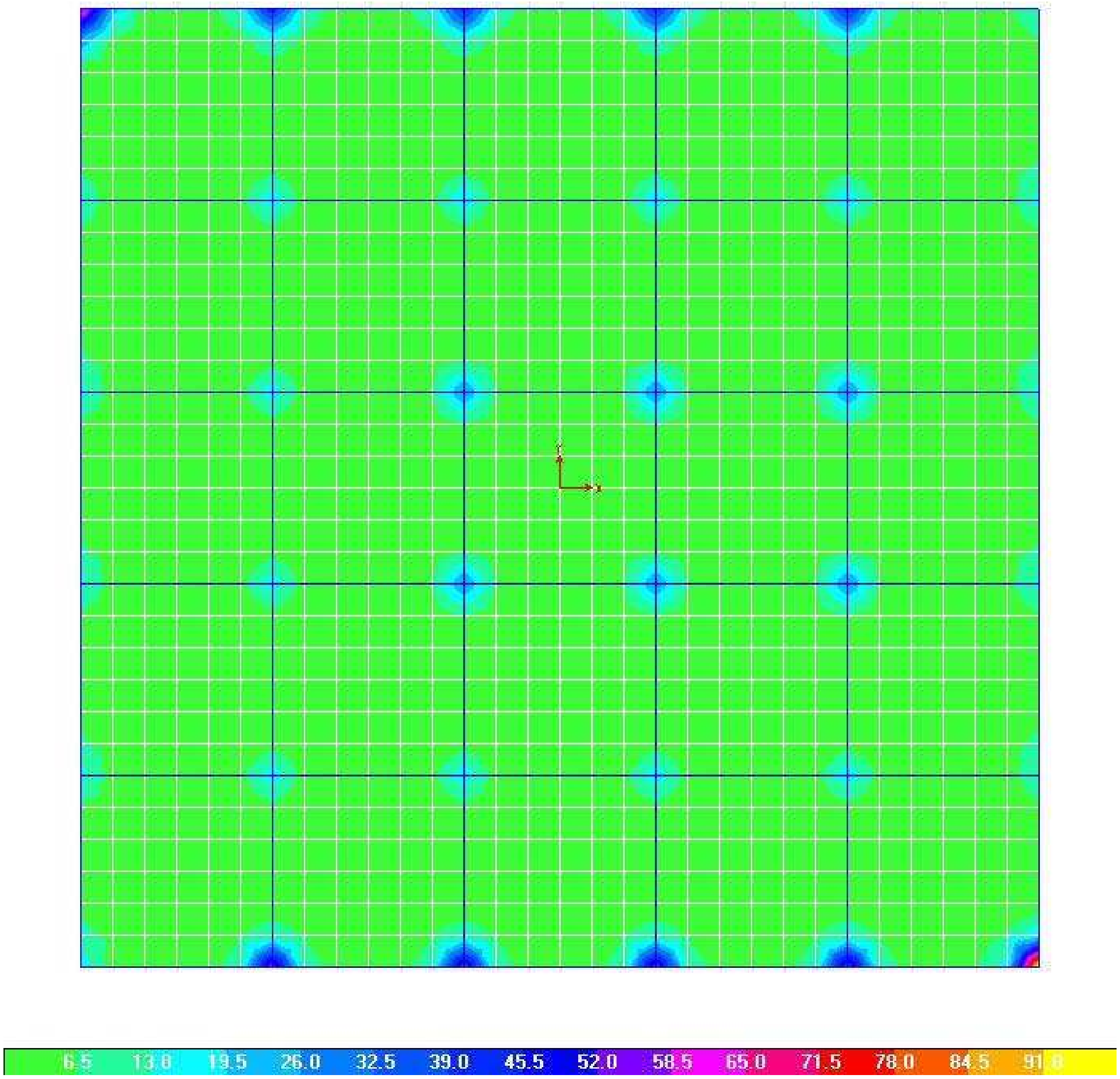

(j) Moment Distribution at 9th Floor (1,000 lb TNT Weight@20 ft Stand-Off Distance)

"Figure 5.54 : Continued"

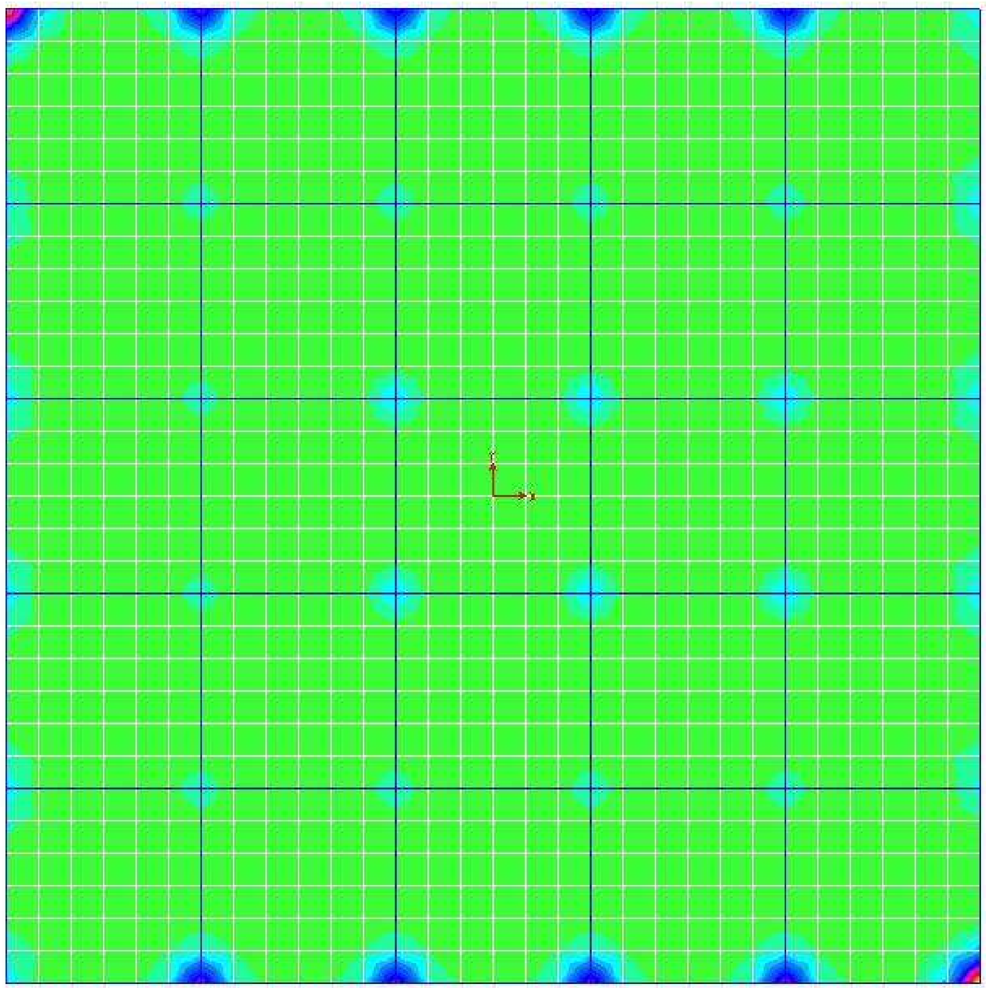

(k) Moment Distribution at Roof (1,000 lb TNT Weight@20 ft Stand-Off Distance)

Table 5.19 : The Results of Rigid Diaphragm Analysis

	1,000 lb @ 20 ft	2,000 lb @ 20 ft	3,000 lb @ 20 ft	4,000 lb @ 20 ft
Floor	Moment (k-in)	Moment (k-in)	Moment (k-in)	Moment (k-in)
Roof	97.0	199.6	309.6	396.2
9th	96.8	197.9	305.8	399.6
8th	87.6	174.4	267.2	348.0
7th	58.8	119.7	186.5	241.3
6th	61.0	127.3	197.4	252.8
5th	50.0	106.2	164.8	213.8
4th	56.6	119.1	185.0	235.4
3rd	49.0	97.7	149.6	190.0
2nd	49.8	100.4	154.3	202.0
1st	64.7	134.7	208.8	268.8

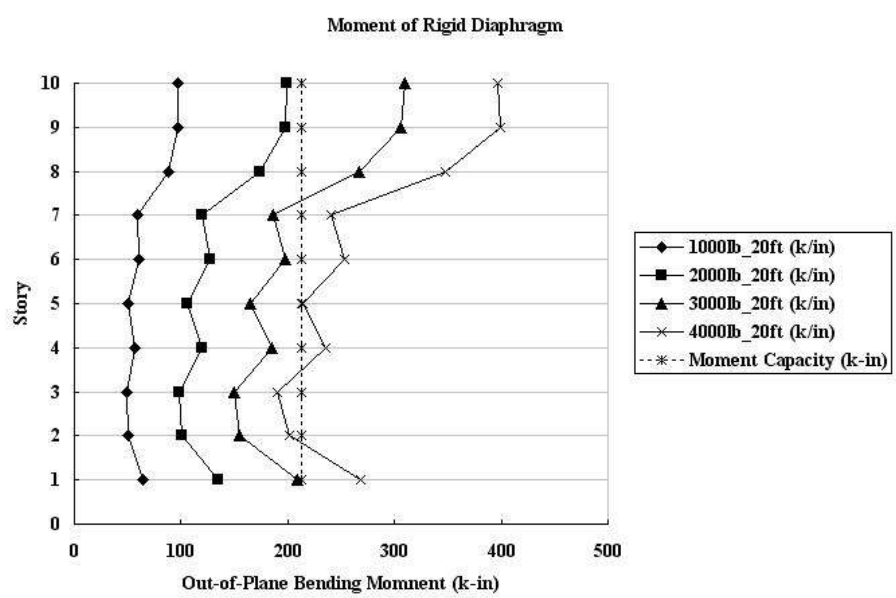

Figure 5.55 : Developed Bending Moment vs. Moment Capacity of Concrete Slab Based on Rigid Diaphragm Analysis

5.5. Nonlinear Structural Response of Ten Story Building

5.5.1. Nonlinear Reponses of Ten Story Building

The time history of the floor displacements obtained from nonlinear analyses is shown in Figure 5.56. Here it can be seen that the displacement for the 4,000 lb @ 20 ft has increased to 28 inches shown in Figure 5.57. In addition, it has been damped out be inelastic deformations that have occurred throughout the frame.

An important parameter in earthquake resistant design is the interstory drift index that is obtained by dividing the maximum relative story displacement by the story height. The UBC'97 requires that for structures having a period greater than 0.7 seconds the interstory drift be limited to 0.02. The graph shown in Figure 5.58 indicates that the drift is slightly satisfied with limit for the 1,000 lb and 2,000 lb TNT weight@20 ft. However, interstory drift ratio of other cases is well above the limiting value.

Nonlinear dynamic analyses can also be used to calculate the demand/capacity (D/C) ratios for the structural members. Calculated demand/capacity ratios for the four loading conditions are shown Figure 5.59 – Figure 5.62. In these figures the largest demands occur in the perimeter moment frames as might be expected. However, there is also a significant demand in the columns of the transverse frames which are normal to the blast loading. The value of D/C ratio is lower than one of D/C ratio obtained linear analyses due to reduction of moment demand.

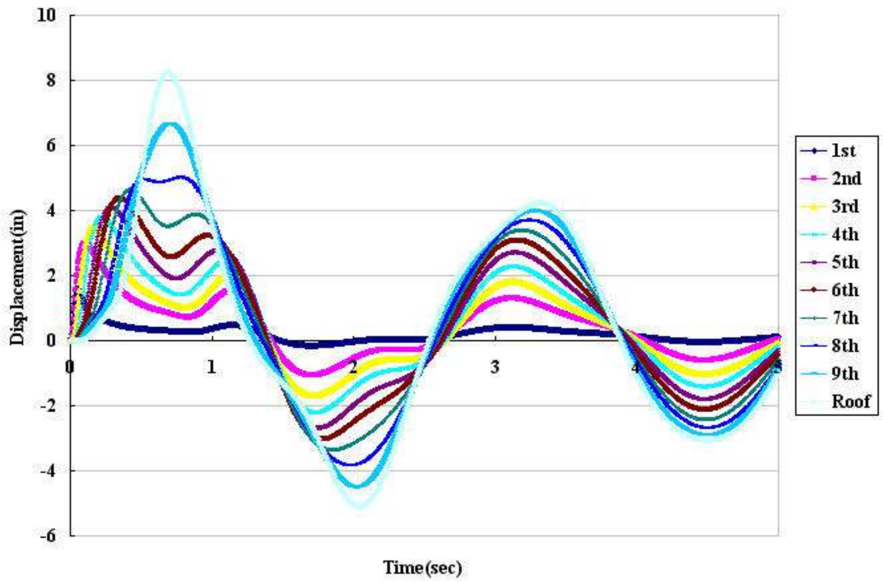

(a) 1,000 lb TNT Weight @ 20 ft Stand-Off Distance

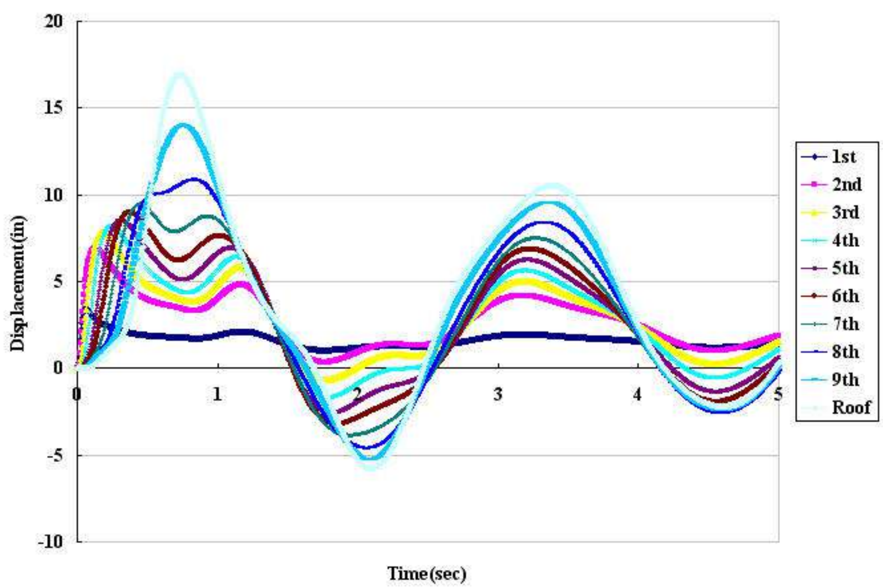

(b) 2,000 lb TNT Weight @ 20 ft Stand-Off Distance

Figure 5.56 : Nonlinear Dynamic Time History

“Figure 5.56 : Continued”

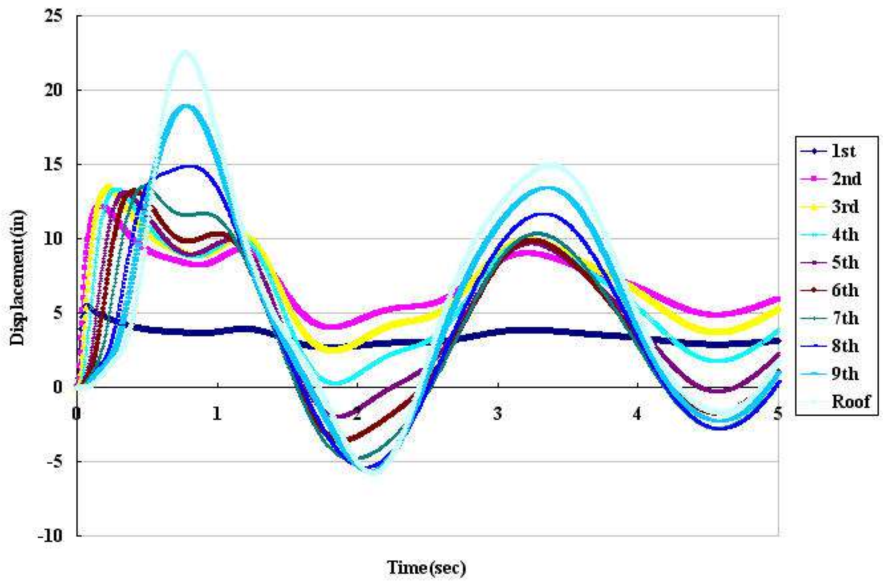

(c) 3,000 lb TNT Weight @ 20 ft Stand-Off Distance

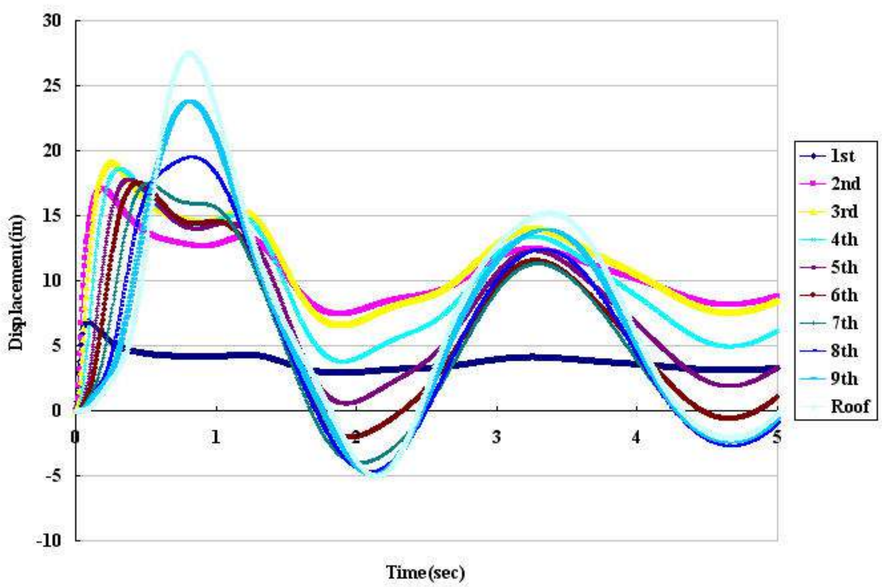

(d) 4,000 lb TNT Weight @ 20 ft Stand-Off Distance

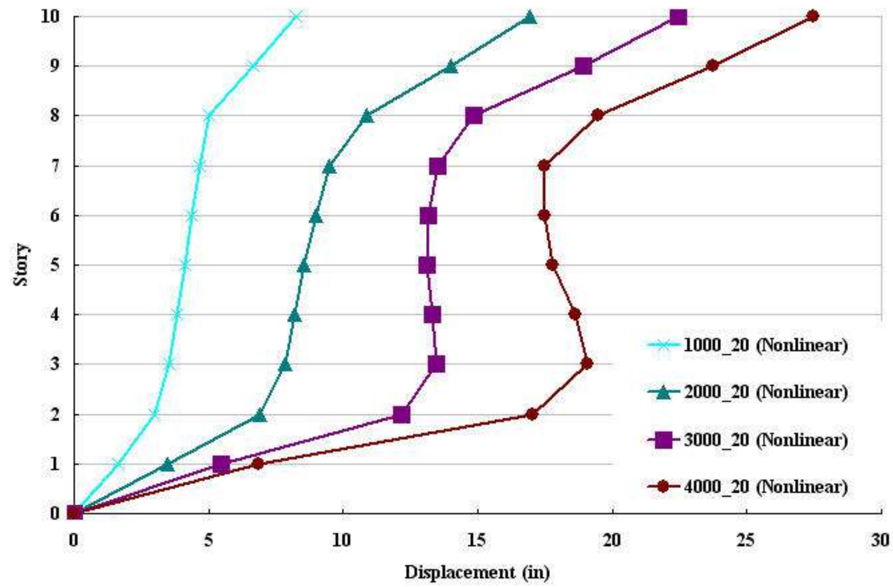

Figure 5.57 : Maximum Deflection on Each Floor By Nonlinear Analysis

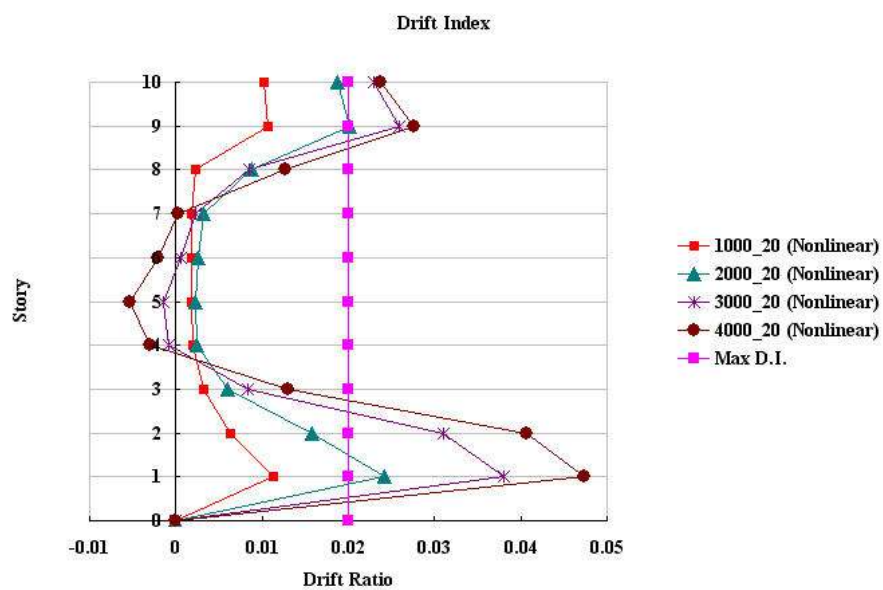

Figure 5.58 : Maximum Drift Ratio Analyzed By Nonlinear Analysis

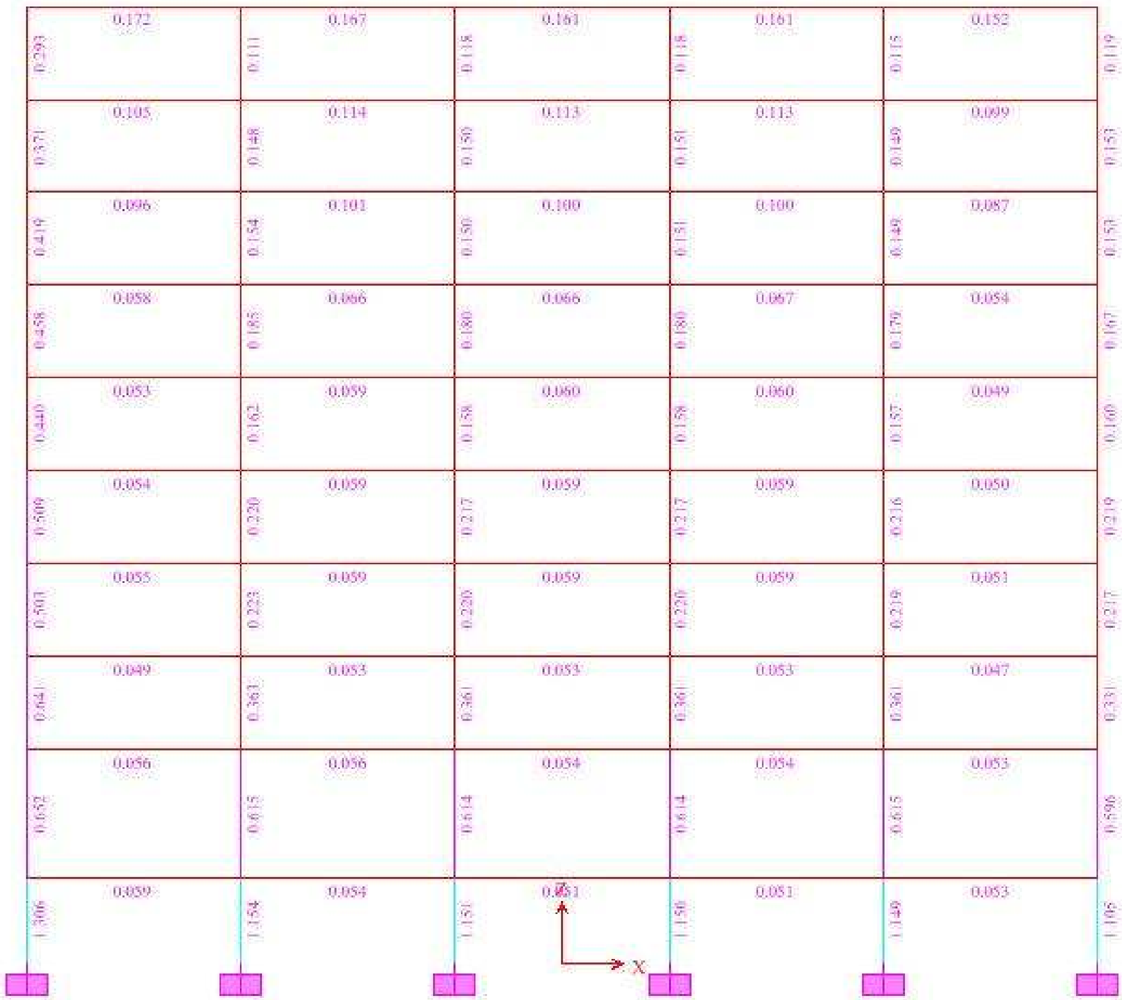

(a) 1,000 lb TNT Weight at 20 ft Stand-Off Distance

Figure 5.59 : Nonlinear Demand/Capacity Ratio on Transverse Direction

"Figure 5.59 : Continued"

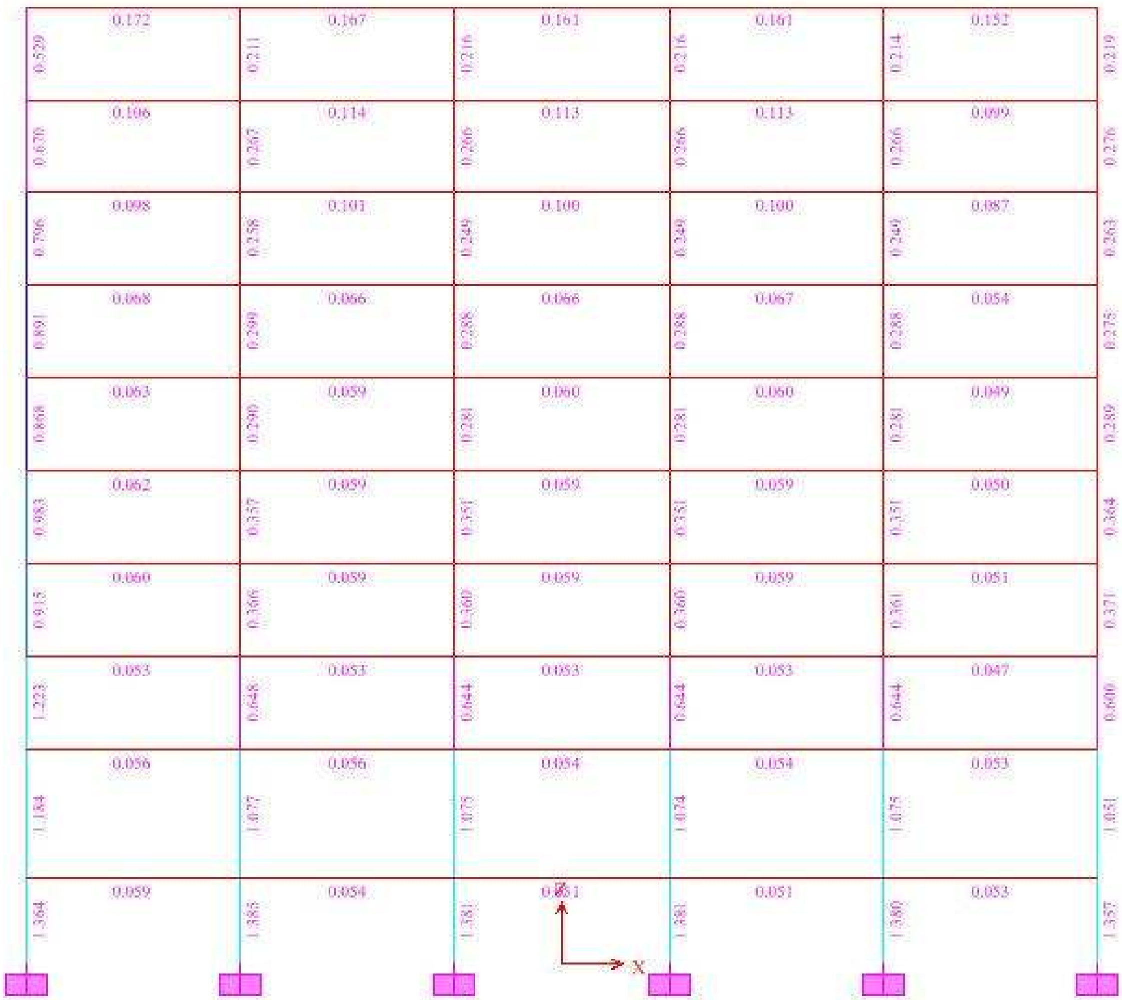

(b) 2,000 lb TNT Weight at 20 ft Stand-Off Distance

"Figure 5.59 : Continued"

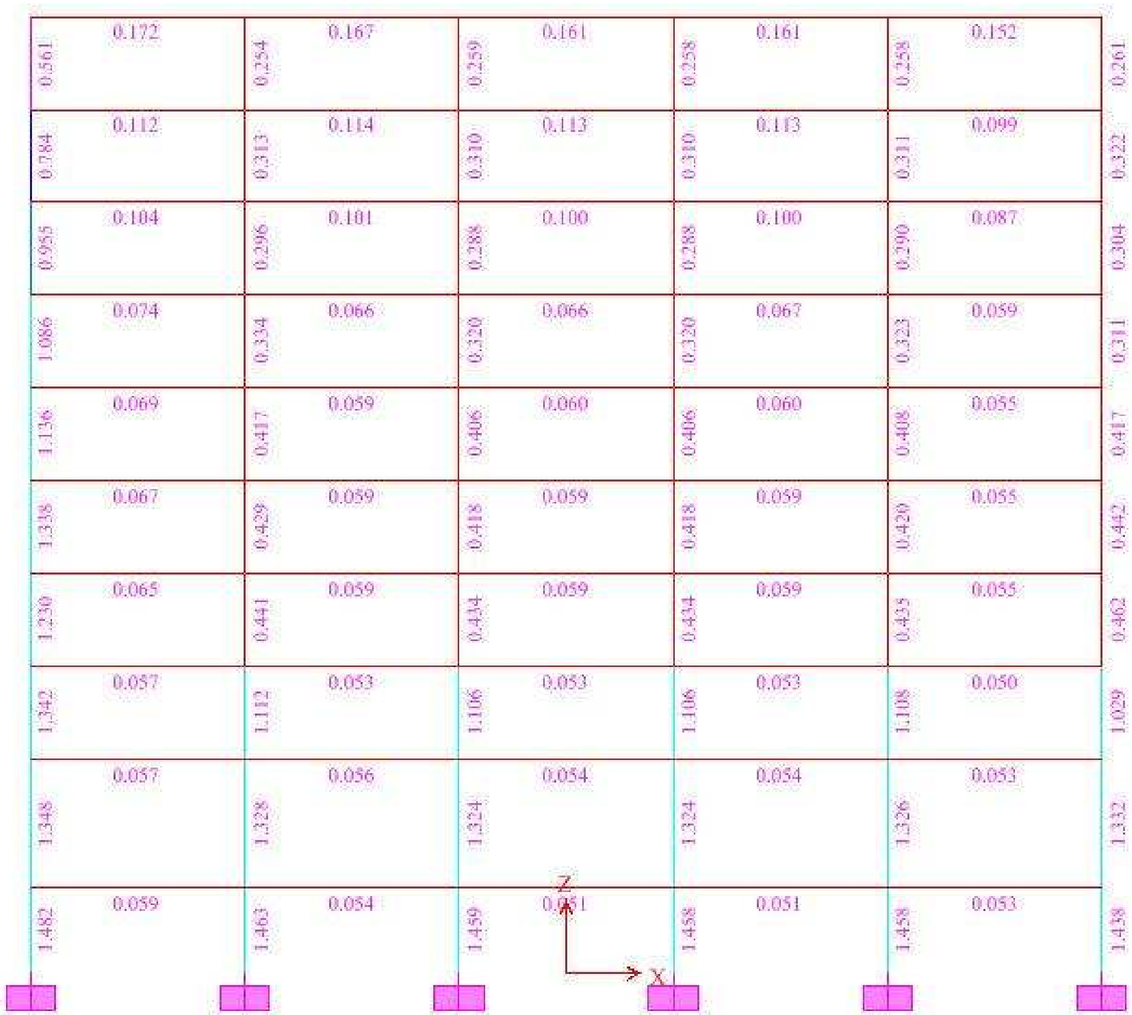

(c) 3,000 lb TNT Weight at 20 ft Stand-Off Distance

“Figure 5.59 : Continued”

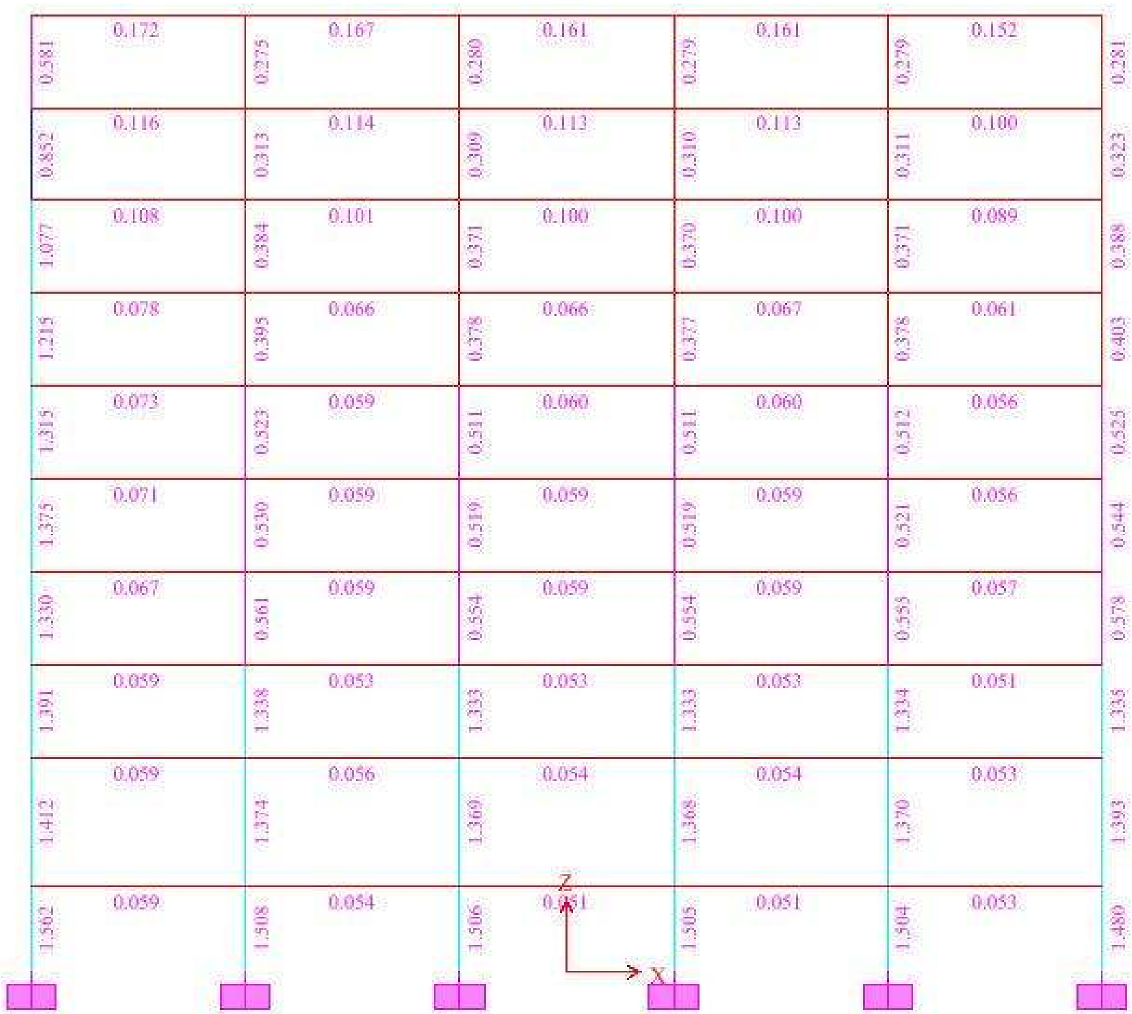

(d) 4,000 lb TNT Weight at 20 ft Stand-Off Distance

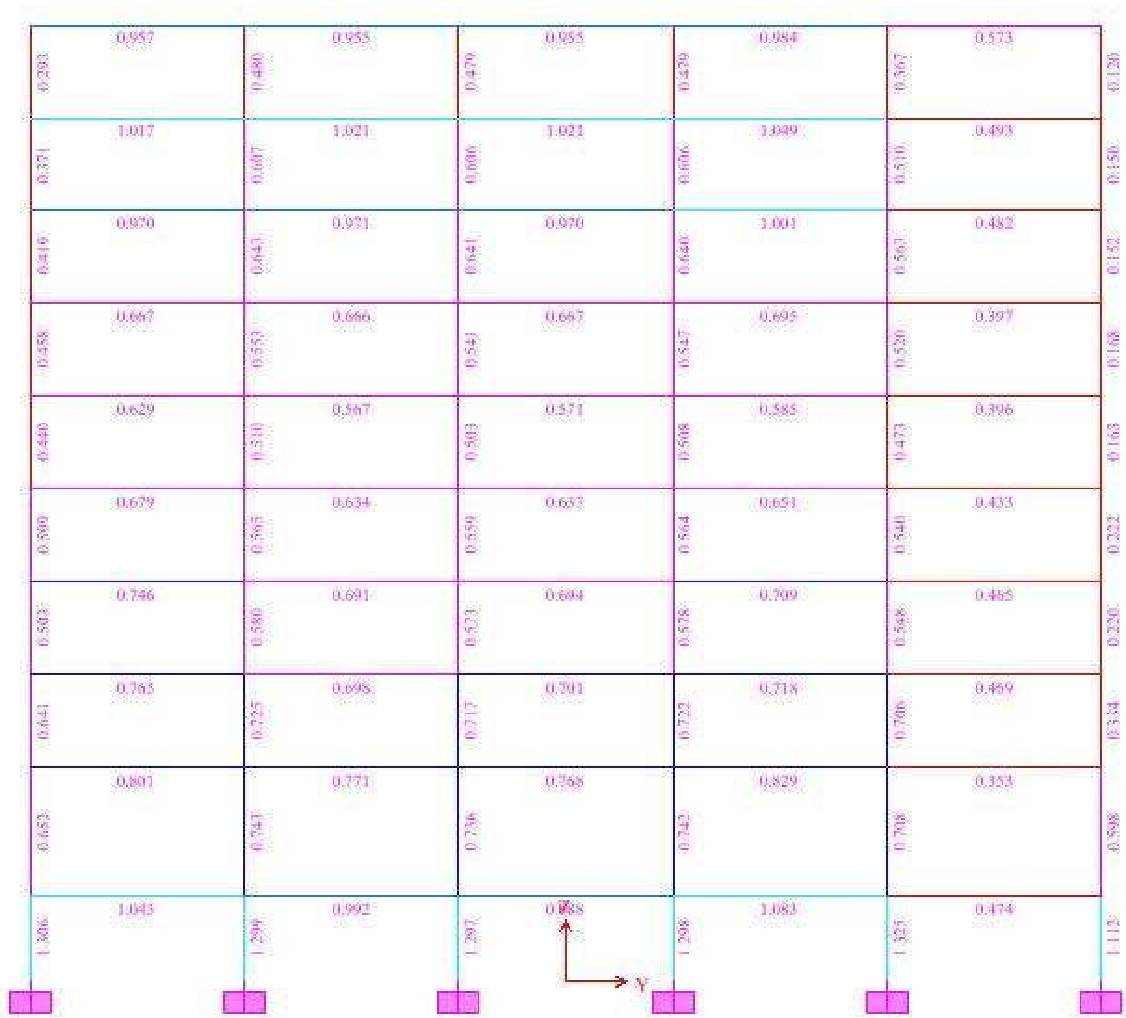

(a) 1,000 lb TNT Weight at 15 ft Stand-Off Distance

Figure 5.60 : Nonlinear Demand/Capacity Ratio on Longitudinal Direction

"**Figure 5.60 : Continued**"

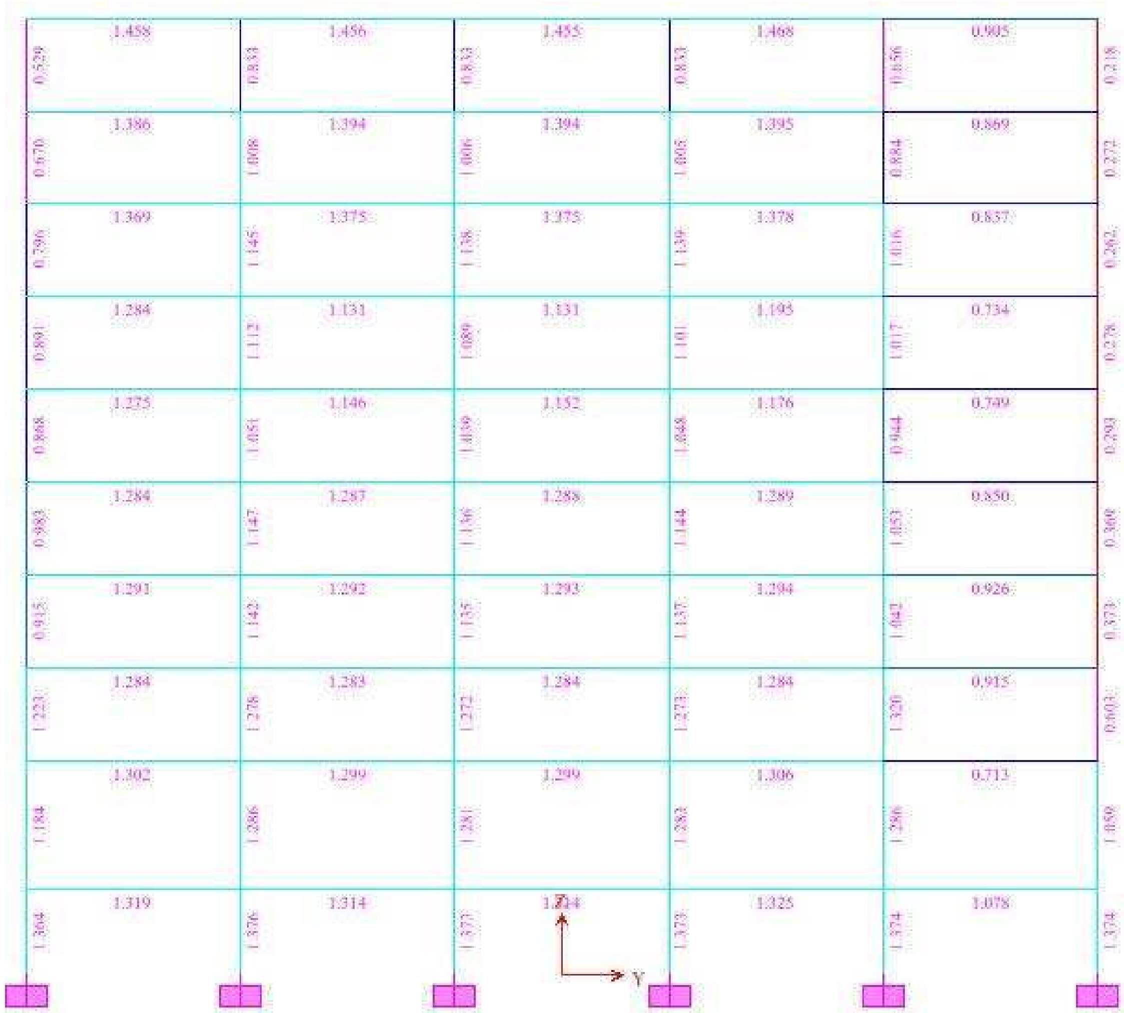

(b) 2,000 lb TNT Weight at 20 ft Stand-Off Distance

“Figure 5.60 : Continued”

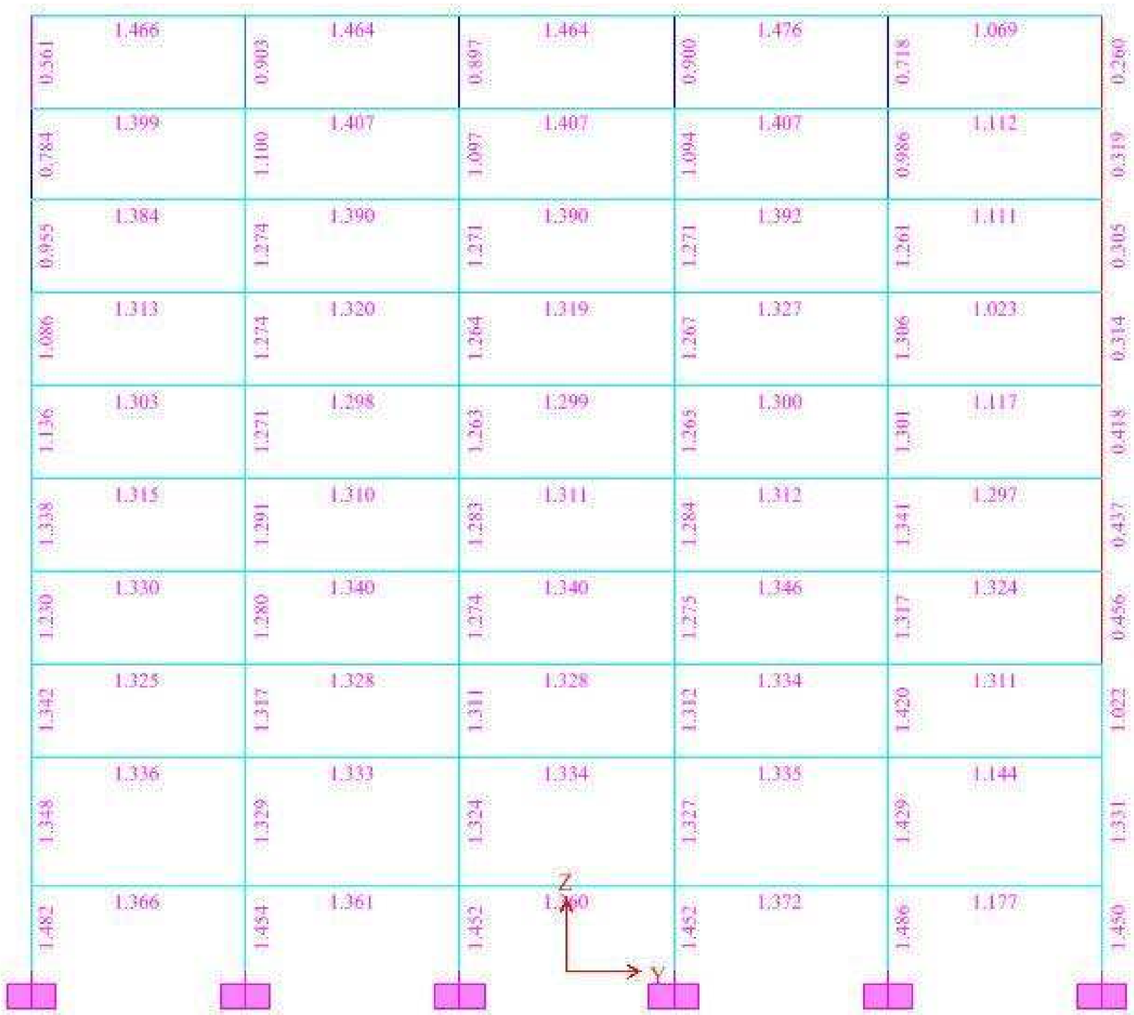

(c) 3,000 lb TNT Weight at 20 ft Stand-Off Distance

“Figure 5.60 : Continued”

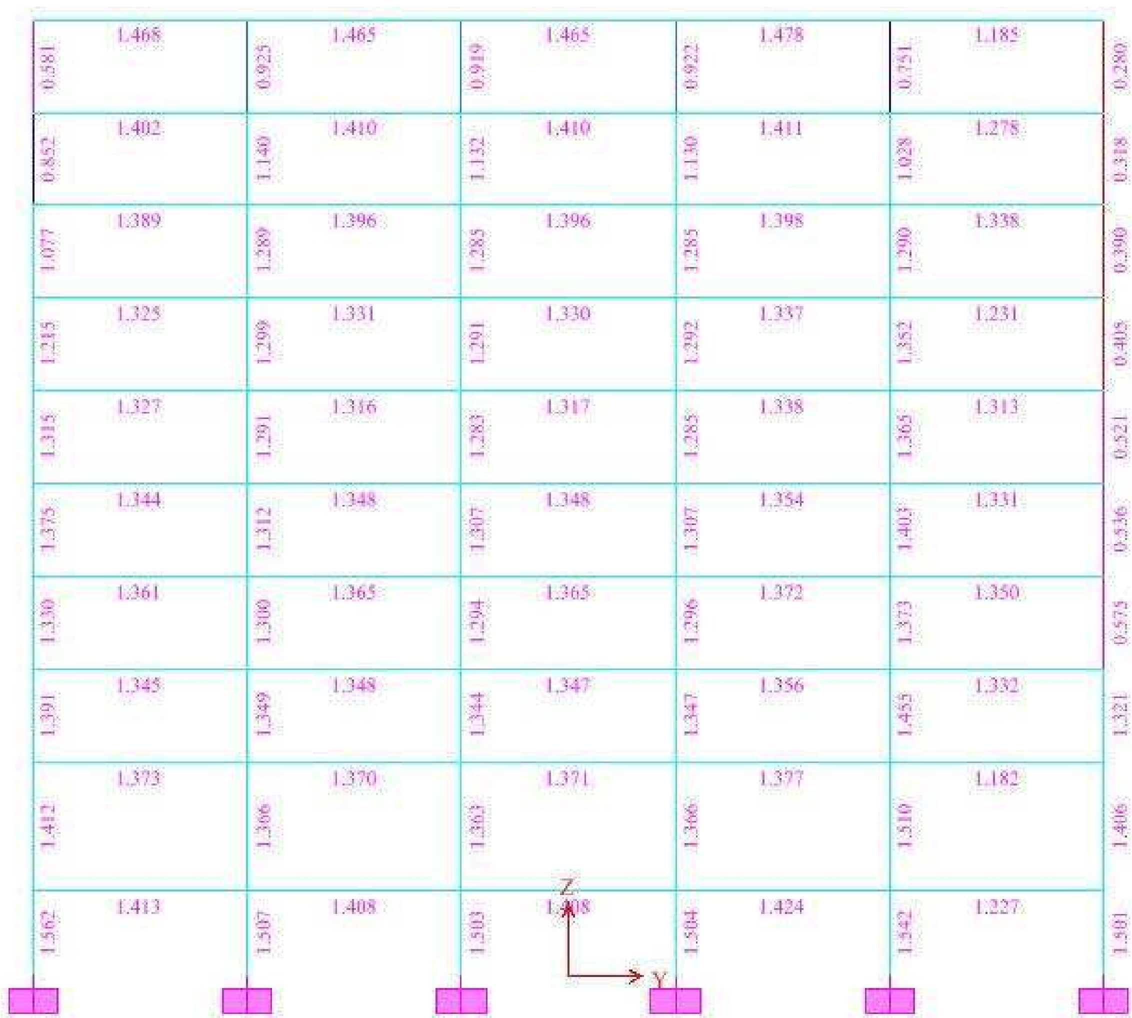

(d) 4,000 lb TNT Weight at 20 ft Stand-Off Distance

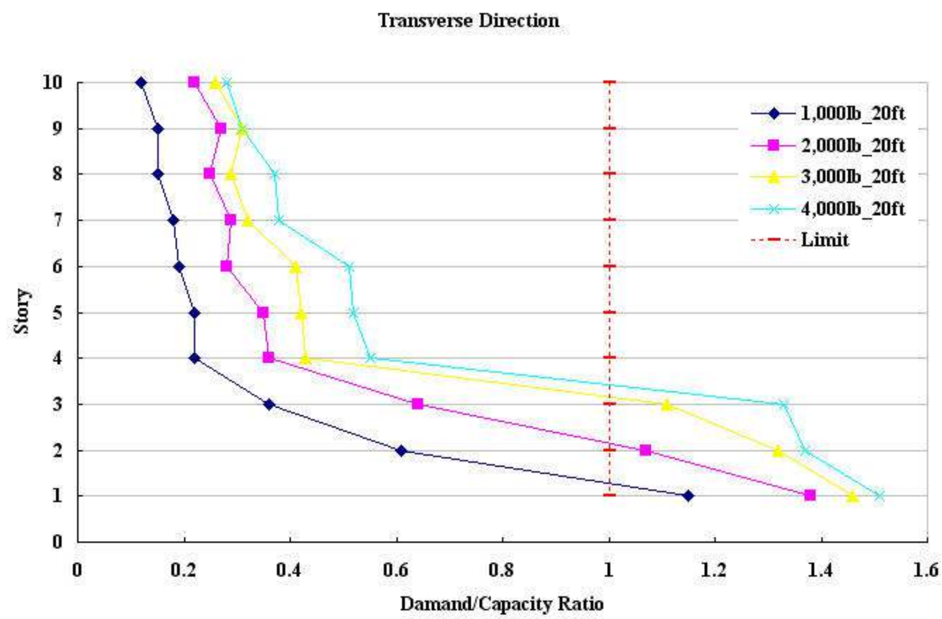

Figure 5.61 : Demand/Capacity Ratio Analyzed by Nonlinear Analysis (Transverse Direction)

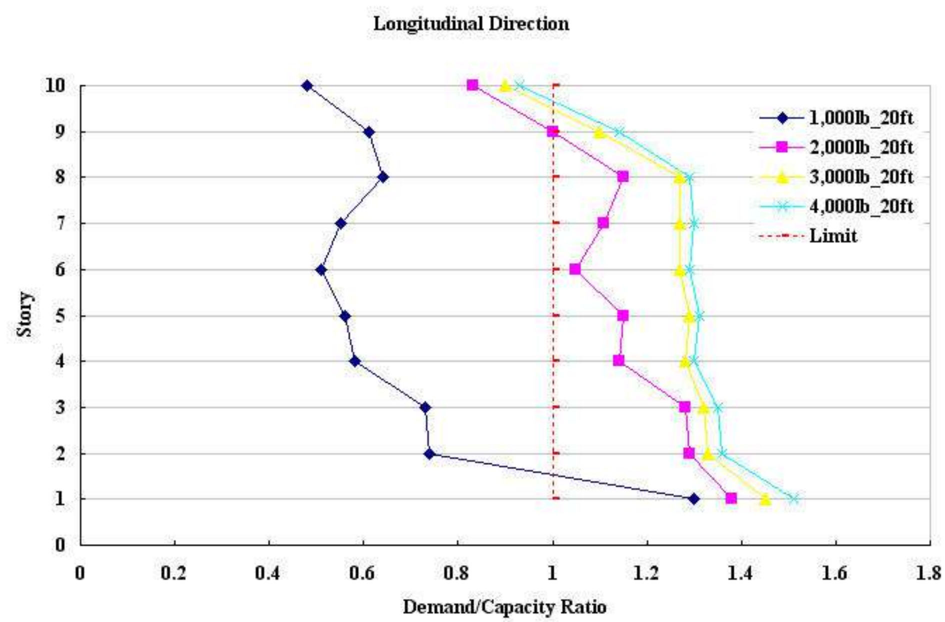

Figure 5.62 : Demand/Capacity Ratio Analyzed by Nonlinear Analysis (Longitudinal Direction)

5.5.2. Nonlinear Plastic Hinge Behavior

The default plastic hinge properties in SAP2000 are used for the analyses. These properties are based on the recommendations made in FEMA-273 for steel moment hinges. The moment-rotation curve that gives the yield value and the plastic deformation following yield is shown in chapter 4.4. The hinge parameters are summarized in chapter 4.4 along with the FEMA condition assessment. To calculate the yield rotation, θy, is also used from FEMA 356 equations as shown in chapter 4.4.

For reference, the member locations and identification numbers are shown in Figure 5.63 and Figure 5.64 for typical transverse and longitudinal frames. The critical members are selected using nonlinear analysis such as two columns of low floor along transverse direction, two columns and two beams along longitudinal direction at low floor and roof. The plastic rotation demands in critical members of the transverse and longitudinal frame are summarized in Figure 5.65 – Figure 5.68.

Demands for the 1,000 lb TNT weight @ 20 ft and 2,000 lb TNT weight @ 20 ft are summarized in Figure 5.65 and Figure 5.66. Figure 5.65 is shown that the columns (1, 11) that exceed the elastic limit have small plastic rotation demands along longitudinal directions. According to the FEMA recommendations, this building would be classified as suitable for immediate occupancy (IO). In Figure 5.66, the behaviors of the longitudinal columns (10, 20) at roof level are linear and similar behaviors can be seen on 1,000 lb TNT weight @ 20 ft case. However, other members that exceed the elastic limit have small plastic rotation demands along both directions.

The demands for extreme condition of 3,000 lb @ 20 ft and 4,000 lb @ 20 ft are summarized in Figure 5.67 and Figure 5.68. Here it can be seen that most cases are over I.O. range and nonlinear with more plastic rotation demands along both directions. However, columns on roof level through longitudinal direction are still in linear ranges.

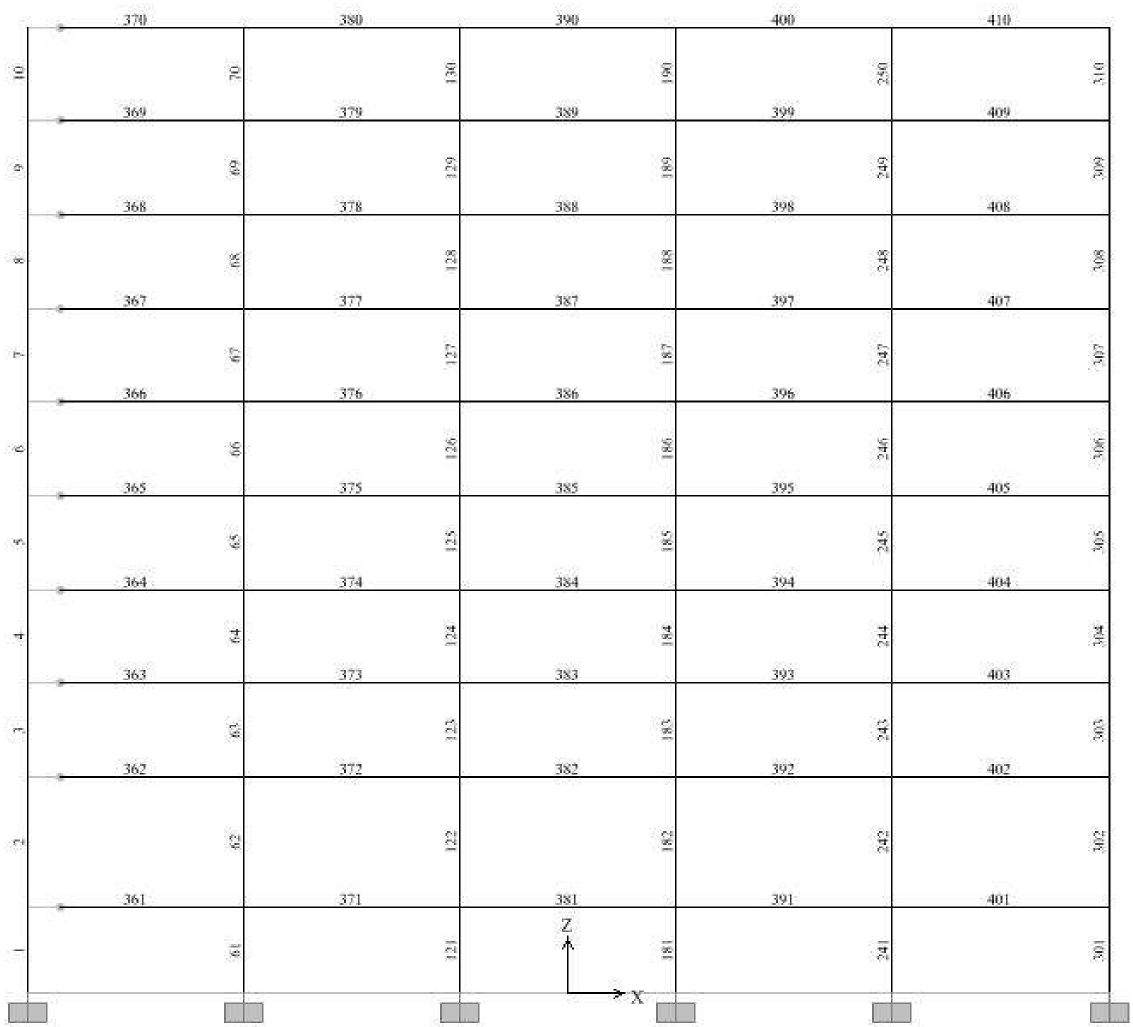

Figure 5.63: Generated Member Numbers along the Transverse Direction

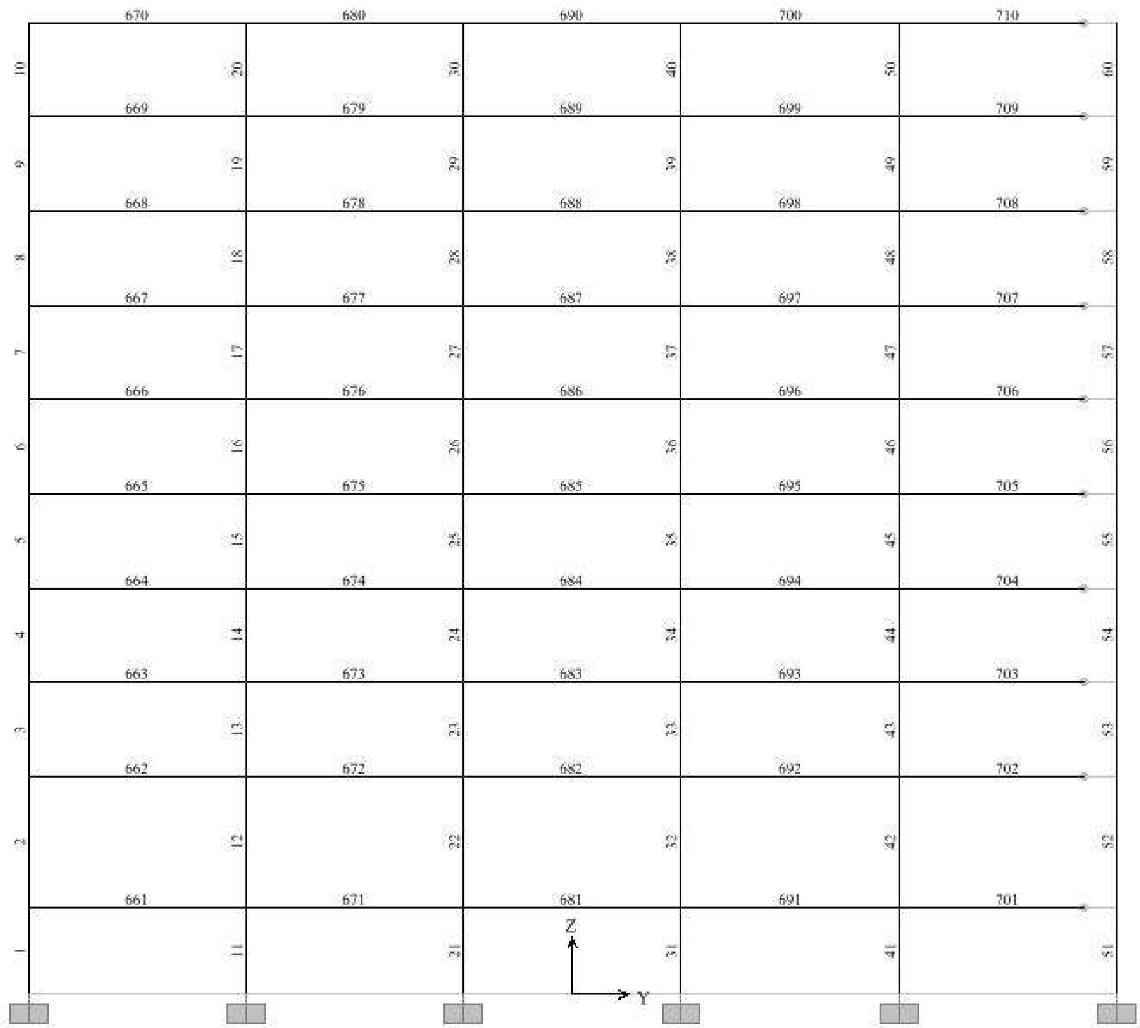

Figure 5.64 : Generated Member Numbers along the Longitudinal Direction

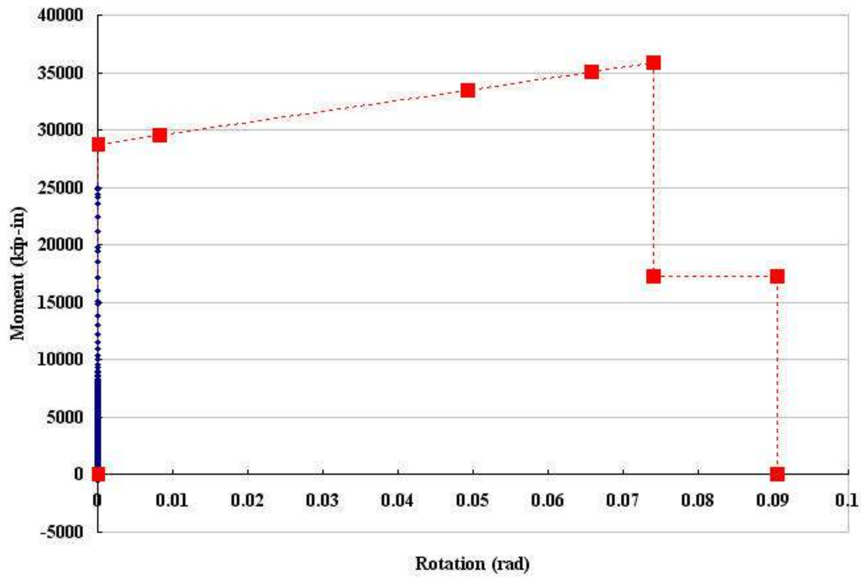

(a) Moment-Rotation Relationship on Transverse Direction (Column 61)

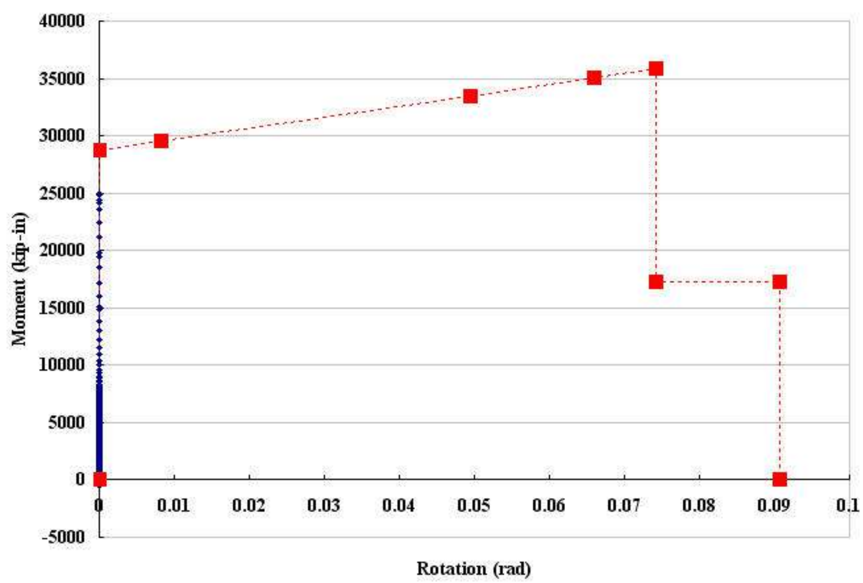

(b) Moment-Rotation Relationship on Transverse Direction (Column 121)

Figure 5.65 : Moment-Rotation Relation In Case of 1,000 lb TNT Weight at 20 ft Stand-Off Distance

“Figure 5.65 : Continued”

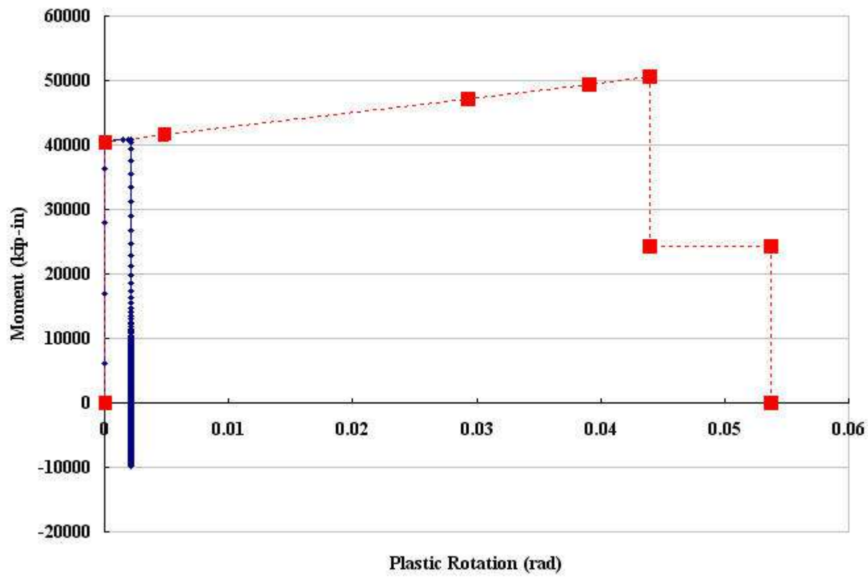

(c) Moment-Rotation Relationship on Longitudinal Direction (Column 1)

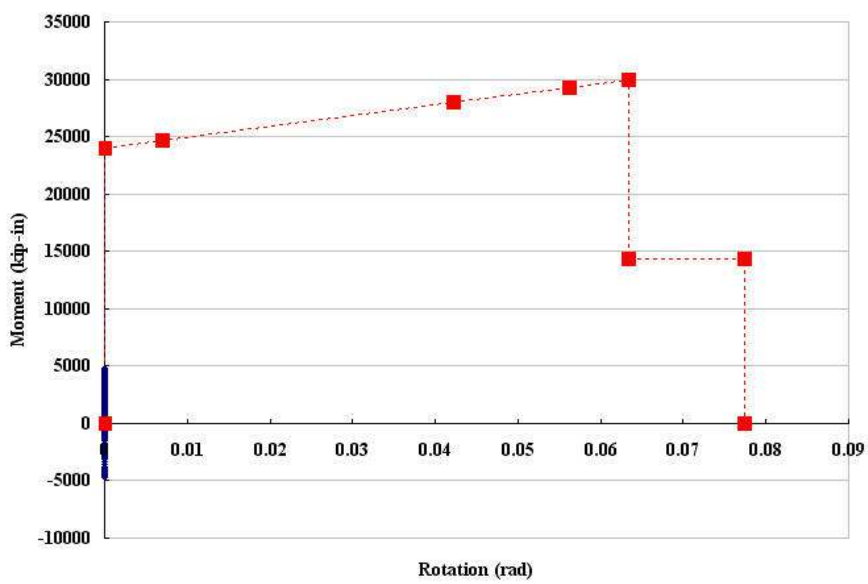

(d) Moment-Rotation Relationship on Longitudinal Direction (Column 10)

“Figure 5.65 : Continued”

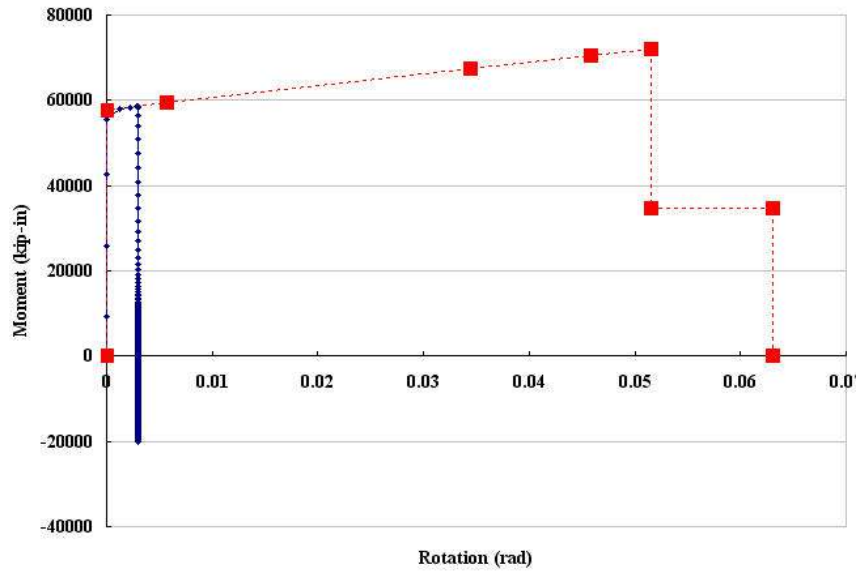

(e) Moment-Rotation Relationship on Longitudinal Direction (Column 11)

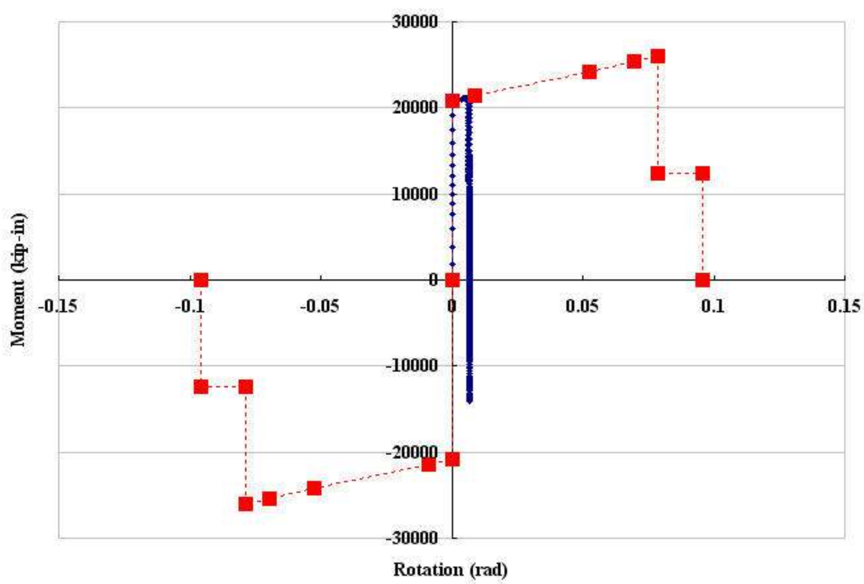

(f) Moment-Rotation Relationship on Longitudinal Direction (Column 20)

“Figure 5.65 : Continued”

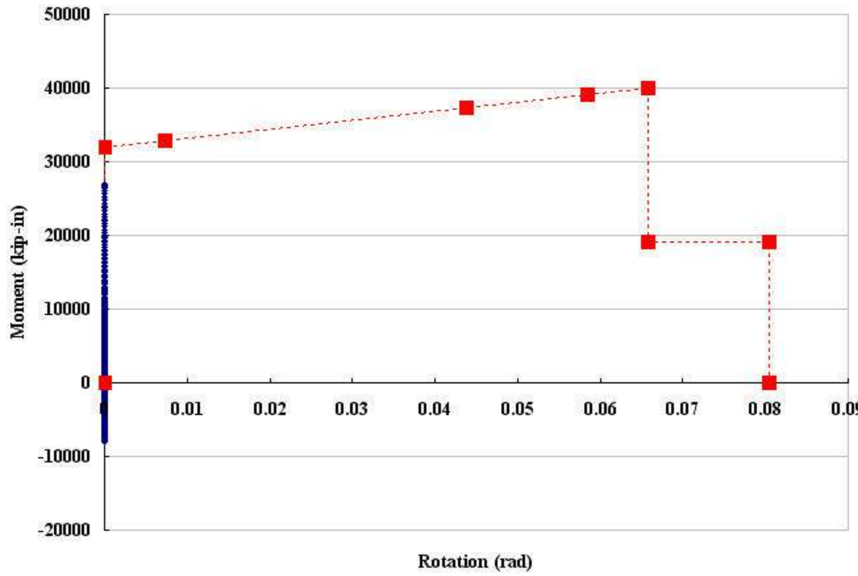

(g) Moment-Rotation Relationship on Longitudinal Direction (Beam 661)

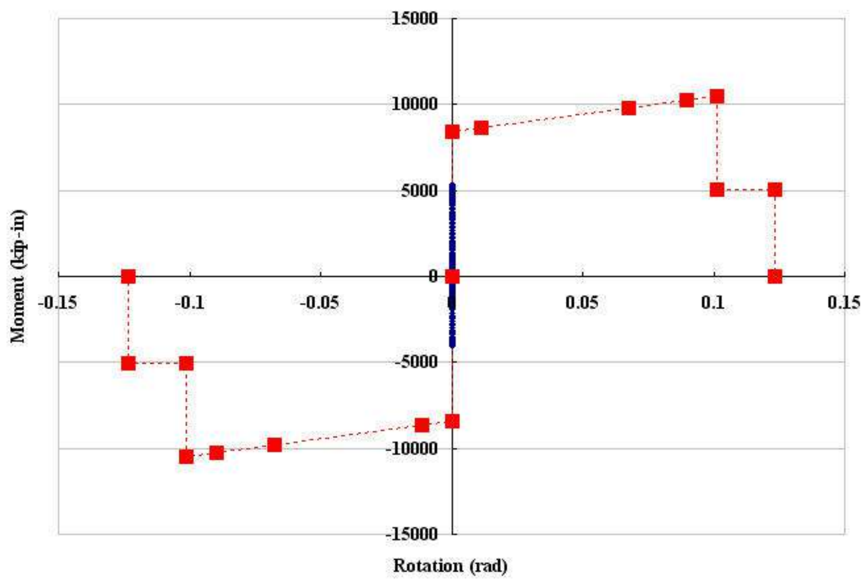

(h) Moment-Rotation Relationship on Longitudinal Direction (Beam 670)

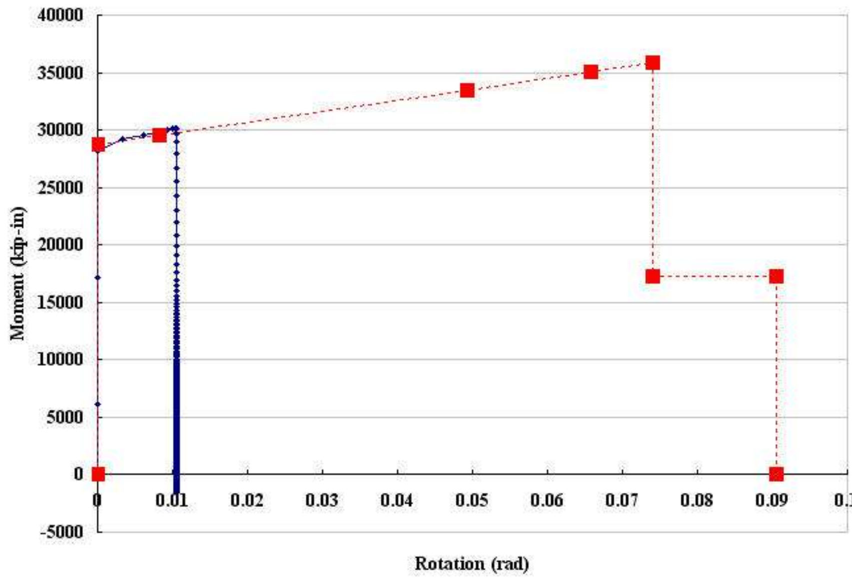

(a) Moment-Rotation Relationship on Transverse Direction (Column 61)

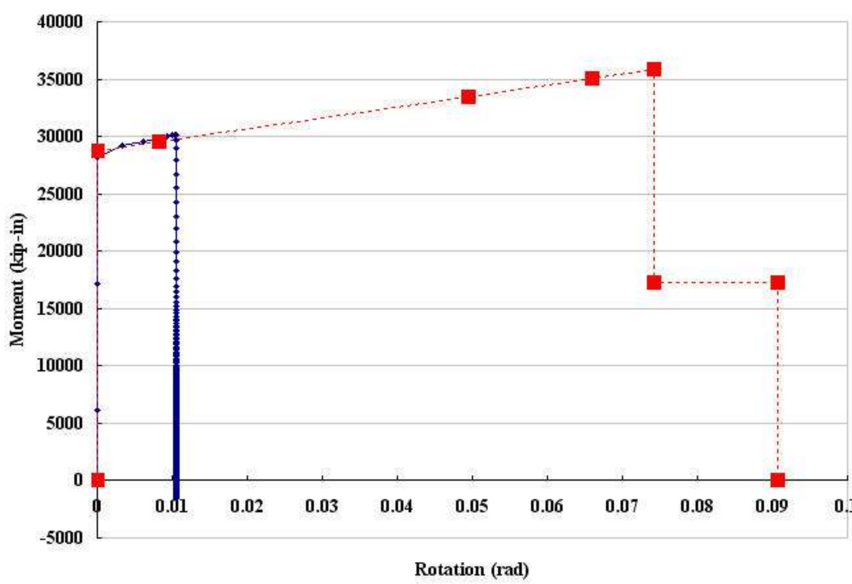

(b) Moment-Rotation Relationship on Transverse Direction (Column 121)

Figure 5.66 : Moment-Rotation Relation In Case of 2,000 lb TNT Weight at 20 ft Stand-Off Distance

"Figure 5.66 : Continued"

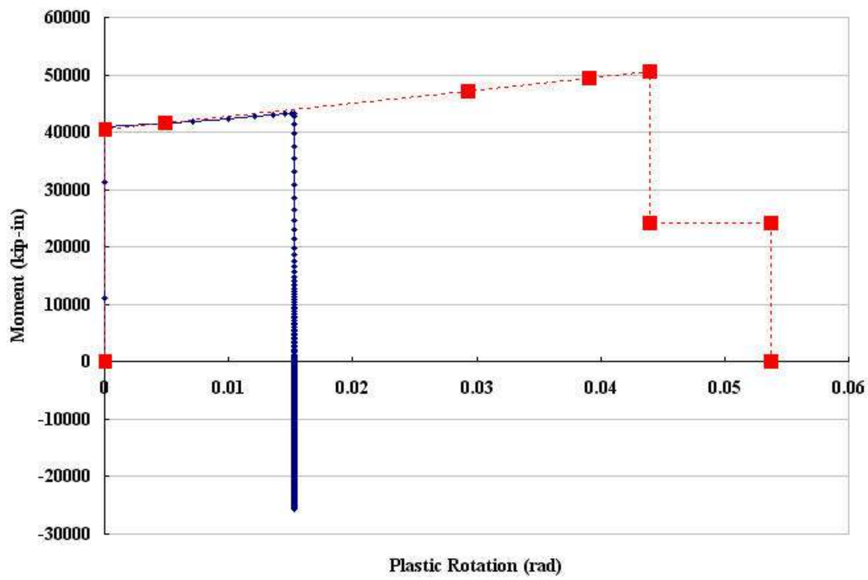

(c) Moment-Rotation Relationship on Longitudinal Direction (Column 1)

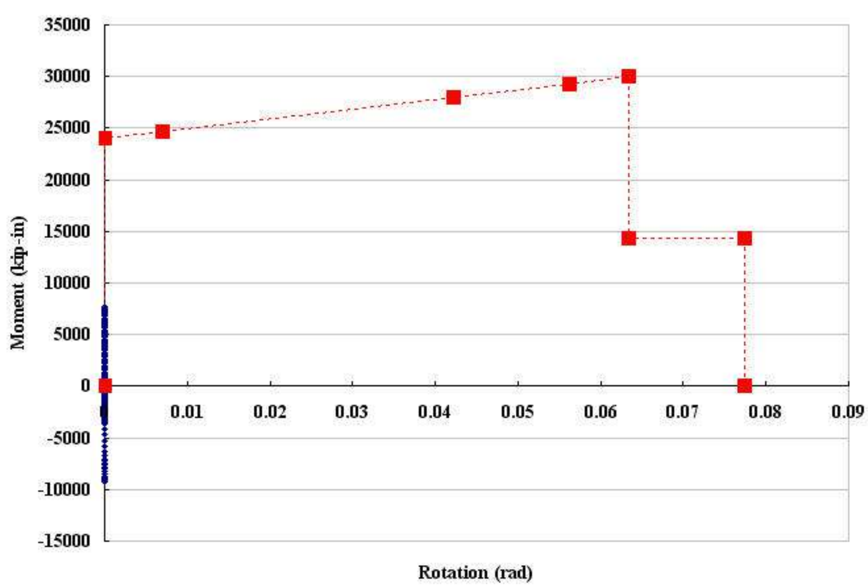

(d) Moment-Rotation Relationship on Longitudinal Direction (Column 10)

“Figure 5.66 : Continued”

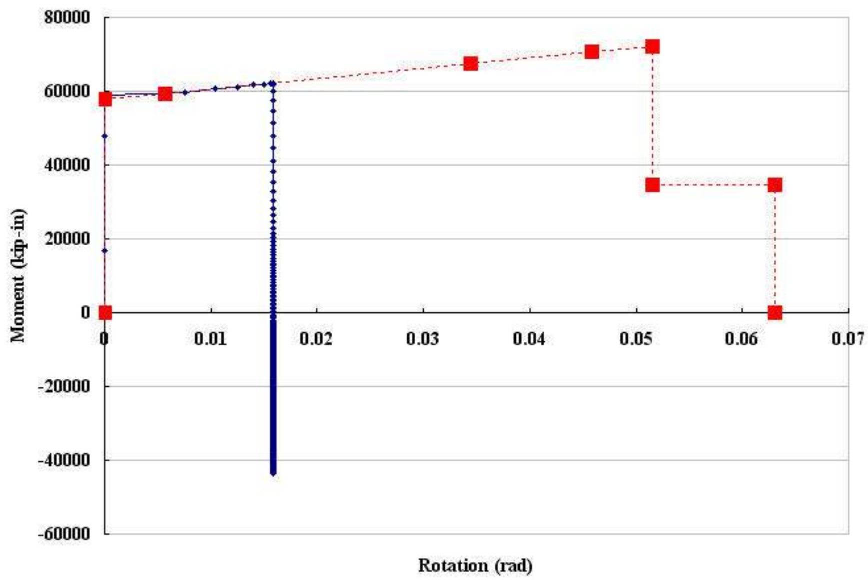

(e) Moment-Rotation Relationship on Longitudinal Direction (Column 11)

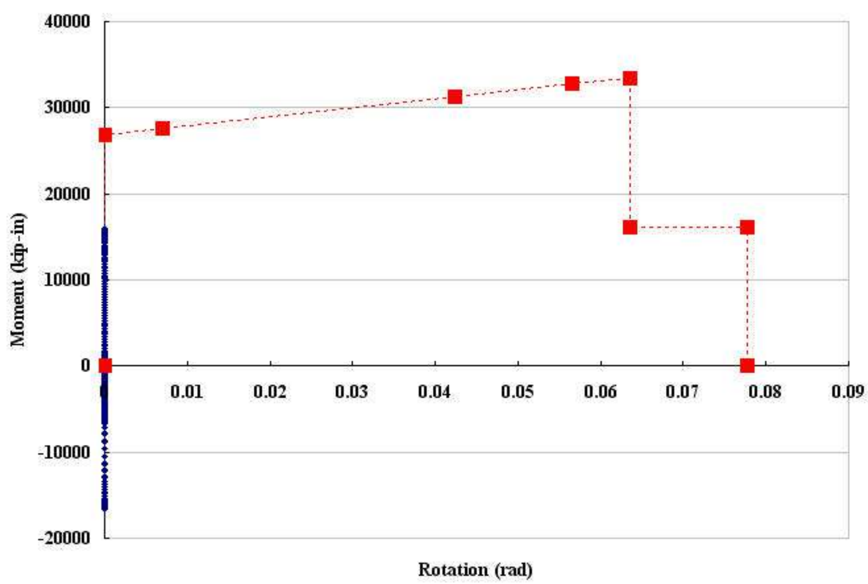

(f) Moment-Rotation Relationship on Longitudinal Direction (Column 20)

"Figure 5.66 : Continued"

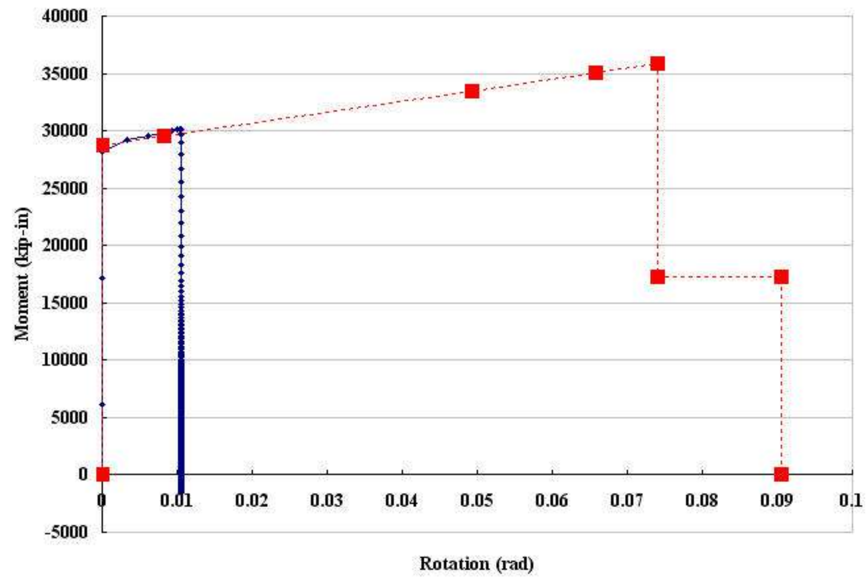

(g) Moment-Rotation Relationship on Longitudinal Direction (Beam 661)

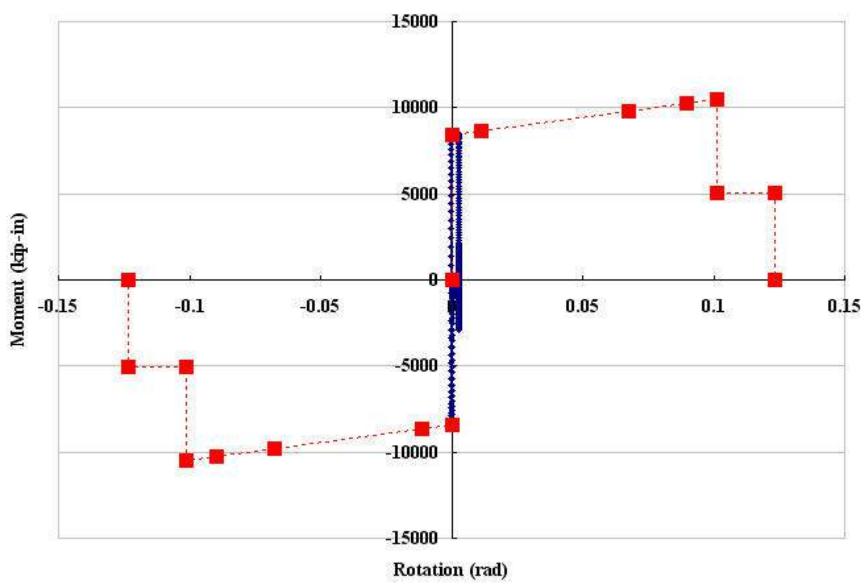

(h) Moment-Rotation Relationship on Longitudinal Direction (Beam 670)

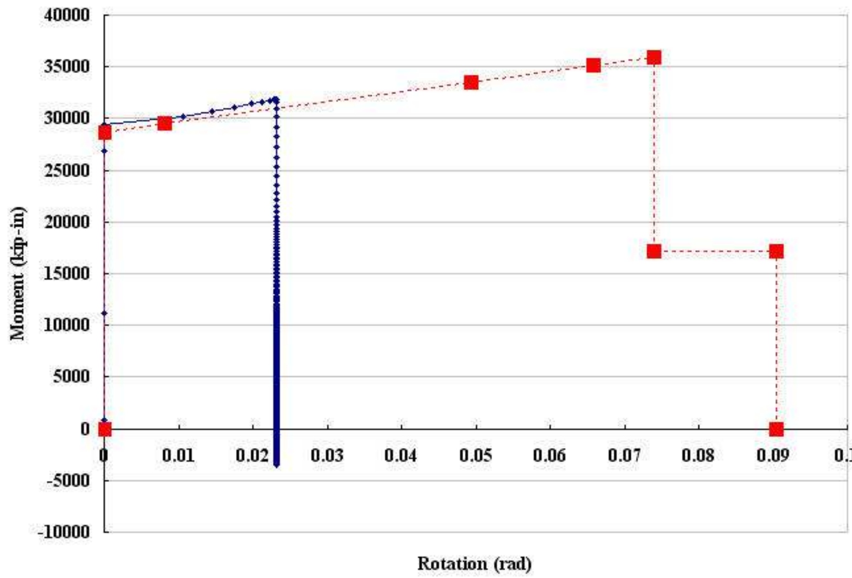

(a) Moment-Rotation Relationship on Transverse Direction (Column 61)

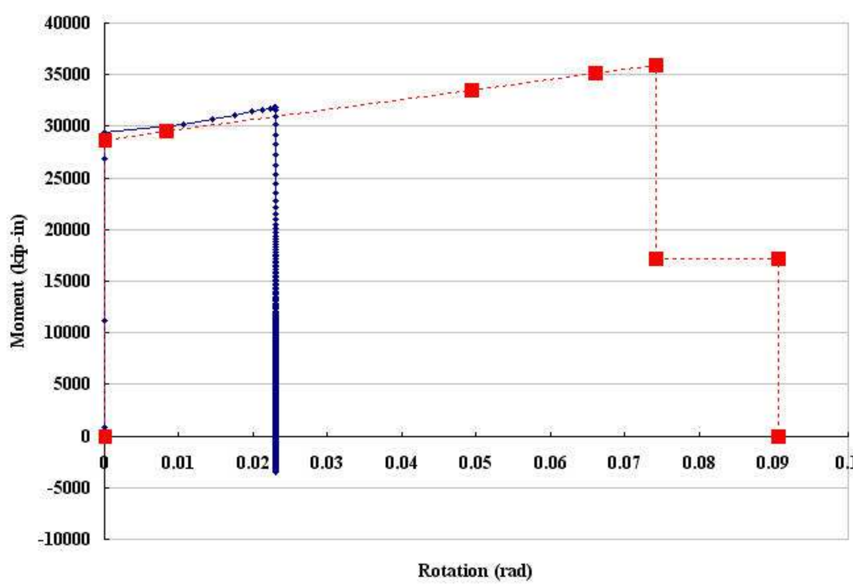

(b) Moment-Rotation Relationship on Transverse Direction (Column 121)

Figure 5.67 : Moment-Rotation Relation In Case of 3,000 lb TNT Weight at 20 ft Stand-Off Distance

"Figure 5.67 : Continued"

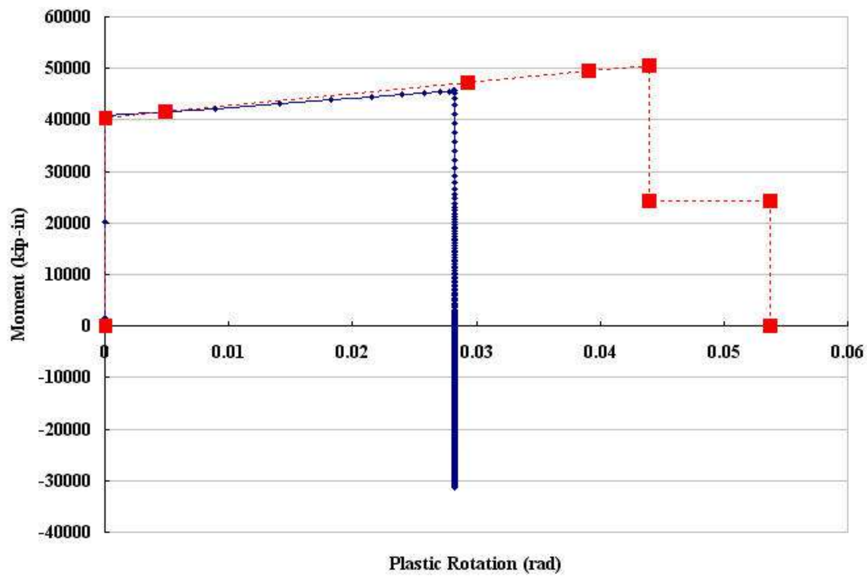

(c) Moment-Rotation Relationship on Longitudinal Direction (Column 1)

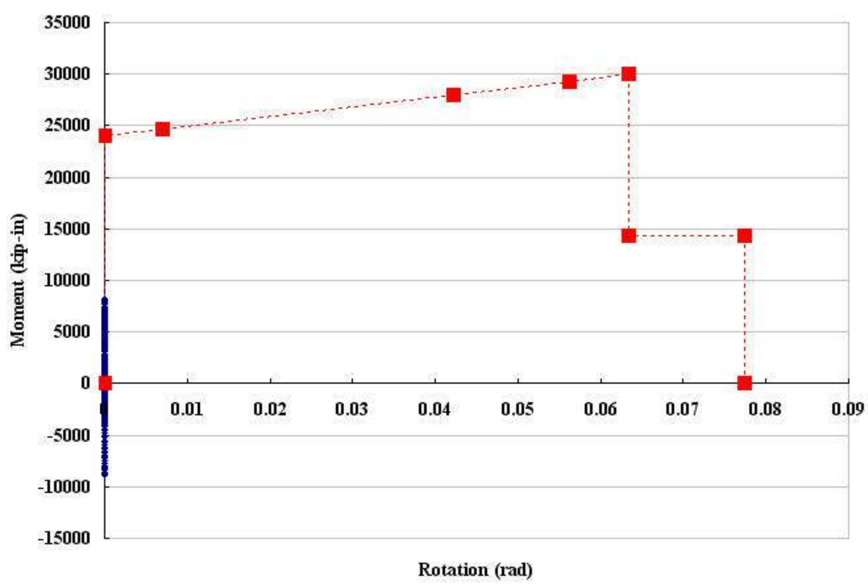

(d) Moment-Rotation Relationship on Longitudinal Direction (Column 10)

“Figure 5.67 : Continued”

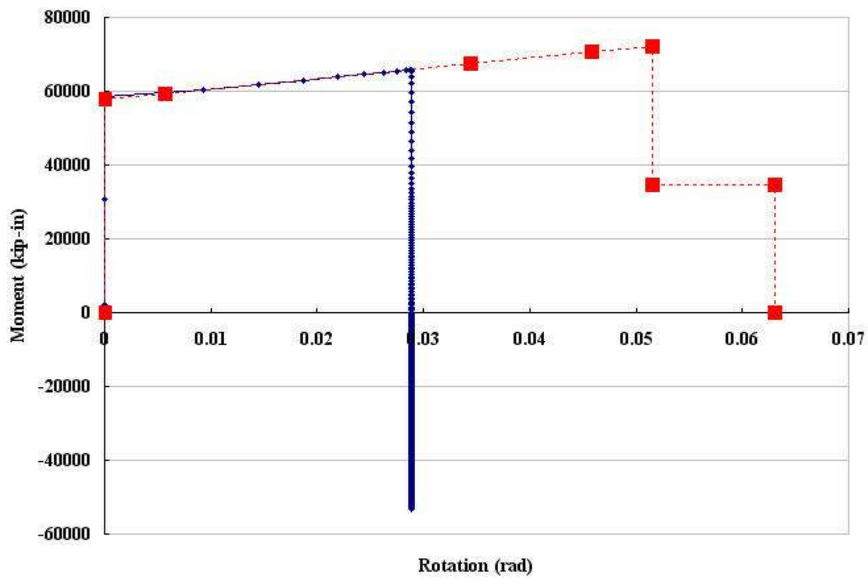

(e) Moment-Rotation Relationship on Longitudinal Direction (Column 11)

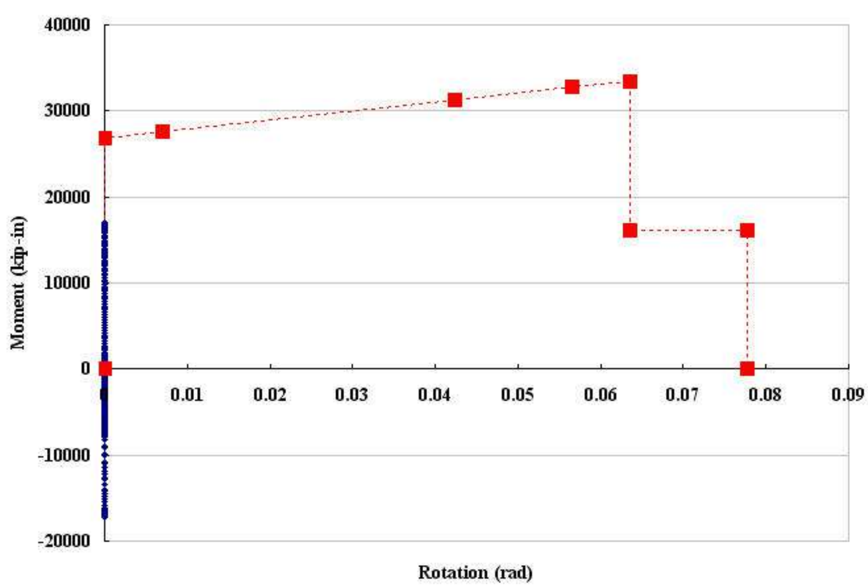

(f) Moment-Rotation Relationship on Longitudinal Direction (Column 20)

"Figure 5.67 : Continued"

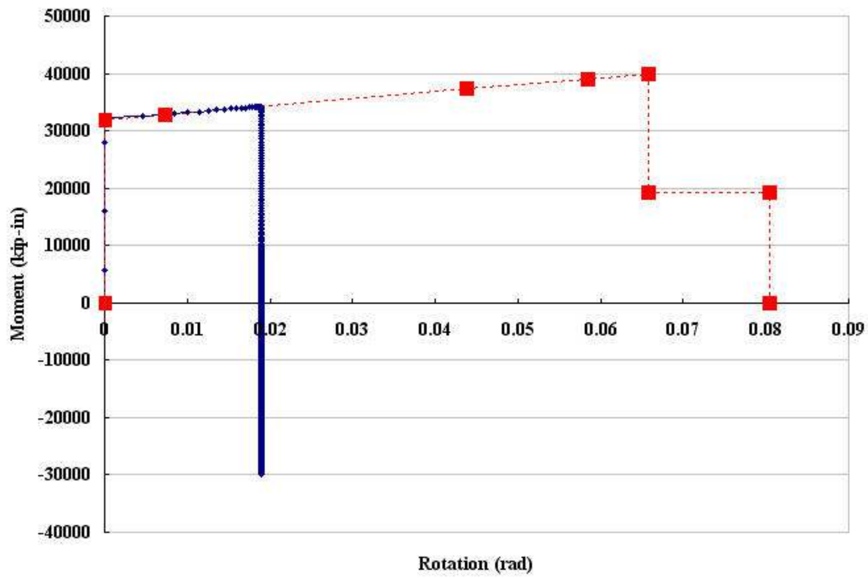

(g) Moment-Rotation Relationship on Longitudinal Direction (Beam 661)

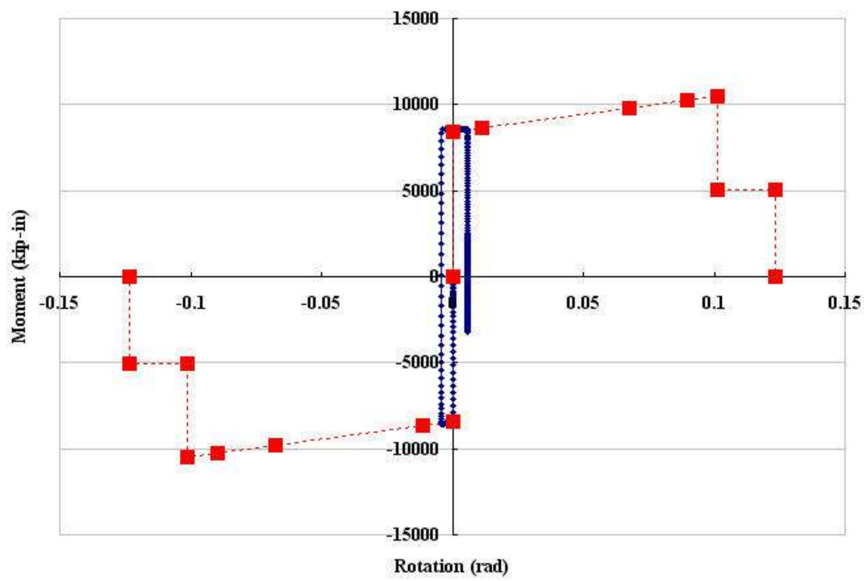

(h) Moment-Rotation Relationship on Longitudinal Direction (Beam 670)

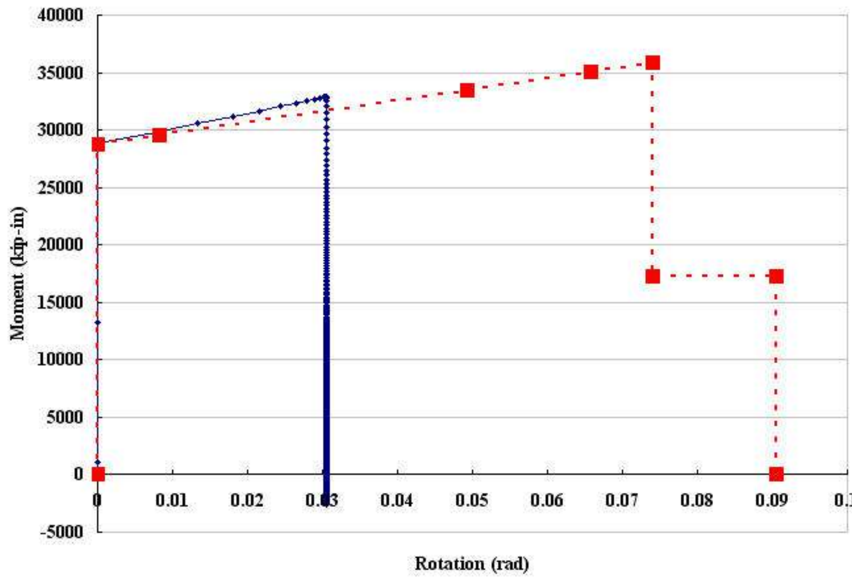

(a) Moment-Rotation Relationship on Transverse Direction (Column 61)

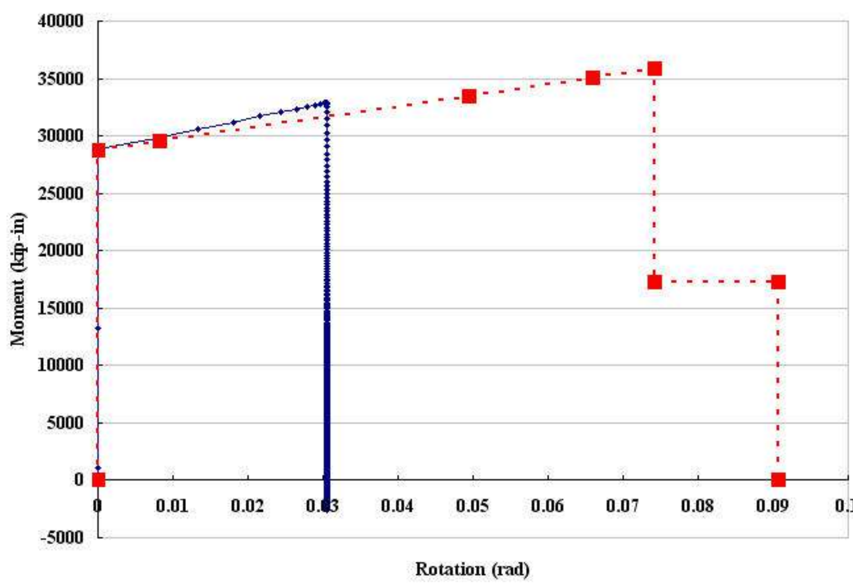

(b) Moment-Rotation Relationship on Transverse Direction (Column 121)

Figure 5.68 : Moment-Rotation Relation In Case of 4,000 lb TNT Weight at 20 ft Stand-Off Distance

“Figure 5.68 : Continued”

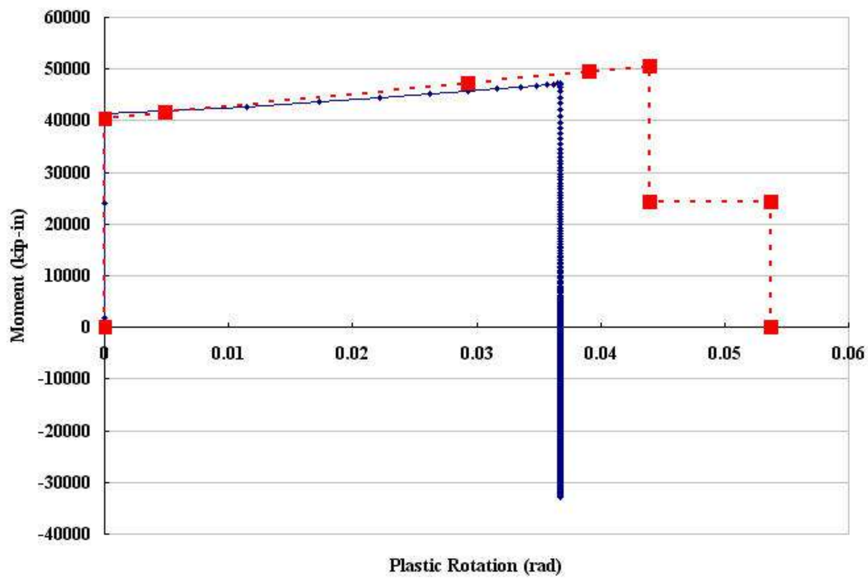

(c) Moment-Rotation Relationship on Longitudinal Direction (Column 1)

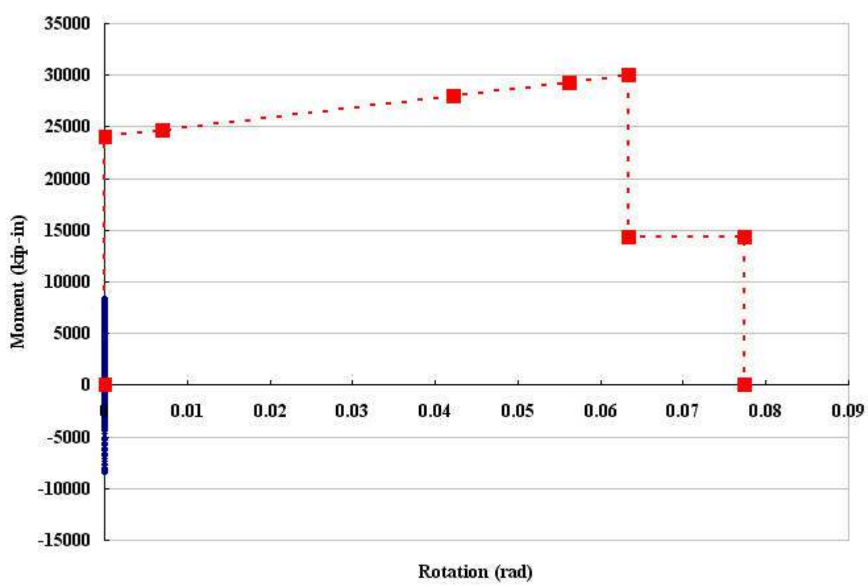

(d) Moment-Rotation Relationship on Longitudinal Direction (Column 10)

“Figure 5.68 : Continued”

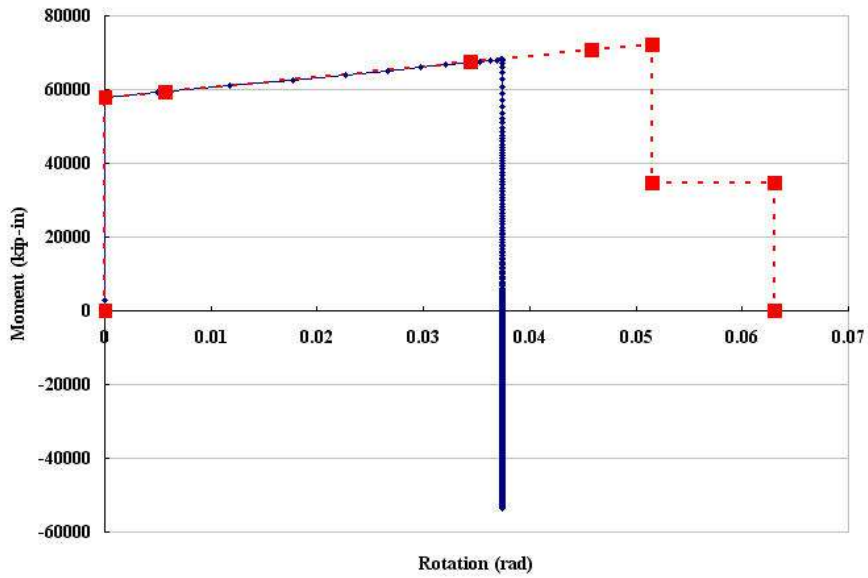

(e) Moment-Rotation Relationship on Longitudinal Direction (Column 11)

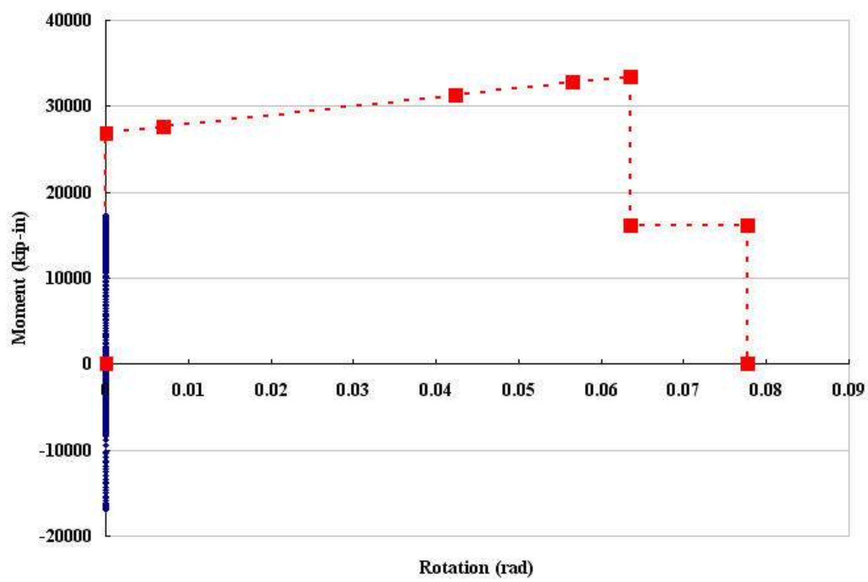

(f) Moment-Rotation Relationship on Longitudinal Direction (Column 20)

"Figure 5.68 : Continued"

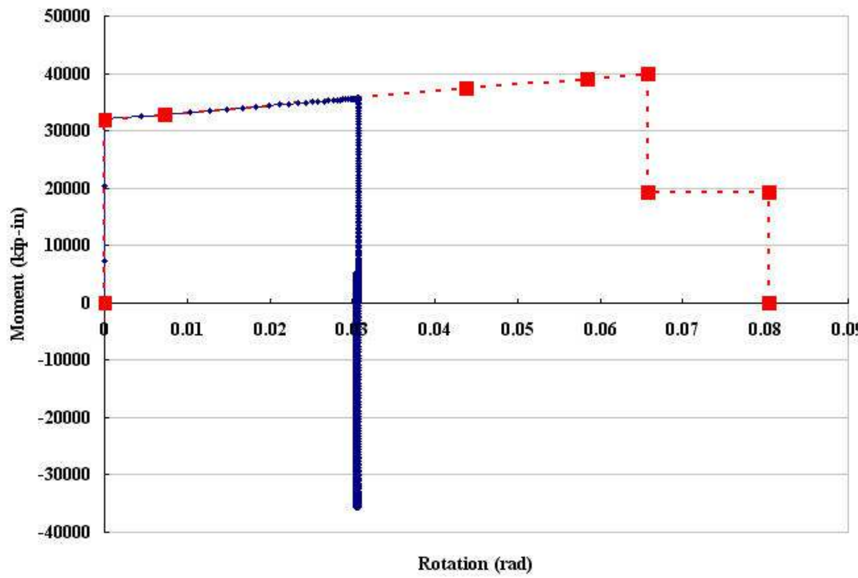

(g) Moment-Rotation Relationship on Longitudinal Direction (Beam 661)

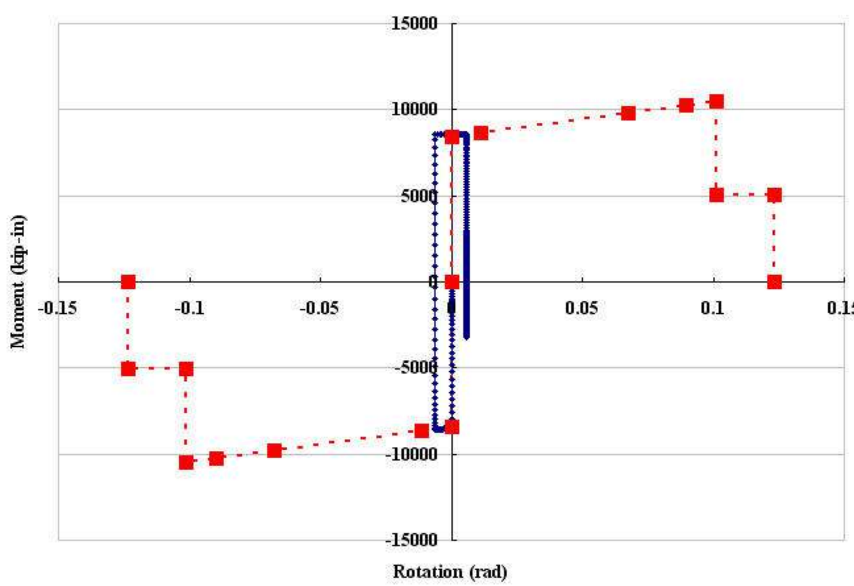

(h) Moment-Rotation Relationship on Longitudinal Direction (Beam 670)

Chapter 6 : Structural Responses of Steel Structure Under Earthquake

To find responses of earthquake ground accelerations, an acceleration record obtained during the Northridge earthquake (1994) is used. The record selected is at the Newhall Fire Station in Northridge earthquake, which is shown in Figure 6.1. This recorded ground acceleration is digitized by 3,000 data points with a 0.02 sec. time interval. As shown in Table 6.1, the maximum acceleration is 554.43 cm/sec/sec (0.57g). To compare the structural responses of recorded earthquake with those of blast loads, the recorded ground acceleration is applied to the three story building and ten story building.

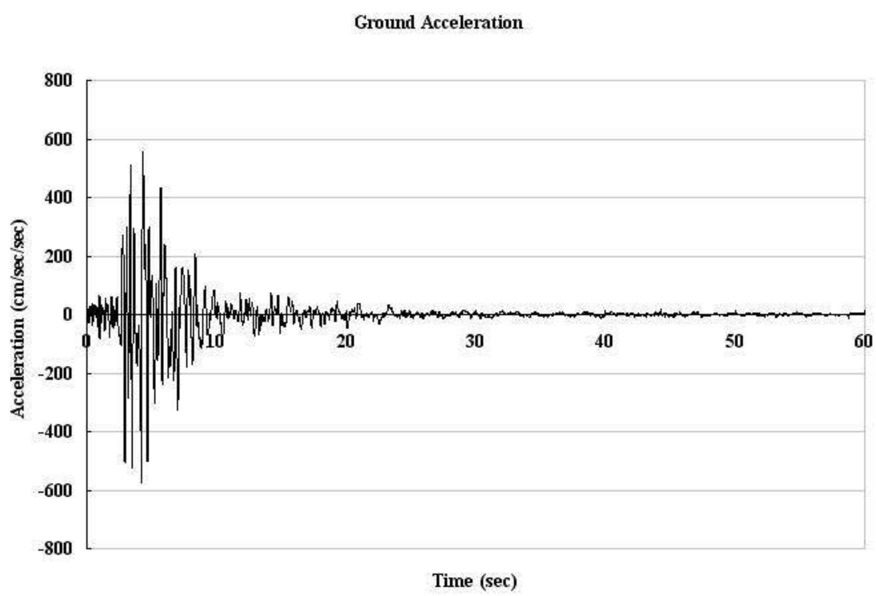

Figure 6.1 : Ground Acceleration of Newhall Fire Station, Northridge Earthquake

Table 6.1 : Ground Motion Record of Northridge Earthquake

Case	Record	No. of Points	Duration (sec)	DT (sec)	PGA (cm/sec2)
NRIDGE 2	Newhall Fire Station Northridge, 1994,	3,000	59.98	0.02	554.43

6.1. Linear Analyses of Three Story Building under Earthquake

From the displacement time histories shown in Figure 6.2 – Figure 6.4, the maximum roof displacement is 16.05 in. at 5.8 sec. for Newhall Fire Station, Northridge earthquake. The other deflections are shown in Table 6.2. In addition, maximum deflection envelope of each floor under recorded ground motion is also shown in Figure 6.5.

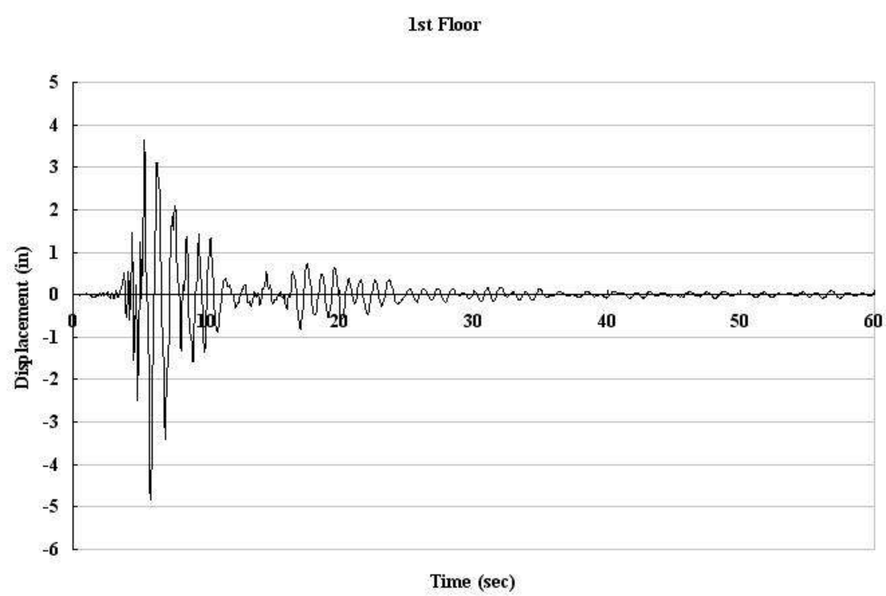

Figure 6.2 : Displacement of at 1st Floor Recorded Ground Motion at Newhall Fire Station

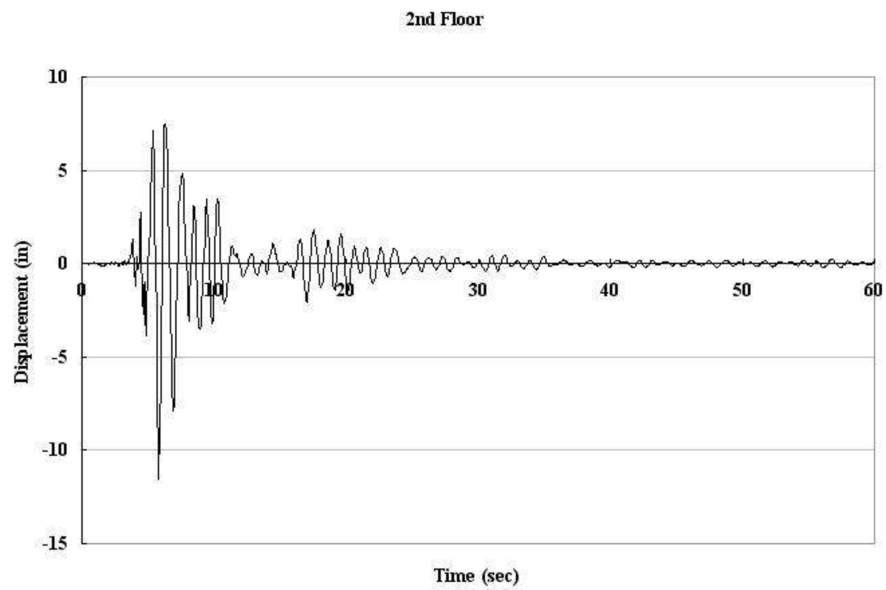

Figure 6.3 : Displacement of at 2nd Floor Recorded Ground Motion at Newhall Fire Station

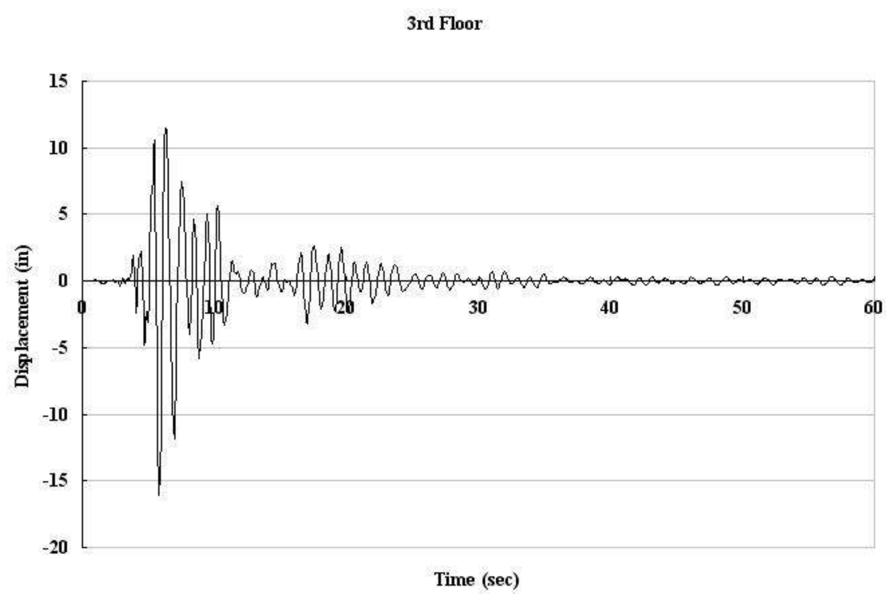

Figure 6.4 : Displacement of at 3rd Floor Recorded Ground Motion at Newhall Fire Station

Table 6.2 : Deflection of Each Floor under Northridge Earthquake

Floor	Record	Time(sec)	Max.Deflection(in)
1st	Newhall Fire Station, Northridge E.Q.	5.8	4.8
2nd	Newhall Fire Station, Northridge E.Q.	5.8	11.53
3rd	Newhall Fire Station, Northridge E.Q.	5.8	16.05

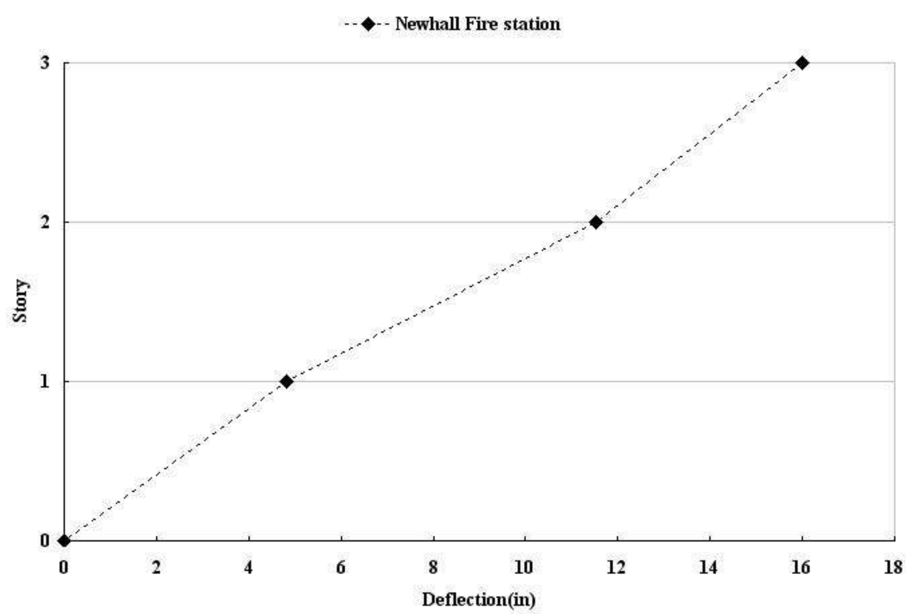

Figure 6.5 : Maximum Deflection Envelope of Each Floor under Recorded Ground Motion at Newhall Fire Station

The code limitation of drift ratio based on UBC'97 is 0.02 and the drift ratio under the ground motion is not satisfied this code limitation as shown in Figure 6.6.

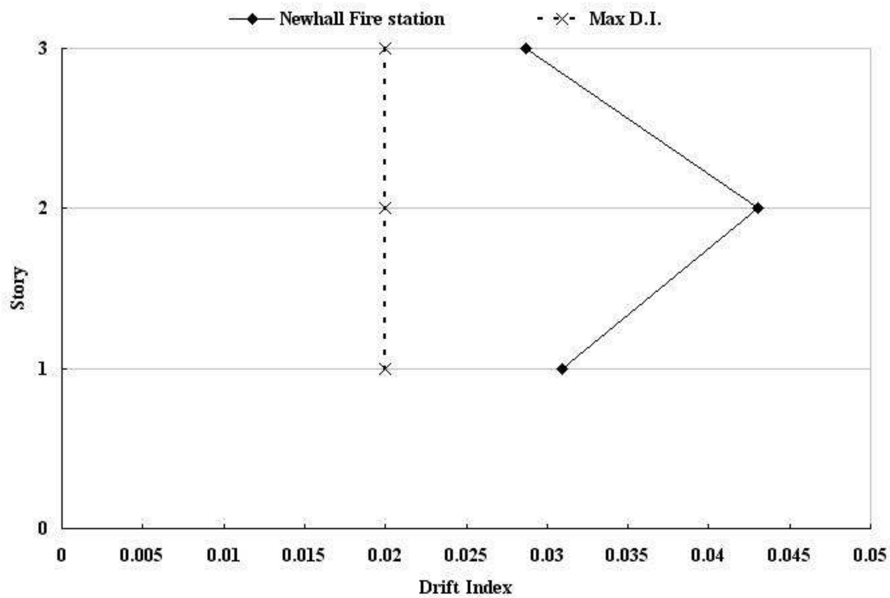

Figure 6.6 : Interstory Drift of Northridge Earthquake

The Demand/Capacity (D/C) ratio of each member is shown in Figure 6.7 – Figure 6.10 where it can be seen that a D/C ratio is over unity at column of 1st floor for the transverse frame and a D/C Ratio is also over unity at MRF frames for longitudinal direction.

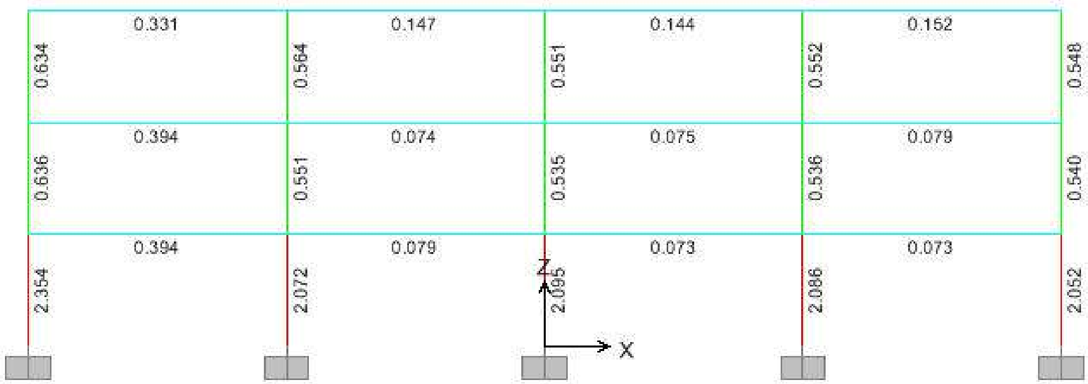

Figure 6.7 : Demand/Capacity Ratio of Transverse Direction on Newhall Fire Station

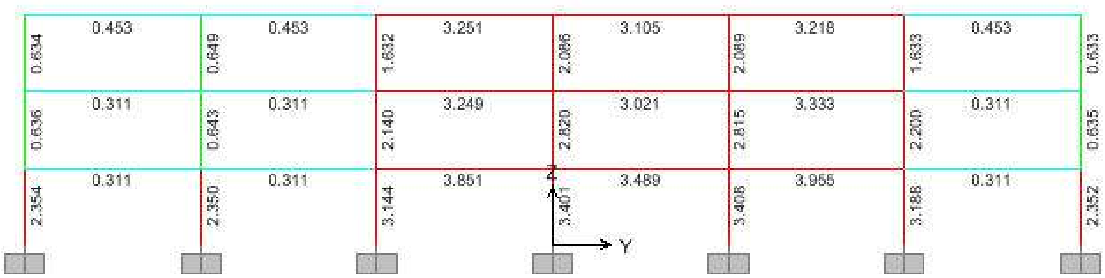

Figure 6.8 : Demand/Capacity Ratio of Longitudinal Direction on Newhall Fire Station

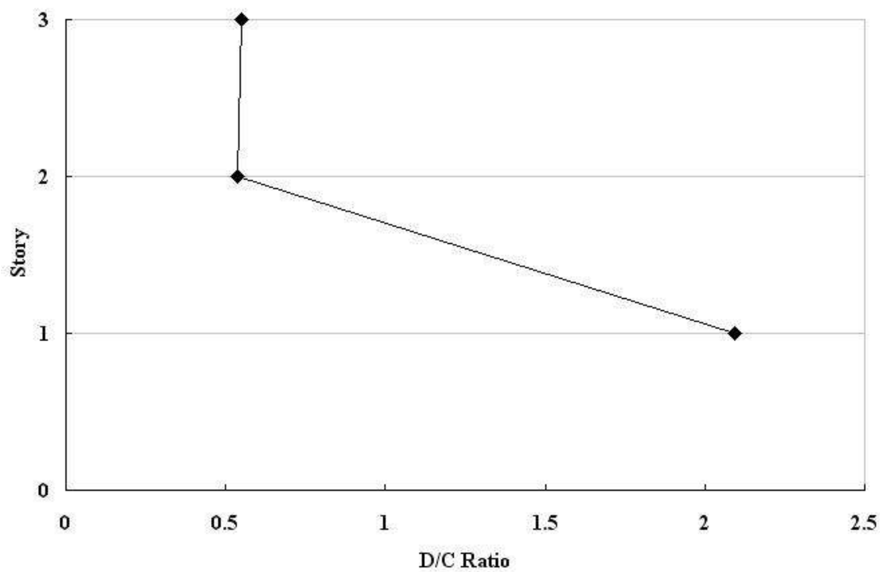

Figure 6.9 : Demand/Capacity Ratio of Newhall Fire Station (Transverse Direction)

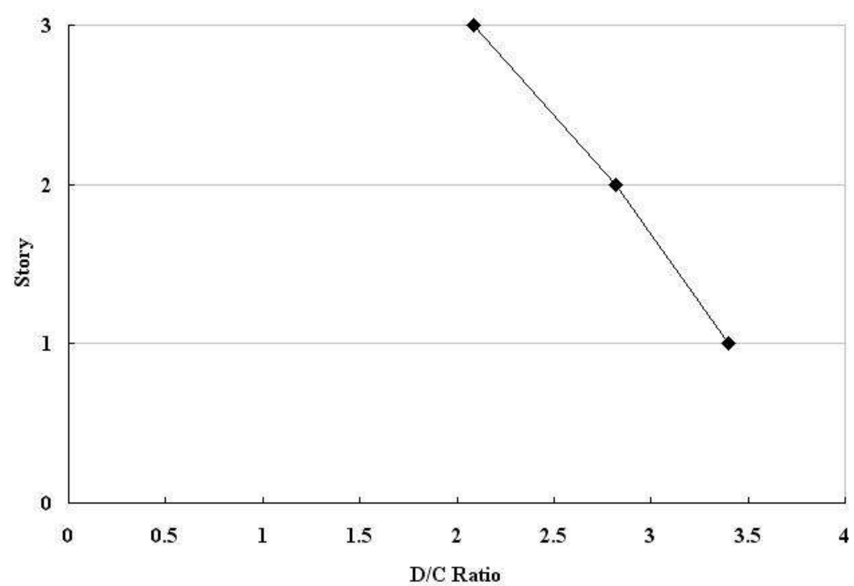

Figure 6.10 : Demand/Capacity Ratio of Newhall Fire Station (Longitudinal Direction)

6.2. Nonlinear Analyses of Three Story Building under Earthquake

6.2.1. Nonlinear Reponses of Three Story Building under Earthquake

The displacement plots at each story obtained from the nonlinear analyses are shown in Figure 6.11 – Figure 6.13. Here it can be seen the displacement has decreased to 3.8 inches at the roof and the limited cycling is occurring about a new equilibrium position in the deformed structure. The other deflections are shown in Table 6.3. In addition, maximum deflection envelope of each floor under recorded ground motion is also shown in Figure 6.14.

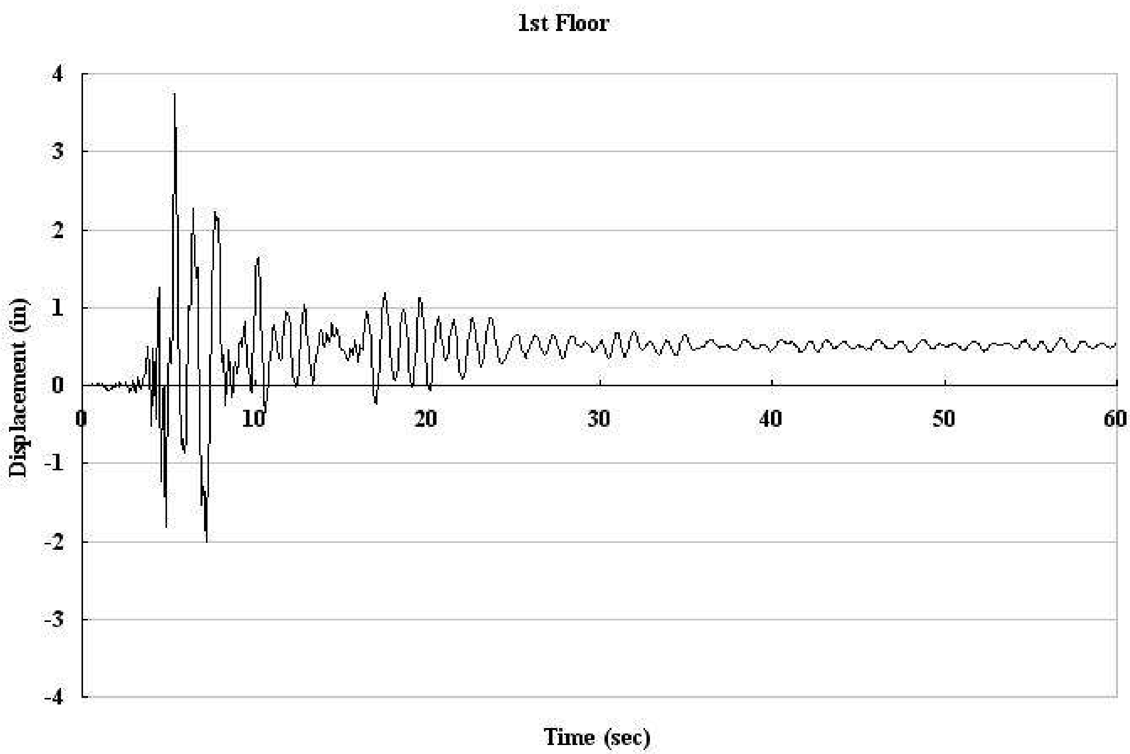

Figure 6.11 : Displacement of at 1st Floor Recorded Ground Motion at Newhall Fire Station

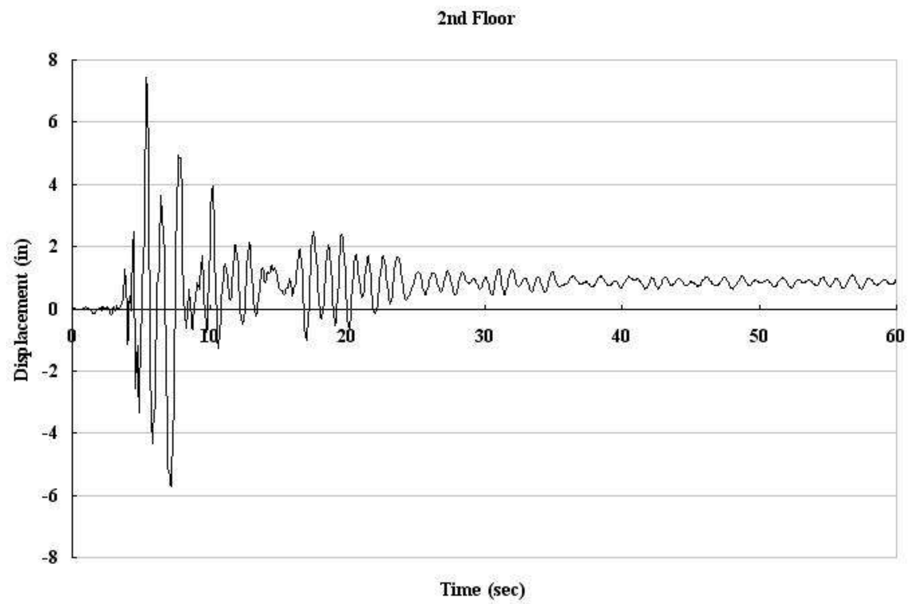

Figure 6.12 : Displacement of at 2nd Floor Recorded Ground Motion at Newhall Fire Station

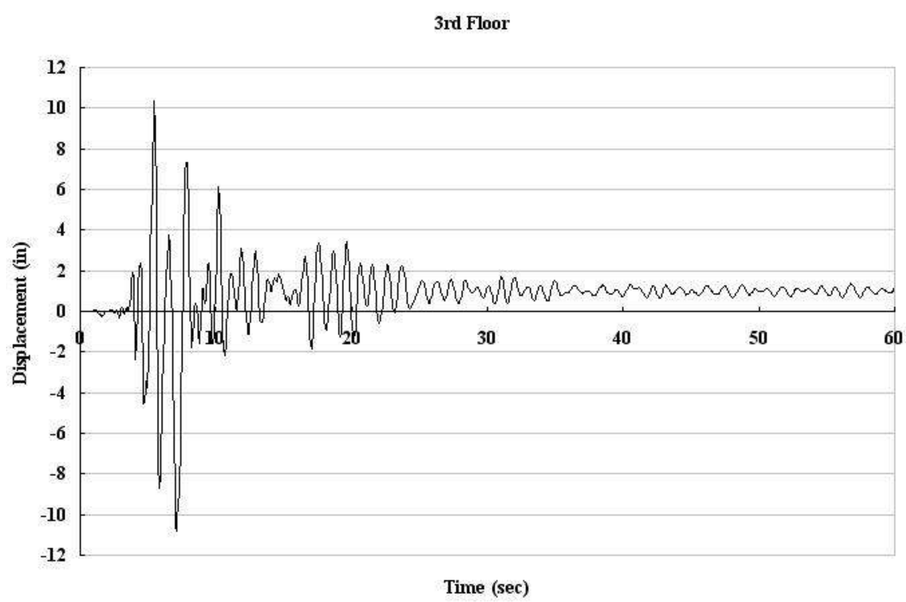

Figure 6.13 : Displacement of at 3rd Floor Recorded Ground Motion at Newhall Fire Station

Table 6.3 : Deflection of Each Floor under Northridge Earthquake

Floor	Record	Time(sec)	Max.Deflection(in)
1st	Newhall Fire Station, Northridge E.Q.	5.4	3.75
2nd	Newhall Fire Station, Northridge E.Q.	5.4	7.45
3rd	Newhall Fire Station, Northridge E.Q.	5.4	10.34

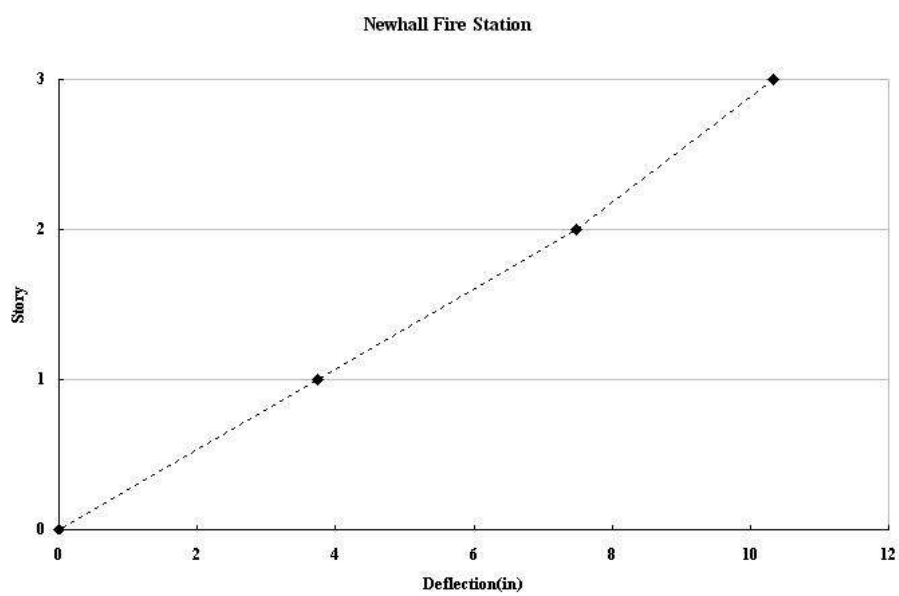

Figure 6.14 : Maximum Deflection Envelope of Each Floor under Recorded Ground Motion at Newhall Fire Station

An important parameter in earthquake resistant design is the interstory drift index that is obtained by dividing the maximum relative story displacement by the story height. The UBC requires that for structures having a period greater than 0.7 seconds the interstory drift be limited to 0.02. The graph shown in Figure 6.15 indicates that the drift is above limiting value at the first and 2nd floor.

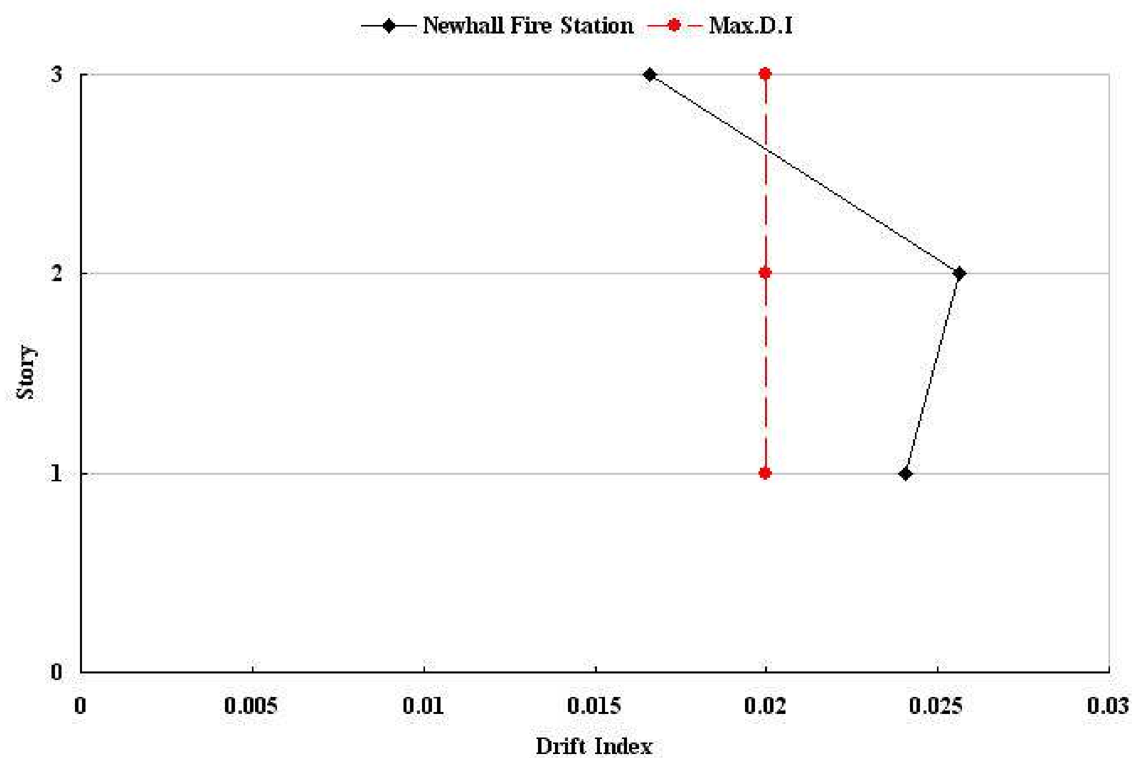

Figure 6.15 : Interstory Drift of Northridge Earthquake

The Demand/Capacity (D/C) ratio of each member is shown in Figure 6.16 – Figure 6.19 where it can be seen that a D/C ratio of the column and girder at the 2nd floor and roof is under unity at the transverse frame but MRF frame for longitudinal direction is still over unity.

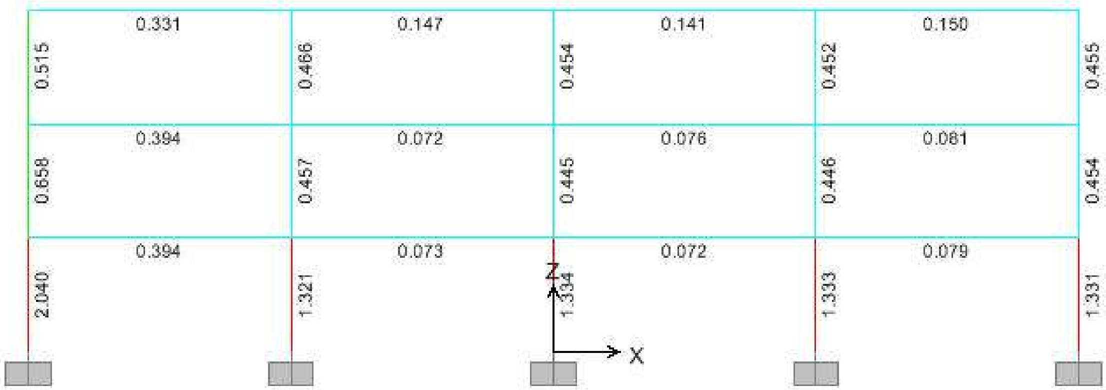

Figure 6.16 : Demand/Capacity Ratio of Transverse Direction under Recorded Ground Motion at Newhall Fire Station

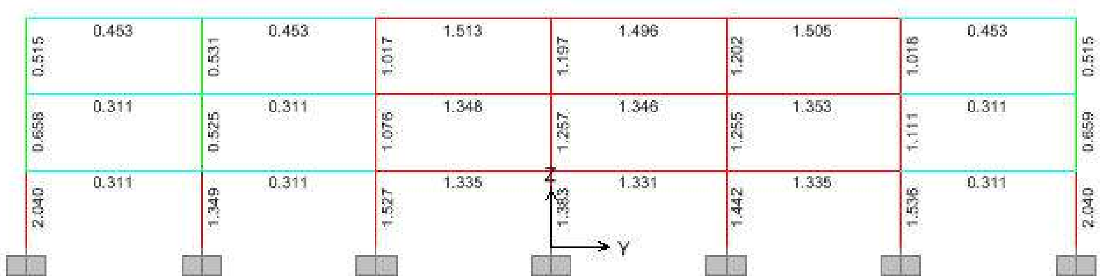

Figure 6.17 : Demand/Capacity Ratio of Longitudinal Direction under Recorded Ground Motion at Newhall Fire Station

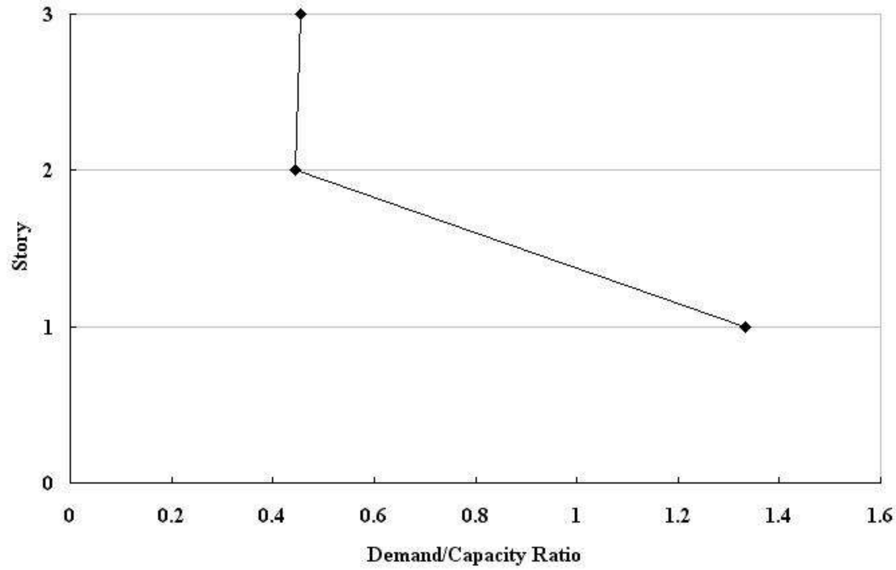

Figure 6.18 : Demand/Capacity Ratio under Recorded Ground Motion at Newhall Fire Station (Transverse Direction)

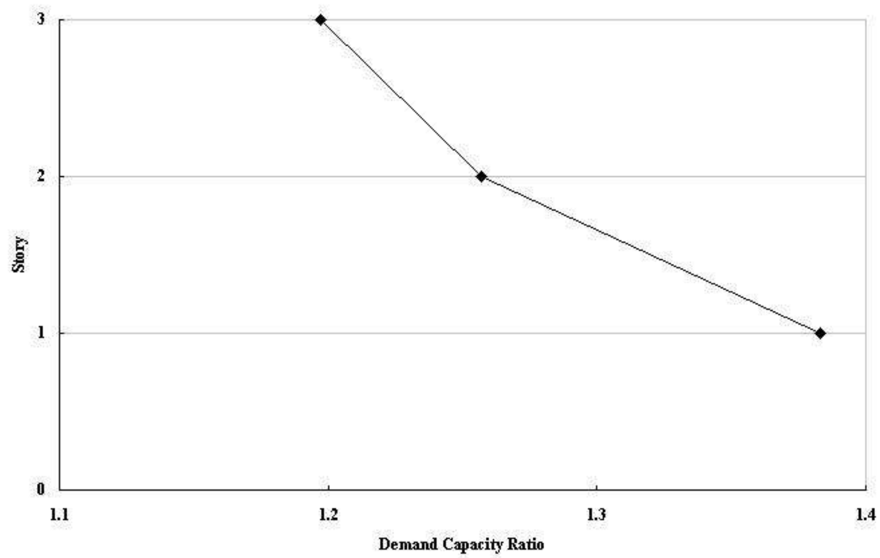

Figure 6.19 : Demand/Capacity Ratio under Recorded Ground Motion at Newhall Fire Station (Longitudinal Direction)

6.2.2. Nonlinear Plastic Hinge Behavior of Three Story Building

The default plastic hinge properties in SAP2000 are also used for the analyses as shown in chapter 4.4.2. These properties are based on the recommendations made in FEMA-273 for steel moment hinges. The moment-rotation curve that gives the yield value and the plastic deformation following yield is shown in Figure 6.20. It should be noted that point IO represents immediate occupancy, LS indicates life safety and CP means collapse prevention. Only the plastic deformation is indicted by the hinge. The hinge parameters are summarized in Figure 4.64 and Table 6.4 along with the FEMA condition assessment. To calculate the yield rotation, θ_y, is used from FEMA 356 equations as shown in chapter 4.4.2.

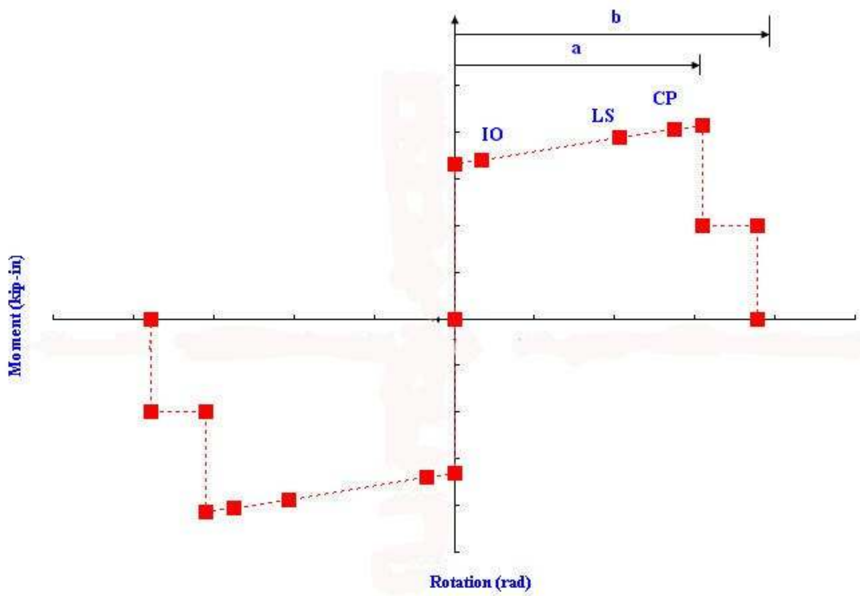

Figure 6.20 : Criteria of Plastic Hinge Behavior

Table 6.4 : Modeling Parameter and Acceptance Criteria for Nonlinear Procedures

Component	Modeling Parameter		Acceptance Parameter		
	Plastic Rotation Angle (radians)		Plastic Rotation Angle (radians)		
	a	b	IO	LS	CP
Beams & Columns	$9\theta_y$	$11\theta_y$	$1\theta_y$	$6\theta_y$	$8\theta_y$

For reference, the member locations and identification numbers are shown in Figure 4.65 and Figure 4.66 for typical transverse and longitudinal frames. The plastic rotation demands in critical members of the transverse and longitudinal frame are summarized in Figure 6.21.

Demands for the earthquake ground motion recorded at the Newhall Fire Station are summarized in Figure 6.21. It is shown that the beams that exceed the elastic limit are nonlinear with plastic rotation demands along longitudinal directions as shown in Figure 6.21. The behaviors of the transverse columns are nonlinear and similar behaviors can be seen on MRF frames through longitudinal direction. According to the FEMA recommendations, this building would be cleared Life Safety (LS).

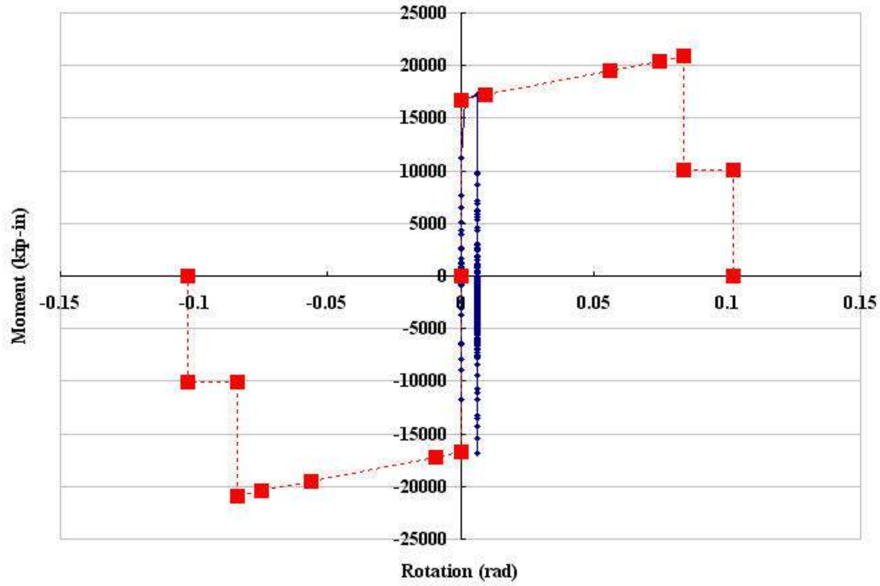

(a) Moment-Rotation Relationship on Transverse Direction (Column 43)

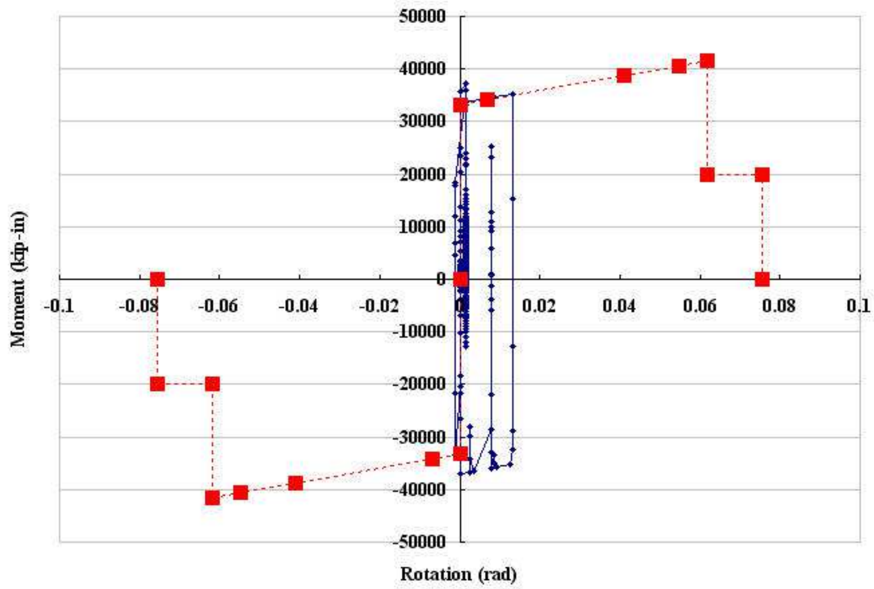

(b) Moment-Rotation Relationship on Longitudinal Direction (Column 10)

Figure 6.21 : Moment-Rotation Relation under Recorded Ground Motion at Newhall Fire Station

“Figure 6.21 : Continued”

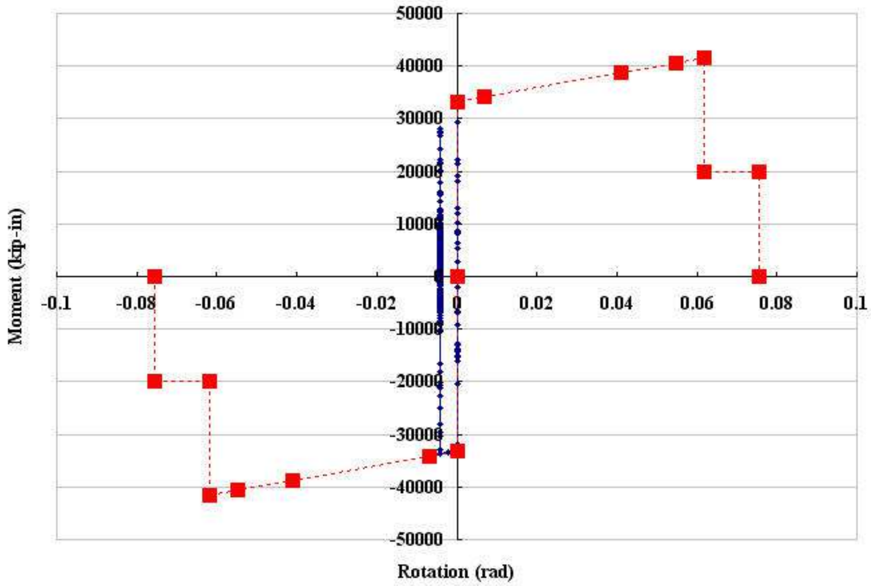

(c) Moment-Rotation Relationship on Longitudinal Direction (Column 11)

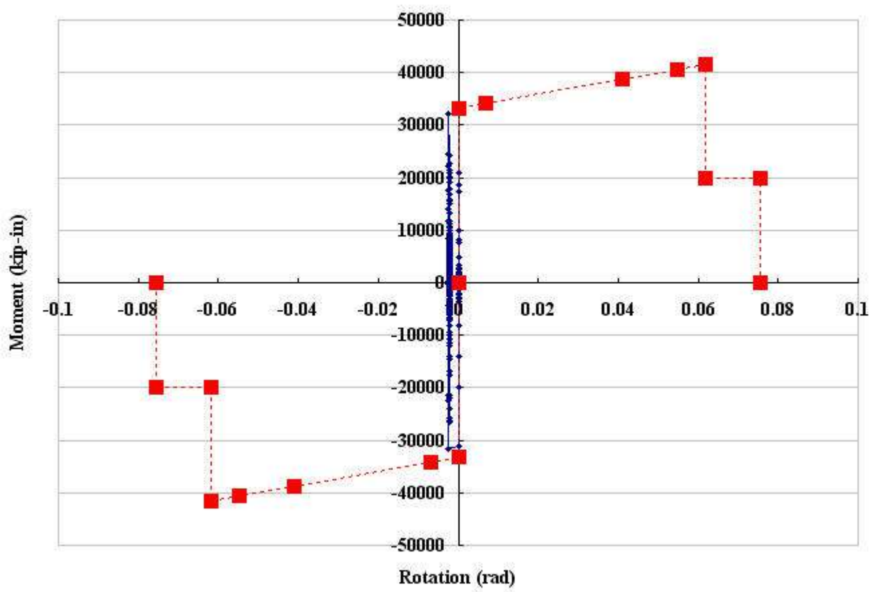

(d) Moment-Rotation Relationship on Longitudinal Direction (Column 12)

"Figure 6.21 : Continued"

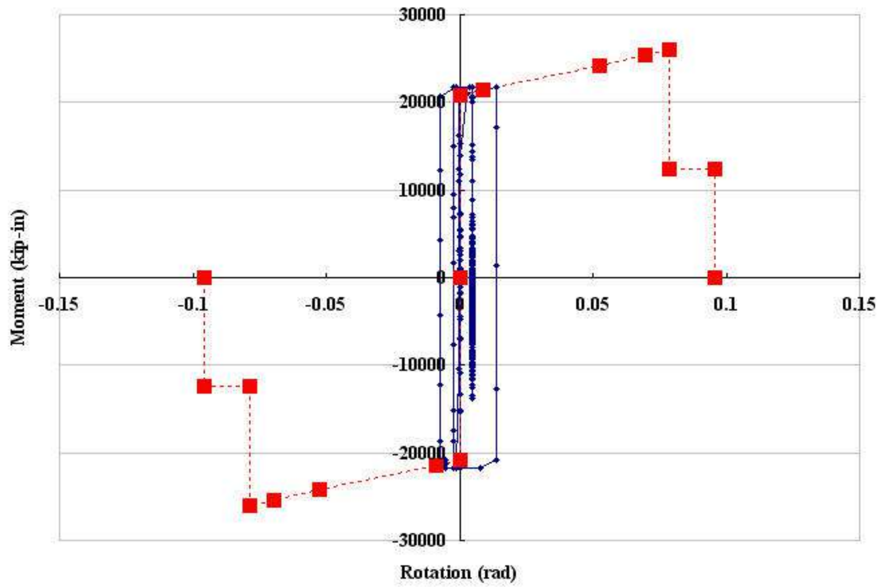

(e) Moment-Rotation Relationship on Longitudinal Direction (Beam 196)

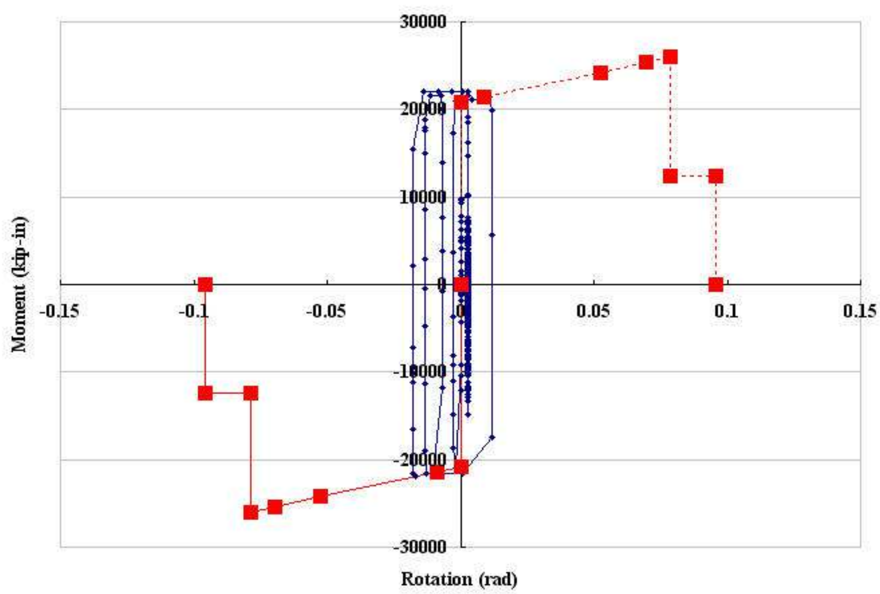

(f) Moment-Rotation Relationship on Longitudinal Direction (Beam 197)

"Figure 6.21 : Continued"

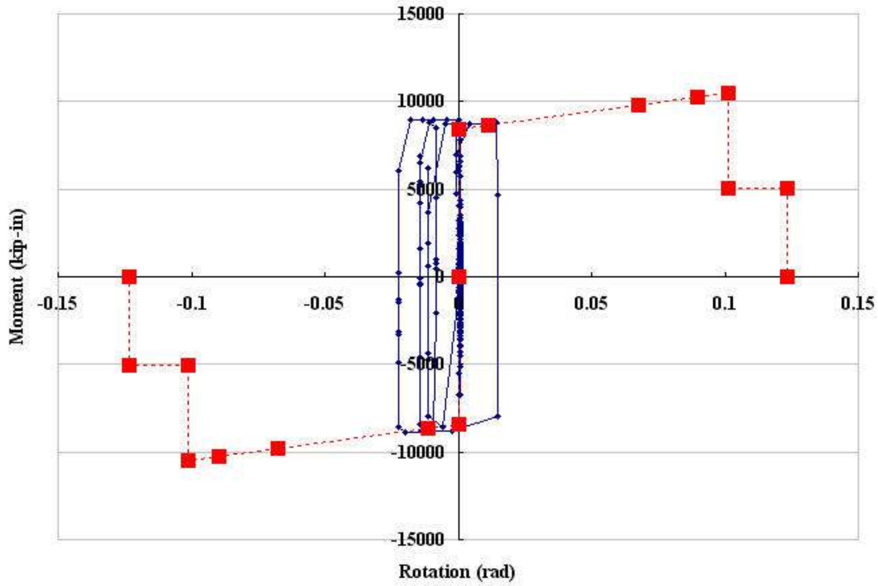

(g) Moment-Rotation Relationship on Longitudinal Direction (Beam 198)

6.3. Linear Analyses of Ten Story Building under Earthquake

In this chapter, similar approach of three story building is applied for ten story building. Using SAP2000 FEM software is also used for linear analyses. The maximum roof displacement is 16.34 in. at 9.8 sec. for Newhall Fire Station ground motion from the time histories shown in Figure 6.22 – Figure 6.25 and shown in Table 6.5

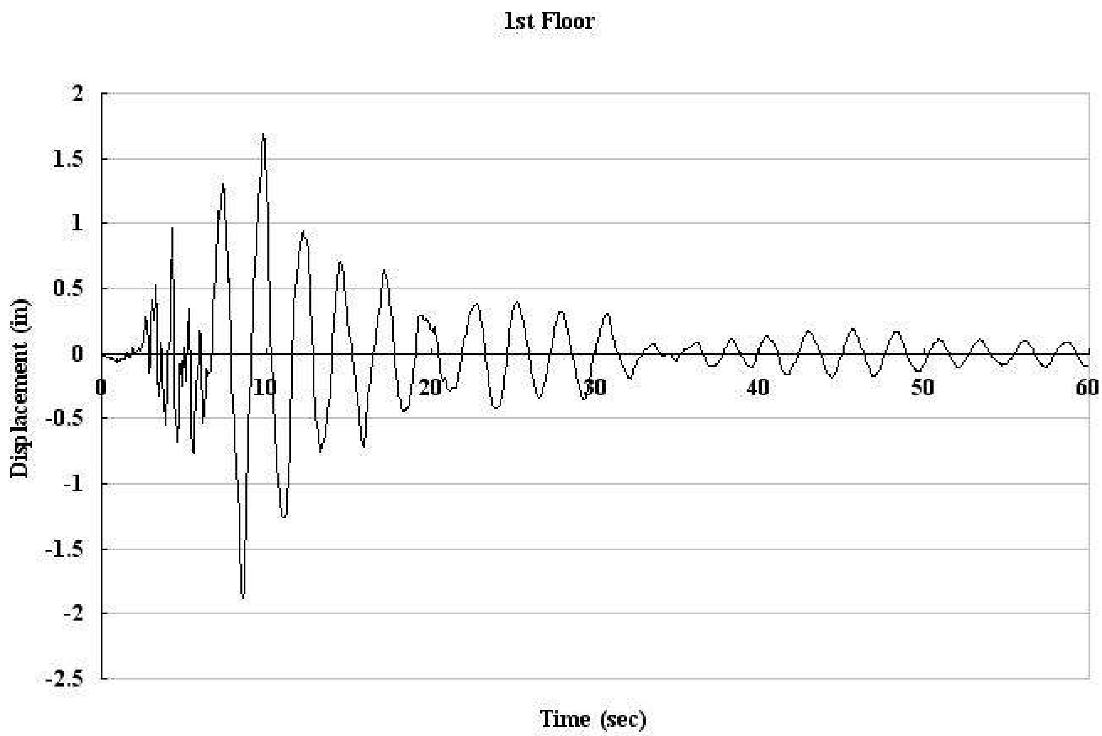

Figure 6.22 : Displacement of at 1st Floor Recorded Ground Motion at Newhall Fire Station

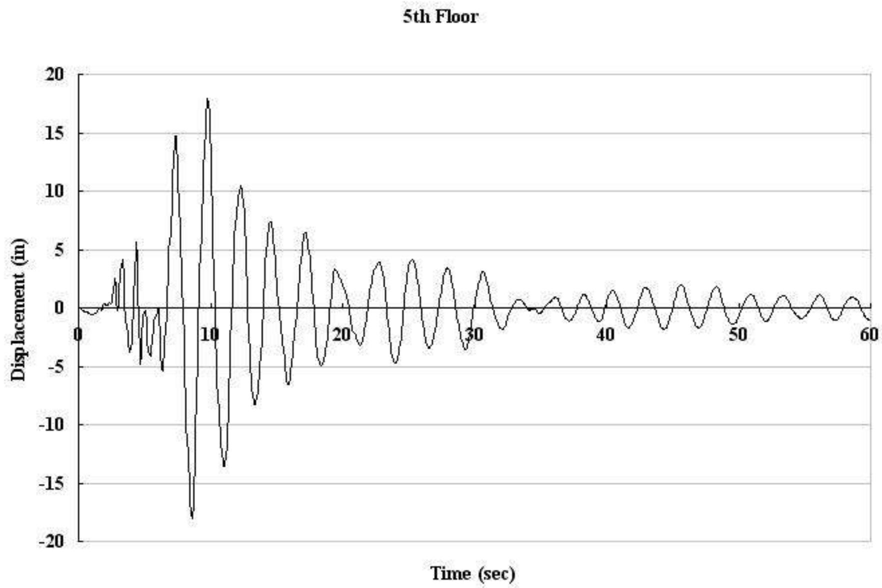

Figure 6.23 : Displacement of at 5th Floor Recorded Ground Motion at Newhall Fire Station

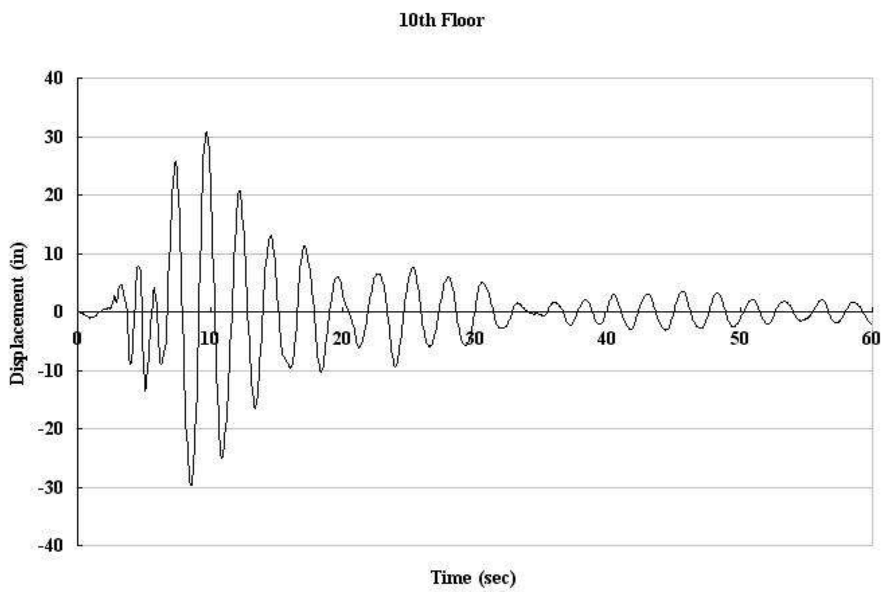

Figure 6.24 : Displacement of at 10th Floor Recorded Ground Motion at Newhall Fire Station

Table 6.5 : Deflection of Each Floor under Northridge Earthquake

Floor	Record	Time(sec)	Max.Deflection (in)
1st	Newhall Fire Station, Northridge E.Q.	8.6	1.87
5^{th}	Newhall Fire Station, Northridge E.Q.	8.6	18.06
10^{th}	Newhall Fire Station, Northridge E.Q.	8.6	30.2

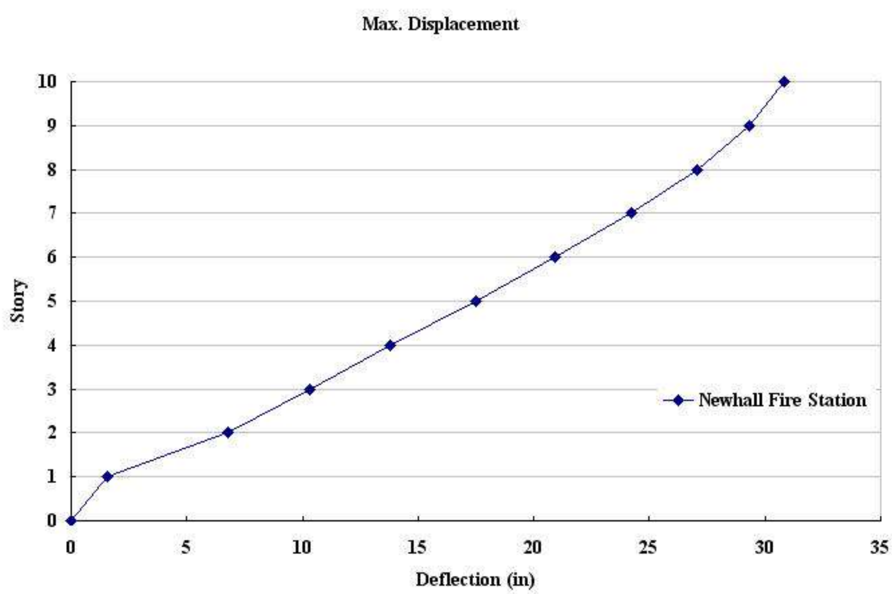

Figure 6.25 : Maximum Deflection Envelope of Each Floor under Northridge Earthquake

The code limitation of drift ratio based on UBC'97 is 0.02 and the responses through 2nd floor and 7th floor of the ground motion is not satisfied this code limitation as shown in Figure 6.26.

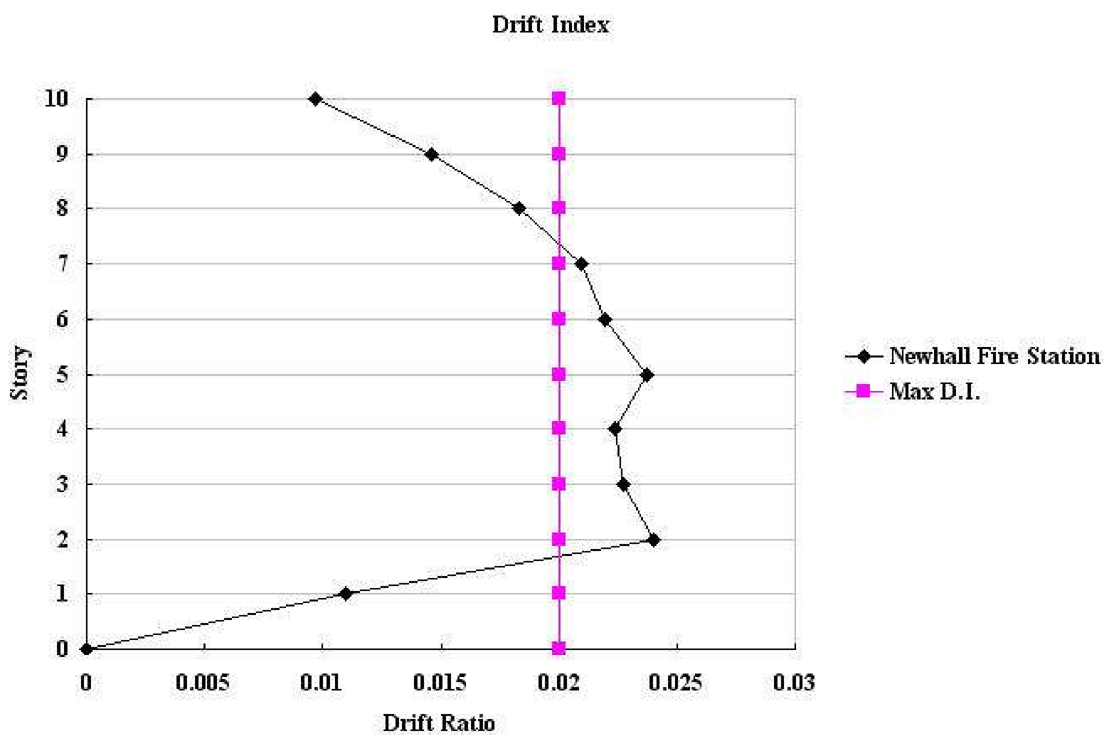

Figure 6.26 : Interstory Drift of Northridge Earthquake

The Demand/Capacity (D/C) ratio of each member is shown in Figure 6.27 – Figure 6.30 where it can be seen that a D/C of transverse direction and longitudinal direction is less than unity but MRF frames through longitudinal direction indicating inelastic behavior.

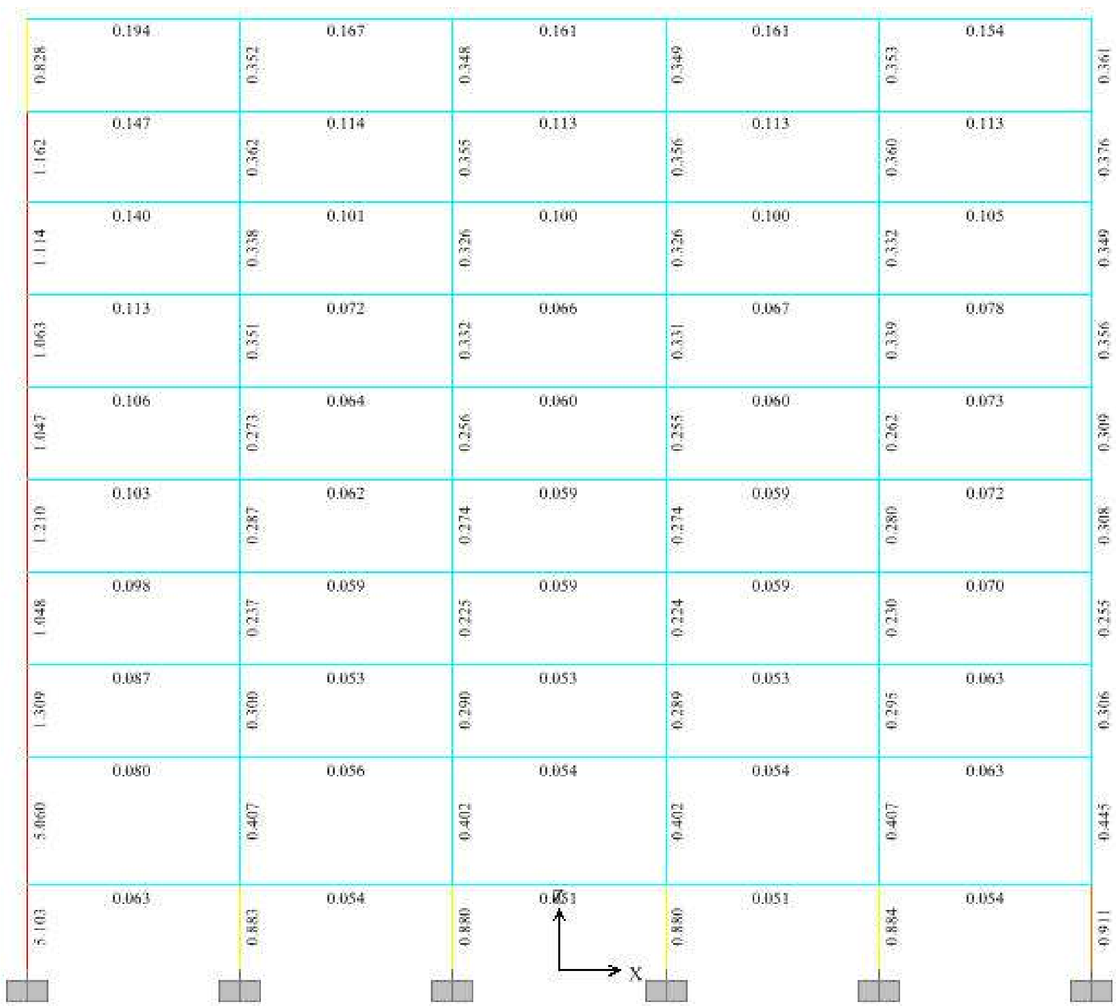

Figure 6.27 : Demand/Capacity Ratio of Transverse Direction under Recorded Ground Motion at Newhall Fire Station

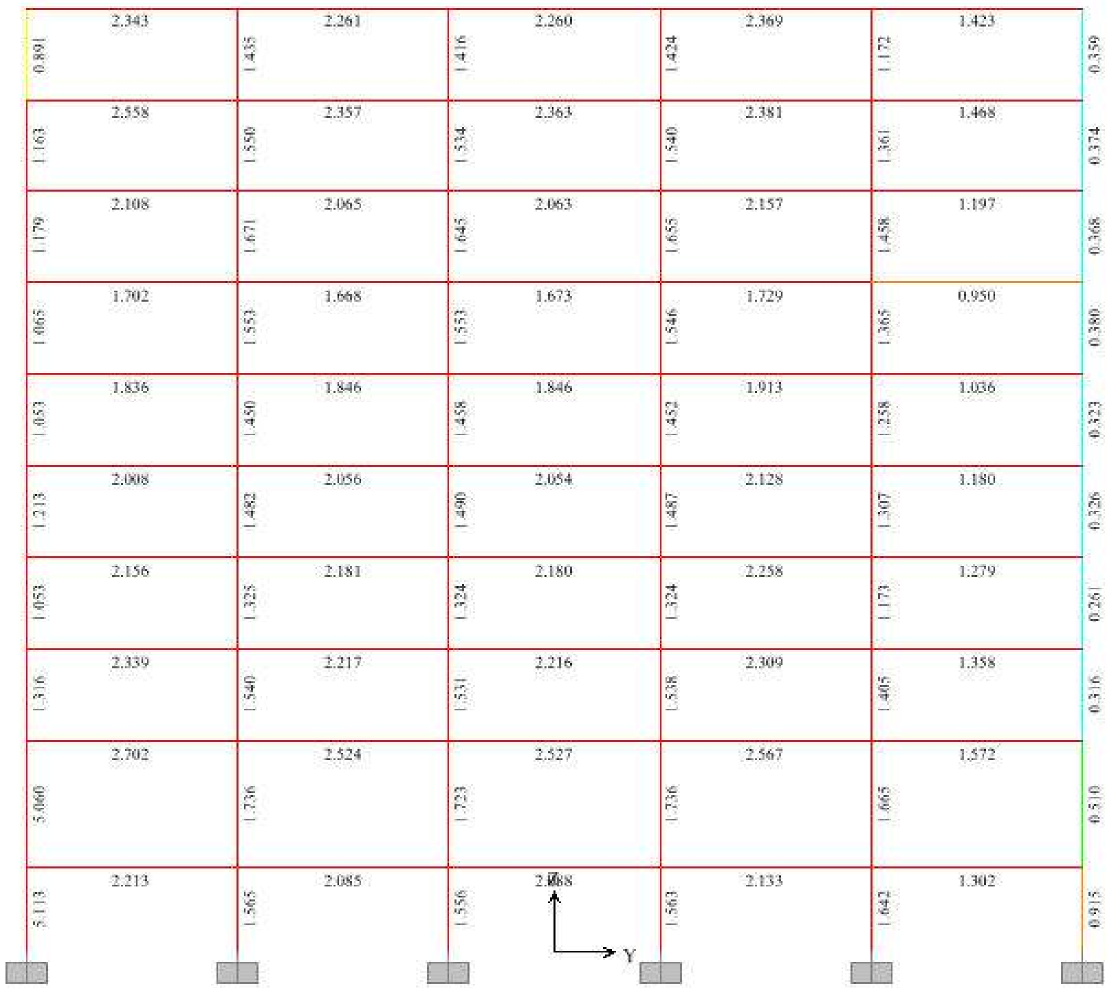

Figure 6.28 : Demand/Capacity Ratio of Longitudinal Direction under Recorded Ground Motion at Newhall Fire Station

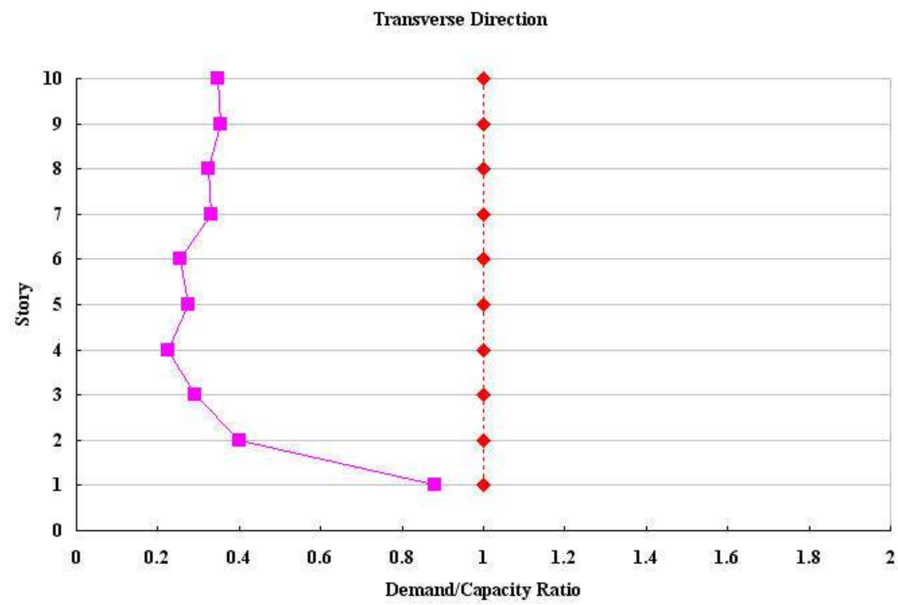

Figure 6.29 : Demand/Capacity Ratio under Recorded Ground Motion at Newhall Fire Station (Transverse Direction)

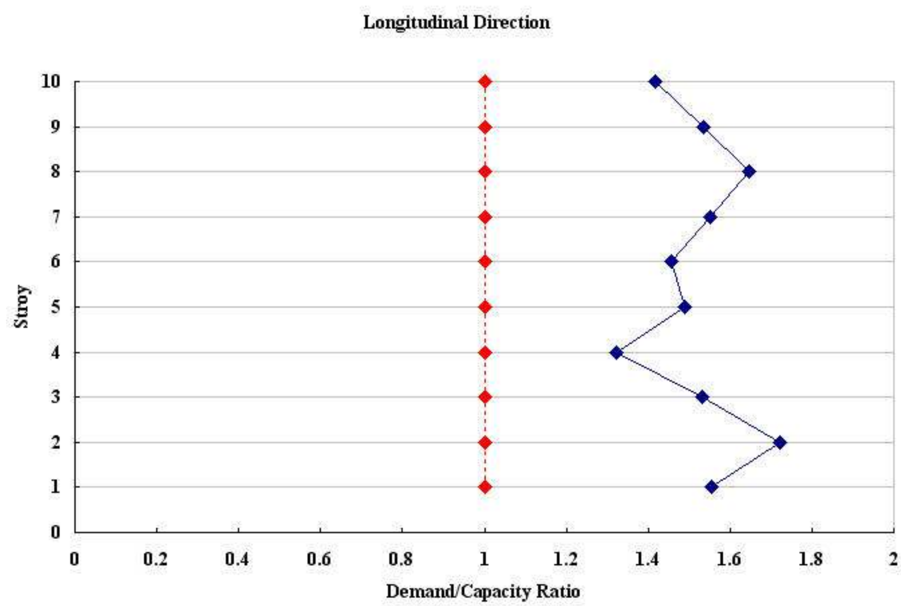

Figure 6.30 : Demand/Capacity Ratio under Recorded Ground Motion at Newhall Fire Station (Longitudinal Direction)

6.4. Nonlinear Analyses of Ten Story Building under Earthquake

6.4.1. Nonlinear Reponses of Ten Story Building under Earthquake

The displacement plots at each story obtained from the nonlinear analyses are shown in Figure 6.31– Figure 6.33. Here it can be seen the displacement has decreased to 25.04 inches at the roof. The other deflections are shown in Table 6.6. In addition, maximum deflection envelope of each floor under recorded ground motion is also shown in Figure 6.34

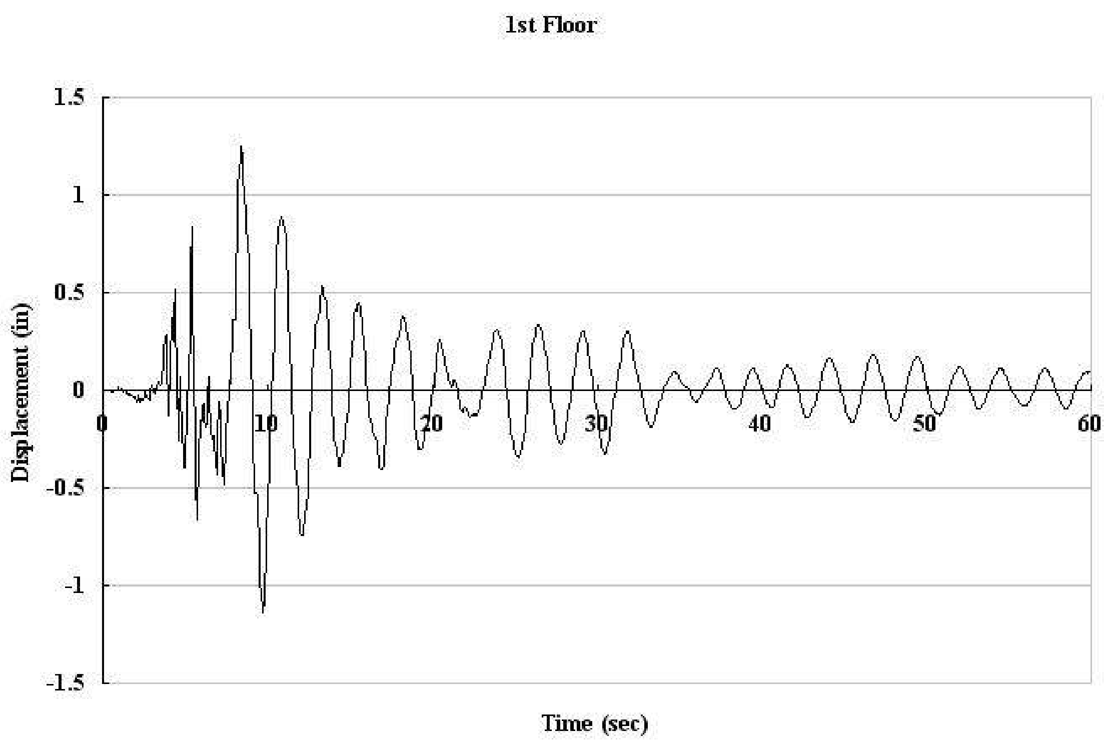

Figure 6.31 : Displacement of at 1st Floor Recorded Ground Motion at Newhall Fire Station

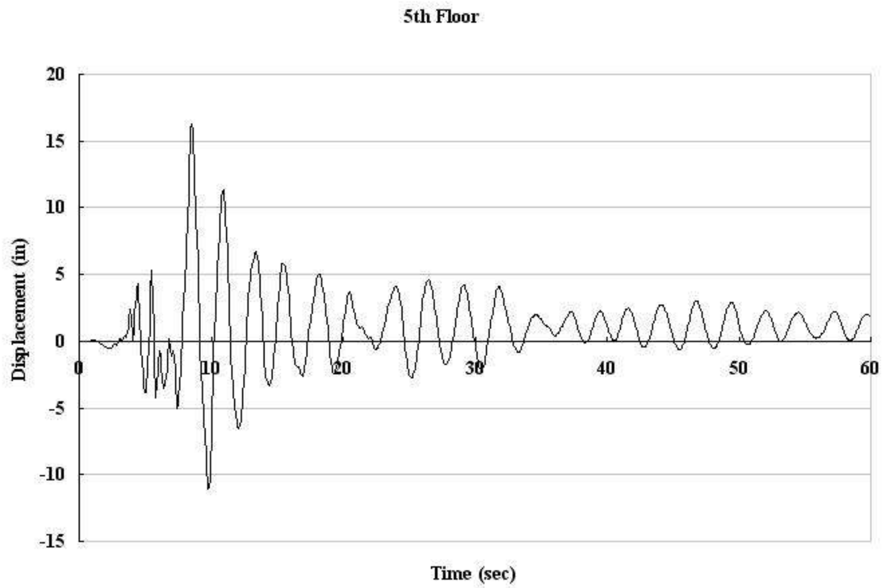

Figure 6.32 : Displacement of at 5th Floor Recorded Ground Motion at Newhall Fire Station

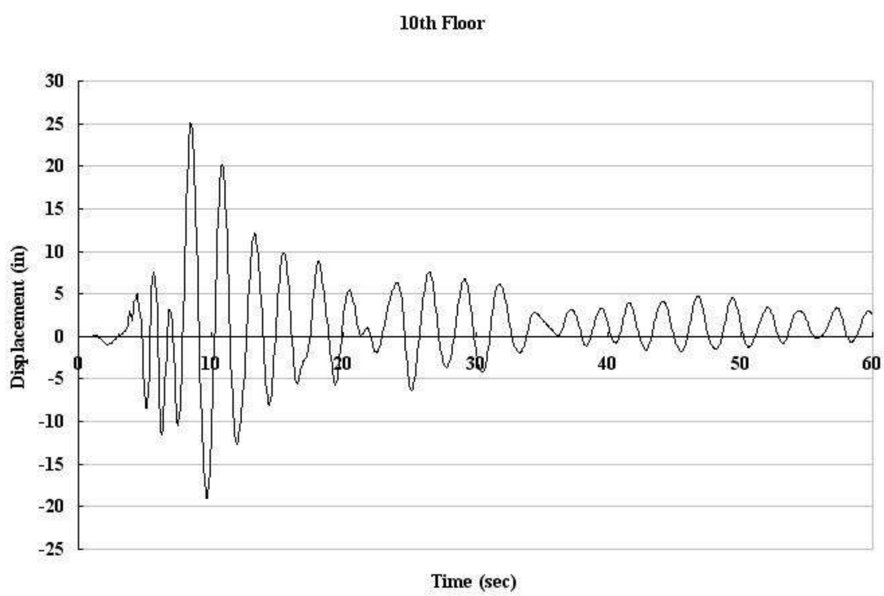

Figure 6.33 : Displacement of at 10th Floor Recorded Ground Motion at Newhall Fire Station

Table 6.6 : Deflection of Each Floor under Northridge Earthquake

Floor	Record	Time(sec)	Max.Deflection (in)
1st	Newhall Fire Station, Northridge E.Q.	8.5	1.25
5th	Newhall Fire Station, Northridge E.Q.	8.5	16.24
10th	Newhall Fire Station, Northridge E.Q.	8.5	25.04

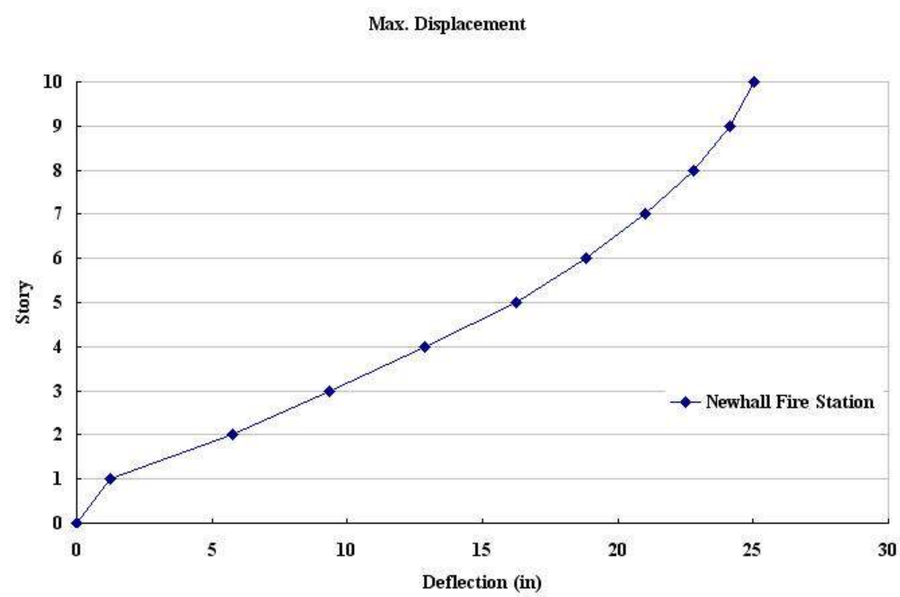

Figure 6.34 : Maximum Deflection Envelope of Each Floor under Northridge Earthquake

The code limitation of drift ratio based on UBC'97 is 0.02 and the responses through 2^{nd} floor and 5^{th} floor of the ground motion is not satisfied this constraint as shown in Figure 6.35

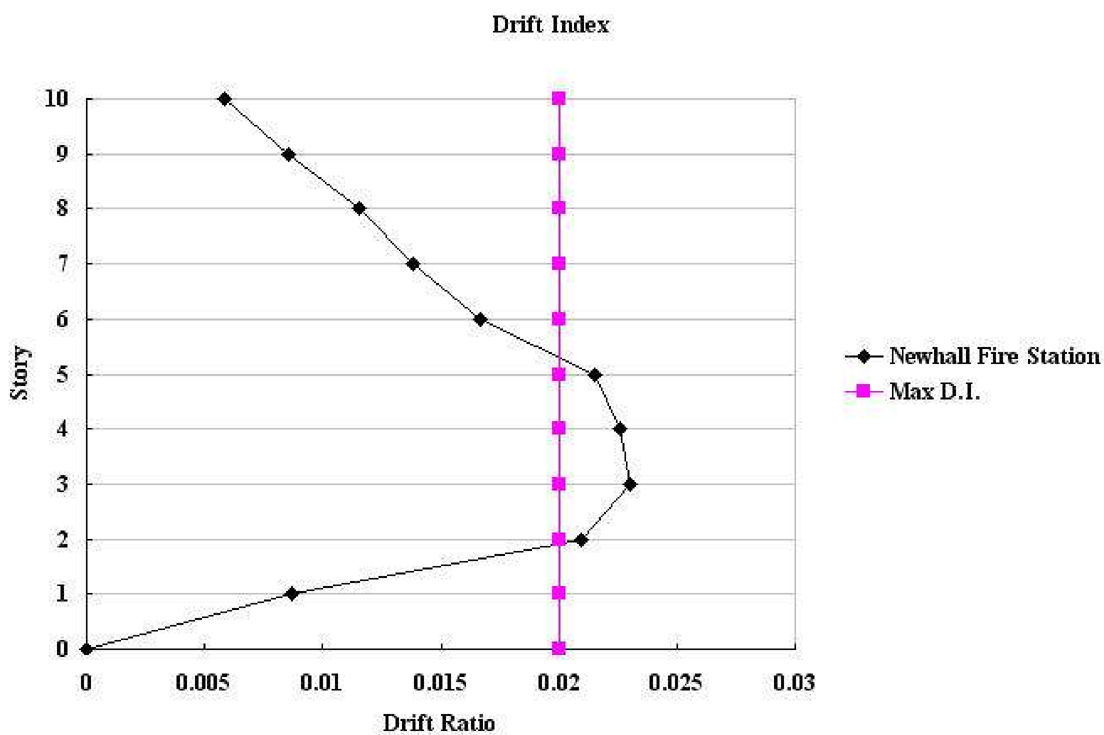

Figure 6.35 : Interstory Drift of Northridge Earthquake

The Demand/Capacity (D/C) ratio of each member is shown in Figure 6.36 - Figure 6.39 where it can be seen that a D/C of transverse direction and longitudinal direction is less than unity but girders of MRF through longitudinal direction indicating inelastic behavior.

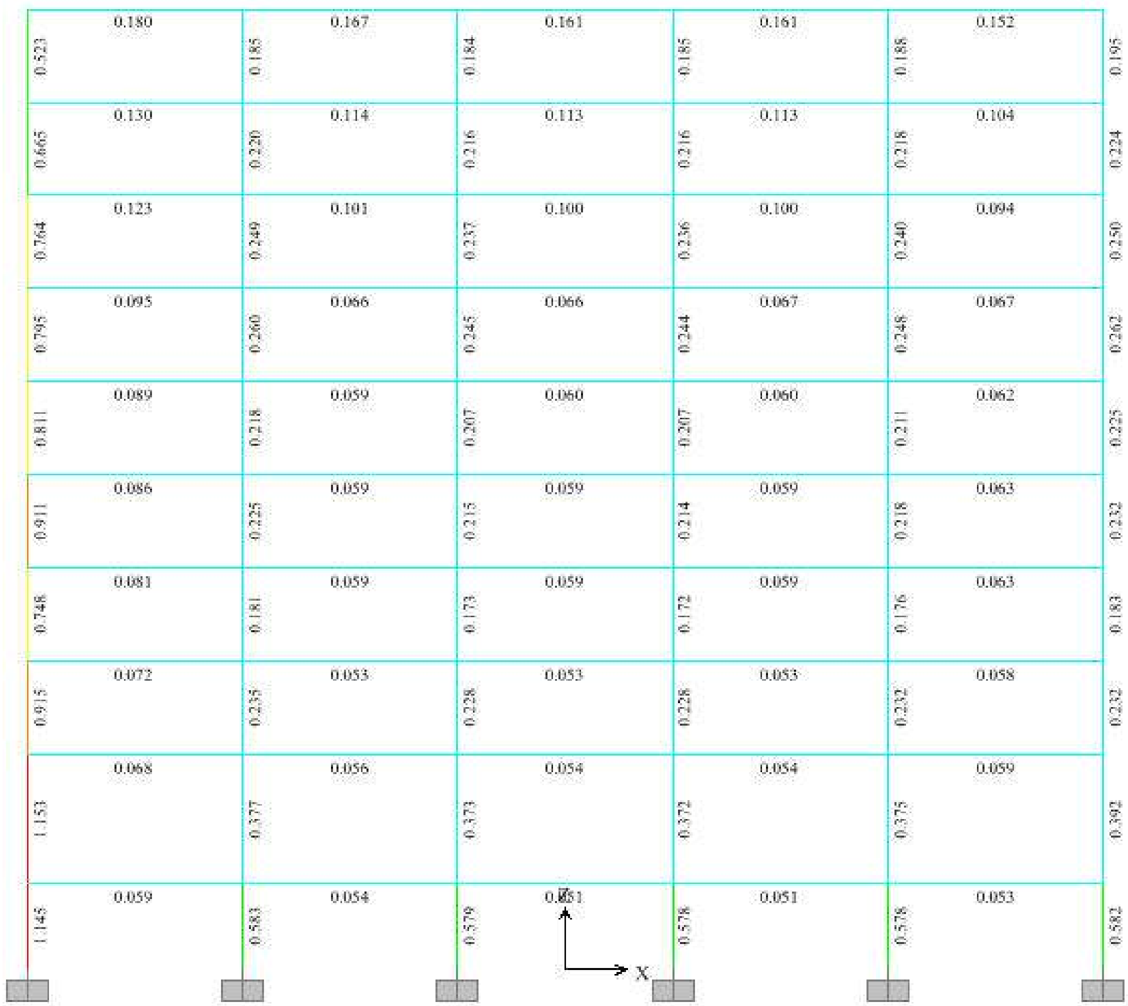

Figure 6.36 : Demand/Capacity Ratio of Transverse Direction under Recorded Ground Motion at Newhall Fire Station

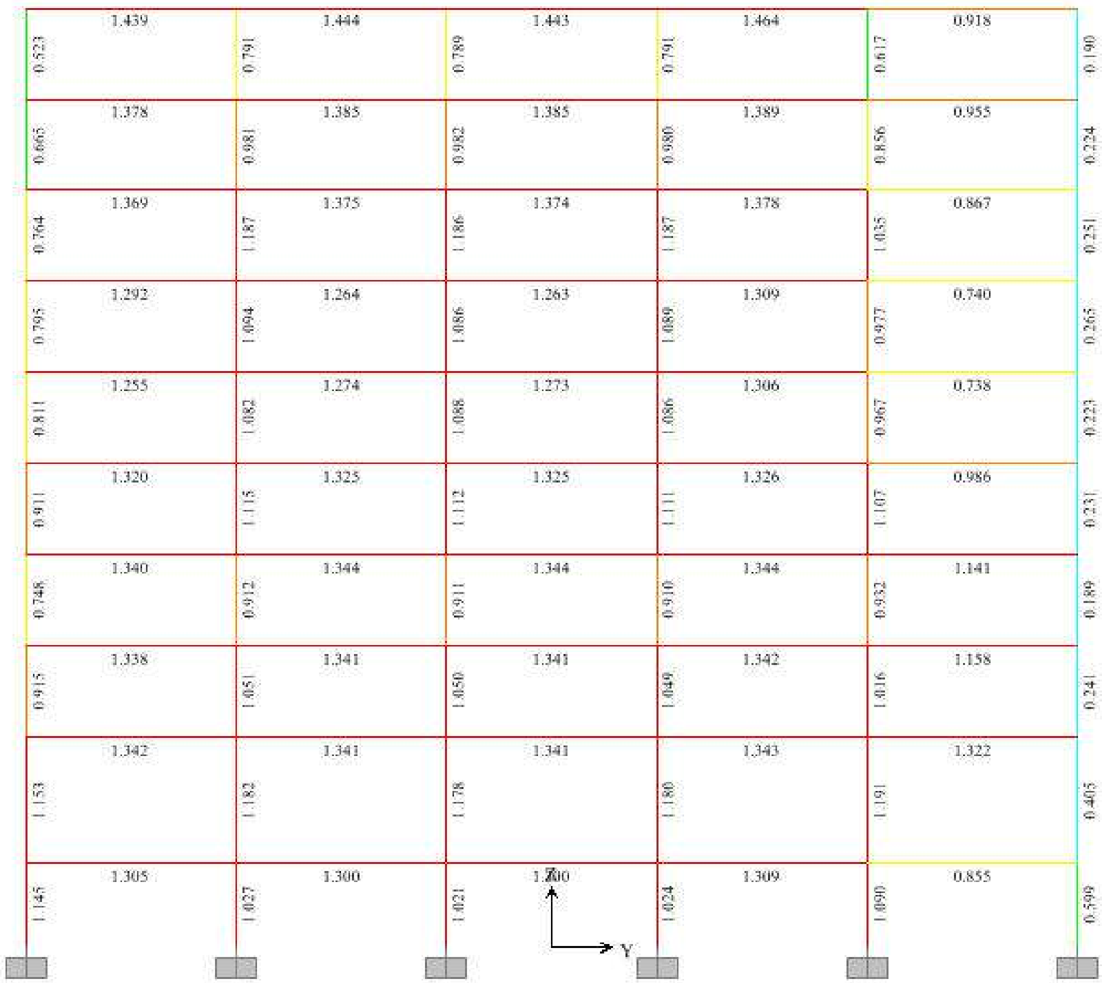

Figure 6.37 : Demand/Capacity Ratio of Longitudinal Direction under Recorded Ground Motion at Newhall Fire Station

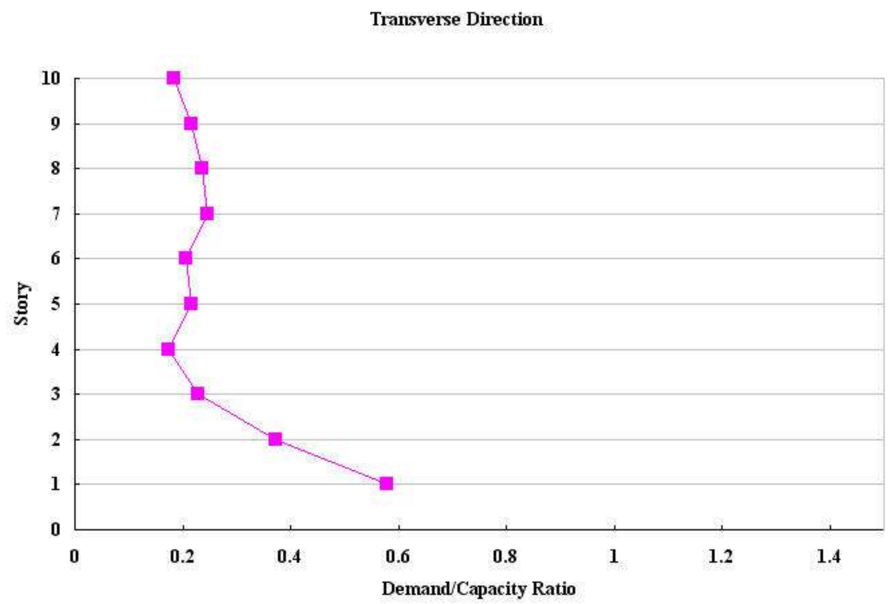

Figure 6.38 : Demand/Capacity Ratio under Recorded Ground Motion at Newhall Fire Station (Transverse Direction)

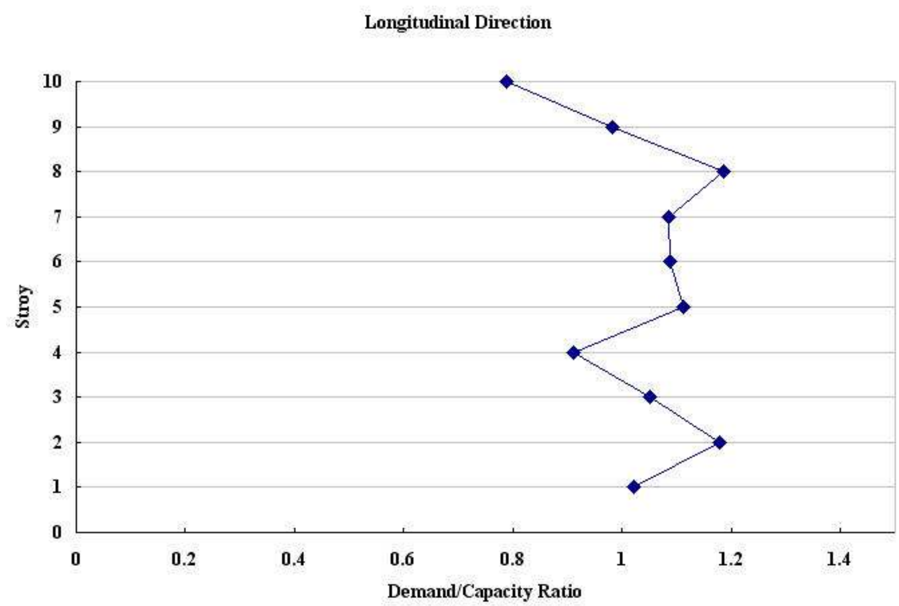

Figure 6.39 : Demand/Capacity Ratio under Recorded Ground Motion at Newhall Fire Station (Longitudinal Direction)

6.4.2. Nonlinear Plastic Hinge Behavior of Ten Story Building

The default plastic hinge properties in SAP2000 are used for nonlinear analyses. These properties are based on the recommendations made in FEMA-273 for steel moment hinges. The moment-rotation curve that gives the yield value and the plastic deformation following yield is shown in chapter 4.4. The hinge parameters are summarized in chapter 4.4 along with the FEMA condition assessment. To calculate the yield rotation, θy, is also used from FEMA 356 equations as shown in chapter 4.4.

The critical members are selected using nonlinear analysis such as one column of 1^{st} floor along transverse direction, one column and two beams along longitudinal direction at 1^{st} floor and roof. The plastic rotation demands in critical members of the transverse and longitudinal frame are summarized in Figure 6.40. The rotation demands of columns in both directions are in elastic range but girders in longitudinal direction are weakly nonlinear behavior in immediate occupancy (IO).

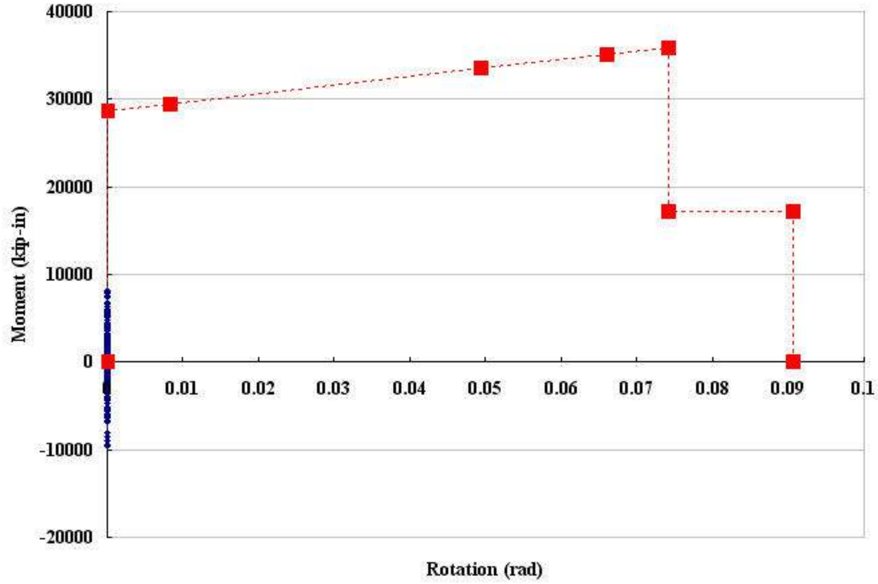

(a) Moment-Rotation Relationship on Transverse Direction (Column 121)

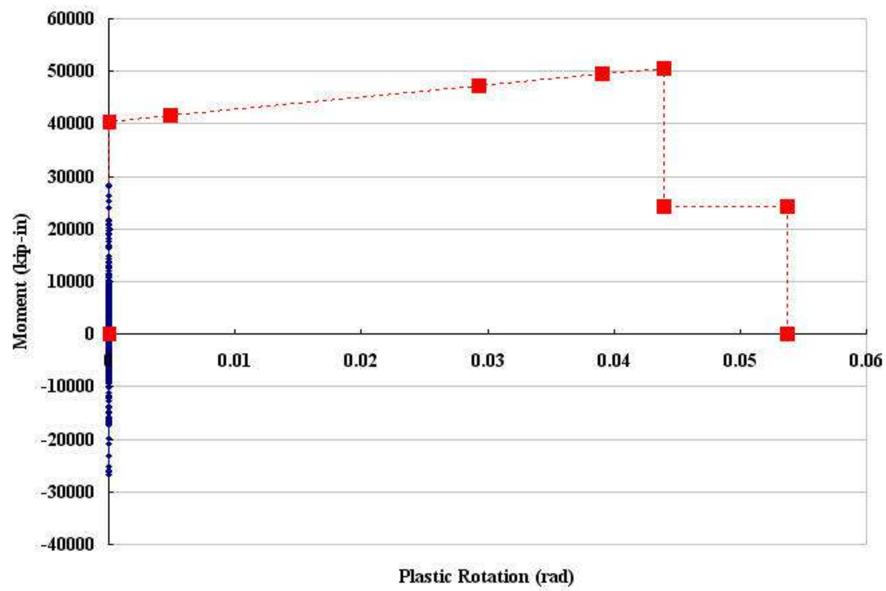

(b) Moment-Rotation Relationship on Longitudinal Direction (Column 1)

Figure 6.40 : Moment-Rotation Relation under Recorded Ground Motion at Newhall Fire Station

“Figure 6.40 : Continued”

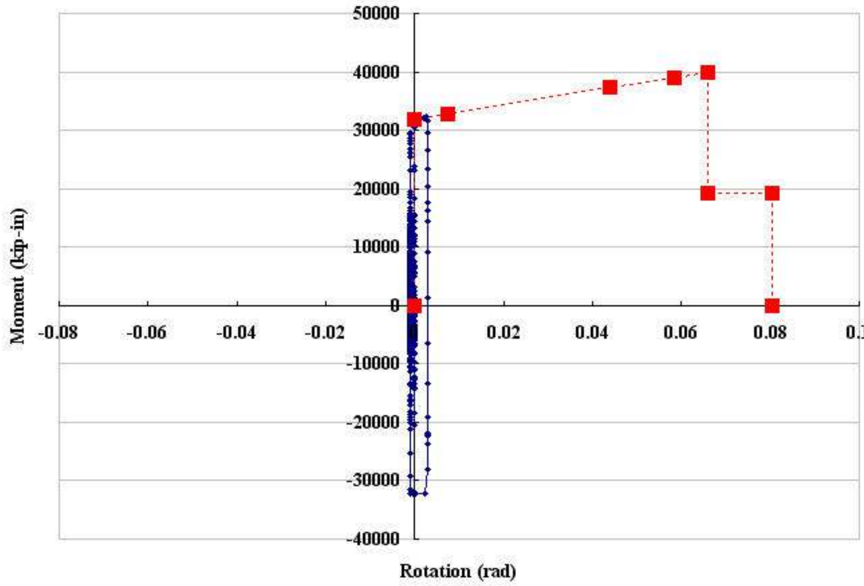

(c) Moment-Rotation Relationship on Longitudinal Direction (Beam 661)

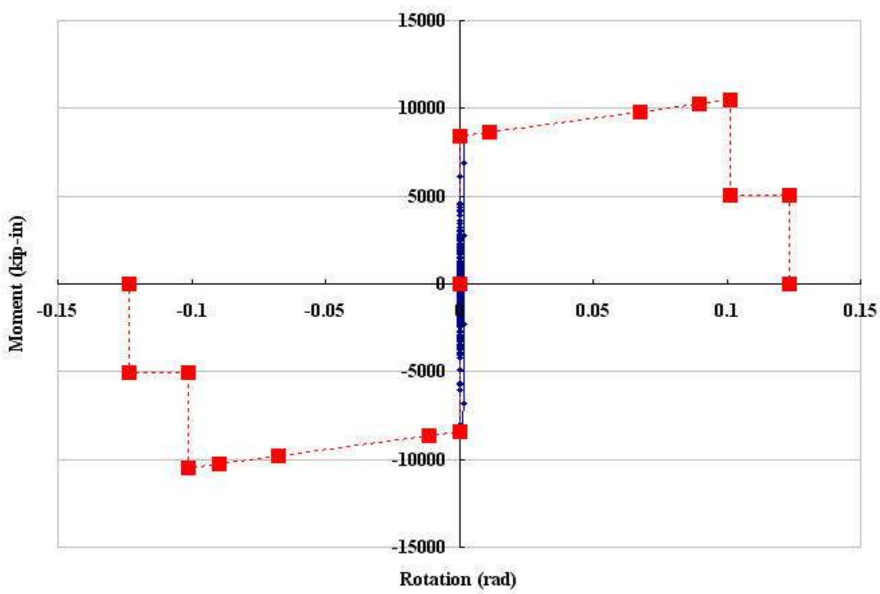

(d) Moment-Rotation Relationship on Longitudinal Direction (Beam 670)

Chapter 7 : Conclusion

The analytical studies are intended to present the responses of low and mid rise steel building structures under blast loads. The analytical results are compared with the current building code requirements for seismic design [28]. Five different sets of finite element models are developed representing two steel structures: the first one is a linear frame model with variable stand off distances; the second one is a linear frame model with variable weights of explosive (TNT); third one is linear diaphragm model with different TNT weights; fourth one is nonlinear frame model with variable TNT weights; while the last one is linear and nonlinear frame model with earthquake case. This study assumes the walls perpendicular to the blast remain intact. This places the maximum horizontal force on the structural frame. The results of this limited study indicate the following:

7.1. Linear Analysis of Three Story Building

1. To investigate the dimension of the blast crater, TM 5-855-1 [26] is used considering explosive weights of 500 lb, 1,000 lb and 2,000 lb. The radii of the crater due to 500 lb, 1,000 lb, 2,000 lb of TNT are all less than the minimum standoff distance used in this study.

2. Considering a 1,000 lb explosive weight, a standoff distance of less than 30 feet does not provide adequate protection for this structure. As results of analysis at 20 ft standoff distance, this structure is not adequate for explosive weights over 1,000 lb TNT.

3. The maximum drift ratio satisfies the UBC'97 code for earthquake with the exception of the following cases ; 1,000 lb at 20 ft or less and 2,000 lb at 20 ft.

4. The constraints of joints (pinned or fixed) and the orientation of column strong axis have a limited effect on the structure for interstory drifts and demand/capacity ratio for weak axis.

5. In flexible diaphragm analysis, the diaphragm is effective in distributing the blast loads from the front face to the other frames on the perimeter. The maximum shear force and bending moment of MRF frames for 2,000 lb, 3,000 lb TNT weight @ 20 ft are exceed the code design values of AISC-LRFD as shown in chapter 4.3. In addition, comparison of in-plane shear on the concrete slab indicates that in-plane shear is over its capacity in blast loads considered as shown in Figure 7.1. If the effective thickness of concrete slab replaces 3.5 inches for 8 inches, the concrete slab can resist for 1,000 lb TNT weight at 20 ft. However, the out-of-plane bending demands are smaller than bending capacity of concrete slab with exception of 3,000 lb TNT weight at 20 ft as shown in Figure 7.2.

6. The maximum shear force and bending moment of MRF frames from rigid diaphragm analysis in 2,000 lb, 3,000 lb TNT weights @ 20 ft also exceed the code design values of AISC-LRFD as shown in chapter 4.3. However, the out-of-plane bending demands are also smaller than bending capacity of concrete slab with exception of 3,000 lb TNT weight at20 ft as shown in Figure 7.3.

7. Comparison with the earthquake response indicates that the maximum displacement of this building for 2,000 lb TNT weight at 20 ft is more than that of earthquake as shown in Figure 7.4.

8. The maximum D/C ratios for the columns in each story of the transverse frame for an explosive weights and ground motion are shown in Figure 7.6. Here it can be seen that the D/C ratio for 500 lb TNT weight at 20 ft and earthquake are less than unity in 2nd floor and roof indicating elastic behavior. The D/C ratio of two blast conditions over 1,000 TNT weight is greater than unity. However, Figure 7.7 shows that the maximum D/C ratios for the columns in each story of the longitudinal frame are greater than unity indicating possible inelastic behavior in all cases.

9. The maximum D/C ratios of columns along longitudinal direction are higher than for the columns along the transverse direction. Because the diaphragm is distributing the blast loads from the front face to the other frames on the parameter as shown in Figure 7.8. The higher D/C ratios and inelastic deformation occur in the longitudinal frame for blast load. In addition, the demand/capacity ratio resulted from rigid diaphragm analysis is higher than that resulted from flexible diaphragm analysis as shown in Figure 7.9 – Figure 7.12.

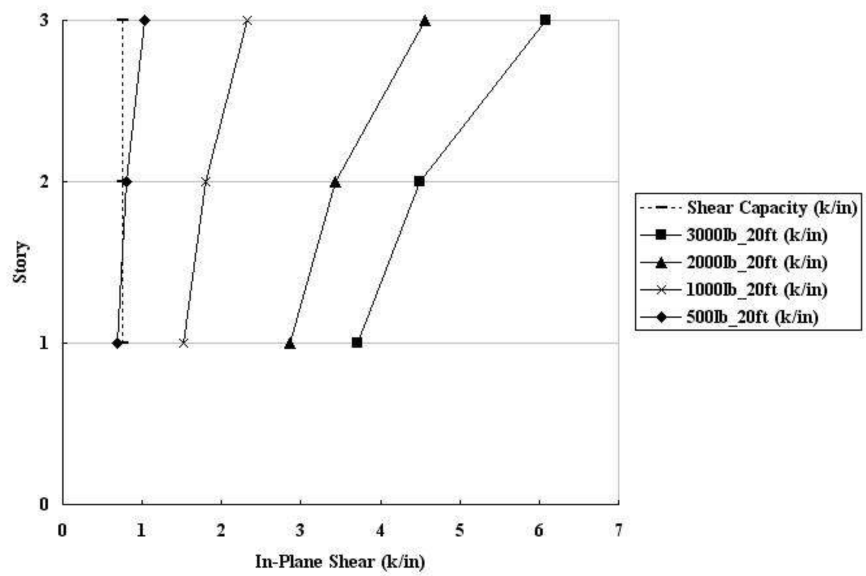

Figure 7.1 : Developed In-Plane Shear vs. Shear Capacity of Concrete Slab Based on Flexible Diaphragm Analysis

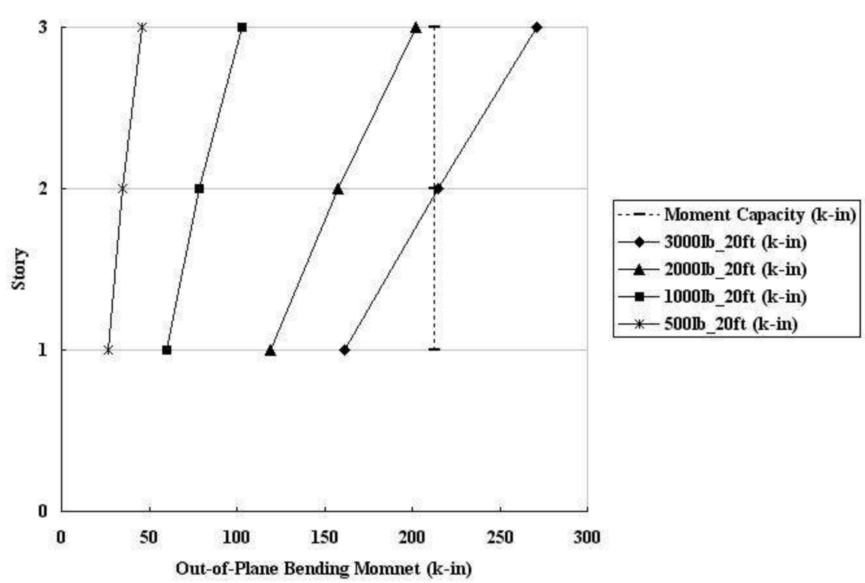

Figure 7.2 : Developed Out-of-Plane Bending Moment vs. Moment Capacity of Concrete Slab Based on Flexible Diaphragm Analysis

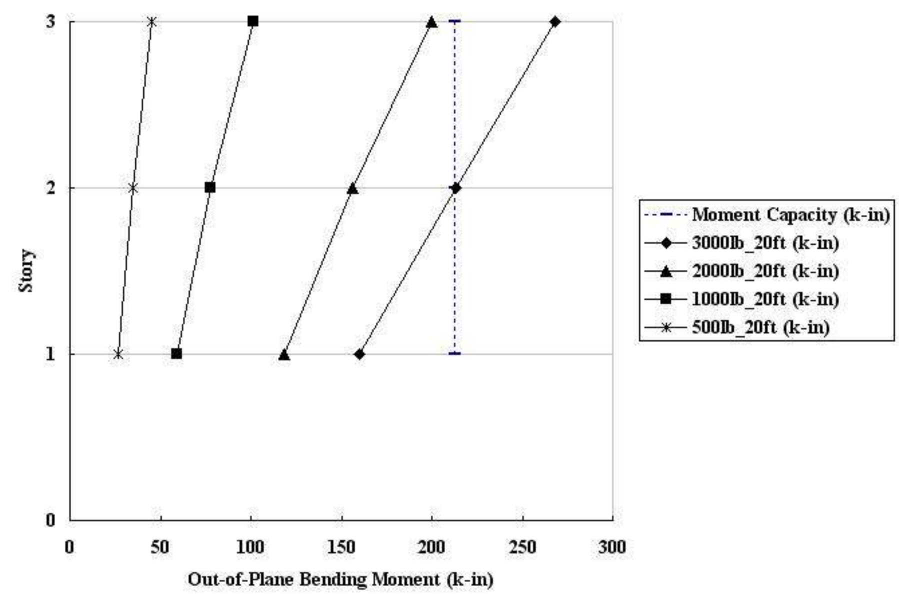

Figure 7.3 : Developed Out-of-Plane Bending Moment vs. Moment Capacity of Concrete Slab Based on Rigid Diaphragm Analysis

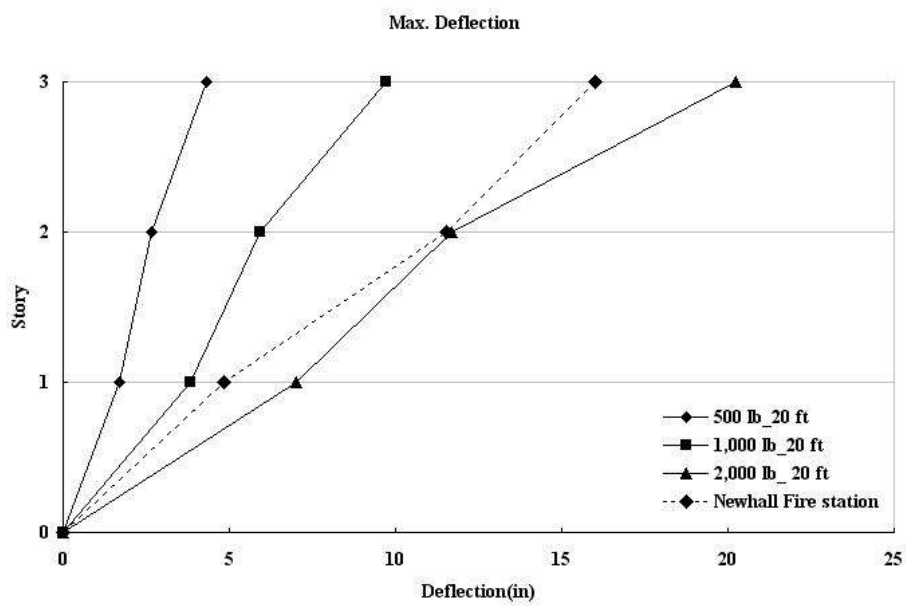

Figure 7.4 : Max. Deflection Envelope of Each Floor under Northridge Earthquake and Blast Loads

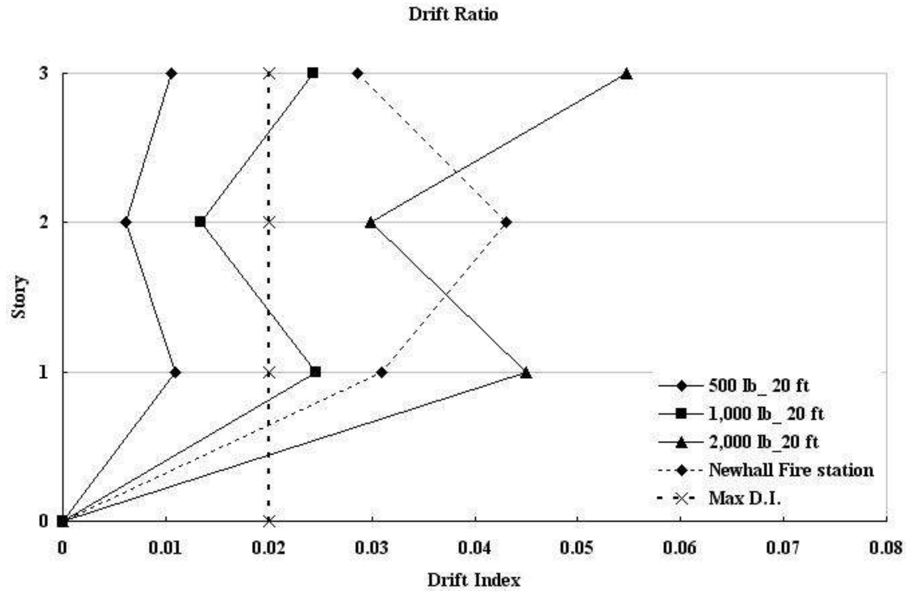

Figure 7.5 : Max. Interstory Drift of Northridge Earthquake and Blast Loads

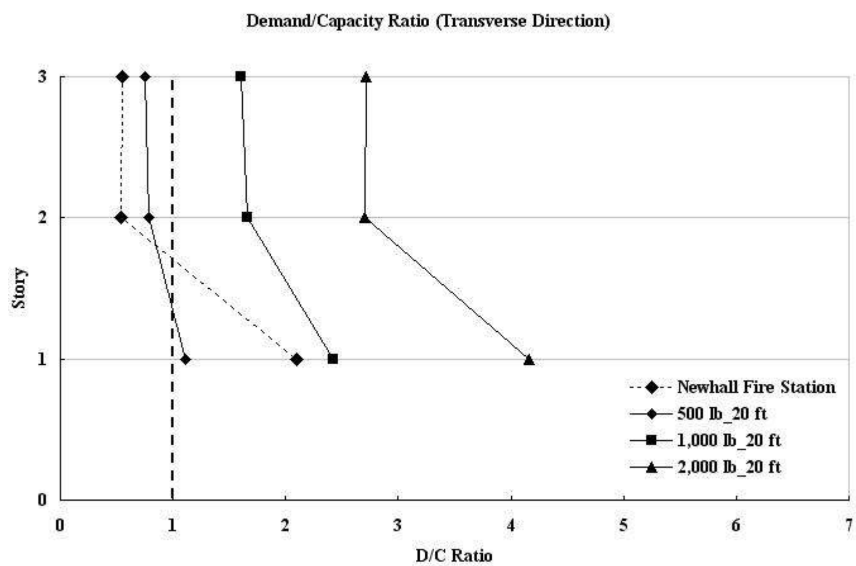

Figure 7.6 : Max. Demand/Capacity Ratio under Blast Loads and Recorded Ground Motion at Newhall Fire Station (Columns along Transverse Direction)

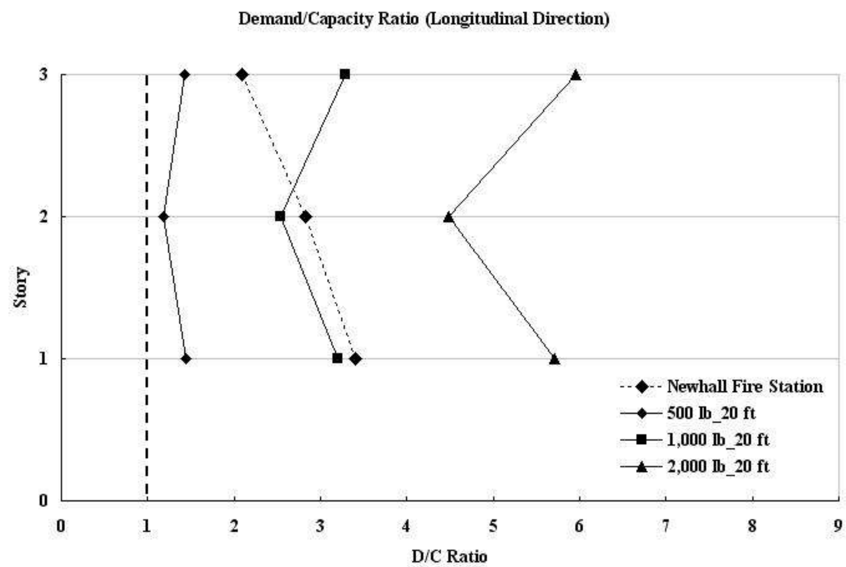

Figure 7.7 : Max. Demand/Capacity Ratio under Blast Loads and Recorded Ground Motion at Newhall Fire Station (Columns along Longitudinal Direction)

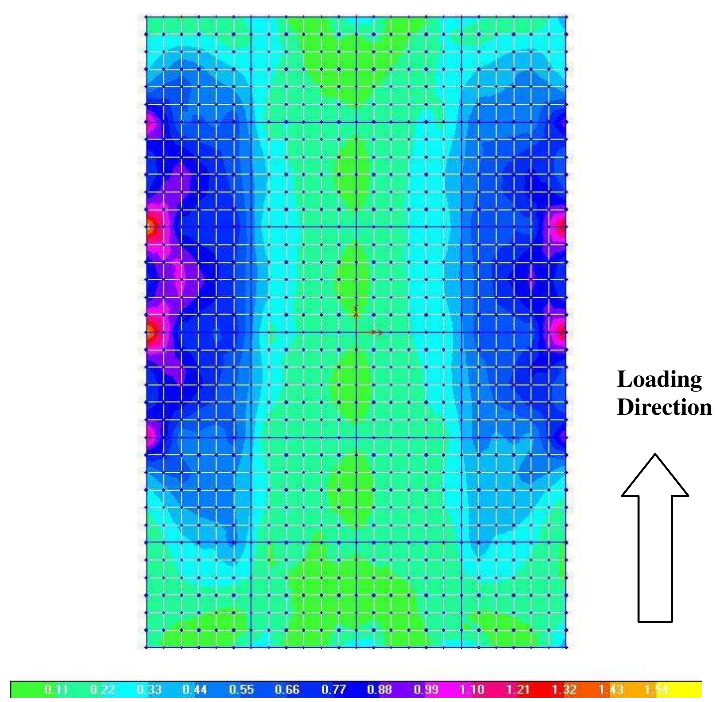

Figure 7.8 : In-Plane Shear Flow Distribution on 3 Story Building

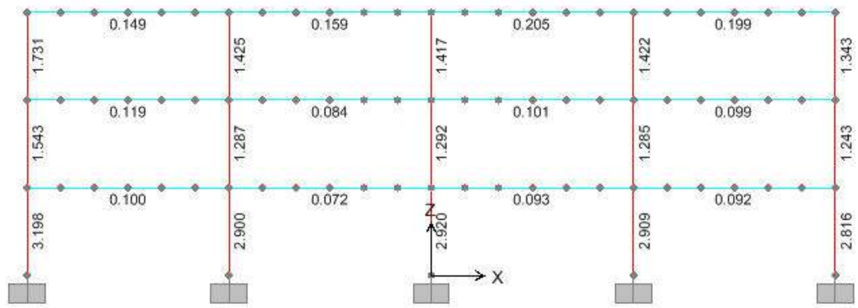

(a) Demand/Capacity Ratio of Transverse Direction (Flexible Diaphragm Analysis)

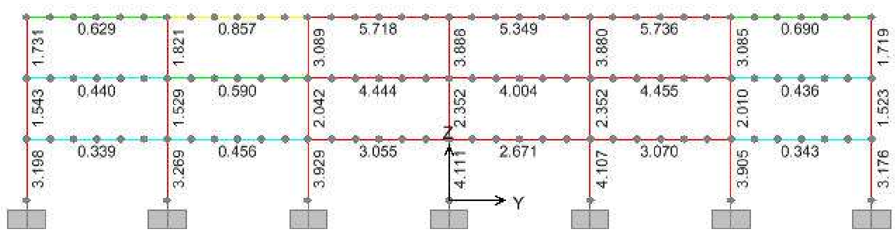

(b) Demand/Capacity Ratio of Longitudinal Direction (Flexible Diaphragm Analysis)

Figure 7.9 : Demand/Capacity Ratio of MRF Frames (Flexible Diaphragm Analysis)

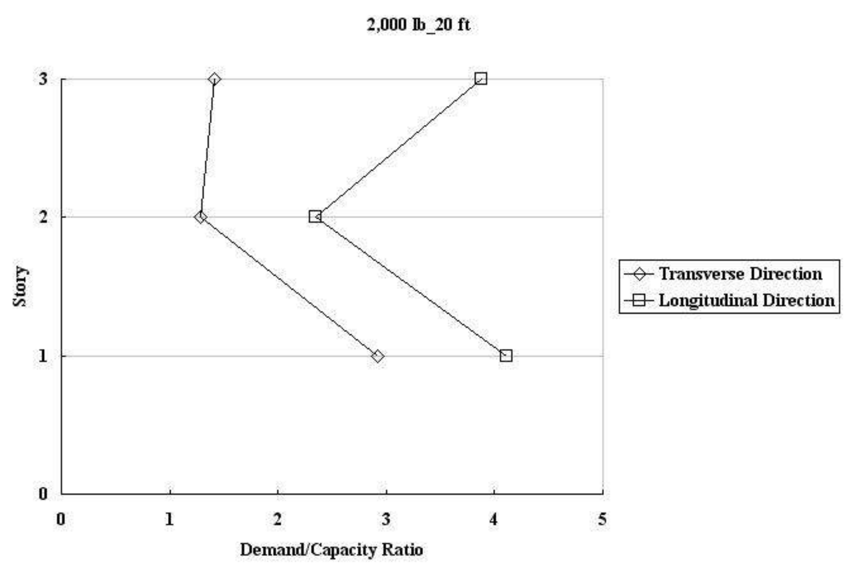

Figure 7.10 : Max. Demand/Capacity Ratio under Blast Load (Columns along Transverse Direction and Longitudinal Direction – Flexible Diaphragm Analysis)

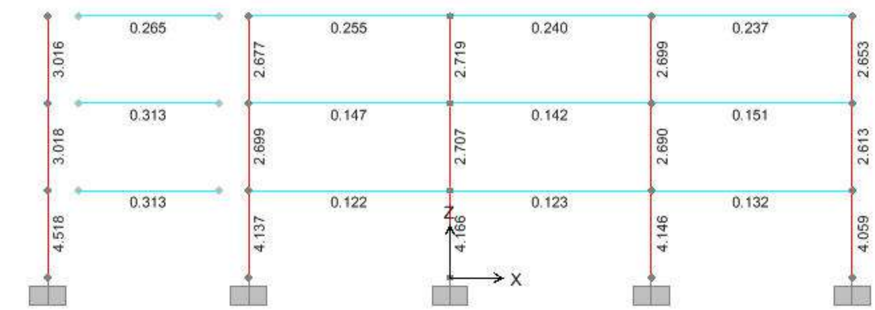

(a) Demand/Capacity Ratio of Transverse Direction (Rigid Diaphragm Analysis)

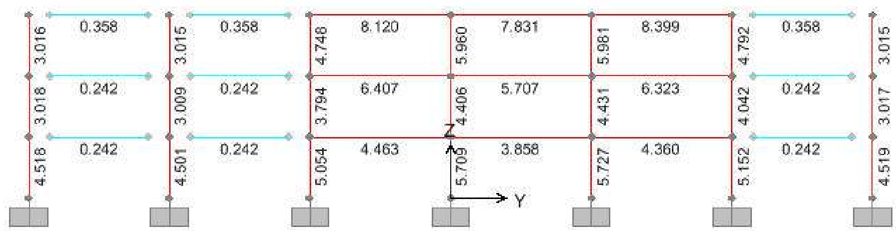

(b) Demand/Capacity Ratio of Longitudinal Direction (Rigid Diaphragm Analysis)

Figure 7.11 : Demand/Capacity Ratio of MRF Frames (Rigid Diaphragm Analysis)

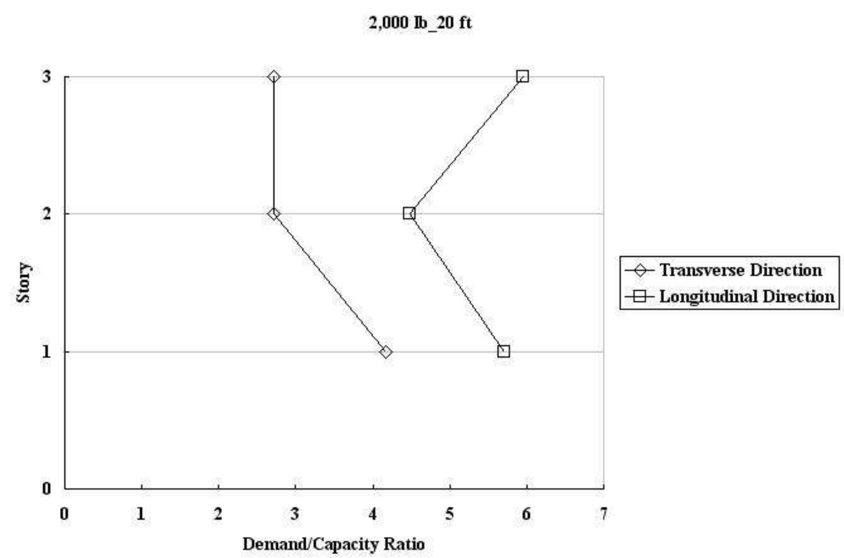

Figure 7.12 : Max. Demand/Capacity Ratio under Blast Load (Columns along Transverse Direction and Longitudinal Direction – Rigid Diaphragm Analysis)

7.2. Nonlinear Analysis of Three Story Building

1. The maximum displacement for 1,000 lb @ 15 ft and 1,000 lb @ 20 ft has similar values. However, the maximum displacement for the 2,000 lb @ 20 ft has increased to 26 inches at roof as shown in Figure 7.13. In addition, the cycling is occurring about new equilibrium position in the deformed structure as shown in chapter 4.4.

2. In Figure 7.14, the drift ratio for the 1,000 lb @ 15 ft and 1,000 lb @ 20 ft exceed limitation of UBC' 97 for earthquake at 1st floor and roof. In addition, for the 2,000 lb @ 20 ft, the interstory drift ratio is also well above the limiting value defined as UBC'97.

3. The value of D/C ratio is lower than one of D/C ratio obtained linear analyses due to reduction of moment demand as shown in Figure 7.15.

4. Comparison with the earthquake response indicates that the displacement of this building for blasts of 15 ft, 20 ft stand-off distances with 1,000 lb TNT weights is basically same as displacement of considered earthquake. However, the displacement of 2,000 lb TNT weight at 20 ft stand-off distance is more than that of considered earthquake as shown in Figure 7.13. The drift ratio of considered earthquake is above the code value with the exception of 3rd floor as shown in Figure 7.14.

5. Nonlinear Demands for the 1,000 lb TNT weight @ 15 ft and 20 ft are summarized in Table 7.1 and Table 7.2. Table 7.1 is shown that the beams and columns that exceed the elastic limit have small plastic rotation demands along both directions. In Table 7.2, the behaviors of the

transverse columns at the roof level are linear and similar behaviors can be seen on 1,000 lb TNT weight at 15 ft. According to the FEMA recommendations, this building would be classified as suitable for life safety (IO).

6. Demands for the condition of 2,000 lb @ 20 ft are summarized in Table 7.3. Here it can be seen that there is yielding in the column over both directions of the frame. The plastic rotation demands range from 0.049 radians at the first floor to 0.030 radians at the roof of longitudinal direction. These range from 0.044 radians at the first floor to 0.009 radians at the roof level of transverse direction. In addition, there is also yielding in the beams over the height of the frame with plastic rotation demands ranging from 0.0459 radians at the 2nd floor to 0.035 at the roof of longitudinal direction. It can be seen that hinge state is classified as suitable for life safety (LS) in case of 2,000 lb TNT weight @ 20 ft.

7. Demands for earthquake recorded Newhall Fire Station are summarized in Table 7.4. It is shown that the columns that exceed the elastic limit have small plastic rotation demands along both directions. However, there is yielding in the longitudinal beams with plastic rotation demands ranging from 0.014 radians at the first floor of longitudinal direction to 0.022 radians at the roof level. It can be seen that hinge state is classified as suitable for life safety (IO) in case of earthquake.

8. As results of nonlinear analysis of 3 story building, columns at the first floor level have a high plastic rotation demand that makes them critical due to maximum horizontal force on the first floor level as shown in Figure 7.17 – Figure 7.19

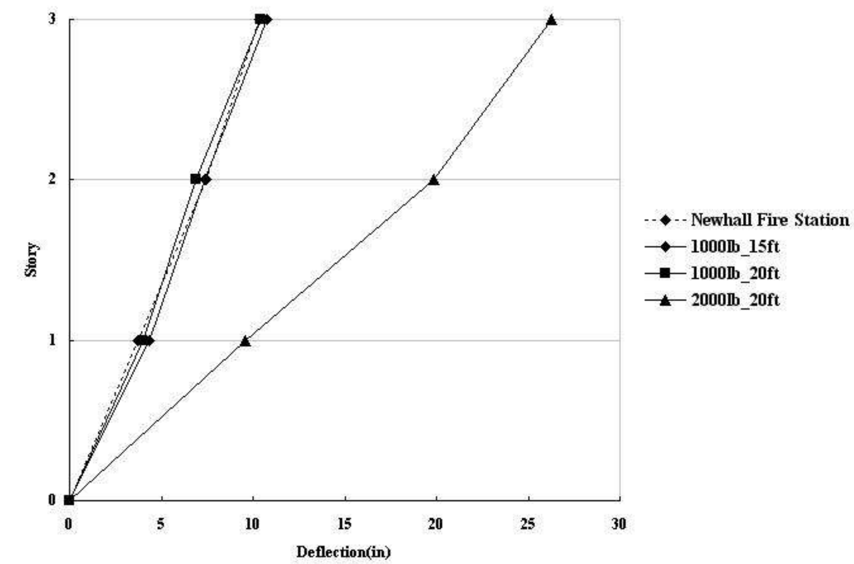

Figure 7.13 : Max. Deflection Envelope of Each Floor under Northridge Earthquake and Blast Loads (Nonlinear Analyses)

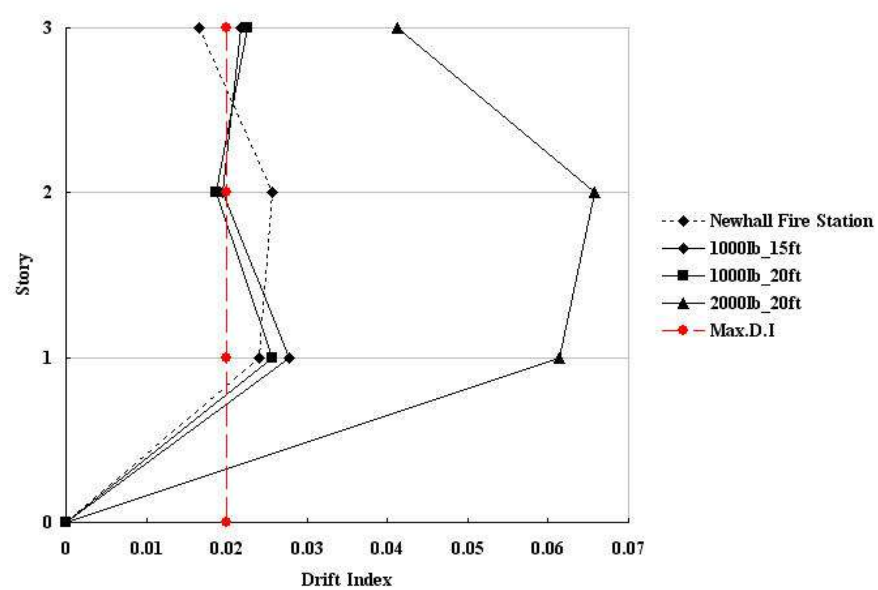

Figure 7.14 : Max. Interstory Drift of Northridge Earthquake and Blast Loads (Nonlinear Analysis)

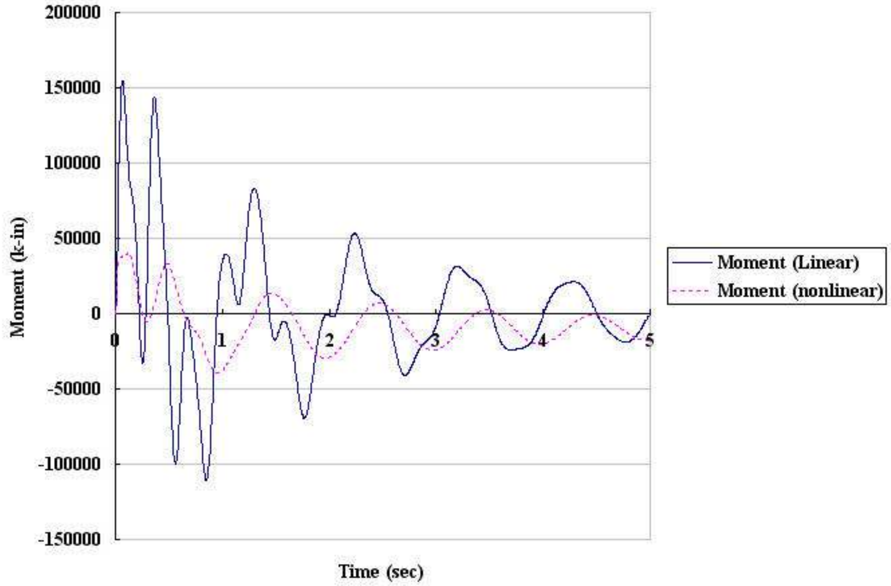

Figure 7.15 : Comparison of Moment Demand Resulted from Linear and Nonlinear Analysis for Longitudinal Column

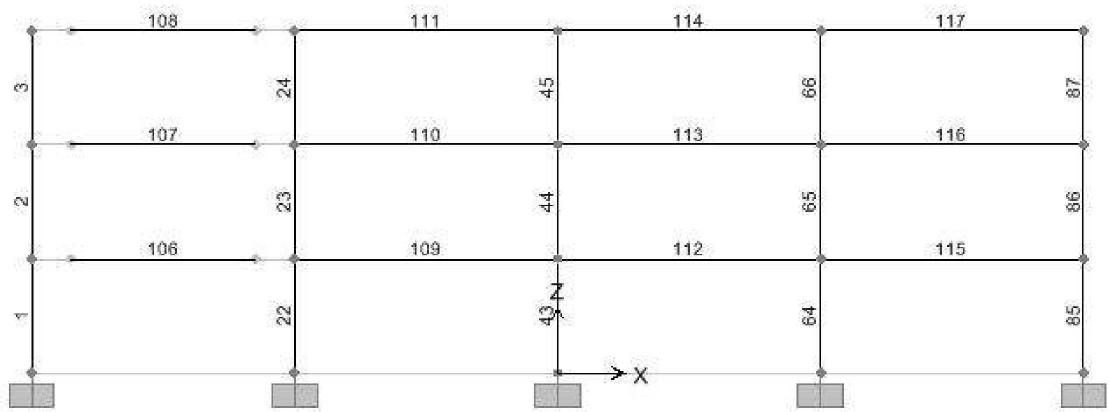

(a) Generated Member Numbers along the Transverse Direction

Figure 7.16 : Generate Member Numbers along Both Directions

"Figure 7.16 : Continued"

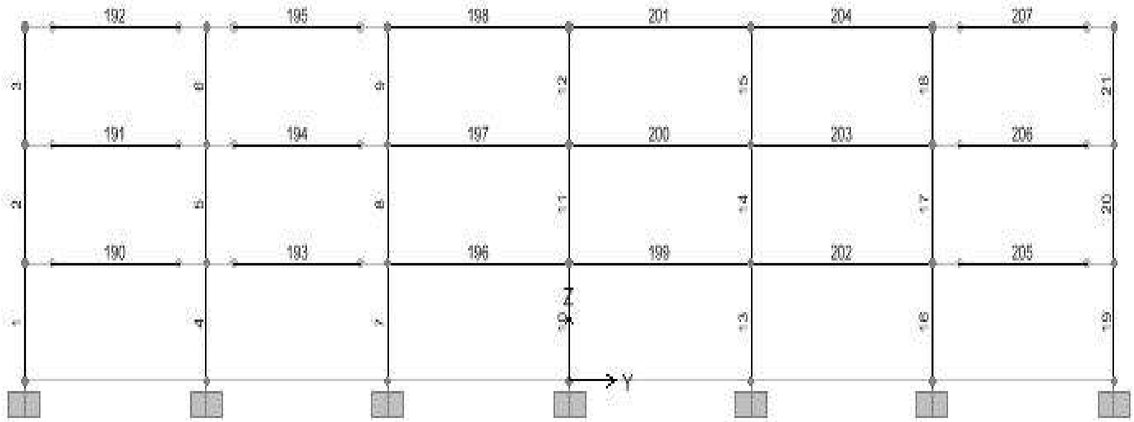

(b) Generated Member Numbers along the Longitudinal Direction

Table 7.1 : Acceptance Criteria for Nonlinear Procedures (1,000 lb @ 15 ft)

Case	Member	Section	θy	θp	a	b	Hinge State
1,000 lb @ 15 ft	Column (Longitudinal)	No. 10 (1^{st} Floor)	0.007	0.0185	0.062	0.076	IO - LS
		No. 11 (2^{nd} Floor)	0.007	0.0018	0.062	0.076	< IO
		No. 12 (Roof)	0.007	0.010	0.062	0.076	IO - LS
	Column (Transverse)	No. 43 (1^{st} Floor)	0.009	0.0144	0.084	0.102	IO - LS
		No. 44 (2^{nd} Floor)	0.009	0.003	0.084	0.102	< IO
		No. 45 (Roof)	0.009	0.000	0.084	0.102	Linear
	Beam (Longitudinal)	No. 196 (1^{st} Floor)	0.009	0.007	0.079	0.096	< IO
		No. 197 (2^{nd} Floor)	0.009	0.016	0.079	0.096	IO - LS
		No. 198 (Roof)	0.011	0.017	0.079	0.124	IO - LS

Where, IO = $1\theta_y$, LS = $6\theta_y$, CP = $8\theta_y$

Table 7.2 : Acceptance Criteria for Nonlinear Procedures (1,000 lb @ 20 ft)

Case	Member	Section	θy	θp	a	b	Hinge State
1,000 lb @ 20 ft	Column (Longitudinal)	No. 10 (1st Floor)	0.007	0.0165	0.062	0.076	IO - LS
		No. 11 (2nd Floor)	0.007	0.0014	0.062	0.076	< IO
		No. 12 (Roof)	0.007	0.0079	0.062	0.076	IO - LS
	Column (Transverse)	No. 43 (1st Floor)	0.009	0.0123	0.084	0.102	IO - LS
		No. 44 (2nd Floor)	0.009	0.0002	0.084	0.102	< IO
		No. 45 (Roof)	0.009	0	0.084	0.102	Linear
	Beam (Longitudinal)	No. 196 (1st Floor)	0.009	0.0062	0.079	0.096	< IO
		No. 197 (2nd Floor)	0.009	0.0157	0.079	0.096	IO - LS
		No. 198 (Roof)	0.011	0.0167	0.079	0.124	IO - LS

Table 7.3 : Acceptance Criteria for Nonlinear Procedures (2,000 lb @ 20 ft)

Case	Member	Section	θy	θp	a	b	Hinge State
2,000 lb @ 20 ft	Column (Longitudinal)	No. 10 (1st Floor)	0.007	0.0493	0.062	0.076	LS - CP
		No. 11 (2nd Floor)	0.007	0.0251	0.062	0.076	IO - LS
		No. 12 (Roof)	0.007	0.030	0.062	0.076	IO - LS
	Column (Transverse)	No. 43 (1st Floor)	0.009	0.044	0.084	0.102	IO - LS
		No. 44 (2nd Floor)	0.009	0.012	0.084	0.102	IO - LS
		No. 45 (Roof)	0.009	0.0092	0.084	0.102	IO - LS
	Beam (Longitudinal)	No. 196 (1st Floor)	0.009	0.035	0.079	0.096	IO - LS
		No. 197 (2nd Floor)	0.009	0.0459	0.079	0.096	IO - LS
		No. 198 (Roof)	0.011	0.0354	0.079	0.124	IO - LS

Table 7.4 : Acceptance Criteria for Nonlinear Procedures (Earthquake)

Case	Member	Section	θy	θp	a	b	Hinge State
Recorded at Newhall Fire Station	Column (Longitudinal)	No. 10 (1st Floor)	0.007	0.013	0.062	0.076	IO -LS
		No. 11 (2nd Floor)	0.007	0.004	0.062	0.076	<IO
		No. 12 (Roof)	0.007	0.003	0.062	0.076	<IO
	Column (Transverse)	No. 43 (1st Floor)	0.009	0.006	0.084	0.102	<IO
	Beam (Longitudinal)	No. 196 (1st Floor)	0.009	0.014	0.079	0.096	IO - LS
		No. 197 (2nd Floor)	0.009	0.018	0.079	0.096	IO - LS
		No. 198 (Roof)	0.011	0.022	0.079	0.124	IO - LS

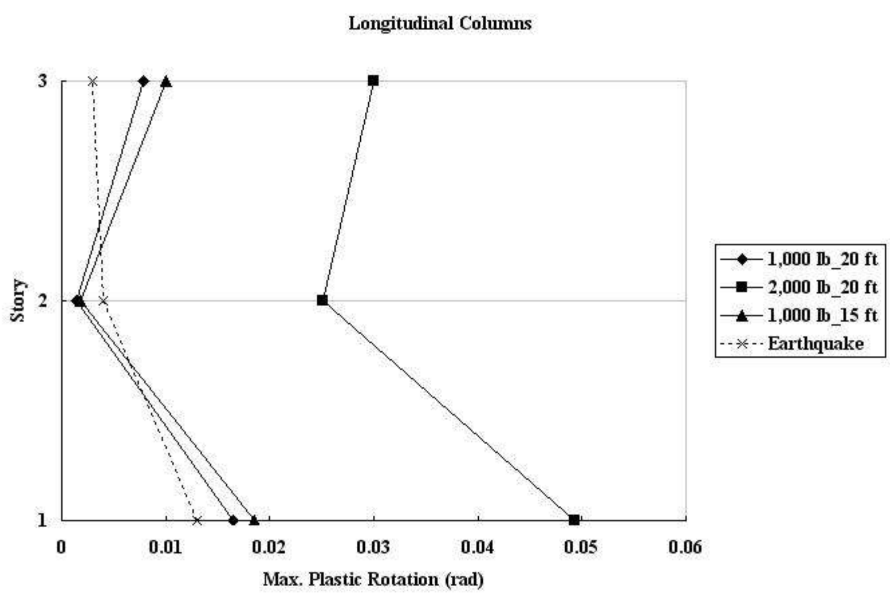

Figure 7.17 : Max. Plastic Rotation at Each Story (Longitudinal Columns)

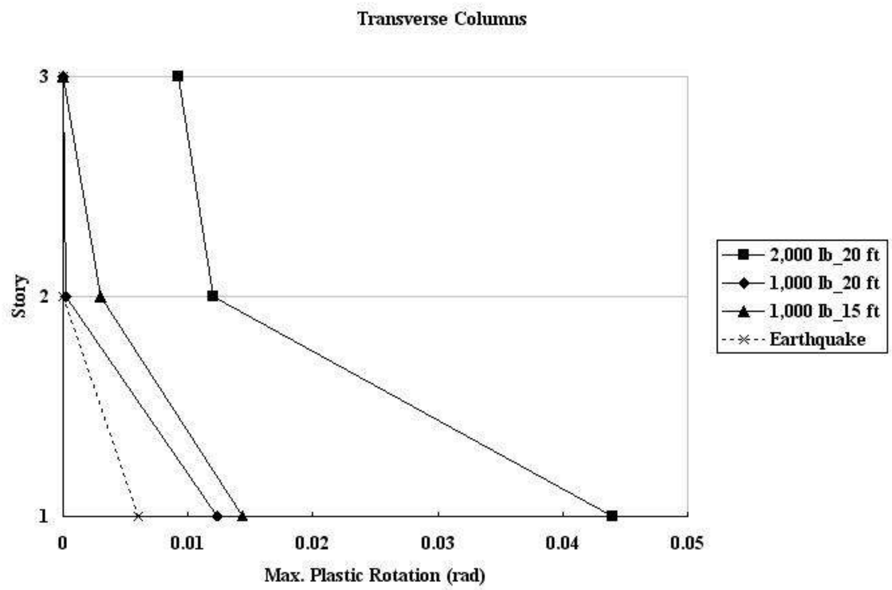

Figure 7.18 : Max. Plastic Rotation at Each Story (Transverse Columns)

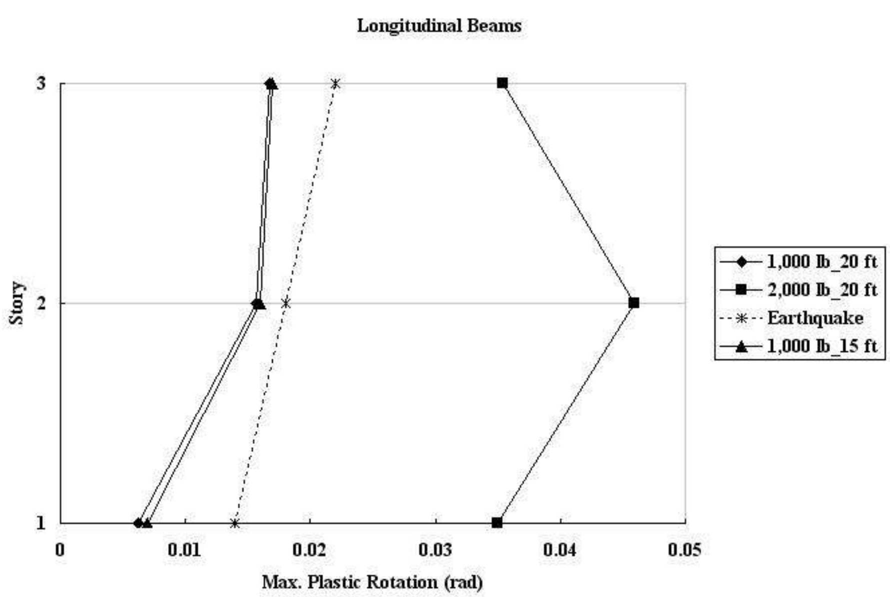

Figure 7.19 : Max. Plastic Rotation at Each Story (Longitudinal Beams)

7.3. Linear Analysis of Ten Story Building

1. Considering the 1,000 lb explosive, this structure is adequate of all considered stand-off distances. As results of analysis with 100 lb, 500 lb, 1,000 lb and 2,000 lb TNT weight at 20 ft stand-off distance, this structure does not provide for protection over 2,000 lb TNT.

2. The drift ratio for all blast loads satisfies the UBC'97 code for earthquake with the exception of 2,000 lb at 20 ft as shown in Figure 7.24. The D/C ratios of transverse direction of blast except for 500 lb TNT weight @ 20 ft are higher than that of the earthquake considered as shown in Figure 7.25. The higher D/C ratios occur in the longitudinal frame (strong axis columns) for both blast and earthquake.

3. As results of analysis with 3,000 lb and 4,000 lb TNT weight at 20 ft standoff distance in chapter 5.3, this structure is also needed adequate protection. The higher D/C ratios also occur in the longitudinal frame for extreme blast load cases. The drift ratios of extreme blast loads exceed the UBC'97 code for earthquake as shown in chapter 5.3.

4. In flexible diaphragm analysis, maximum shear force and bending moment of MRF frames for 2,000 lb, 3,000 lb, 4,000 lb TNT weight @ 20 ft are exceed the code design values of AISC-LRFD as shown in chapter 5.4. In addition, comparison of in-plane shear on the concrete slab indicates that in-plane shear is over its capacity in blast loads considered as shown in Figure 7.20. However, the out-of-plane bending demands are smaller than bending capacity of concrete slab with exception of 3,000 lb and 4,000 lb TNT weight @ 20 ft as shown in Figure 7.21.

5. The rigid diaphragm is effective in distributing the blast loads from the front face to the other frames on the perimeter. Maximum shear force and bending moment of MRF frames resulted from both analyses in 2,000 lb, 3,000 lb, 4,000 lb TNT weights @ 20 ft are also exceed the code design values of AISC-LRFD as shown in chapter 5.4. However, the out-of-plane bending demands are smaller than bending capacity of concrete slab with exception of 3,000 lb and 4,000 lb TNT weight @ 20 ft as shown in Figure 7.22. In addition, maximum shear force and bending moment of MRF frames are almost same in flexible and rigid diaphragm analysis as shown in chapter 5.4.

6. Comparison with the earthquake response indicates that the maximum displacement of this building for a blast is less than that of earthquake as shown in Figure 7.23. The code limitation of drift ratio based on UBC'97 for earthquake is 0.02 and the responses of all loadings satisfy code limitation with the exception of the 2,000 lb TNT weight @ 20 ft and earthquake considered as shown in Figure 7.24. However the drift is only 0.029 of 2,000 lb TNT which should be sustained with proper welded connections.

7. The maximum D/C ratios for the columns in each story of the transverse frame for an explosive weights and ground motion are shown in Figure 7.25. Here it can be seen that the D/C ratios are less than unity indicating elastic behavior except case of 2,000 lb TNT. However, Figure 7.26 shows that the maximum D/C ratios for the columns in each story of the longitudinal frame are over unity in cases of 1,000 lb, 2,000 lb TNT weights and earthquake.

8. The maximum D/C ratios of columns along longitudinal direction are higher than for the columns along the transverse direction. Because the diaphragm is distributing the blast loads from the front face to the other frames on the parameter as shown in Figure 7.27. The higher D/C ratios and inelastic deformation occur in the longitudinal frame for blast load. In addition, the demand/capacity ratio resulted from rigid diaphragm analysis is slightly higher than that resulted from flexible diaphragm analysis as shown in Figure 7.28 – Figure 7.31.

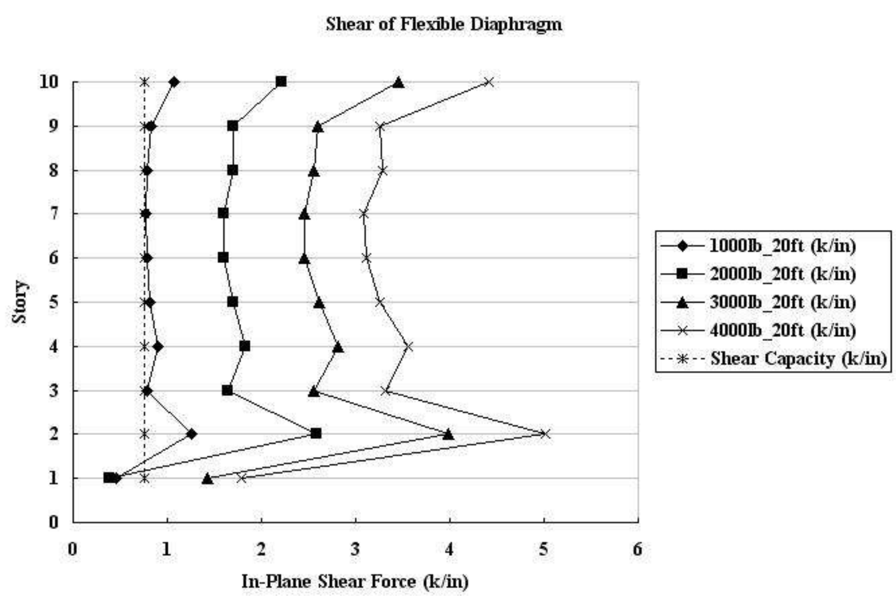

Figure 7.20 : Developed In-Plane Shear vs. Shear Capacity of Concrete Slab Based on Flexible Diaphragm Analysis

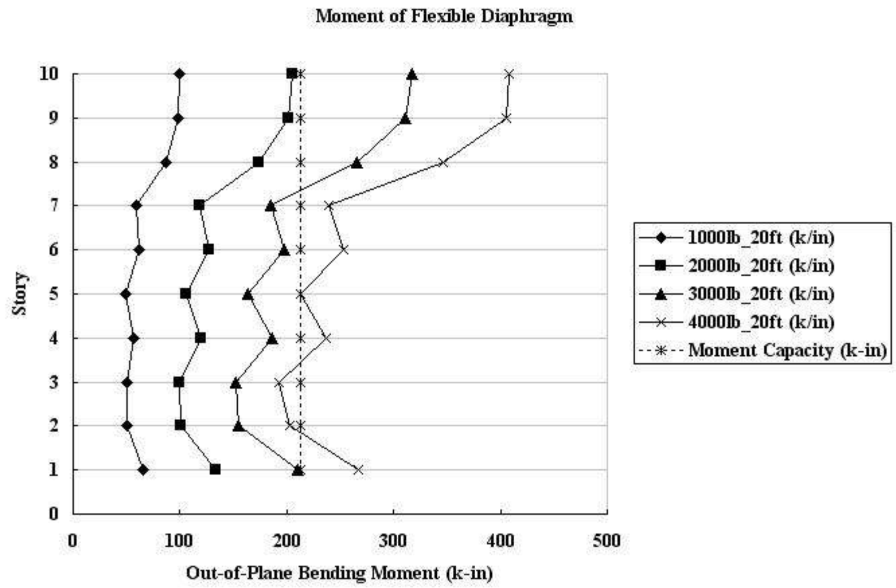

Figure 7.21 : Developed Out-of-Plane Bending Moment vs. Moment Capacity of Concrete Slab Based on Flexible Diaphragm Analysis

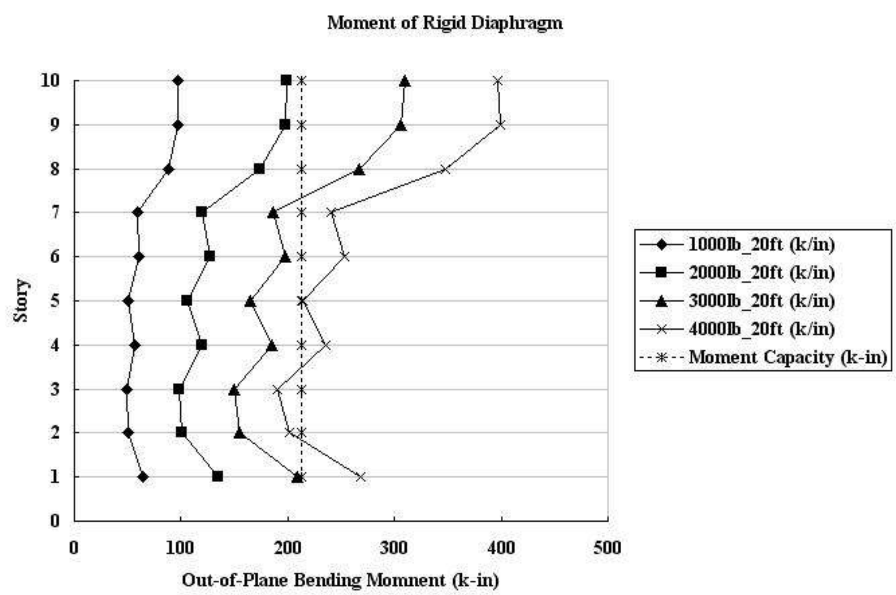

Figure 7.22 : Developed Out-of-Plane Bending Moment vs. Moment Capacity of Concrete Slab Based on Rigid Diaphragm Analysis

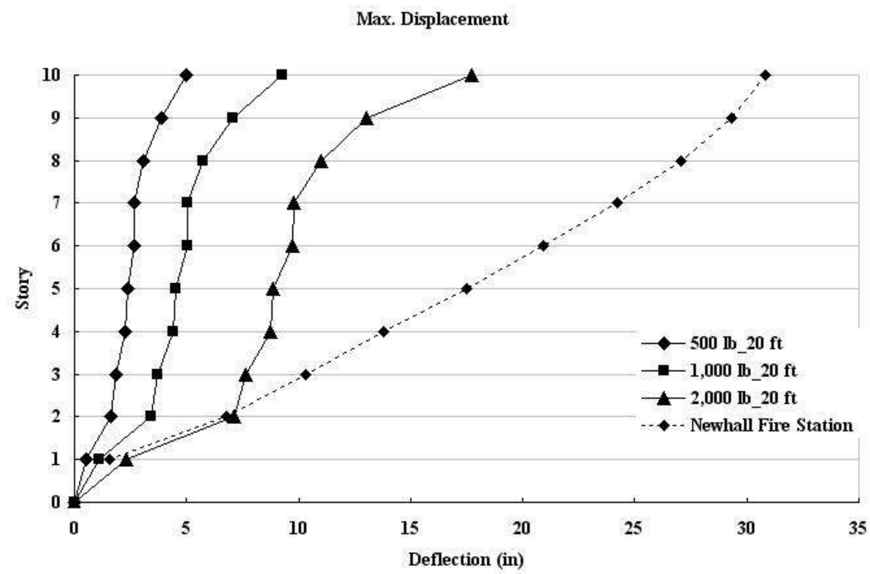

Figure 7.23 : Max. Deflection Envelope of Each Floor under Northridge Earthquake and Blast Loads

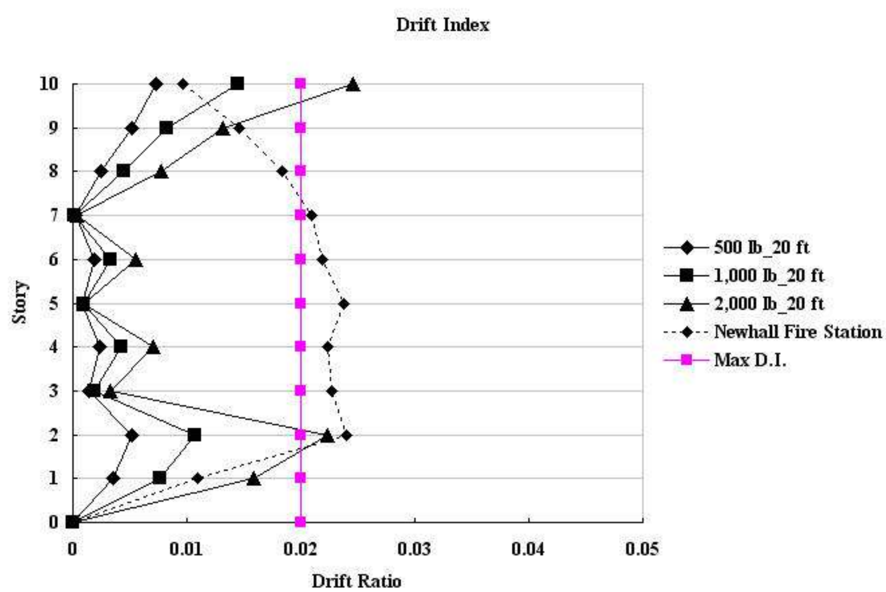

Figure 7.24 : Max. Interstory Drift of Northridge Earthquake and Blast Loads

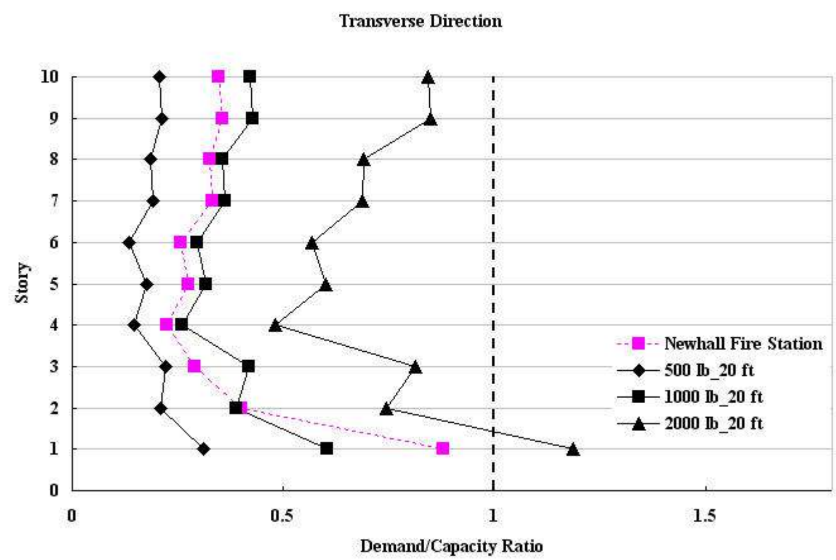

Figure 7.25 : Max. Demand/Capacity Ratio under Blast Loads and Recorded Ground Motion at Newhall Fire Station (Columns along Transverse Direction)

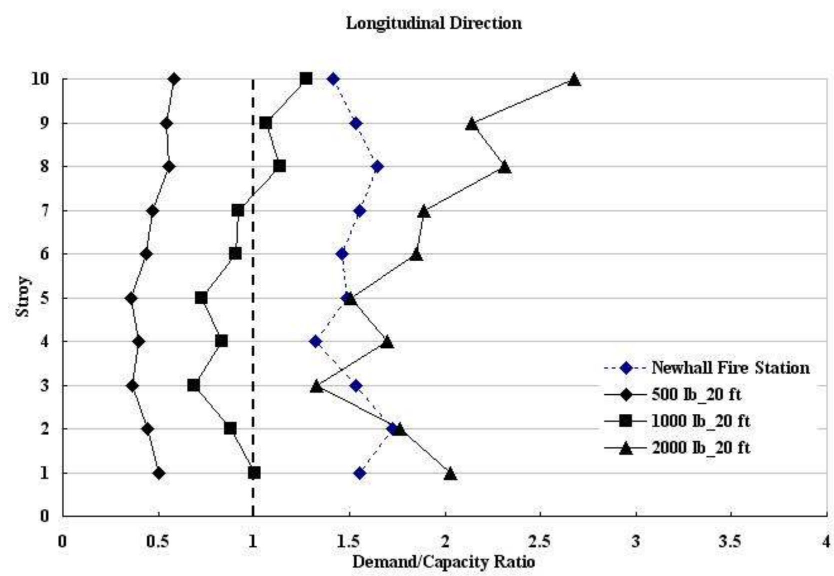

Figure 7.26 : Max. Demand/Capacity Ratio under Blast Loads and Recorded Ground Motion at Newhall Fire Station (Columns along Longitudinal Direction)

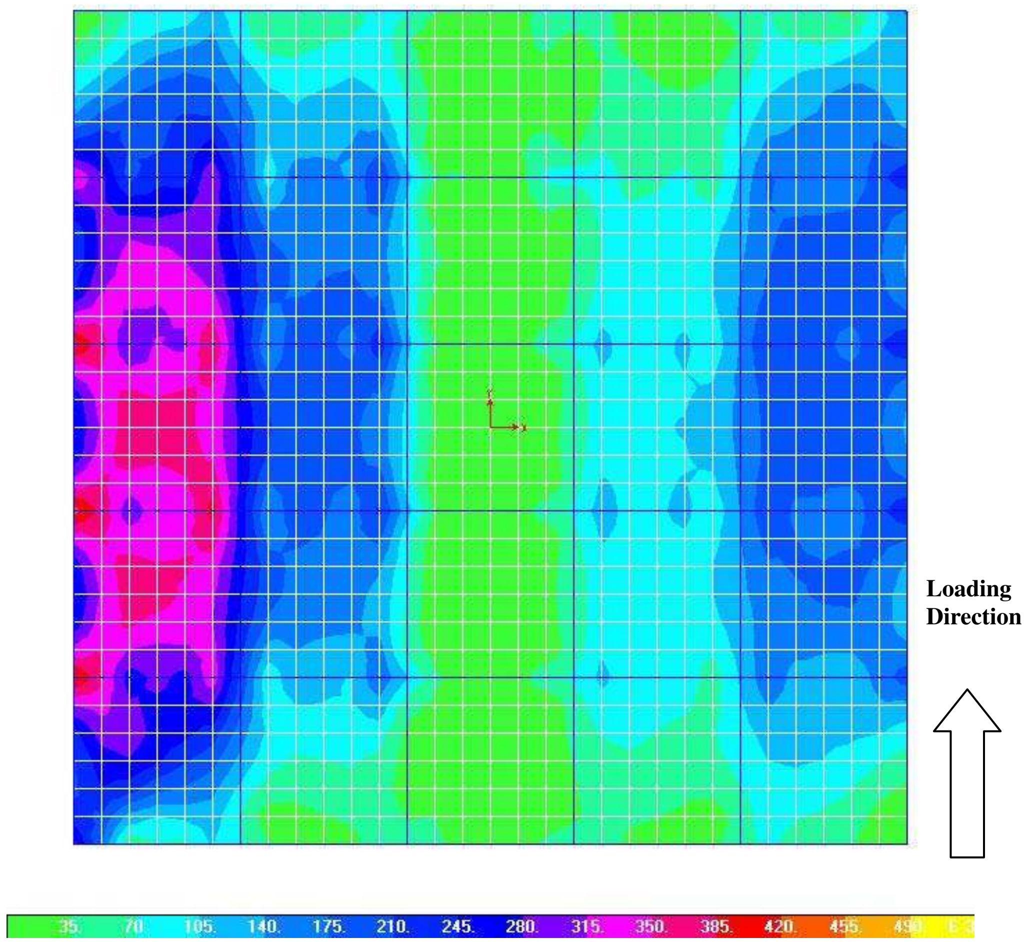

Figure 7.27 : In-Plane Shear Flow Distribution on 10 Story Building

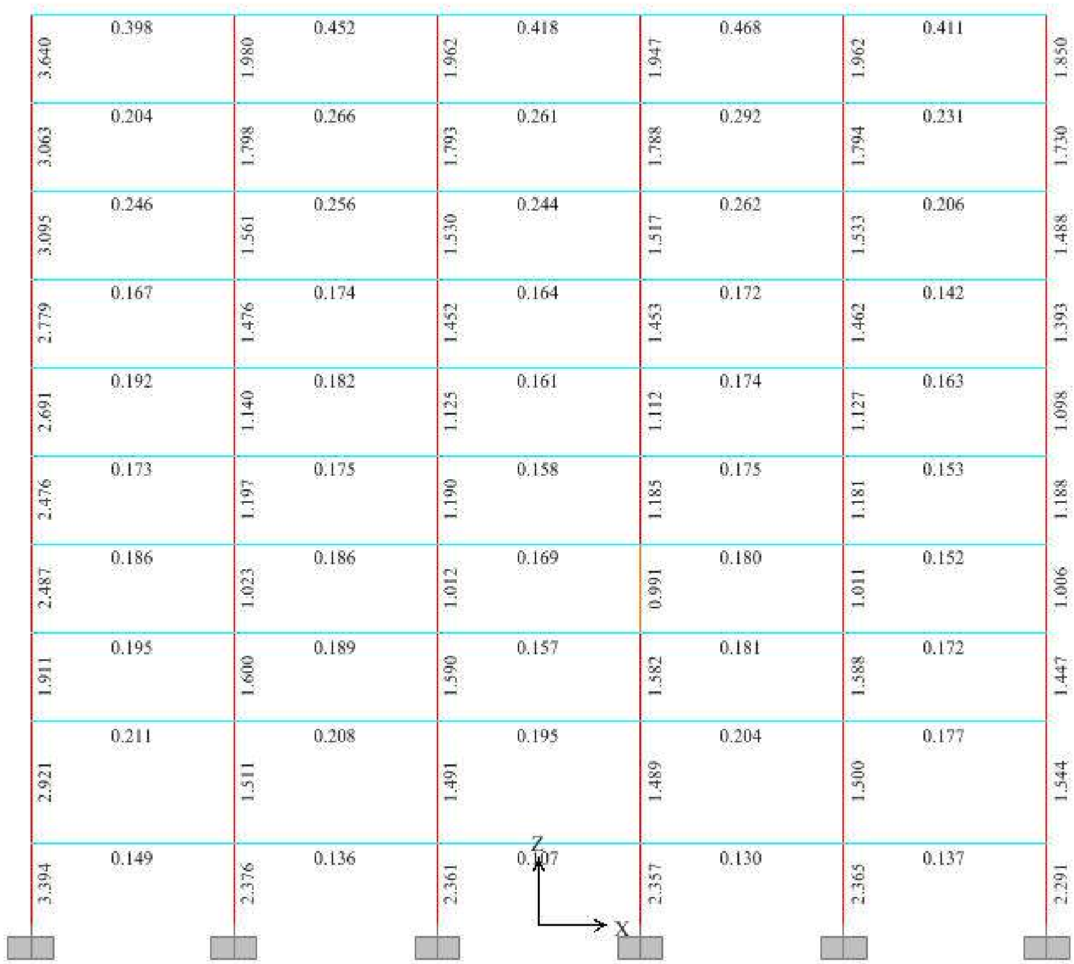

(a) Demand/Capacity Ratio of Transverse Direction (Flexible Diaphragm Analysis)

Figure 7.28 : Demand/Capacity Ratio of MRF Frames (Flexible Diaphragm)

"Figure 7.28 : Continued"

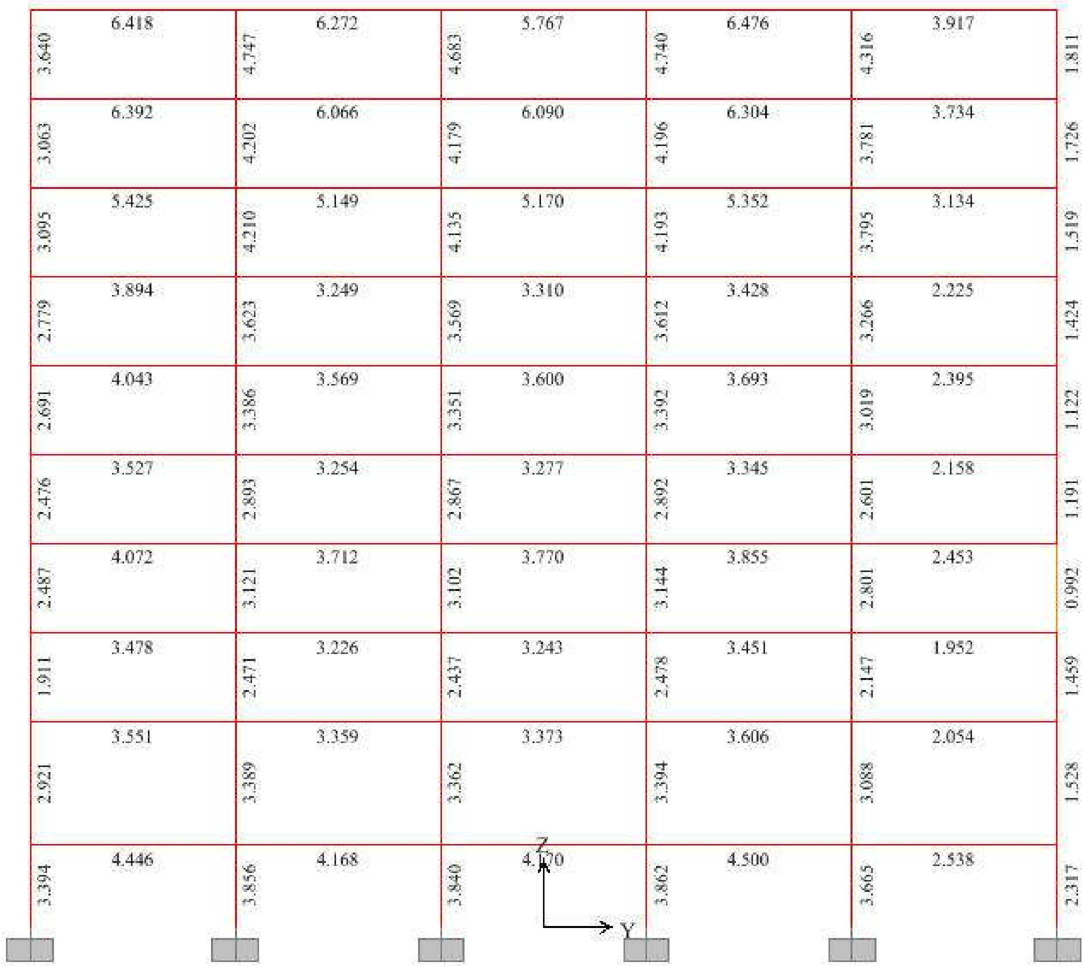

(b) Demand/Capacity Ratio of Longitudinal Direction (Flexible Diaphragm Analysis)

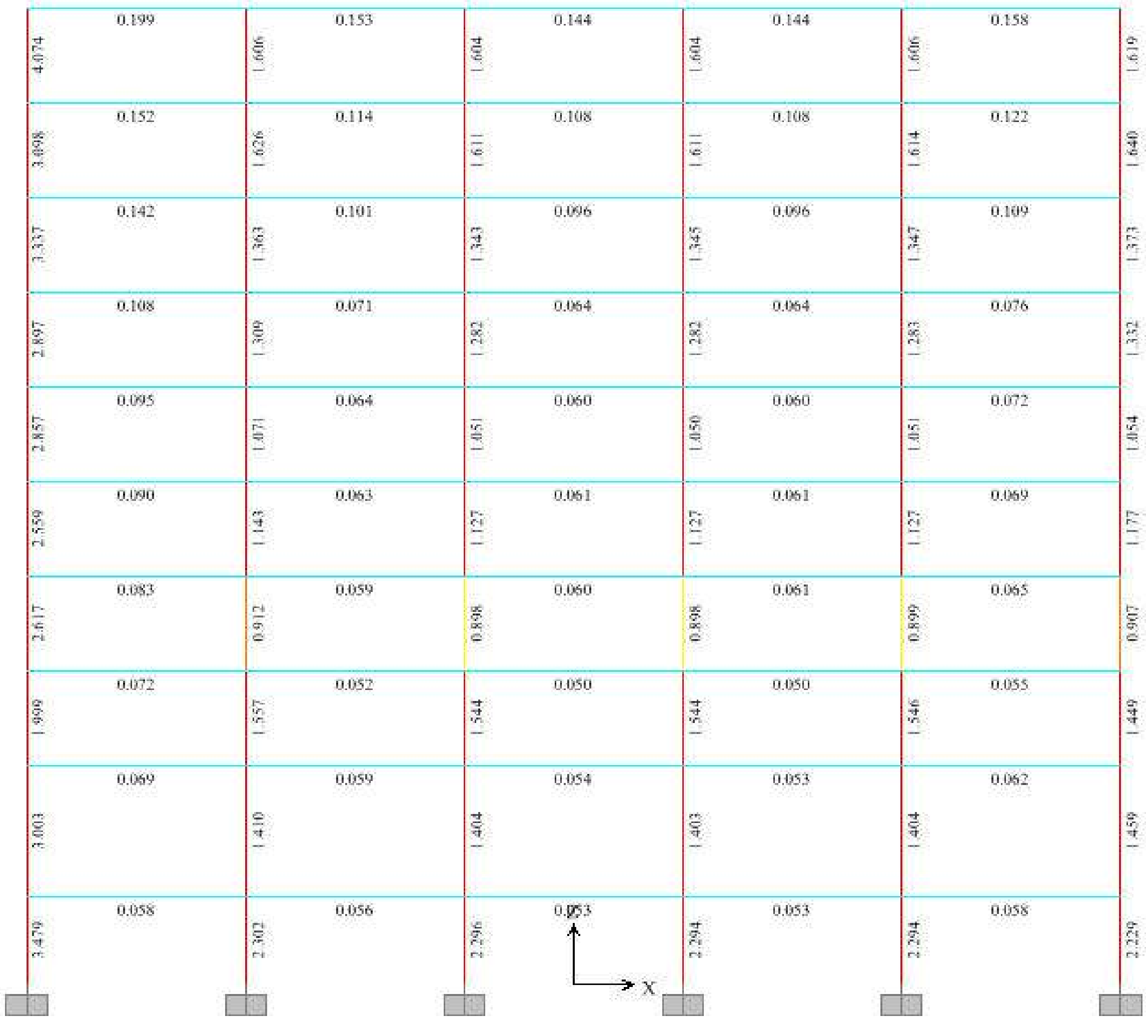

(a) Demand/Capacity Ratio of Transverse Direction (Rigid Diaphragm Analysis)

Figure 7.29 : Demand/Capacity Ratio of MRF Frames (Rigid Diaphragm Analysis)

“Figure 7.29 : Continued”

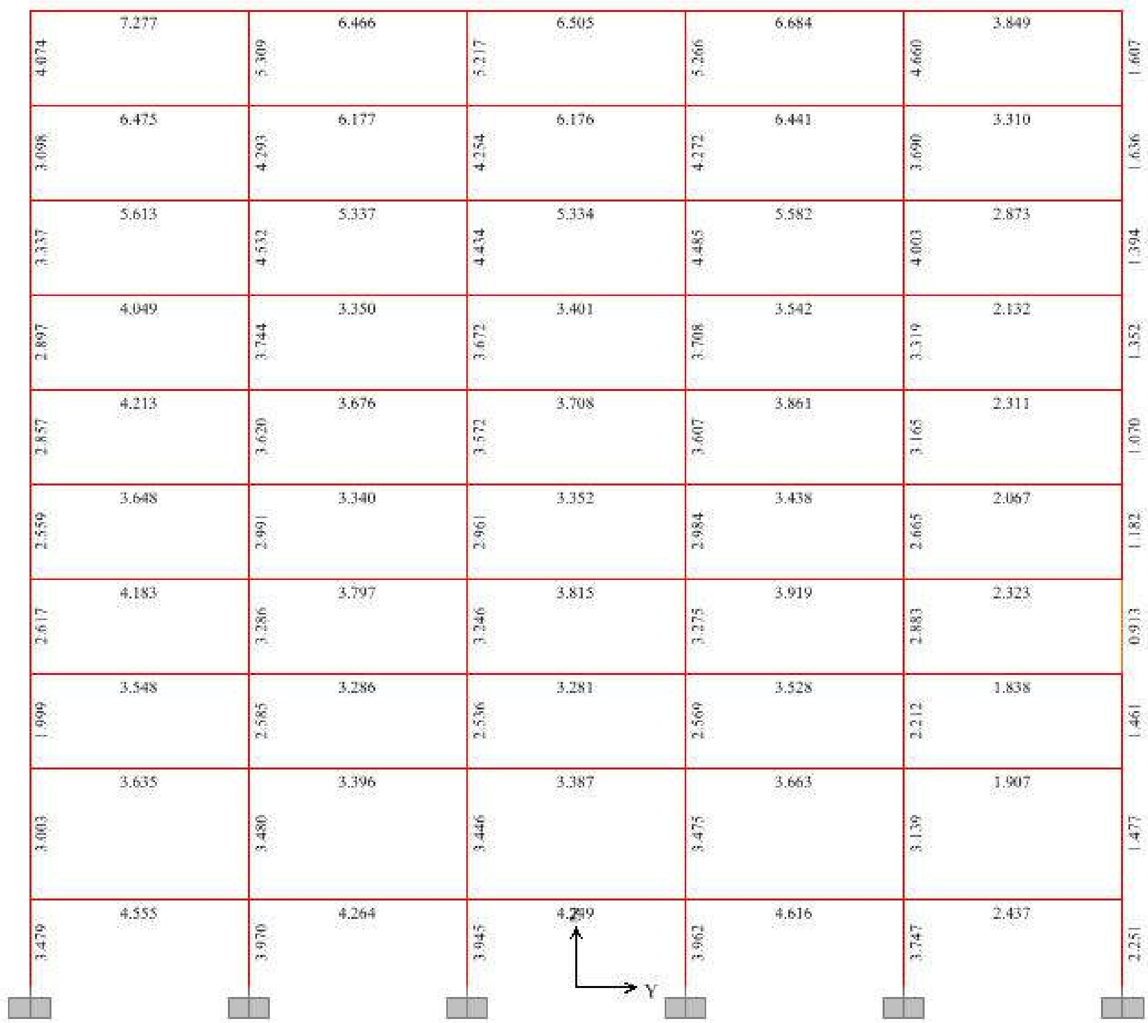

(b) Demand/Capacity Ratio of Longitudinal Direction (Rigid Diaphragm Analysis)

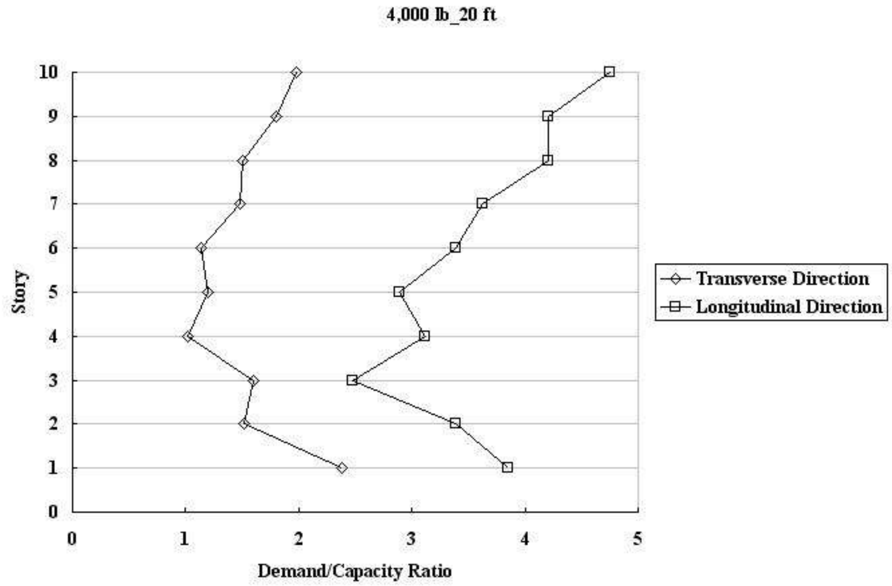

Figure 7.30 : Max. Demand/Capacity Ratio under Blast Load (Columns along Transverse Direction and Longitudinal Direction – Flexible Diaphragm Analysis)

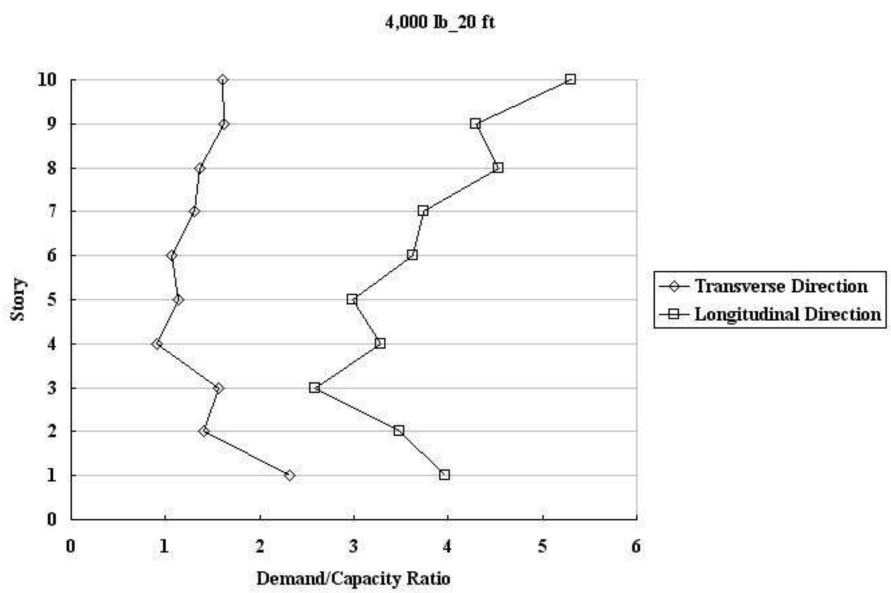

Figure 7.31 : Max. Demand/Capacity Ratio under Blast Load (Columns along Transverse Direction and Longitudinal Direction – Rigid Diaphragm Analysis)

7.4. Nonlinear Analysis of Ten Story Building

1. The maximum displacement through 6th floor and 9th floor in case of earthquake is greater than that of blast loads. However, in cases of 3,000 lb and 4,000 lb TNT weights at 20 ft stand-off distance, the displacement of earthquake is less through the first floor and 5th floor as shown in Figure 7.32.

2. An important parameter in earthquake resistant design is the interstory drift index that is obtained by dividing the maximum relative story displacement by the story height. The UBC requires that for structures having a period greater than 0.7 seconds the interstory drift be limited to 0.02. As results of nonlinear analysis for blast loads, the drift ratio is above the code limitation in case of 3,000 lb and 4,000 lb TNT weights at 20 ft stand-off distance. In case of earthquake, the drift ratio is well satisfied with limiting code value in exception through 3rd floor and 5th floor as shown in Figure 7.33.

3. The value of demand/capacity ratio is lower than one of D/C ratio obtained linear analysis due to reduction of moment demand as shown in Figure 7.34.

4. Demands for the 1,000 lb TNT weight @ 20 ft and 2,000 lb TNT weight @ 20 ft are summarized in Table 7.5 and Table 7.6. Table 7.5 is shown that the columns (1, 11) at 1st floor that exceed the elastic limit have small plastic rotation demands along longitudinal directions. According to the FEMA recommendations, this building would be classified as suitable for immediate occupancy (IO). In Table 7.6, the behaviors of the longitudinal columns (10, 20) at roof level are linear and other members that exceed the elastic limit have small plastic rotation demands along both directions.

5. The demands for extreme condition of 3,000 lb @ 20 ft and 4,000 lb @ 20 ft are summarized in Table 7.7 and Table 7.8. Here it can be seen that most cases have more plastic rotation demands along both directions than previous cases. However, columns (10, 20) on roof level through longitudinal direction are still in linear ranges. According to the recommendations of FEMA, this building under 3,000 lb TNT weight and 4,000 lb TNT weight at 20 ft would be classified as suitable for life safety (LS) and collapse prevention (CP) respectively. Demands for earthquake recorded Newhall Fire Station are summarized in Table 7.9. It is shown that the demands of column of both directions are still elastic but girders have small plastic rotation demands along longitudinal direction. According to the FEMA recommendations, this building would be classified as suitable for immediate occupancy (IO)

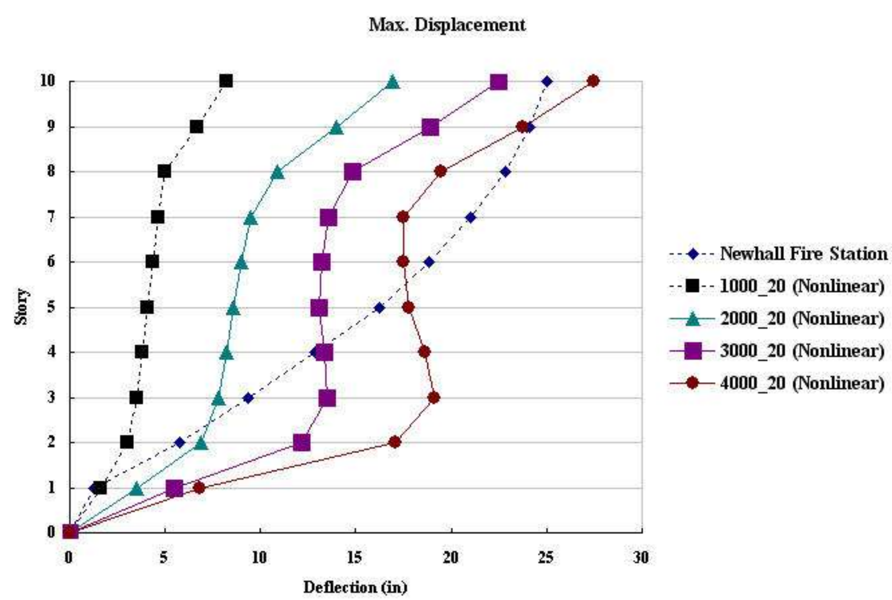

Figure 7.32 : Max. Deflection Envelope of Each Floor under Northridge Earthquake and Blast Loads

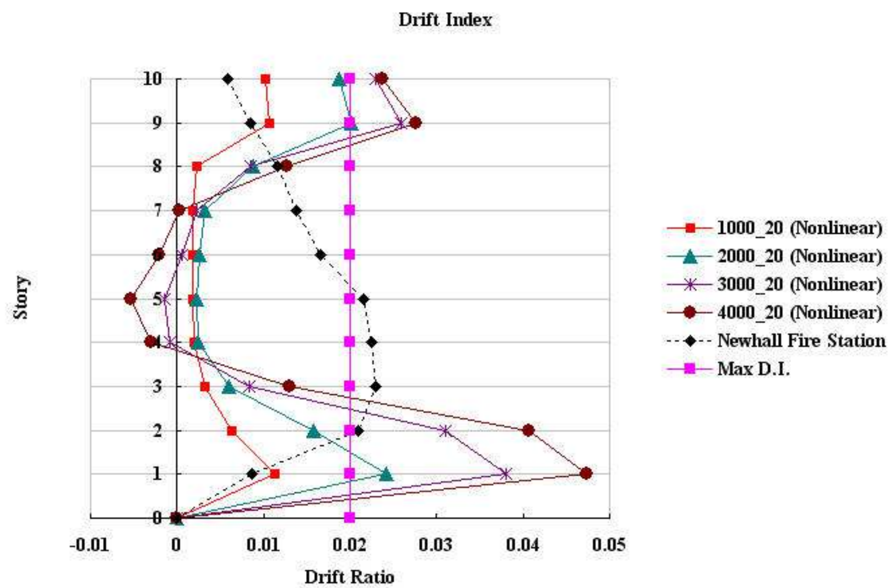

Figure 7.33 : Max. Interstory Drift of Northridge Earthquake and Blast Loads

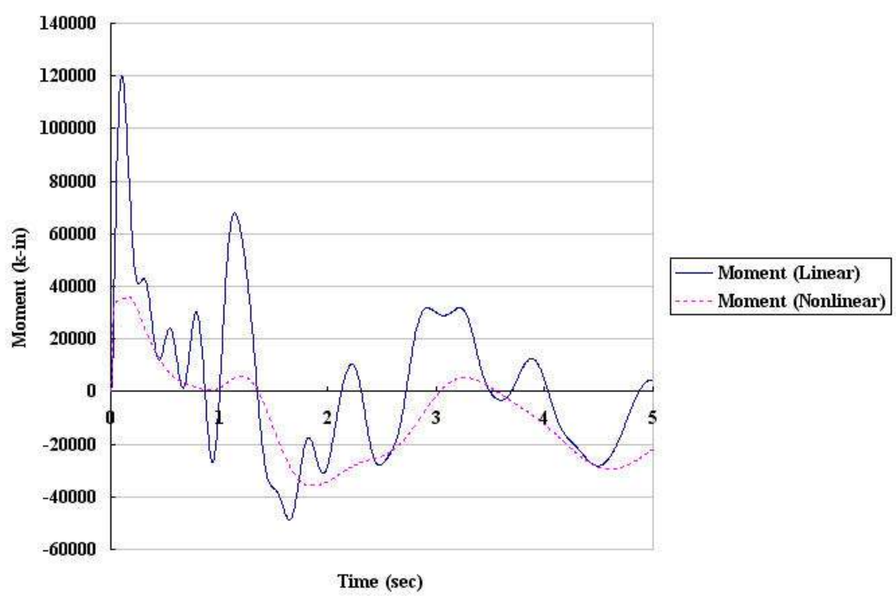

Figure 7.34 : Comparison of Moment Demand Resulted from Linear and Nonlinear Analysis for Longitudinal Girder

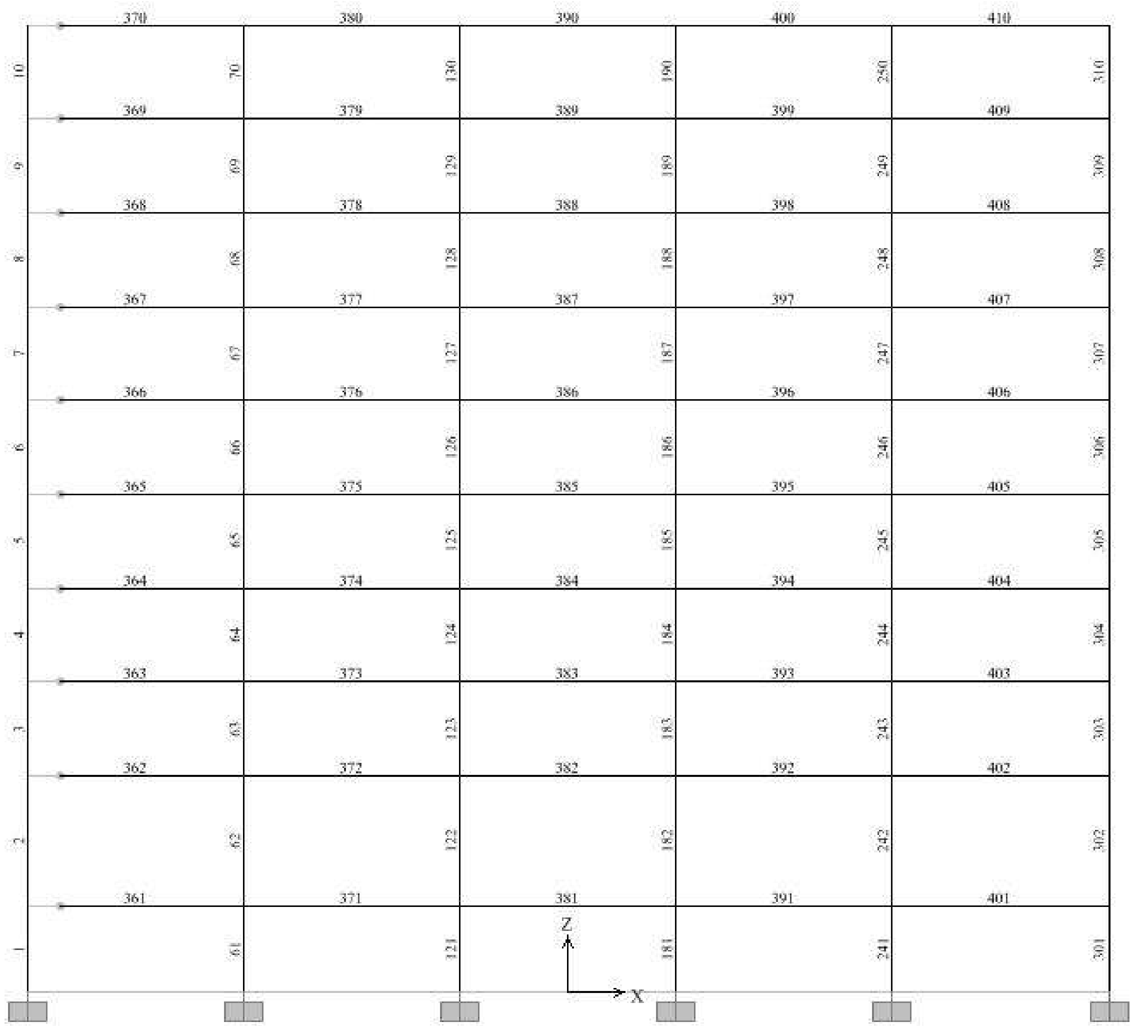

(a) Generated Member Numbers along the Transverse Direction

Figure 7.35 : Generate Members along Both Direction

“Figure 7.35 : Continued”

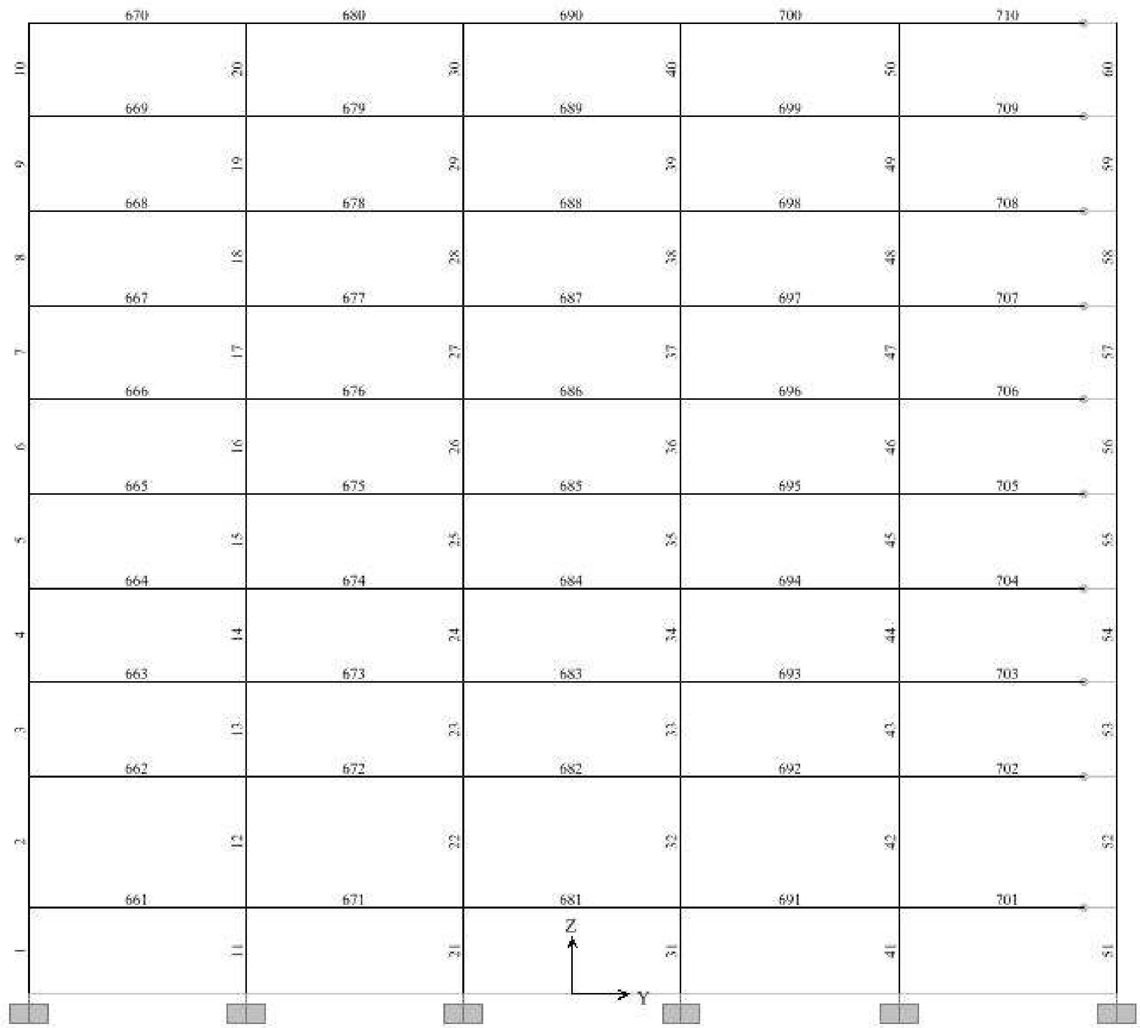

(b) Generated Member Numbers along the Longitudinal Direction

Table 7.5 : Acceptance Criteria for Nonlinear Procedures (1,000 lb @ 20 ft)

Case	Member	Section	θy	θp	a	b	Hinge State
1,000 lb @ 20 ft	Column (Longitudinal)	No. 1 (1st Floor)	0.0061	0.0021	0.0554	0.0677	< IO
		No. 10 (Roof)	0.0071	0	0.0643	0.0786	Linear
		No. 11 (1st Floor)	0.0058	0.0030	0.0524	0.0640	< IO
		No. 20 (Roof)	0.0070	0	0.0636	0.0777	Linear
	Column (Transverse)	No. 61 (1st Floor)	0.0080	0	0.0743	0.0908	Linear
		No. 121 (1st Floor)	0.0080	0	0.0743	0.0908	Linear
	Beam (Longitudinal)	No. 661 (1st Floor)	0.0070	0	0.0658	0.0805	Linear
		No. 670 (1st Floor)	0.0110	0	0.1011	0.1236	Linear

Table 7.6 : Acceptance Criteria for Nonlinear Procedures (2,000 lb @ 20 ft)

Case	Member	Section	θy	θp	a	b	Hinge State
2,000 lb @ 20 ft	Column (Longitudinal)	No. 1 (1st Floor)	0.0061	0.0153	0.0554	0.0677	IO - LS
		No. 10 (Roof)	0.0071	0	0.0643	0.0786	Linear
		No. 11 (1st Floor)	0.0058	0.0158	0.0524	0.0640	IO - LS
		No. 20 (Roof)	0.0070	0	0.0636	0.0777	Linear
	Column (Transverse)	No. 61 (1st Floor)	0.0080	0.0105	0.0743	0.0908	IO - LS
		No. 121 (1st Floor)	0.0080	0.0105	0.0743	0.0908	IO - LS
	Beam (Longitudinal)	No. 661 (1st Floor)	0.0070	0.0078	0.0658	0.0805	IO - LS
		No. 670 (1st Floor)	0.0110	0.0029	0.1011	0.1236	< IO

Table 7.7 : Acceptance Criteria for Nonlinear Procedures (3,000 lb @ 20 ft)

Case	Member	Section	θy	θp	a	b	Hinge State
3,000 lb @ 20 ft	Column (Longitudinal)	No. 1 (1st Floor)	0.0061	0.02830	0.0554	0.0677	IO - LS
		No. 10 (Roof)	0.0071	0	0.0643	0.0786	Linear
		No. 11 (1st Floor)	0.0058	0.02892	0.0524	0.0640	IO - LS
		No. 20 (Roof)	0.0070	0	0.0636	0.0777	Linear
	Column (Transverse)	No. 61 (1st Floor)	0.0080	0.02311	0.0743	0.0908	IO - LS
		No. 121 (1st Floor)	0.0080	0.02311	0.0743	0.0908	IO - LS
	Beam (Longitudinal)	No. 661 (1st Floor)	0.0070	0.01899	0.0658	0.0805	IO - LS
		No. 670 (1st Floor)	0.0110	0.0058	0.1011	0.1236	< IO

Table 7.8 : Acceptance Criteria for Nonlinear Procedures (4,000 lb @ 20 ft)

Case	Member	Section	θy	θp	a	b	Hinge State
4,000 lb @ 20 ft	Column (Longitudinal)	No. 1 (1st Floor)	0.0061	0.0367	0.0554	0.0677	LS - CP
		No. 10 (Roof)	0.0071	0	0.0643	0.0786	Linear
		No. 11 (1st Floor)	0.0058	0.0375	0.0524	0.0640	LS – CP
		No. 20 (Roof)	0.0070	0	0.0636	0.0777	Linear
	Column (Transverse)	No. 61 (1st Floor)	0.0080	0.0305	0.0743	0.0908	IO - LS
		No. 121 (1st Floor)	0.0080	0.0305	0.0743	0.0908	IO - LS
	Beam (Longitudinal)	No. 661 (1st Floor)	0.0070	0.0307	0.0658	0.0805	IO - LS
		No. 670 (1st Floor)	0.0110	0.006	0.1011	0.1236	< IO

Table 7.9 : Acceptance Criteria for Nonlinear Procedures (Earthquake)

Case	Member	Section	θy	θp	a	b	Hinge State
Recorded At Newhall Fire Station	Column (Longitudinal)	No. 1 (1st Floor)	0.0061	0	0.0554	0.0677	Linear
	Column (Transverse)	No. 121 (1st Floor)	0.0080	0	0.0743	0.0908	Linear
	Beam (Longitudinal)	No. 661 (1st Floor)	0.0070	0.002	0.0658	0.0805	< IO
		No. 670 (1st Floor)	0.0110	0.002	0.1011	0.1236	< IO

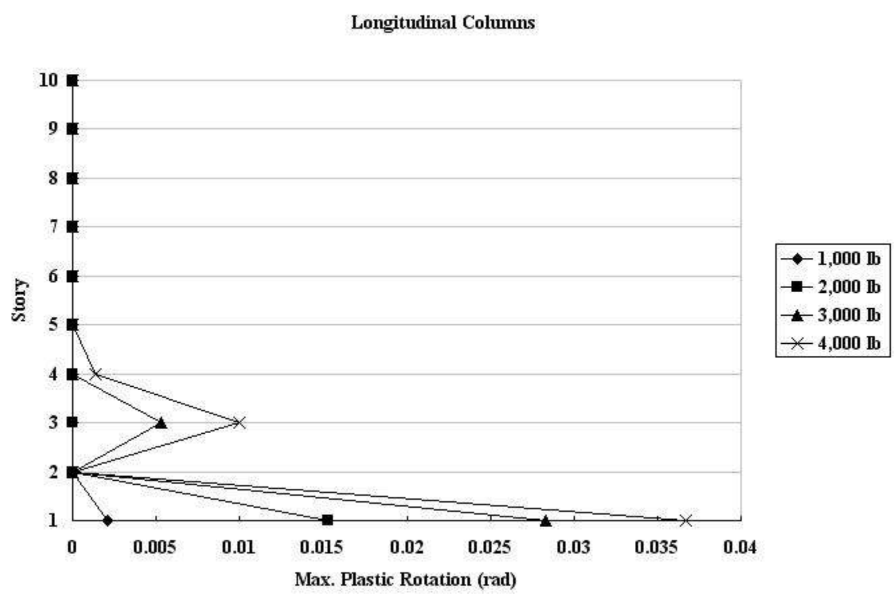

Figure 7.36 : Max. Plastic Rotation at Each Story (Longitudinal Columns)

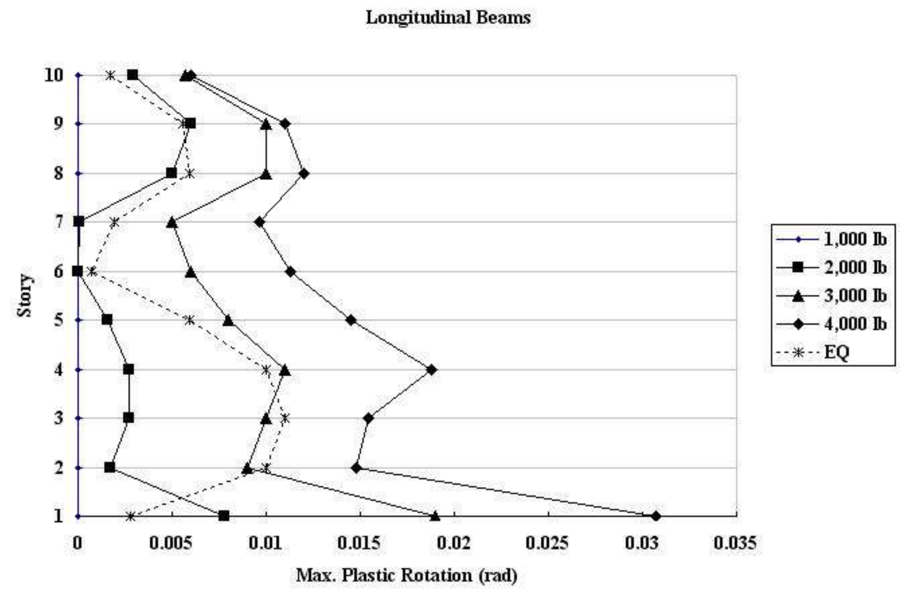

Figure 7.37 : Max. Plastic Rotation at Each Story (Longitudinal Beams)

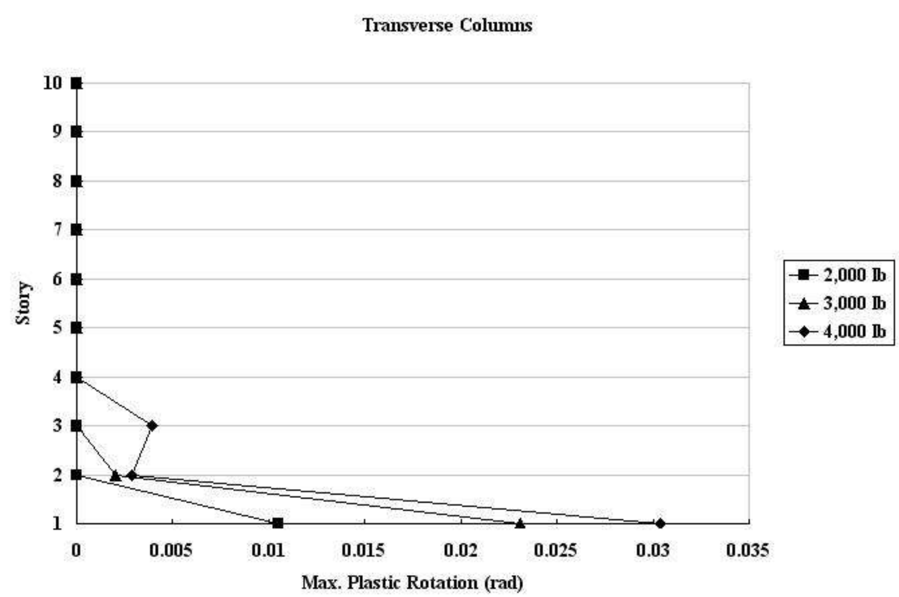

Figure 7.38 : Max. Plastic Rotation at Each Story (Transverse Columns)

7.5. Comparison of Single-Degree of Freedom analysis Between Steel and Concrete Column on Murrah Building

The Murrah building represents one structural system, a reinforced concrete ordinary moment frame (OMF), gravity –load-resisting system with reinforced concrete shear walls used to resist lateral wind loads [14]. The structure was a nine story building reinforced concrete frame. However, the principal exterior columns supporting the transfer girder and the floor slabs of the building did not provide any deliberate resistance against a vehicular bomb attack. In this chapter, substituting concrete column used in murrah building for steel column used in chapter 5, the effect of steel column is investigated using single degree of freedom analysis [5]. As indicated in Figure 7.33, its response to blast load is approximated as a simply supported beam between the first- and third floor elevations [5]. The column resisted blast loads about its weak axis as shown in Figure 7.34. The blast loads was 4,000 lb TNT weight at 14 ft and it directly removed a principal exterior column [14].

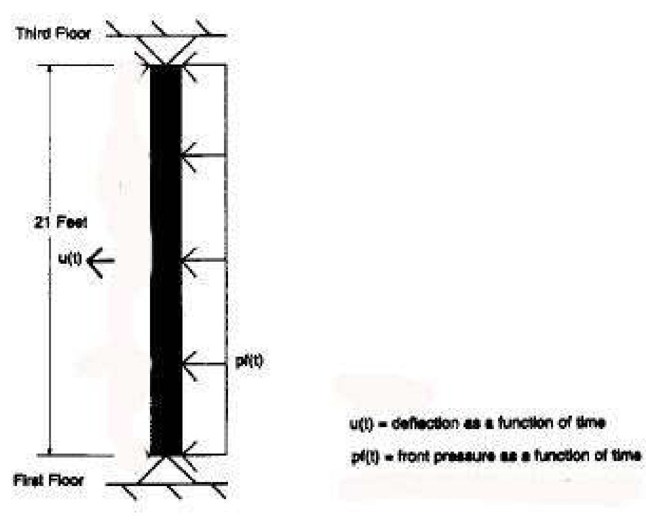

Figure 7.39 : Model of Column (Single Degree of Freedom)

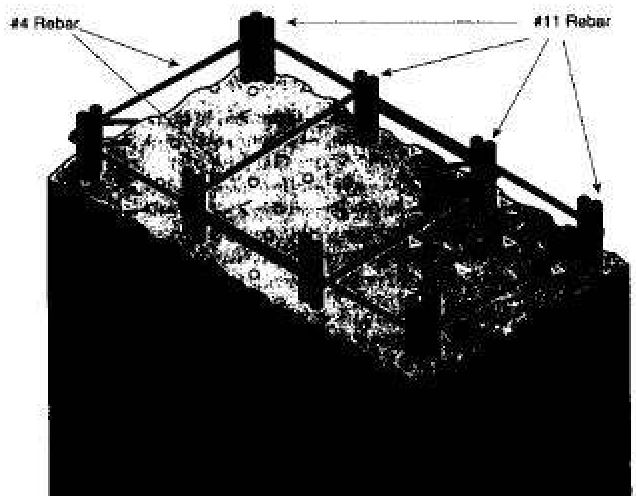

Figure 7.40 : Cross Section of Column

On the front face of this column, the blast load rises abruptly to the reflected pressure, 1,400 lb per square inch [14]. Therefore this blast load is used in this chapter to compare concrete and steel column. Table 7.10 contain the nominal flexural strength of the concrete column section and used in the calculations. The flexural strength was based on the following expression.

$$M_u = A_s f_y \left(1 - 0.5 \frac{\rho f_y}{0.85 f_c^{'}} \right)$$

Where, Mu = flexural moment strength of a reinforced section; As = total cross-sectional area of tensile reinforcement; fy = yielding strength of the tensile reinforcement; d = distance from top fiber in compression to centroid of tensile reinforcement

Table 7.10 : Calculated Flexural Strength of Concrete Column

Measurement	Concrete Column (Murrah Building)
width (in)	36
Effective depth (in)	20
Number of bars	11
Bar area (sq. in)	1.56
Sum area (sq. in)	15.6
Flexural Moment Strength (thousand of pound-feet)	1270.94

Note : Concrete design strength = 4,000 lb per sq in. Steel design yield stress = 60,000 lb per sq in.

Table 7.11 is shown that material properties of steel column used in chapter 5. These data is used to calculate period, plastic moment and maximum resistance.

Table 7.11 : Material Properties of Steel Column Used in Chapter 5

Measurement	Steel Column about Weak Axis (W14*500)	Steel Column about Strong Axis (W14*500)
Width (in)	19.6	17
Depth (in)	17	19.6
Plastic Modulus of Strong Axis (cu. in)	-	1050
Plastic Modulus of Weak Axis (cu. in)	522	-
Yield stress (lb per sq. in)	29000000	29000000

Table 7.12 : The results of Single Degree of Freedom Analysis

Results	Concrete Column	Steel Column with Weak Axis	Steel Column with Strong Axis
T_d/T	0.32	0.38	0.65
R/F	0.11	0.11	0.28
Required Ductility Ratio	60	62	40

The results of single degree of freedom analysis are shown in Table 7.12. It indicates that required ductility ratio [5] of concrete column and steel column with weak axis is similar value but steel column with strong axis has reduction of 35%.

7.6. Comparison of the Murrah Building and 10 Story Building

According to The Oklahoma City Bombing [14], it is inferred that the blast was equivalent to the detonation of 4,000 lb of TNT at 14 ft. The blast caused the removal of nearest column (G20) by brisance as well as the shear failure of columns G16 and G24 as shown in Figure 7.41. With this loss of three intermediate principal columns, the transfer girder supporting the upper portion of the building on the west side collapsed.

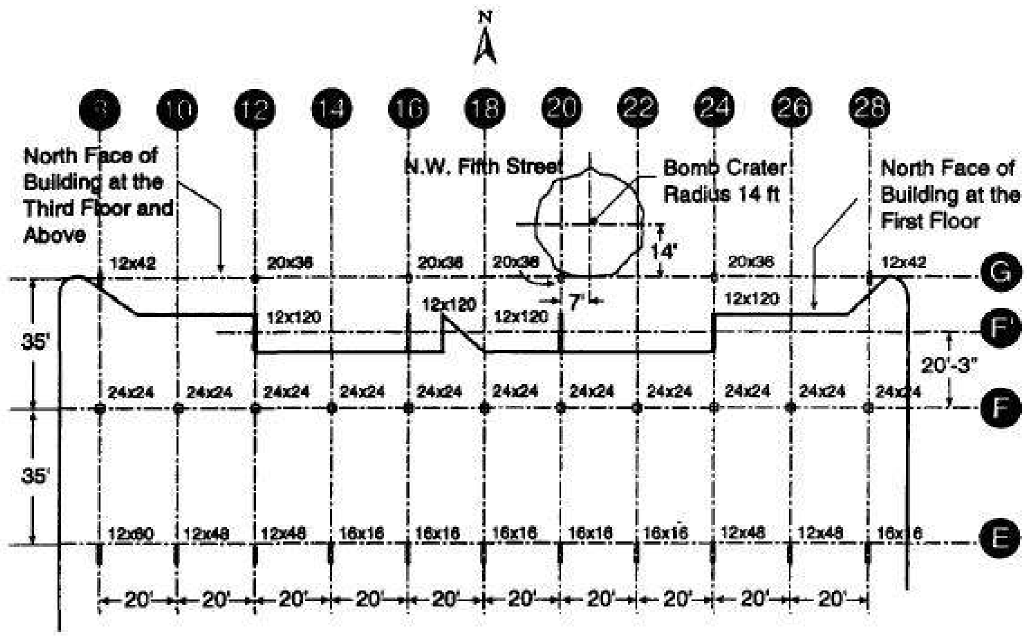

Figure 7.41 : Column Locations and Dimensions

To compare 10 story building with Murrah building, same blast loads and stand-off distance are applied to 10 story building. The demand/capacity ratio of critical structural elements to this loading (4,000 lb TNT weight at 14 ft) is computed using flexible diaphragm and rigid diaphragm analysis. As results of two analyses, the higher D/C ratios occur in columns at 1st

floor level through both directions. In addition, the D/C ratio of longitudinal direction is higher than that of transverse direction as shown in Figure 7.42 – Figure 7.45. It is indicated that the diaphragm is distributing the blast loads from the front face to the other frames on the perimeter provided it remains intact.

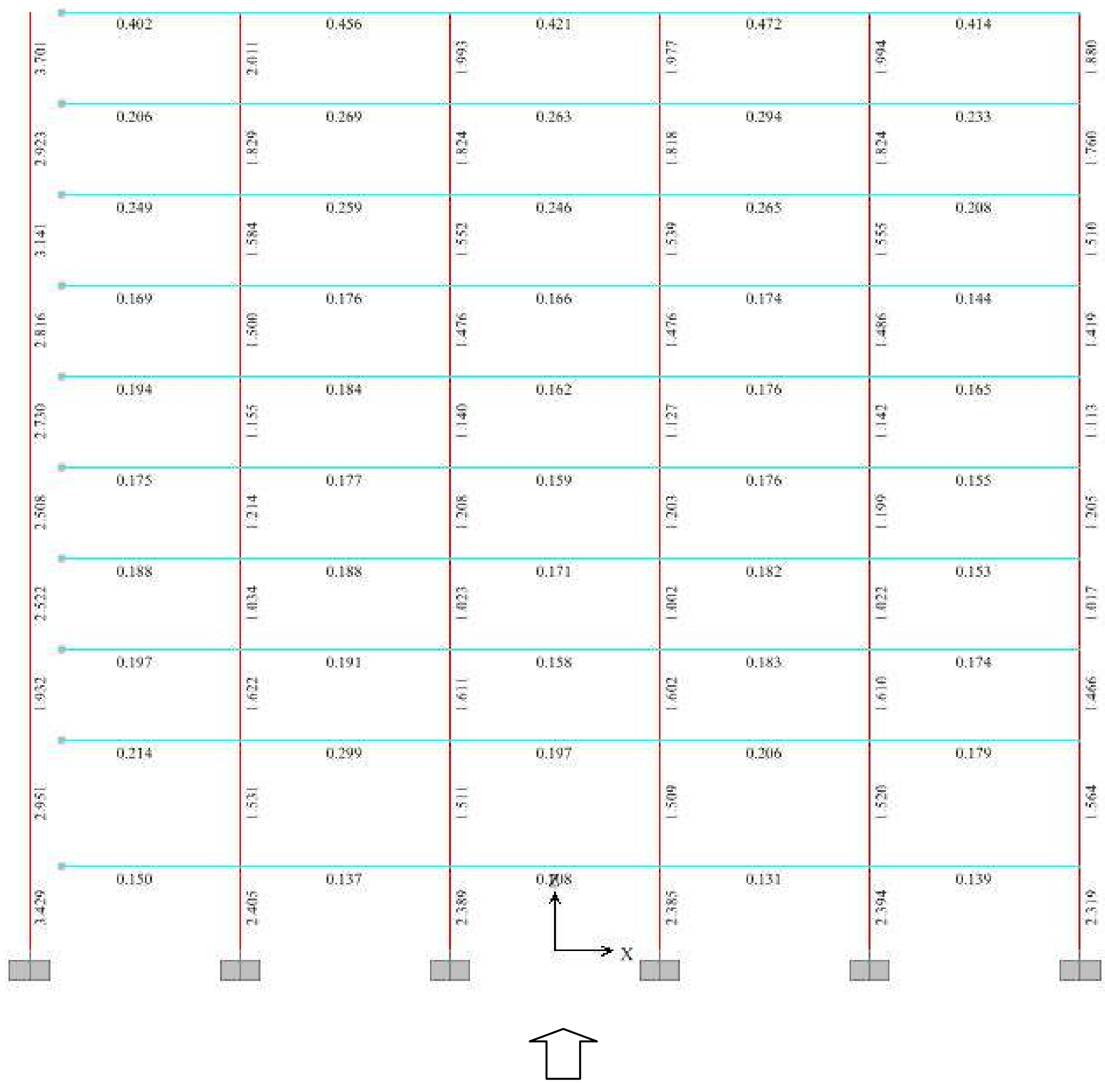

(a) Demand/Capacity Ratio of Transverse Direction (Flexible Diaphragm Analysis)

Figure 7.42 : Demand/Capacity Ratio of MRF Frames (Flexible Diaphragm)

“Figure 7.42 : Continued”

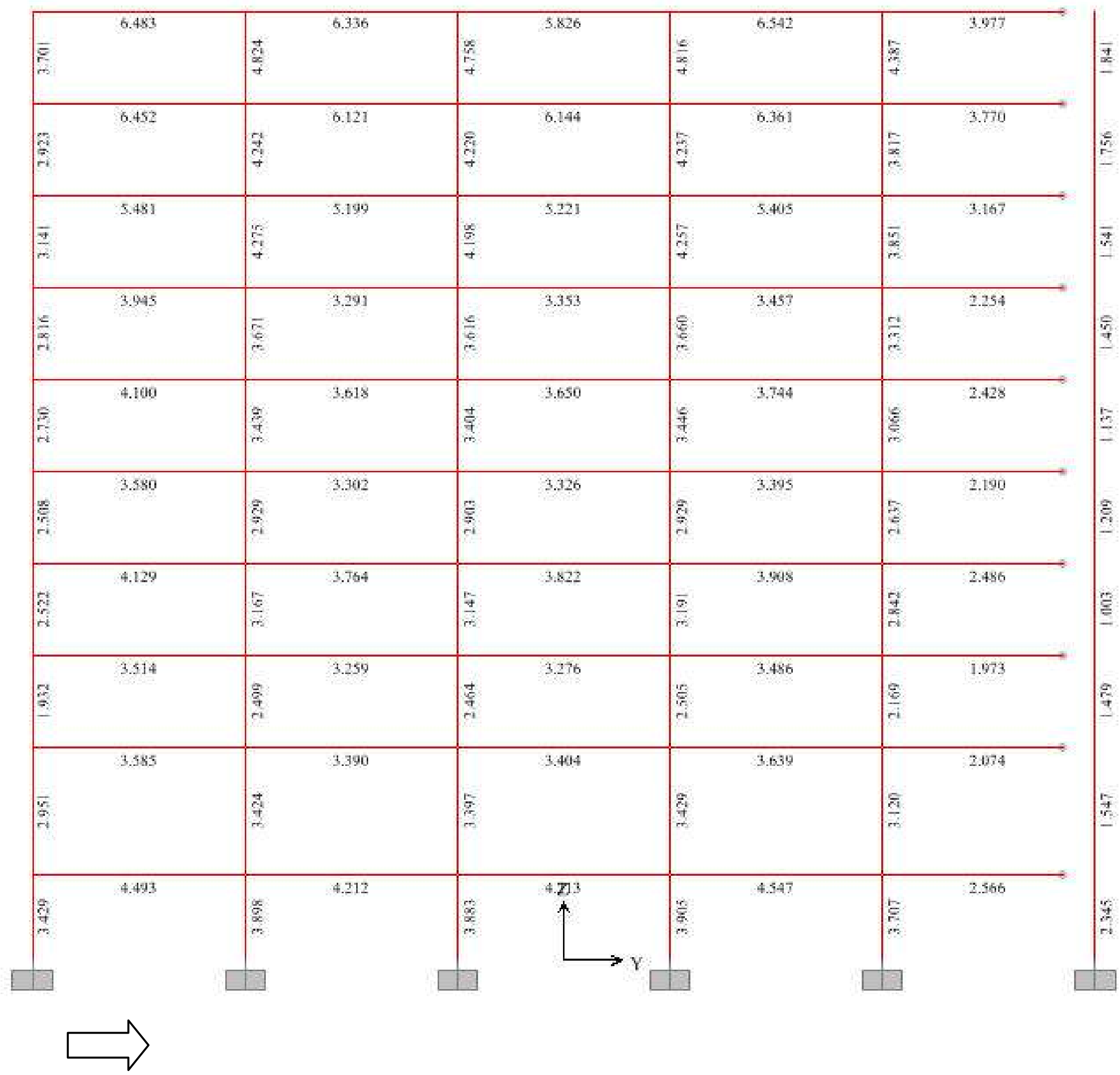

(b) Demand/Capacity Ratio of Longitudinal Direction (Flexible Diaphragm Analysis)

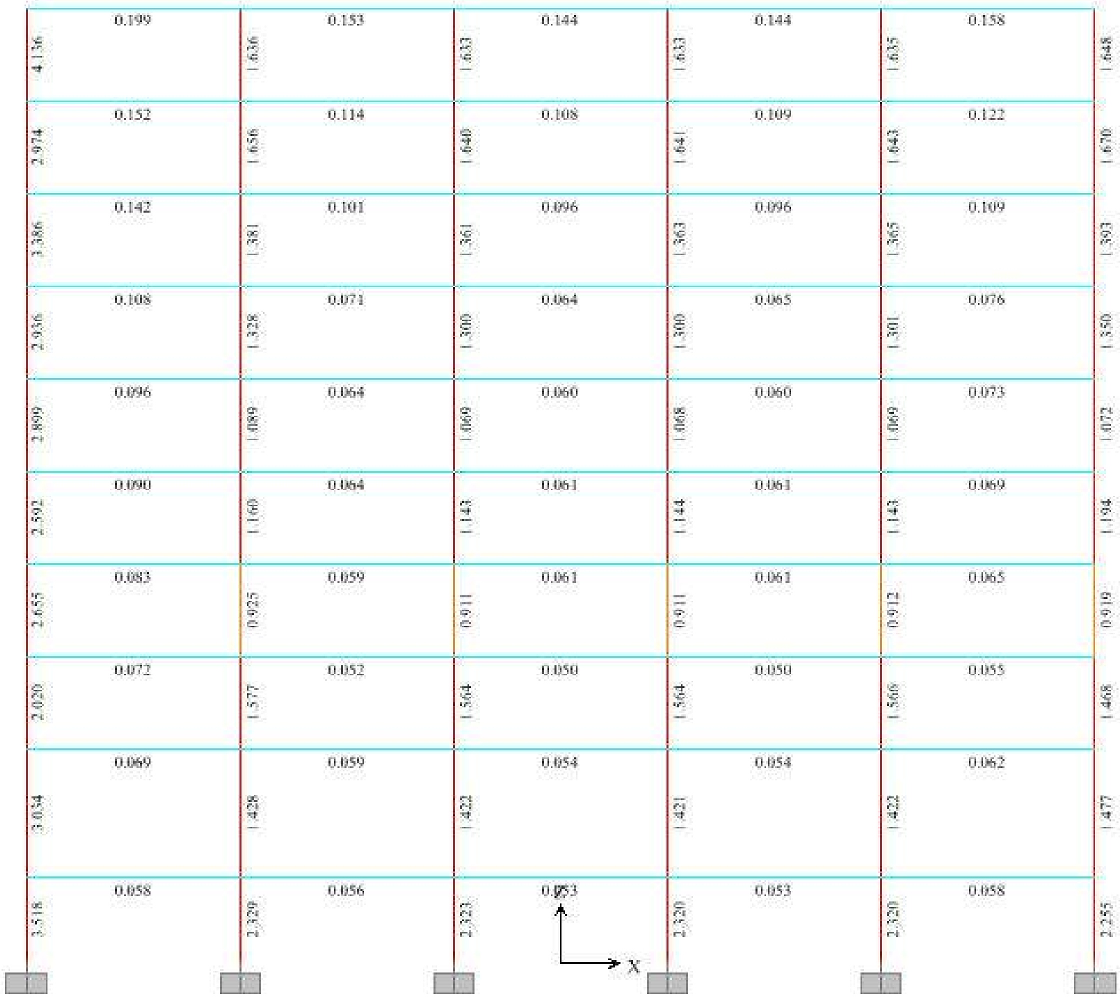

(a) Demand/Capacity Ratio of Transverse Direction (Rigid Diaphragm Analysis)

Figure 7.43 : Demand/Capacity Ratio of MRF Frames (Rigid Diaphragm Analysis)

"Figure 7.43 : Continued"

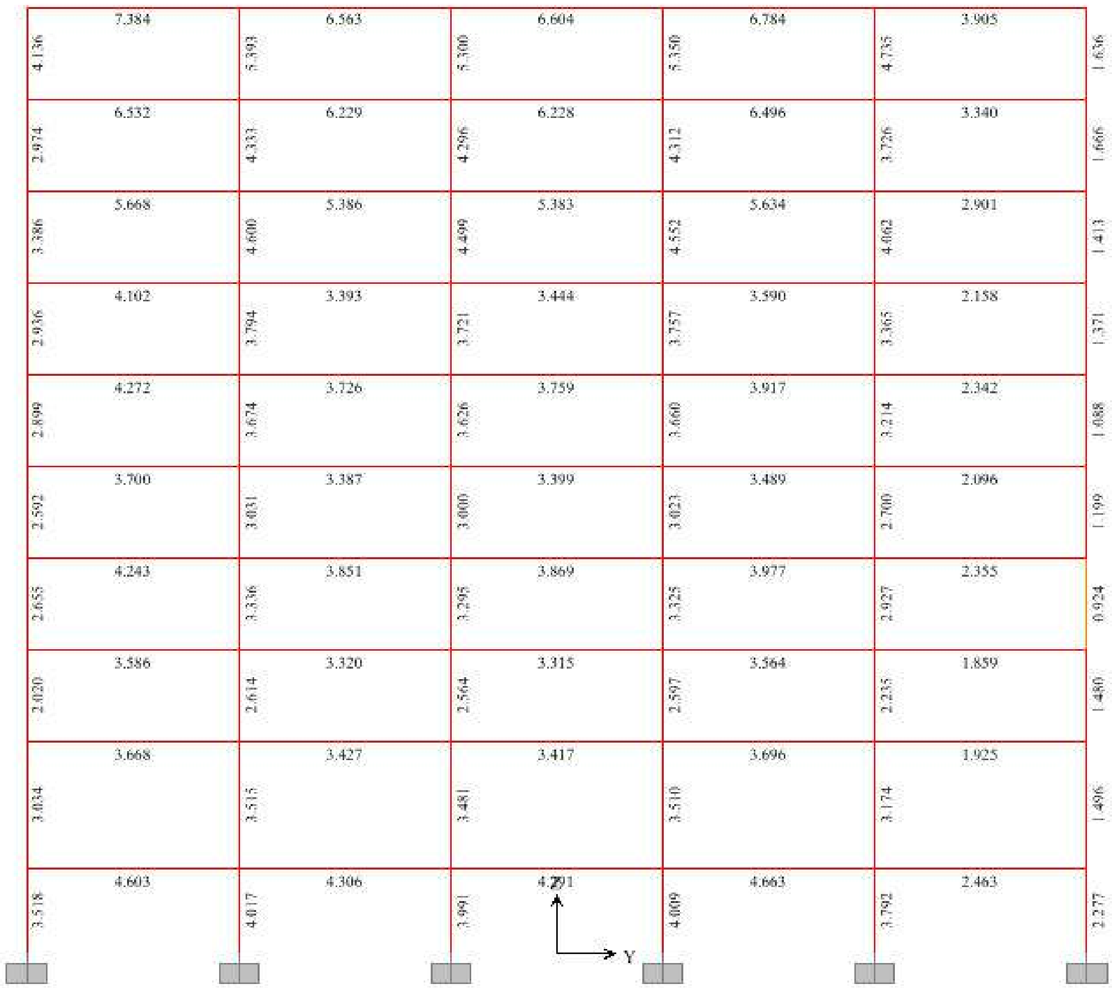

(b) Demand/Capacity Ratio of Longitudinal Direction (Rigid Diaphragm Analysis)

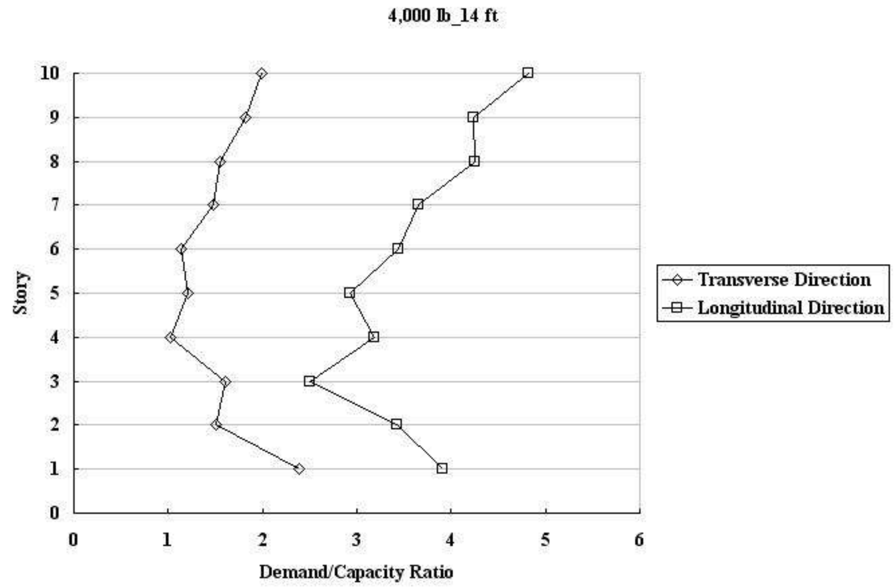

Figure 7.44 : Max. Demand/Capacity Ratio under Blast Load (Columns along Transverse Direction and Longitudinal Direction – Flexible Diaphragm Analysis)

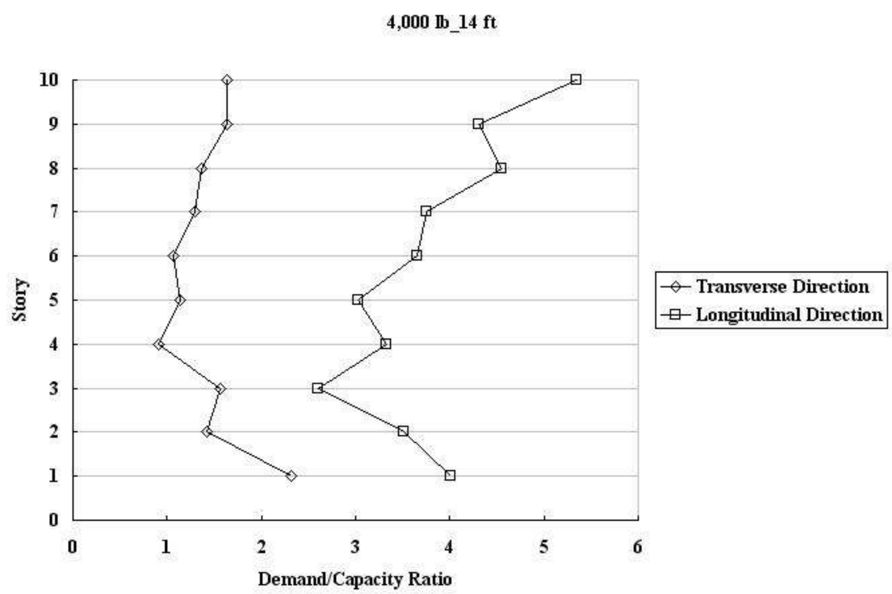

Figure 7.45 : Max. Demand/Capacity Ratio under Blast Load (Columns along Transverse Direction and Longitudinal Direction – Rigid Diaphragm Analysis)

References

[1] American Concrete Institute. (1989). “Building coded requirements for reinforced concrete [ACI 318-89]”. Detroit, Mich.

[2] AISC. “Load and Resistance Factor Design Specification for Structural Steel”, 2001. Buildings, AISC, Chicago, IL.

[3] AT blast version 2.0. Applied Research Associates, Inc., Vicksburg, Miss., 2,000.

[4] Brode H.L., “Numerical solution of spherical blast wave”., Journal of Applied Physics, American institute of Physics, New York, 1964.

[5] Biggs, John M., “Introduction to Structural Dynamics”, McGrew-Hill, 1964.

[6] Baker, W.E.. “Explosions in Air”. University of Texas Press, Austin, TX., 1973.

[7] Beshara, F.B.A. Modeling of Blast Loading on Aboveground Structures — “General Phenomenology and External Blast”, Computers & Structures, Vol. 51, No. 5., 1994. pp. 585-596.

[8] Conrath, E.J., Krauthammer, T., Marchand, K.A., and Mlakar, P.F. Structural “Design for Physical Security” State of the Practice. ASCE, Reston, VA., 1999.

[9] Federal Emergency Management Agency(2,000). “Prestandard and Commentary for the Seismic Rehabilitation of Buildings”, FEMA356, November 2,000.

[10] Federal Emergency Management Agency(2003). “Reference Manual to Mitigate Potential Terrorist Attacks Against Buildings”, FEMA426, December 2003.

[11] ICBO, “Uniform Building Code, Vol. 2”, Whittier, CA, 1997.

[12] ICBO, “Uniform Building Code, Vol. 2”, Whittier, CA, 1994.

[13] Joshep W. Tedesco, William G. McDougal, C. Allen Ross., “Structural Dynamics Theory and Applications”, Addison-Wesley., 1999.

[14] John R. Hayes, Jr., Stanley C. Woodson, Robert G. Pekelnicky, Chris D. Poland, W. Gene Corley, and Mete Sozen., “Can Strengthening for Earthquake Improve Blast and Progressive Collapse Resistance?”, Journal of Structural Engineering, vol. 131, No.8, August1, 2005. pp1157 – 1177.

[15] Krauthammer, T. “Blast-resistant Structural Concrete and Steel Connections”, International Journal of Impact Engineering, Vol. 22, No. 9-10, pp. 887-910., 1999

[16] Longinow, A. and Mniszewski, K.R. “Protecting Buildings Against Vehicle Bomb Attacks”, Practice Periodical on Structural Design and Construction, Vol. 1, No. 1, pp. 51-54., 1996.

[17] Longinow A, and Mniszewski KR., “Protecting buildings against vehicle bomb attacks., Practice Periodical on Structural Design and Construction”, ASCE, New York, pp. 51-54, 1996.

[18] Miyamoto, H.K. and Taylor, D. “Structural Control of Dynamic Blast Loading”, Advanced Technology in Structural Engineering, Proceedings from Structures Congress, ASCE, Reston, VA., 2,000.

[19] Norris, C. H., Hansen, R. J., Holley, M. J., Biggs, J. M., Namyet, S., and Minami, J. K., “Structural Design for Dynamic Loads”, McGraw Hill, New York, 1959.

[20] Newmark, N. M. and Hansen, R. J., “Design of blast resistant structures”, shock and vibration Handbook, Vol. 3, Eds. Harris and Crede. McGrew-Hill, New York, USA. 1961.

[21] SAP2000, Version 9, Computers and Structures, Inc., Berkeley, CA, 2004.

[22] SAP2000, Version 14, Computers and Structures, Inc., Berkeley, CA, 2007.

[23] SDI “Steel Deck Institute”, Standard for Composite Steel Floor Deck, ANSI/SDI C1.0 – 2006

[24] Smith P. D. and Hetherington J. G. “Blast and Ballistic Loading of Structures”, Butterworth-Heinemann, 1994.

[25] UFC 4-010-01, “DoD Minimum Antiterrorism Standards for Buildings”, U. S. Department of Defense, 31 July 2002.

[26] U.S. Department of the Army. “Fundamentals of Protective Design for Conventional Weapons”, TM 5-855-1. Washington, DC, Headquarters, U.S. Department of the Army., 1986.

[27] U.S. Department of the Army. “Structures to Resist the Effects of Accidental Explosions”, TM 5-1300, Navy NAVFAC P-397, AFR 88-2., Washington, DC, U.S. Department of the Army, Navy and Air Force., 1990.

[28] Uniform Building Code 1997, Structural Engineering Design Provisions (Uniform Building Code Vol 2: Structural Engineering Design Provisions)

Appendix A : Comparisons of ATBLAST and CONWEP

A.1. The Incident Pressure and Reflected Pressure of ATBLAST Program

Table A. 1 : Incident Pressure (2,000 lb TNT Weight @ 900 ft -1,000 ft, ATBLAST)

Range (ft)	Velocity (ft/msec)	Time of Arrival (msec)	Pressure (psi)	Impulse (psi-msec)	Load Duration (msec)
900	1.13	717.16	0.56	15.8	56.57
910	1.13	726.01	0.55	15.63	56.8
920	1.13	734.84	0.54	15.46	57.04
930	1.13	743.68	0.53	15.29	57.27
940	1.13	752.51	0.53	15.13	57.51
950	1.13	761.33	0.52	14.97	57.74
960	1.13	770.15	0.51	14.81	57.98
970	1.13	778.96	0.5	14.65	58.22
980	1.13	787.77	0.5	14.5	58.46
990	1.13	796.58	0.49	14.35	58.69
1,000	1.13	805.37	0.48	14.21	58.93

Table A. 2 : Reflected Pressure (2,000 lb TNT Weight @ 900 ft -1,000 ft, ATBLAST)

Range (ft)	Velocity (ft/msec)	Time of Arrival (msec)	Pressure (psi)	Impulse (psi-msec)	Load Duration (msec)
900	1.13	717.16	1.14	27.97	49.21
910	1.13	726.01	1.12	27.64	49.39
920	1.13	734.84	1.1	27.33	49.58
930	1.13	743.68	1.09	27.02	49.76
940	1.13	752.51	1.07	26.72	49.95
950	1.13	761.33	1.05	26.43	50.14
960	1.13	770.15	1.04	26.14	50.34
970	1.13	778.96	1.02	25.85	50.53
980	1.13	787.77	1.01	25.58	50.73
990	1.13	796.58	0.99	25.31	50.92
1,000	1.13	805.37	0.98	25.04	51.12

Table A. 3 : Incident Pressure (2,000 lb TNT Weight @ 500 ft -600 ft, ATBLAST)

Range (ft)	Velocity (ft/msec)	Time of Arrival (msec)	Pressure (psi)	Impulse (psi-msec)	Load Duration (msec)
500	1.15	364.75	1.19	28.08	47.31
510	1.15	373.4	1.16	27.55	47.58
520	1.15	382.07	1.13	27.03	47.85
530	1.15	390.76	1.1	26.54	48.11
540	1.15	399.46	1.08	26.07	48.36
550	1.15	408.17	1.05	25.61	48.61
560	1.15	416.89	1.03	25.17	48.86
570	1.15	425.62	1.01	24.74	49.1
580	1.15	434.37	0.99	24.33	49.34
590	1.15	443.12	0.97	23.93	49.58
600	1.15	451.89	0.95	23.54	49.81

Table A. 4 : Reflected Pressure (2,000 lb TNT Weight @ 900 ft -1,000 ft, ATBLAST)

Range (ft)	Velocity (ft/msec)	Time of Arrival (msec)	Pressure (psi)	Impulse (psi-msec)	Load Duration (msec)
500	1.15	364.75	2.45	51.68	42.15
510	1.15	373.4	2.39	50.62	42.37
520	1.15	382.07	2.33	49.61	42.58
530	1.15	390.76	2.27	48.63	42.79
540	1.15	399.46	2.22	47.69	43
550	1.15	408.17	2.17	46.78	43.2
560	1.15	416.89	2.12	45.91	43.39
570	1.15	425.62	2.07	45.07	43.58
580	1.15	434.37	2.02	44.26	43.77
590	1.15	443.12	1.98	43.48	43.95
600	1.15	451.89	1.94	42.72	44.13

Table A. 5 : Incident Pressure (2,000 lb TNT Weight @ 300 ft - 400 ft, ATBLAST)

Range (ft)	Velocity (ft/msec)	Time of Arrival (msec)	Pressure (psi)	Impulse (psi-msec)	Load Duration (msec)
300	1.19	194.72	2.32	46	39.58
310	1.19	203.08	2.22	44.57	40.14
320	1.18	211.45	2.13	43.23	40.68
330	1.18	219.83	2.04	41.96	41.18
340	1.18	228.24	1.96	40.77	41.67
350	1.18	236.65	1.88	39.64	42.13
360	1.17	245.09	1.81	38.58	42.57
370	1.17	253.53	1.75	37.57	42.99
380	1.17	262	1.69	36.61	43.4
390	1.17	270.48	1.63	35.7	43.79
400	1.17	278.97	1.58	34.84	44.17

Table A. 6 : Reflected Pressure (2,000 lb TNT Weight @ 300 ft - 4,000 ft, ATBLAST)

Range (ft)	Velocity (ft/msec)	Time of Arrival (msec)	Pressure (psi)	Impulse (psi-msec)	Load Duration (msec)
300	1.19	194.72	4.97	88.5	35.59
310	1.19	203.08	4.74	85.47	36.07
320	1.18	211.45	4.53	82.64	36.52
330	1.18	219.83	4.33	79.99	36.95
340	1.18	228.24	4.15	77.5	37.36
350	1.18	236.65	3.98	75.16	37.76
360	1.17	245.09	3.83	72.96	38.13
370	1.17	253.53	3.68	70.89	38.5
380	1.17	262	3.55	68.92	38.84
390	1.17	270.48	3.42	67.06	39.18
400	1.17	278.97	3.31	65.3	39.5

Table A. 7 : Incident Pressure (2,000 lb TNT Weight @ 50 ft -150 ft, ATBLAST)

Range (ft)	Velocity (ft/msec)	Time of Arrival (msec)	Pressure (psi)	Impulse (psi-msec)	Load Duration (msec)
50	2.53	10.49	71.47	237.55	6.65
60	2.15	14.76	46.92	199.37	8.5
70	1.91	19.66	32.98	172.23	10.44
80	1.74	25.1	24.47	152.27	12.45
90	1.62	31.02	18.94	136.97	14.47
100	1.53	37.34	15.16	124.8	16.46
110	1.47	44	12.48	114.82	18.4
120	1.42	50.95	10.51	106.44	20.26
130	1.38	58.13	9.01	99.26	22.03
140	1.35	65.51	7.85	93.02	23.7
150	1.32	73.06	6.93	87.52	25.27

Table A. 8 : Reflected Pressure (2,000 lb TNT Weight @ 50 ft -150 ft, ATBLAST)

Range (ft)	Velocity (ft/msec)	Time of Arrival (msec)	Pressure (psi)	Impulse (psi-msec)	Load Duration (msec)
50	2.53	10.49	316.85	687.68	4.34
60	2.15	14.76	182.03	547.87	6.02
70	1.91	19.66	114.62	453.97	7.92
80	1.74	25.1	77.72	386.84	9.95
90	1.62	31.02	55.94	336.62	12.04
100	1.53	37.34	42.23	297.71	14.1
110	1.47	44	33.15	266.71	16.09
120	1.42	50.95	26.86	241.47	17.98
130	1.38	58.13	22.33	220.54	19.75
140	1.35	65.51	18.96	202.9	21.4
150	1.32	73.06	16.4	187.84	22.91

A.2. Input Procedure and Reflected Pressure of CONWEP Program

1. Select types of Blast

```
    CONVENTIONAL WEAPONS EFFECTS

            MAIN MENU

     SELECT FROM THE FOLLOWING:

     1. Airblast
     2. Fragment penetration
     3. Projectile penetration
     4. Projectile path into earth
     5. Shaped charge penetration
     6. Cratering
     7. Ground shock
     8. Change weapon
     9. Change units
    10. Exit

    Enter Selection...   1
```

2. Select Units and Types of Air Blast

```
     6. Cratering
     7. Ground shock
     8. Change weapon
     9. Change units
    10. Exit

    Enter Selection...   1


  Use (1) U.S. or (2) SI units? 1


            AIRBLAST MENU

     SELECT FROM THE FOLLOWING:

 1. Aboveground detonation
 2. Pressure attenuation in a tunnel
 3. Internal detonation
 4. Subsurface detonation
 5. Loads on structures
 6. Return to main menu

 Enter Selection ...   5
```

3. Select of Weapon and Weight

Name		Constant Bx (3)	Constant fps	Eqv. Weight for Pressure	Eqv. Weight for Impulse
1. TNT		0.30	7600.	1.00	1.00
2. ANFO (AmNi/Fuel Oil)	(2)	unknown	unknown	0.820	0.820
3. Composition A-3		0.22	8300.	1.09	1.07
4. Composition B		0.22	8800.	1.11	0.980
5. Composition C-4	(1)	0.22	8300.	1.37	1.19
6. HBX-1		0.26	8100.	1.17	1.16
7. H-6		0.28	8600.	1.38	1.15
8. Octal(75/25)	(1,2)	0.22	9500.	1.06	1.06
9. RDX	(1)	0.22	9300.	1.14	1.09
10. Pentolite		0.25	8100.	1.42	1.00
11. Tritonal	(1)	0.22	7600.	1.07	0.960
12. Other					

Note: (1) - Assumed Bx = Bx for A-3
(2) - Assumed equivalent weight for impulse = equivalent weight for pressure
(3) - Bx is in units of oz.**1/2 / in.**7/6

Enter selection 1

Enter weight of explosives, lb 2000

4. Direction of Target

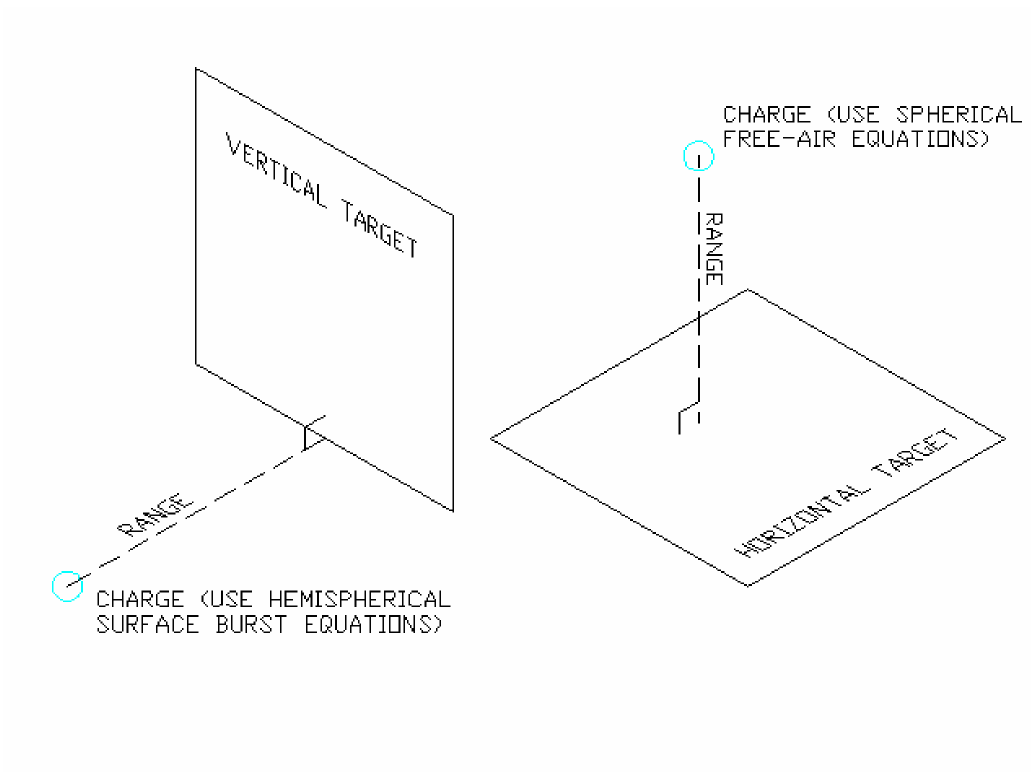

5. Enter Stand-off Distance

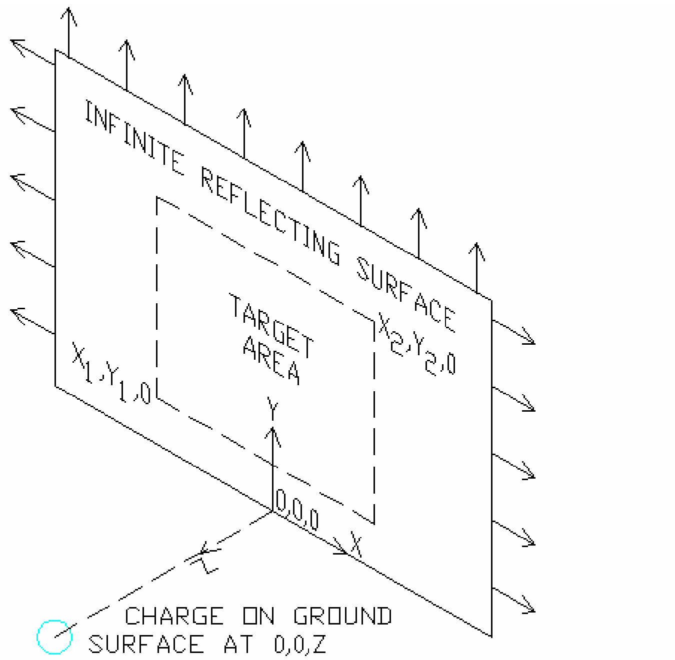


```
Enter standoff distance Z, feet   (0 to abort)...  970
```

6. Answers of CASE1

```
***************** ANSWERS **********************
Charge weight, lb ..................     2000.
Equivalent weight of TNT, lb ........    2000.
Horizontal range, feet   ...........     970.0

                  YIELDS

Peak pressure, psi .................     1.032
 at X =    0.0000E+00 feet
    Y =    0.0000E+00 feet
Minimum pressure, psi ..............     1.028
 at X =    -60.00      feet
    Y =     39.00      feet
Total impulse, lb-sec ..............   0.1740E+05
Average impulse, psi-msec ..........     25.82


          Press <Enter> to continue ...
```

7. Plot Peak Pressure of CASE 1, 2, 3 and 4

Peak Pressure Distribution

Charge Weight, lb .... 2000.
TNT Equivalent, lb .... 2000.
Range, feet 970.0
Peak Pressure, psi 1.032

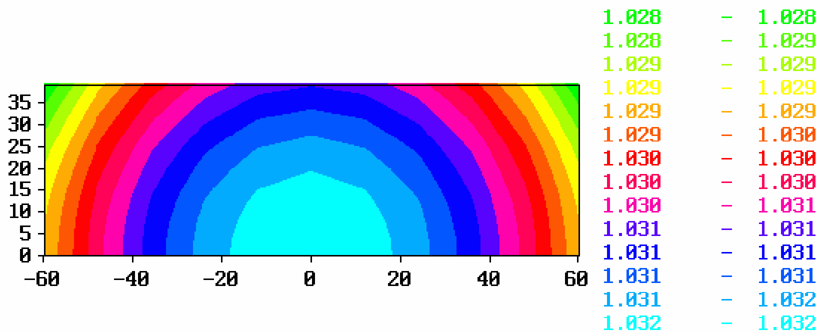

Peak Pressure Distribution

Charge Weight, lb .... 2000.
TNT Equivalent, lb .... 2000.
Range, feet 575.0
Peak Pressure, psi 2.043

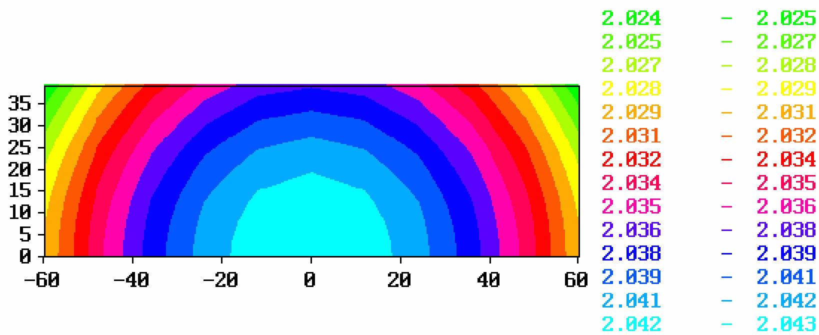

Peak Pressure Distribution

```
Charge Weight, lb ........ 2000.
TNT Equivalent, lb ....... 2000.
Range, feet   ............ 335.0
Peak Pressure, psi ....... 4.192
```

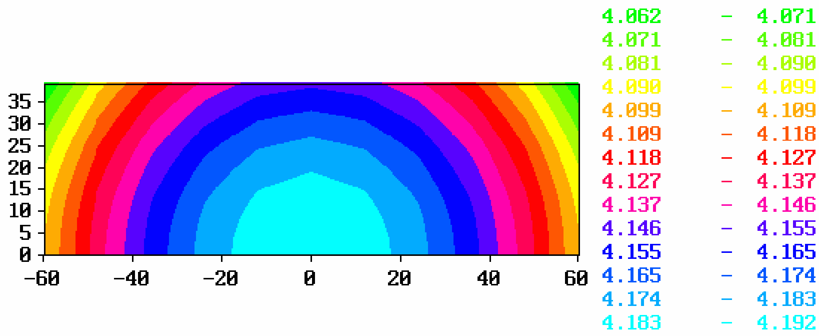

Peak Pressure Distribution

```
Charge Weight, lb ........ 2000.
TNT Equivalent, lb ....... 2000.
Range, feet   ............ 123.0
Peak Pressure, psi ....... 25.05
```

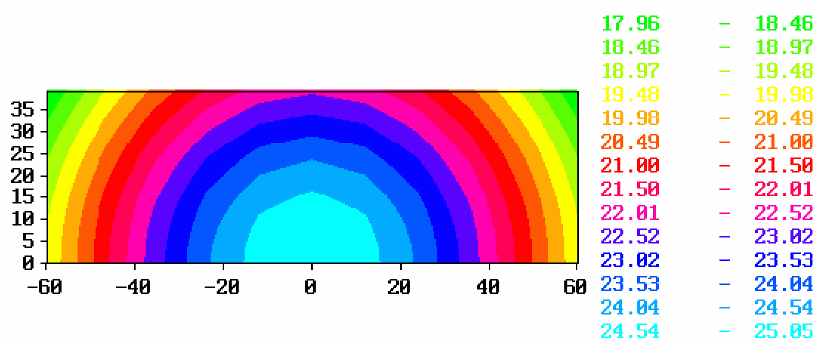

Appendix B : Demand/Capacity Ratio of 3 Story Building

B.1. Variable Stand-off Distance

CASE 1 : Moment Released

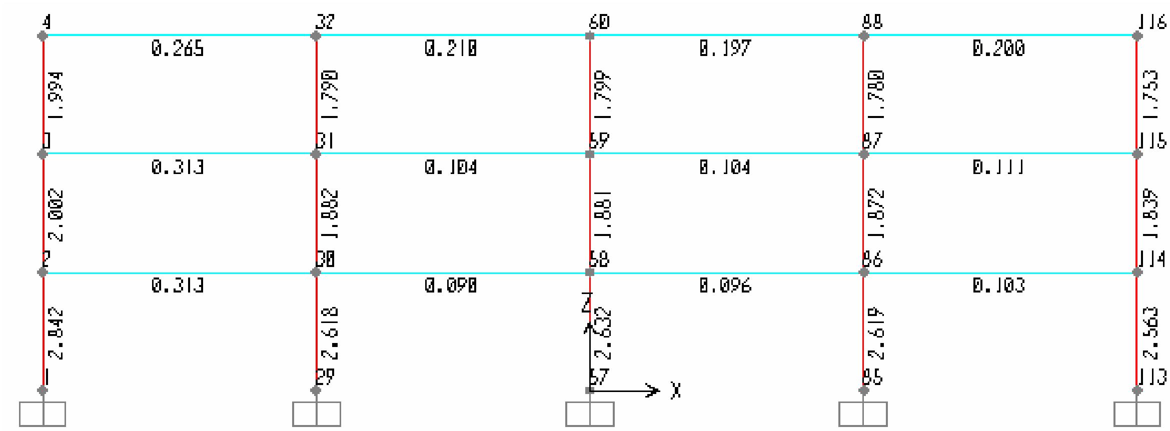

(a) 1,000 lb Weight at 15 ft Stand-off

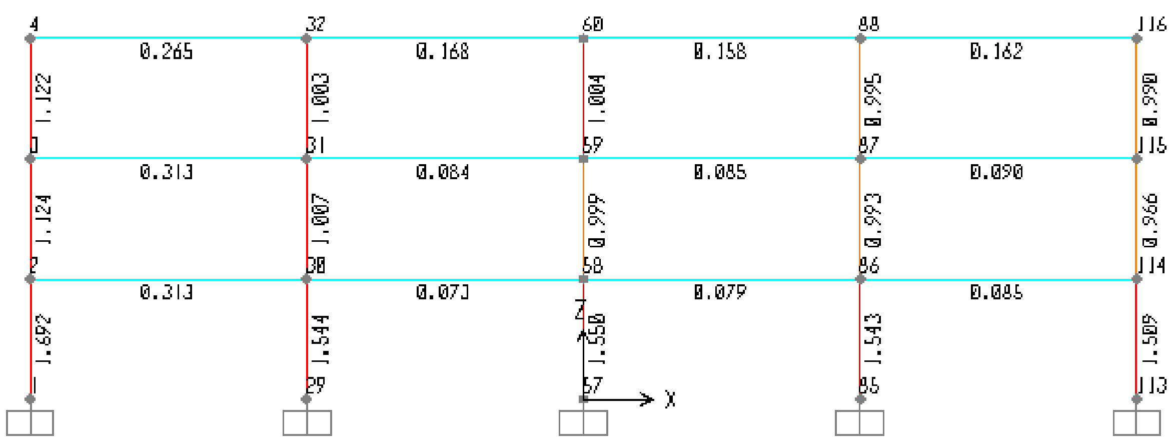

(b) 1,000 lb Weight at 30 ft Stand-off

Figure B. 1 : Demand/Capacity Ratio on Transverse MRF to Variable Stand-Off Distances (Moment Released)

"**Figure B.1 : Continued**"

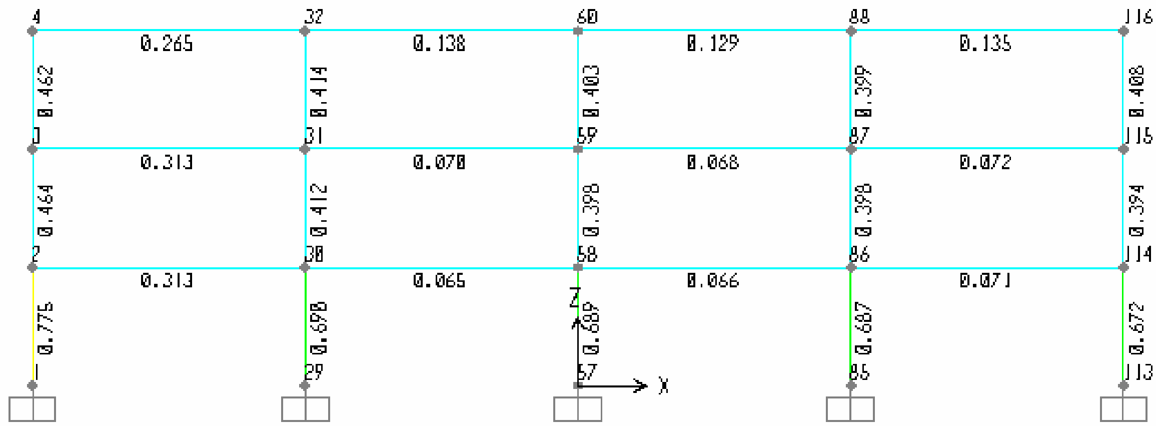

(c) Demand/capacity ratio with 1,000 lb Weight at 50 ft Stand-off

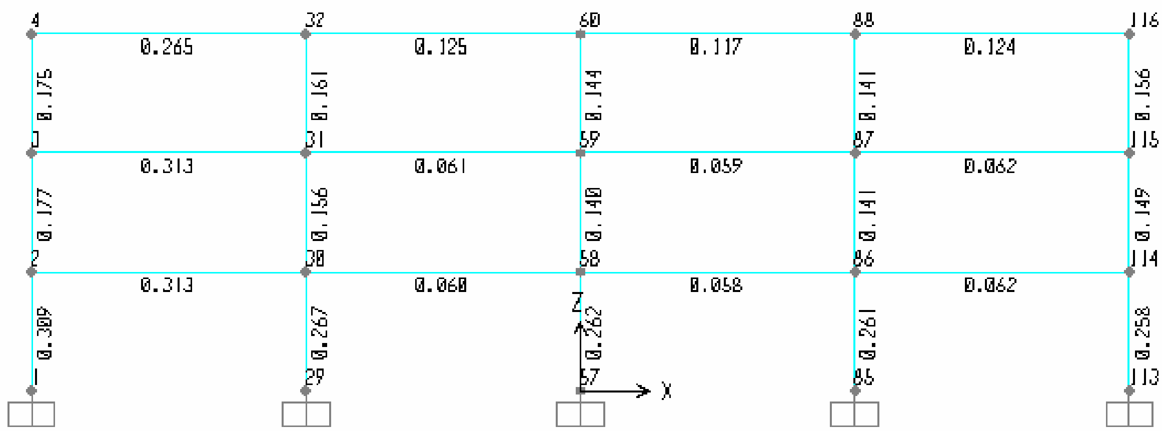

(d) Demand/capacity ratio with 1,000 lb Weight at 100 ft Stand-off

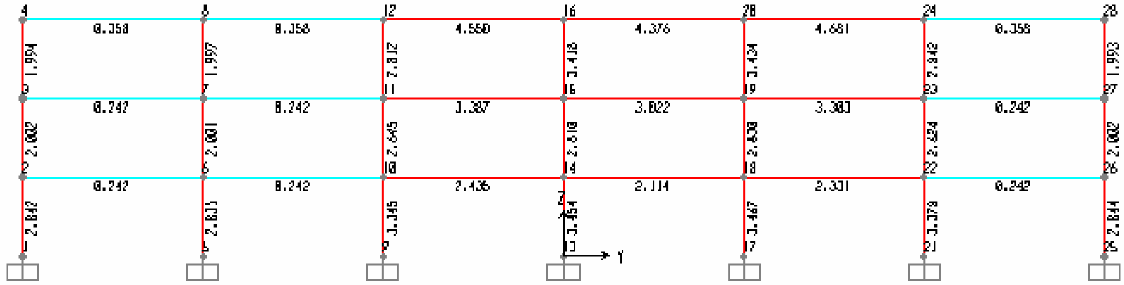

(a) 1,000 lb Weight at 15 ft Stand-off

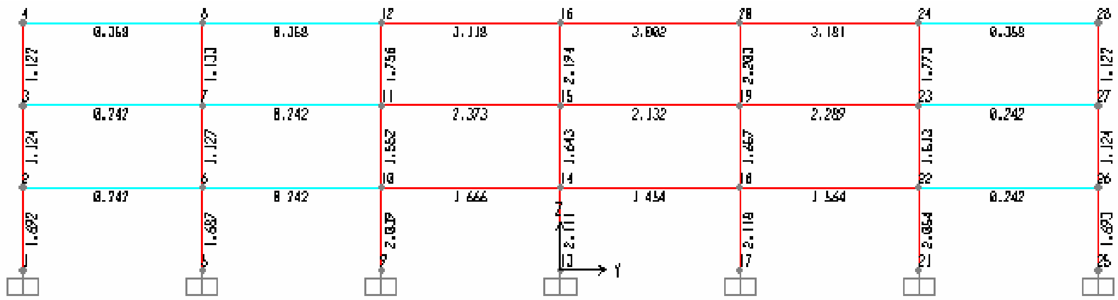

(b) 1,000 lb Weight at 30 ft Stand-off

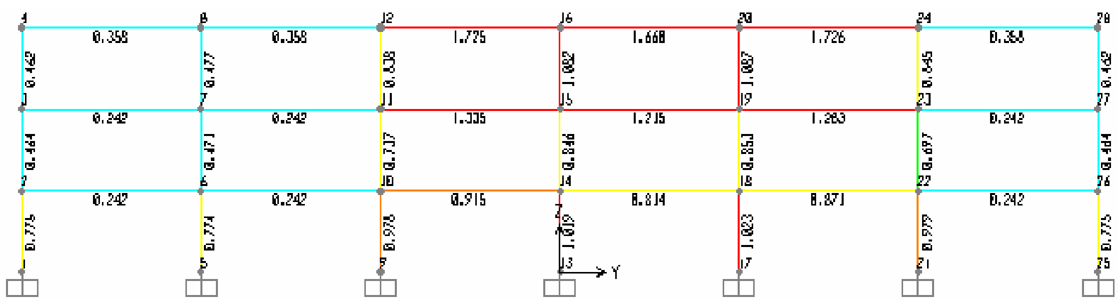

(c) 1,000 lb Weight at 50 ft Stand-off

Figure B. 2 : Demand/Capacity Ratio on Longitudinal MRF to Variable Stand-Off Distances (Moment Released)

“Figure B.2 : Continued”

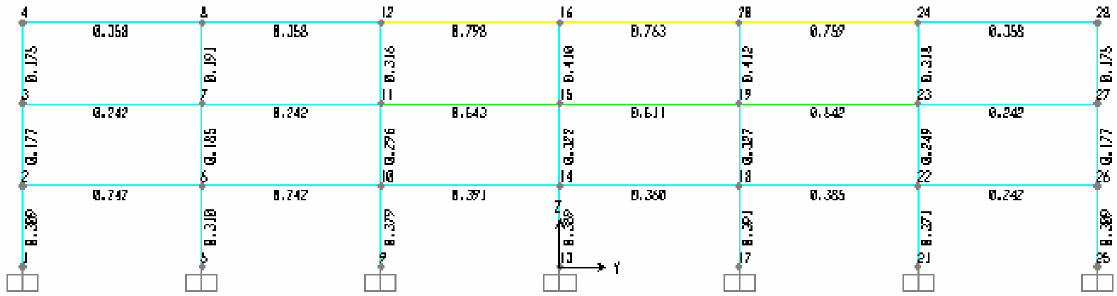

(d) 1,000 lb Weight at 100 ft Stand-off

CASE 2 : Moment Fixed

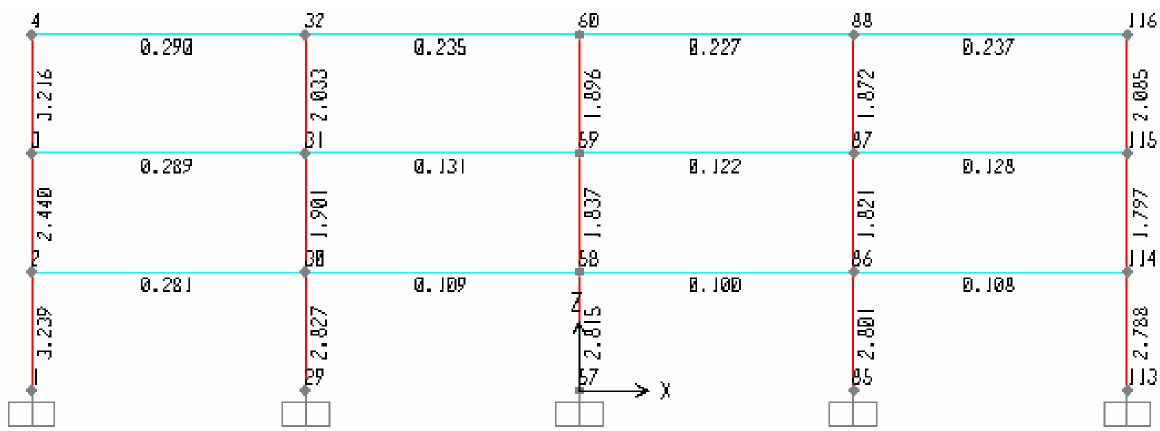

(a) 1,000 lb Weight at 15 ft Stand-off

Figure B. 3 : Demand/Capacity Ratio on Transverse MRF to Variable Stand-Off Distances (Moment Fixed)

“Figure B.3 : Continued”

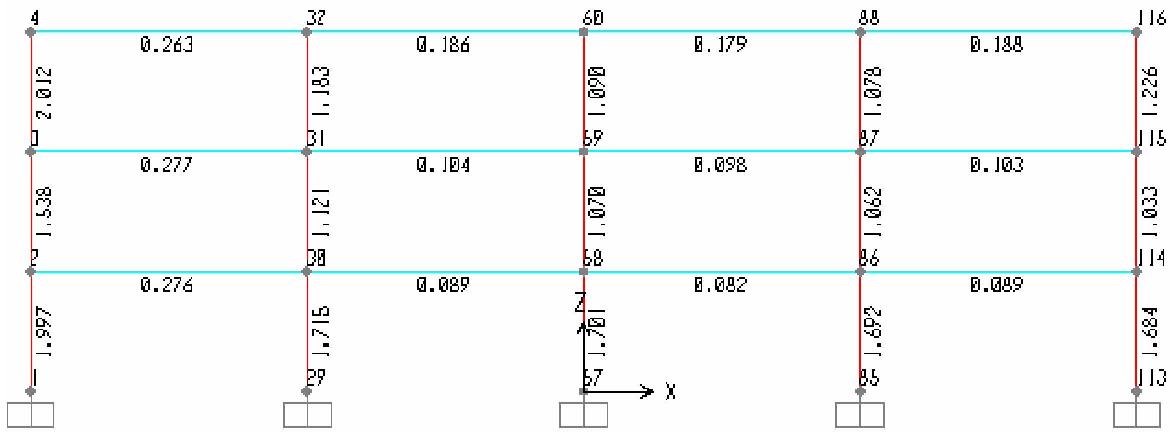

(b) Demand/capacity ratio with 1,000 lb Weight at 30 ft Stand-off

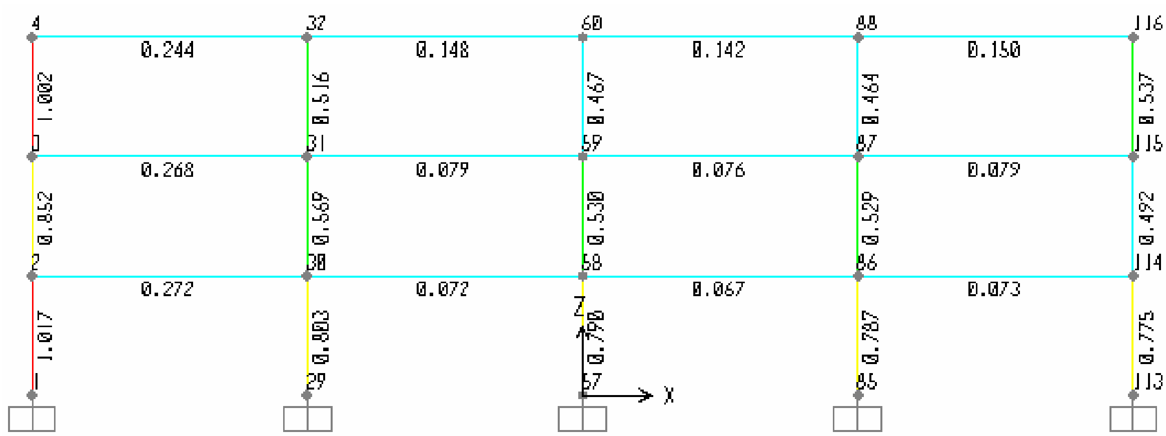

(c) Demand/capacity ratio with 1,000 lb Weight at 50 ft Stand-off

“Figure B.3 : Continued”

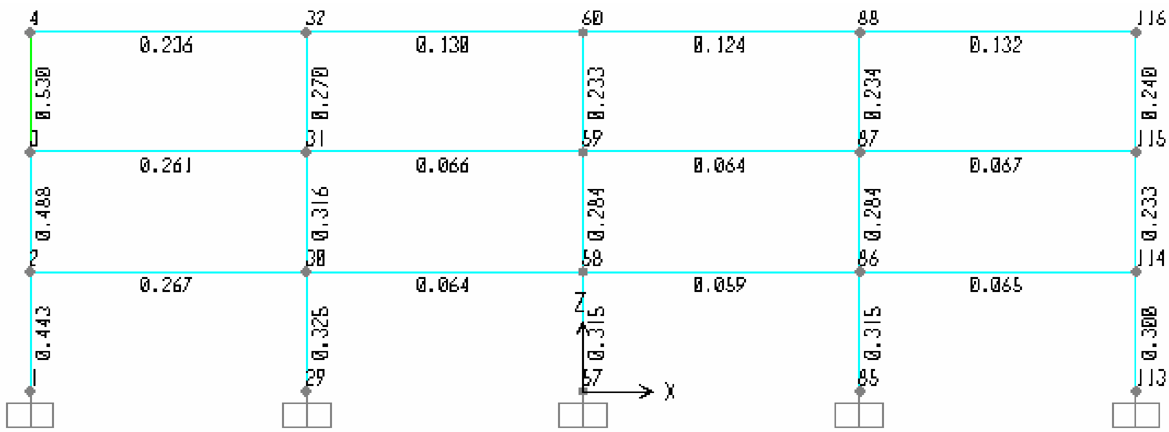

(d) Demand/capacity ratio with 1,000 lb Weight at 100 ft Stand-off

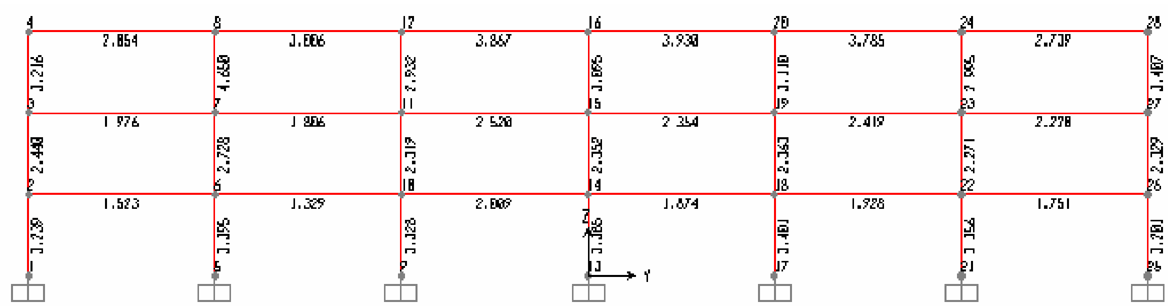

(a) 1,000 lb Weight at 15 ft Stand-off

Figure B. 4 : Demand/Capacity Ratio on Longitudinal MRF to Variable Stand-Off Distances (Moment Fixed)

“Figure B.4 : Continued”

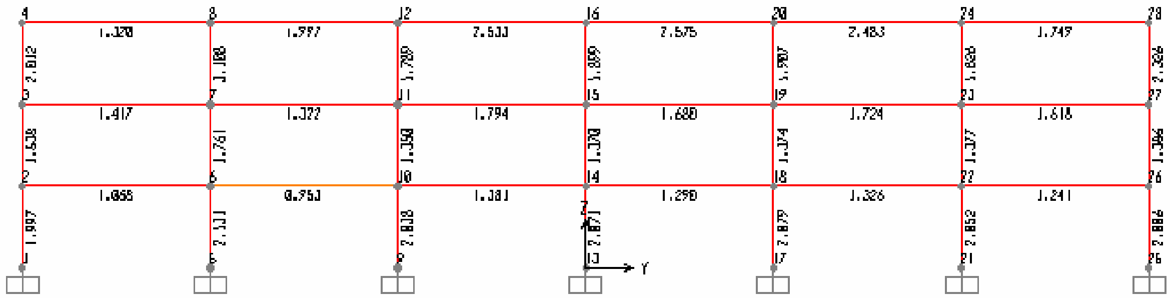

(b) 1,000 lb Weight at 30 ft Stand-off

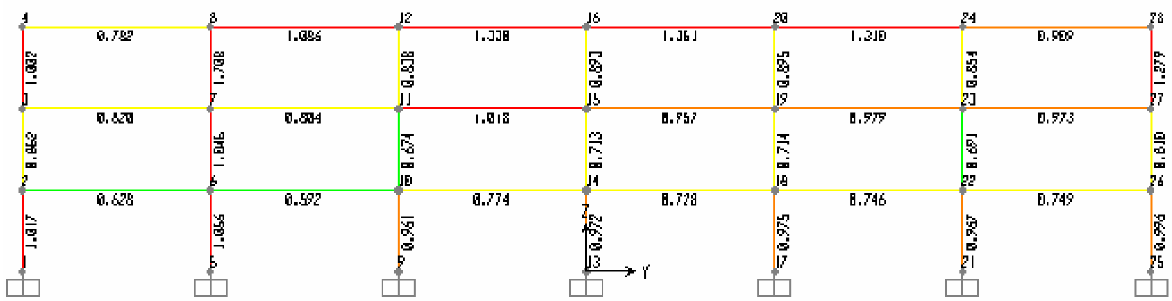

(c) 1,000 lb Weight at 50 ft Stand-off

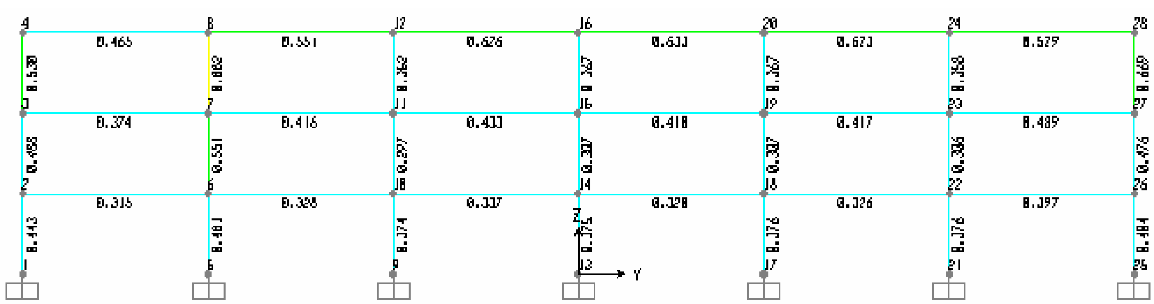

(d) Demand/capacity ratio with 1,000 lb Weight at 100 ft Stand-off

CASE 3 : Moment Fixed (Alternative Rotation)

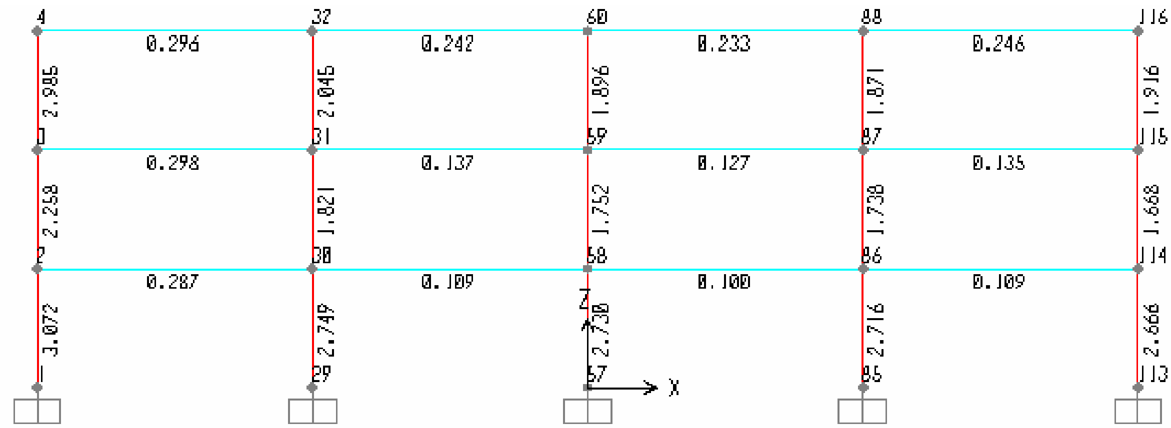

(a) 1,000 lb Weight at 15 ft Stand-off

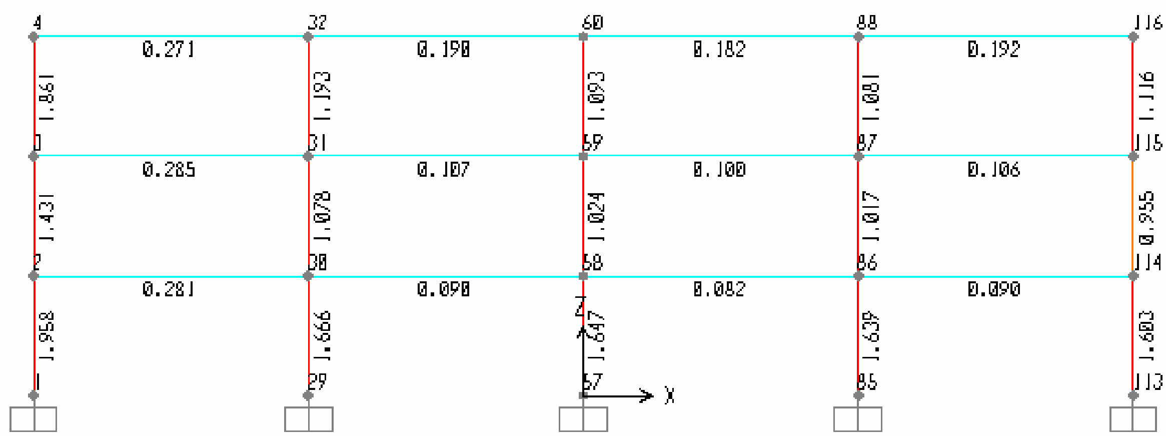

(b) 1,000 lb Weight at 30 ft Stand-off

Figure B. 5 : Demand/Capacity Ratio on Transverse MRF to Variable Stand-Off Distances (Moment Fixed (Alternative Rotation))

“Figure B.5 : Continued”

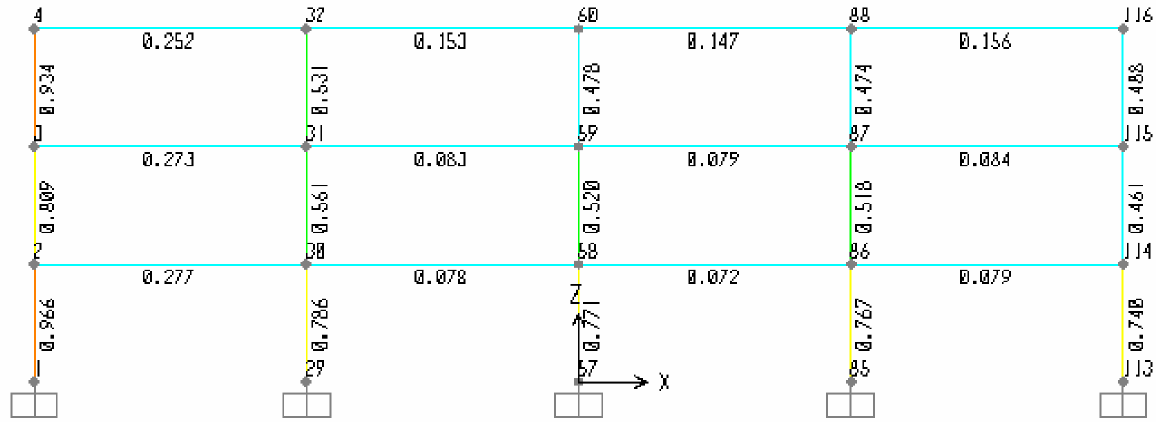

(c) 1,000 lb Weight at 50 ft Stand-off

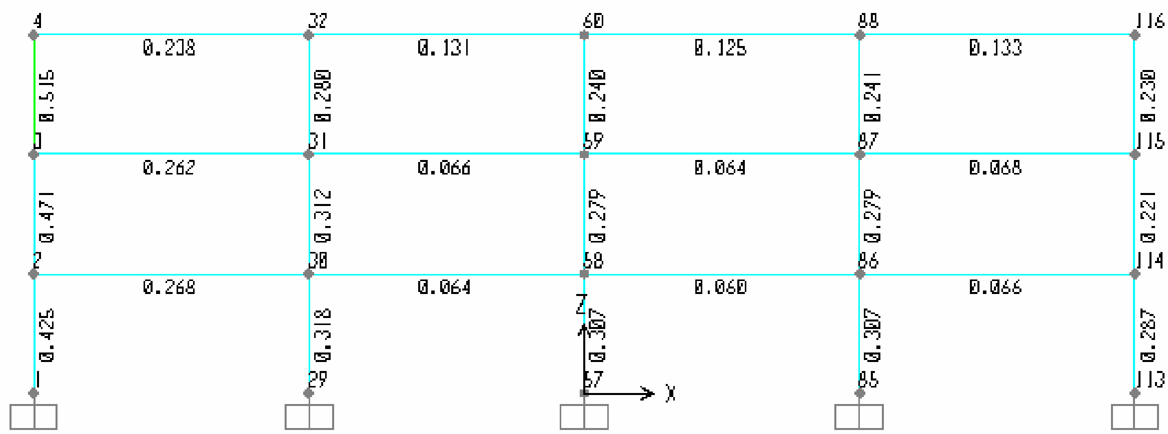

(d) 1,000 lb Weight at 100 ft Stand-off

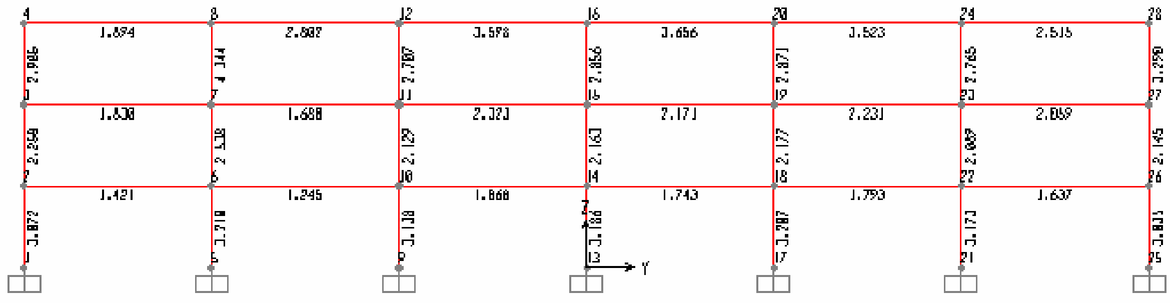

(a) 1,000 lb Weight at 15 ft Stand-off

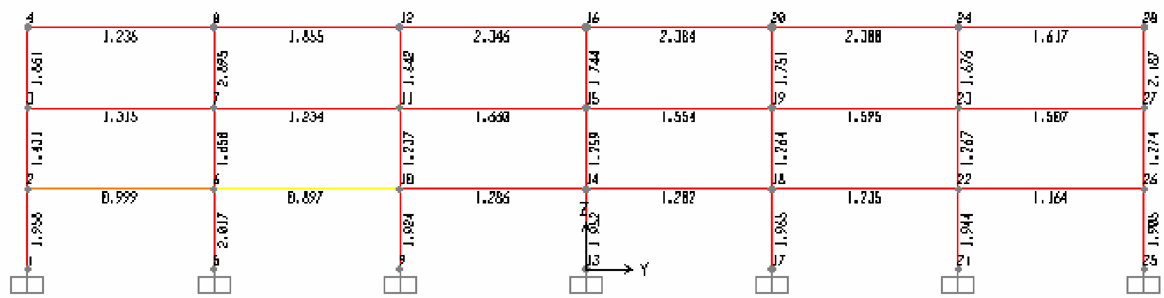

(b) 1,000 lb Weight at 30 ft Stand-off

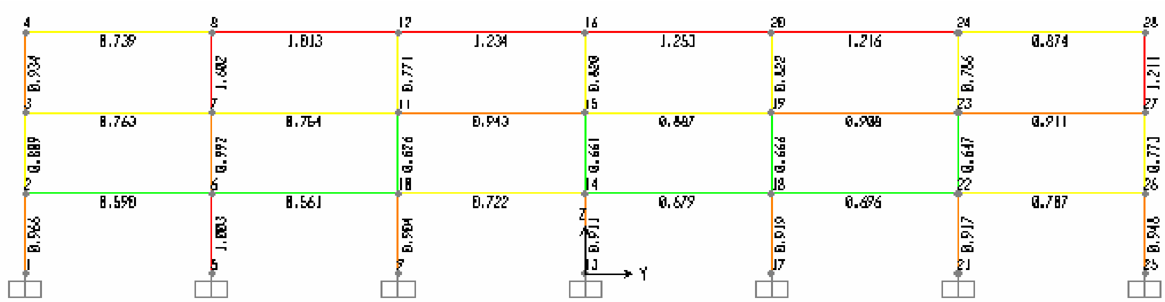

(c) 1,000 lb Weight at 50 ft Stand-off

Figure B. 6 : Demand/Capacity Ratio on Longitudinal MRF to Variable Stand-Off Distances (Moment Fixed (Alternative Rotation))

"Figure B.6 : Continued"

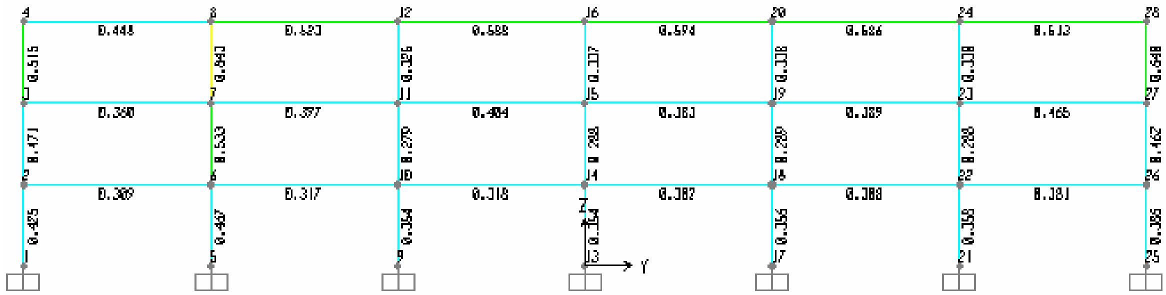

(d) 1,000 lb Weight at 100 ft Stand-off

B.2. Variable TNT Weights

Case 1 : Moment Released

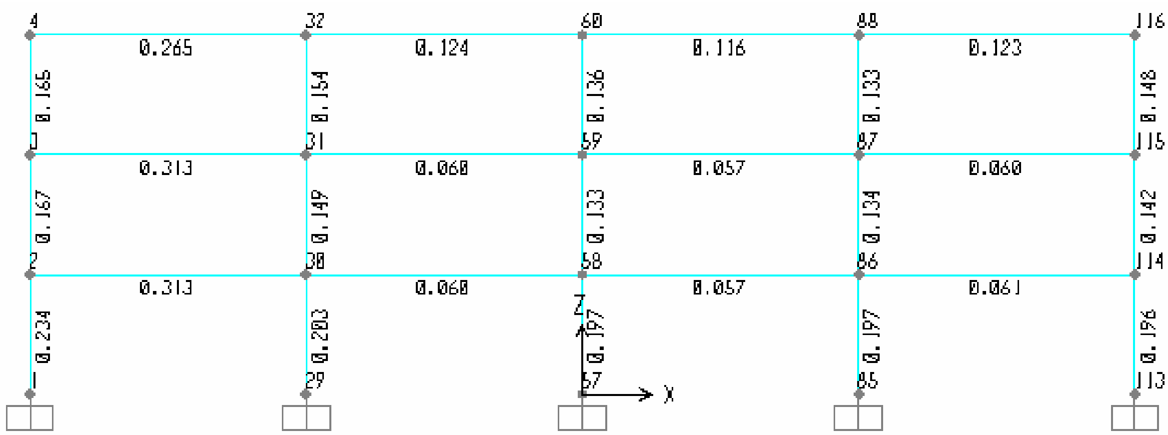

(a) 100 lb Weight at 20 ft Stand-Off

Figure B. 7 : Demand/Capacity Ratio on Transverse MRF to Variable TNT Weight (Moment Released)

“Figure B.7 : Continued”

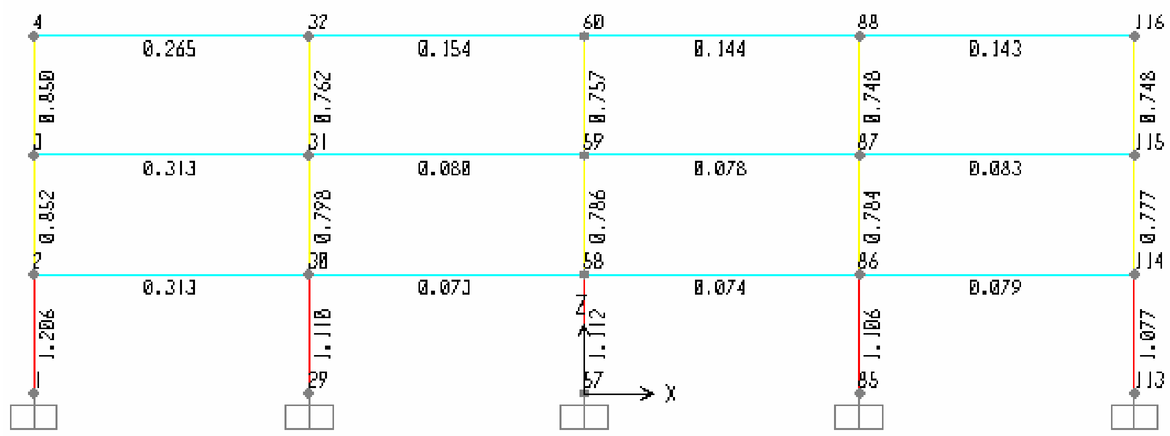

(b) 500 lb Weight at 20 ft Stand-Off

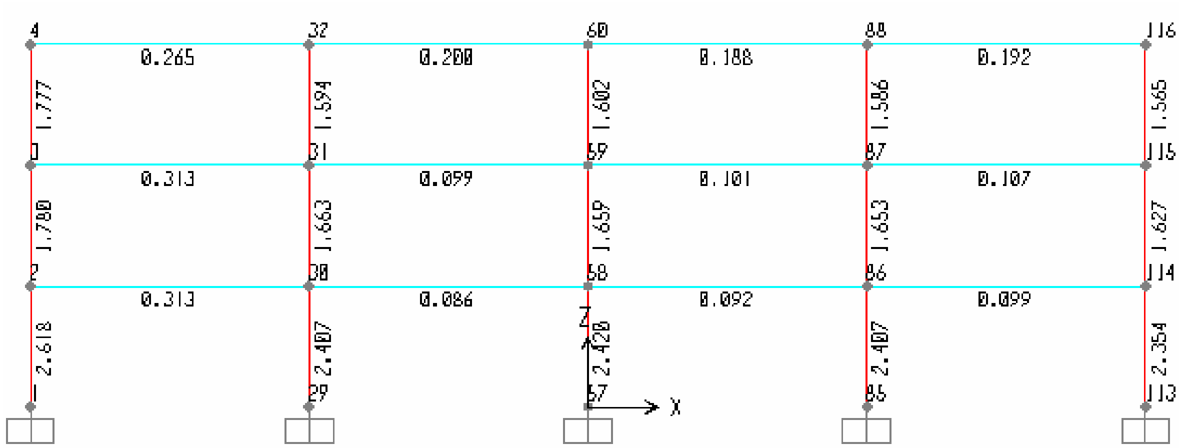

(c) 1,000 lb Weight at 20 ft Stand-Off

"Figure B.7 : Continued"

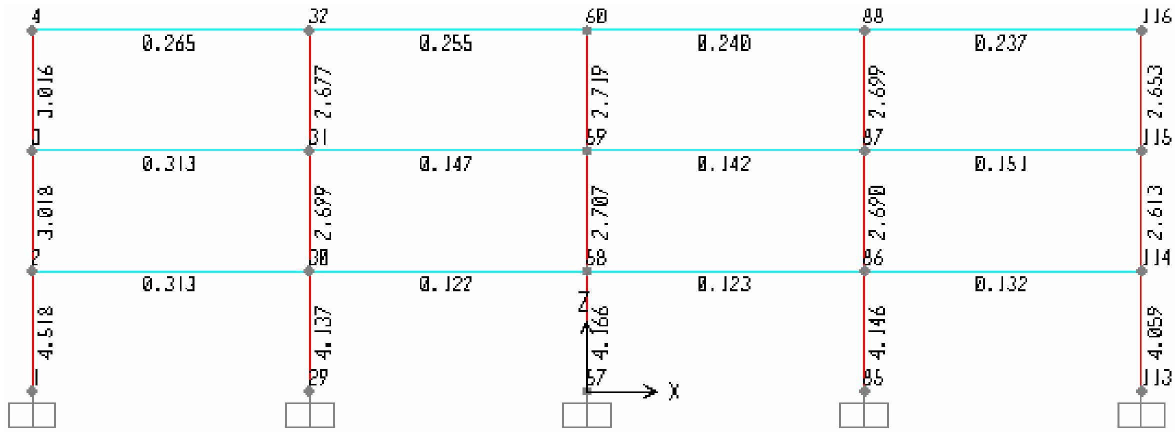

(d) 2,000 lb Weight at 20 ft Stand-off

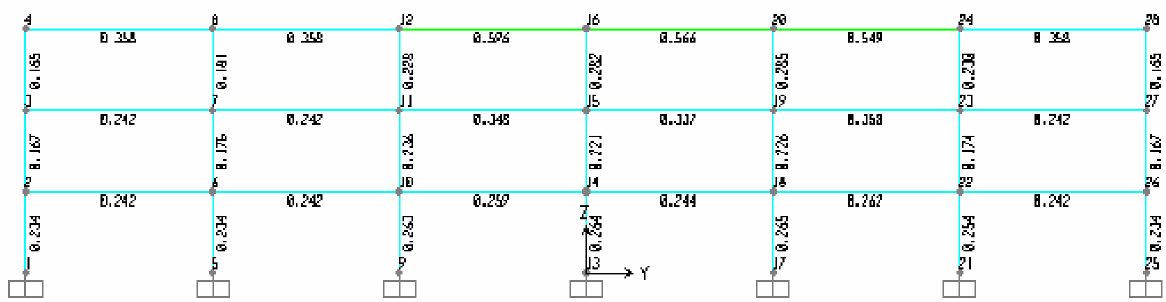

(a) 100 lb Weight at 20 ft Stand-off

Figure B. 8 : Demand/Capacity Ratio on Longitudinal MRF to Variable TNT Weight (Moment Released)

"Figure B.8 : Continued"

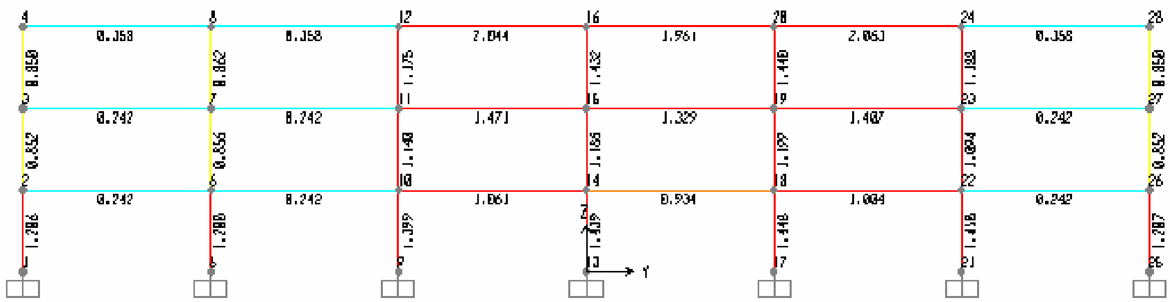

(b) 500 lb Weight at 20 ft Stand-off

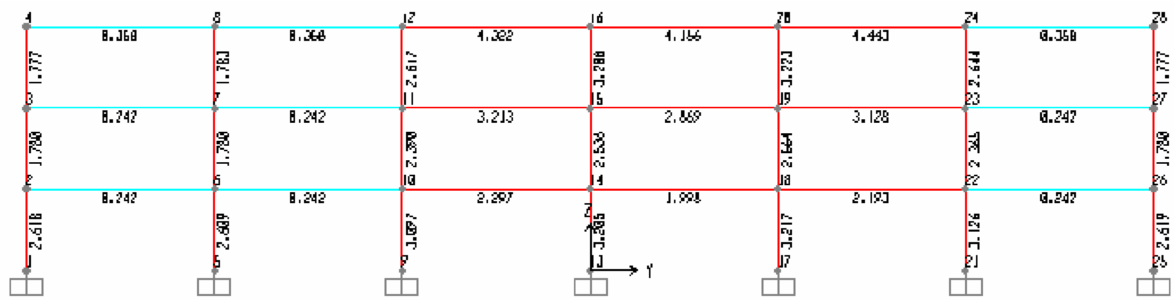

(c) 1,000 lb Weight at 20 ft Stand-off

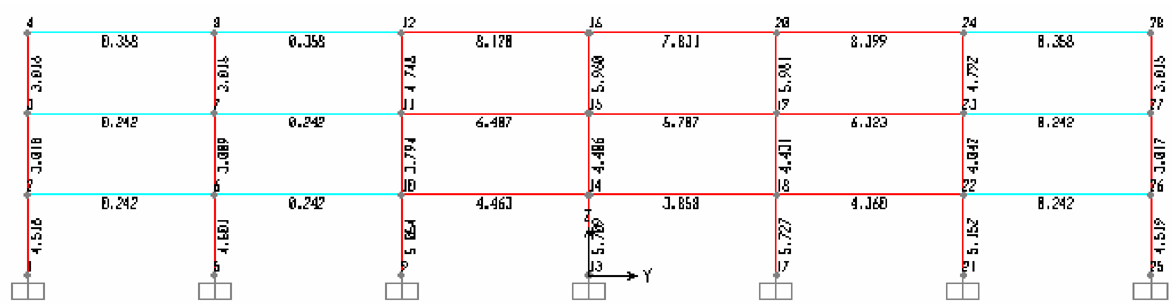

(d) 2,000 lb TNT Weight at 20 ft Stand-off

CASE 2 : Moment Fixed

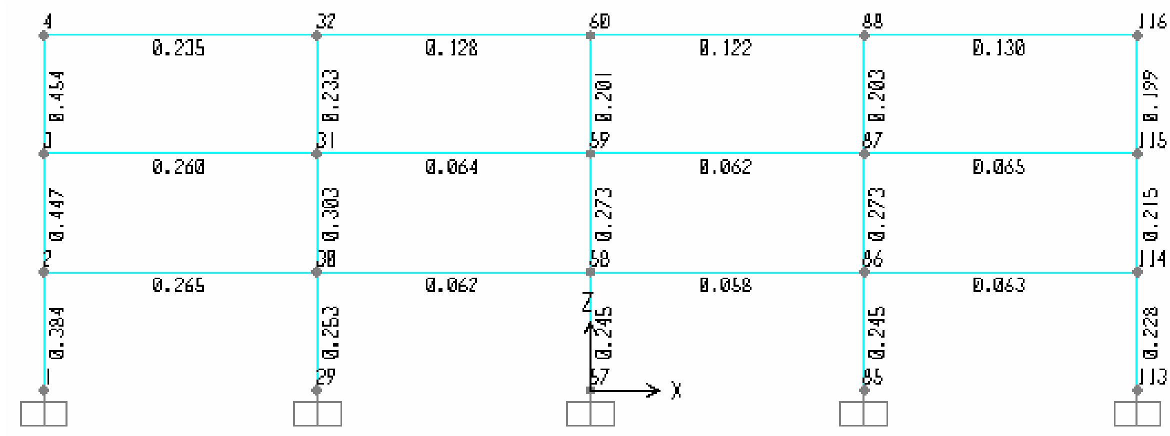

(a) 100 lb TNT Weight at 20 ft Stand-off

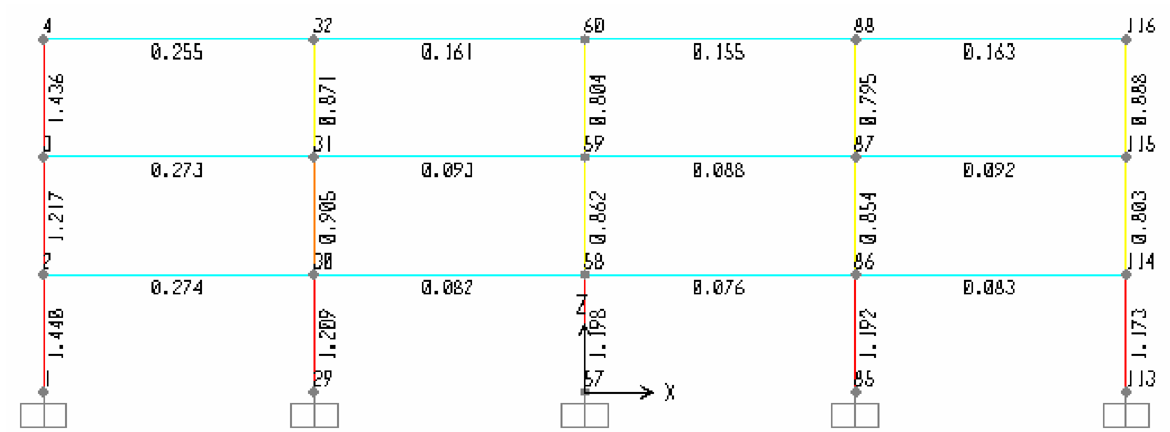

(b) 500 lb TNT Weight at 20 ft Stand-off

Figure B. 9 : Demand/Capacity Ratio on Transverse MRF to Variable TNT Weight (Moment Fixed)

“Figure B.9 : Continued”

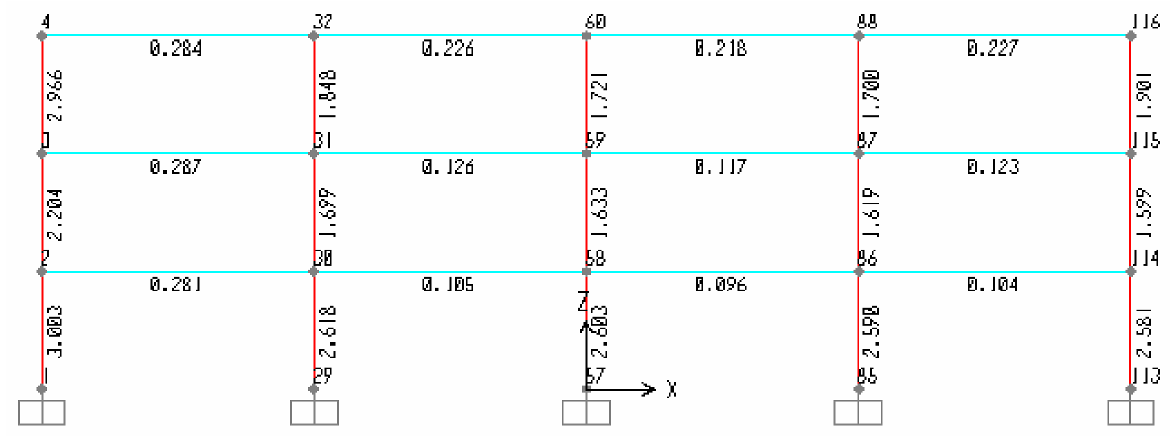

(c) 1,000 lb TNT Weight at 20 ft Stand-off

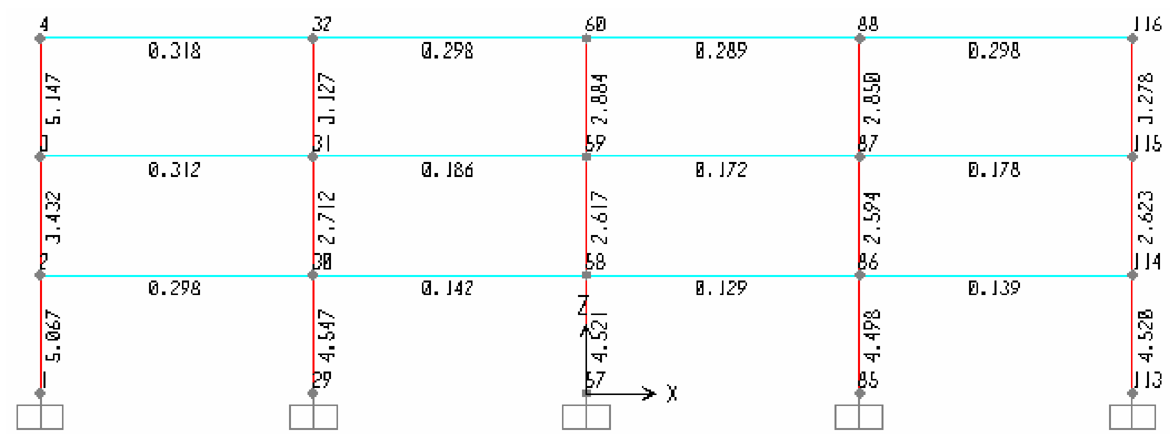

(d) 2,000 lb TNT Weight at 20 ft Stand-off

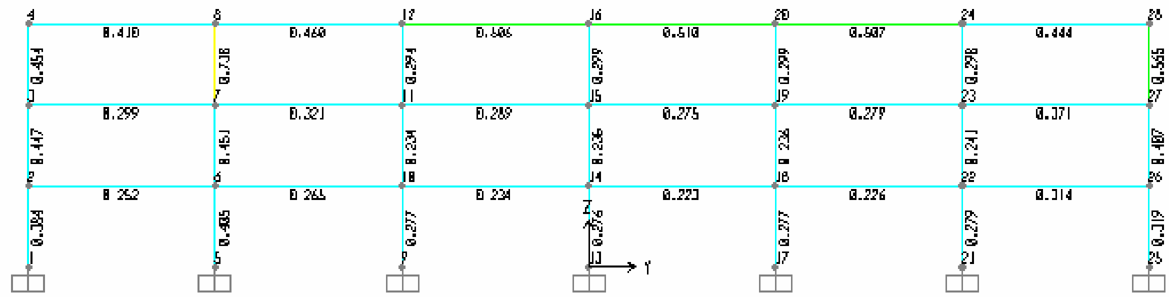

(a) 100 lb TNT Weight at 20 ft Stand-off

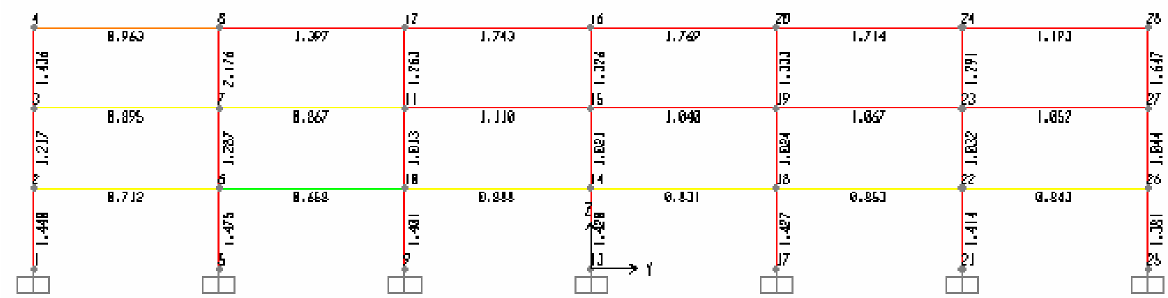

(b) 500 lb TNT Weight at 20 ft Stand-off

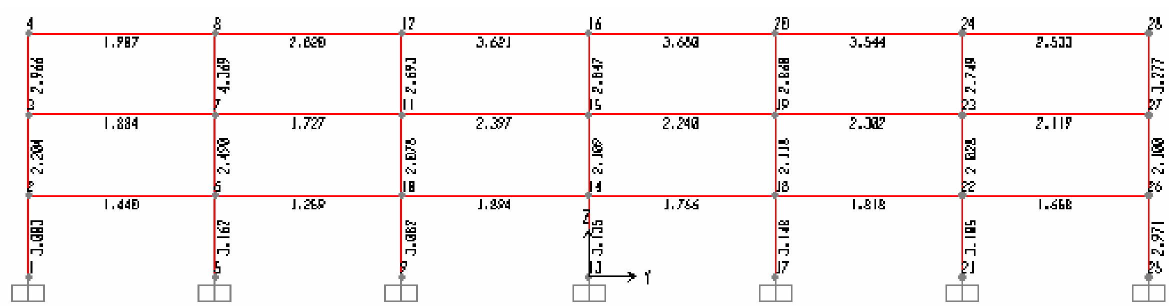

(c) 1,000 lb TNT Weight at 20 ft Stand-off

Figure B. 10 : Demand/Capacity Ratio on Longitudinal MRF to Variable TNT Weight (Moment Fixed)

“Figure B.10 : Continued”

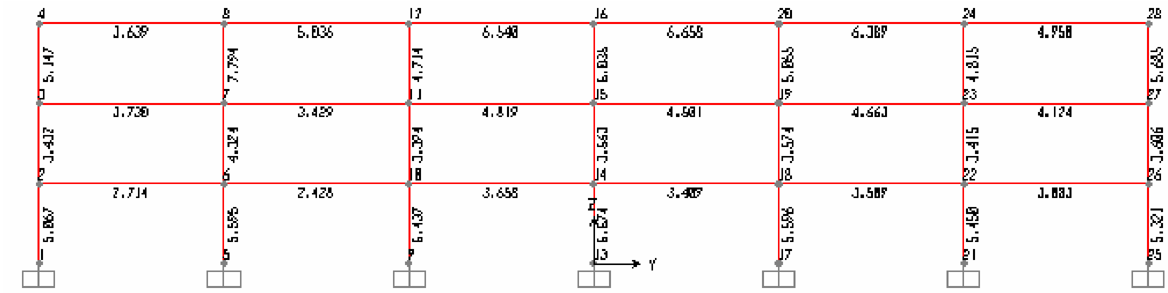

(d) 2,000 lb TNT Weight at 20 ft Stand-off

CASE 3 : Moment Fixed (Alternative Rotation)

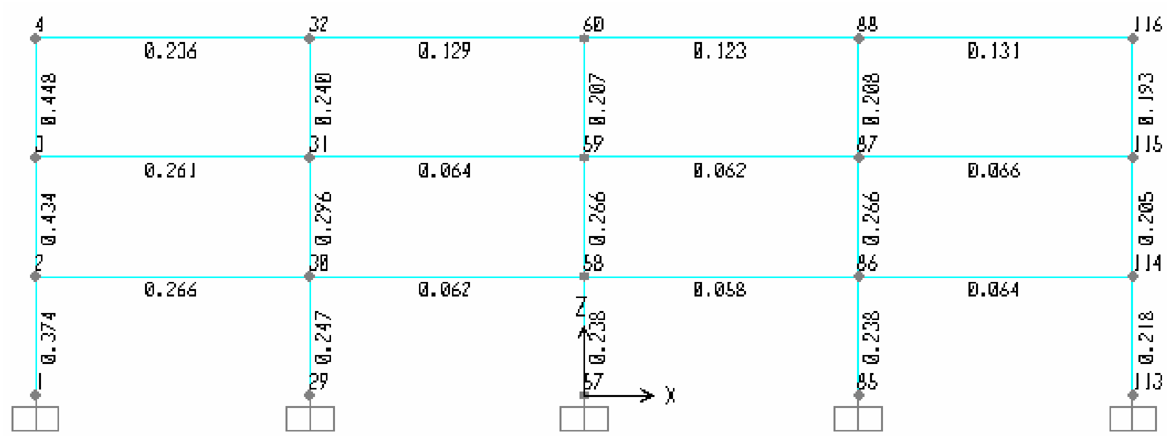

(a) 100 lb TNT Weight at 20 ft Stand-off

Figure B. 11 : Demand/Capacity Ratio on Transverse MRF to Variable TNT Weight (Moment Fixed (Alternative Rotation))

“Figure B.11 : Continued”

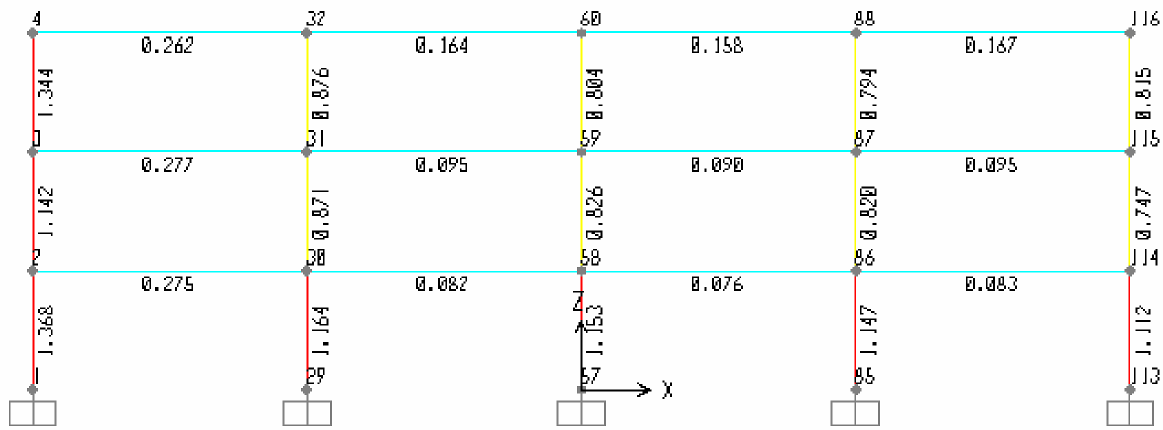

(b) 500 lb TNT Weight at 20 ft Stand-off

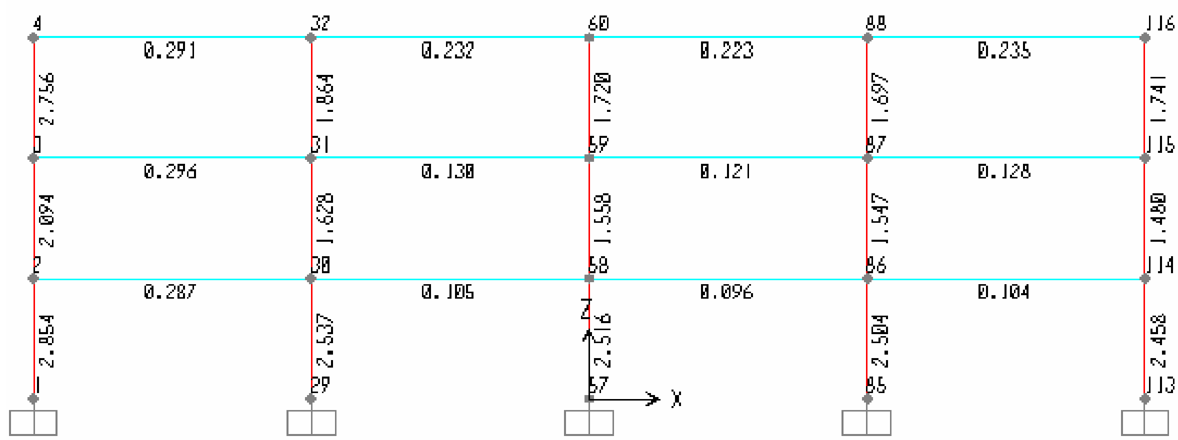

(c) 1,000 lb TNT Weight at 20 ft Stand-off

"Figure B.11 : Continued"

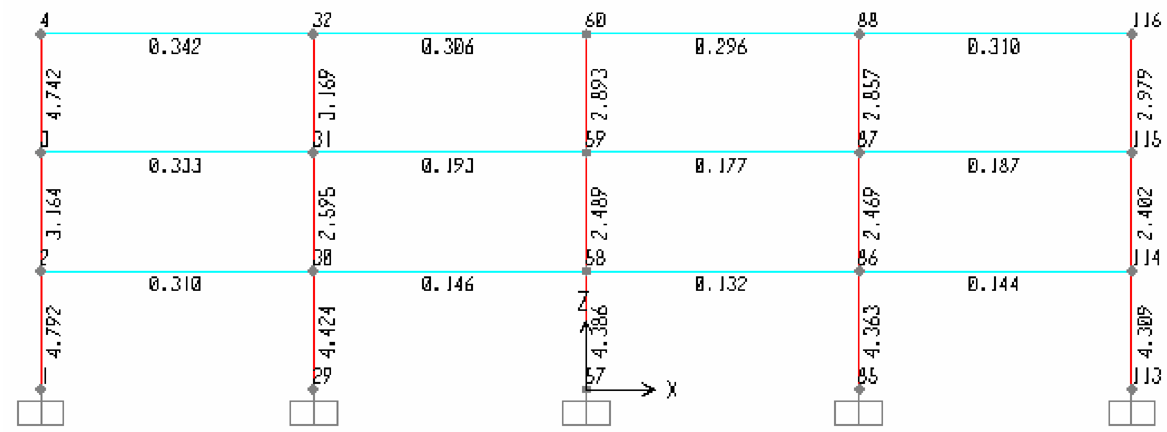

(d) 2,000 lb TNT Weight at 20 ft Stand-off

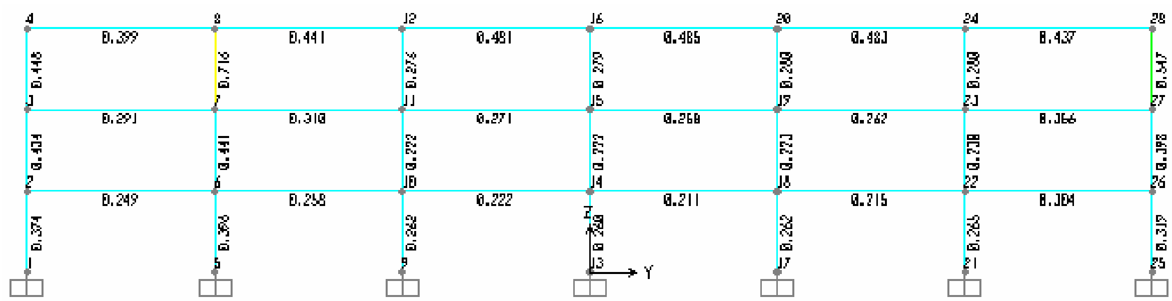

(a) 100 lb TNT Weight at 20 ft Stand-off

Figure B. 12 : Demand/Capacity Ratio on Longitudinal MRF to Variable TNT Weight (Moment Fixed (Alternative Rotation))

"**Figure B.12 : Continued**"

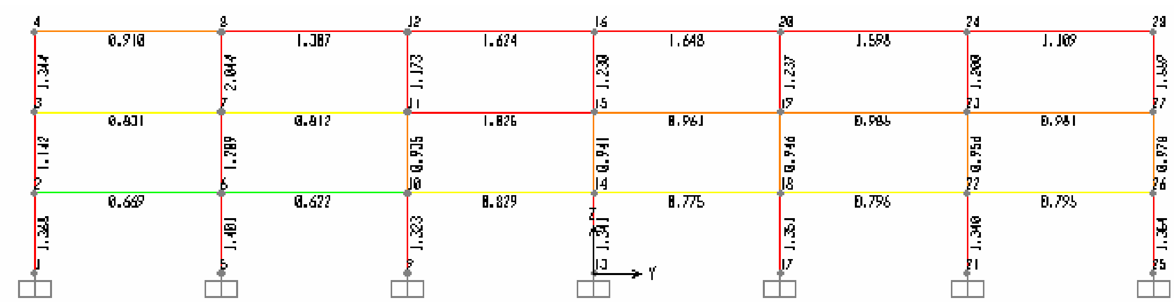

(b) 500 lb TNT Weight at 20 ft Stand-off

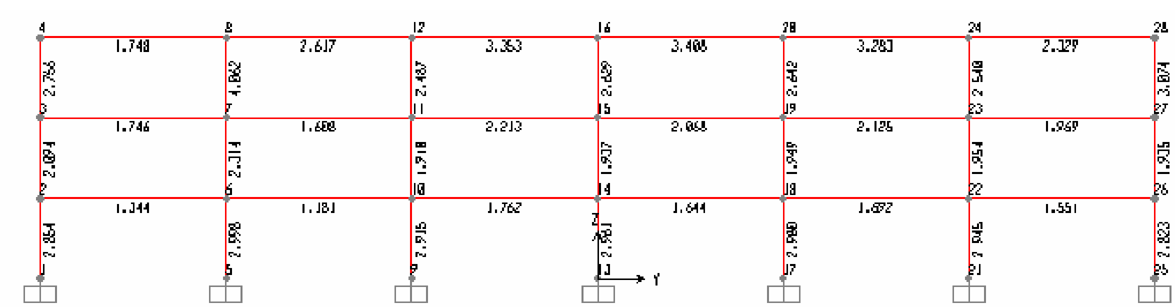

(c) 1,000 lb TNT Weight at 20 ft Stand-off

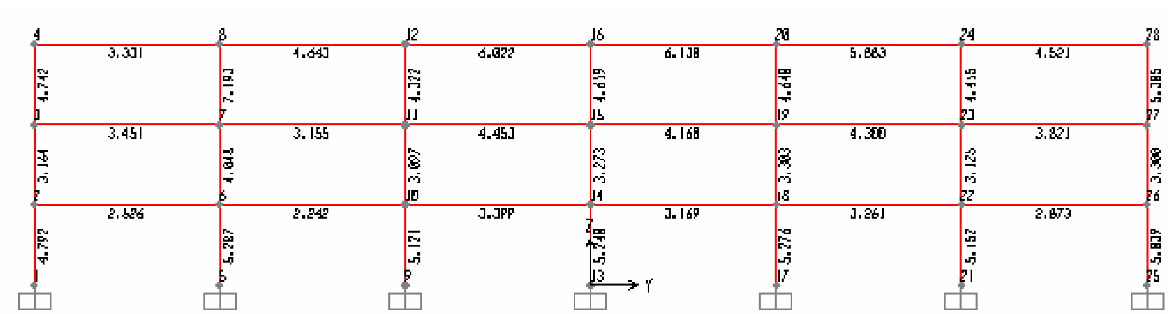

(d) 2,000 lb TNT Weight at 20 ft Stand-off

Appendix C : Calculation of Effective Thickness for Composite Slab

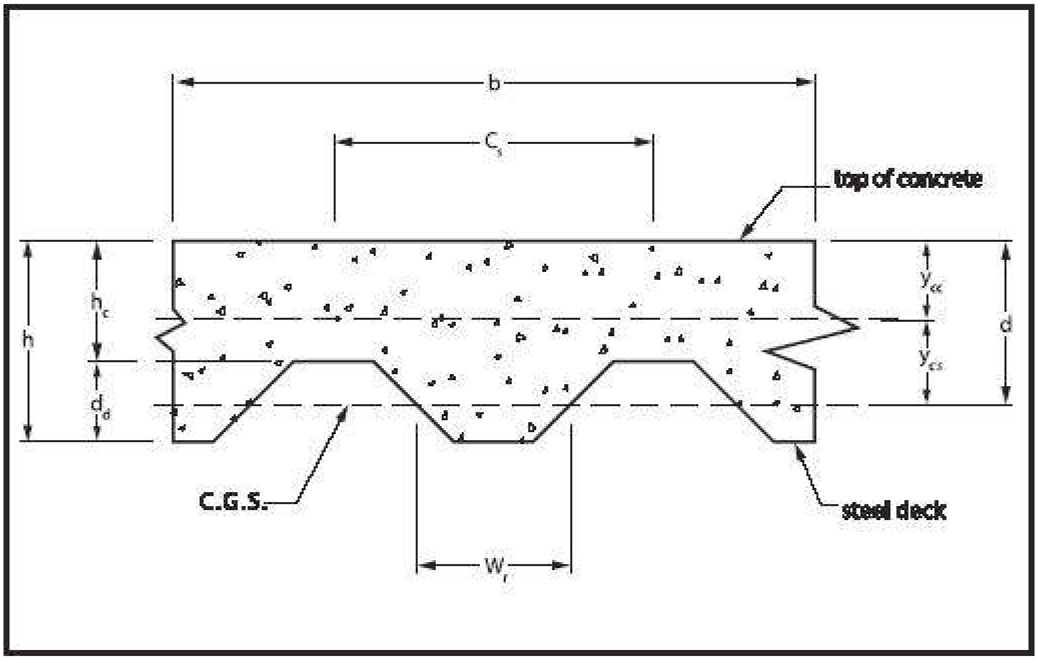

Figure C. 1 : The dimension of Composite Slab [23]

Note : 1. Section shows non-cellular deck. Section shall be either cellular, a blend of cellular and non-cellular deck, or non-cellular deck

2. C.G..S. = centroidal axis of full cross section of steel deck (3.64 in)

3. Cs = pitch (12 in)

4. N.A. = neutral axis of transformed composite section

5. Wr = average rib width (6 in)

Moment of Inertia of Uncracked Section

For the uncracked moment of inertia

$$y_{cc} = \frac{0.5bh_c^2 + nA_s d + W_r d_d\left(h - 0.5d_d\right)\dfrac{b}{C_s}}{bh_c + nA_s + W_r d_d\,\dfrac{b}{C_s}}$$

= 2.46 in

y_{cs} = d – y_{cc} = 1.18 in

The uncracked moment of inertia is

$$I_u = \frac{bh_c^3}{12n} + \frac{bh_c}{n}\left(y_{cc} - 0.5h_c\right)^2 + I_{sf} + A_s y_{cs}^2 + \left(\frac{W_r b d_d}{nC_s}\right)\left[\frac{d_d^2}{12} + \left(h - y_{cc} - 0.5d_d\right)^2\right]$$

= 33.09 in^4

Where

As = area of steel deck per unit slab width = 1.85 in^2

b = unit slab width (12 inches in imperial units) = 24 in

d = distance from top of concrete to centroid of steel deck = 3.64 in

n = modular ratio = Es/Ec = 8

I_{sf} = the moment of inertia of the full (unreduced) steel deck per unit slab width = 1.51 in^4

hc = 2.5 in

$w_r = 6$ in

$d_d = 3$ in

$h = 5.5$ in

$c_s = 12$ in

Therefore, the thickness of transformed concrete is **3.5 in**